

Molecular Zinc(I) Dimers, Zinc(II) Hydrides, and Cations: Synthesis, and Catalytic Applications with Mechanistic Insights

By

RAJATA KUMAR SAHOO

CHEM11201704023

**National Institute of Science Education and Research Bhubaneswar,
Odisha – 752050**

*A thesis submitted to the
Board of Studies in Chemical Sciences
In partial fulfillment of requirements
for the Degree of*

DOCTOR OF PHILOSOPHY

of

HOMI BHABHA NATIONAL INSTITUTE



June, 2023

Homi Bhabha National Institute¹

Recommendations of the Viva Voce Committee

As members of the Viva Voce Committee, we certify that we have read the dissertation prepared by **Rajata Kumar Sahoo** entitled “**Molecular Zinc(I) Dimers, Zinc(II) Hydrides, and Cations: Synthesis, and Catalytic Applications with Mechanistic Insights**” and recommend that it may be accepted as fulfilling the thesis requirement for the award of Degree of Doctor of Philosophy.

Chairman – Dr. Moloy Sarkar



Date: 24.08.23

Guide / Convener – Dr. Sharanappa Nembenna



Date: 24/8/23

Examiner – Prof. Dr. Ganesan Prabu Sankar



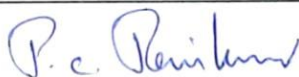
Date: 24/08/2023

Member 1 – Dr. Bhargava B.L.



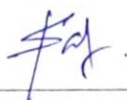
Date: 24.08.2023

Member 2 – Dr. P. C. Ravikumar



Date: 24/08/2023

Member 3 – Dr. Shantanu Pal




Date: 24/8/23.

Final approval and acceptance of this thesis is contingent upon the candidate's submission of the final copies of the thesis to HBNI.

I/We hereby certify that I/we have read this thesis prepared under my/our direction and recommend that it may be accepted as fulfilling the thesis requirement.

Date: 24.08.2023

Place: NISER, Bhubaneswar



(Dr. Sharanappa Nembenna)
Guide

¹ This page is to be included only for final submission after successful completion of viva voce.

STATEMENT BY AUTHOR

This dissertation has been submitted in partial fulfillment of requirements for an advanced degree at Homi Bhabha National Institute (HBNI) and is deposited in the library to be made available to borrowers under rules of the HBNI.

Brief quotations from this dissertation are allowable without special permission, provided that accurate acknowledgement of source is made. Requests for permission for extended quotation from or reproduction of this manuscript in whole or in part may be granted by the Competent Authority of HBNI when in his or her judgment the proposed use of the material is in the interests of scholarship. In all other instances, however, permission must be obtained from the author.

Rajata Kumar Sahoo

Rajata Kumar Sahoo

DECLARATION

I, hereby declare that the investigation presented in the thesis has been carried out by me. The work is original and has not been submitted earlier as a whole or in part for a degree / diploma at this or any other Institution / University.

Rajata Kumar Sahoo
Rajata Kumar Sahoo

List of Publications

Journal Published

(#pertaining to the thesis)

1. **#Sahoo, R. K.**; Mahato, M.; Jana, A.; Nembenna, S. Zinc Hydride-Catalyzed Hydrofunctionalization of Ketones. *J. Org. Chem.* **2020**, 85, 11200-11210.
2. **#Sahoo, R. K.**; Sarkar, N.; Nembenna, S. Zinc Hydride Catalyzed Chemoselective Hydroboration of Isocyanates: Amide Bond Formation and C=O Bond Cleavage. *Angew. Chem. Int. Ed.* **2021**, 60, 11991-12000.
3. **#Sahoo, R. K.**; Rajput, S.; Patro, A. G.; Nembenna, S. Synthesis of low oxidation state zinc(I) complexes and their catalytic studies in the dehydroborylation of terminal alkynes. *Dalton Trans.* **2022**, 51, 16009-16016.
4. **#Sahoo, R. K.**; Sarkar, N.; Nembenna, S. Intermediates, Isolation and Mechanistic Insights into Zinc Hydride-Catalyzed 1,2-Regioselective Hydrofunctionalization of N-Heteroarenes. *Inorg. Chem.* **2023**, 62, 304-317.
5. **#Sahoo, R. K.**; Patro, A. G.; Sarkar, N.; Nembenna, S. Comparison of Two Zinc Hydride Precatalysts for Selective Dehydrogenative Borylation of Terminal Alkynes: A Detailed Mechanistic Study. *ACS Omega* **2023**, 8, 3452-3460.
6. **#Sahoo, R. K.**; Patro, A. G.; Sarkar, N.; Nembenna, S. Zinc Catalyzed Hydroelementation (HE; E = B, C, N, and O) of Carbodiimides: Intermediates Isolation and Mechanistic Insights. *Organometallics* **2023**, 42, 1746–1758 (**Special Issue: Advances and Applications in Catalysis with Earth-Abundant Metals**).
7. **#Sahoo, R. K.**; Nembenna, S. Zinc Catalyzed Chemoselective Reduction of Nitriles

-
- to N-Silylimines through Hydrosilylation: Insights into the Reaction Mechanism. *Inorg. Chem.* **2023**, 62, 12213-12222.
8. #**Sahoo, R. K.**; Rajput, S.; Dutta, S.; Sahu, K.; Nembenna, S. Zinc Hydride Catalyzed Dihydroboration of Isonitriles and Nitriles: Mechanistic Studies with the Structurally Characterized Zinc Intermediates. *Organometallics* **2023**, DOI: <https://doi.org/10.1021/acs.organomet.3c00281>.
9. Sarkar, N.; **Sahoo, R. K.**; Mukhopadhyay, S.; Nembenna, S. Organoaluminum Cation Catalyzed Selective Hydrosilylation of Carbonyls, Alkenes, and Alkynes. *Eur. J. Inorg. Chem.* **2022**, e202101030 (*Invited, Main group catalysis*).
10. Sarkar, N.; **Sahoo, R. K.**; Patro, A. G.; Nembenna, S. Aluminum-Catalyzed Selective Hydroboration of Carbonyls and Dehydrocoupling of Alcohols, Phenols, Amines, Thiol, Selenol, Silanols with HBpin. *Polyhedron* **2022**, 222, 115902 (*Invited, Part of Special Issue: Catalytic Applications of Main group Compounds; Edited by Gerard Parkin*).
11. Sarkar, N.; **Sahoo, R. K.**; Nembenna, S. Aluminum-Catalyzed Selective Hydroboration of Esters and Epoxides to Alcohols: C-O bond Activation. *Chem. Eur. J.* **2023**, 29, e202203023.
12. Sarkar, N.; **Sahoo, R. K.**; Nembenna, S. Aluminum Catalyzed Selective Reduction of Heteroallenes via Hydroboration: Amide Bond Construction and C=X (X= O, S, Se) Bond Activation. *Eur. J. Org. Chem.* **2022**, e202200941.
13. Khuntia, A. P.; Sarkar, N.; Patro, G.; **Sahoo, R. K.**; Nembenna, S. Germanium Hydride Catalyzed Selective Hydroboration and Cyanosilylation of Ketones. *Eur. J. Inorg. Chem.* **2022**, e202200209 (*Invited, Main group catalysis*).

-
14. Nayak, D. K; Sarkar, N.; Sampath, C. M.; **Sahoo, R. K.**; Nembenna, S. Organoaluminum Catalyzed Guanylation and Hydroboration Reactions of Carbodiimides. *Z. Anorg. Allg. Chem.* **2022**, e202200116 (*Invited Article*).

Manuscript Communicated

15. # **Sahoo, R. K.**; Mukhopadhyay, S.; Rajput, S.; Jana, A.; Nembenna, S. Conjugated Bis-Guanidine (CBG) Ligand Based Neutral and Cationic Zinc Alkyls, Halide, and Hydride Complexes: Synthesis, Characterization, and Catalytic Application in Cyanosilylation of Ketones. (*Manuscript submitted*).
16. Patro, A. G.;[‡] **Sahoo, R. K.**;[‡] Nembenna, S. Zinc Hydride Catalyzed Hydroboration of Esters and Epoxides. (*Manuscript submitted*) ([‡] *equally contributed*).

Book Chapter:

17. Nembenna, S. Sarkar, N.; **Sahoo, R. K.**; Mukhopadhyay, *Organometallic Complexes of the Alkaline Earth Metals*, Book Chapter, In *Comprehensive Organometallic Chemistry IV* **2022** (*Invited*). DOI: 10.1016/B978-0-12-820206-7.00173-6.

Rajata Kumar Sahoo
Rajata Kumar Sahoo

CONFERENCE AND PRESENTATIONS

1. **Poster Presentation:** 'XVIII International Symposium at MTIC- Modern Trends in Inorganic Chemistry' held at IIT Guwahati, Assam (11th-13th December 2019).
2. **Poster Presentation:** '2nd International Conference on Main Group Molecules to Materials (MMM-II)' held at NISER, Bhubaneswar (13th-15th December 2021).
3. **Oral Presentation:** '35th Annual Conference of Orissa Chemical Society' held at North Odisha University (18th-19th December 2021). **"Achieved Prof. Sripati Pani Memorial Award for best Research Article (2021)."**
4. **Poster Presentation:** '1st International RSC-IISER Desktop Seminar with Dalton Transactions' Twitter Conference (9th-12th May 2022).
5. **Poster Presentation:** '1st HBNI Interaction Meeting in Chemical Sciences' held at NISER, Bhubaneswar (18th-20th Jan 2023). **"Received The Best Poster Award."**
6. **Poster Presentation:** 'International Conference on Main Group Synthesis and Catalysis' held at IISER Trivandrum, Kerala (9th-12th Feb. 2023). **"Received The Best Poster Award."**

Rajata Kumar Sahoo
Rajata Kumar Sahoo

Dedicated to My Beloved Brother
Mr. Amitabh Sahoo

ACKNOWLEDGEMENTS

“If we knew what it was we were doing, it would not be called research, would it?”

(Albert Einstein)

Over the last five years, I have received constant support and encouragement from a large number of people. I sincerely thank everyone who made this dissertation possible. First of all, I would like to express my deepest gratitude to my supervisor, **Dr. Sharanappa Nembenna**. He always guided me in the right direction. I have learned a lot from him, and I could not have finished my thesis work without his assistance. Your patience and continuous support helped me overcome numerous crisis situations and complete this dissertation. You have been an inspiration to me.

I sincerely thank Prof. A. Srinivasan, Director (Officiating) of NISER, and Prof. Sudhakar Panda, former Director of NISER.

It gives me immense pleasure to thank my thesis monitoring committee members, Dr. Moloy Sarkar, Dr. Bhargava B.L., Dr. P. C. Ravikumar, and Dr. Shantanu Pal, for their insightful comments, constructive criticisms, and kind support during my research.

I want to express my heartfelt thanks to all other faculty members and staff of the School of Chemical Sciences for providing a healthy research atmosphere. I am also grateful to Prof. A. Srinivasan, Dr. Moloy Sarkar, Dr. Prasenjit Mal, Dr. U. Lourderaj, Dr. V. Krishnan, Dr. Sharanappa Nembenna, and Dr. Bidraha Bagh for teaching me through my course work in NISER, which helped to strengthen my knowledge.

I thank all my teachers, who helped me a lot before starting my research work, especially Mrs. Shasmita Panda (who saw the potential in me and helped me to perceive it), Mr. Naresh Mohapatra, Dr. Kshiroda Ojha, Dr. Hirak Chakraborty, and Dr. Nabakrushna Behera, for their valuable suggestions and direction.

My warmest thanks to my loving seniors, friends, and juniors both inside and outside the lab, Dr. Mamata Mahato, Dr. Satya Ranjan Behera, Dr. Achinta Jana, and Dr. Ashim Bashiya, for their valuable time in sharing my research problems and personal dilemmas whenever I needed it.

I thank all my present and past labmates, Dr. Mamata Mahato, Dr. Nabin Sarkar, Subhadeep Bera, Dr. Ashim Bashiya, A Ganesh Patro, Deepak Nayak, Bikash Ranjan Jally, Sayantan Mukhopadhyay, Sagrika Rajput, Sneha Dutta, and Smruti Rani Pradhan, for the stimulating discussions and good times I shared over the past five years.

I am also thankful to Dr. Achinta Jana, and Dr. Kasturi Sahu, for solving a few of my crystals. I thank NISER, HBNI, DAE, and SERB for their research and financial support throughout the whole research process.

I would like to acknowledge them, whose names I unintentionally missed out on despite their unconditional help for my Ph.D. work.

I am grateful to Dr. Satya Ranjan Behera for your constant support; you are always there for me when I am in trouble. You have taken care of me like an elder brother. Thank you so much for everything.

I thank my close friends Rajesh Behera, Susanta Parida, and Sadhya Rani Nayak for their support and for always cherishing our time spent together.

My Brother, Rajendra Kumar Sahoo (Tuku Nana), he is an amazing indivisual. I couldn't have asked for anyone better. You have been an inspiration and someone I always look up to. Thank you for always giving valuable inputs and encouraging me.

My deepest gratitude goes to my elder brother Amitabh Sahoo for raising me to be the person I am today, giving me freedom, believing in me, and supporting me in every way possible. Also, always think about the well-being of the family. I dedicate this thesis to you.

I wish to express my hearty gratitude and a deep sense of reverence to my beloved father Chintamani Sahoo, mother Sailabala Sahoo, sister-in-law, sister, brother-in-law, and all my family members (from my side and my wife's side) for their affection, cooperation, inspiration, and good wishes.

Thanks to all my family children, Lucky, Divansh, and Gudulu, for their love and affection.

Finally, I would like to thank my wife, Madhusmita Sahoo (Rinky), for her help, discussed ideas, and continuous support (mental and motivational); without her, I may never have completed this thesis. Thank you very much for supporting my family and being my best friend.

Last but not least, my sincere thanks to almighty **God**...

Rajata Kumar Sahoo
Rajata Kumar Sahoo

TABLE OF CONTENTS

Contents	Page No.
Synopsis	23-33
List of Schemes	34-37
List of Figures	38-40
List of Tables	41-42
List of Abbreviations	43-45
 CHAPTER 1: Introduction	 46-80
1.1 Introduction of Conjugated Bis-Guanidine (CBG) Ligands	46
1.1.1 Synthesis and Reactivity of Carbodiimides	46
1.1.2 Synthesis and Coordination Modes of Bulky CBG Ligand	47
1.2 Complexes of C/N-Donor Ligand with Zinc	48
1.2.1 A General Overview about Zinc Metal	48
1.2.2 Reported Zinc-Zinc Bonded Complexes	49
1.2.2.1 Synthetic Methods to Molecular Zinc-Zinc Bonded Complexes	51
1.2.3 Reported Molecular Zinc Hydride Complexes	51
1.2.3.1 Synthetic Methods to Molecular Zinc Hydrides	53
1.2.4 Reported Cationic Zinc Complexes	54
1.3 Catalytic Activity of Reagent/Molecular-based Zinc Complexes	55
1.3.1 Zinc-Mediated C-H Borylation of Terminal Alkynes	55
1.3.2 Hydrofunctionalization of Ketones and Chemoselective Hydroboration of Isocyanates	56

1.3.2.1	Part A: Hydroboration and Hydrosilylation of Ketones	56
1.3.2.2	Part B: Chemoselective Reduction of Isocyanates via Hydroboration: Amide Bond Formation and Hydrodeoxygenation	58
1.3.3	Hydroelementation of Carbodiimides	59
1.3.4	Chemoselective Hydrofunctionalization of Nitrile and Isocyanides	61
1.3.4.1	Part A: Dihydroboration of Nitrile and Isocyanides	61
1.3.4.2	Part B: Chemoselective Reduction of Nitriles to N-Silylimines Through Hydrosilylation	63
1.3.5	Metal-Catalyzed 1, 2-Regioselective Hydroboration and Hydrosilylation of N-Heteroarenes	64
1.3.6	Zinc Hydride Mediated Dehydrogenative Borylation of Terminal Alkynes	65
1.3.7	Metal-Catalyzed Cyanosilylation of Ketones	67
1.4	Aim, Scope, and Objective of the Current Work	67
1.5	References	68-80
CHAPTER 2:	Synthesis of Low Oxidation State Zinc(I) Complexes and Their Catalytic Studies in Dehydroborylation of Terminal Alkynes	81-102
	Abstract	81
2.1	Introduction	81
2.2	Results and Discussions	83
2.3	Conclusions	90
2.4	Experimental Section	91
2.4.1	Stoichiometric Experiments	91

2.4.2	X-ray Crystallographic Data	94
2.5	Appendix	96
2.6	References	96-99
	^1H and $^{13}\text{C}\{^1\text{H}\}$ NMR Spectra of the Selected Compounds	99-102
CHAPTER 3A:	Zinc Hydride Catalyzed Hydrofunctionalization of Ketones	103-126
	Abstract	103
3.A.1	Introduction	103
3.A.2	Results and Discussions	105
3.A.3	Conclusions	113
3.A.4	Experimental Section	114
3.A.4.1	Synthesis of Zinc Based Complexes	114
3.A.4.2	Crystallographic Data	116
3.A.5	Appendix	117
3.A.6	References	117-122
	^1H and $^{13}\text{C}\{^1\text{H}\}$ NMR Spectra of the Selected Compounds	122-126
CHAPTER 3B:	Zinc Hydride Catalyzed Chemoselective Hydroboration of Isocyanates: Amide Bond Formation and C=O Bond Cleavage	127-158
	Abstract	127

3.B.1	Introduction	127
3.B.2	Results and Discussions	130
3.B.2.1	Monohydroboration	130
3.B.2.2	Dihydroboration	135
3.B.2.3	Hydrodeoxygenation: N-Boryl Methyl Amines	135
3.B.2.4	Kinetics	139
3.B.2.5	Intermolecular Chemoselective Reactions	140
3.B.2.6	Control Experiments	142
3.B.2.7	Catalytic Cycle	144
3.B.3	Conclusions	146
3.B.4	Experimental Section	146
3.B.4.1	X-ray Crystallography	149
3.B.5	Appendix	151
3.B.6	References	151-156
	^1H and $^{13}\text{C}\{^1\text{H}\}$ NMR Spectra of the Selected Compounds	156-158
CHAPTER 4:	Zinc Catalyzed Hydroelementation (HE; E = B, C, N, O) of Carbodiimides: Intermediates Isolation and Mechanistic Insights	159-196
	Abstract	159
4.1	Introduction	160

4.2	Results and Discussions	162
4.2.1	Addition of HBpin to Carbodiimides	162
4.2.2	Addition of Alkynes to Carbodiimides (CDIs)	166
4.2.3	Addition of Primary Amines to Diisopropylcarbodiimide	169
4.2.4	Addition of Alcohols to Diisopropylcarbodiimide	170
4.2.5	Large Scale Reactions	170
4.2.6	Stoichiometric Experiments for B-H Addition to Carbodiimides	171
4.2.7	Stoichiometric Experiments for C-H Addition to Carbodiimides	174
4.2.8	Catalytic Cycle for Hydroboration of Carbodiimides	177
4.2.9	Catalytic Cycles for C, N, and O-H Addition to Carbodiimides	177
4.3	Conclusions	178
4.4	Experimental Section	179
4.4.1	Stoichiometric Experiments	180
4.4.2	X-ray Crystallographic Data	183
4.5	Appendix	186

4.6	References	187-191
	^1H and $^{13}\text{C}\{^1\text{H}\}$ NMR Spectra of the Selected Compounds	192-196
CHAPTER	Zinc Hydride Catalyzed Dihydroboration of Isonitriles and Nitriles:	197-222
5A:	Mechanistic Studies with the Structurally Characterized Zinc Intermediates	
	Abstract	197
5.A.1	Introduction	197
5.A.2	Results and Discussions	200
5.A.2.1	Isonitrile Hydroboration	200
5.A.2.2	Nitrile Hydroboration	202
5.A.2.3	Intermolecular Chemoselective Reactions	205
5.A.2.4	Scale-up Reactions	206
5.A.2.5	Stoichiometric Experiments for Hydroboration of Isonitriles and Nitriles	206
5.A.2.6	Catalytic Cycle for Hydroboration of Isonitriles	210
5.A.2.7	Catalytic Cycle for Hydroboration of Nitriles	211
5.A.3	Conclusions	212
5.A.4	Experimental Section	213
5.A.4.1	Stoichiometric Experiments	214
5.A.4.2	X-ray Crystallographic Data	216

5.A.5	Appendix	217
5.A.5	References	218-221
	^1H and $^{13}\text{C}\{^1\text{H}\}$ NMR Spectra of the Selected Compounds	221-222
CHAPTER 5B:	Zinc Catalyzed Chemoselective Reduction of Nitriles to N-Silylimines Through Hydrosilylation: Insights into the Reaction Mechanism	223-254
	Abstract	223
5.B.1	Introduction	223
5.B.2	Results and Discussions	226
5.B.2.1	Synthetic Utility	237
5.B.3	Conclusions	238
5.B.4	Experimental Section	239
5.B.4.1	Stoichiometric Experiments	240
5.B.4.2	X-ray Crystallographic Data	244
5.B.5	Appendix	248
5.B.6	References	248-252
	^1H and $^{13}\text{C}\{^1\text{H}\}$ NMR Spectra of the Selected Compounds	252-254
CHAPTER 6:	Intermediates, Isolation and Mechanistic Insights into Zinc Hydride Catalyzed 1, 2-Regioselective Hydrofunctionalization of N-Heteroarenes	255-295

	Abstract	255
6.1	Introduction	255
6.2	Results and Discussions	258
6.2.1	Hydroboration of Pyridines	258
6.2.2	Hydroboration of N-Heteroarenes	261
6.2.3	Hydrosilylation of N-Heteroarenes	263
6.2.4	Stoichiometric Experiments for 1,2-Regioselective Hydroboration	267
6.2.5	Stoichiometric Experiments for Bis-Hydrosilylation	271
6.2.6	Stoichiometric Experiments for Mono-Hydrosilylation	275
6.2.7	The Mechanism for 1,2-Regioselective Hydroboration of N-Heteroarenes.	277
6.2.8	The Mechanism for 1,2-Regioselective Hydrosilylation of N-Heteroarenes	277
6.3	Conclusions	279
6.4	Experimental Section	280
6.4.1	Stoichiometric Experiments	281

6.4.2	X-ray Crystallographic Data	286
6.5	Appendix	288
6.6	References	288-292
	^1H and $^{13}\text{C}\{^1\text{H}\}$ NMR Spectra of the Selected Compounds	292-295
CHAPTER 7:	Comparison of Two Zinc Hydride Precatalysts for Selective Dehydrogenative Borylation of Terminal Alkynes: A Detailed Mechanistic Study	296-320
	Abstract	296
7.1	Introduction	296
7.2	Results and Discussions	299
7.3	Conclusions	308
7.4	Experimental Section	309
7.4.1	X-ray Crystallographic Data	314
7.5	Appendix	315
7.6	References	316-318
	^1H and $^{13}\text{C}\{^1\text{H}\}$ NMR Spectra of the Selected Compounds	319-320
CHAPTER 8:	Conjugated Bis-Guanidine (CBG) Ligand Based Neutral and Cationic Zinc Alkyls, Halide, and Hydride Complexes: Synthesis,	321-344

Characterization, and Catalytic Application in Cyanosilylation of Ketones		
	Abstract	321
8.1	Introduction	322
8.2	Results and Discussions	323
8.2.1	Synthesis and Characterization of CBG Ligated Zinc (II) Alkyls, Halide, Hydride, and their Corresponding Cationic Complexes	323
8.2.2	TMSCN Addition in Ketones	328
8.2.3	Scale-up Reaction	331
8.2.4	Catalytic Cycle for Cyanosilylation of Carbonyls	331
8.3	Conclusions	332
8.4	Experimental Section	333
8.4.1	X-ray Crystallography	338
8.5	References	341-344
Thesis Summary:		345

SYNOPSIS OF Ph. D. THESIS

- 1. Name of the Student:** Rajata Kumar Sahoo
- 2. Name of the Constituent Institution:** National Institute of Science Education and Research (NISER)
- 3. Enrolment No.:** CHEM11201704023
- 4. Title of the Thesis:** Molecular Zinc(I) Dimers, Zinc(II) Hydrides, and Cations: Synthesis, and Catalytic Applications with Mechanistic Insights
- 5. Board of Studies:** Chemical Sciences, NISER

Abstract

Zinc is one of life's most important and essential elements and has many applications, from enzymes to medicine. Many ligated zinc complexes have been developed to understand and study the coordination environment surrounding zinc ions in natural, biologically active zinc-containing molecules.

This current work presents the synthesis of conjugated bis-guanidinate (CBG) stabilized unusual Zn(I) dimers, Zn(II) hydrides, and cations and their catalytic application towards hydrofunctionalization and cyanosilylation of unsaturated functional groups. Additionally, low valent Zn(I) dimers are used as pre-catalysts for the dehydroborylation of terminal alkynes. Further, molecular CBG Zn(II) hydrides were synthesized and thoroughly characterized. Moreover, zinc hydrides are used as efficient catalysts for different organic transformations such as hydrofunctionalization of ketones, chemoselective hydroboration of isocyanates, chemoselective reduction of nitriles and isonitriles and regioselective hydrofunctionalization of

N-heteroarenes. Apart from this, CBG-stabilized zinc alkyls, halide, and hydride and their corresponding alkyl and halide cations are isolated. The cationic zinc iodide complex effectively catalyzes the cyanosilylation of ketones under mild conditions. Moreover, we explored a series of stoichiometric experiments and structurally characterized intermediates to prove the mechanistic cycles. The synthesis and catalytic outcomes of molecular CBG zinc(I) dimers, zinc(II) hydrides, and cationic complexes have opened opportunities to design efficient catalysts, reduce other challenging organic transformations, and understand their reaction mechanisms.

The thesis has been divided into eight chapters.

Chapter 1. Introduction

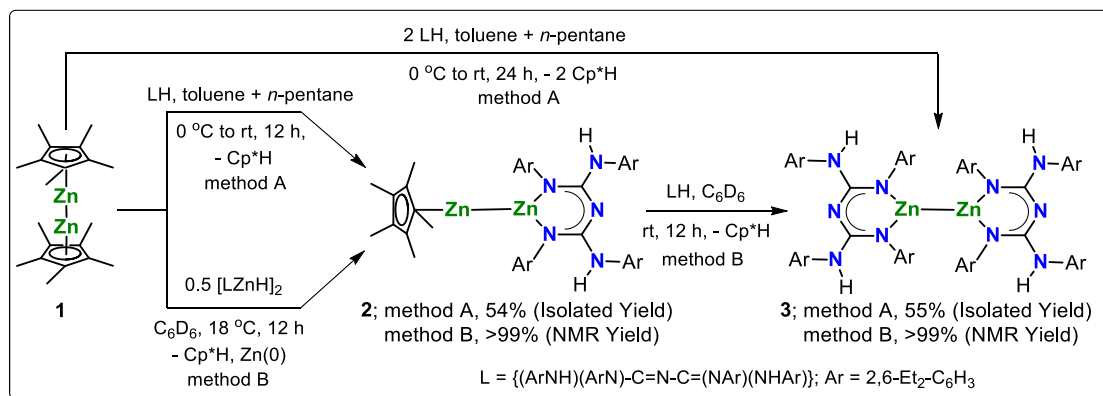
This chapter summarizes the fundamental introduction to the work done throughout the thesis. Next is a basic introduction to synthesizing conjugated bis-guanidine (CBG) ligands and their coordination chemistry with various metals. In addition, a review of previous literature reports on the synthesis and catalytic application of unusual low-oxidation state zinc(I) dimers, heteroleptic zinc(II) hydrides, and cationic complexes has been provided. Finally, this thesis's aim, scope, and objectives were designed based on previous literature reports.

Chapter 2. Synthesis of Low Oxidation State Zinc(I) Complexes and Their Catalytic Studies in Dehydroborylation of Terminal Alkynes.

2.1 Synthesis of heteroleptic and homoleptic zinc(I) complexes and its characterization

Treatment of Cp^*_2Zn_2 ($\text{Cp}^* = 1,2,3,4,5\text{-pentamethyl cyclopentadienide}$) with an equimolar amount of CBG ligand (LH) [$\text{L} = \{(\text{ArNH})(\text{ArN})\text{-C=N-C}=(\text{NAr})(\text{NHAr})\}$; $\text{Ar} = 2,6\text{-Et}_2\text{-C}_6\text{H}_3$] or 0.5 equiv. $[\text{LZnH}]_2$ to afford a heteroleptic zinc(I) complex (Cp^*ZnZnL). Compound **2** is

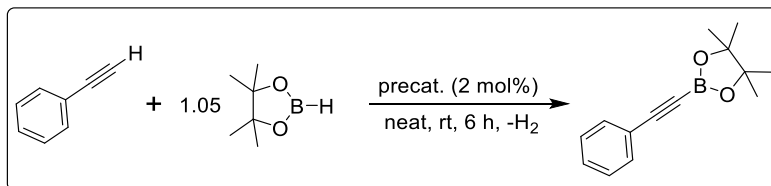
characterized by NMR and HRMS analysis. In addition, the homoleptic zinc(I) complex can be synthesized by deprotonating the free ligand (LH) with Cp^*Zn_2 or Cp^*ZnZnL (Scheme 1). Single-crystal X-ray diffraction analysis has confirmed the synthesis of compound **3**.



Scheme 1. Synthesis of CBG-supported zinc(I) complexes **2** and **3**.

2.2 Catalytic activity: Dehydrogenative borylation of terminal alkynes.

These heteroleptic and homoleptic zinc(I) complexes were used as pre-catalysts for the dehydroborylation of terminal alkynes to corresponding alkynyl borates with excellent conversions (Scheme 2). The active catalyst involved in the catalytic cycle was confirmed by reacting compound **2** or compound **3** with terminal alkyne resulting in the formation of CBG stabilized zinc acetylide complex, **5**.



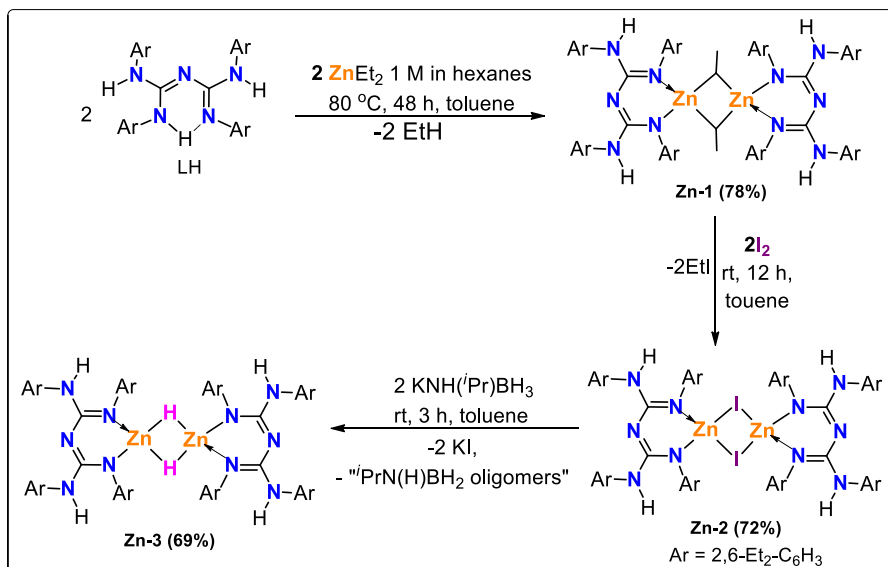
Scheme 2. Dehydrogenative borylation of terminal alkynes pre-catalyzed by compound **2** or **3**.

Chapter 3. This chapter has been divided into two parts, i.e., parts A and B.

Part A: Zinc Hydride-Catalyzed Hydrofunctionalization of Ketones

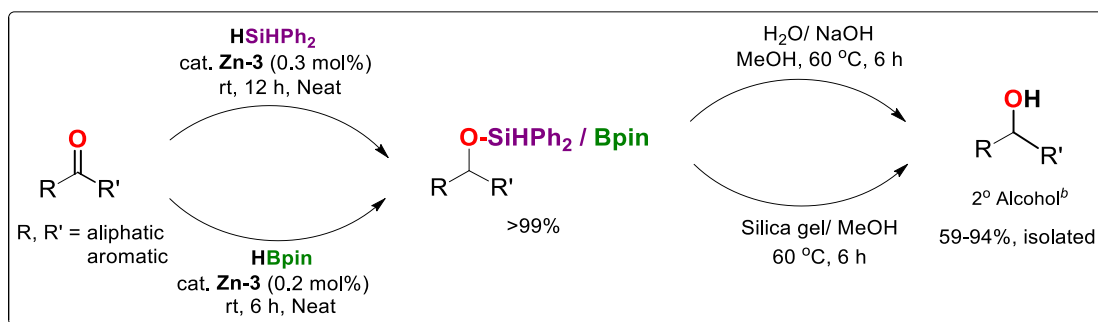
3.1 Synthesis of (*Diethyl*CBG) zinc hydride complex and its characterization

This part describes the synthesis and catalytic application of CBG-supported zinc(II) hydride complexes. The reaction of the conjugated bis-guanidine (CBG) ligand with ZnEt_2 in toluene afforded the complex $[\text{LZnEt}]_2$ (**Zn-1**) and the evolution of ethane gas. Further, complex **Zn-1**, upon treatment with iodine (I_2), formed $[\text{LZnI}]_2$. Furthermore, a reaction between compound **Zn-2** and two equiv. of $[\text{KNH}(\textit{i}\text{Pr})\text{BH}_3]$ in toluene led to the formation of $[\text{LZnH}]_2$ (**Zn-3**) (Scheme 3). Multi-nuclear NMR and HRMS analysis confirmed all compounds **Zn-1**- **Zn-3**. Moreover, compounds **Zn-2** and **Zn-3** are characterized by X-ray studies.



Scheme 3. Synthesis of CBG-supported zinc complexes **Zn-1**- **Zn-3**.

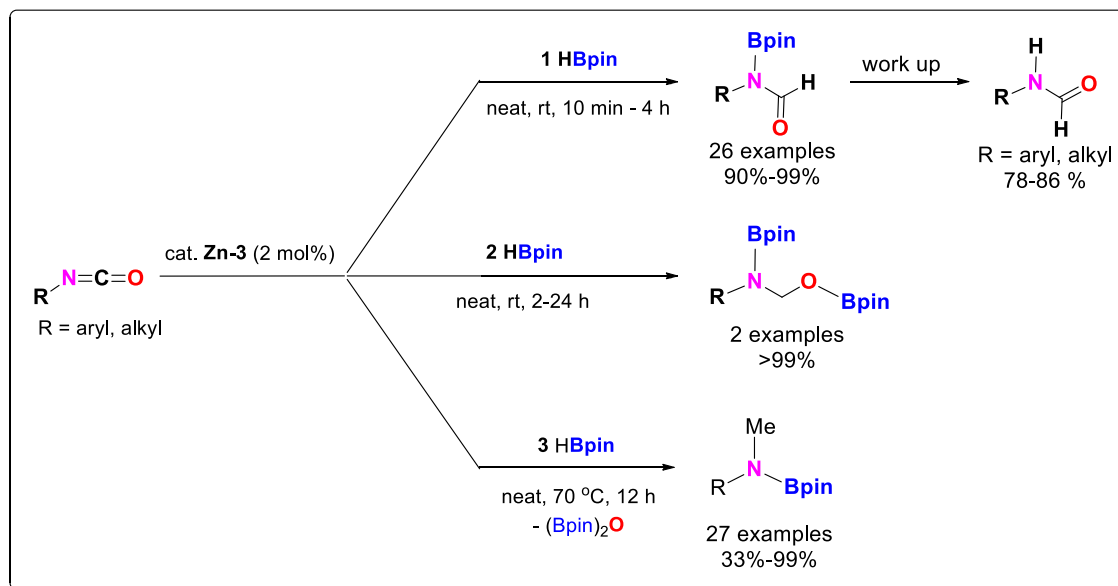
Compound **Zn-3** was an efficient catalyst for reducing ketones through hydroboration and hydrosilylation into corresponding boryl and silyl ethers. Further, borylated and silylated ethers undergo hydrolysis to produce secondary alcohols with satisfactory yields (Scheme 4).



Scheme 4. Compound **Zn-3** catalyzed hydrofunctionalization of ketones.

Part B: Zinc Hydride Catalyzed Chemoselective Hydroboration of Isocyanates: Amide Bond Formation and C=O Bond Cleavage.

This part reveals zinc hydride-catalyzed chemoselective reduction of isocyanates. The zinc hydride complex **Zn-3** has shown excellent catalytic activity towards mono- and di-hydroboration of isocyanates into N-boryl formamide and bis(boryl) hemiaminal products with quantitative conversions.



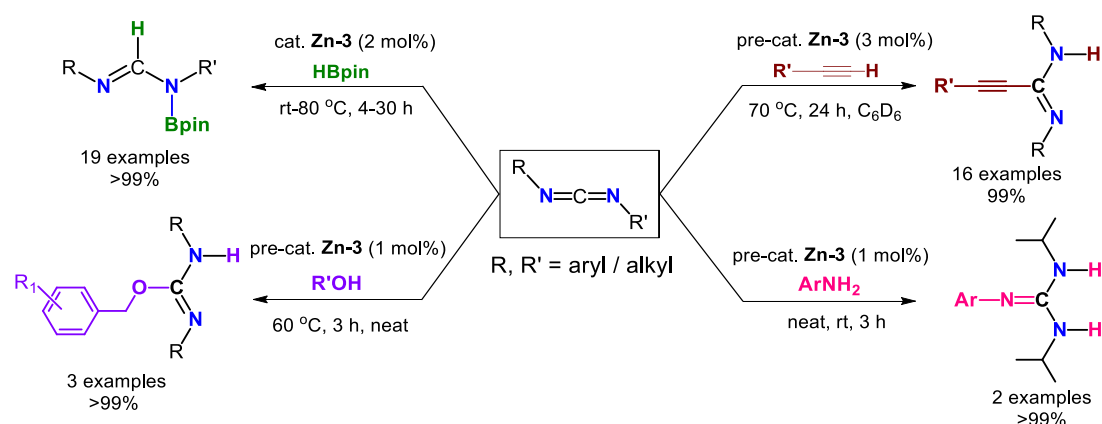
Scheme 5. Chemoselective hydroboration of isocyanates catalyzed by $[LZnH]_2$ complex (**Zn-3**).

Further, complex **Zn-3** was employed for the hydrodeoxygenation of isocyanates into N-methyl amines under neat conditions (Scheme 5). The reaction mechanism is established by isolating the

key intermediates. The DiethylCBGZnH reacting with isocyanates led to zinc formamidate and boryloxide complexes. These intermediates are confirmed by NMR, mass, and X-ray studies.

Chapter 4. Zinc Catalyzed Hydroelementation (HE; E = B, C, N, and O) of Carbodiimides: Intermediates Isolation and Mechanistic Insights.

Chapter 4 contains the single and efficient CBG zinc hydride (**Zn-3**) complex that performs various E-H (E = B, C, N, and O) additions to the carbodiimides with a broad range of substrate scope under mild conditions. The zinc hydride complex is used as an effective catalyst for the hydroboration of a vast range of carbodiimides into N-boryl formamidines under mild conditions. Further, compound **Zn-3** was used as a pre-catalyst for reducing carbodiimides with alkynes, amines, and alcohols, producing propiolamidines, guanidines, and isoureas, respectively (Scheme 6).



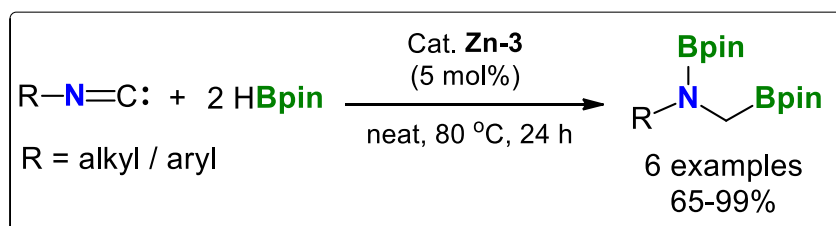
Scheme 6. Hydroelementation of carbodiimides catalyzed by $[\text{LZnH}]_2$ complex (**Zn-3**)

Moreover, we isolated several active catalysts and key intermediates to establish the catalytic cycles. Compound **Zn-3** was treated with carbodiimide, alkyne, amine, and alcohol, isolating CBG-stabilized zinc amidinate, zinc acetylide, zinc anilide, and zinc alkoxide complexes, which are characterized by NMR, HRMS, and X-ray single-crystal diffraction studies.

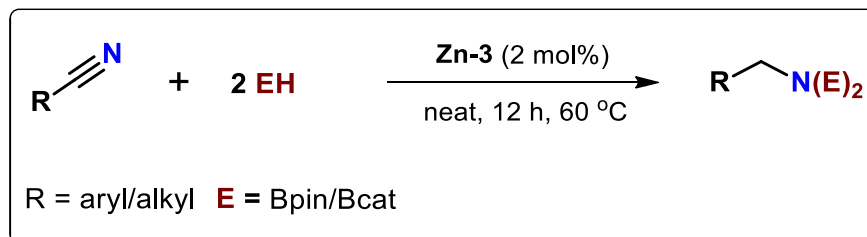
Chapter 5. This chapter has been divided into two parts, i.e., parts A and B.

Part A: Zinc Hydride Catalyzed Dihydroboration of Isonitriles and Nitriles: Mechanistic Studies with the Structurally Characterized Zinc Intermediates

This part presents the dihydroboration of isonitriles and nitriles with two equiv. of HBpin or HBcat into di(boryl)amines in the presence of a zinc hydride catalyst (**Zn-3**) (Scheme 7-8).



Scheme 7. Hydroboration of isonitriles catalyzed by **Zn-3** catalyst.



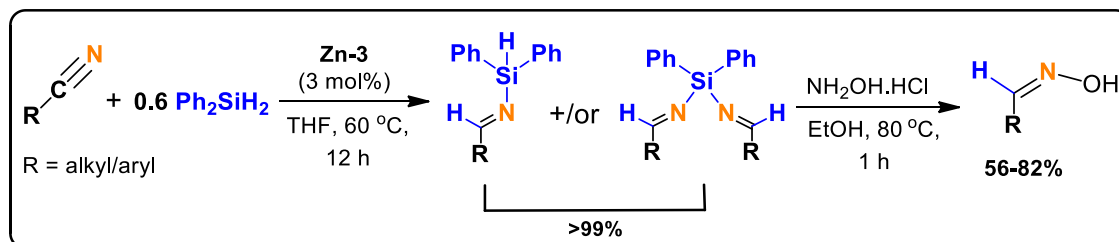
Scheme 8. Hydroboration of nitriles catalyzed by compound **Zn-3**.

We have isolated and characterized the key intermediates by NMR, mass, and X-ray analysis involved in the dihydroboration of isonitriles and nitriles.

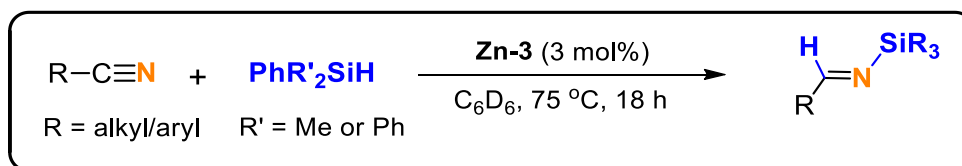
Part B: Zinc Catalyzed Chemoselective Reduction of Nitriles to N-Silylimines Through Hydrosilylation: Insights into the Reaction Mechanism.

In this part, we described the chemoselective reduction of nitrile to N-silylimines via hydrosilylation under mild conditions. Next, N-silylimines, after workup, produce oximes with good to excellent yields (Scheme 9). We can isolate the active catalysts, i.e., CBG or NacNac zinc

vinylidenamido complexes, by the reaction between the pre-catalysts and 2 equiv. of 4-(methylthio)benzonitrile. These active catalysts are characterized by single-crystal X-ray analysis.



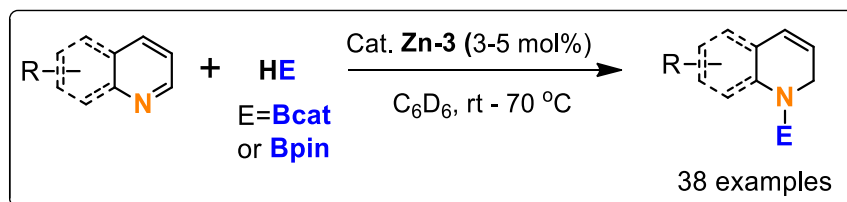
Scheme 9. Zinc-catalyzed Chemoselective Mono-Hydrosilylation of Nitriles with Ph_2SiH_2 .



Scheme 10. Zinc-catalyzed Chemoselective Mono-Hydrosilylation of Nitriles with PhMe_2SiH , Ph_3SiH , and TMSH.

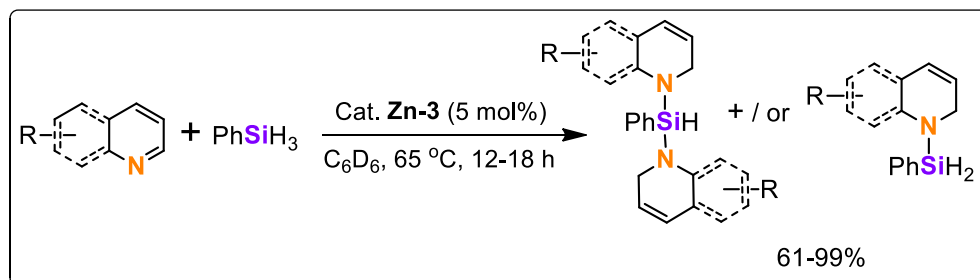
Chapter 6. Intermediates, Isolation and Mechanistic Insights into Zinc Hydride Catalyzed 1, 2-Regioselective Hydrofunctionalization of N-Heteroarenes

In this chapter, I studied the catalytic activity of molecular zinc hydride complex towards 1,2-regioselective hydrofunctionalization of N-heteroarenes was studied. The hydroboration of pyridines or N-heteroarenes to exclusive 1,2-hydroborated products was obtained in the presence of 3-5 mol% of catalyst **Zn-3** (Scheme 11).



Scheme 11. 1, 2-Regioselective hydroboration of N-heteroarenes catalyzed by $[\text{LZnH}]_2$ complex (**Zn-3**).

Further, the catalytic activity of catalyst **Zn-3** has been examined to reduce N-heteroarenes with phenylsilane. In this reaction, the quantitative amount of 1,2-hydrosilylated products has been noticed (Scheme 12).



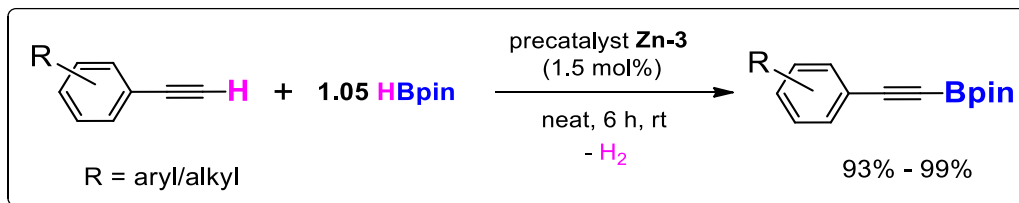
Scheme 12. 1, 2-Regioselective hydrosilylation of N-heteroarenes catalyzed by [LZnH]₂ complex(**Zn-3**).

We have shown intermediates isolation and several stoichiometric experiments to propose the catalytic cycles. The monomeric zinc hydride complex was synthesized by the reaction between [LZnH]₂ (**Zn-3**) or [L'ZnH]₂ (**Zn-3'**) and 4-methyl pyridine.

Further, 0.5 equiv. of catalyst, **Zn-3** or **Zn-3'** treated with 2.0 equiv. of isoquinoline in toluene resulted in the zinc amide complexes characterized by NMR, HRMS, and X-ray analysis.

Chapter 7. Comparison of Two Zinc Hydride Precatalysts for Selective Dehydrogenative Borylation of Terminal Alkynes: A Detailed Mechanistic Study.

Compounds **Zn-3** and **Zn-3'** were employed as pre-catalysts for the selective dehydroborylation of terminal alkynes to alkynyl borates with quantitative conversion under a low catalyst load (Scheme 13). The active catalysts CBG or Nacnac-supported zinc alkynyl complexes are synthesized by compound **Zn-3** or **Zn-3'** and two equiv. of phenylacetylene in *d*₈-toluene at ambient temperature. These compounds were characterized by multi-nuclear NMR, HRMS, IR, and X-ray studies.

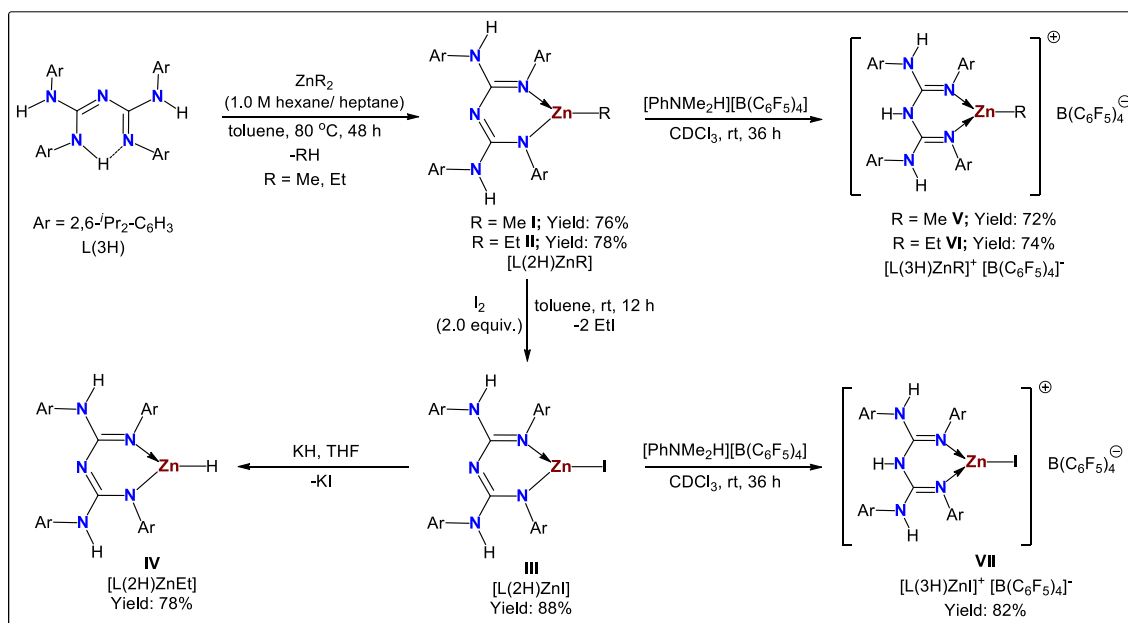


Scheme 13. Dehydrogenative borylation of terminal alkynes catalyzed by $[\text{L}^1\text{ZnH}]_2$ precatalyst (**Zn-3**).

Chapter 8. Conjugated Bis-Guanidine (CBG) Ligand Based Neutral and Cationic Zinc Alkyls, and Halide Compounds: Synthesis, Characterization, and Catalytic Application in Cyanosilylation of Ketones.

8.1 Synthesis of (*Dipp*CBG) zinc-alkyls, halide, hydride and their cationic (alkyls and halide) complexes.

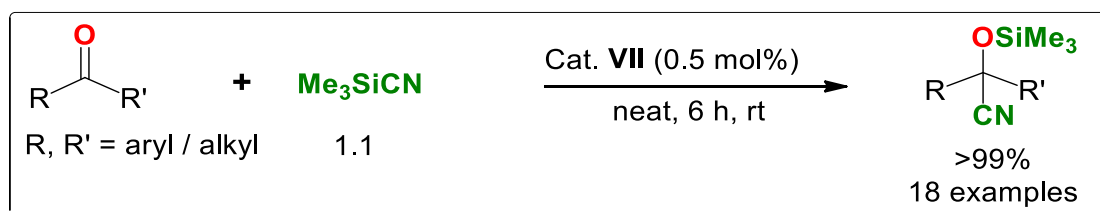
The CBG-stabilized organozinc compounds $[\text{L}(2\text{H})\text{ZnR}]$, $\text{R} = \text{Me}$ (**I**), Et (**II**) have been achieved by the reaction between free ligand (**LH**) ($\text{L} = \{(\text{ArHN})(\text{ArN})-\text{C}=\text{N}-\text{C}=(\text{NAr})(\text{NHAr})\}$; $\text{Ar} = 2,6\text{-}i\text{Pr}_2\text{-C}_6\text{H}_3$) and dialkylzinc reagent (ZnR_2 , $\text{R} = \text{Me}$, Et , 1.0 M hexane or heptane) in toluene with the evolution of methane or ethane gas (Scheme 14).



Scheme 14. Synthesis of CBG-supported neutral and cationic zinc complexes (**I** to **VII**).

Next, compound **I** or **II** was treated with 2 equiv. of molecular iodine (I_2) in toluene at room temperature gave the DippCBG zinc iodide complex (**III**) a good yield. Further, the ^{Dipp}CBG zinc hydride complex (**IV**) is prepared by a salt metathesis reaction between compound **III** and potassium hydride in THF (tetrahydrofuran) at room temperature.

Again, the reaction between compounds (**I** to **III**) and $[PhNMe_2H][B(C_6F_5)_4]$ reagent in $CDCl_3$ at room temperature produced the monomeric zinc alkyl cations $[L(3H)ZnR]^+[B(C_6F_5)_4]^-$ ($R = Me$ (**V**), Et (**VI**) or zinc halide cation $[L(3H)ZnI]^+[B(C_6F_5)_4]^-$ (**VII**) in good yields (Scheme 14). All the neutral and cationic zinc compounds (**I** to **VII**) were characterized by multi-nuclear NMR, HRMS, and X-ray studies. Compound **VII** was an effective catalyst for the cyanosilylation of ketones into their corresponding cyanohydrin products (Scheme 15).



Scheme 15. Substrate scope for cyanosilylation of ketones catalyzed by ^{Dipp}LZnI cationic complex (**VII**).

Summary of the work:

- In summary, we have shown the synthesis of low oxidation state zinc(I) complexes bearing bulky conjugated bis-guanidinate (CBG) ligand and their catalytic applications in the dehydroborylation of terminal alkynes.
- Synthesis and structural characterization of monomeric and dimeric CBG zinc (II) hydride complexes was achieved. Moreover, zinc hydrides are used as catalysts in the hydrofunctionalization of a wide range of unsaturated functional groups (chemoselective and regioselective).
- CBG-supported neutral and cationic zinc complexes have been isolated; subsequently, the catalytic activity of zinc halide cation complex for the cyanosilylation of ketones was investigated.

	LIST OF SCHEMES	Page No.
1	Scheme 1.1. Synthesis of bulky symmetrical and unsymmetrical carbodiimides	46
2	Scheme 1.2. Synthesis of bulky N-donor ligands from CDI	47
3	Scheme 1.3. Synthesis of symmetrical bulky conjugated bis-guanidine ligand (1-4).	47
4	Scheme 1.4. Common synthetic routes for the formation of zinc-zinc bonded complexes	51
5	Scheme 1.5. General synthetic routes for the formation of molecular zinc hydrides	53
6	Scheme 1.6. Dehydroborylation of terminal alkynes	55
7	Scheme 1.7. Hydrosilylation and hydroboration of ketones	56
8	Scheme 1.8. Chemoselective hydroboration of isocyanates	58
9	Scheme 1.9. Hydroboration of carbodiimides	59
10	Scheme 1.10. C-H, and O-H addition to carbodiimides	60
11	Scheme 1.11. Hydroboration of isonitriles	62
12	Scheme 1.12. Hydroboration of nitriles	62
13	Scheme 1.13. Chemoselective mono-hydrosilylation of nitriles with PhMe ₂ SiH, Ph ₃ SiH and TMDS	63
14	Scheme 1.14. 1, 2-Selective hydrofunctionalization of N-heteroarenes	64
15	Scheme 1.15. Dehydroborylation of terminal alkynes	65
16	Scheme 1.16. Canosilylation of ketones	67
17	Scheme 2.1. Low oxidation state metal complexes with M-M bond in catalysis	82
18	Scheme 2.2. Synthesis of zinc-zinc bonded complexes 2 and 3	84
19	Scheme 2.3. Stoichiometric experiments	89
20	Scheme 2.4. Proposed mechanism for the dehydroborylation of terminal alkynes	90
21	Scheme 3.A.1. Synthesis of CBG-Supported Zinc Complexes 1- 3	106
22	Scheme 3.A.2. Substrate scope for compound 3 -catalyzed hydrosilylation and hydroboration of ketones	108
23	Scheme 3.A.3. Bulk scale hydroboration of acetophenone with HBpin	110
24	Scheme 3.A.4. Competitive hydrosilylation and hydroboration reaction	111
25	Scheme 3.A.5. Intermolecular chemoselective reactions	112

26	Scheme 3.A.6. Proposed mechanism for the zinc catalyzed hydrosilylation and hydroboration of ketones	113
27	Scheme 3.B.1. Monohydroboration of isocyanates catalyzed by [LZnH] ₂ complex(I).	133
28	Scheme 3.B.2. Dihydroboration of isocyanates catalyzed by [LZnH] ₂ complex (I)	135
29	Scheme 3.B.3. Deoxygenative hydroboration of isocyanates catalyzed by [LZnH] ₂ complex (I)	138
30	Scheme 3.B.4. Intermolecular chemoselective hydroboration catalyzed by [LZnH] ₂ complex (I)	141
31	Scheme 3.B.5. Control experiments	143
32	Scheme 3.B.6. Proposed mechanism	145
33	Scheme 4.1. Hydroboration of carbodiimides catalyzed by [LZnH] ₂ complex(1)	164
34	Scheme 4.2. Substrate scope for C-H addition to carbodiimides pre-catalyzed by 1	168
35	Scheme 4.3. Substrate scope for guanylation of DIC with 1° aryl amines pre-catalyzed by 1	169
36	Scheme 4.4. Substrate scope for alcohol addition to carbodiimide pre-catalyzed by 1	170
37	Scheme 4.5. Scale up reactions for E-H addition to DIC	171
38	Scheme 4.6. Stoichiometric experiments for hydroboration of carbodiimides	172
39	Scheme 4.7. Stoichiometric experiments for hydroacetylenation of carbodiimides	175
40	Scheme 4.8. Stoichiometric experiments for N-H and O-H addition to carbodiimides	176
41	Scheme 4.9. Proposed mechanism for CDIs hydroboration catalyzed by compound 1	177
42	Scheme 4.10. Proposed mechanism for synthesis of propiolamidines	178
43	Scheme 5.A.1. Hydroboration of isonitriles catalyzed by Zn-1 catalyst	201
44	Scheme 5.A.2. Hydroboration of nitriles catalyzed by Zn-1	203
45	Scheme 5.A.3. Hydroboration of nitriles catalyzed by compound Zn-1	204
46	Scheme 5.A.4. Intermolecular chemoselective reactions by Zn-1 catalyst	205
47	Scheme 5.A.5. Scale-up reactions	206
48	Scheme 5.A.6. Stoichiometric experiments for hydroboration of isonitriles	207

49	Scheme 5.A.7. Stoichiometric experiments for hydroboration of nitriles	208
50	Scheme 5.A.8. Proposed mechanism for hydroboration of isonitriles	211
51	Scheme 5.A.9. Proposed mechanism for hydroboration of nitriles	212
52	Scheme 5.B.1. Zinc-catalyzed chemoselective mono-hydrosilylation of nitriles with PhMe ₂ SiH, Ph ₃ SiH, and TMDS	232
53	Scheme 5.B.2. Mechanistic studies for partial hydrosilylation of nitriles	234
54	Scheme 5.B.3. Proposed mechanism for the hydrosilylation of nitriles	237
55	Scheme 6.1. Catalytic selective hydrofunctionalization of N-heteroarenes	257
56	Scheme 6.2. 1, 2-Selective hydroboration of pyridines catalyzed by [LZnH] ₂ complex(I)	259
57	Scheme 6.3. 1, 2-Selective hydroboration of N-heteroarenes catalyzed by [LZnH] ₂ complex(I)	261
58	Scheme 6.4. 1, 2-Selective hydrosilylation of N-heteroarenes catalyzed by [LZnH] ₂ complex(I)	263
59	Scheme 6.5. Competitive and exchange reaction between phenylsilane and pinacolborane with N-heteroarenes	264
60	Scheme 6.6. Intermolecular chemoselective reactions	266
61	Scheme 6.7. Stoichiometric experiments for hydroboration of N-heteroarenes	267
62	Scheme 6.8. Mechanistic studies for bis-hydrosilylation of N-heteroarenes	272
63	Scheme 6.9. Stoichiometric experiments for mono-hydrosilylation of N-heteroarenes	275
64	Scheme 6.10. Proposed mechanism for the 1,2-regioselective hydroboration of N-heteroarenes	278
65	Scheme 6.11. Proposed mechanism for the 1,2-regioselective hydrosilylation of N-heteroarenes	279
66	Scheme 7.1. Metal-catalyzed dehydroborylation of terminal alkynes	297
67	Scheme 7.2. Dehydrogenative borylation of terminal alkynes catalyzed by [L ¹ ZnH] ₂ precatalyst (I)	300
68	Scheme 7.3. Intermolecular chemoselective reactions	302
69	Scheme 7.4. Stoichiometric experiments for dehydroborylation of terminal alkynes	304
70	Scheme 7.5. Proposed mechanism for the dehydroborylation of terminal alkynes	308

71	Scheme 8.1. Synthesis of CBG-supported neutral and cationic zinc compounds (Zn-1 - Zn-7)	324
72	Scheme 8.2. Substrate scope for canosilylation of ketones catalyzed by cationic zinc complex (Zn-7)	330
73	Scheme 8.3. Gram-scale cyanosilylation of benzaldehyde and acetophenone catalyzed by Zn-7	331
74	Scheme 8.4. Proposed mechanism for cyanosilylation of carbonyls catalyzed by Zn-7	332

	LIST OF FIGURES	Page No.
1	Figure 1.1. Coordination modes of CBGs	48
2	Figure 1.2. Selected examples of low oxidation Zn(I) dimers with Zinc-Zinc Bonds	50
3	Figure 1.3. Selected examples of molecular zinc hydrides	52
4	Figure 1.4. Selected reports of cationic zinc complexes	54
5	Figure 1.5. Mg(I) and Zn(I) dimers in catalysis	56
6	Figure 1.6. Reported zinc-based hydrosilylation and hydroboration of ketones	57
7	Figure 1.7. Plausible catalytic cycle for hydrosilylation of carbonyls by Parkin and co-workers	57
8	Figure 1.8. Report on metal-catalyzed reduction of isocyanates via hydroboration	58
9	Figure 1.9. Previous reports on main-group metal-mediated hydroboration of carbodiimides	60
10	Figure 1.10. Previous reports on zinc-catalyzed C-H and O-H addition to carbodiimides	61
11	Figure 1.11. Plausible catalytic cycle for hydroboration and hydroalkynylation of carbodiimides by Hill and co-workers	61
12	Figure 1.12. Previous reports on metal-catalyzed hydroboration of isonitriles and nitriles	62
13	Figure 1.13. Previous reports on zinc-catalyzed chemoselective mono-hydrosilylation of nitriles	64
14	Figure 1.14. Reports on zinc-catalyzed 1,2-regioselective hydroboration and hydrosilylation of N-heteroarenes	65
15	Figure 1.15. Reported zinc-catalyzed C-H borylation of terminal alkynes	66
16	Figure 1.16. Plausible catalytic cycle for dehydroborylation of terminal alkynes by Ingleson and co-workers	66
17	Figure 2.1. Annotated ^1H NMR stack plot of the reaction between Cp^*_2Zn_2 and 2.0 equiv. of LH	85
18	Figure 2.2. Molecular structures of 3 (left) and 5 (right)	88

19	Figure 2.3. – 2.8. ^1H and $^{13}\text{C}\{^1\text{H}\}$ NMR spectrum of selected compounds	99-102
20	Figure 3.A.1. Previously reported selected zinc hydride catalysts for (A-G) hydrosilylation and (D, E) hydroboration of ketones and present work.	104
21	Figure 3.A.2. The solid-state structure of 2	107
22	Figure 3.A.3. – 3.A.10. ^1H and $^{13}\text{C}\{^1\text{H}\}$ NMR spectrum of selected compounds	122-126
23	Figure 3.B.1. Production of formamides and N-methyl amines from isocyanates	128
24	Figure 3.B.2. Molecular structures of 2d (left) and 2ee (right)	134
25	Figure 3.B.3. Stacked ^1H NMR spectra (400 MHz) for the reaction of 4-Bromophenyl isocyanate (1n) (0.3 mmol, 1.0 equiv.) and pinacolborane (0.9 mmol, 3.0 equiv.), and catalyst I (2 mol%) in THF- d_8 .	139
26	Figure 3.B.4. The plot of [product] versus time for hydroboration of 4-BrPhNCO catalyzed by 2 mol% I at rt-70 °C.	140
27	Figure 3.B.5. Molecular structures of II (left) and IV (right)	144
28	Figure 3.B.6. – 3.B.9. ^1H and $^{13}\text{C}\{^1\text{H}\}$ NMR spectrum of selected compounds	156-158
29	Figure 4.1. Metal-catalyzed E-H addition to carbodiimides	161
30	Figure 4.2. Molecular structure of 3q	166
31	Figure 4.3. Annotated ^1H NMR stack plot for the stoichiometric hydroboration of DIC with 1 in C_6D_6	172
32	Figure 4.4. Molecular structures of compounds Zn-1' (left) and Zn-2' (right)	173
33	Figure 4.5. Molecular structures of compounds Zn-4 (left) and Zn-5 (right)	176
34	Figure 4.6. – 4.15. ^1H and $^{13}\text{C}\{^1\text{H}\}$ NMR spectrum of selected compounds	192-196
35	Figure 5.A.1. Metal-catalyzed dihydroboration of isonitriles and nitriles	199
36	Figure 5.A.2. CBG-based zinc(II) hydride complex (Zn-1)	200
37	Figure 5.A.3. Molecular structures of compounds Zn-2 (left), and Zn-3 (right)	209
38	Figure 5.A.4. Annotated ^1H NMR (400 MHz) stack plot of the stoichiometric hydroboration of benzonitrile with Zn-1 in C_6D_6 .	210
39	Figure 5.A.5. – 5.A.7. ^1H and $^{13}\text{C}\{^1\text{H}\}$ NMR spectrum of selected compounds	221-222
40	Figure 5.B.1. Chemoselective synthesis of N-silylimine	225
41	Figure 5.B.2. CBG and NacNac stabilized zinc(II) hydride complexes	226
42	Figure 5.B.3. Molecular structures of compounds Zn-1' (left) and Zn-2' (right)	236

43	Figure 5.B.4. – 5.B.6. X-ray crystallographic data of compounds 2i'' , 2y'' and 7b	244-245
44	Figure 5.B.7. – 5.B.10. ^1H and $^{13}\text{C}\{^1\text{H}\}$ NMR spectrum of selected compounds	252-254
45	Figure 6.1. Molecular structures of compounds IIA' (left), III' (middle), and III (right)	268
46	Figure 6.2. Annotated ^1H NMR (400 MHz) stack plot of the stoichiometric hydroboration of isoquinoline with I in C_6D_6	270
47	Figure 6.3. Annotated ^1H NMR (400 MHz) stack plot of the stoichiometric hydrosilylation of isoquinoline with catalyst I in C_6D_6	273
48	Figure 6.4. Annotated ^1H NMR (400 MHz) stack plot of the stoichiometric hydrosilylation of 3-methyl quinoline with catalyst I in C_6D_6	276
49	Figure 6.5. X-ray crystallographic data of compound 4f	286
50	Figure 6.6. – Figure 6.11. ^1H and $^{13}\text{C}\{^1\text{H}\}$ NMR spectrum of selected compounds	292-295
51	Figure 7.1. Molecular structures of compounds II (left) and IV (right)	306
52	Figure 7.2. – 7.5. ^1H and $^{13}\text{C}\{^1\text{H}\}$ NMR spectrum of selected compounds	319-320
53	Figure 8.1. Molecular structures of Zn-1 (upper left), Zn-2 (upper right), Zn-3 (lower left), and Zn-4 (lower right)	325
54	Figure 8.2. Molecular structure of Zn-5 (left), Zn-6 (middle), Zn-7 (right)	326
55	Figure 8.3. Two bonding modes	328

	LIST OF TABLES	Page No.
1	Table 2.1. Optimization of compound 3 pre-catalyzed dehydroborylation of phenylacetylene	86
2	Table 2.2. Dehydrogenative borylation of terminal alkynes precatalyzed by compound 3	87
3	Table 2.3. Crystallographic data and refinement parameters for compounds 3 and 5	95
4	Table 3.A.1. Hydroboration of acetophenone catalyzed by 3 .	111
5	Table 3.A.2. Crystallographic data and refinement parameters for compound 2	117
6	Table 3.B.1. Optimization of zinc hydride catalyzed hydroboration of <i>p</i> -tolyl isocyanate	131
7	Table 3.B.2. Optimization of zinc hydride catalyzed hydroboration of <i>p</i> -tolyl isocyanate	137
8	Table 3.B.3. Crystallographic data and refinement parameters for compounds II , IV , 2d and 2ee	150
9	Table 4.1. Optimization table of [LZnH] ₂ complex (1) catalyzed hydroboration of <i>N,N'</i> -diisopropylcarbodiimide (DIC)	163
10	Table 4.2. Optimization table of [LZnH] ₂ complex (1) pre-catalyzed phenylacetylene addition to <i>N,N'</i> -diisopropylcarbodiimide (DIC).	167
11	Table 4.3. Crystallographic data and refinement parameters for compounds Zn-1' , Zn-2' , Zn-4 , and Zn-5 .	185
12	Table 4.4. Crystallographic data and refinement parameters for compound 3q	186
13	Table 5.A.1. Optimization table of Zn-1 catalyzed hydroboration of benzonitrile	202
14	Table 5.A.2. Crystallographic data and refinement parameters for compounds Zn-2 and Zn-3	217
15	Table 5.B.1. Optimization of zinc catalyzed chemoselective hydrosilylation of benzonitrile with Ph ₂ SiH ₂ .	227
16	Table 5.B.2. Screening of silanes in the hydrosilylation of benzonitrile by pre-catalyst Zn-1 or Zn-2	228
17	Table 5.B.3. Zinc-catalyzed chemoselective mono-hydrosilylation of nitriles with Ph ₂ SiH ₂	230

18	Table 5.B.4. Crystallographic data and refinement parameters for compounds Zn-1' , Zn-2' , 2i'' , and 2y''	246
19	Table 5.B.5. Crystallographic data and refinement parameters for compounds 3h , 3w , and 7b	247
20	Table 6.1. Crystallographic data and refinement parameters for compounds IIA' , III' , III , and 4f	287
21	Table 7.1. Comparison of TON and TOF for dehydroborylation of terminal alkynes of selected substrates with precatalysts I , III and catalyst A	303
22	Table 7.2. Crystallographic data and refinement parameters for compounds II and IV	315
23	Table 8.1. Optimization table of zinc-catalyzed cyanosilylation of acetophenone	329
24	Table 8.2. Crystallographic data and refinement parameters for compounds Zn-1 - Zn-4	339
25	Table 8.3. Crystallographic data and refinement parameters for compounds Zn-5 - Zn-7	340

List of Abbreviations Used

Å	Angstrom
Ar	Aryl/Aromatic
()°	Angle
Br	Bromine
br	Broad
C ₆ D ₆	Deuterated Benzene
°C	Degree Celcius
δ	Chemical Shift
Calcd.	Calculated
cat.	Catalyst
CBG	Conjugated Bis-Guanidinate
Cp*	1,2,3,4,5-Pentamethyl Cyclopentadienide
<i>J</i>	Coupling Constant in NMR
Cl	Chlorine
CDCl ₃	Deuterated Chloroform
HBcat	Catecholborane
CN (C≡N)	Cyanide / Nitrile
CHN	Carbon/Hydrogen/Nitrogen
CDI	Carbodiimide
CCDC	Cambridge Crystallographic Data Centre
HBcat	Catecholborane
d	Doublet, Days
dd	Doublet of a Doublet
Diethyl	2,6-Et ₂ -C ₆ H ₃
Dipp	2,6- ^{<i>i</i>} Pr ₂ -C ₆ H ₃
DIC	diisopropylcarbodiimide
DHP	Dihydropyridine
equiv.	Equivalent
ESI-TOF	Electrospray ionization time-of-flight

Et	Ethyl
g	Gram
h	Hour
HRMS	High-Resolution Mass Spectrometry
HDO	Hydrodeoxygenation
Hz	Hertz
IR	Infrared
NC (N=C)	Isocyanide / Isonitrile / Carbylamine
Int	Intermediate
IS	Internal standard
K	Kelvin
M ⁺	Molecular ion
mp	Melting point
Me	Methyl
Mes	2,4,6-Me ₃ -C ₆ H ₂
m	Multiplet
mg	Microgram
μl	Microlitre
mL	Milliliter
mmol	Millimole
mol	Mole
M	Molar
MS	Mass Spectra, Molecular Sieves
M/Z	Mass to charge ratio
NO ₂	Nitro
NMR	Nuclear Magnetic Resonance
ppm	Parts Per Million
HBpin	Pinacolborane
Py	Pyridine
Ph ₂ SiH ₂	diphenyl silane
q	Quartet in NMR

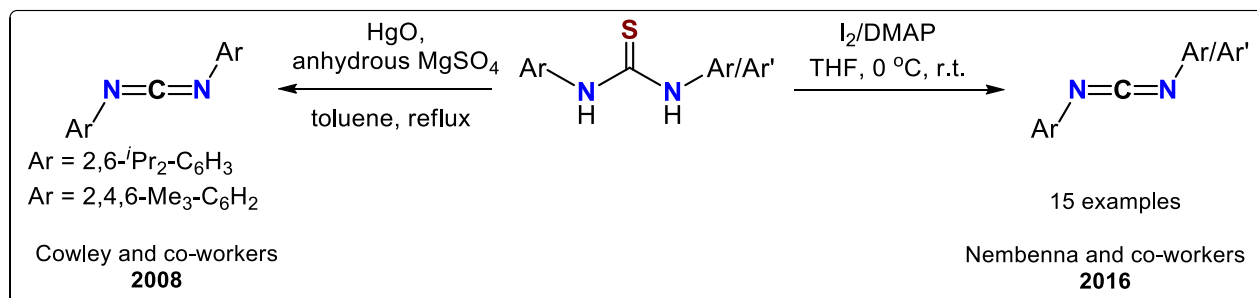
rt	Room Temperature
s	Singlet, Seconds
ν	Stretching Frequency
s	Singlet in NMR
sept	Septet in NMR
σ	Sigma
TON	Turnover Number
TOF	Turnover Frequency
CF ₃	Trifluoromethyl
Tol-d8	Deuterated Toluene
t	Triplet
Tol	Toluene
THF	Tetrahydrofuran
λ	Wavelength
TMS	Trimethylsilyl
XRD	X-Ray diffraction
Xyl	2,6-Me ₂ -C ₆ H ₃
Zn	Zinc

Chapter1: Introduction

1.1 Introduction of Conjugated Bis-Guanidine (CBG) Ligands

1.1.1 Synthesis and Reactivity of Carbodiimides

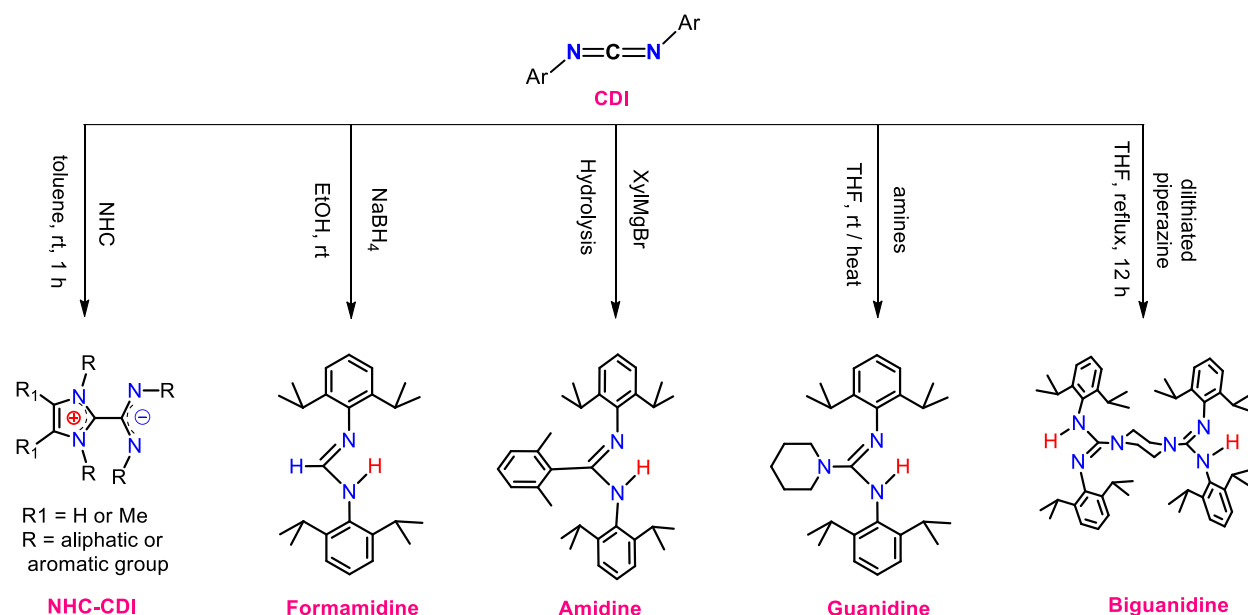
Carbodiimides (CDIs) are a unique class of most reactive organic compounds containing an $N=C=N$ core.¹ These are broadly applied in synthesizing nucleotides, peptides, lactams, antibiotics, and a wide range of N-donor ligands.² Weith first discovered the molecular structure of carbodiimide (CDI) in 1874.³ Later, Cowley and co-workers reported the desulfurization of 1,3-diaryl substituted thioureas to afford bulky *N,N'*-diaryl carbodiimides by using toxic HgO and anhydrous $MgSO_4$.⁴ Recently, Nembenna and co-workers established a metal-free approach to synthesizing symmetrical and unsymmetrical bulky diaryl carbodiimides via desulfurization of thioureas using DMAP and I_2 in THF.^{2f}



Scheme 1.1. Synthesis of bulky symmetrical and unsymmetrical carbodiimides

As illustrated in Scheme 1.2, diaryl carbodiimides are suitable precursors for synthesizing various bulky N-donor ligands, including N-heterocyclic carbene-carbodiimide adducts (NHC-CDI), formamidines, amidines, guanidine, and biguanidine.^{5a-5d}

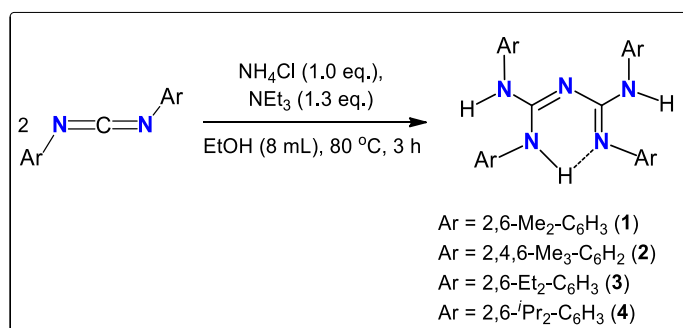
In 1861, Adolph Strecker first introduced the guanidines. Guanidines are essential organic compounds containing a CN_3 core. Similarly, biguanides are used in medicinal chemistry,



Scheme 1.2. Synthesis of bulky N-donor ligands from CDI

especially in drugs for diabetes.⁶ The unsubstituted biguanides were first reported by Rathke group in 1879.⁷ Subsequently, Eckert-Maksic and co-workers prepared hexasubstituted biguanides.⁸ Very recently, Kretschmer and co-workers synthesized 3,4-ethylene-bridged 1,1,2,5-tetrasubstituted biguanides.⁹

1.1.2 Synthesis and Coordination Modes of Bulky CBG Ligand



Scheme 1.3. Synthesis of symmetrical bulky conjugated bis-guanidine ligand (**1-4**).

NacNac or β -diketiminate N-donor ligands are very popular and extensively used in the coordination chemistry of almost all the elements of the periodic table.^{5e, 5f} Unsubstituted and

substituted biguanides are known in the literature. However, tetraaryl-substituted conjugated bis-guanidines (NacNac analogs) are not known in the literature. Recently, our group reported a series of symmetrical and unsymmetrical conjugated bis-guanidine (CBG) ligands.¹⁰ When two equiv. of carbodiimides were reacted with one equiv. of NH_4Cl and 1.3 equiv. of NEt_3 in ethanol, conjugated bis-guanidine (CBG) was afforded in good yield (Scheme 1.3).

We observed five coordination modes (**A–E**) for tetra-aryl substituted CBGs (Figure 1).¹¹ Two types of bonding modes are observed regarding zinc metal, i.e., LX (**A**) and L_2 (**E**). Like, other N-donor ligands such as tetra-substituted guanidines (four-membered metallacycles) and NacNac,¹² one can expect interesting coordination chemistry of these new CBGs with all elements of the periodic table.

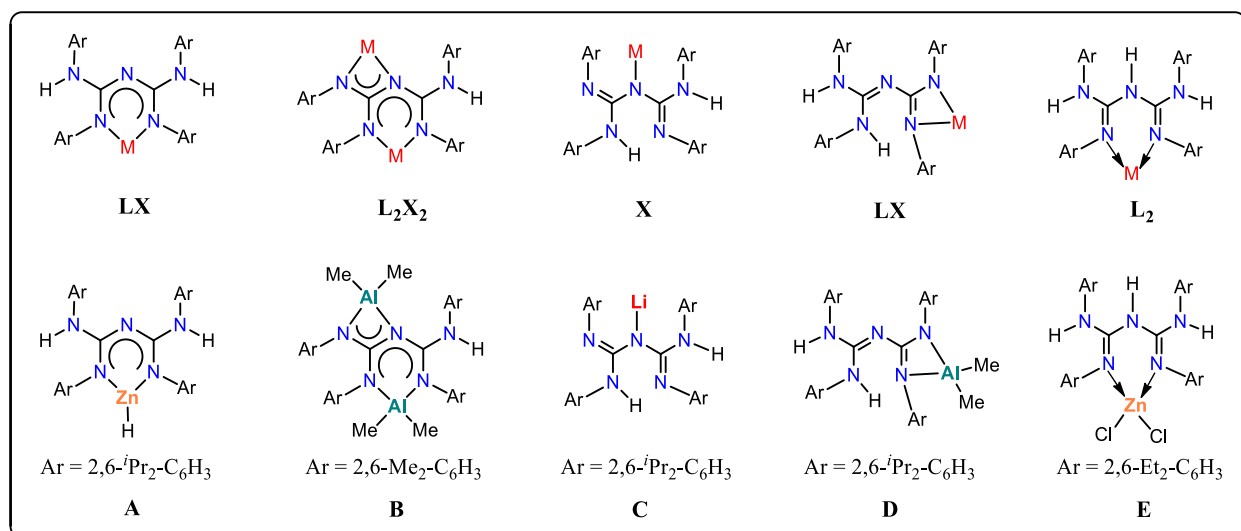


Figure 1.1. Coordination modes of CBGs.

1.2 Complexes of C/N-Donor Ligand with Zinc

1.2.1 A General Overview about Zinc Metal

Zinc is the twenty-fourth (0.007%) most abundant element in the earth's crust. In nature, zinc exists in high concentrations in ores, mainly in sulfide and oxide forms. Furthermore, the zinc-containing important minerals are sphalerite (ZnS , ~60% concentration of zinc), wurtzite, smithsonite, and

hemimorphite.¹³ Additionally, zinc is a lower toxic metal in comparison to other metals. Every human body contains nearly 2-3 g of zinc. It is a part of more than 300 enzymes.¹⁴ As a result, it is a useful component in pharmaceutical synthesis.

On the other hand, diethyl zinc, the first constituted organometallic compound, was introduced by Edward Frankland in 1849.¹⁵ Since then, various stoichiometric applications of zinc have been documented, including the Reformatskii reaction, the Negishi coupling reaction, and the Fukuyama reaction, which are ground-breaking chemical transformations in organic chemistry.¹⁶ However, the application of zinc catalysis in the organic transformation was less developed compared to other metals.

Zinc is placed between transition metals and the main group elements in the periodic table with an electron configuration of $[\text{Ar}] 3d^{10} 4s^2$. The zinc atom has filled d-shells; the main oxidation states are Zn(0) and Zn(II). The valence electronic configuration of the zinc atom is similar to that of the alkaline earth metals. In the M^{II} state, the Group 12 elements are well known. However, the M^{I} state in the form of M_2^{2+} ions is very important for mercury, but there are very few reports for zinc and cadmium. This is due to the large ionization enthalpy of the Hg atom, which is in turn due to the relativistic stabilization of its 6s orbital.¹⁷ In 2004, Carmona and co-workers introduced the first stable zinc(I) dimers with a zinc-zinc bond, i.e., decamethyldizincocene ($\text{Cp}^*\text{ZnZnCp}^*$).¹⁸ Moreover, zinc lacks distinctive redox chemistry compared to other transition metals.¹⁹ Therefore, the zinc atom differs from transition metals and is more closely related to the group 2 metals, particularly magnesium.^{19a, 20}

1.2.2 Reported Zinc-Zinc Bonded Complexes

Metal-metal bonds in molecules and clusters are of interest in various areas of chemical science.²¹ Traditionally, metal-metal bonds have focused on transition metals, particularly compounds

containing multiple bonds between metal atoms.²⁰⁻²¹ Recently, Power and co-workers discovered stable chromium compounds containing fivefold bonding between two chromium centers.²² The Jones group recently introduced the bulky ligand stabilized first Mg(I) complex.²³ There are also a few zinc-zinc bonded complexes known in the literature.^{19b, 24}

In this regard, the Carmona group reported the first cp^* stabilized zinc(I) dimer in 2004, which was unexpectedly formed by the reaction between ZnEt_2 and $\text{Zn}(\text{Cp}^*)_2$ through a reductive coupling reaction with a low yield.¹⁸ However, this compound is highly thermally unstable. So, further chemistry from $\text{Cp}^*\text{ZnZnCp}^*$ complex is difficult. Thus, many scientists have developed thermally stable zinc(I) complexes.^{21c, 24-25} In this context, several N-donor ligand-stabilized unusual zinc(I) dimers have been documented to understand the construction of zinc-zinc bonded complexes. Sterically bulky and chelating ligands are ideal candidates for synthesizing zinc-zinc bonded complexes in a low oxidation state.^{21c, 24-25, 25d, 25e, 26}

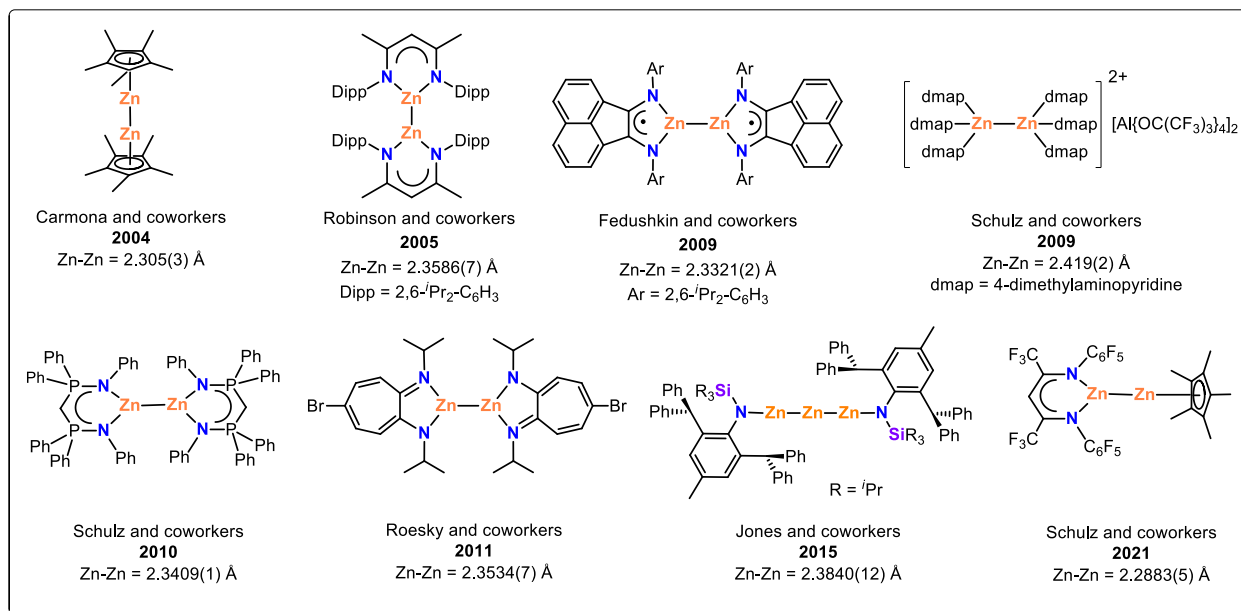


Figure 1.2. Selected examples of low oxidation Zn(I) dimers with Zinc-Zinc Bonds.

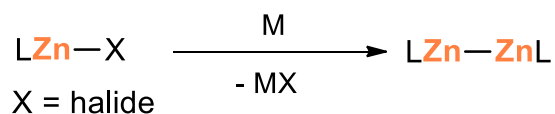
Robinson and coworkers reported the second example of zinc (I) dimer complex stabilized by the DippNacNac ligand.^{25e} In 2009, Schulz and coworkers prepared a dicationic zinc-zinc bonded

complex stabilized by 4-dimethylaminopyridine.^{26e} The Roesky research group recently synthesized amino troponimine ligand-based zinc(I) dimers.^{25c} Schulz and coworkers recently presented a NacNac stabilized heteroleptic Zn-Zn bonded complex.^{25b} All these compounds shown in Figure 1.2 are confirmed by X-ray single-crystal diffraction studies. The Zn-Zn bond lengths in these complexes lie between 2.30–2.41 Å.^{18, 21c, 25b-e, 26b, 26e}

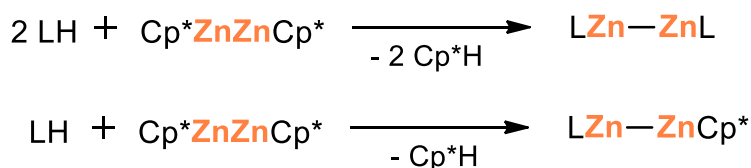
1.2.2.1 Synthetic Methods to Molecular Zinc-Zinc Bonded Complexes

There are mainly two methods to synthesize zinc-zinc bonded complexes: the reduction method and the deprotonation method.^{18, 21c, 25b-e, 26b, 26e, 27} The reduction of molecular zinc halide complexes with alkali metals (such as Na, K, etc.) afforded low oxidation state zinc-zinc bonded complexes (Scheme 1.4.a).^{26b, 27}

a) Reduction method



b) Deprotonation method



Scheme 1.4. Common synthetic routes for the formation of zinc-zinc bonded complexes.

Alternatively, unusual zinc-zinc bonded complexes can be obtained by reacting a suitable ligand with Cp*ZnZnCp* by the protonation of Cp* (Scheme 1.4.b).^{25b, 25d}

1.2.3 Reported Molecular Zinc Hydride Complexes

Schlesinger and coworkers first introduced the parent zinc dihydride (ZnH₂) in 1947.²⁸ Many synthetic protocols have been developed to date in order to prepare ZnH₂. However, the exact

structure is unknown.²⁹ Further, it suffers from several drawbacks, such as insoluble in organic solvents, pyrophoric, polymeric in nature, difficult to crystalize, and thermally unstable. Thus, many research groups developed several methods to prepare heteroleptic zinc hydrides. In this context, the Goel group synthesized the first stable organozinc hydride complex, PhZn_2H_3 , in 1977.³⁰ Later, the Parkin research group used a bulky spectator ligand to report the first example of a monomeric zinc hydride complex.³¹

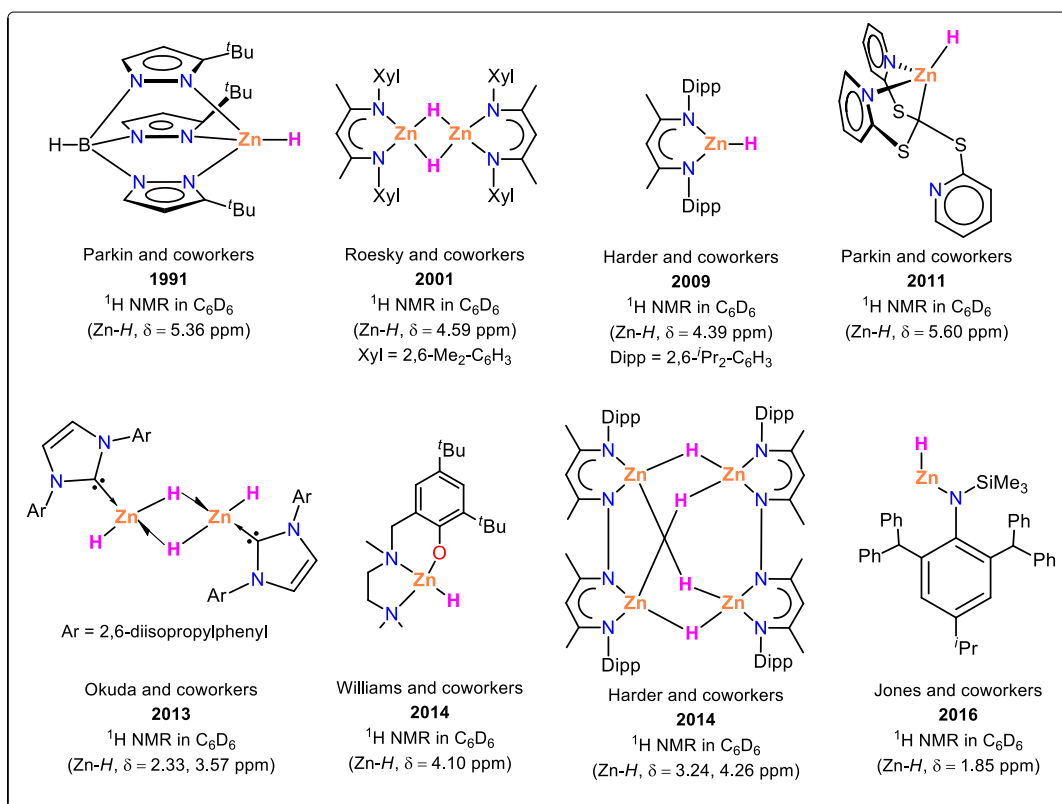


Figure 1.3. Selected examples of molecular zinc hydrides.

After that, many research groups reported mononuclear, dinuclear, and tetranuclear zinc hydride complexes.³¹⁻³² In 2013, the Okuda group introduced a structurally characterized and soluble N-heterocyclic carbene (NHC)-based zinc dihydride complex.^{32a} Recently, Jones and coworkers prepared a low-coordinate zinc hydride complex.^{32c} All zinc hydride complexes were characterized

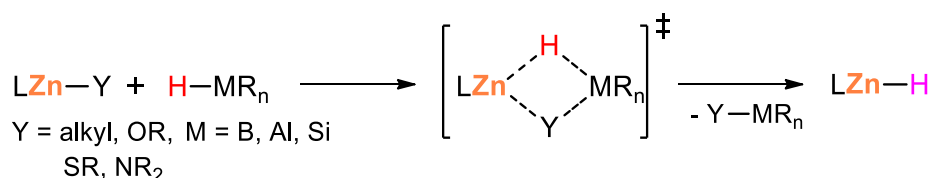
by NMR spectroscopy. The ^1H NMR spectra reveal a signature peak due to the Zn-H moiety in the range of 1.85–5.60 ppm in C_6D_6 (Figure 1.3).³¹⁻³²

1.2.3.1 Synthetic Methods to Molecular Zinc Hydrides

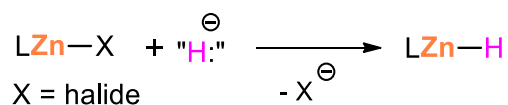
Considering the natural abundance, cheaper, low toxicity, and biocompatibility of zinc metal, the well-characterized molecular zinc hydride complexes become highly interesting in the different challenging organic transformations and hydrogen storage materials. Thus, over the last few years, zinc hydride complexes have been widely used as active catalytic species in different organic transformations such as hydroelementation, hydrogenation, hydroamination, hydroacetylation, cyanosilylation, etc.³³

As I mentioned earlier, molecular zinc hydride complexes are valuable starting materials for catalysis, so several synthetic methods have been developed to synthesize molecular zinc hydrides.^{33f} Organozinc compounds (such as alkyls, OR, SR, or NR_2) can be converted into molecular zinc hydrides upon reacting with silanes via σ -bond metathesis (Scheme 1.5.a).

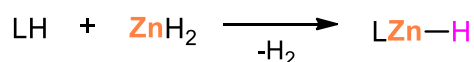
a) Hydride/Heteroatom Metathesis



b) Hydride/Halide Metathesis



c) Deprotonation method



Scheme 1.5. General synthetic routes for the formation of molecular zinc hydrides.

Alternatively, zinc halide complexes react with alkali metal hydrides (such as NaH, KH, $\text{KNH}(\text{iPr})\text{BH}_3$, or LiHBEt_3) to produce Zn-H bonds (Scheme 1.5.b). Additionally, zinc hydride complexes can be synthesized via deprotonation by reacting a suitable ligand with parent ZnH_2 (Scheme 1.5.c).

1.2.4 Reported Cationic Zinc Complexes

Lewis acid chemistry has been attractive in catalysis and small molecule activation in the last few decades.³⁴ In this regard, several cationic zinc complexes have been synthesized (Figure 1.4).³⁵ Recently, molecular zinc cations have been used as catalysts in various organic transformations such as hydrosilylation of carbonyls, CO_2 , nitrile, alkene, alkyne, and hydroamination reactions. Additionally, it was used for ring-opening polymerization of esters and carbonates.^{34-35, 35g, 35h} Moreover, a few molecular zinc hydride cations were synthesized and applied in catalysis.^{35b, 35d}

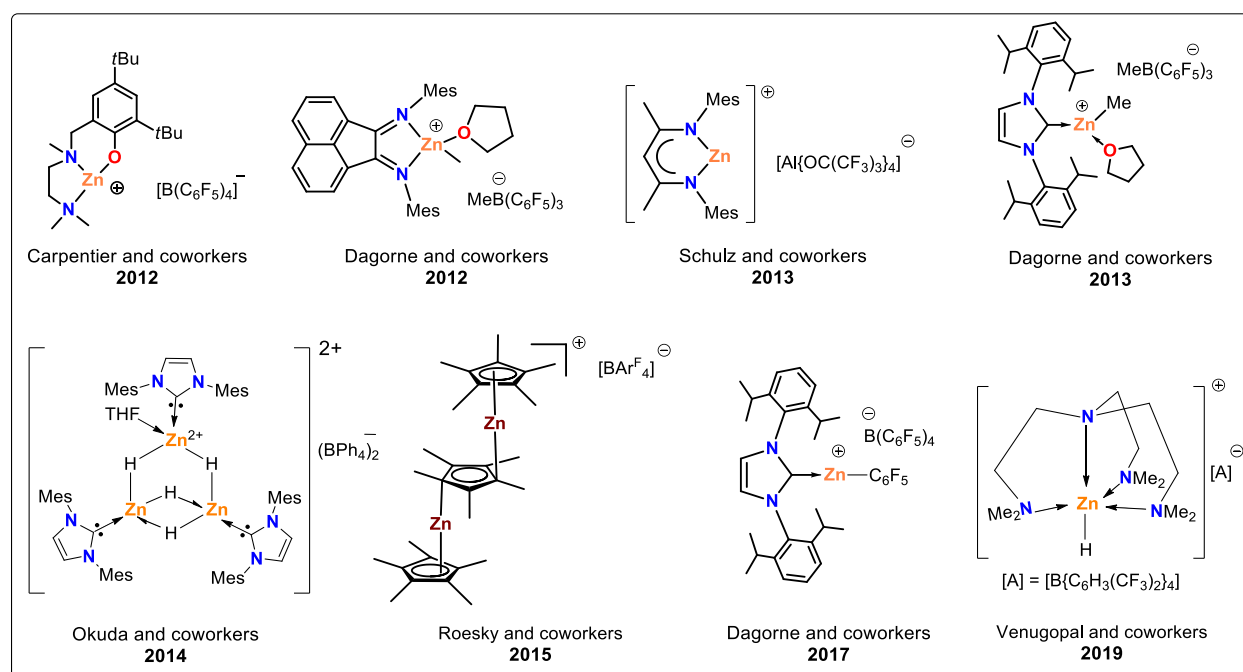


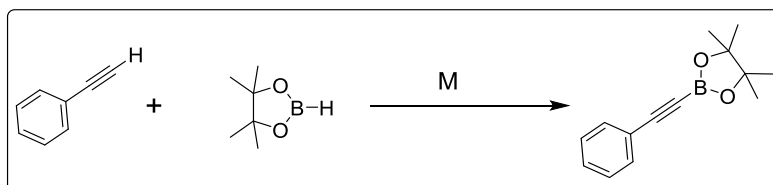
Figure 1.4. Selected reports of cationic zinc complexes.

1.3 Catalytic Activity of Reagent/Molecular-based Zinc Complexes

Zinc is earth-abundant, cheaper, and non-toxic compared to other precious metals. Thus, the use of zinc-based reagents and complexes is promoted in catalysis such as C-C, C-N, and C-O bond formation reactions, reductions of unsaturated compounds, transformations of carbon dioxide, hydroamination reactions, Friedel-Crafts reactions, oxidative coupling reactions, oxidation reactions, and depolymerizations.^{33f, 36} This wide application motivated the development of effective zinc-based catalysts for challenging unsaturated organic transformations.

1.3.1 Zinc-Mediated C-H Borylation of Terminal Alkynes

The catalytic dehydroborylation of terminal alkynes with pinacolborane is a mild approach to synthesizing organoboranes. These organoboranes are used as an intermediate for different chemical transformations and medicinal chemistry.³⁷



Scheme 1.6. Dehydroborylation of terminal alkynes.

On the other hand, metal-metal bonded complexes in catalysis are underdeveloped. In this regard, Ma and coworkers reported that Mg(I) dimers are used as pre-catalysts for the hydroboration of different organic substrates like aldehydes, ketones, carbonates, esters, carbon dioxide, epoxide, alkynes, and nitriles.³⁸ Similarly, Roesky and coworkers utilized zinc(I) complexes for the hydroamination reactions.³⁹ However, low-oxidation state metal-metal bonded complex catalyzed dehydroborylation of alkynes is unknown. There is a handful of reports on zinc-based dehydroborylation of terminal alkynes.⁴⁰

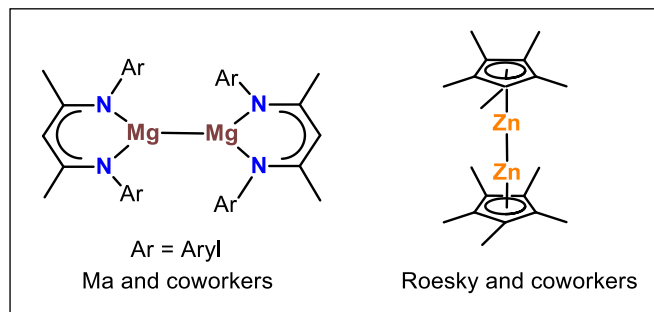
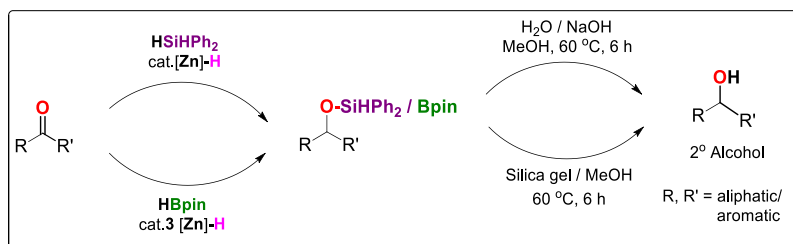


Figure 1.5. Mg(I) and Zn(I) dimers in catalysis.

1.3.2 Hydrofunctionalization of Ketones and Chemoselective Hydroboration of Isocyanates

1.3.2.1. Part A: Hydroboration and Hydrosilylation of Ketones

The silyl ethers or borate esters are important intermediates for synthesizing alcohols.⁴¹ The synthetic methods involve hydrosilylation or hydroboration of carbonyls to afford the desired silyl ethers or borate esters. In 1960, Calas et al. described the first hydrosilylation of carbonyl compounds using ZnCl_2 as a reagent. After that, many reports are there for the transition and main-group metals catalyzed hydrosilylation and hydroboration of carbonyl compounds.^{33f, 41a, 41c} In this regard, earth-abundant, cheaper, and non-toxic zinc complexes are ideal candidates for the hydrofunctionalization of aldehydes and ketones. A wide array of zinc-catalyzed reductions of carbonyls have been reported.^{32c, 35b, 35d, 42} In 2013, Nikonov and coworkers reported that $\text{Dipp}^{\text{Nac}}\text{Nac}$ zinc hydride catalyzed the hydrosilylation of ketones.^{42a}



Scheme 1.7. Hydrosilylation and hydroboration of ketones.

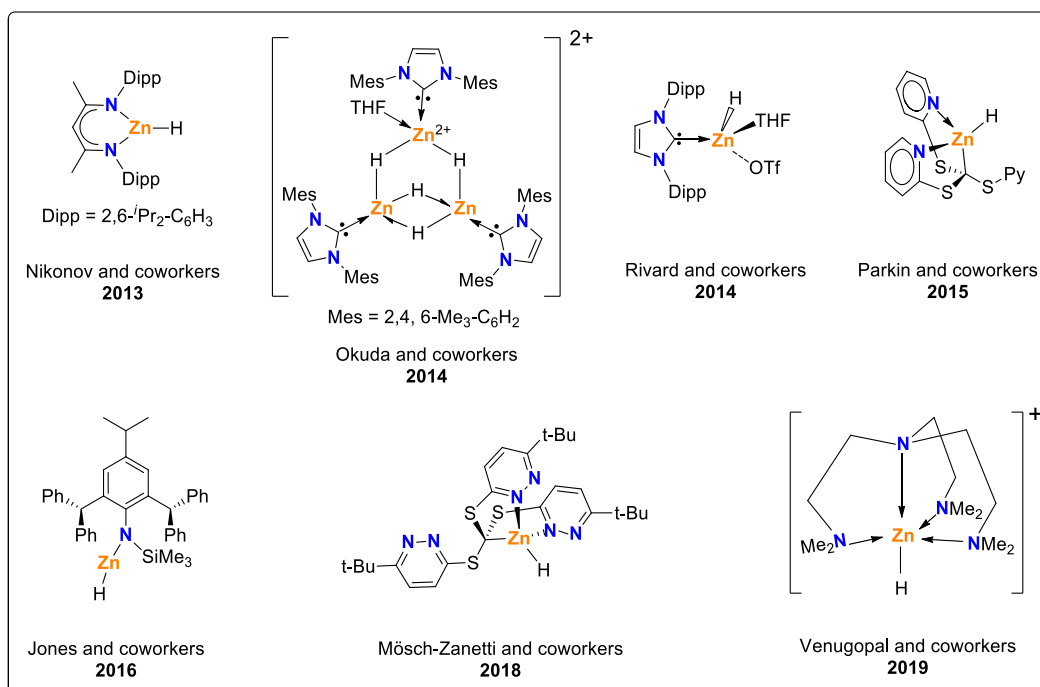


Figure 1.6. Reported zinc-based hydrosilylation and hydroboration of ketones.

Subsequently, many groups established hydrosilylation and hydroboration of ketones using molecular zinc hydride-based catalysts. In 2015, Parkin and co-workers reported aldehydes and ketones hydrosilylation using a zinc hydride catalyst.^{42c} The plausible mechanism of this transformation is shown in Figure 1.7.^{42c}

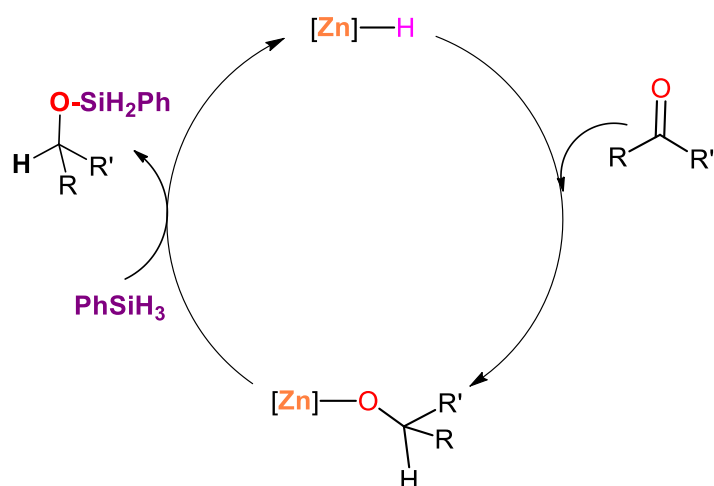
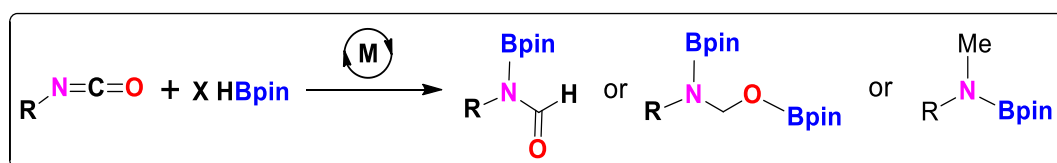


Figure 1.7. Plausible catalytic cycle for hydrosilylation of carbonyls by Parkin and co-workers.

In the first step, the unsaturated C=O bond of carbonyls inserted into the Zn-H bond yielded the corresponding zinc alkoxide intermediate. Followed by reacting with phenylsilane via σ -bond metathesis to give the desired product and regeneration of the catalyst.^{42c}

1.3.2.2. Part B: Chemoselective Reduction of Isocyanates via Hydroboration: Amide Bond Formation and Hydrodeoxygenation.

Isocyanates are essential starting materials for the formation of amide compounds. These amides produce heterocycles, drug molecules, and agricultural applications.⁴³



Scheme 1.8. Chemoselective hydroboration of isocyanates

Thus, developing a methodology to synthesize amide is highly desirable. Many synthetic procedures have been established for forming amides; however, these protocols have many drawbacks.⁴⁴

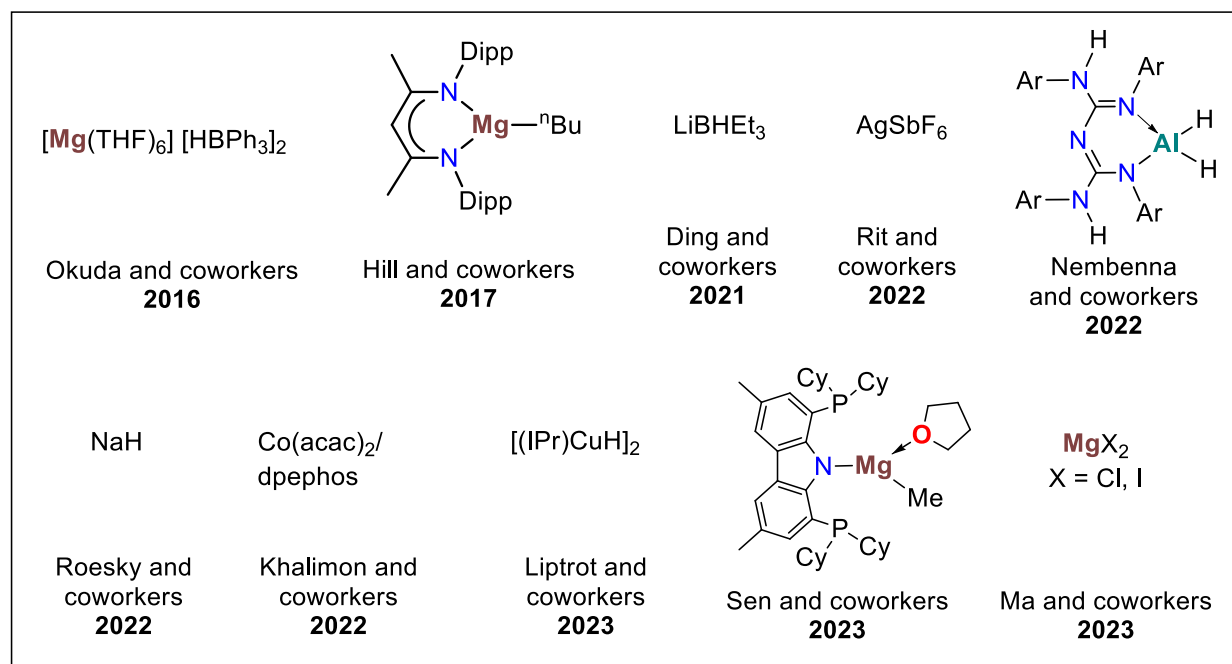


Figure 1.8. Report on metal-catalyzed reduction of isocyanates via hydroboration.

The partial reduction of isocyanates mediated by the Schwartz reagent (Cp_2ZrClH) was performed by Pace and coworkers in 2016.⁴⁵ Subsequently, Okuda and Hill groups independently utilized magnesium-based complexes for the hydroboration of isocyanates.⁴⁶ Later, many groups reported metal-catalyzed hydroboration of isocyanates, as shown in Figure 1.8.⁴⁶⁻⁴⁷ Recently, Khalimon established catalyst-free vs. cobalt-catalyzed hydroboration of isocyanates in 2022.^{47c}

1.3.3 Hydroelementation of Carbodiimides

The heterocumulenes are necessary starting materials for synthesizing formamidine, propiolamidine, guanidine, and urea products, which are found in material chemistry, coordination compounds, and medicinal applications.^{10a, 48} The hydroelementation of carbodiimides plays a crucial role in synthesizing carbon-carbon and carbon-heteroatom bonds. Due to their wide application, many researchers are developing suitable catalysts for the hydroelementation of heterocumulenes.



Scheme 1.9. Hydroboration of carbodiimides

Recently, there have been some reports on the transition metal-catalyzed hydroboration of carbodiimides.⁴⁹ In the last few years, only a handful of reports on molecular main group metal-based hydroboration of carbodiimides have been established.^{46a, 50}

In 2016, the Hill group established the magnesium-catalyzed hydroboration of carbodiimides to N-boryl formamidine.⁵⁰ⁱ Subsequently, a few main-group metal-based catalysts employed in converting carbodiimides into formamidines are shown in Figure 1.9.^{46a, 49-50} However, there are no reports on zinc-based hydroboration of carbodiimides.

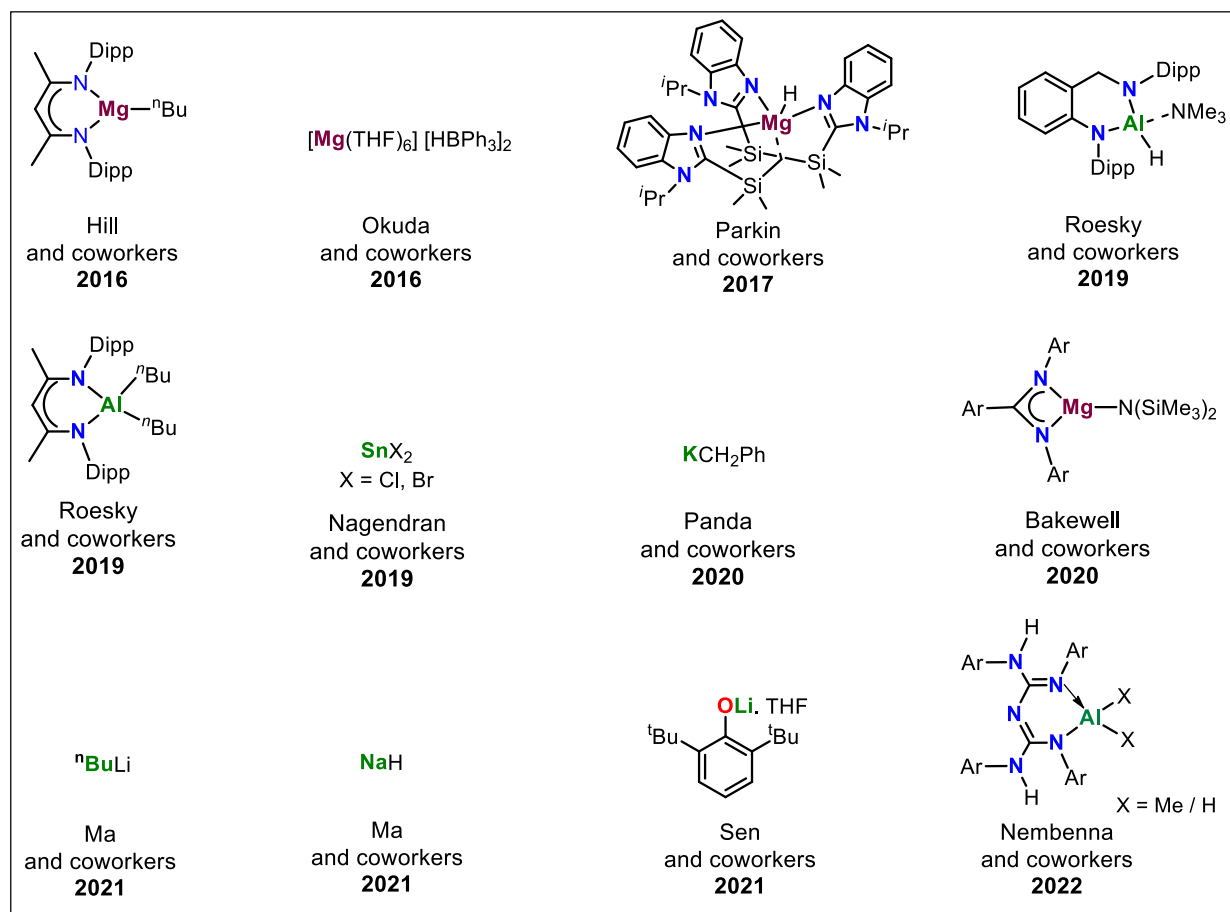
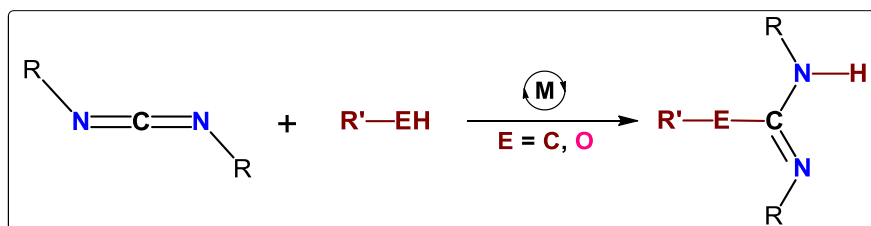


Figure 1.9. Previous reports on main-group metal-mediated hydroboration of carbodiimides.

In 2017, Carrillo–Hermosilla and coworkers reported diethylzinc pre-catalyzed hydroalkynylation of carbodiimides into propiolamidines.⁵¹ Very recently, García-Vivó used ZnEt_2 as a pre-catalyst for activating carbodiimides by alcohols into corresponding urea with good yields.⁵²



Scheme 1.10. C-H, and O-H addition to carbodiimides.

In 2016, Hill and co-workers reported the plausible mechanism for the B-H and C-H additions to carbodiimides by a magnesium-based complex, as depicted in Figure 1.11.⁵⁰ⁱ The catalytic cycles

initiate with the formation of a magnesium-hydride complex, followed by the hydrozincation of the carbodiimide substrate, generating a magnesium amidinate complex.

ZnEt₂	ZnEt₂
Carrillo-Hermosilla and coworkers 2017	García-Vivó and coworkers 2022

Figure 1.10. Previous reports on zinc-catalyzed C-H and O-H addition to carbodiimides.

The magnesium amidinate intermediate reacting with pinacolborane undergoes σ -bond metathesis to produce N-boryl formamidines as the desired product and rebirth of the active catalyst. Similarly, the authors proposed a plausible catalytic cycle for the hydroalkynylation of carbodiimide, as shown in Figure 1.11.

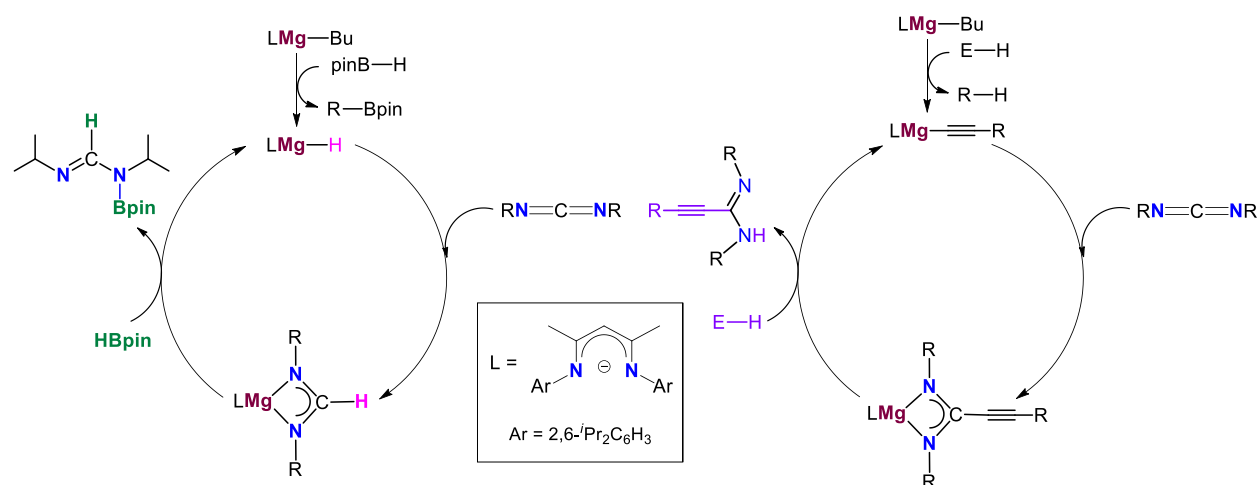
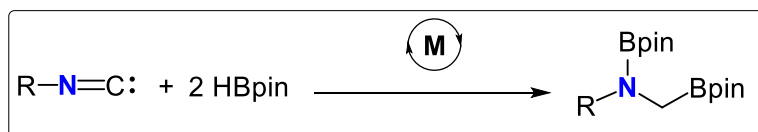


Figure 1.11. Plausible catalytic cycle for hydroboration and hydroalkynylation of carbodiimides by Hill and co-workers.

1.3.4 Chemoselective Hydrofunctionalization of Nitrile and Isocyanides

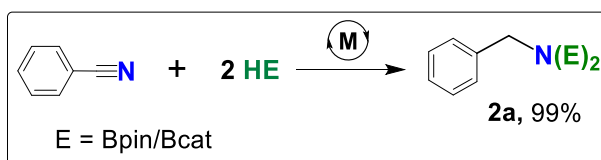
1.3.4.1. Part A: Dihydroboration of Nitrile and Isocyanides

The double activation of isonitriles and nitriles afforded amines, which are broadly used in the pharmaceutical industry, dyes, and agrochemicals.⁵³



Scheme 1.11. Hydroboration of isonitriles.

In 2015, Figueroa and coworkers reported mono-hydroboration of isonitriles even at higher temperatures.⁵⁴ Subsequently, Hill groups introduced dihydroboration of isocyanides by employing the *Dipp*NacNac magnesium-based complex.⁵⁵



Scheme 1.12. Hydroboration of nitriles.

Next, the Nembenna group established the aluminum-catalyzed direduction of isonitriles with HBpin into 1,1-bis(boryl)amines at elevated temperatures.^{50g} There are various reports on transition metal-based dihydroboration of nitriles.^{50c, 50g, 56}

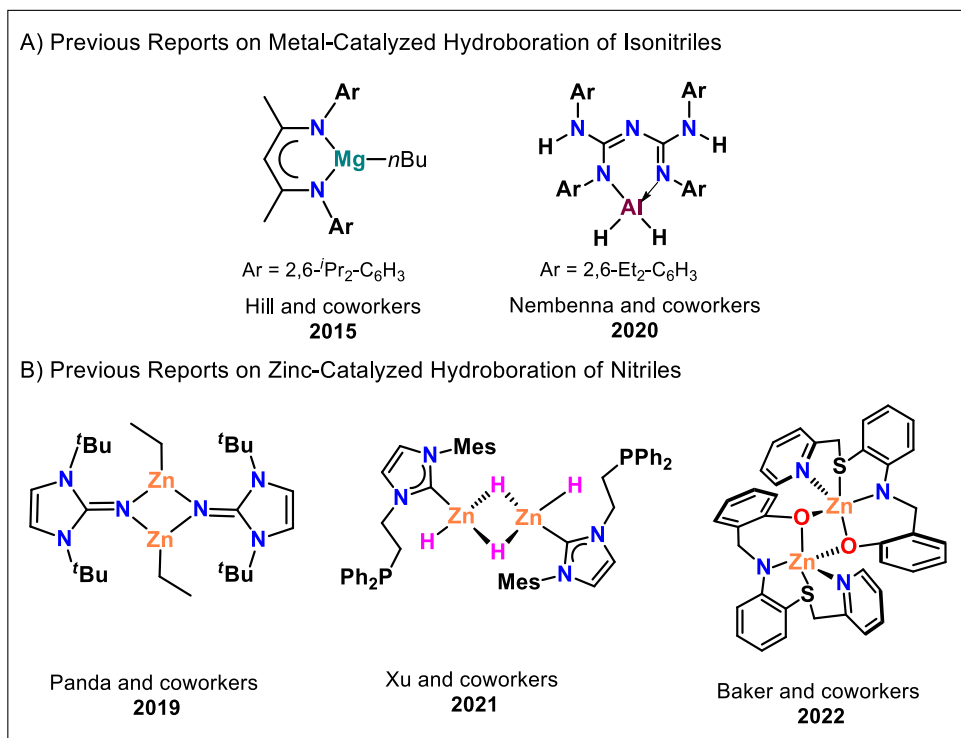


Figure 1.12. Previous reports on metal-catalyzed hydroboration of isonitriles and nitriles.

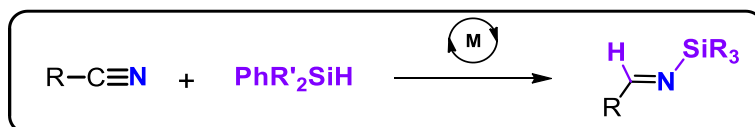
Nikonov and co-workers introduced dihydroboration of nitriles to 1,2-bis(boryl)amines by using a $(2,6\text{-}^i\text{Pr}_2\text{-C}_6\text{H}_3\text{N})\text{Mo}(\text{H})(\text{Cl})(\text{PMe}_3)_3$ complex.^{56f} After that, Panda, Xu, and Baker's research groups described molecular zinc-based hydroboration of nitriles with pinacolborane.^{56b, 56d, 56h}

1.3.4.2. Part B: Chemoselective Reduction of Nitriles to N-Silylimines Through Hydrosilylation

Organosilicon species are essential precursors for industries, medicinal chemistry, and silicon-containing polymers. In addition, the N-silylated imines are suitable starting materials for forming nitrogen-containing organic compounds and are used in laboratory methodology.⁵⁷

The synthesis of N-silylimines is challenging because they are further reduced to produce disilylamine products. Because of the importance of N-silylimines, many research groups are developing different protocols for synthesizing these precious N-silylimines.

Roschow, Spunta, Mulvey, and Walsh groups independently reported the synthesis of N-silylimines by adding a stoichiometric amount of sodium or lithium hexamethyldisilylamides to aldehydes.⁵⁸ In 1986, Panunzio and coworkers reported the chemoselective hydrosilylation of nitriles to N-silylimines by using $\text{LiAl}(\text{L})_3\text{H}$ (L = triethoxy/*n*-butyl diisopropyl).⁵⁹ Above traditional methods have several drawbacks, including the use of stoichiometric metal reagents, huge metal waste generation, and safety risks. Following these reports, significant advancements in hydrosilylation techniques using metal-based catalysts were discovered. Calas et al. reported that ZnCl_2 catalyzed the first chemoselective hydrosilylation of nitriles with triethylsilane.⁶⁰



Scheme 1.13. Chemoselective mono-hydrosilylation of nitriles with PhMe_2SiH , Ph_3SiH and TMS.

Later, transition and main-group element based compounds have been used as catalysts for chemoselective hydrosilylation of nitriles to N-silylimines.⁶¹ In this background, earth-abundant, inexpensive, and biocompatible zinc complexes are ideal candidates for such transformation. Nikonov and Okuda's groups independently described zinc-catalyzed Si-H addition in nitriles under mild conditions.^{35d, 42a}

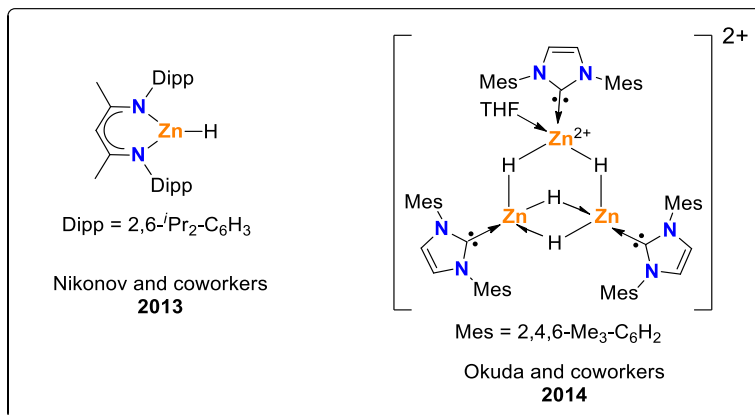
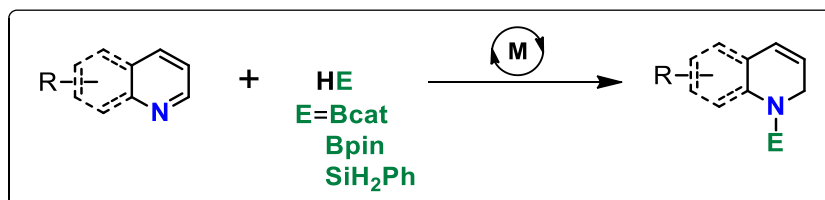


Figure 1.13. Previous reports on zinc-catalyzed chemoselective mono-hydrosilylation of nitriles.

1.3.5 Metal-Catalyzed 1, 2-Regioselective Hydroboration and Hydrosilylation of N-Heteroarenes

The catalytic reduction of N-heteroarenes afforded nitrogen heterocycles, which play a vital role in natural products, biological transformations, and agrochemical industries.⁶² To selectively synthesize precious dihydropyridines, many synthetic approaches have been developed. In traditional protocols, metal hydrides or alkali metal hydrides have been used to synthesize dihydropyridines.



Scheme 1.14. 1, 2-Selective hydrofunctionalization of N-heteroarenes.

However, the disadvantage of this method is the large quantity of waste generated.⁶³ Therefore, reducing N-heteroarenes with borane or silane reagents in the presence of transition metal catalysts would be an effective alternative.⁶⁴ Considering the low abundance, precious and toxic transition metal catalysts cause serious problems. As a result, there has been a lot of interest in switching to earth-abundant, inexpensive, and non-toxic zinc metals. In this regard, Nikonov and co-workers introduced the first example of zinc-catalyzed hydroboration and hydrosilylation of N-heteroarenes in 2017.⁶⁵ Recently, the Yao group extended the hydrofunctionalization of N-heteroarenes under mild conditions.⁶⁶

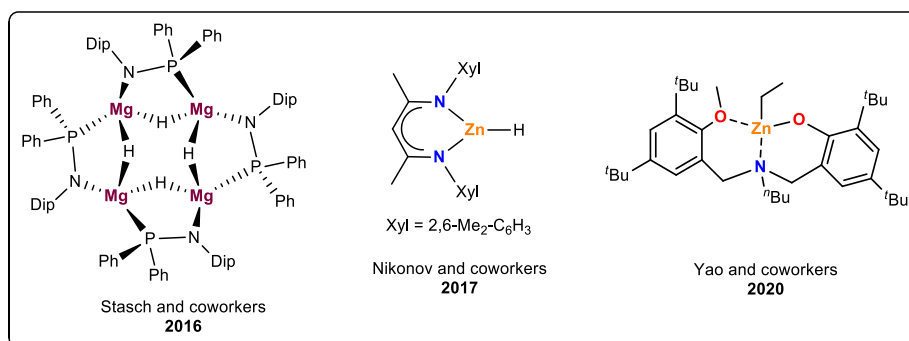
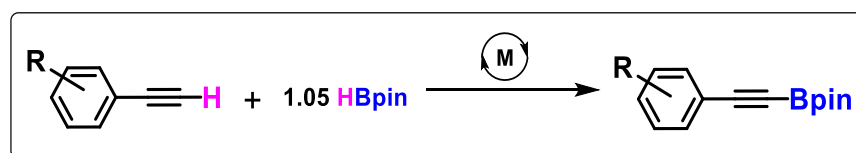


Figure 1.14. Reports on zinc-catalyzed 1,2-regioselective hydroboration and hydrosilylation of N-heteroarenes.

1.3.6 Zinc Hydride Mediated Dehydrogenative Borylation of Terminal Alkynes

The hydroboration and dehydroborylation of alkynes afforded precious organoboranes. This product is used for the synthesis of medicinal and industrial species.³⁷ Previously, the organoboranes were synthesized by using an equimolar quantity of organomagnesium reagents.⁶⁷



Scheme 1.15. Dehydroborylation of terminal alkynes.

This method has many disadvantages, including poor functional group tolerance, producing a large amount of waste, and safety issues. Thus, catalytic hydroboration and dehydroborylation of alkynes into organoboranes is a safe protocol.

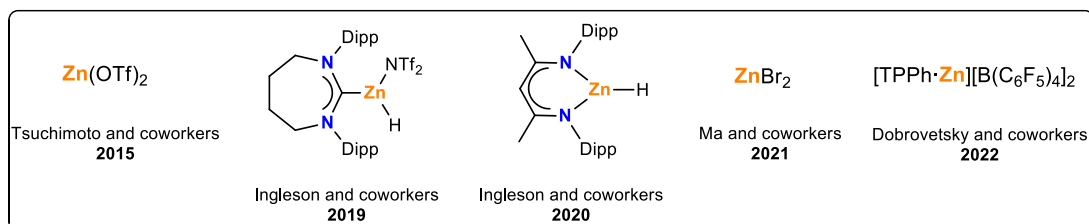


Figure 1.15. Reported zinc-catalyzed C-H borylation of terminal alkynes.

The hydroboration of terminal alkynes is saturated compared to the dehydroborylation reaction.^{50g.}

⁶⁸ Ozerov and coworkers introduced the first report in 2013 by using an iridium-based catalyst for the dehydroborylation of terminal alkynes to alkynyl boronates.⁶⁹

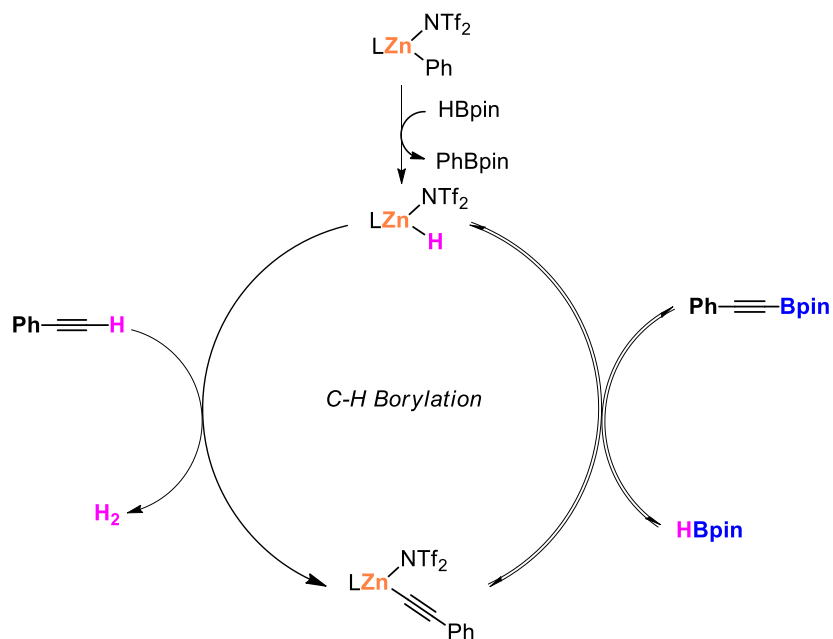


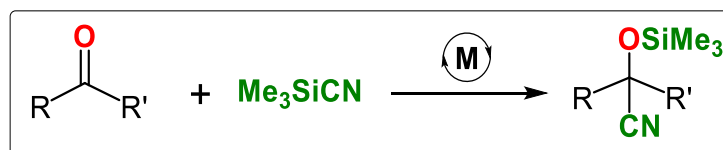
Figure 1.16. Plausible catalytic cycle for dehydroborylation of terminal alkynes by Ingleson and coworkers.

Later, the groups of Tsuchimoto, Ingleson, Ma, and Dobrovetsky individually established zinc-catalyzed dehydroborylation of terminal alkynes to organoboranes.^{40, 70} Ingleson established a

plausible mechanism for the dehydroborylation of alkynes based upon several stoichiometric experiments, as shown in Figure 1.16.^{40b}

1.3.7 Metal-Catalyzed Cyanosilylation of Ketones.

The catalytic cyanosilylation of carbonyls with trimethylsilyl cyanide is a gentle approach for producing cyanohydrins widely used in pharmaceuticals and agriculture.⁷¹ There are several transition and main group metal complexes have been used as catalysts for the cyanosilylation of carbonyls.^{71a, 72} Zinc is concerned, there are two reports in the literature.^{33d, 73} Lewis acid is an attractive tool for cyanosilylation reactions. In this regard, only a few cationic main-group complexes have been used for cyanosilylation reactions.⁷⁴ Although a hand full of examples of molecular zinc cationic complexes were reported and used in catalysis.^{34, 35g} However, there are no reports on the catalytic cyanosilylation of carbonyls catalyzed by molecular zinc cationic compounds.



Scheme 1.16. Canosilylation of ketones.

1.4 Aim, Scope, and Objective of the Current Work

The synthesis, reactivity, and catalysis of zinc-based complexes are well-established in the literature. However, there were few examples of catalytic reactions involving low-oxidation-state zinc(I) dimers, zinc(II) hydrides, and cationic complexes.

Schlesinger and coworkers discovered the parent zinc dihydride (ZnH₂), but it suffers from several drawbacks, such as being pyrophoric, thermally unstable, insoluble in organic solvents, and polymeric. Therefore, many scientists developed several heteroleptic zinc hydride complexes.

However, their utilization in different organic transformations such as hydroboration, hydrosilylation, hydrogenation, hydroamination, and hydroalkylation reactions is limited. Furthermore, fewer examples of zinc(I) dimers and zinc(II) cations are used in catalysis, including a lack of mechanistic details.

Based on these facts, the current work's goal is as follows:

- To isolate unusual zinc(I) complexes bearing CBG ligand and their catalytic applications.
- To employ monomeric and dimeric CBG zinc hydride complexes as catalytically active species in the hydrofunctionalization of unsaturated functional groups and to investigate the detailed mechanistic insights.
- To synthesize CBG-stabilized neutral and cationic zinc complexes and their practical application in cyanosilylation reactions.

1.5 References

1. *Chemistry and Technology Carbodiimides*. John Wiley & Sons, Ltd.: **2007**.
2. (a) Barman, M. K.; Nembenna, S. *RSC Adv.* **2016**, *6*, 338-345; (b) Edelmann, F. T. *Chem. Soc. Rev.* **2009**, *38*, 2253-2268; (c) Holthausen, M. H.; Colussi, M.; Stephan, D. W. *Chem. Eur. J.* **2015**, *21*, 2193-2199; (d) Jones, C. *Coord. Chem. Rev.* **2010**, *254*, 1273-1289; (e) Maity, A. K.; Fortier, S.; Griego, L.; Metta-Magaña, A. J. *Inorg. Chem.* **2014**, *53*, 8155-8164; (f) Peddaraao, T.; Baishya, A.; Barman, M. K.; Kumar, A.; Nembenna, S. *New J. Chem.* **2016**, *40*, 7627-7636; (g) Williams, A.; Ibrahim, I. T. *Chem. Rev.* **1981**, *81*, 589-636; (h) Williams, A.; Ibrahim, I. T. *J. Am. Chem. Soc.* **1981**, *103*, 7090.
3. Weith, W. *Ber. Dtsch. Chem. Ges.* **1874**, *7*, 10.
4. Findlater, M.; Hill, N. J.; Cowley, A. H. *Dalton Trans.* **2008**, 4419-4423.

-
5. (a) Baishya, A.; Kumar, L.; Barman, M. K.; Biswal, H. S.; Nembenna, S. *Inorg. Chem.* **2017**, *56*, 9535-9546; (b) Baishya, A.; Kumar, L.; Barman, M. K.; Peddarao, T.; Nembenna, S. *ChemistrySelect* **2016**, *1*, 498-503; (c) Baishya, A.; Peddarao, T.; Barman, M. K.; Nembenna, S. *New J. Chem.* **2015**, *39*, 7503-7510; (d) T. Boéré, R.; Klassen, V.; Wolmershäuser, G. *J. Chem. Soc., Dalton Trans.* **1998**, 4147-4154; (e) Tsai, Y.-C. *Coord. Chem. Rev.* **2012**, *256*, 722-758; (f) Webster, R. L. *Dalton Trans.* **2017**, *46*, 4483-4498.
 6. (a) Berlinck, R. G. S. *Nat. Prod. Rep.* **1996**, *13*, 377-409; (b) Berlinck, R. G. S.; Trindade-Silva, A. E.; Santos, M. F. C. *Nat. Prod. Rep.* **2012**, *29*, 1382-1406; (c) Durant, G. J. *Chem. Soc. Rev.* **1985**, *14*, 375-398; (d) Ishikawa, T.; Kumamoto, T. *Synthesis* **2006**, 737-752; (e) Santos, M. F. C.; Harper, P. M.; Williams, D. E.; Mesquita, J. T.; Pinto, É. G.; da Costa-Silva, T. A.; Hajdu, E.; Ferreira, A. G.; Santos, R. A.; Murphy, P. J.; Andersen, R. J.; Tempone, A. G.; Berlinck, R. G. S. *J. Nat. Prod.* **2015**, *78*, 1101-1112.
 7. Rathke, B. *Ber. Dtsch. Chem. Ges.* **1879**, *12*, 776-78.
 8. Glasovac, Z.; Troselj, P.; Jusinski, I.; Margetic, D.; Eckert-Maksic, M. *Synlett* **2013**, *24*, 2540-2544.
 9. Dehmel, M.; Vass, V.; Prock, L.; Görls, H.; Kretschmer, R. *Inorg. Chem.* **2020**, *59*, 2733-2746.
 10. (a) Peddarao, T.; Baishya, A.; Sarkar, N.; Acharya, R.; Nembenna, S. *Eur. J. Inorg. Chem.* **2021**, 2034-2046; (b) Sahoo, R. K.; Sarkar, N.; Nembenna, S. *Angew. Chem. Int. Ed.* **2021**, *60*, 11991-12000.
 11. (a) Green, M. L. H. *J. Organomet. Chem.* **1995**, *500*, 127-148; (b) Peddarao, T.; Sarkar, N.; Nembenna, S. *Inorg. Chem.* **2020**, *59*, 4693-4702; (c) unpublished results.

-
12. (a) Antiñolo, A.; Carrillo-Hermosilla, F.; Fernández-Galán, R.; Montero-Rama, M. P.; Ramos, A.; Villaseñor, E.; Rojas, R. S.; Rodríguez-Diéguez, A. *Dalton Trans.* **2016**, *45*, 15350-15363; (b) Edelmann, F. T. *Chem. Soc. Rev.* **2012**, *41*, 7657-7672; (c) Klementyeva, S. V.; Sukhikh, T. S.; Abramov, P. A.; Poddel'sky, A. I. *Molecules* **2023**, *28*, 1994; (d) Willcocks, A. M.; Robinson, T. P.; Roche, C.; Pugh, T.; Richards, S. P.; Kingsley, A. J.; Lowe, J. P.; Johnson, A. L. *Inorg. Chem.* **2012**, *51*, 246-257; (e) Zhong, M.; Sinhababu, S.; Roesky, H. W. *Dalton Trans.* **2020**, *49*, 1351-1364.
13. (a) Fleischer, M. *J. Chem. Educ.* **1954**, *31*, 446; (b) Kaur, K.; Gupta, R.; Saraf, S. A.; Saraf, S. K. *Compr. Rev. Food Sci. Food Saf.* **2014**, *13*, 358-376.
14. (a) Dudev, T.; Lim, C. *Chem. Rev.* **2003**, *103*, 773-788; (b) Frieden, E. *J. Chem. Educ.* **1985**, *62*, 917.
15. Seyferth, D. *Organometallics* **2004**, *23*, 1172-1172.
16. (a) Reformatsky, S. *Ber. Dtsch. Chem. Ges.* **1887**, *20*, 1210-1211; (b) Fürstner, A. *Synthesis* **1989**, 571-590; (c) Simmons, H. E.; Smith, R. D. *J. Am. Chem. Soc.* **1958**, *80*, 5323-5324; (d) Nakamura, E.; Sekiya, K.; Kuwajima, I. *Tetrahedron Lett.* **1987**, *28*, 337-340; (e) Negishi, E.; King, A. O.; Okukado, N. *J. Org. Chem.* **1977**, *42*, 1821-1823.
17. (a) Cotton, F. A.; Wilkinson, G.; Bochmann, M.; Murillo, C. *Advanced Inorganic Chemistry*, 6th ed., Wiley, **1998**; (b) Wiberg, N. *Holleman-Wiberg Inorganic Chemistry*, 34th ed., 101st printing, Academic Press, New York, **2001**.
18. Resa, I.; Carmona, E.; Gutierrez-Puebla, E.; Monge, A. *Science* **2004**, *305*, 1136-1138.
19. (a) Jensen, W. B. *J. Chem. Educ.* **2003**, *80*, 952; (b) Li, T.; Schulz, S.; Roesky, P. W. *Chem. Soc. Rev.* **2012**, *41*, 3759-3771.
20. Carmona, E.; Galindo, A. *Angew. Chem. Int. Ed.* **2008**, *47*, 6526-6536.
-

-
21. (a) *Metal-Metal Bonding*. [In: *Struct. Bonding (Berlin, Ger.)*, 2010; 136]. Springer GmbH: 2010; (b) Berry, J. F.; Lu, C. C. *Inorg. Chem.* **2017**, *56*, 7577-7581; (c) Hicks, J.; Underhill, E. J.; Kefalidis, C. E.; Maron, L.; Jones, C. *Angew. Chem. Int. Ed.* **2015**, *54*, 10000-10004; (d) Powers, I. G.; Uyeda, C. *ACS Catal.* **2017**, *7*, 936-958; (e) Schmid, G.; Bäumle, M.; Geerkens, M.; Heim, I.; Osemann, C.; Sawitowski, T. *Chem. Soc. Rev.* **1999**, *28*, 179-185; (f) Balakrishna, M. S. *Polyhedron* **2018**, *143*, 2-10; (g) Joseph, B.; Prakash, R.; Dorcet, V.; Roisnel, T.; Halet, J.-F.; Ghosh, S. *Organometallics* **2020**, *39*, 2942-2946.
22. Nguyen, T.; Sutton, A. D.; Brynda, M.; Fettingner, J. C.; Long, G. J.; Power, P. P. *Science* **2005**, *310*, 844-847.
23. Green, S. P.; Jones, C.; Stasch, A. *Science* **2007**, *318*, 1754-1757.
24. Juckel, M.; Dange, D.; de Bruin-Dickason, C.; Jones, C. Z. *Anorg. Allg. Chem.* **2020**, *646*, 603-608.
25. (a) Gondzik, S.; Bläser, D.; Wölper, C.; Schulz, S. *Chem. Eur. J.* **2010**, *16*, 13599-13602; (b) Li, B.; Huse, K.; Wölper, C.; Schulz, S. *Chem. Commun.* **2021**, *57*, 13692-13695; (c) Nayek, H. P.; Lühl, A.; Schulz, S.; Köppe, R.; Roesky, P. W. *Chem. Eur. J.* **2011**, *17*, 1773-1777; (d) Schulz, S.; Gondzik, S.; Schuchmann, D.; Westphal, U.; Dobrzycki, L.; Boese, R.; Harder, S. *Chem. Commun.* **2010**, *46*, 7757-7759; (e) Wang, Y.; Quillian, B.; Wei, P.; Wang, H.; Yang, X.-J.; Xie, Y.; King, R. B.; Schleyer, P. V. R.; Schaefer, H. F.; Robinson, G. H. *J. Am. Chem. Soc.* **2005**, *127*, 11944-11945.
26. (a) Fedushkin, I. L.; Eremenko, O. V.; Skatova, A. A.; Piskunov, A. V.; Fukin, G. K.; Ketkov, S. Y.; Irran, E.; Schumann, H. *Organometallics* **2009**, *28*, 3863-3868; (b) Fedushkin, I. L.; Skatova, A. A.; Ketkov, S. Y.; Eremenko, O. V.; Piskunov, A. V.; Fukin, G. K. *Angew. Chem. Int. Ed.* **2007**, *46*, 4302-4305; (c) Hicks, J.; Jones, C. *Inorg. Chem.*
-

- 2013**, 52, 3900-3907; (d) Schulz, S. *Chem. Eur. J.* **2010**, 16, 6416-6428; (e) Schulz, S.; Schuchmann, D.; Krossing, I.; Himmel, D.; Bläser, D.; Boese, R. *Angew. Chem. Int. Ed.* **2009**, 48, 5748-5751; (f) Schulz, S.; Schuchmann, D.; Westphal, U.; Bolte, M. *Organometallics* **2009**, 28, 1590-1592; (g) Wang, Y.; Quillian, B.; Yang, X.-J.; Wei, P.; Chen, Z.; Wannere, C. S.; Schleyer, P. v. R.; Robinson, G. H. *J. Am. Chem. Soc.* **2005**, 127, 7672-7673.
27. Zhu, Z.; Brynda, M.; Wright, R. J.; Fischer, R. C.; Merrill, W. A.; Rivard, E.; Wolf, R.; Fettingner, J. C.; Olmstead, M. M.; Power, P. P. *J. Am. Chem. Soc.* **2007**, 129, 10847-10857.
28. Finholt, A. E.; Bond, A. C., Jr.; Wilzbach, K. E.; Schlesinger, H. I. *J. Am. Chem. Soc.* **1947**, 69, 2692-2696.
29. (a) Barbaras, G. D.; Dillard, C.; Finholt, A. E.; Wartik, T.; Wilzbach, K. E.; Schlesinger, H. I. *J. Am. Chem. Soc.* **1951**, 73, 4585-4590; (b) Greene, T. M.; Brown, W.; Andrews, L.; Downs, A. J.; Chertihin, G. V.; Runeberg, N.; Pyykko, P. *J. Phys. Chem.* **1995**, 99, 7925-7934; (c) Ritter, F.; Morris, L. J.; McCabe, K. N.; Spaniol, T. P.; Maron, L.; Okuda, J. *Inorg. Chem.* **2021**, 60, 15583-15592; (d) Shayesteh, A.; Appadoo, D. R. T.; Gordon, I. E.; Bernath, P. F. *J. Am. Chem. Soc.* **2004**, 126, 14356-14357; (e) Wang, X.; Andrews, L. *J. Phys. Chem. A* **2004**, 108, 11006-11013; (f) Watkins, J. J.; Ashby, E. C. *Inorg. Chem.* **1974**, 13, 2350-2354.
30. Ashby, E. C.; Goel, A. B. *J. Organomet. Chem.* **1977**, 139, C89-C91.
31. Han, R.; Gorrell, I. B.; Looney, A. G.; Parkin, G. *J. Chem. Soc., Chem. Commun.* **1991**, 717-719.
32. (a) Rit, A.; Spaniol, T. P.; Maron, L.; Okuda, J. *Angew. Chem. Int. Ed.* **2013**, 52, 4664-4667; (b) Brown, N. J.; Harris, J. E.; Yin, X.; Silverwood, I.; White, A. J. P.; Kazarian, S.

- G.; Hellgardt, K.; Shaffer, M. S. P.; Williams, C. K. *Organometallics* **2014**, *33*, 1112-1119;
- (c) Dawkins, M. J. C.; Middleton, E.; Kefalidis, C. E.; Dange, D.; Juckel, M. M.; Maron, L.; Jones, C. *Chem. Commun.* **2016**, *52*, 10490-10492; (d) Hao, H.; Cui, C.; Roesky, H. W.; Bai, G.; Schmidt, H.-G.; Noltemeyer, M. *Chem. Commun.* **2001**, 1118-1119; (e) Intemann, J.; Sirsch, P.; Harder, S. *Chem. Eur. J.* **2014**, *20*, 11204-11213; (f) Sattler, W.; Parkin, G. *J. Am. Chem. Soc.* **2011**, *133*, 9708-9711; (g) Spielmann, J.; Piesik, D.; Wittkamp, B.; Jansen, G.; Harder, S. *Chem. Commun.* **2009**, 3455-3456.
33. (a) Baker, G. J.; White, A. J. P.; Casely, I. J.; Grainger, D.; Crimmin, M. R. *J. Am. Chem. Soc.* **2023**, *145*, 7667-7674; (b) Bhattacharjee, J.; Sachdeva, M.; Banerjee, I.; Panda, T. K. *J. Chem. Sci.* **2016**, *128*, 875-881; (c) Jochmann, P.; Stephan, D. W. *Angew. Chem. Int. Ed.* **2013**, *52*, 9831-9835; (d) Ma, Z.; Aliyeva, V. A.; Tagiev, D. B.; Zubkov, F. I.; Guseinov, F. I.; Mahmudov, K. T.; Pombeiro, A. J. L. *J. Organomet. Chem.* **2020**, *912*, 121171; (e) Paul, S.; Morgante, P.; MacMillan, S. N.; Autschbach, J.; Lacy, D. C. *Chem. Eur. J.* **2022**, *28*, e202201042; (f) Roy, M. M. D.; Omaña, A. A.; Wilson, A. S. S.; Hill, M. S.; Aldridge, S.; Rivard, E. *Chem. Rev.* **2021**, *121*, 12784-12965; (g) Sahoo, R. K.; Patro, A. G.; Sarkar, N.; Nembenna, S. *Organometallics* **2023**, DOI: <https://doi.org/10.1021/acs.organomet.2c00610>; (h) Zhang, B.; Ma, X.; Yan, B.; Ni, C.; Yu, H.; Yang, Z.; Roesky, H. W. *Dalton Trans.* **2021**, *50*, 15488-15492.
34. (a) Dagorne, S. *Synthesis* **2018**, *50*, 3662-3670; (b) Suresh, P.; Prabusankar, G. *J. Chem. Sci.* **2014**, *126*, 1409-1415.
35. (a) Brignou, P.; Guillaume, S. M.; Roisnel, T.; Bourissou, D.; Carpentier, J.-F. *Chem. Eur. J.* **2012**, *18*, 9360-9370; (b) Chambenahalli, R.; Andrews, A. P.; Ritter, F.; Okuda, J.; Venugopal, A. *Chem. Commun.* **2019**, *55*, 2054-2057; (c) Chilleck, M. A.; Hartenstein, L.;

- Braun, T.; Roesky, P. W.; Braun, B. *Chem. Eur. J.* **2015**, *21*, 2594-2602; (d) Rit, A.; Zanardi, A.; Spaniol, T. P.; Maron, L.; Okuda, J. *Angew. Chem. Int. Ed.* **2014**, *53*, 13273-13277; (e) Romain, C.; Rosa, V.; Fliedel, C.; Bier, F.; Hild, F.; Welter, R.; Dagorne, S.; Avilés, T. *Dalton Trans.* **2012**, *41*, 3377-3379; (f) Scheiper, C.; Schulz, S.; Wölper, C.; Bläser, D.; Roll, J. Z. *Anorg. Allg. Chem.* **2013**, *639*, 1153-1159; (g) Schnee, G.; Fliedel, C.; Avilés, T.; Dagorne, S. *Eur. J. Inorg. Chem.* **2013**, 3699-3709; (h) Specklin, D.; Hild, F.; Fliedel, C.; Gourlaouen, C.; Veiros, L. F.; Dagorne, S. *Chem. Eur. J.* **2017**, *23*, 15908-15912.
36. (a) Enthaler, S. *ACS Catal.* **2013**, *3*, 150-158; (b) Lennartson, A. *Nat. Chem.* **2014**, *6*, 166-166; (c) Wu, X.-F.; Neumann, H. *Adv. Synth. Catal.* **2012**, *354*, 3141-3160; (d) Chambenahalli, R.; Bhargav, R. M.; McCabe, K. N.; Andrews, A. P.; Ritter, F.; Okuda, J.; Maron, L.; Venugopal, A. *Chem. Eur. J.* **2021**, *27*, 7391-7401; (e) Mannarsamy, M.; Nandeshwar, M.; Muduli, G.; Prabusankar, G. *Chem. Asian J.* **2022**, *17*, e202200594.
37. (a) Hartwig, J. F. *Acc. Chem. Res.* **2012**, *45*, 864-873; (b) Lennox, A. J. J.; Lloyd-Jones, G. C. *Chem. Soc. Rev.* **2014**, *43*, 412-443; (c) Suzuki, A. *Angew. Chem. Int. Ed.* **2011**, *50*, 6722-6737.
38. (a) Cao, X.; Li, J.; Zhu, A.; Su, F.; Yao, W.; Xue, F.; Ma, M. *Org. Chem. Front.* **2020**, *7*, 3625-3632; (b) Cao, X.; Wang, W.; Lu, K.; Yao, W.; Xue, F.; Ma, M. *Dalton Trans.* **2020**, *49*, 2776-2780; (c) Li, J.; Luo, M.; Sheng, X.; Hua, H.; Yao, W.; Pullarkat, S. A.; Xu, L.; Ma, M. *Org. Chem. Front.* **2018**, *5*, 3538-3547.
39. (a) Lühl, A.; Hartenstein, L.; Blechert, S.; Roesky, P. W. *Organometallics* **2012**, *31*, 7109-7116; (b) Lühl, A.; Pada Nayek, H.; Blechert, S.; Roesky, P. W. *Chem. Commun.* **2011**, *47*, 8280-8282.

-
40. (a) Luo, M.; Qin, Y.; Chen, X.; Xiao, Q.; Zhao, B.; Yao, W.; Ma, M. *J. Org. Chem.* **2021**, *86*, 16666-16674; (b) Procter, R. J.; Uzelac, M.; Cid, J.; Rushworth, P. J.; Ingleson, M. J. *ACS Catal.* **2019**, *9*, 5760-5771; (c) Tsuchimoto, T.; Utsugi, H.; Sugiura, T.; Horio, S. *Adv. Synth. Catal.* **2015**, *357*, 77-82; (d) Uzelac, M.; Yuan, K.; Ingleson, M. J. *Organometallics* **2020**, *39*, 1332-1338.
41. (a) Ai, W.; Zhong, R.; Liu, X.; Liu, Q. *Chem. Rev.* **2019**, *119*, 2876-2953; (b) Shegavi, M. L.; Bose, S. K. *Catal. Sci. Technol.* **2019**, *9*, 3307-3336; (c) Wei, D.; Darcel, C. *Chem. Rev.* **2019**, *119*, 2550-2610.
42. (a) Boone, C.; Korobkov, I.; Nikonov, G. I. *ACS Catal.* **2013**, *3*, 2336-2340; (b) Lummis, P. A.; Momeni, M. R.; Lui, M. W.; McDonald, R.; Ferguson, M. J.; Miskolzie, M.; Brown, A.; Rivard, E. *Angew. Chem. Int. Ed.* **2014**, *53*, 9347-9351; (c) Sattler, W.; Ruccolo, S.; Rostami Chaijan, M.; Nasr Allah, T.; Parkin, G. *Organometallics* **2015**, *34*, 4717-4731; (d) Tüchler, M.; Gärtner, L.; Fischer, S.; Boese, A. D.; Belaj, F.; Mösch-Zanetti, N. C. *Angew. Chem. Int. Ed.* **2018**, *57*, 6906-6909.
43. (a) Bruffaerts, J.; von Wolff, N.; Diskin-Posner, Y.; Ben-David, Y.; Milstein, D. *J. Am. Chem. Soc.* **2019**, *141*, 16486-16493; (b) Majewski, M. W.; Miller, P. A.; Oliver, A. G.; Miller, M. J. *J. Org. Chem.* **2017**, *82*, 737-744.
44. (a) Leong, B.-X.; Teo, Y.-C.; Condamines, C.; Yang, M.-C.; Su, M.-D.; So, C.-W. *ACS Catal.* **2020**, *10*, 14824-14833; (b) Valeur, E.; Bradley, M. *Chem. Soc. Rev.* **2009**, *38*, 606-631.
45. (a) Pace, V.; de la Vega-Hernández, K.; Urban, E.; Langer, T. *Org. Lett.* **2016**, *18*, 2750-2753; (b) Pace, V.; Monticelli, S.; de la Vega-Hernández, K.; Castoldi, L. *Org. Biomol. Chem.* **2016**, *14*, 7848-7854.
-

-
46. (a) Mukherjee, D.; Shirase, S.; Spaniol, T. P.; Mashima, K.; Okuda, J. *Chem. Commun.* **2016**, 52 (89), 13155-13158; (b) Yang, Y.; Anker, M. D.; Fang, J.; Mahon, M. F.; Maron, L.; Weetman, C.; Hill, M. S. *Chem. Sci.* **2017**, 8, 3529-3537.
47. (a) Du, Z.; Behera, B.; Kumar, A.; Ding, Y. *J. Organomet. Chem.* **2021**, 950, 121982; (b) English, L. E.; Horsley Downie, T. M.; Lyall, C. L.; Mahon, M. F.; McMullin, C. L.; Neale, S. E.; Saunders, C. M.; Liptrot, D. J. *Chem. Commun.* **2023**, 59, 1074-1077; (c) Gudun, K. A.; Tussupbayev, S.; Slamova, A.; Khalimon, A. Y. *Org. Biomol. Chem.* **2022**, 20, 6821-6830; (d) Kumar, R.; Sharma, V.; Banerjee, S.; Vanka, K.; Sen, S. S. *Chem. Commun.* **2023**, 59, 2255-2258; (e) Ni, C.; Ma, X.; Yang, Z.; Roesky, H. W. *ChemistrySelect* **2022**, 7, e202202878; (f) Pandey, V. K.; Sahoo, S.; Rit, A. *Chem. Commun.* **2022**, 58, 5514-5517; (g) Sarkar, N.; Sahoo, R. K.; Nembenna, S. *Eur. J. Org. Chem.* **2022**, e202200941; (h) Shi, J.; Luo, M.; Zhang, X.; Yuan, T.; Chen, X.; Ma, M. *Org. Biomol. Chem.* **2023**, 21, 3628-3635.
48. (a) Carrillo-Hermosilla, F.; Fernández-Galán, R.; Ramos, A.; Elorriaga, D. *Molecules* **2022**, 27, 5962; (b) Smith, R. C.; Protasiewicz, J. D. *J. Am. Chem. Soc.* **2004**, 126, 2268-2269; (c) Zarate, G. S.; Santana, G. A.; Bastida, A.; Revuelta, J. *Curr. Org. Chem.* **2014**, 18, 2711-2749.
49. (a) Khononov, M.; Fridman, N.; Tamm, M.; Eisen, M. S. *Eur. J. Org. Chem.* **2020**, 3153-3160; (b) Liu, H.; Kulbitski, K.; Tamm, M.; Eisen, M. S. *Chem. Eur. J.* **2018**, 24, 5738-5742; (c) Rezaei Bazkiaei, A.; Findlater, M.; Gorden, A. E. V. *Org. Biomol. Chem.* **2022**, 20, 3675-3702.
50. (a) Bakewell, C. *Dalton Trans.* **2020**, 49, 11354-11360; (b) Bisai, M. K.; Gour, K.; Das, T.; Vanka, K.; Sen, S. S. *J. Organomet. Chem.* **2021**, 949, 121924; (c) Ding, Y.; Ma, X.;
-

- Liu, Y.; Liu, W.; Yang, Z.; Roesky, H. W. *Organometallics* **2019**, *38*, 3092-3097; (d) Panda, T. K.; Banerjee, I.; Sagar, S. *Appl. Organomet. Chem.* **2020**, *34*, e5765; (e) Patel, M.; Desai, B.; Sheth, A.; Dholakiya, B. Z.; Naveen, T. *Asian J. Org. Chem.* **2021**, *10*, 3201-3232; (f) Rauch, M.; Ruccolo, S.; Parkin, G. *J. Am. Chem. Soc.* **2017**, *139*, 13264-13267; (g) Sarkar, N.; Bera, S.; Nembenna, S. *J. Org. Chem.* **2020**, *85*, 4999-5009; (h) Shen, Q.; Ma, X.; Li, W.; Liu, W.; Ding, Y.; Yang, Z.; Roesky, H. W. *Chem. Eur. J.* **2019**, *25*, 11918-11923; (i) Weetman, C.; Hill, M. S.; Mahon, M. F. *Chem. Eur. J.* **2016**, *22*, 7158-7162; (j) Yan, B.; He, X.; Ni, C.; Yang, Z.; Ma, X. *ChemCatChem* **2021**, *13*, 851-854.
51. Martínez, A.; Moreno-Blázquez, S.; Rodríguez-Diéguez, A.; Ramos, A.; Fernández-Galán, R.; Antiñolo, A.; Carrillo-Hermosilla, F. *Dalton Trans.* **2017**, *46*, 12923-12934.
52. Ramos, A.; Carrillo-Hermosilla, F.; Fernández-Galán, R.; Elorriaga, D.; Naranjo, J.; Antiñolo, A.; García-Vivó, D. *Organometallics* **2022**, *41*, 2949-2957.
53. (a) Carey, J. S.; Laffan, D.; Thomson, C.; Williams, M. T. *Org. Biomol. Chem.* **2006**, *4*, 2337-2347; (b) Martin, R.; Buchwald, S. L. *Acc. Chem. Res.* **2008**, *41*, 1461-1473; (c) Pelckmans, M.; Renders, T.; Van de Vyver, S.; Sels, B. F. *Green Chem.* **2017**, *19*, 5303-5331; (d) Torborg, C.; Beller, M. *Adv. Synth. Catal.* **2009**, *351*, 3027-3043.
54. Barnett, B. R.; Moore, C. E.; Rheingold, A. L.; Figueroa, J. S. *Chem. Commun.* **2015**, *51*, 541-544.
55. Weetman, C.; Hill, M. S.; Mahon, M. F. *Chem. Commun.* **2015**, *51*, 14477-14480.
56. (a) Ataie, S.; Baker, R. T. *Inorg. Chem.* **2022**, *61*, 19998-20007; (b) Ataie, S.; Ovens, J. S.; Tom Baker, R. *Chem. Commun.* **2022**, *58*, 8266-8269; (c) Banerjee, I.; Anga, S.; Bano, K.; Panda, T. K. *J. Organomet. Chem.* **2019**, *902*, 120958; (d) Das, S.; Bhattacharjee, J.; Panda, T. K. *New J. Chem.* **2019**, *43*, 16812-16818; (e) Geri, J. B.; Szymczak, N. K. *J. Am. Chem.*

- Soc.* **2015**, *137*, 12808-12814; (f) Khalimon, A. Y.; Farha, P.; Kuzmina, L. G.; Nikonov, G. I. *Chem. Commun.* **2012**, *48*, 455-457; (g) Pradhan, S.; Sankar, R. V.; Gunanathan, C. *J. Org. Chem.* **2022**, *87*, 12386-12396; (h) Wang, X.; Xu, X. *RSC Adv.* **2021**, *11*, 1128-1133; (i) Weetman, C.; Anker, M. D.; Arrowsmith, M.; Hill, M. S.; Kociok-Köhn, G.; Liptrot, D. J.; Mahon, M. F. *Chem. Sci.* **2016**, *7*, 628-641.
57. (a) Fessenden, R.; Fessenden, J. S. *Chem. Rev.* **1961**, *61*, 361-388; (b) Liu, Z.; Li, M.; Deng, G.; Wei, W.; Feng, P.; Zi, Q.; Li, T.; Zhang, H.; Yang, X.; Walsh, P. J. *Chem. Sci.* **2020**, *11*, 7619-7625; (c) Melen, R. L. *Chem. Soc. Rev.* **2016**, *45*, 775-788; (d) Ruecker, C. *Chem. Rev.* **1995**, *95*, 1009-1064; (e) Shirobokov, O. G.; Kuzmina, L. G.; Nikonov, G. I. *J. Am. Chem. Soc.* **2011**, *133*, 6487-6489; (f) Tanabe, Y.; Nishibayashi, Y. *Coord. Chem. Rev.* **2019**, *389*, 73-93.
58. (a) Cainelli, G.; Giacomini, D.; Panunzio, M.; Martelli, G.; Spunta, G. *Tetrahedron Lett.* **1987**, *28*, 5369-5372; (b) Chan, L.-H.; Roschow, E. G. *J. Organomet. Chem.* **1967**, *9*, 231-250; (c) Gentner, T. X.; Mulvey, R. E. *Angew. Chem. Int. Ed.* **2021**, *60*, 9247-9262.
59. (a) Andreoli, P.; Cainelli, G.; Contento, M.; Giacomini, D.; Martelli, G.; Panunzio, M. *Tetrahedron Lett.* **1986**, *27*, 1695-1698; (b) Barluenga, J.; Aznar, F.; Valdés, C. *Angew. Chem. Int. Ed.* **2004**, *43*, 343-345.
60. Calas, R.; Frainnet, E.; Bazouin, A. *C.R. Acad. Sci.* **1961**, *252*, 420-422.
61. (a) Garduño, J. A.; Flores-Alamo, M.; García, J. J. *ChemCatChem* **2019**, *11*, 5330-5338; (b) Khalimon, A. Y.; Simionescu, R.; Kuzmina, L. G.; Howard, J. A. K.; Nikonov, G. I. *Angew. Chem. Int. Ed.* **2008**, *47*, 7701-7704; (c) Peterson, E.; Khalimon, A. Y.; Simionescu, R.; Kuzmina, L. G.; Howard, J. A. K.; Nikonov, G. I. *J. Am. Chem. Soc.* **2009**, *131*, 908-909.

-
62. (a) Eisner, U.; Kuthan, J. *Chem. Rev.* **1972**, *72*, 1-42; (b) Liu, Z.; Chen, L.; Li, J.; Liu, K.; Zhao, J.; Xu, M.; Feng, L.; Wan, R.-z.; Li, W.; Liu, L. *Org. Biomol. Chem.* **2017**, *15*, 7600-7606; (c) Michael, J. P. *Nat. Prod. Rep.* **2003**, *20*, 476-493; (d) Thiele, B.; Rieder, O.; Golding, B. T.; Müller, M.; Boll, M. *J. Am. Chem. Soc.* **2008**, *130*, 14050-14051; (e) Welsch, M. E.; Snyder, S. A.; Stockwell, B. R. *Curr. Opin. Chem. Biol.* **2010**, *14*, 347-361; (f) Yu, H.-C.; Islam, S. M.; Mankad, N. P. *ACS Catal.* **2020**, *10*, 3670-3675.
63. (a) Birch, A. J.; Karakhanov, E. A. *J. Chem. Soc., Chem. Commun.* **1975**, 480-481; (b) Danishefsky, S.; Cavanaugh, R. *J. Am. Chem. Soc.* **1968**, *90*, 520-521.
64. (a) Chong, C. C.; Kinjo, R. *ACS Catal.* **2015**, *5*, 3238-3259; (b) Fohlmeister, L.; Stasch, A. *Chem. Eur. J.* **2016**, *22*, 10235-10246; (c) McLellan, R.; Kennedy, A. R.; Mulvey, R. E.; Orr, S. A.; Robertson, S. D. *Chem. Eur. J.* **2017**, *23*, 16853-16861.
65. Lortie, J. L.; Dudding, T.; Gabidullin, B. M.; Nikonov, G. I. *ACS Catal.* **2017**, *7*, 8454-8459.
66. Wang, X.; Zhang, Y.; Yuan, D.; Yao, Y. *Org. Lett.* **2020**, *22*, 5695-5700.
67. (a) Bose, S. K.; Mao, L.; Kuehn, L.; Radius, U.; Nekvinda, J.; Santos, W. L.; Westcott, S. A.; Steel, P. G.; Marder, T. B. *Chem. Rev.* **2021**, *121*, 13238-13341; (b) Mkhaliid, I. A. I.; Barnard, J. H.; Marder, T. B.; Murphy, J. M.; Hartwig, J. F. *Chem. Rev.* **2010**, *110*, 890-931; (c) Tian, Y.-M.; Guo, X.-N.; Braunschweig, H.; Radius, U.; Marder, T. B. *Chem. Rev.* **2021**, *121*, 3561-3597.
68. (a) Fontaine, F.-G.; Rochette, É. *Acc. Chem. Res.* **2018**, *51*, 454-464; (b) Guo, J.; Cheng, Z.; Chen, J.; Chen, X.; Lu, Z. *Acc. Chem. Res.* **2021**, *54*, 2701-2716.
69. Lee, C.-I.; Zhou, J.; Ozerov, O. V. *J. Am. Chem. Soc.* **2013**, *135*, 3560-3566.
-

-
70. Jaiswal, K.; Groutchik, K.; Bawari, D.; Dobrovetsky, R. *ChemCatChem* **2022**, *14*, e202200004.
71. (a) Kurono, N.; Ohkuma, T. *ACS Catal.* **2016**, *6*, 989-1023; (b) North, M.; Usanov, D. L.; Young, C. *Chem. Rev.* **2008**, *108*, 5146-5226.
72. (a) Cui, X.; Xu, M.-C.; Zhang, L.-J.; Yao, R.-X.; Zhang, X.-M. *Dalton Trans.* **2015**, *44*, 12711-12716; (b) Harinath, A.; Bhattacharjee, J.; Nayek, H. P.; Panda, T. K. *Dalton Trans.* **2018**, *47*, 12613-12622; (c) Khuntia, A. P.; Sarkar, N.; Patro, A. G.; Sahoo, R. K.; Nembenna, S. *Eur. J. Inorg. Chem.* **2022**, *2022*, e202200209; (d) Pahar, S.; Kundu, G.; Sen, S. S. *ACS Omega* **2020**, *5*, 25477-25484; (e) Saravanan, P.; Anand, R. V.; Singh, V. K. *Tetrahedron Lett.* **1998**, *39*, 3823-3824; (f) Sen, N.; Khan, S. *Chem. Asian J.* **2021**, *16*, 705-719; (g) Wang, W.; Luo, M.; Li, J.; Pullarkat, S. A.; Ma, M. *Chem. Commun.* **2018**, *54*, 3042-3044; (h) Yang, Z.; Yi, Y.; Zhong, M.; De, S.; Mondal, T.; Koley, D.; Ma, X.; Zhang, D.; Roesky, H. W. *Chem. Eur. J.* **2016**, *22*, 6932-6938.
73. Gassman, P. G.; Talley, J. J. *Tetrahedron Lett.* **1978**, *19*, 3773-3776.
74. (a) Rawat, S.; Bhandari, M.; Prashanth, B.; Singh, S. *ChemCatChem* **2020**, *12*, 2407-2411; (b) Sharma, M. K.; Sinhababu, S.; Mukherjee, G.; Rajaraman, G.; Nagendran, S. *Dalton Trans.* **2017**, *46*, 7672-7676.

Chapter 2

Synthesis of Low Oxidation State Zinc(I) Complexes and Their Catalytic Studies in Dehydroborylation of Terminal Alkynes

Published:

Sahoo, R. K.; Rajput, S.; Patro, A. G.; Nembenna, S. *Dalton Trans.* **2022**, 51, 16009-16016.

Abstract

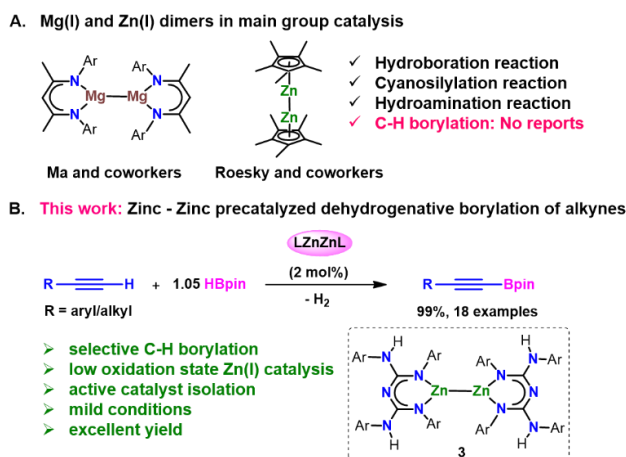
A new example of a structurally characterized conjugated bis-guanidinate (CBG) supported zinc (I) dimer, i.e., LZnZnL (**3**) ($\text{L} = \{(\text{ArNH})(\text{ArN})-\text{C}=\text{N}-\text{C}=(\text{NAr})(\text{NHAr})\}$; $\text{Ar} = 2,6\text{-Et}_2\text{-C}_6\text{H}_3$) with a Zn-Zn bond is reported. Moreover, homoleptic (**3**) and heteroleptic (Cp^*ZnZnL , **2**, ($\text{Cp}^* = 1,2,3,4,5\text{-pentamethyl cyclopentadienide}$)) zinc (I) dimers are used as precatalysts in the dehydroborylation of a wide array of terminal alkynes. Furthermore, the active catalyst, CBG zinc acetylide ($\text{LZn}-\text{C}\equiv\text{C}-\text{Ph}-4\text{-Me}$)₂, (**5**), is isolated and confirmed by X-ray crystal structure analysis. A series of stoichiometric experiments have been performed to propose a plausible reaction mechanism.

2.1. Introduction

The syntheses of low oxidation state metal-metal bonded complexes have attracted interest in several areas of chemical science due to their unique properties.¹ In 2004, Carmona and coworkers reported the first covalent zinc-zinc bonded complex Cp^*_2Zn_2 ($\text{Cp}^* = 1,2,3,4,5\text{-pentamethyl cyclopentadienide}$).² Later, synthesis and reactivity studies of low-oxidation state zinc complexes with Zn-Zn bonds showed progress.³ In 2007, Jones and coworkers reported the first example of β -diketiminato stabilized magnesium(I) dimer with an Mg-Mg bond.⁴ There are few reports concerning low oxidation state metal-metal bonded Zn(I) and Mg(I) dimers in catalysis. In 2018, Ma and coworkers reported that an Mg(I) dimer, i.e., $(^{\text{Xyl}}\text{NacnacMg})_2$, pre-catalyzed the cyanosilylation of ketones.⁵ Afterward, the same group reported the hydroboration of carbonyl

compounds such as aldehydes, ketones, esters, carbonates, CO₂, and epoxides using Mg(I) dimers as pre-catalysts.⁶ Further, Ma and coworkers described unsymmetrical β -diketimate Mg(I) dimers as pre-catalysts for the hydroboration of alkynes and nitriles.⁷ Although mechanisms are unclear, presumably, L'MgH is active species in such hydroboration reactions.⁸

Likewise, a few examples of low oxidation state zinc (I) complexes in catalysis are known. In 2011, Roesky and coworkers demonstrated Cp*₂Zn₂ as a catalyst for the hydroamination reaction for the first time.⁹ Later, the authors compared the catalytic efficiency of Cp*₂Zn₂ with those of Cp*₂Zn and commercially available ZnEt₂ in hydroamination reactions (Scheme 2.1.A).¹⁰ To explore the catalytic activity of the Zn(I) compound, herein, we investigated the Zn(I) pre-catalyzed dehydroborylation of terminal alkynes for the first time. Organoboranes are in high demand because of their wide range of applications in many chemical transformations and provide valuable intermediates in medicinal and organic chemistry.¹¹



Scheme 2.1. Low oxidation state metal complexes with M-M bond in catalysis.

Compared to the well-established hydroboration of alkynes,^{8, 12} there are few reports on selective dehydroborylation of terminal alkynes using transition¹³ and main group¹⁴ metal catalysts. As Earth-abundant, less toxic, and cheaper zinc catalysis is concerned, there have been a few examples

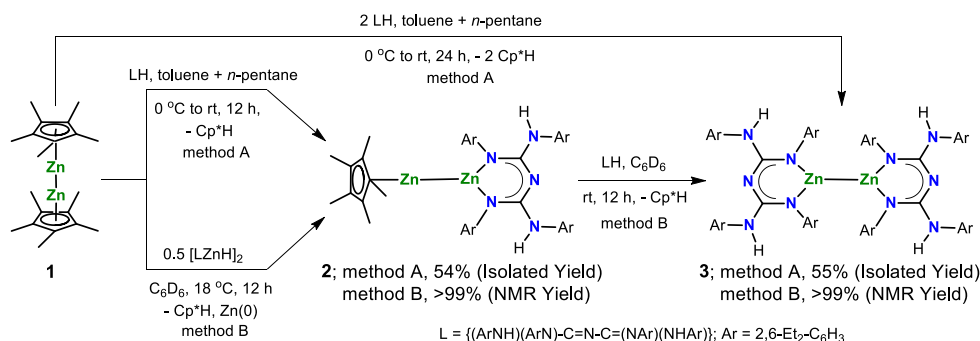
of dehydrogenative borylation of alkynes; however, these procedures suffer from low selectivity, extra additives, solvent use, and high catalyst loadings.¹⁵ Thus, designing a new example of a Zn(I) complex and applying it in catalysis under mild conditions are highly attractive.

Herein, we report new examples of Zn(I) dimers and their catalytic studies in the C-H borylation of terminal alkynes. (Scheme 2.1.B). Actually, zinc(I) complexes are used as precatalysts in this investigation; however, the actual catalyst is a zinc(II) complex, which is in line with earlier Zn(II)¹⁵ and Mg(I)⁵⁻⁸ catalysis.

2.2. Results and Discussion

Recently, we have introduced a β -diketiminato analogue, conjugated bis-guanidine (CBG) and its coordination chemistry, and CBG metal complexes in catalysis.^{12b, 16} The synthesis of zinc(I) dimers is well-established; however, the application of zinc(I)-dimers in catalysis is scarce.^{3a} Thus, we aimed to synthesize a new class of zinc(I) complexes and study their catalytic application in the C-H borylation of terminal alkynes. Complex (**2**) can be synthesized in two ways. The reaction of Cp^*_2Zn_2 ($\text{Cp}^* = 1,2,3,4,5\text{-pentamethyl cyclopentadienide}$) with 1.0 equiv. of the CBG ligand (LH ($\text{L} = \{(\text{ArNH})(\text{ArN})\text{-C=N-C=(NAr)(NHAr)}\}$; $\text{Ar} = 2,6\text{-Et}_2\text{-C}_6\text{H}_3$)) in a mixture of toluene and *n*-pentane at 0 °C to room temperature for 12 h afforded the heteroleptic complex Cp^*ZnZnL in 54% isolated yield (method A). Alternatively, a reaction between Cp^*_2Zn_2 and 0.5 equiv. of $[\text{LZnH}]_2$ at 18 °C for 12 h in C_6D_6 resulted in the formation of Cp^*ZnZnL (**2**) in 99% NMR yield (method B). The ^1H and $^{13}\text{C}\{^1\text{H}\}$ NMR and HRMS studies confirm the formation of compound **2**. The ^1H NMR spectra indicate the production of compound **2** by the disappearance of the N-*H*...N *proton* of the free ligand (LH) (12.96 ppm) or the LZnH (5.00 ppm) peak. A new characteristic peak for the backbone NH moiety of compound **2** was observed at 4.92 ppm.

The homoleptic compound **3** can be synthesized by adding 2 equiv. of LH to Cp^*_2Zn_2 (method A, 55% isolated yield) or adding of 1.0 equiv. of LH to compound **2** (method B, >99% NMR yield). Moreover, compound **3** was confirmed by NMR, HRMS, and single-crystal X-ray diffraction studies. The appearance of a characteristic peak at 4.80 ppm corresponds to the backbone Ar-NH of compound **3**, and the complete disappearance of the more acidic proton of LH (12.96 ppm)^{16a} indicates the formation of compound **3**.



Scheme 2.2. Synthesis of zinc-zinc bonded complexes **2** and **3**.

Single crystals of compound **3** suitable for X-ray diffraction were grown from benzene solution at room temperature within 3 days. Compound **3** crystallizes in the monoclinic system with the $C2/c$ space group (Scheme 2.2). The Zn1-Zn1' bond distance of compound **3** (2.4072(3) Å) is longer than those of previously reported zinc (I) dimers ($^{\text{Dipp}}\text{NacnacZn}$)₂^{3d} (2.3586(7) Å) and ($^{\text{Mes}}\text{NacnacZn}$)₂^{3e} (2.3813(8) Å). The Zn-N bond distances for compound **3**, i.e., Zn1-N1 2.0021(12) Å and Zn1-N2 2.0035(13) Å, are in good agreement with the previously reported Zn-N bond distances of the ($^{\text{Dipp}}\text{NacnacZn}$)₂^{3d} (Zn1-N1 2.005(3), Zn1-N2 2.013(3) Å) and ($^{\text{Mes}}\text{NacnacZn}$)₂^{3e} (Zn1-N1 2.005(2), Zn1-N2 2.000(3) Å) complexes. Nevertheless, the N1-Zn1-N2 bite angle of complex **3** (91.08(5)°), which is acute compared to the bite angles of ($^{\text{Dipp}}\text{NacnacZn}$)₂ (93.65(13)°) and ($^{\text{Mes}}\text{NacnacZn}$)₂ (93.8(2)°) (*vide infra*, Fig. 2.2, left).

The sequential formation of compounds **2** and **3** was evaluated by *in situ* recording the ^1H NMR spectra of a reaction of Cp^*_2Zn_2 and LH at 1:2 molar ratio from 18 °C to room temperature up to 24 h. Initially, the formation of compound **2** was confirmed by the appearance of a characteristic downfield peak (NH) at 4.92 ppm. After 12 h, a characteristic peak at 4.80 ppm emerged, corresponding to the backbone ArN-*H* resonance of compound **3**. Finally, an exclusive formation of compound **3** was observed, as shown in Fig. 2.1.

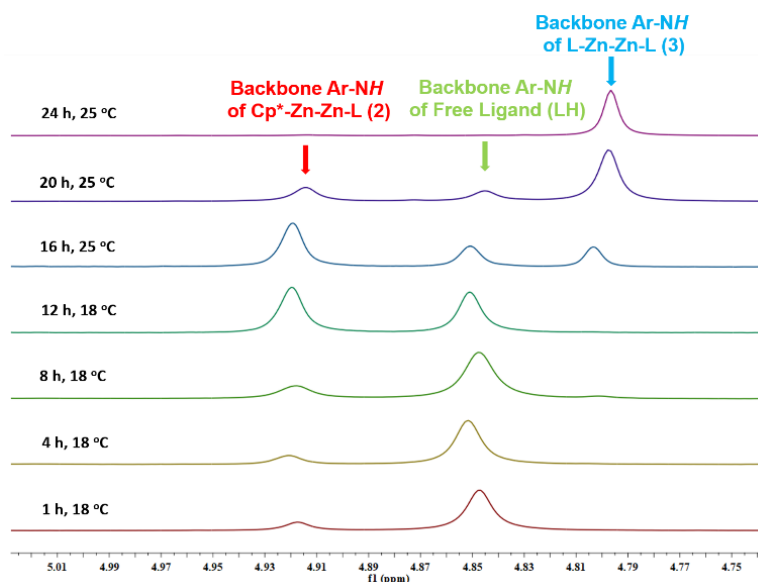


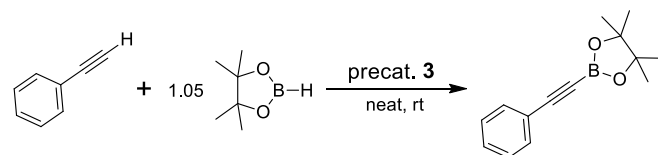
Figure 2.1. Annotated ^1H NMR stack plot of the reaction between Cp^*_2Zn_2 and 2.0 equiv. of LH.

Next, we explored the catalytic study of newly synthesized CBG zinc(I) dimers in the C-H borylation of terminal alkynes. We chose phenylacetylene as a model substrate. The reaction of phenylacetylene and pinacolborane (HBpin) with 10 mol% precatalyst **3** afforded a quantitative amount of the dehydroborylated product **7a** after 12 h at room temperature (Table 2.1, entry 2).

Further lowering the precatalyst loading from 10 to 2 mol% and shortening the reaction time from 12 to 6 h resulted in no change in the yield. In the absence of precatalyst **3**, the reaction of phenylacetylene with HBpin did not afford the alkynyl borate product at rt after 6 h. The optimization table suggests that all compounds (**1**, **2**, and **3**) show high catalytic

efficiency under mild conditions, whereas compounds **2** and **3** show slightly better selectivity than compound **1**.

Table 2.1. Optimization of compound **3** pre-catalyzed dehydroborylation of phenylacetylene^a



Entry	Pre-cat.	mol %	Time (h)	Conv. (%)
1	---	No catalyst	6	0
2	3	10	12	99
3	3	5	12	99
4	3	3	12	99
5	3	2	12	99
6	3	2	6	99
7	1	2	6	95
8	2	2	6	99

^a Reaction conditions: Terminal alkynes (0.3 mmol, 1.0 equiv.), pinacolborane (0.315 mmol, 1.05 equiv.), precatalyst **3** (2 mol%), 6 h at r.t under N₂. The NMR yield was determined by ¹H and ¹³C{¹H} NMR spectroscopy based on alkyne consumption and the appearance of the Bpin peak confirmed the product.

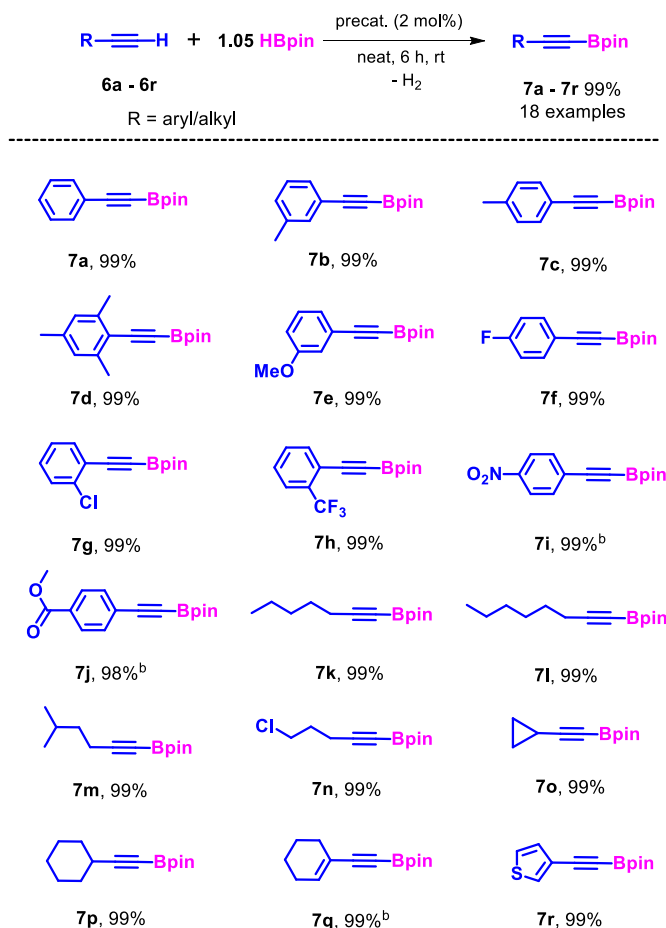
Under the optimized conditions, we investigated a broad range of terminal alkynes, including electron-donating (**6a-6e**) and withdrawing substituents (**6f-6j**), long-chain (**6k-6n**) and cyclic alkynes (**6o-6q**), and heterocyclic system (**6r**). All products **7a-7r** were characterized by ¹H and ¹³C{¹H} NMR spectroscopic methods (Table 2.2).

We performed stoichiometric experiments to understand the mechanism for terminal alkyne's Zn(I) precatalyzed dehydrogenative borylation. In the initial stage, a reaction of compound **2** with 1.0 equiv. 4-ethynyltoluene (**6c**) in toluene resulted in the formation of CBG zinc acetylide complex **5** after 6 h at 70 °C (Scheme 2.3(i)). Alternatively, the CBG zinc acetylide complex can be synthesized by the reaction of compound **3** with 2 equiv. of 4-ethynyltoluene (**6c**) at 80 °C for 36 h in toluene (Scheme 2.3(ii)). The active catalyst **5** was confirmed by NMR, HRMS, and single-crystal X-ray diffraction analysis. The NMR spectra show the formation of product **5** by the complete disappearance of the alkynyl

proton ($-\text{C}\equiv\text{CH}$) of compound **6c** and downfield shifting of the backbone Ar-NH moiety from 4.92 ppm of compound **2** or 4.80 ppm of compound **3** to 5.04 ppm.

Furthermore, a solution of compound **5** in toluene was kept at $-20\text{ }^{\circ}\text{C}$, and we noticed the formation of single crystals after 24 h. The CBG zinc acetylide is dimeric, in which each zinc atom is distorted tetrahedral and attached to two N atoms of the CBG ligand, and the other two sites are occupied by the C atoms of bridged acetylene moieties.

Table 2.2. Dehydrogenative borylation of terminal alkynes precatalyzed by compound **3**^a



^a Reaction conditions: Terminal alkynes (0.3 mmol, 1.0 equiv.), pinacolborane (0.315 mmol, 1.05 equiv.), precatalyst **3** (2 mol%), at r.t. under N_2 . ^bFor **6i**, **6j**, and **6q**, NMR yields were determined by ^1H NMR spectroscopy using mesitylene as an internal standard. The NMR yield was determined by ^1H and $^{13}\text{C}\{^1\text{H}\}$ NMR spectroscopy based on alkyne consumption and the appearance of the Bpin peak confirmed the product.

The bond distance of Zn1-C1, 2.0181(15) Å in compound **5** is longer than those of Ingleson's NHC Zn-bis-alkynyl complex,^{15b} Zn-C = 1.969(4) and 1.959(4) Å, and Yang's N,N'-Zn alkynyl complex,¹⁷ Zn1-C1 1.970(4) Å. However, the C1-C2 bond length, 1.187(2) Å, is comparable with NHC Zn-bis alkynyl complex^{15b} (1.197(4) and 1.179(4) Å) and shorter than that of the N, N'-Zn alkynyl complex¹⁷ (1.213(5) Å) (Fig. 2.2, right). We presume that the above two bond parameters suggest that compound **5** is more active and selective than the N,N'-Zn alkynyl complex to afford alkynyl boronates. Afterward, the zinc alkynyl complex **5** was treated with 2.0 equiv. of HBpin which undergoes σ -bond metathesis to produce the dehydroborylation product **7c** and complex **4** with 25 % conversion observed by ¹H and ¹¹B NMR studies.

The ¹H and ¹¹B NMR spectra confirm the formation of product **7c** by the generation of new characteristic peaks at 1.02 and 24.5 ppm corresponding to the *Bpin* moiety of **7c**. After heating the reaction mixture at 80 °C for 12 h no change was observed in the equilibrium position (Scheme 2.3(iii)).

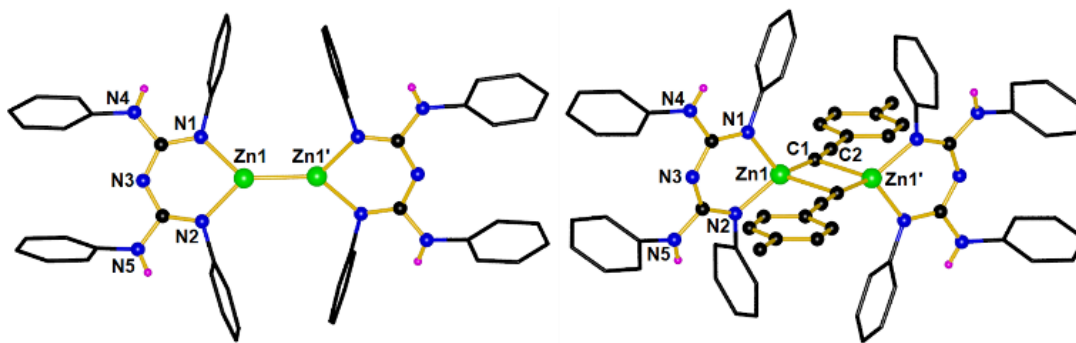
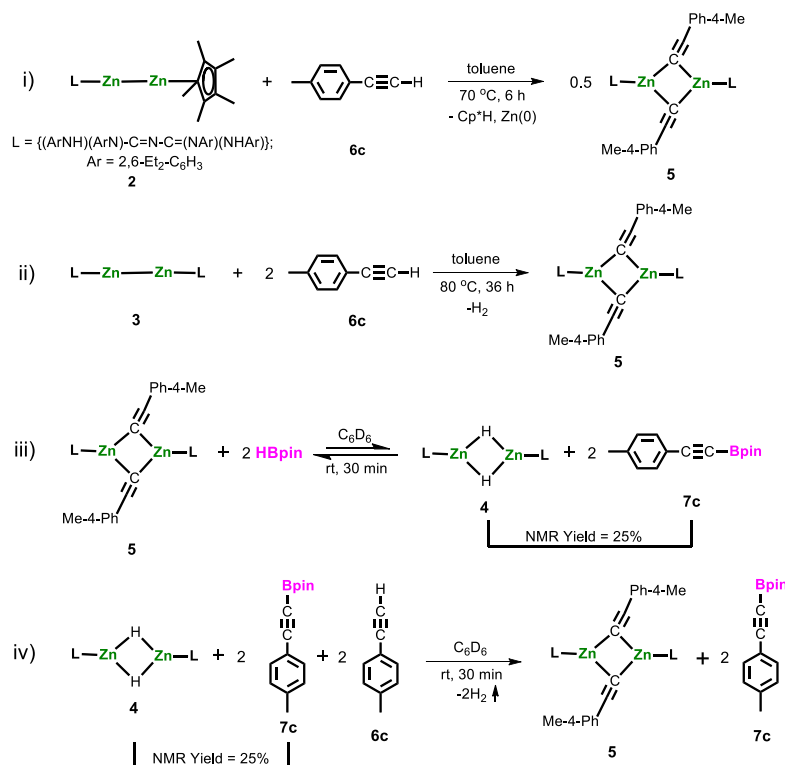


Figure 2.2. Molecular structures of **3** (left) and **5** (right). All the hydrogen atoms (except for H(4), H(5)), and ethyl groups have been removed for clarity. Selected bond lengths (Å) and angles (°), For **3**: Zn1-Zn1' 2.4072(3), Zn1-N1 2.0021(12), Zn1-N2 2.0035(13); N1-Zn1-N2 91.08(5), N1-Zn1- Zn1' 134.92(4), N2-Zn1- Zn1' 134.00(4). For **5**: Zn1-Zn1' 3.0400(4), Zn1-N1 1.9709(13), Zn1-N2 1.9663(13), Zn1-C1 2.0181(15), Zn1-C1' 2.3360(16), C1-C2 1.187(2); N1-Zn1-N2 94.76(5), N1-Zn1-C1 119.73(6), N2-Zn1-C1 122.42(6), C1-Zn1-C1' 91.75(6), Zn1-C1-Zn1' 88.25(6).

Finally, two equiv. of 4-ethynyltoluene are added to the reaction mixture containing a solution of compounds **4** and **7c** with 25% conversion in C_6D_6 after 30 min indicating the complete formation of product **7c** and the rebirth of catalyst **5** (Scheme 2.3(iv)). The multinuclear magnetic resonance spectra confirm the quantitative formation of product **7c** and compound **5** by the appearance of the corresponding new characteristic peaks at 1.02 (the *Bpin* moiety of **7c**) and 5.04 ppm (the backbone Ar-NH moiety of compound **5**), respectively (Scheme 2.3).

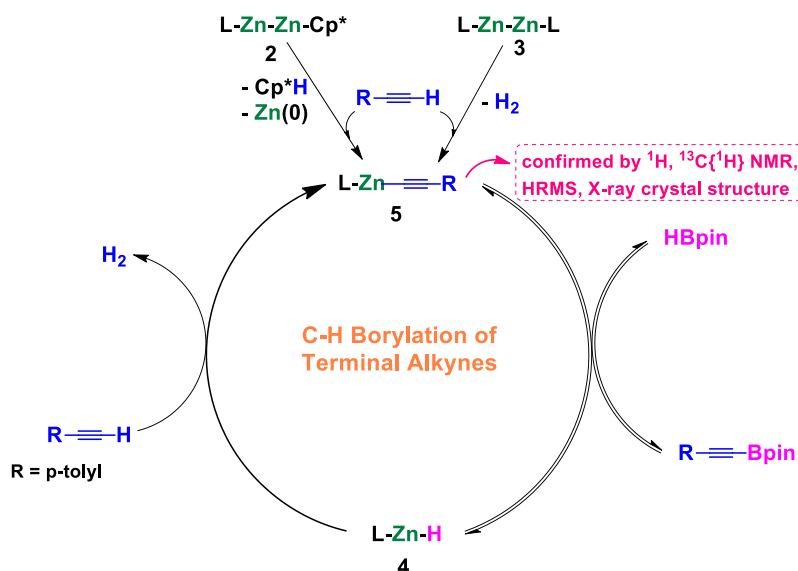
A plausible reaction mechanism for the zinc(I) precatalyzed selective dehydrogenative borylation of terminal alkynes to alkynyl borates has been investigated based on the stoichiometric experiments and active catalyst isolation.



Scheme 2.3. Stoichiometric experiments.

In the first step, compound **2** reacts with the terminal alkyne affording active catalyst **5** by a disproportionation reaction by eliminating $Zn(0)$ and Cp^*H . Alternatively, the zinc acetylide (**5**)

can be synthesized by the reaction between compound **3** and 4-ethynyltoluene, liberating H₂ gas.^{3g} Next, complex **5** reacts with HBpin, giving the complex LZnH (**4**) and alkynyl borate in an equilibrium position *via* Zn-C/B-H σ -bond metathesis. Finally, compound **4**, treated with another molecule of the terminal alkyne, stops the equilibrium reaction between compound **5** and **7c** and produces a quantitative amount of the corresponding alkynyl borate product (**7c**) along with the recovery of the active catalyst (**5**), and closes the catalytic cycle (Scheme 2.4).



Scheme 2.4. Proposed mechanism for the dehydroborylation of terminal alkynes.

2.3. Conclusion

In summary, this protocol adds a new example to the small class of structurally characterized low oxidation state zinc complexes with Zn-Zn bonds. The homoleptic precatalyst **3** shows exceptional selective catalytic performance for the C-H borylation of terminal alkynes under mild conditions. The mechanism is established depending on the active catalyst isolation and stoichiometric experiments. The active catalyst CBG zinc acetylide (**5**) is characterized by NMR, HRMS, and X-ray crystal studies. Moreover, applying zinc(I) dimers in homogenous catalysis could provide insights to synthetic chemists to help design M-M bonded catalysts for organic transformations. Currently, the reactivity and catalytic studies of CBG zinc (I) are ongoing in our laboratory.

2.4. Experimental Section

General procedures

Unless stated, manipulations were performed under a dinitrogen atmosphere using standard glovebox and Schlenk techniques. NMR spectra were recorded on Jeol-400 MHz spectrometer and Bruker NMR spectrometers at 400 MHz (^1H), 101 MHz ($^{13}\text{C}\{^1\text{H}\}$), and 128.36 MHz (^{11}B). ^1H NMR and $^{13}\text{C}\{^1\text{H}\}$ NMR chemical shifts are referenced to residual protons or carbons in the deuterated solvent. ^{11}B were calibrated using an external reference of $\text{BF}_3\cdot\text{Et}_2\text{O}$. Multiplicities are reported as singlet (s), doublet (d), triplet (t), quartet (q), and multiplet (m). Chemical shifts are reported in ppm. Coupling constants are reported in Hz. The crystal data were collected on a Rigaku Oxford diffractometer at 100 K. Selected data collection parameters, and other crystallographic results are summarized in Table 2.3. Mass spectrometry analyses were carried out on Bruker micrOTOF-Q II and Waters XevoG2 XS Q-TOF mass spectrometers. The melting points of compounds **2**, **3**, and **5** were measured using Stuart SMP 10 instrument.

Materials:

Solvents were purified by distillation over Na/ benzophenone. Deuterated chloroform (CDCl_3) was dried on molecular sieves, and benzene- d_6 (C_6D_6) was dried over Na/K alloy and distilled. The ligand L(3H) ($\text{L} = \{(\text{ArNH})(\text{ArNH})-\text{C}=\text{N}-\text{C}=(\text{NAr})(\text{NHAr})\}$; $\text{Ar} = 2,6\text{-Et}_2\text{-C}_6\text{H}_3$)]^{16a-c} and $\text{Cp}^*_2\text{Zn}^{2+}$ are prepared according to reported literature procedures. For catalysis reactions, sealed reaction vials or J. Young valve-sealed NMR tubes were properly oven-dried before being used. Chemicals and reagents were purchased from Sigma-Aldrich Co. Ltd., Merck India Pvt. Ltd., and TCI chemicals were used without purification.

2.4.1. Stoichiometric Experiments

Synthesis of compound (2) {NMR scale}

A solution of Cp^*_2Zn_2 (0.015 g, 25 °C, 0.037 mmol) in C_6D_6 taken in a J. Young valve NMR tube was treated with LH (0.023 g, 0.037 mmol) at 18 °C after 12 h which resulted in the formation of compound **2** with the elimination of Cp^*H as observed by ^1H NMR spectroscopy. Alternatively, compound **2** was synthesized in a J. Young valve NMR tube containing a solution of Cp^*_2Zn_2 (0.020 g, 25 °C, 0.05 mmol) in C_6D_6 was treated with $[\text{LZnH}]_2$ (0.035 g, 0.025 mmol), at 18 °C for 12 h with the elimination of Cp^*H and $\text{Zn}(0)$ as characterized by NMR spectroscopy.

Reaction scale:

Diethyl^lCBGH (0.35 g, 0.55 mmol) dissolved in 10 mL of toluene was added at 0 °C to a solution of (0.22 g, 0.55 mmol) of Cp^*_2Zn_2 in 5 mL of *n*-pentane and the mixture stirred for 5 h at 0 °C, followed by 7 h at room temperature. The solvent was removed in a vacuum resulting in a pale yellow solid compound and dried thoroughly. The resultant solid was dissolved in 10 mL toluene and filtered. The filtrate was concentrated, yielding **2** as a pale yellow solid. (0.265 g, 54 %); m.p. 170-180 °C. ^1H NMR (400 MHz, C_6D_6) δ 7.13 – 7.07 (m, 6H), 6.90 (t, J = 6.8 Hz, 2H), 6.66 – 6.64 (m, 4H), 4.92 (s, 2H), 3.05 – 2.96 (m, 4H), 2.69 – 2.59 (m, 4H), 2.41 – 2.31 (m, 4H), 2.21 – 2.12 (m, 4H), 1.93 (s, 15H), 1.32 (t, J = 6.8 Hz, 12H), 0.96 (t, J = 6.7 Hz, 12H). $^{13}\text{C}\{^1\text{H}\}$ NMR (101 MHz, C_6D_6) δ 156.4, 142.9, 141.1, 138.8, 135.3, 126.5, 126.2, 125.4, 125.2, 107.9, 24.9, 24.4, 14.8, 14.2, 9.9. HRMS (ASAP/Q-TOF) m/z : $[\text{M}]^+$ Calcd for $\text{C}_{52}\text{H}_{69}\text{N}_5\text{Zn}_2$ 893.4136, Found: 893.4119.

Synthesis of precatalyst (3) {NMR scale}

A solution of compound **2** (0.037 mmol) in C_6D_6 taken in a J. Young valve NMR tube was treated with LH (0.023 g, 0.037 mmol) at room temperature for 12 h, resulting in the

formation of compound **3** with the elimination of Cp*H as observed by ^1H NMR spectroscopy.

Reaction scale:

Alternatively, (0.35 g, 0.55 mmol) of $^{\text{Diethyl}}$ CBGH dissolved in 10 mL of toluene was added at 0 °C to a solution of (0.11 g, 0.28 mmol) Cp^*_2Zn_2 in 5 mL of *n*-pentane and the mixture was stirred for 6 h at 0 °C, followed by 18 h at room temperature. The solvent was removed in a vacuum resulting in a white solid compound and dried thoroughly. The resultant solid was dissolved in benzene, filtered, and stored at room temperature, giving block-shaped colorless crystals suitable for single crystal X-ray diffraction within 3 days. (0.214 g, 55 %); m.p. 210-220 °C. ^1H NMR (400 MHz, C_6D_6) δ 7.14 – 7.03 (m, 12H), 6.87 – 6.85 (d, J = 6.9 Hz, 4H), 6.63 – 6.61 (d, J = 7.2 Hz, 8H), 4.80 (s, 4H), 2.76 – 2.61 (m, 8H), 2.51 – 2.46 (m, 8H), 2.35 – 2.30 (m, 8H), 2.15 – 2.10 (m, 8H), 1.22 (t, J = 6.5 Hz, 24H), 0.92 (t, J = 6.6 Hz, 24H). $^{13}\text{C}\{^1\text{H}\}$ NMR (101 MHz, C_6D_6) δ 155.8, 144.2, 141.0, 138.2, 135.6, 125.9, 125.2, 125.1, 124.7, 24.8, 23.8, 14.2, 13.3. HRMS (ASAP/Q-TOF) m/z : $[\text{M}]^+$ Calcd for $\text{C}_{42}\text{H}_{54}\text{N}_5\text{Zn}$ 692.3671, Found: 692.3593.

Synthesis of the active catalyst $[\text{LZnCC}(\text{C}_6\text{H}_5\text{-4-Me})_2]$, (5**) {NMR scale}**

A solution of complex **2** (0.020 g, 25 °C, 0.022 mmol) in C_6D_6 taken in a J. Young valve NMR tube was treated with 4-ethynyltoluene (0.022 mmol) and the reaction mixture was heated at 70 °C for 6 h, resulting in the formation of compound **5** with the elimination of Zn(0) and Cp*H as characterized by NMR spectroscopy.

Reaction scale:

42.60 μL (0.34 mmol) of 4-ethynyltoluene in 5 mL of toluene was added to a reaction mixture of complex **2** (0.300 g, 0.34 mmol) in 10 mL of toluene at room temperature

through a cannula transfer. The reaction mixture was heated at 70 °C for 6 h. The resulting reaction mixture containing zinc metal was filtered. The filtrate was concentrated and stored at – 20 °C for 24 h, yielding compound **5** as block-shaped colorless crystals suitable for single crystal X-ray diffraction (0.195 g, 71 %).

An alternative way to the synthesis of the active catalyst [LZnCC(C₆H₅-4-Me)]₂, (5**) {reaction scale}**

36.65 µL (0.29 mmol) of 4-ethynyltoluene in 5 mL of toluene was added to a reaction mixture of complex **3** (0.200 g, 0.14 mmol) in 8 mL of toluene at room temperature through a cannula transfer. The reaction mixture was heated at 80 °C for 36 h. The resulting reaction mixture was concentrated and stored at – 20 °C for 24 h, yielding **5** as a white crystalline solid. (0.180 g, 78 %); m.p. 185 – 190 °C. ¹H NMR (400 MHz, C₆D₆) δ 7.25 – 7.23 (d, *J* = 7.7 Hz, 4H), 7.15 (s, 4H), 7.13 – 7.06 (m, 8H), 6.90 (t, *J* = 7.5 Hz, 4H), 6.69 – 6.67 (d, *J* = 7.5 Hz, 4H), 6.65 – 6.63 (d, *J* = 7.6 Hz, 8H), 5.06 (s, 4H), 3.17 – 3.08 (m, 8H), 2.78 – 2.69 (m, 8H), 2.41 – 2.32 (m, 8H), 2.21 – 2.12 (m, 8H), 1.89 (s, 3H), 1.38 (t, *J* = 7.5 Hz, 24H), 0.95 (t, *J* = 7.6 Hz, 24H). ¹³C{¹H} NMR (101 MHz, C₆D₆) δ 157.5, 142.0, 141.1, 139.0, 136.3, 135.1, 131.9, 128.4, 126.7, 126.3, 125.9, 125.2, 122.7, 100.7, 24.9, 24.3, 20.8, 14.4, 14.2. HRMS (ASAP/Q-TOF) *m/z*: [M + H]⁺ Calcd for C₅₁H₆₂N₅Zn 808.4297, Found: 808.4210.

2.4.2. X-ray Crystallographic Data

The single crystals of compounds **3** and **5** were crystallized from benzene and toluene as colorless blocks. The crystal data of compounds **3** and **5** were collected on a Rigaku Oxford diffractometer at 100 K. Selected data collection parameters and other crystallographic results are summarized in Table 2.3.

Table 2.3. Crystallographic data and refinement parameters for compounds **3** and **5**.

Compound	3	5
Empirical Formula	C ₈₄ H ₁₀₈ N ₁₀ Zn ₂	C ₁₀₂ H ₁₂₂ N ₁₀ Zn ₂
CCDC	2179810	2179805
Molecular mass	1388.54	1618.83
Temperature (K)	100	100
Wavelength (Å)	0.71073	0.71073
Size(mm)	0.2×0.18×0.18	0.2×0.18×0.17
Crystal system	monoclinic	Triclinic
Space group	C2/c	P-1
a (Å)	18.0369(4)	12.89300(10)
b (Å)	16.9127(4)	12.9295(2)
c (Å)	27.6720(6)	14.8009(2)
α (deg)°	90	77.6300(10)
β (deg)°	104.820(2)	71.4150(10)
γ (deg)°	90	71.6870(10)
Volume (Å ³)	8160.6(3)	2202.29(5)
Z	4	1
Calculated density (g/cm ³)	1.130	1.221
Absorption coefficient (mm ⁻¹)	0.635	0.598
F(000)	2968.0	864.0
Theta range for data collection (deg)°	6.64 to 50.694	6.692 to 52.74
Limiting indices	-20 ≤ h ≤ 21, -19 ≤ k ≤ 20, -33 ≤ l ≤ 33	-16 ≤ h ≤ 16, -16 ≤ k ≤ 16, -18 ≤ l ≤ 18
Reflections collected	34530	38471
Independent reflections	7460 [R _{int} = 0.0335, R _{sigma} = 0.0231]	8979 [R _{int} = 0.0343, R _{sigma} = 0.0246]
Completeness to theta	99 %	99 %
Absorption correction	Empirical	Empirical
Data / restraints / parameters	7460 / 0 / 441	8979 / 0 / 517
Goodness – of–fit on F ²	1.057	1.047
Final R indices [I>2 sigma(I)]	R ₁ = 0.0305, wR ₂ = 0.0807	R ₁ = 0.0348, wR ₂ = 0.0936

The structure was determined using direct methods employed in *ShelXT*,²¹ *OleX*,²² and refinement was carried out using least-square minimization implemented in *ShelXL*.²³ All non-hydrogen atoms were refined with anisotropic displacement parameters. Hydrogen atom positions were fixed geometrically in idealized positions and were refined using a riding model.

2.5. Appendix: All general experimental information, stoichiometric reactions, analytical data, and spectral data were available in published paper. *Dalton Trans.* **2022**, *51*, 16009–16016.

2.6. References

1. Schmid, G.; Bäumle, M.; Geerkens, M.; Heim, I.; Osemann C.; Sawitowski, T. *Chem. Soc. Rev.* **1999**, *28*, 179–185.
2. Resa, I.; Carmona, E.; Gutierrez-Puebla E.; Monge, A.; *Science* **2004**, *305*, 1136–1138.
3. (a) Li, T.; Schulz S.; Roesky, P. W.; *Chem. Soc. Rev.* **2012**, *41*, 3759–3771; (b) Nayek, H. P.; Luehl, A.; Schulz, S.; Koeppe R.; Roesky, P. W.; *Chem. Eur. J.* **2011**, *17*, 1773–1777; (c) Li, B.; Huse, K.; Wölper C.; Schulz, S.; *Chem. Commun.* **2021**, *57*, 13692–13695; (d) Wang, Y.; Quillian, B.; Wei, P.; Wang, H.; Yang, X. J.; Xie, Y.; King, R. B.; Schleyer, P. V. R.; Schaefer, H. F.; Robinson, G. H. *J. Am. Chem. Soc.* **2005**, *127*, 11944–11945; (e) Schulz, S.; Schuchmann, D.; Westphal U.; Bolte, M. *Organometallics* **2009**, *28*, 1590–1592; (f) Schulz, S.; Gondzik, S.; Schuchmann, D.; Westphal, U.; Dobrzycki, L.; Boese, R.; Harder, S.; *Chem. Commun.* **2010**, *46*, 7757–7759; (g) Fedushkin, I. L. ; Eremenko, O. V.; Skatova, A. A.; Piskunov, A. V.; Fukin, G. K.; Ketkov, S. Y.; Irran E.; Schumann, H. *Organometallics* **2009**, *28*, 3863–3868.
4. Green, S. P.; Jones, C.; Stasch, A. *Science* **2007**, *318*, 1754–1757.

-
5. Wang, W.; Luo, M.; Li, J.; Pullarkat, S. A.; Ma, M. *Chem. Commun.* **2018**, *54*, 3042–3044.
 6. (a) Cao, X.; Wang, W.; Lu, K.; Yao, W.; Xue, F.; Ma, M. *Dalton Trans.* **2020**, *49*, 2776–2780; (b) Cao, X.; Li, J.; Zhu, A.; Su, F.; Yao, W.; Xue, F.; Ma, M. *Org. Chem. Front.* **2020**, *7*, 3625–3632.
 7. Li, J.; Luo, M.; Sheng, X.; Hua, H.; Yao, W.; Pullarkat, S. A.; Xu, L.; Ma, M. *Org. Chem. Front.* **2018**, *5*, 3538–3547.
 8. Jones, D. D. L.; Matthews, A. J. R.; Jones, C. *Dalton Trans.* **2019**, *48*, 5785–5792.
 9. Luehl, A.; Nayek, H. P.; Blechert, S.; Roesky, P. W. *Chem. Commun.* **2011**, *47*, 8280–8282.
 10. Luehl, A.; Hartenstein, L.; Blechert, S.; Roesky, P. W. *Organometallics* **2012**, *31*, 7109–7116.
 11. (a) Suzuki, A. *Angew. Chem., Int. Ed.* **2011**, *50*, 6722–6737; (b) Lennox, A. J. J.; Lloyd-Jones, G. C. *Chem. Soc. Rev.* **2014**, *43*, 412–443; (c) Hartwig, J. F. *Acc. Chem. Res.* **2012**, *45*, 864–873; (d) Pécharman, A.-F.; Colebatch, A. L.; Hill, M. S.; McMullin, C. L.; Mahon, M. F.; Weetman, C. *Nature Commun.* **2017**, *8*, 15022.
 12. (a) Fontaine, F.-G.; Rochette, É. *Acc. Chem. Res.* **2018**, *51*, 454–464; (b) Sarkar, N.; Bera, S.; Nembenna, S. *J. Org. Chem.* **2020**, *85*, 4999–5009; (c) Mandal, S.; Mandal, S.; Geetharani, K. *Chem. Asian J.* **2019**, *14*, 4553–4556; (d) Magre, M.; Maity, B.; Falconnet, A.; Cavallo, L.; Rueping, M. *Angew. Chem., Int. Ed.* **2019**, *58*, 7025–7029; (e) Zhong, M.; Gagné, Y.; Hope, T. O.; Pannecoucke, X.; Frenette, M.; Jubault, P.; Poisson, T. *Angew. Chem. Int. Ed.* **2021**, *60*, 14498–14503; (f) Guo, J.; Cheng, Z.; Chen, J.; Chen, X.; Lu, Z. *Acc. Chem. Res.* **2021**, *54*, 2701–2716.

-
13. (a) Lee, C.-I.; Zhou, J.; Ozerov, O. V. *J. Am. Chem. Soc.* **2013**, *135*, 3560–3566; (b) Romero, E. A.; Jazzar, R.; Bertrand, G. *Chem. Sci.* **2017**, *8*, 165–168; (c) Wei, D.; Carboni, B.; Sortais, J.-B.; Darcel, C. *Adv. Synth. Catal.* **2018**, *360*, 3649–3654.
14. Willcox, D. R.; De Rosa, D. M.; Howley, J.; Levy, A.; Steven, A.; Nichol, G. S.; Morrison, C. A.; Cowley, M. J.; Thomas, S. P. *Angew. Chem. Int. Ed.* **2021**, *60*, 20672–20677.
15. (a) Uzelac, M.; Yuan, K.; Ingleson, M. J. *Organometallics* **2020**, *39*, 1332–1338; (b) Procter, R. J.; Uzelac, M.; Cid, J.; Rushworth, P. J.; Ingleson, M. J.; *ACS Catal.* **2019**, *9*, 5760–5771; (c) Tsuchimoto, T.; Utsugi, H.; Sugiura, T.; Horio, S.; *Adv. Synth. Catal.* **2015**, *357*, 77–82; (d) Luo, M.; Qin, Y.; Chen, X.; Xiao, Q.; Zhao, B.; Yao, W.; Ma, M. *J. Org. Chem.* **2021**, *86*, 16666–16674; (e) Jaiswal, K.; Groutchik, K.; Bawari, D.; Dobrovetsky, R.; *ChemCatChem*, **2022**, *14*, e202200004.
16. (a) Sahoo, R. K.; Sarkar, N.; Nembenna, S. *Angew. Chem. Int. Ed.* **2021**, *60*, 11991–12000; (b) Peddaraao, T.; Baishya, A.; Sarkar, N.; Acharya, R.; Nembenna, S. *Eur. J. Inorg. Chem.* **2021**, 2034–2046; (c) Sahoo, R. K.; Mahato, M.; Jana A.; Nembenna, S. *J. Org. Chem.* **2020**, *85*, 11200–11210; (d) Sarkar, N.; Sahoo, R. K.; Patro A. G.; Nembenna, S. *Polyhedron*, **2022**, *222*, 115902; (e) Peddaraao, T.; Sarkar N.; Nembenna, S. *Inorg. Chem.* **2020**, *59*, 4693–4702.
17. Gao, J.; Li, S.; Zhao, Y.; Wu, B.; Yang, X.-J. *Organometallics* **2012**, *31*, 2978–2985.
18. Hu, J.-R.; Liu, L.-H.; Hu, X.; Ye, H.-D. *Tetrahedron* **2014**, *70*, 5815–5819.
19. Ho, H. E.; Asao, N.; Yamamoto, Y.; Jin, T. *Org. Lett.* **2014**, *16*, 4670–4673.
20. Desrosiers, V.; Garcia, C. Z.; Fontaine, F.-G. *ACS Catal.* **2020**, *10*, 11046–11056.
21. Sheldrick, G. *Acta Crystallogr. C.* **2015**, *71*, 3–8.
-

22. Dolomanov, O. V.; Bourhis, L. J.; Gildea, R. J.; Howard, J. A. K.; Puschmann, H. J. *Appl. Crystallogr.* **2009**, 42, 339-341.
23. (a) Sheldrick, G. M. *Acta Crystallogr., Sect. A: Found. Crystallogr.* **2008**, 64, 112-122; (b) Sheldrick, G. M. *Acta Crystallogr., Sect. A: Found. Adv.* **2015**, 71, 3-8.

NMR spectra

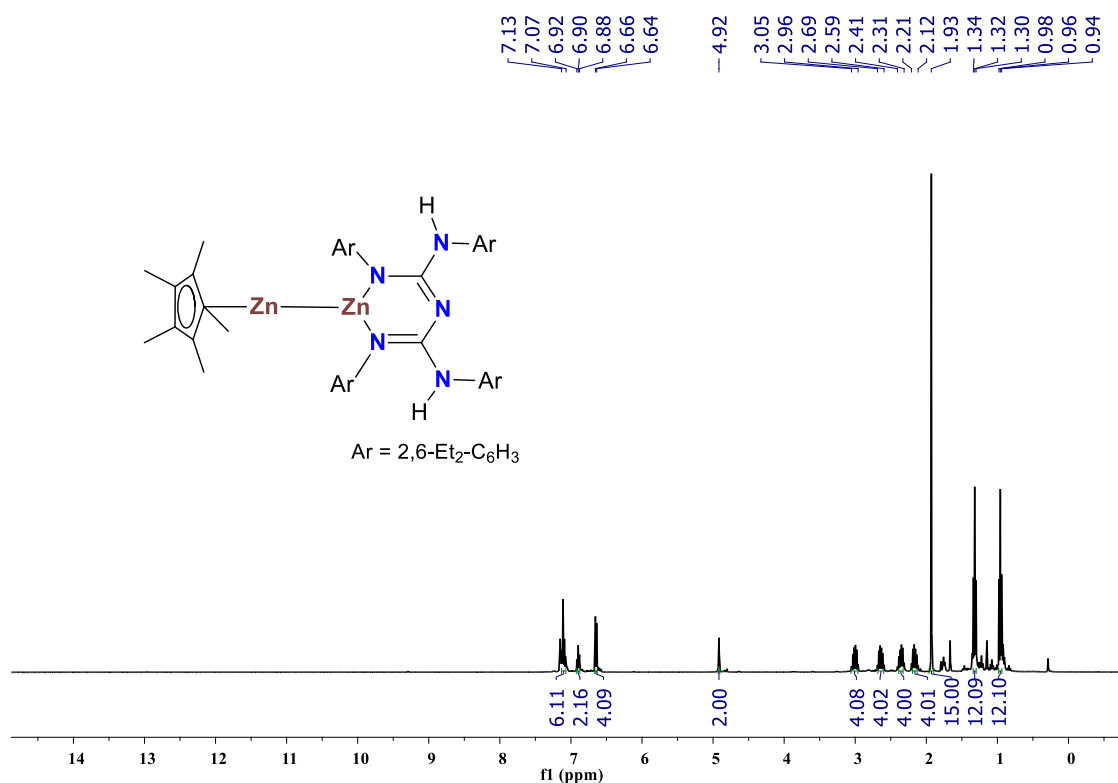


Figure 2.3. ^1H NMR spectrum of compound **2** (400 MHz, CDCl_3) {Reaction scale}.

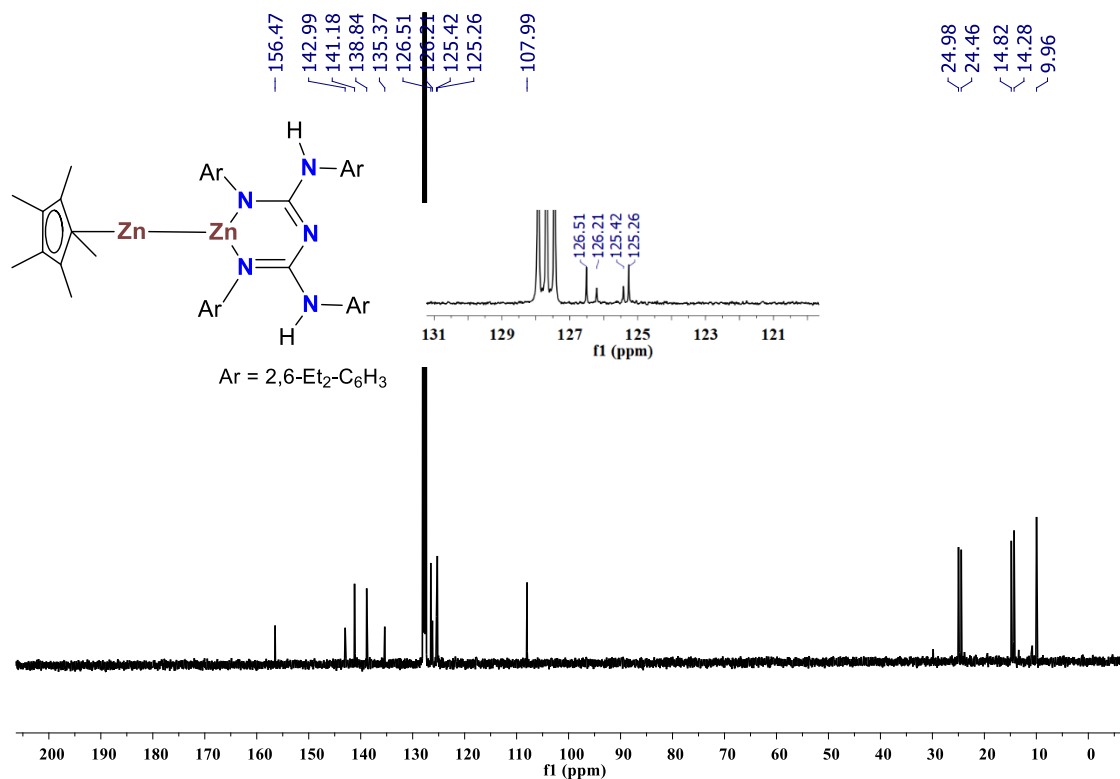


Figure 2.4. $^{13}\text{C}\{^1\text{H}\}$ NMR spectrum of compound **2** (101 MHz, C₆D₆) {Reaction scale}.

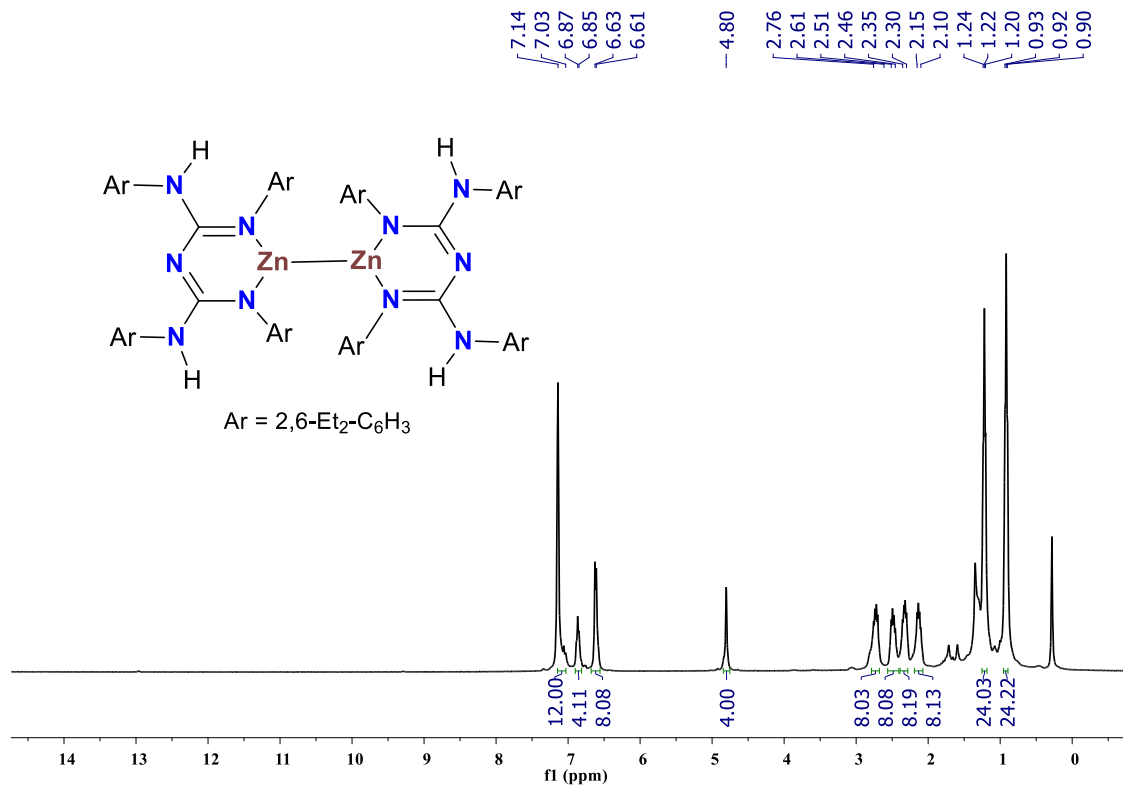


Figure 2.5. ^1H NMR spectrum of compound **3** (400 MHz, C₆D₆) {Reaction scale}.

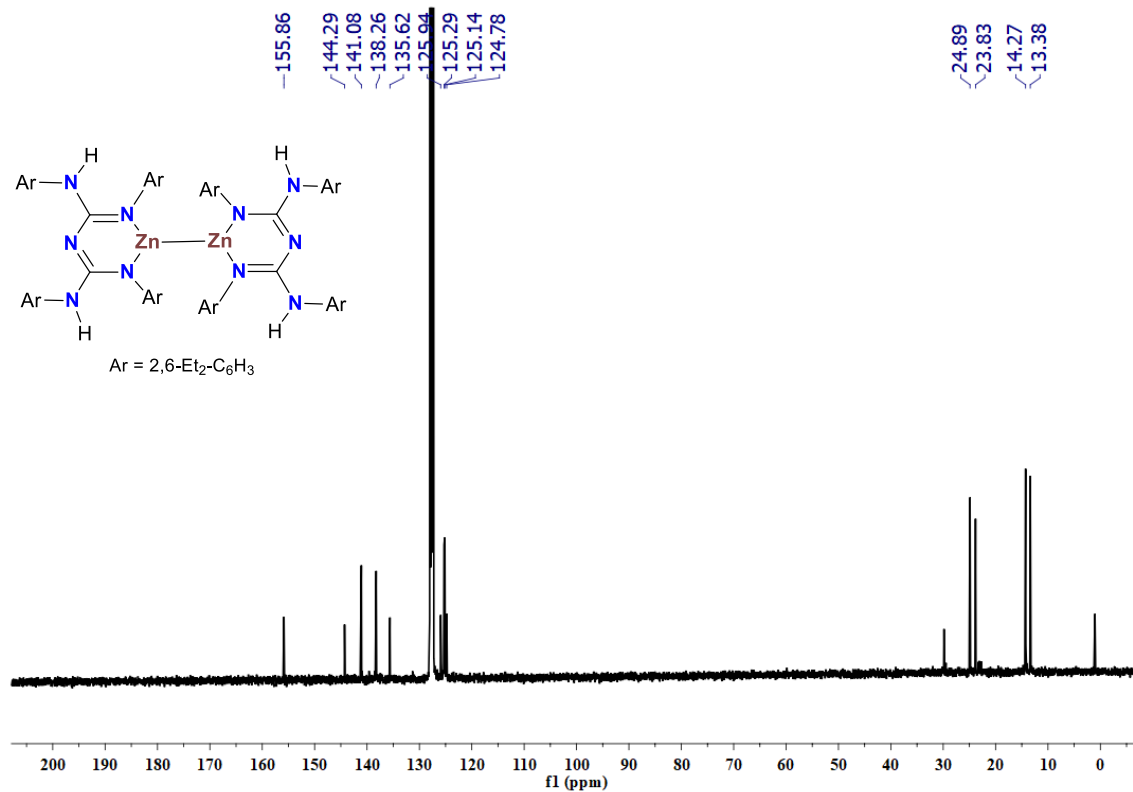


Figure 2.6. ¹³C{¹H} NMR spectrum of compound **3** (101 MHz, C₆D₆) {Reaction scale}.

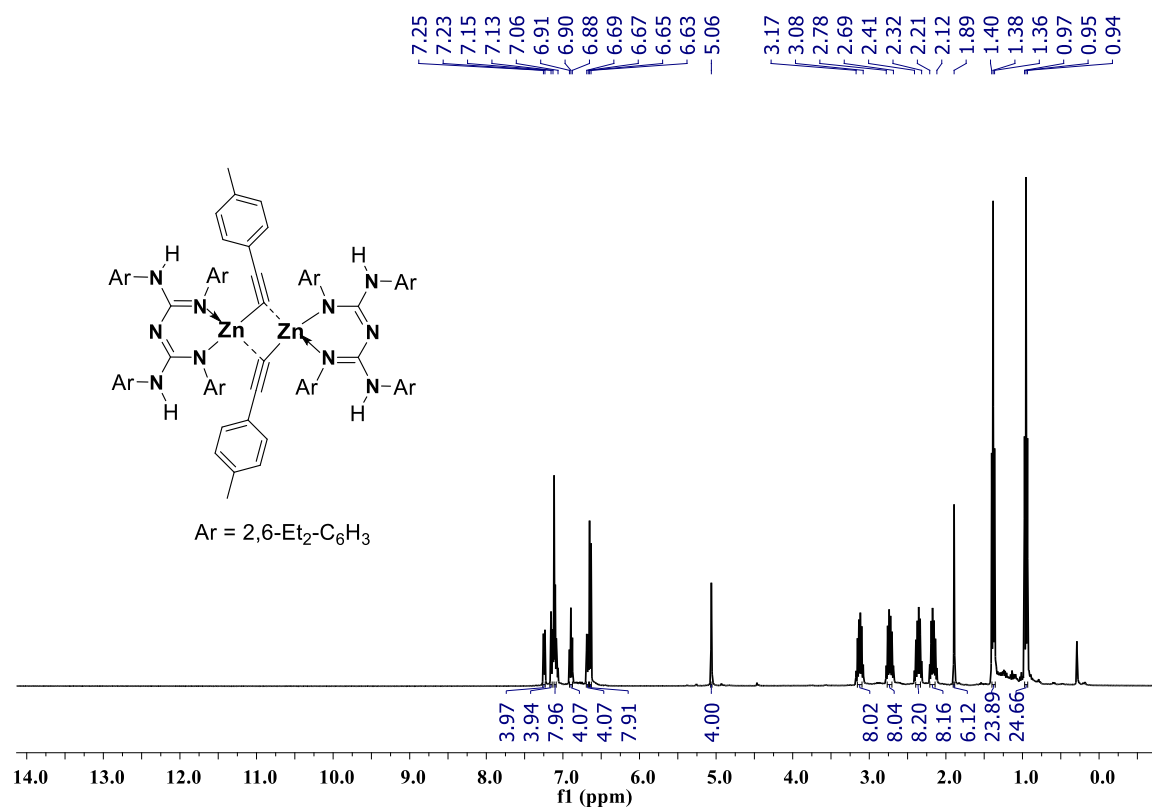


Figure 2.7. ¹H NMR spectrum of compound **5** (400 MHz, C₆D₆).

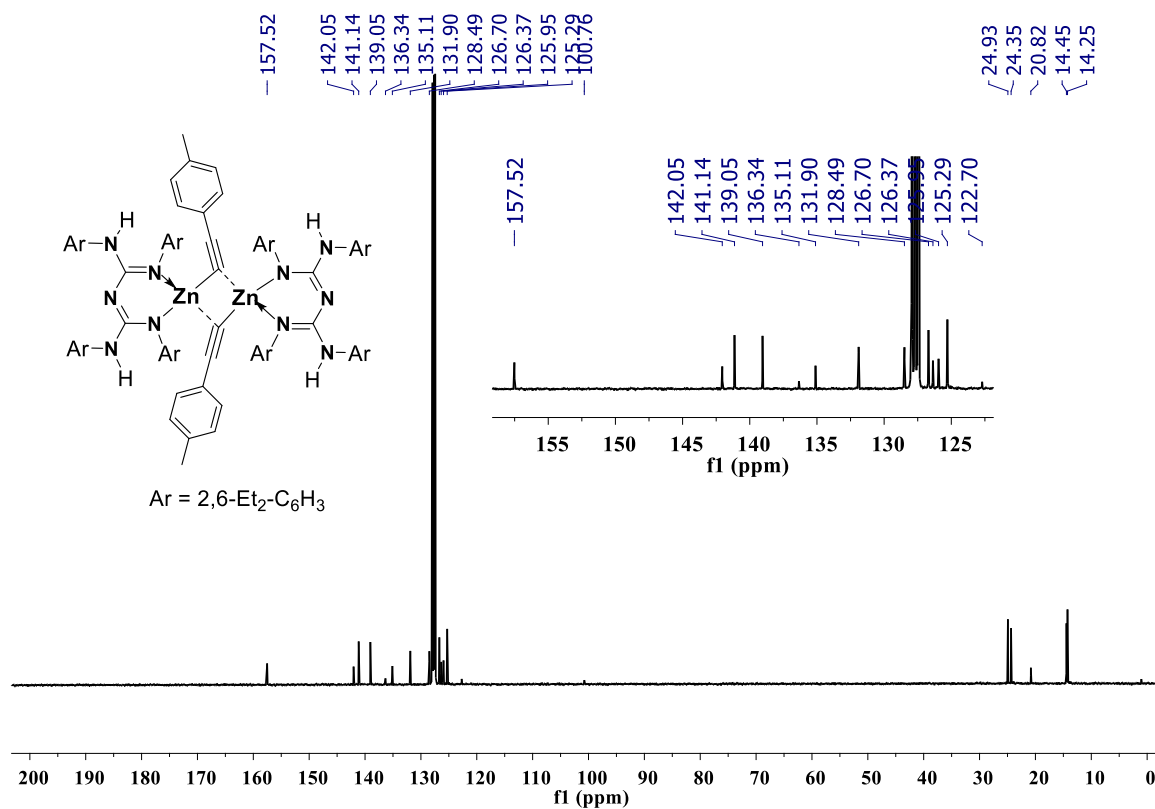


Figure 2.8. $^{13}\text{C}\{^1\text{H}\}$ NMR spectrum of compound **5** (101 MHz, C_6D_6).

Chapter 3A

Zinc Hydride Catalyzed Hydrofunctionalization of Ketones

Published:

Sahoo, R. K.; Mahato, M.; Jana, A.; Nembenna, S. *J. Org. Chem.* **2020**, 85, 11200-11210.

Abstract

Three new dimeric bis-guanidinate zinc(II) alkyl, halide, and hydride complexes [LZnEt]₂ (**1**), [LZnI]₂ (**2**) and [LZnH]₂ (**3**) were prepared. Compound **3** was successfully employed for the hydrosilylation and hydroboration of a vast number of ketones. The catalytic performance of **3** in the hydroboration of acetophenone exhibits a turnover frequency, reaching up to 5800 h⁻¹, outperforming that of reported zinc hydride catalysts. Notably, both intra- and intermolecular chemoselective hydrosilylation and hydroboration reactions have been investigated.

3.A.1. Introduction

The catalytic hydrofunctionalization of ketones with silanes or HBpin is undoubtedly a practical methodology for the syntheses of silyl ethers or borate esters, which are extensively utilized as intermediates for the syntheses of alcohols.¹ The design of inexpensive and sustainable homogenous metal catalysts, particularly, metal hydrides, is very desirable. In this context, an earth-abundant, environmentally friendly, cheaper, and biocompatible zinc² element fits the bill entirely.

In 1947, Schlesinger reported the synthesis of zinc dihydride.³ To date, several synthetic routes are available for the preparation of zinc dihydride⁴ (ZnH₂)_∞, it is a white solid, for which the exact structure is not clear. Moreover, it is thermally unstable and poorly soluble in organic solvents. This motivated many synthetic chemists to prepare neutral heteroleptic zinc hydrides.⁵ Such zinc

hydrides are not only important reducing agents but they can also be model compounds for enzyme mimicking, as precursors in material science and catalysts for various organic transformations.⁶

As far as zinc-catalyzed hydrofunctionalization of carbonyls is concerned, there are reports on zinc-catalyzed hydrosilylation of carbonyls.⁷ Mainly, Parkin et al.,⁸ Nikonov et al.,⁹ Okuda et al.,¹⁰ Rivard et al.,¹¹ Jones et al.,¹² Mösch-Zanetti et al.,¹³ and Venugopal et al.¹⁴ independently reported zinc hydride-catalyzed hydrosilylation of ketones (Figure 3.A.1A-G). Surprisingly, examples of zinc-catalyzed hydroboration of ketones are scarce.¹⁵ To our knowledge, there are only two examples on the hydroboration of ketones catalyzed by molecular zinc-hydrides (Figure 3.A.1D,E).^{11,12} It should be noted that no zinc

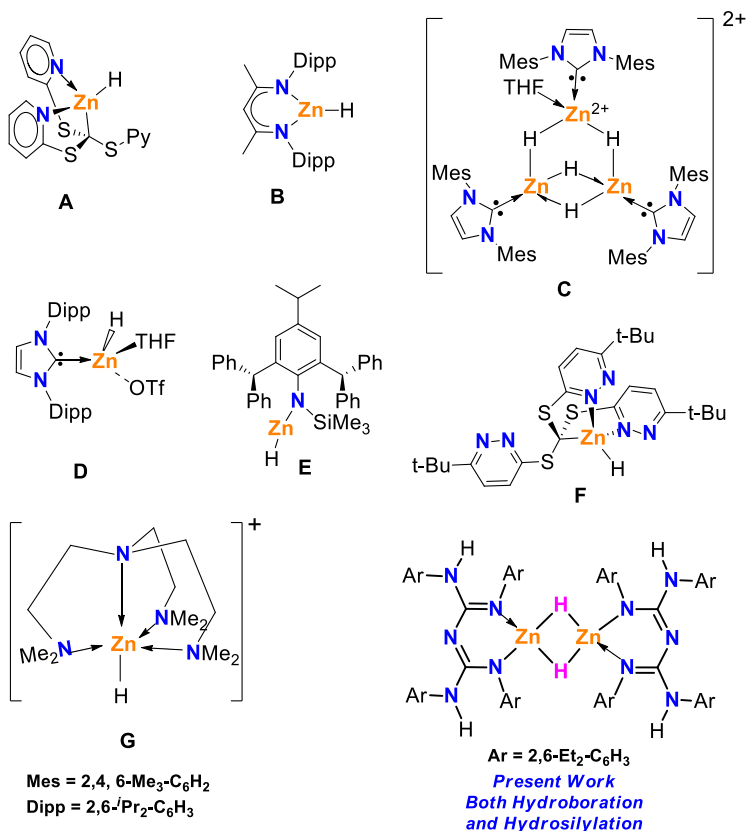


Figure 3.A.1. Previously reported selected zinc hydride catalysts for (A-G) hydrosilylation and (D,E) hydroboration of ketones and present work.

catalysts are available in literature, which performs for both hydrosilylation and hydroboration of many ketones (bifunctional), except **D** and **E**, which are limited to only one substrate. However, very recently, the Baker group reported a copper-based catalyst for hydroboration and hydrosilylation of carbonyls.¹⁶

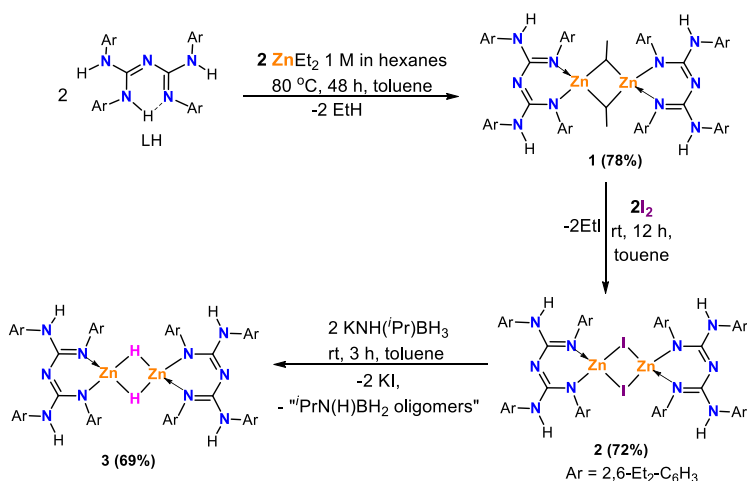
Recently our group reported inexpensive and sustainable aluminum-based catalysts bearing conjugated bis-guanidinate (CBG) anions for the hydroboration of carbonyl compounds and other challenging unsaturated organic substrates.¹⁷ A few examples of biguanide- or CBG-supported zinc complexes are known in literature.¹⁸ However, a β -diketiminato analogue, *i.e.*, CBG-supported zinc hydride, is not known in literature.

Thus, herein, we report the synthesis of three new examples of molecular CBG zinc alkyl, halide, and hydride complexes. Further, zinc hydride-catalyzed hydrosilylation, and hydroboration of a broad range of ketones have been investigated. Moreover, we designed a new, sustainable, and easily accessible catalyst containing only C, H, N, and Zn elements. We are employing the lowest catalyst loading (0.05 %) for the hydroboration of acetophenone.

3.A.2. Results and Discussion

A new example of the β -diketiminato analogue, *i.e.*, conjugated bis-guanidinate (CBG)-stabilized dimeric zinc hydride, can be accessed in three steps: i) Deprotonation of a free CBG ligand: a treatment of LH [$L = \{(\text{ArHN})(\text{ArN})-\text{C}=\text{N}-\text{C}=(\text{NAr})(\text{NHAr})$; $\text{Ar} = 2,6\text{-Et}_2\text{-C}_6\text{H}_3\}$] with ZnEt_2 in toluene afforded $[\text{LZnEt}]_2$ (**1**) in 78% yield. ii) Alkyl-halide exchange: a reaction between compound **1** and two equivalents of molecular iodine in toluene resulted in $[\text{LZnI}]_2$ (**2**) in 72% yield. iii) Salt-metathesis reaction: Compound **2** upon treatment with $[\text{KNH}(\textit{iPr})\text{BH}_3]$ in toluene allowed the formation of $[\text{LZnH}]_2$ (**3**) in 69% yield (Scheme 3.A.1). All three CBG Zn(II)

complexes are air and moisture sensitive and thermally stable. Compounds **1-3** were characterized by ^1H and $^{13}\text{C}\{^1\text{H}\}$ NMR and mass spectrometric analyses. Moreover, the molecular structure of CBG Zn(II) iodide (**2**) is established by single-crystal X-ray diffraction studies¹⁹, which is dimeric. The ^1H NMR spectrum of **1** shows one quartet at -0.08 ppm and one triplet at 0.60 ppm in CDCl_3 , corresponding to four and six protons for ZnCH_2CH_3 and ZnCH_2CH_3 , respectively, and also, a singlet peak at 5.01 equivalent to four protons of the side-arm ArNH parts of the ligand.



Scheme 3.A.1. Synthesis of CBG-Supported Zinc Complexes **1-3**.

The $^{13}\text{C}\{^1\text{H}\}$ NMR show typical ZnCH_2CH_3 and ZnCH_2CH_3 resonances at -2.3 and 11.5 ppm, respectively. Complete disappearance of ZnCH_2CH_3 and ZnCH_2CH_3 proton resonances in ^1H NMR and ZnCH_2CH_3 carbon resonances in $^{13}\text{C}\{^1\text{H}\}$ NMR in C_6D_6 , which indicated the formation of compound $[\text{LZnI}]_2$ (**2**). The ^1H NMR spectrum of **3** in C_6D_6 displays the Zn-H hydride resonance at 4.52 ppm (4.50 ppm in d_8 -toluene), a good agreement with the bridged four-coordinate heteroleptic zinc hydride complexes reported in literature (4.57 – 4.59 ppm).^{5e} The $^{13}\text{C}\{^1\text{H}\}$ NMR spectra of compounds **1-3** display a unique resonance for the N3C carbon atom at 156.6, 157.5, and 157.2 ppm, respectively. The crystals of **2** suitable for single-crystal X-ray diffraction analysis were crystallized from toluene solution at -5°C . The compound **2** crystallizes in the triclinic system

with the $P\bar{1}$ space group. The molecular structure of compound **2** is depicted in figure 3.A.2. The solid-state structure of **2** shows that each zinc atom is coordinated to two N atoms from the CBG ligand in N, N' chelate fashion and two- bridged iodide moieties to form a distorted tetrahedral geometry.

The Zn1–I1 and Zn1–I1' bond distances in **2** are 2.5819(15) (Å) and 2.7702(16) (Å), which are comparable to Zn–I bond distances of the analogous $\text{DippNacnacZn}(\mu\text{-I})_2\text{Li}(\text{OEt}_2)_2$ complex, [Zn–I(1) 2.6142(8) Å and Zn–I(2) 2.6648(8) Å].²⁰ The N–M–N bite angle of the compound **2** is N1–Zn1–N4 95.7(3)°, which is acute when compared to the bond angle in $\text{DippNacnacZn}(\mu\text{-I})_2\text{Li}(\text{OEt}_2)_2$ (N1–Zn1–N2 98.78(15)°).

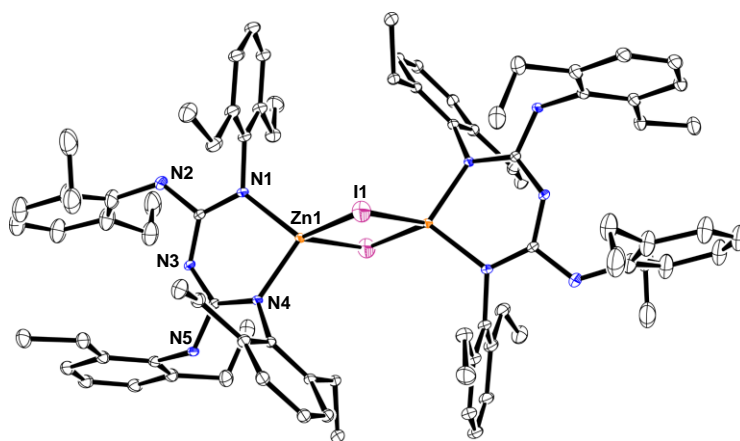
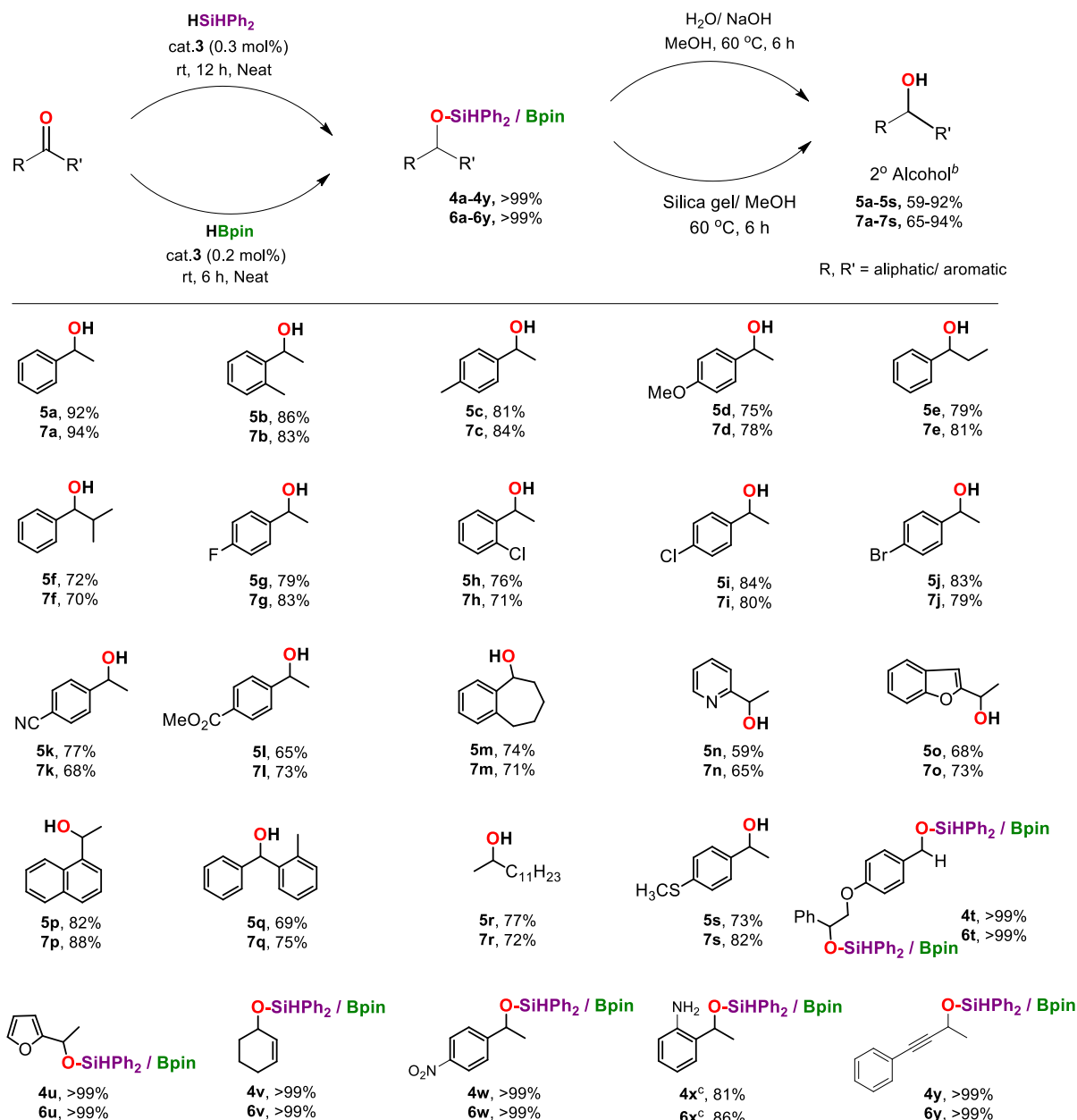


Figure 3.A.2. The solid-state structure of **2**. H atoms are omitted for clarity. Selected bond lengths (Å) and bond angles (°): Zn1–N1 1.956(8), Zn1–N4 1.943(8), Zn1–I1 2.5819(15), Zn1–I1' 2.7702(16), Zn1–Zn1' 2.4819(19); N1–Zn1–N4 95.7(3), N1–Zn1–I1 119.5(2), N4–Zn1–I1 112.2(2), I1–Zn1–I1' 104.04 (5), and Zn1–I1–Zn1' 75.59 (5).

X-ray diffraction studies confirm that compound **3** is in a dimeric form. However, despite several attempts, weakly diffracting crystals led to relatively poor data collection.¹⁹ Further, a temperature-dependent NMR (toluene- d_8 , 298–358 K) studies have been performed to know the solution structure of compound **3**. These experiments indicate that a temperature-variable dimer-monomer equilibrium exists. The dimeric μ -hydride, $[\text{LZnH}]_2$ complex presents at 298 K, and the



Scheme 3.A.2. Substrate scope for compound 3-catalyzed hydrosilylation and hydroboration of ketones.^a

^aReaction conditions for hydrosilylation and hydroboration: all reactions were carried out with ketones (1 mmol), diphenyl silane (1.1 mmol) or pinacolborane (1.1 mmol), 0.3 and 0.2 mol % of 3 for hydrosilylation and hydroboration, respectively for all ketones, except for 4t and 6t, 0.5 mol% of 3 and diphenylsilane (2.2 mmol) or pinacolborane (2.2 mmol) were used, at rt. for 6 h for

hydroboration and 12 h for hydrosilylation under N₂; ^bIsolated yields were determined after column chromatography. ^cNitromethane was used as an internal standard for the substrates 4x and 6x and reaction timings 8 and 1.5 h, respectively.

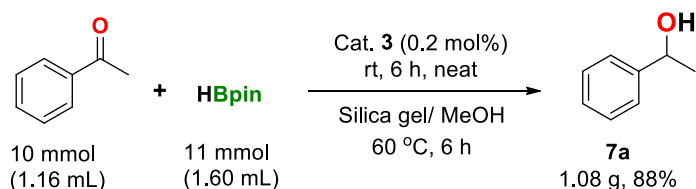
equilibrium shifted toward a monomeric complex, LZnH, at increasing temperatures. As a result, increasing the temperature from 298 to 358 K results in a decrease in the Zn-H chemical shift from 4.50 to 4.19 ppm and shows a change in the coordination geometry of the complex at increasing temperature. Hence, a temperature-dependent dimer-monomer equilibrium is controlled by the dinuclear species at 298 K, while a monomeric species is at elevated temperatures.²¹

Considering the fewer reports on highly efficient zinc catalysts for hydroboration and hydrosilylation of ketones, we aimed to explore CBG ZnH-catalyzed hydrofunctionalization of ketones. We chose a diphenylsilane, Ph₂SiH₂ as a hydride source for hydrosilylation, because this reagent is much ideal in terms of cost for the small and medium scale industries.^{1a} The reaction of acetophenone and diphenylsilane with 5 mol % catalyst **3** gave quantitative conversion to the hydrosilylation product after 12 h at room temperature. Lowering the catalyst loadings to 3.0, 1.0, and 0.3 mol % gave quantitative conversion at the same reaction conditions. However, at a loading of the 0.3 mol % catalyst, we observed a 93% yield of the product within 8 h. Thus, 1.0 mmol of acetophenone and 1.1 mmol of Ph₂SiH₂ and 0.3 mol% of catalyst loading at room temperature in the neat condition are the optimized conditions for hydrosilylation reaction. A vast range of substrates has been investigated including electron-donating (**5b-5f**, **5s**), electron-withdrawing substituents (**5g-5l**), a seven-membered ring attached with a phenyl ring (**5m**), heterocycles (**5n-5o**), a fused system (**5p**), substituted benzophenone (**5q**) and long-chain aliphatic ketone (**5r**) as well as some exotic ketones (**4t-4y**) (Scheme 3.A.2). It is worthy to note that compound **3** is capable of catalyzing the insertion of 2-acetyl pyridine into all two of the Si-H bonds of Ph₂SiH₂ to afford **4n'**, which upon hydrolysis yielded **5n**.

In each case, the hydrolysis of the silylated ethers resulted in the formation of secondary alcohols with good to excellent yields (59-92%, **5a-5s**). ^1H and $^{13}\text{C}\{^1\text{H}\}$ NMR spectra of silylated ethers (**4a-4y**) are provided in the Supporting Information.

Examining whether B-H bond activation could be augmented to the catalyst **3**; we investigated the hydroboration reaction with the same ketone substrates. The reaction of acetophenone and HBpin with 0.2 mol % catalyst **3** gave quantitative conversion to the hydroboration product after 6 h at room temperature.

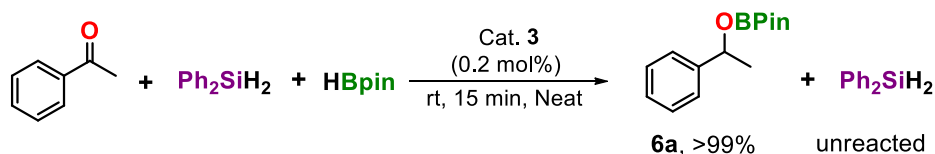
With these optimized conditions in hand, we determined to expand the same ketone substrates, which employed for the hydrosilylation reaction. To our delight, in all instances, a quantitative conversion of ketones into their corresponding boronates esters (**6a-6y**) was observed. The good to excellent yield of alcohol was noticed upon the hydrolysis of the boronated esters (65-94%, **7a-7s**, Scheme 3.A.2). The ^1H and $^{13}\text{C}\{^1\text{H}\}$ NMR spectra for boronate esters (**6a-6y**) and alcohols (**7a-7s**) can be found in the Supporting Information.



Scheme 3.A.3. Bulk scale hydroboration of acetophenone with HBpin

Further, a bulk scale hydroboration reaction was performed to verify the practical applicability of this protocol. Strikingly, a 10 mmol scale reaction of acetophenone under standard reaction conditions forming a quantitative yield of boronate ester, which upon hydrolysis yielded the alcohol **7a** in 88 % (Scheme 3.A.3).

It is important to note that the substrate scope includes excellent tolerance of amine, nitro, nitrile, ester, heterocycle, alkene, and alkyne functionalities in both hydrosilylation and hydroboration reactions (intramolecular chemoselectivity). It is no surprise that the substrate bearing the aldehyde functional group (**4t** or **6t**) was not tolerated in both hydrosilylation and hydroboration under reaction conditions. Remarkably, hydroboration proceeded more efficiently than hydrosilylation.



Scheme 3.A.4. Competitive hydrosilylation and hydroboration reaction

Next, a one-pot reaction of acetophenone, with both diphenylsilane and HBpin in the presence of catalyst **3** (0.2 mol %) under neat conditions at room temperature for 15 min, has been carried out, which showed the formation of **6a** alone in quantitative yield (Scheme 3.A.4).

Table 3.A.1. Hydroboration of acetophenone catalyzed by **3**.^a

CC(=O)c1ccccc1 + HBpin $\xrightarrow{\text{Cat. 3}}$ CC(OBpin)c1ccccc1

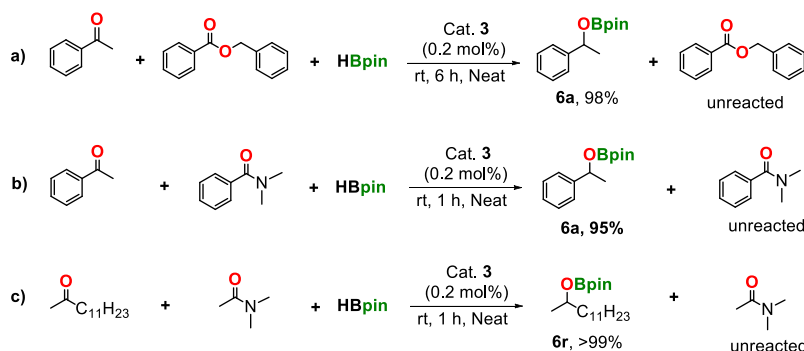
6a

entry	cat. (mol%)	time (h)	yield (%)	TON	TOF (h ⁻¹)
1	0.2	6	>99	500	83
2	0.2	1	>99	500	500
3	0.2	0.25	>99	500	2000
4	0.1	1	>99	1000	1000
5	0.075	0.5	>99	1333	2666
6	0.05	0.5	>99	2000	4000
7	0.05	0.334	97	1940	5800

^aReaction conditions: catalyst (x mol %, 100 μ L from stock solution in toluene), acetophenone (1 mmol), HBpin (1.11 mmol) at rt. Yields were determined by ¹H NMR spectroscopy using nitromethane as an internal standard. TON was calculated through the dividing number of moles of the product by the number of moles of catalyst used. TOF was determined to divide TON by time of reaction.

We were curious to know the catalytic efficiency of compound **3** for the hydroboration of acetophenone. Under the optimized conditions, the reactions of HBpin and acetophenone with a catalyst loading of 0.2 mol % provided a >99 % conversion within 6 h (TOF 83 h⁻¹).

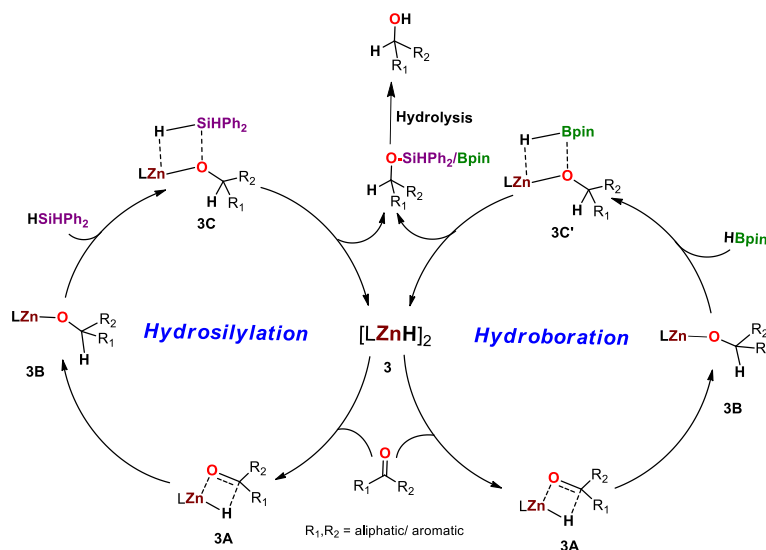
We noticed the >99% conversion of acetophenone into corresponding boronate ester at room temperature with a turnover number and frequency 1940 and 5800 h⁻¹, respectively (see Table 3.A.1, entry 5). To the best of our knowledge, CBG Zn(II) hydride catalysts (**3**) exhibited the highest catalytic activity as compared with molecular zinc hydride catalysts reported in literature for the ketone hydroboration reaction (see Table S3).^{11,12}



Scheme 3.A.5. Intermolecular chemoselective reactions

We are further excited to investigate the catalytic efficiency of **3** in the intermolecular chemoselectivity hydroboration between ketone and ester or amide. Thus, when acetophenone was mixed with benzyl benzoate and HBpin under optimized conditions, a 98% yield of hydroboration of ketone was noticed in the choice of ester. Likewise, acetophenone provides the corresponding boronate ester in a 95 % yield in preference to the N,N'-dimethyl benzamide. Similarly, 2-tridecanone, N,N'-dimethylacetamide, and HBpin were reacted together with catalyst **3**, which solely yielded **6a** in a quantitative yield in preference to amide (Scheme 3.A.5).

In all three cases, only ketones were reduced in preferences to other reducible functionalities. We established the mechanism as earlier described by others for the metal hydride-catalyzed hydrofunctionalization reactions.¹ The insertion of Zn-H moiety into C=O functionality of ketone yielded the zinc alkoxide, LZnOR (**3B**), via intermediate **3A**. Next, a reaction of **3B** with Ph₂SiH₂ or HBpin affords silyl ether or boronate ester via **3C** or **3C'** along with the restoration of the LZnH catalyst (Scheme 3.A.6). Further, to confirm the formation of reactive intermediate **3B**, a stoichiometric reaction of LZnH with benzophenone has been carried out. The ¹H and ¹³C NMR indicated the formation of [LZnOCHPh₂], **3B**, and corresponding peaks for OCH appeared at 6.36 and 77.2 ppm in ¹H and ¹³C {¹H} NMR, respectively.



Scheme 3.A.6. Proposed mechanism for the zinc catalyzed hydrosilylation and hydroboration of ketones

3.A.3. Conclusion

In summary, the first examples of β -diketiminato analogues, *i.e.*, CBG-supported zinc alkyl (**1**), halide (**2**), and hydride (**3**) complexes have been reported. Moreover, we have exemplified earth-abundant, cheaper, and easily accessible, [LZnH]₂ (**3**) as an efficient catalyst for hydrosilylation and hydroboration of many ketones under mild conditions. It is noted that reported examples of zinc-based catalysts for hydrosilylation and hydroboration reactions require high catalyst loading

(5-10 mol %), limited substrate scope, and longer reaction times. This work presents a remarkably active ketone reduction *via* the insertion/heterolytic cleavage mechanistic pathway.

3.A.4. Experimental Section

All manipulations were performed under a nitrogen atmosphere using standard glove box and Schlenk techniques unless otherwise stated. The ligand LH ($L = \{(ArNH)(ArN)-C=N-C=(NAr)(NHAr)\}$; $Ar = 2,6-Et_2-C_6H_3$) was synthesized by using a protocol developed in our laboratory.²² Diethyl zinc solution, 1 M in hexanes, was procured from Sigma Aldrich. Iodine granules were purchased from Spectrochem. The hydride source $[KNH(^iPr)BH_3]$ was prepared as per the reported procedure.^{5c} The solvents used for the synthesis and NMR experiments were dried, distilled, and degassed before use by standard methods.²³ The 1H , $^{13}C\{^1H\}$ NMR spectra were recorded on 400 MHz Bruker AV spectrometer. The chemical shifts (δ ppm) in 1H and $^{13}C\{^1H\}$ NMR spectra were referenced to the deuterated solvents' residual proton signals. The crystal data of compound **2** were collected on a Rigaku Oxford diffractometer at 120 K. Selected data collection parameters, and other crystallographic results are summarized in Table 3.A.2. The structure was determined using direct methods employed in *ShelXT*,²⁴ *Olex*,²⁵ and refinement was carried out using least-square minimization implemented in *ShelXL*.²⁶ All non-hydrogen atoms were refined with anisotropic displacement parameters. Hydrogen atom positions were fixed geometrically in idealized positions and were refined using a riding model. High-resolution mass spectra (HRMS) were recorded on a Bruker micrOTOF-Q II spectrometer.

3.A.4.1. Synthesis of Zinc Based Complexes

Synthesis of $[LZnEt]_2$ (**1**)

A 1.5 g (2.38 mmol) of LH was dissolved in ~20 mL of toluene. Next, a diethylzinc solution (2.5 mL, 2.5 mmol, 1 M in hexanes) was added at room temperature. It was then heated at 80 °C in oil

bath for 2 days. The clear solution was filtered through a Celite. The desired product **1** was isolated as colorless crystalline compound after removing the entire solution in high vacuum. (1.340 g, yield 78%); Mp 178–182 °C. ^1H NMR (400 MHz, 25 °C, CDCl_3) δ 7.16–7.14 (d, $^3J_{\text{HH}} = 7.1$ Hz, 8H), 7.11–7.07 (m, 4H), 6.84 (t, $^3J_{\text{HH}} = 7.5$ Hz, 4H), 6.63–6.61 (d, $^3J_{\text{HH}} = 7.5$ Hz, 8H), 5.01 (s, 4H), 2.93–2.85 (m, 8H), 2.70–2.61 (m, 8H), 2.42–2.33 (m, 8H), 2.17–2.12 (m, 8H), 1.29 (t, $^3J_{\text{HH}} = 7.5$ Hz, 24H), 0.92 (t, $^3J_{\text{HH}} = 7.5$ Hz, 24H), 0.60 (t, $^3J_{\text{HH}} = 8.0$ Hz, 6H), –0.08 (q, $^3J_{\text{HH}} = 8.1$ Hz, 4H). $^{13}\text{C}\{^1\text{H}\}$ NMR (100 MHz, CDCl_3) δ 156.6, 143.0, 141.4, 138.9, 135.2, 126.3, 126.2, 125.3, 125.3, 24.9, 24.2, 14.4, 14.3, 11.5, –2.3. HRMS (ESI) m/z : $[\text{M}/2 + \text{H}]^+$ Calcd for $\text{C}_{44}\text{H}_{59}\text{N}_5\text{Zn}$ 722.4135; Found: 722.4094.

Synthesis of $[\text{LZnI}]_2$ (**2**)

A 0.7 g (0.48 mmol) of compound **1** dissolved in ~15 mL of dry toluene. Also, 0.25 g (0.99 mmol) of iodine was dissolved in ~10 mL of dry toluene in another Schlenk tube. Then the solution of iodine was added dropwise to the $[\text{LZnEt}]_2$ (**1**) solution. Immediately after the addition, a rose red could be observed. The reaction mixture was stirred for 12 h, during this period a pale yellow solution was observed. Then the volatiles were evacuated, to the yellow powder a dry toluene was added. The product **2** was crystallized in the form of block shaped crystals suitable for X-ray diffraction at –5 °C after 12 h. (0.573 g, yield 72%); Mp 238–242 °C. ^1H NMR (400 MHz, 25 °C, C_6D_6) δ 7.10 (s, 12H), 6.87 (t, $^3J_{\text{HH}} = 7.5$ Hz, 4H), 6.62–6.60 (d, $^3J_{\text{HH}} = 7.5$ Hz, 8H), 5.08 (s, 4H), 3.08–3.04 (m, 8H), 2.74–2.69 (m, 8H), 2.36–2.28 (m, 8H), 2.18–2.12 (m, 8H), 1.32 (t, $^3J_{\text{HH}} = 7.4$ Hz, 24H), 0.94 (t, $^3J_{\text{HH}} = 7.5$ Hz, 24H). $^{13}\text{C}\{^1\text{H}\}$ NMR (100 MHz, C_6D_6) δ 157.5, 141.0, 140.8, 138.8, 134.7, 126.6, 126.5, 126.4, 125.2, 24.8, 24.3, 14.3, 14.1. HRMS (ESI) m/z : $[\text{M}/2 + \text{H}]^+$ Calcd for $\text{C}_{42}\text{H}_{54}\text{IN}_5\text{Zn}$ 820.2788, Found: 820.2819.

Synthesis of [LZnH]₂ (3)

A 0.85 g (0.52 mmol) of compound **2** was dissolved in ~10 mL of dry toluene. Also, 0.121 g (1.08 mmol) of [KNH(*i*Pr)BH₃] was dissolved in another Schlenk tube. Then, the solution of compound **2** was added to the [KNH(*i*Pr)BH₃] solution. The reaction mixture was stirred for 3h. Then the mixture was filtered through Celite and removed the solvent in vacuo to yield a white crystalline solid. (0.501 g, yield 69%); Mp 229–233 °C. ¹H NMR (400 MHz, C₆D₆) δ 7.10–7.08 (m, 12H), 6.90 (t, ³J_{HH} = 7.6 Hz, 4H), 6.66–6.64 (d, ³J_{HH} = 7.6 Hz, 8H), 5.00 (s, 4H), 4.52 (s, 2H, ZnH), 3.08–2.99 (m, 8H), 2.76–2.66 (m, 8H), 2.42–2.33 (m, 8H), 2.22–2.13 (m, 8H), 1.30 (t, ³J_{HH} = 7.5 Hz, 24H), 0.96 (t, ³J_{HH} = 7.6 Hz, 24H). ¹³C{¹H} NMR (100 MHz, C₆D₆) δ 157.2, 142.6, 141.1, 138.8, 135.2, 126.7, 126.3, 125.7, 125.2, 24.9, 24.2, 14.4, 14.2. ¹H NMR (400 MHz, *d*₈-toluene) δ 7.05 (s, 12H), 6.83 (t, ³J_{HH} = 7.6 Hz, 4H), 6.58–6.56 (d, ³J_{HH} = 7.6 Hz, 8H), 4.96 (s, 4H), 4.50 (s, 2H), 3.02–2.92 (m, 8H), 2.76–2.66 (m, 8H), 2.38–2.28 (m, 8H), 2.18–2.10 (m, 8H), 1.29 (t, ³J_{HH} = 7.5 Hz, 24H), 0.93 (t, ³J_{HH} = 7.6 Hz, 24H). ¹³C{¹H} NMR (100 MHz, *d*₈-toluene) δ 157.6, 142.6, 141.4, 139.2, 135.4, 126.9, 126.7, 126.2, 125.6, 25.2, 24.6, 14.6, 14.5. HRMS (ESI) *m/z*: [M/2 + H]⁺ Calcd for C₄₂H₅₅N₅Zn 694.3822, Found: 694.3816.

3.A.4.2. Crystallographic Data

The single crystal of compound **2** was crystalized from toluene at -5 °C as colorless blocks after 12 h. The crystal data of compound **2** were collected on a Rigaku Oxford diffractometer at 120 K. Selected data collection parameters and other crystallographic results are summarized in Table 3.A.2. The structure was determined using direct methods employed in *ShelXT*,²⁴ *OleX*,²⁵ and refinement was carried out using least-square minimization implemented in *ShelXL*.²⁶ All non-hydrogen atoms were refined with anisotropic displacement parameters. Hydrogen atom positions were fixed geometrically in idealized positions and were refined using a riding model.

Table 3.A.2. Crystallographic data and refinement parameters for compound **2**

Compound	2
Formula	C ₈₄ H ₁₀₈ N ₁₀ I ₂ Zn ₂
Formula mass	1642.34
<i>T</i> /K	110(2)
λ /Å	1.54184
Crystal dimensions/mm	0.12×0.09×0.08
Crystal system	Triclinic
Space group	<i>P</i> 1̄
<i>a</i> /Å	13.5467(2)
<i>b</i> /Å	15.2671(3)
<i>c</i> /Å	19.7699(3)
α /°	107.173(2)
β /°	100.8440(10)
γ /°	90.3100(10)
<i>V</i> /Å ³	3828.64(12)
<i>Z</i>	2
<i>D</i> _c /g cm ⁻³	1.425
μ /mm ⁻¹	7.487
<i>F</i> (000)	1696
θ Range/°	3.247–68.435
Measured reflections	52497
Independent reflections/ <i>R</i> _{int}	11738/0.0981
Parameters	898
<i>R</i> ₁ (<i>I</i> > 2σ(<i>I</i>)) ^a	0.1292
<i>wR</i> ₂ (all data) ^b	0.3923
Goodness-of-fit on <i>F</i> ²	1.709
$\Delta\rho_{\text{max, min}}$ /e Å ⁻³	3.671, -3.871

3.A.5. Appendix: All general experimental information, stoichiometric reactions, analytical data, and spectral data were available in published paper. *J. Org. Chem.* **2020**, 85, 11200–11210.

3.A.6. References

- (a) Raya-Barón, Á.; Oña-Burgos, P.; Fernández, I. *ACS Catal.* **2019**, 9, 5400–5417; (b) Liu, Y.; Zhang, D.; Ma, Y.; Li, J.; Bai, Y.; Peng, J. *Curr. Org. Synth.* **2019**, 16, 276–282; (c) Bleith,

- T.; Gade, L. H. *J. Am. Chem. Soc.*, **2016**, *138*, 4972–4983; (d) Riener, K.; Högerl, M. P.; Gigler, P.; Kühn, F. E. *ACS Catal.* **2012**, *2*, 613–621; (e) Shegavi, M. L.; Bose, S. K. *Catal. Sci. Technol.* **2019**, *9*, 3307–3336; (f) Chong, C. C.; Kinjo, R. *ACS Catal.* **2015**, *5*, 3238–3259; (g) Tamang, S. R.; Findlater, M. *Molecules* **2019**, *24*, 3194; (h) Ai, W.; Zhong, R.; Liu, X.; Liu, Q. *Chem. Rev.* **2019**, *119*, 2876–2953; (i) Wei, D.; Darcel, C. *Chem. Rev.* **2019**, *119*, 2550–2610.
2. Parkin, G. *Chem. Rev.* **2004**, *104*, 699–768.
 3. Finholt, A. E.; Bond, A. C., Jr.; Schlesinger, H. I. *J. Am. Chem. Soc.* **1947**, *69*, 1199–1203.
 4. Watkins, J. J.; Ashby, E. C. *Inorg. Chem.* **1974**, *13*, 2350–2354.
 5. (a) Hao, H.; Cui, C.; Roesky, H. W.; Bai, G.; Schmidt, H.-G.; Noltemeyer, M. *Chem. Commun.* **2001**, 1118–1119; (b) Ballmann, G.; Grams, S.; Elsen, H.; Harder, S. *Organometallics* **2019**, *38*, 2824–2833; (c) Spielmann, J.; Piesik, D.; Wittkamp, B.; Jansen, G.; Harder, S. *Chem. Commun.* **2009**, 3455–3456; (d) Mukherjee, D.; Ellern, A.; Sadow, A. D. *J. Am. Chem. Soc.* **2010**, *132*, 7582–7583; (e) Wiegand, A.-K.; Rit, A.; Okuda, J. *Coord. Chem. Rev.* **2016**, *314*, 71–82; (f) Jochmann, P.; Stephan, D. W. *Angew. Chem., Int. Ed.* **2013**, *52*, 9831–9835.
 6. (a) Procter, R. J.; Uzelac, M.; Cid, J.; Rushworth, P. J.; Ingleson, M. J. *ACS Catal.* **2019**, *9*, 5760–5771; (b) Uzelac, M.; Yuan, K.; Ingleson, M. J. *Organometallics* **2020**, *39*, 1332–1338; (c) Enthaler, S. *ACS Catal.* **2013**, *3*, 150–158; (d) Wu, X.-F. *Chem. - Asian J.* **2012**, *7*, 2502–2509.
 7. (a) Alshakova, I. D.; Nikonov, G. I. *Synthesis*, **2019**, *51*, 3305–3312; (b) Dagorne, S. *Synthesis* **2018**, *50*, 3662–3670; (c) Revunova, K.; Nikonov, G. I. *Dalton Trans.* **2015**, *44*, 840–866; (d) Feng, G.; Du, C.; Xiang, L.; del Rosal, I.; Li, G.; Leng, X.; Chen, E. Y. X.; Maron, L.; Chen,

-
- Y. *ACS Catal.* **2018**, 8, 4710–4718; (e) Rauch, M.; Parkin, G. *J. Am. Chem. Soc.* **2017**, 139, 18162–18165; (f) Li, Y.; Junge, K.; Beller, M. in *Zinc Catalysis*, **2015**, 5–32.
8. Sattler, W.; Ruccolo, S.; Chaijan, M. R.; Allah, T. N. and Parkin, G. *Organometallics* **2015**, 34, 4717–4731.
9. Boone, C.; Korobkov, I.; Nikonov, G. I. *ACS Catal.* **2013**, 3, 2336–2340.
10. Rit, A.; Zanardi, A.; Spaniol, T. P.; Maron, L.; Okuda, J. *Angew. Chem., Int. Ed.* **2014**, 53, 13273–13277.
11. Lummis, P. A.; Momeni, M. R.; Lui, M. W.; McDonald, R.; Ferguson, M. J.; Miskolzie, M.; Brown, A.; Rivard, E. *Angew. Chem., Int. Ed.* **2014**, 53, 9347–9351.
12. Dawkins, M. J. C.; Middleton, E.; Kefalidis, C. E.; Dange, D.; Juckel, M. M.; Maron, L.; Jones, C. *Chem. Commun.* **2016**, 52, 10490–10492.
13. Tüchler, M.; Gärtner, L.; Fischer, S.; Boese, A. D.; Belaj, F.; Mösch-Zanetti, N. C. *Angew. Chem., Int. Ed.* **2018**, 57, 6906–6909.
14. Chambenahalli, R.; Andrews, A. P.; Ritter, F.; Okuda, J.; Venu gopal, A. *Chem. Commun.* **2019**, 55, 2054–2057.
15. (a) Kumar, G. S.; Harinath, A.; Narvariya, R.; Panda, T. K. *Eur. J. Inorg. Chem.* **2020**, 467–474; (b) Mukherjee, D.; Wiegand, A. -K.; Spaniol, T. P.; Okuda, J. *Dalton Trans.* **2017**, 46, 6183–6186.
16. Elsby, M. R.; Baker, R. T. *Chem. Commun.* **2019**, 55, 13574–13577.
17. (a) Sarkar, N.; Bera, S.; Nembenna, S. *J. Org. Chem.* **2020**, 85, 4999–5009; (b) Peddarao, T.; Sarkar, N.; Nembenna, S. *Inorg. Chem.* **2020**, 59, 4693–4702; (c) Jakhar, V. K.; Barman, M. K.; Nembenna, S. *Org. Lett.* **2016**, 18, 4710–4713.

-
18. (a) Dehmel, M.; Vass, V.; Prock, L.; Goerls, H.; Kretschmer, R. *Inorg. Chem.* **2020**, *59*, 2733–2746. (b) Ray, P. *Chem. Rev.* **1961**, *61*, 313–359.
19. CCDC for compound **2**: 199416. Note that X-ray diffraction studies confirm that both compounds **1** and **3** are in dimeric in form. However, despite several attempts, poor quality crystals of compounds **1** and **3** obtained by crystallization.
20. Prust, J.; Most, K.; Müller, I.; Stasch, A.; Roesky, H. W.; Usón, I. *Eur. J. Inorg. Chem.* **2001**, 1613–1616.
21. (a) Brown, N. J.; Harris, J. E.; Yin, X.; Silverwood, I.; White, A. J. P.; Kazarian, S. G.; Hellgardt, K.; Shaffer, M. S. P.; Williams, C. K. *Organometallics* **2014**, *33*, 1112–1119. (b) Rit, A.; Spaniol, T. P.; Maron, L.; Okuda, J. *Organometallics* **2014**, *33*, 2039–2047.
22. Peddaraao, T.; Baishya, A.; Sarkar, N.; Acharya, R.; Nembenna, S. *Manuscript Submitted*.
23. Armarego, W. F.; Chai, C. L. L. “Purification of laboratory chemicals” **2013**, Elsevier, UK.
24. Sheldrick, G. M. Crystal structure refinement with SHELXL. *Acta Crystallogr., Sect. C: Struct. Chem.* **2015**, *71*, 3–8.
25. Dolomanov, O. V.; Bourhis, L. J.; Gildea, R. J.; Howard, J. A. K.; Puschmann, H. *J. Appl. Crystallogr.* **2009**, *42*, 339–341.
26. (a) Sheldrick, G. M. *Acta Crystallogr., Sect. A: Found. Crystallogr.* **2008**, *64*, 112–122. (b) Sheldrick, G. M. *Acta Crystallogr., Sect. A: Found. Adv.* **2015**, *71*, 3–8.
27. Tafazolian, H.; Yoxtheimer, R.; Thakuri, R. S.; Schmidt, J. A. R. *Dalton Trans*, **2017**, *46*, 5431–5440.
28. Brunner, H.; Obermann, U. *Chem. Ber.* **1989**, *122*, 499–507.
29. Tan, M.; Zhang, Y.; Ying, J. Y. *Adv. Synth. Catal.* **2009**, *351*, 1390–1394.
30. Monney, A.; Nastri, F.; Albrecht, M. *Dalton Trans.* **2013**, *42*, 5655–5660.
-

31. Yang, J.; Tilley, T. D. *Angew. Chem. Int. Ed.* **2010**, *49*, 10186–10188.
32. Valyaev, D. A.; Wei, D.; Elangovan, S.; Cavailles, M.; Dorcet, V.; Sortais, J. -B.; Darcel, C.; Lugan, N. *Organometallics* **2016**, *35*, 4090-4098.
33. Daisuke, I.; Miyuki, H.; Kohta, I.; Tetsuo, O.; Yoshihiko, I. *Chem. Lett.* **2007**, *36*, 366-367.
34. Orr, S. A.; Kelly, J. A.; Boutland, A. J.; Blair, V. L. *Chem. – Eur. J.* **2020**, *26*, 4947-4951.
35. Tapu, D.; Buckner, O. J.; Boudreaux, C. M.; Norvell, B.; Vasiliu, M.; Dixon, D. A.; McMillen, C. D. *J. Organomet. Chem.* **2016**, *823*, 40-49.
36. Bisai, M. K.; Das, T.; Vanka, K.; Sen, S. S. *Chem. Commun.* **2018**, *54*, 6843-6846.
37. Yan, D.; Dai, P.; Chen, S.; Xue, M.; Yao, Y.; Shen, Q.; Bao, X. *Org. Biomol. Chem.* **2018**, *16*, 2787-2791.
38. Wang, W.; Shen, X.; Zhao, F.; Jiang, H.; Yao, W.; Pullarkat, S. A.; Xu, L.; Ma, M. *J. Org. Chem.* **2018**, *83*, 69-74.
39. Zhang, G.; Zeng, H.; Wu, J.; Yin, Z.; Zheng, S.; Fettingner, J. C. *Angew. Chem. Int. Ed.* **2016**, *55*, 14369–14372.
40. Li, L.; Liu, E.; Cheng, J.; Zhang, G. *Dalton Trans.* **2018**, *47*, 9579-9584.
41. Sarkar, N.; Mahato, M.; Nembenna, S. *Eur. J. Inorg Chem.* **2020**, 2295-2301.
42. Huang, Z.; Liu, D.; -Bunquin, J. C.; Zhang, G.; Yang, D.; -Encarnación, J. M. L.; Xu, Y.; Ferrandon, M. S.; Niklas, J.; Poluektov, O. G.; Jellinek, J.; Lei, A.; Bunel, E. E.; Delferro, M. *Organometallics*, **2017**, *36*, 3921-3930.
43. Guo, J.; Chen, J.; Lu, Z. *Chem. Commun.* **2015**, *51*, 5725-5727.
44. Wu, Y.; Shan, C.; Ying, J.; Su, J.; Zhu, J.; Liu, L. L.; Zhao, Y. *Green Chem.* **2017**, *19*, 4169-4175.

45. Baratta, W.; Benedetti, F.; Zotto, A. D.; Fanfoni, L.; Felluga, V.; Magnolia, S.; Putignano, E.; Rigo, P. *Organometallics* **2010**, 29, 3563-3570.
46. Qi, X.; Zheng, T.; Zhou, J.; Dong, Y.; Zuo, X.; Li, X.; Sun, H.; Fuhr, O.; Fenske, D. *Organometallics* **2019**, 38, 268-277.
47. Baishya, A.; Baruah, S.; Geetharani, K. *Dalton Trans.* **2018**, 47, 9231-9236.
48. Nicholson, K.; Dunne, J.; Bell, P. D.; Garcia, A. B.; Bage, A. D.; Docherty J. H.; Hunt, T. A.; Langer, T.; Thomas, S. P. *ChemRxiv* **2020**, 1-168.
49. Chardon, A.; Rouden, J.; Blanchet, J. *Eur. J. Org. Chem.* **2019**, 995-998.

NMR Spectra

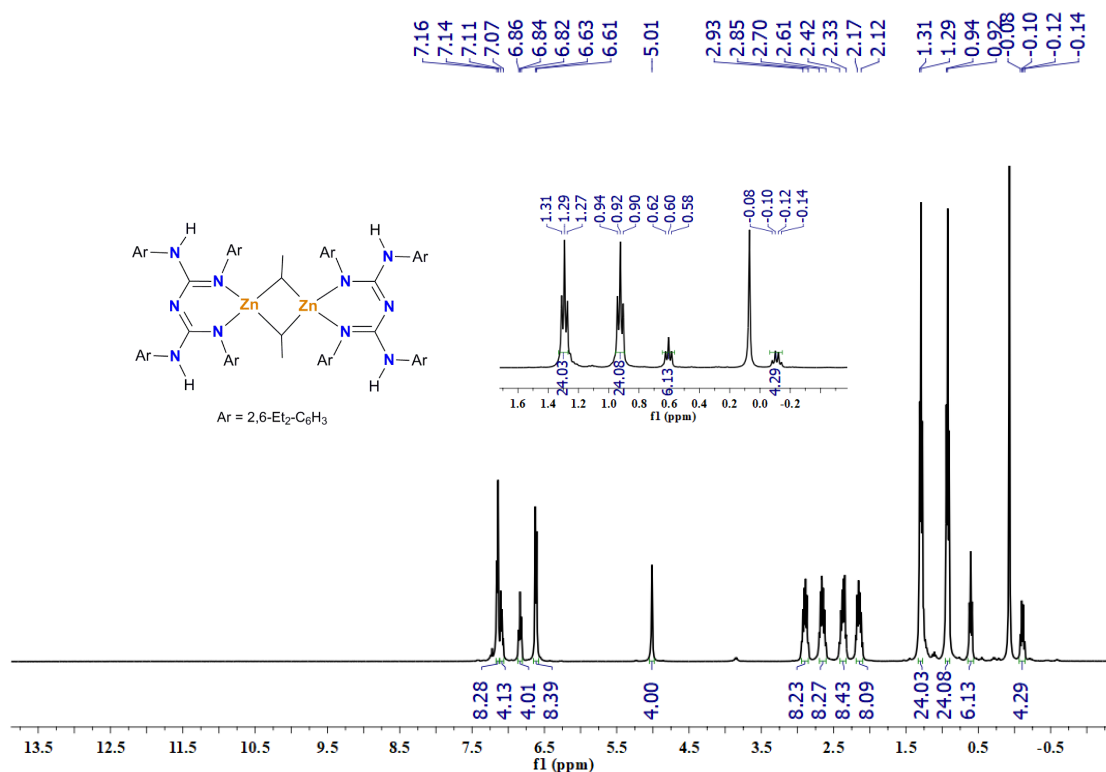


Figure 3.A.3. 1H NMR (400 MHz, 25 °C, $CDCl_3$) spectrum of $[LZnEt]_2$, **1**.

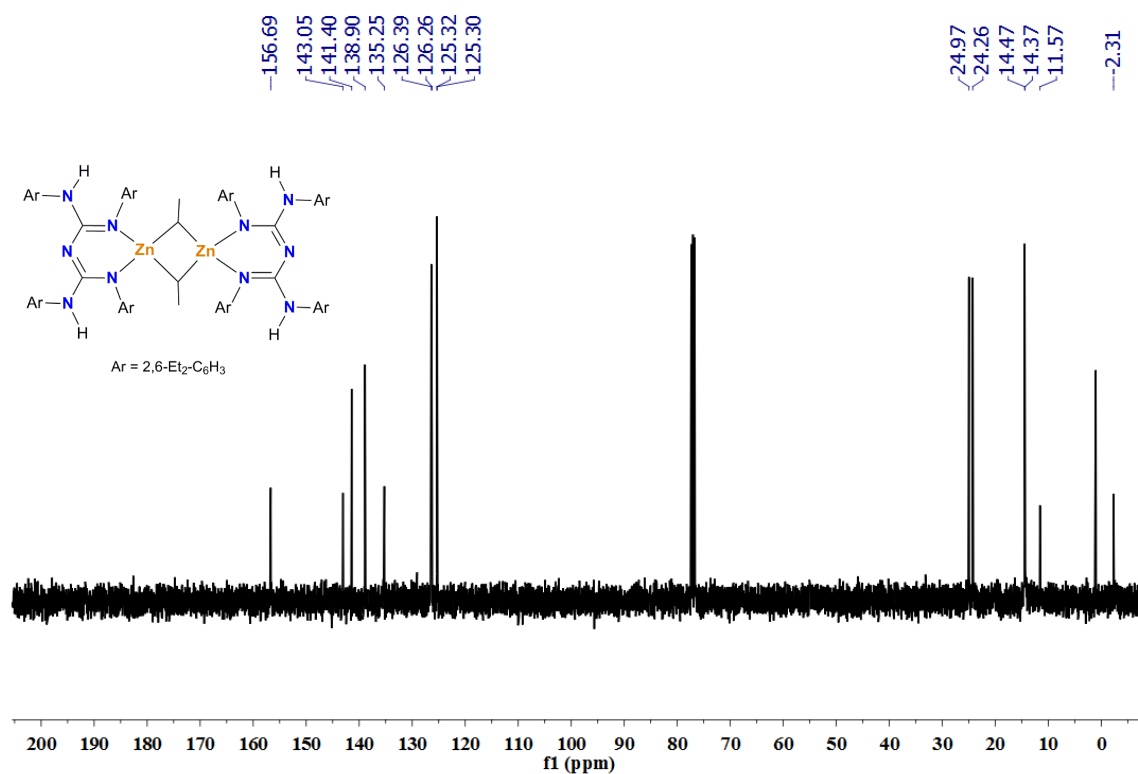


Figure 3.A.4. $^{13}C\{^1H\}$ NMR (100 MHz, 25 °C, $CDCl_3$) spectrum of $[LZnEt]_2$, **1**.

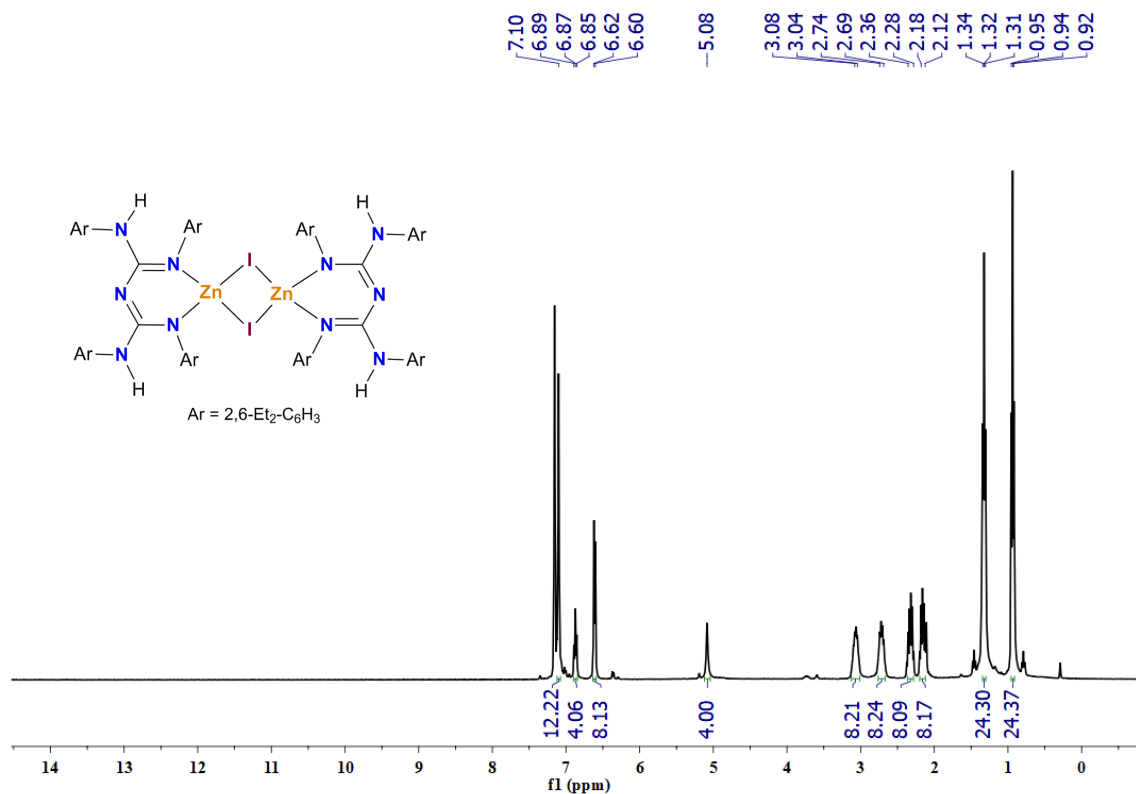


Figure 3.A.5. 1H NMR (400 MHz, 25 °C, C_6D_6) spectrum of $[LZnI]_2$, **2**.

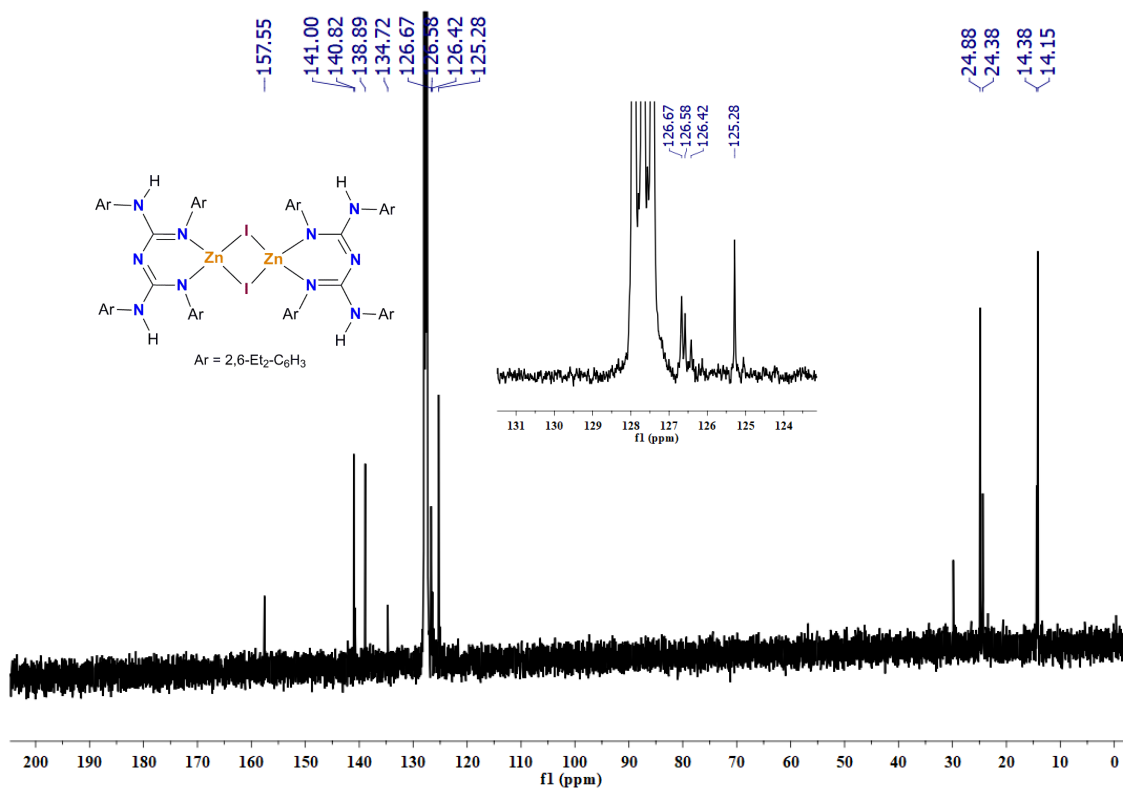


Figure 3.A.6. $^{13}C\{^1H\}$ NMR (100 MHz, 25 °C, C_6D_6) spectrum of $[LZnI]_2$, **2**.

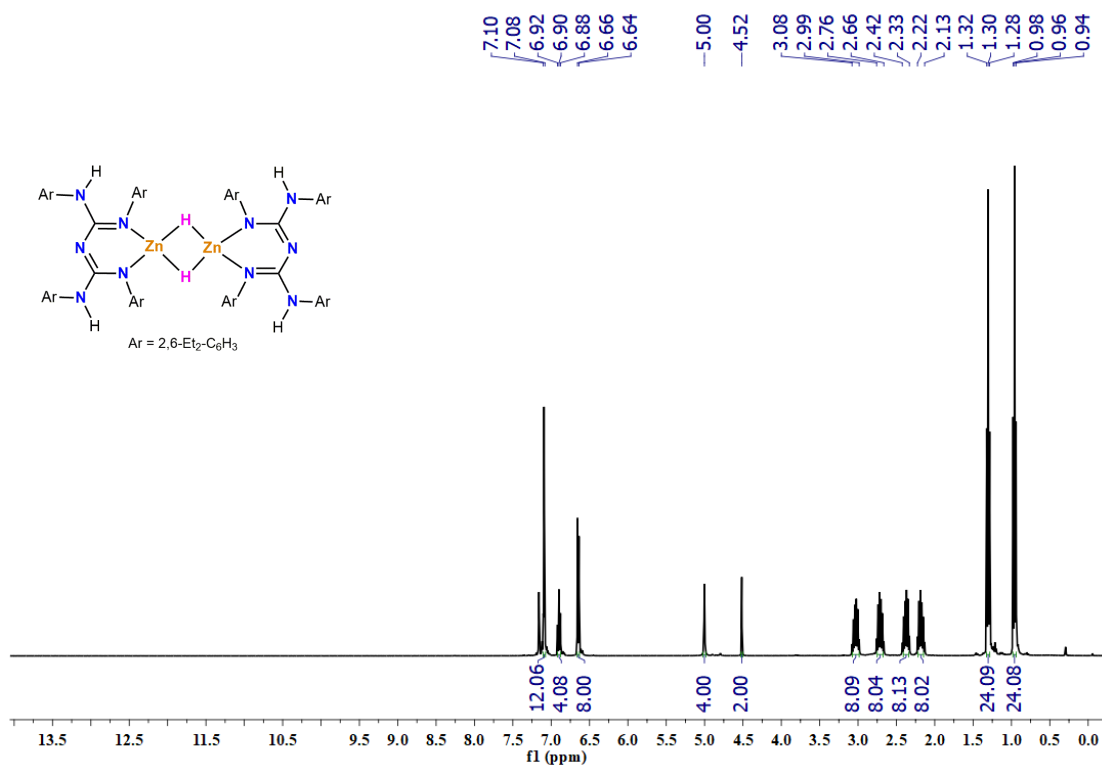


Figure 3.A.7. 1H NMR (400 MHz, 25 °C, C_6D_6) spectrum of $[LZnH]_2$, **3**.

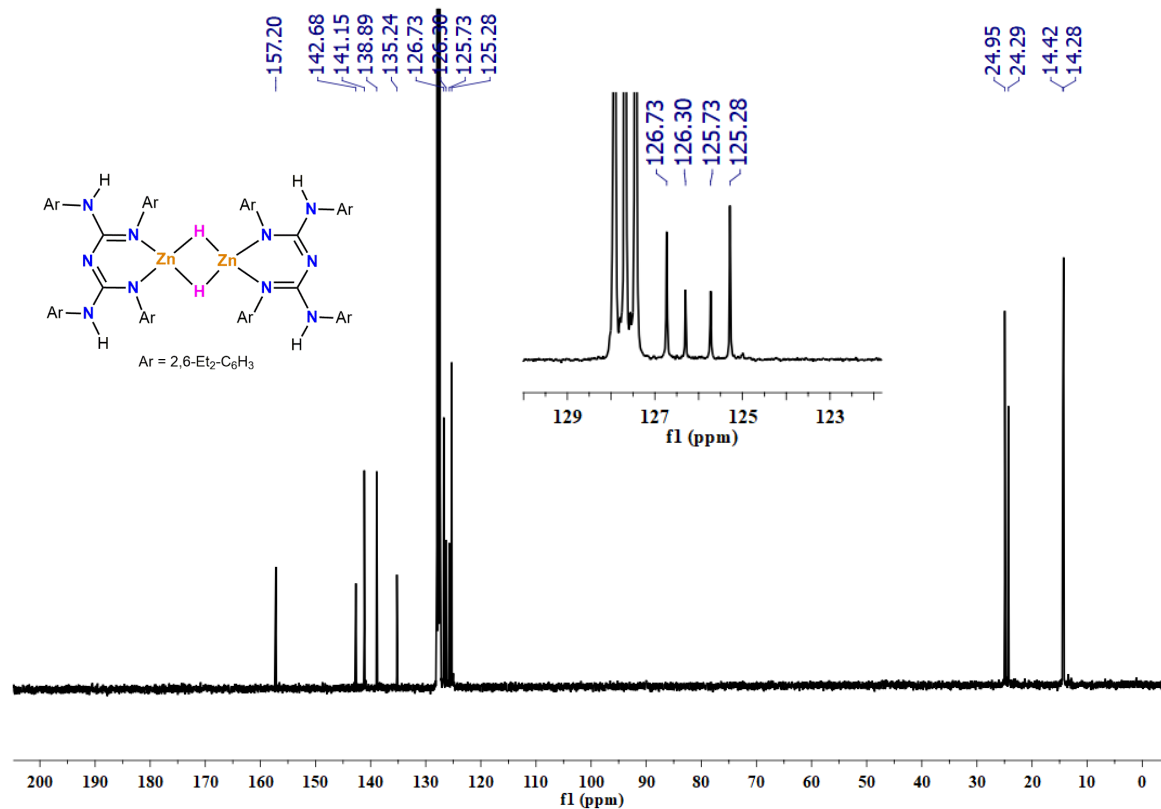


Figure 3.A.8. $^{13}C\{^1H\}$ NMR (100 MHz, 25 °C, C_6D_6) spectrum of $[LZnH]_2$, **3**.

1H , $^{13}C\{^1H\}$ NMR Spectra of Stoichiometric Reaction

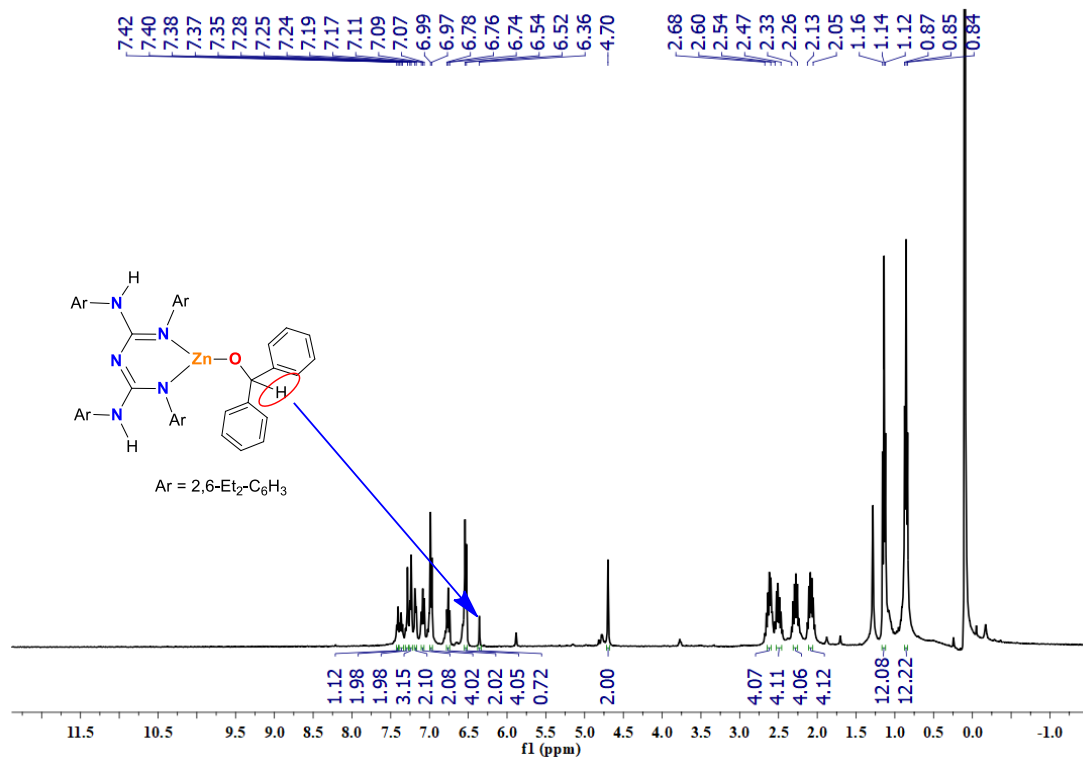


Figure 3.A.9. 1H NMR (400 MHz, 25 °C, $CDCl_3$) spectrum of $LZnOCHPh_2$, **(3B)**

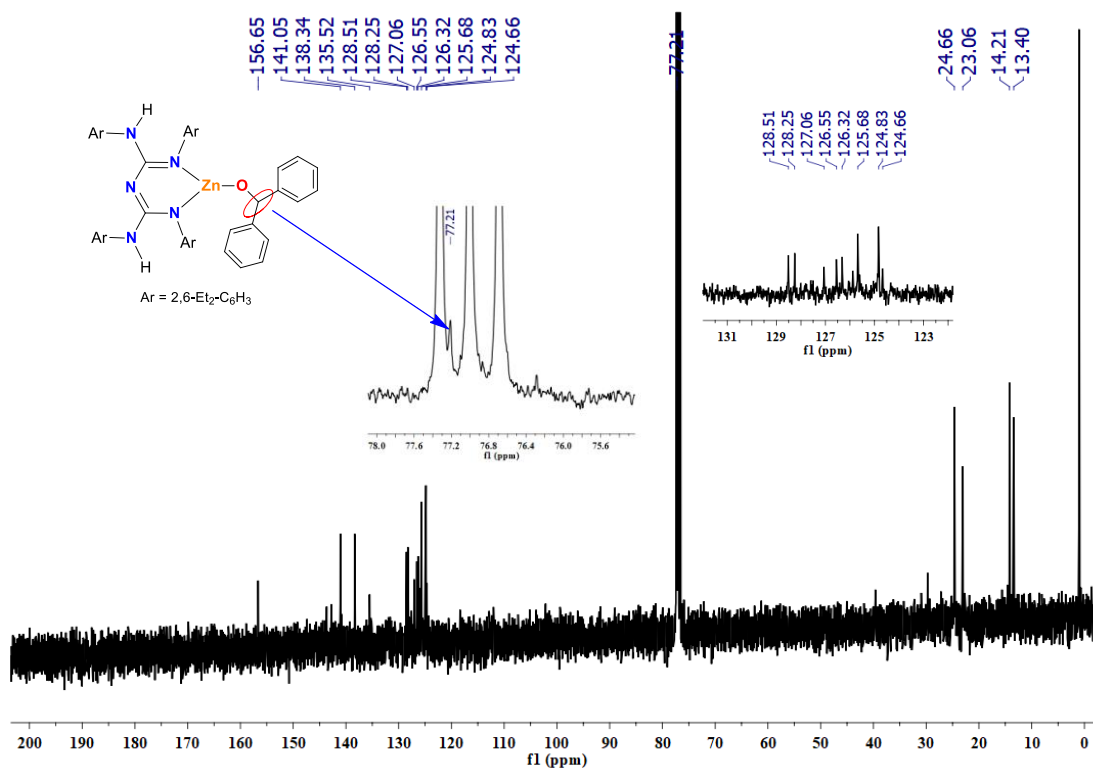


Figure 3.A.10. $^{13}\text{C}\{^1\text{H}\}$ NMR (400 MHz, 25 °C, CDCl_3) spectrum of LZnOCHPh_2 , (**3B**).

Chapter 3B

Zinc Hydride Catalyzed Chemoselective Hydroboration of Isocyanates: Amide Bond Formation and C=O Bond Cleavage

Published:

Sahoo, R. K.; Sarkar, N.; Nembenna, S. *Angew. Chem. Int. Ed.* **2021**, *60*, 11991-12000.

Abstract

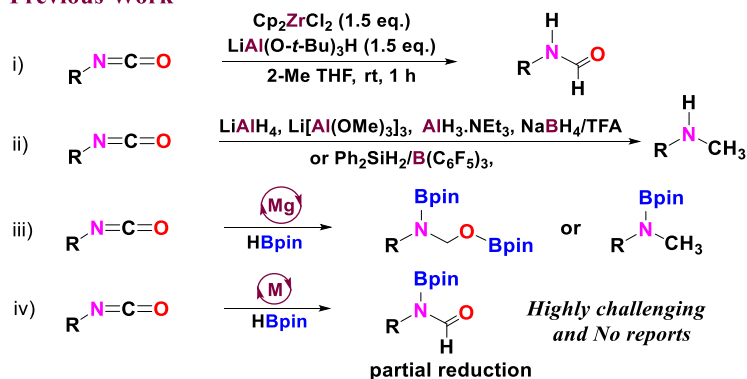
Herein, a remarkable conjugated bis-guanidinate (CBG) supported zinc hydride, [$\{LZnH\}_2$; L = $\{(ArHN)(ArN)-C=N-C=(NAr)(NHAr)$; Ar = 2,6-Et₂-C₆H₃}] (**I**) catalyzed partial reduction of heteroallenes via hydroboration is reported. A large number of aryl and alkyl isocyanates, including electron-donating and withdrawing groups, undergo reduction to obtain selectively N-boryl formamide, bis(boryl) hemiaminal and N-boryl methyl amine products. The compound **I** effectively catalyzes the chemoselective reduction of various isocyanates, in which the construction of the amide bond occurs. Isocyanates undergo a deoxygenation hydroboration reaction, in which the C=O bond cleaves, leading to N-boryl methyl amines. Several functionalities such as nitro, cyano, halide, and alkene groups are well-tolerated. Furthermore, a series of kinetic, control experiments and structurally characterized intermediates suggest that the zinc hydride species are responsible for all reduction steps and breaking the C=O bond.

3.B.1. Introduction

Isocyanates are cheaper and commercially available feedstocks that are very useful in numerous organic transformations.¹ These are essential precursors for the synthesis of extremely important amides.² In particular, formamides are necessary starting materials to produce useful heterocycles, bioactive compounds, and drugs.³ Generally, these formamides can be accessed using formylating agents such as formic acid, formaldehyde, formate, chloral, and carbon dioxide, thereby producing

a considerable waste.⁴ Conventional methods for amide bond creation are based on C-N bond-forming strategies utilizing carboxylic acid derivatives and amines.⁵ Formamides can be produced easily by the direct coupling of methanol with amines using organic or inorganic supported metal catalysts (C-N bond formation).⁶ Also, the recent trend of making amides involves metal-catalyzed C-C coupling with isocyanates.⁷

Previous Work



This Work

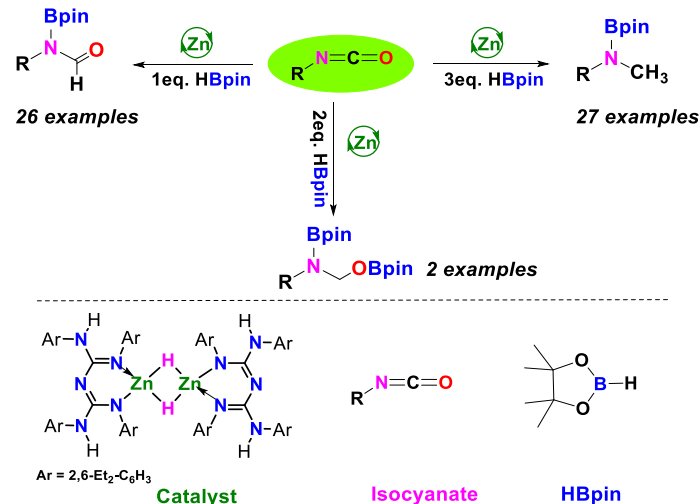


Figure 3.B.1. Production of formamides and N-methyl amines from isocyanates

Pace and coworkers reported the *in situ* generated Schwartz reagent (Cp_2ZrClH) mediated chemoselective reduction of isocyanates to formamides.^{2a,8} Before this elegant work, there were reports on amide synthesis by Grignard or other metal reagents and isocyanates' reaction.⁹

Despite the tremendous work on the metal-catalyzed hydroboration of unsaturated organic molecules,¹⁰ including heteroallenes such as carbon dioxide¹¹ and carbodiimides,¹² there have been no hydroboration reports of isocyanates to N-boryl formamides in the literature (*vide infra*). Nonetheless, to the best of our knowledge, there have been very few reports on selective monohydrosilylation of isocyanates to N-silyl formamide¹³ and hydrogenation of isocyanates to formamides.¹⁴

N-methyl amines are key intermediates in the production of fine chemicals, dyes, and natural products.¹⁵ Typically, the selective N-alkylation of primary amines utilizing CH₃I and (CH₃)₂SO₄ is challenging, and usually, over methylation occurs. Other methods are the metal-catalyzed reduction of CO₂ surrogates¹⁶ and direct amine alkylation with alcohols.¹⁷ However, these methods suffer from the use of hazardous chemicals and harsh reaction conditions.

Rueping et al. have shown the magnesium catalyzed hydroboration of formamide to N-methyl amine product.¹⁸ In 2015, Beller and coworkers reported commercially available Karstadt's complex/2,2':6',2''-terpyridine (tpy) catalyzed reductive methylation of amines with carbonates.¹⁹ In 2009, Zhang et al. reported the metal-free reduction of isocyanates to N-methyl amine using a Ph₂SiH₂/B(C₆F₅)₃ catalytic system.²⁰ Besides, there have been reports on the reduction of isocyanates by using stoichiometric amounts of metal reagents.²¹

As far as metal-catalyzed reduction of isocyanates is concerned, as shown in Figure 3.B.1, the ideal catalyst for the desired transformations should possess few significant features: a) Partial (chemoselective) reduction of isocyanates *via* hydroboration, the formation of N-boryl formamide, b) Reduction of isocyanates without cleavage of a C=O bond, N-, O- bis(boryl) hemiaminal c) Deoxygenated hydroboration of isocyanates that can lead to the formation of N-boryl methyl amines in which cleavage of C=O bond should occur.

In this context, Okuda group reported magnesium catalyzed dihydroboration of ^{tert}Butyl isocyanate with HBpin to N-, O-bis (boryl) hemiaminal.²² The metal-catalyzed deoxygenated reduction of amides to amines²³ is known, however as far as hydrodeoxygenation (HDO) of isocyanates is concerned, there are only three examples, including recently published two patents and one research paper in the literature.²⁴ In 2017, Hill and coworkers reported magnesium catalyzed hydroboration of isocyanates to N-boryl methyl amines.²⁵ The authors observed N-borylated formamide and N-,O-bis(boryl) hemiaminal species as intermediates during the reductive catalysis.

The catalytic application of molecular zinc hydrides in homogenous catalysis has advanced rapidly in recent years.²⁶ More recently, we developed a new β -diketiminato analogue, conjugated bis-guanidinate(CBG) stabilized zinc hydride complex, [$\{LZnH\}_2$; $L = \{(ArHN)(ArN)-C=N-C=(NAr)(NHAr)$; $Ar = 2,6-Et_2-C_6H_3\}$] (**I**) and used as a catalyst for hydrosilylation and hydroboration of ketones.²⁷ Herein, we report the unprecedented zinc hydride (**I**) catalyzed mono hydroboration, i.e., partial reduction of a wide range of aryl and alkyl isocyanates to N-borylated formamides for the first time. Further, zinc catalyzed dihydroboration and deoxygenated hydroboration of isocyanates to afford N-, O-bis(boryl) hemiaminal, and N-boryl methyl amines, respectively, have been investigated.

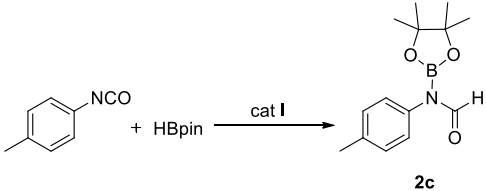
3.B.2. Results and Discussion

3.B.2.1. Monohydroboration

We began our study by exploring the conditions for the zinc catalyzed isocyanate monohydroboration reaction (Table 3.B.1). The reaction of 1:1 stoichiometric amounts of *p*-tolyl isocyanate and HBpin with 10 mol% catalyst **I** in a neat condition gave quantitative conversion to the monohydroborated product, N-borylated formamide after 6 h at room temperature. Decreasing

the catalyst loadings from 8 to 2 mol% gave a full conversion within 2 h in neat conditions. Moreover, the same reaction was performed in solvents such as benzene, toluene, THF, and acetonitrile by using a 2 mol % catalyst; in all cases, we observed the formation of the desired product in a quantitative yield. A negligible conversion (~3 %) was noticed in the absence of catalyst **I**, displaying that zinc hydride complex is necessary for isocyanates hydroboration. Next, we investigated the substrate scope of this zinc catalyzed organoisocyanates hydroboration reaction with favorable reaction conditions.

Table 3.B.1. Optimization of zinc hydride catalyzed hydroboration of *p*-tolyl isocyanate.^a



2c

entry	cat (mol%)	solvent	time (h)	yield (%) ^b
1	0	neat	2	3
2	10	neat	6	>99
3	8	neat	4	>99
4	5	neat	3	>99
5	3	neat	2	>99
6	2	neat	2	>99
7	0.5	neat	1	>99
8	0.25	neat	1	98
9	2	benzene	2	>99
10	2	toluene	2	>99
11	2	THF	2	>99
12	2	acetonitrile	2	>99

^aReaction conditions: *p*-tolyl isocyanate (0.3 mmol, 1.0 equiv.), pinacolborane (0.3 mmol, 1.0 equiv.), catalyst **I** (2 mol%, 8.0 mg), 2 h at rt under N₂. ^bYield was calculated by ¹H NMR spectroscopy based on isocyanate consumption and identified the NCHO signal at 8.93 ppm confirmed the product.

A wide range of aryl mono and diisocyanate and cyclic and acyclic (long-chain) alkyl isocyanates have been studied. All reactions went to completion within 4 h to afford quantitative yield (>99%) selective monohydroborated product, N-boryl formamide. The CBG zinc hydride proved to be a prototype chemoselective catalyst for synthesizing formamides from isocyanates. The various aryl mono isocyanates, including electron-donating (**1a-1h**) and withdrawing groups (**1i-1o**), were quantitatively converted into corresponding N-boryl formamide products (**2a-2h** and **2i-2o**). 4-Biphenyllyl and 1-Naphthyl isocyanates were also fully converted into corresponding N-boryl formamides (**2p** and **2q**).

A more difficult substrate, 1,4-phenylene diisocyanate, could be converted into a quantitative yield of 1,4-phenylene di-N-boryl formamide (**2r**). It is quite challenging due to the selective N-boryl formylation of diisocyanates vs. monoisocyanates. Both cyclic and acyclic isocyanates are also transformed into corresponding N-boryl formamides in quantitative yields (**2s-2z**) (Scheme 3.B.1). We did not observe any other side products in these reactions. Interestingly, we observed excellent chemoselectivity in the presence of other reducible functionalities such as nitro, cyano, halide, and alkene groups. We noticed that isocyanates bearing electron-withdrawing groups react much faster than those bearing electron-donating groups, owing to their high electrophilicity of the isocyanates' carbon atom. We calculated turn over number (TON) and turn over frequency (TOF) for one representative example, aryl isocyanate, i.e., *p*-tolyl isocyanate (**1c**), showcasing the high efficiency of the catalyst **I**. The catalytic performance of catalyst **I** in the monohydroboration of *p*-tolyl isocyanate exhibits TON 400 and TOF 400 h⁻¹ (Table 3.B.1, entry 8).

for 15 min; and **2i** – **2o** stirred for 10 min. The yield was calculated by ^1H NMR spectroscopy based on isocyanate consumption and identified the NCHO signal confirmed the product. Formamide (**2ee**, **2ff**, **2mm**, **2yy**) was isolated as a mixture of s-cis and s-trans isomers after hydrolysis in methanol. ^bcatalyst (0.25 mol %, 100 μL from stock solution in THF), *p*-tolyl isocyanate (0.3 mmol, 1.0 equiv.), pinacolborane (0.3 mmol, 1.0 equiv.), at rt. ^cFor **2r**, pinacolborane (0.6 mmol, 2.0 equiv.) was used. ^dFor **2u**, the yield was determined by ^1H NMR spectroscopy using nitromethane as the internal standard.

All N-boryl formamides (**2a-2z**) were characterized by multinuclear (^1H , $^{13}\text{C}\{^1\text{H}\}$ and ^{11}B) magnetic resonance and mass spectrometry methods. The ^1H NMR spectra exhibit a characteristic NCHO peak in the range of 8.55-9.19 ppm. The $^{13}\text{C}\{^1\text{H}\}$ NMR spectra of each reveal a signature peak for the NCHO in the range of 164.4-167.4 ppm. Moreover, the compound **2d**, N-boryl^{xyl}formamide, was confirmed by single-crystal X-ray structural analysis (Figure 3.B.2, left).

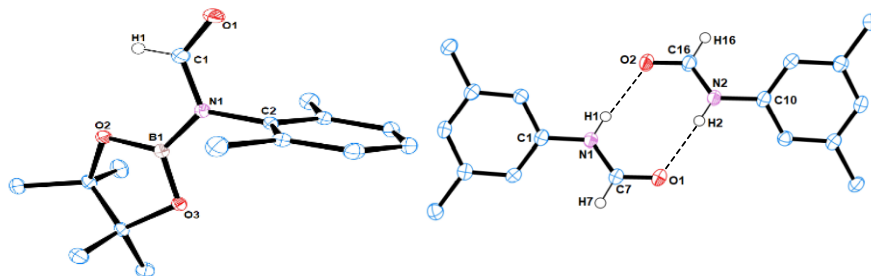


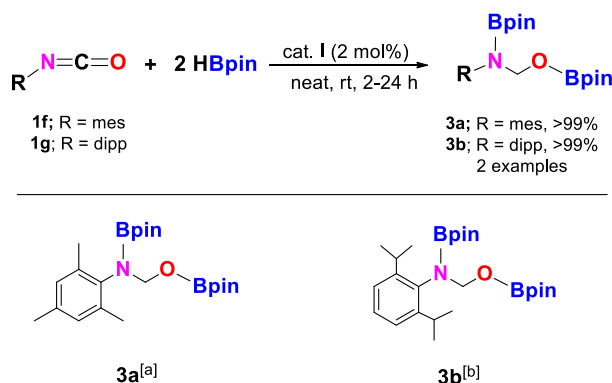
Figure 3.B.2. Molecular structures of **2d** (left) and **2ee** (right). The thermal ellipsoids are shown at 50% probability, and all the hydrogen atoms (except for H(1) from structure **2d** and H(7), H(16), from structure **2ee**) are deleted for clarity. Selected bond lengths (\AA) and angles (deg), For **2d** (left): O1–C1 1.2115(13), N1–C1 1.3718(13), N1–B1 1.4446(13), N1–C2 1.4485(12). O1–C1–N1 124.97(10), C1–N1–B1 119.88(9), C1–N1–C2 117.43(8). For **2ee** (right): O1–C7 1.2265(17), N1–C7 1.3443(18), N1–C1 1.4100(17). O1–C7–N1 124.64(13), C7–N1–C1 125.84(12). O2–C16 1.2327(17), N2–C16 1.3383(18), N2–C10 1.4144(17). O2–C16–N2 124.85(13), C16–N2–C10 124.22(12).

Bond parameters are consistent with Hill's only example of structurally characterized N-Borylated formamide, DippN(Bpin)HC(O).²⁵ Four examples of N-boryl formamides have been performed in 1 mmol scale reactions; moreover, these N-boryl formamides were hydrolyzed into their corresponding free formamides in 78-86% yields. These formamides were characterized by ^1H and $^{13}\text{C}\{^1\text{H}\}$ NMR spectra. The spectral data were well in agreement with those reported in the

literature.²⁸ Next, compound **2ee** was confirmed by single-crystal X-ray diffraction analysis. Compound **2ee** exists as a dimer in the solid-state, in which N-H...O hydrogen bonds link the molecules into the dimeric structure (Figure 3.B.2, right).

3.B.2.2. Dihydroboration

The addition of two equivalents of HBpin to either MesNCO (**1f**) or DippNCO (**1g**) in the presence of a zinc hydride catalyst 2 mol % at room temperature resulted in N-, O-bis(boryl) hemiaminal product (Scheme 3.B.2). In these cases, two hydride moieties were added to the electrophilic central carbon atom of bulky isocyanate, and two Bpin moieties were attached to both nucleophilic N and O atoms. Further, we attempted to expand the substrate scope with a few more aryl and alkyl isocyanate dihydroboration reactions. In all cases, the mixture of products was observed.



Scheme 3.B.2. Dihydroboration of isocyanates catalyzed by [LZnH]₂ complex (**I**).

Reaction conditions: ^a2,4,6-Trimethylphenyl isocyanate (0.3 mmol, 1.0 equiv.), pinacolborane (0.6 mmol, 2.0 equiv.), catalyst **I** (2 mol%), 2 h at rt under N₂. ^b2,6-Diisopropylphenyl isocyanate (0.3 mmol, 1.0 equiv.), pinacolborane (0.66 mmol, 2.2 equiv.), catalyst **I** (2 mol%), 24 h at rt under N₂. The yield was calculated by ¹H NMR spectroscopy based on isocyanate consumption and identified the NCH₂OBpin signal confirmed the product.

3.B.2.3. Hydrodeoxygenation: N-Boryl Methyl Amines

As mentioned before, as far as metal-catalyzed hydrodeoxygenation of isocyanates to N-boryl methyl amines is concerned, there are only three examples in the literature.

Thus, we decided to investigate the same isocyanates' deoxygenated hydroboration with HBpin by using catalyst **I**. We chose the same *p*-tolyl isocyanate as a model substrate for the deoxygenated hydroboration reaction. The reaction of *p*-tolyl isocyanate and HBpin in a 1:3 molar ratio with 10 mol % catalyst **I** in neat conditions at 70 °C temperature for 12 h gave the exclusively N-boryl methyl amine in a quantitative yield. A similar reaction conditions in the absence of catalyst **I**, we observed the mixture of products. We identified them as N-boryl formamide, N-, O-bis-(boryl) hemiaminal, and N-boryl methyl amine in a ratio 24:7:27 along with 42% unreacted *p*-tolyl isocyanate. Next, the same reaction was performed under similar conditions using lower catalyst loadings from 8 to 2 mol%. We noticed the formation of the N-boryl methyl amine product in a quantitative yield. No change in the yield was observed when the reactions were carried out in the solvents such as benzene, THF, toluene, and acetonitrile in standard reaction conditions (Table 3.B.2).

Further, we decided to extend the same isocyanate substrates with the optimized conditions in hand, utilized for the monohydroboration reaction. To our pleasure, in all cases (except **4w**), a quantitative conversion of isocyanates into their related N-borylated methyl amine was noticed (**4a-4z**) (Scheme 3.B.3). Like monohydroboration reaction, we observed the tolerance of halide, cyano, nitro, and alkene functionalities. However, it is worthy to note that a reaction of 4-cyano phenyl isocyanate treated with 5.0 equiv. HBpin in the presence of the catalyst **I** at room temperature for 24 h yielded the solely 4-cyano methyl N-boryl methyl amine product and the cyano group is untouched. However, the same reaction was carried out at higher temperatures (70 °C and 48h), both nitrile and NCO groups were reduced. The 1,4-phenylene diisocyanate (**1r**) upon treatment with 6.0 equiv. of HBpin at standard reaction conditions resulted in a quantitative yield of **4r**.

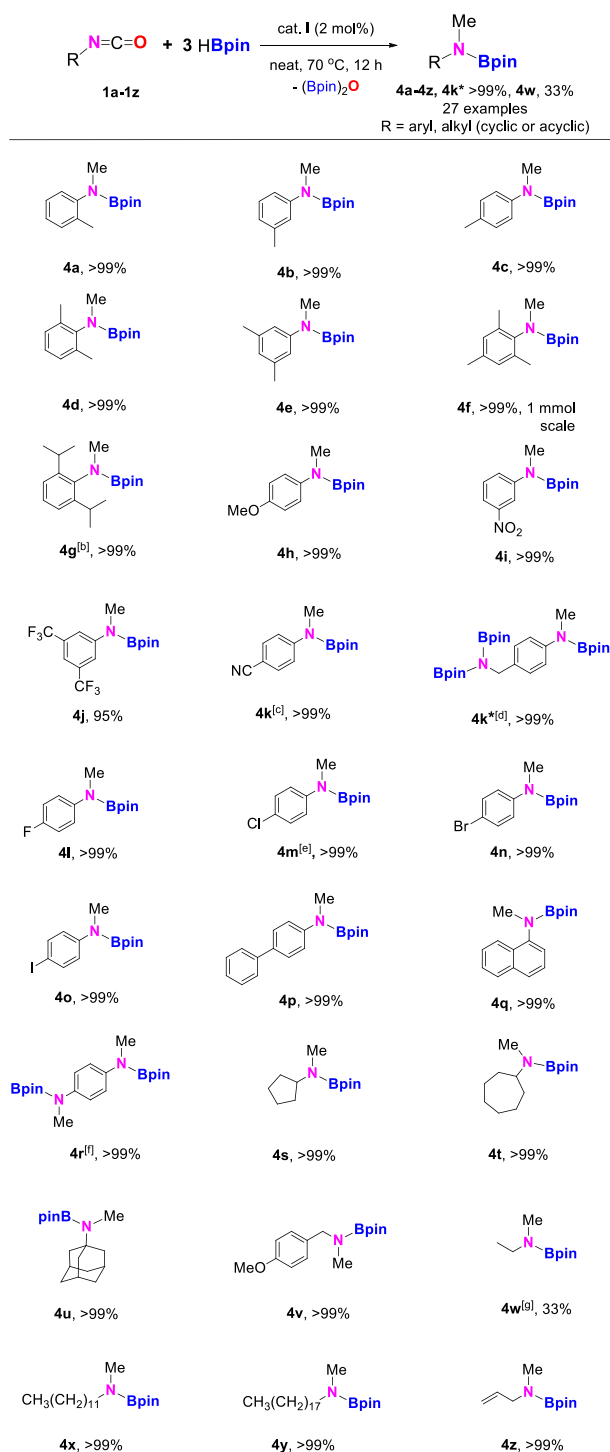
Table 3.B.2. Optimization of zinc hydride catalyzed hydroboration of *p*-tolyl isocyanate.^a

4c

entry	cat (mol%)	solvent	time (h)	yield (%) ^b
1	0	neat	12	27
2	10	neat	12	>99
3	8	neat	12	>99
4	5	neat	12	>99
5	2	neat	12	>99
6	2	benzene	12	>99
7	2	toluene	12	>99
8	2	THF	12	>99
9	2	acetonitrile	12	>99

^aReaction conditions: *p*-tolyl isocyanate (0.3 mmol, 1.0 equiv.), pinacolborane (0.9 mmol, 3.0 equiv.), catalyst **I** (2 mol%, 8.0 mg), 12 h at 70 °C under N₂. O(Bpin)₂ is the side product. ^bThe yield was calculated by ¹H NMR spectroscopy based on isocyanate consumption and identified the NCH₃ signal at 3.07 ppm confirmed the product.

It was observed that isocyanates bearing electron-withdrawing groups require less reaction time than the electron-donating groups. All N-boryl methyl amine products were characterized by multinuclear (¹H, ¹³C{¹H} and ¹¹B) magnetic resonance and mass spectrometric techniques. All N-boryl methylamine and side product, bis(boryl)oxide, O(Bpin)₂²⁹ were characterized by the occurrence of a singlet methyl ¹H NMR resonance in the range 2.10-3.14 ppm and a singlet resonance in the upfield region, which corresponds to twenty-four protons of O(Bpin)₂. The ¹³C{¹H} NMR spectra exhibit an N-CH₃ in the range of 28-38 ppm. The ¹¹B NMR spectra of each reveal two peaks, one peak for the N-B resonance at ca. 20.20-24.68, which was assigned to N-boryl methyl amine product and a byproduct peak of O(Bpin)₂.



Scheme 3.B.3. Deoxygenative hydroboration of isocyanates catalyzed by [LZnH]₂ complex (**I**)^a

^aReaction conditions: isocyanates (0.3 mmol, 1.0 equiv.), pinacolborane (0.9 mmol, 3.0 equiv.), catalyst **I** (2 mol%), 12 h at 70 °C under N₂. The yield was calculated by ¹H NMR spectroscopy based on isocyanate consumption and identified the NCH₃ signal confirmed the product. ^bFor **4g**, 18 h. ^cFor **4k**, pinacolborane

(5.0 eq.), neat, rt, 24 h was used. ^dFor **4k***, pinacolborane (5.0 eq.), neat, 70 °C, 48 h was used. ^eFor **4m**, rt, 2 h. ^fFor **4r**, pinacolborane (6.0 eq.), neat, 70 °C, 12 h was used. ^gFor **4w**, the yield was determined by ¹H NMR spectroscopy using nitromethane as the internal standard.

3.B.2.4. Kinetics

The catalytic reactivity was evaluated by *in situ* monitoring (¹H NMR spectroscopy) of a reaction of HBpin and *p*-Bromophenyl isocyanate (**1n**) catalyzed by 2 mol% of **I** at rt to 70 °C. Figure 3.B.3 demonstrates the reaction's progress over 360 minutes and reveals a successive formation of N-boryl formamide, N-, O-bis-(boryl) hemiaminal, and N-boryl methyl amine products. In the initial stages of the reaction, the formation of the N-boryl formamide, 4-BrPh(Bpin)HC(O) (**2n**), was confirmed by the emergence of a downfield singlet peak at 8.81 ppm at room temperature (indicated by ♦ Figure 3.B.3).

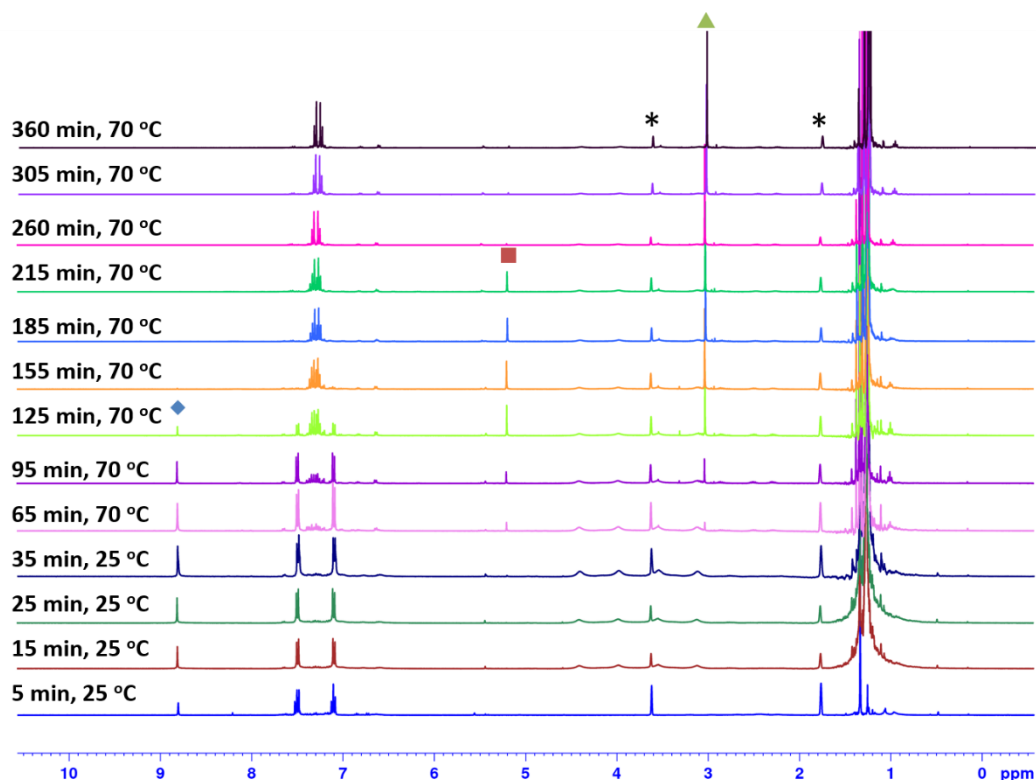


Figure 3.B.3. Stacked ¹H NMR spectra (400 MHz) for the reaction of 4-Bromophenyl isocyanate (**1n**) (0.3 mmol, 1.0 equiv.) and pinacolborane (0.9 mmol, 3.0 equiv.), and catalyst **I** (2 mol%) in THF-d₈. Spectra recorded at different temperature and time intervals between T = 25 °C to 70 °C and t = 5 min-360 min

respectively. \blacklozenge = 4-BrPhN(Bpin)HC(O), \blacksquare = 4-BrPhN(Bpin)CH₂OBpin, \blacktriangle = 4-BrPhN(Bpin)CH₃, * = residuals peak of THF-d₈.

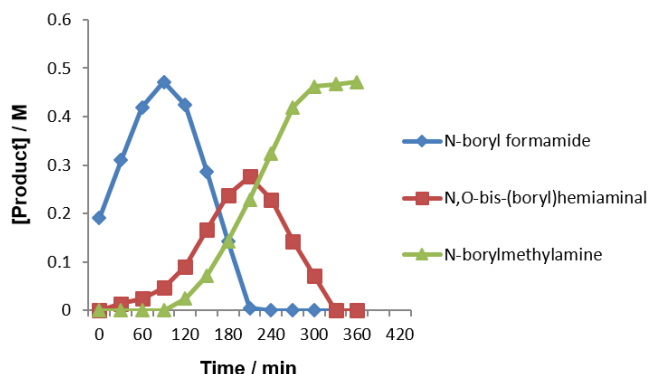


Figure 3.B.4. The plot of [product] versus time for hydroboration of 4-BrPhNCO catalyzed by 2 mol% **I** at rt-70 °C. \blacklozenge = 4-BrPhN(Bpin)HC(O), \blacksquare = 4-BrPhN(Bpin)CH₂OBpin, \blacktriangle = 4-BrPhN(Bpin)CH₃

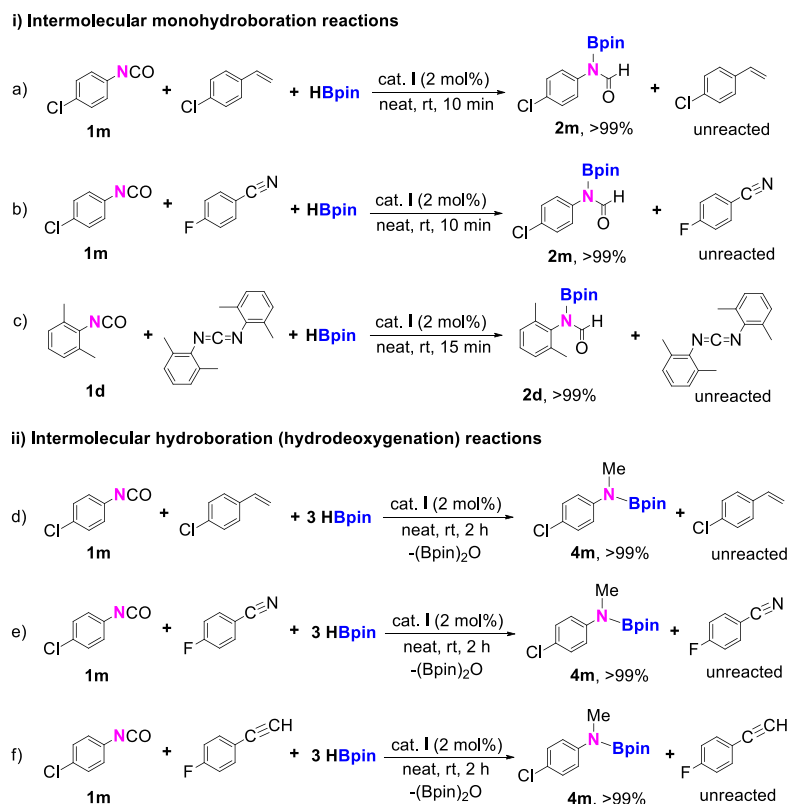
Next, when raised the temperature to 70 °C, the appearance of characteristic peaks at 3.03 ppm and 5.20 ppm corresponding to N-borylated methyl amine (\blacktriangle) and N-, O-(bis)-boryl hemiaminal (\blacksquare) products and complete disappearance of 4-BrPhN(Bpin)HC(O) (**2n**) was noticed. After completing 360 minutes, an exclusively hydrodeoxygenated product (C=O bond cleavage), N-boryl methyl amine, 4-BrPhN(Bpin)Me (**4n**), along with O(Bpin)₂, and no other side products were observed.

Kinetics experiments suggest that the reaction proceeds through a sequential order of mechanism and give evidence for primarily formed formamide and hemiaminal re-insertion into the catalytic cycle for further reduction to N-methyl amine (Figure 3.B.4). The N-methyl amine formation represents a sigmoidal curve akin to previous work on magnesium mediated hydrodeoxygenation of isocyanates described by Hill and coworkers.

3.B.2.5. Intermolecular Chemoselective Reactions

Most importantly, we have further shown zinc hydride catalyzed intermolecular chemoselective hydroboration of isocyanates over alkene, nitrile, carbodiimide, and alkyne substrates for the

partial (monohydroboration) and full reduction reactions. One equivalent *p*-chlorophenyl isocyanate, 1 equiv. *p*-chloro styrene and HBpin were mixed with catalyst **I** (2 mol%) under neat conditions at ambient temperature for 10 minutes, which afforded the N-borylated formamide in the quantitative yield in preference to the *p*-chlorostyrene. Similarly, at the same reaction conditions, *p*-chlorophenyl isocyanate gives the monohydroborated product, N-borylated formamide, in a quantitative yield over *p*-fluorobenzonitrile. Next, equimolar amounts of 2,6-dimethyl phenyl isocyanate and ^{xy}lcarbodiimide and HBpin were mixed with catalyst **I** under solvent-free conditions at room temperature for 15 minutes, which produced the N-borylated formamide over the aryl carbodiimide (Scheme 3.B.4). We further examined the catalytic performance of **I** in the intermolecular chemoselective deoxygenative reduction between isocyanate and alkene or nitrile or alkyne.



Scheme 3.B.4. Intermolecular chemoselective hydroboration catalyzed by [LZnH]₂ complex (**I**).

Thus, one equivalent of *p*-chlorophenyl isocyanate, 1.0 equiv. *p*-chloro styrene and 3.0 equiv. HBpin were combined with catalyst **I** (2 mol%) under neat conditions at ambient temperature for 2 h, which provided the N-boryl methyl amine in the full conversion of aryl isocyanate priority the alkene. Likewise, at similar reaction conditions, *p*-chlorophenyl isocyanate was reduced to N-boryl methyl amine in a quantitative yield over either nitrile or alkyne (Scheme 3.B.4).

3.B.2.6. Control Experiments

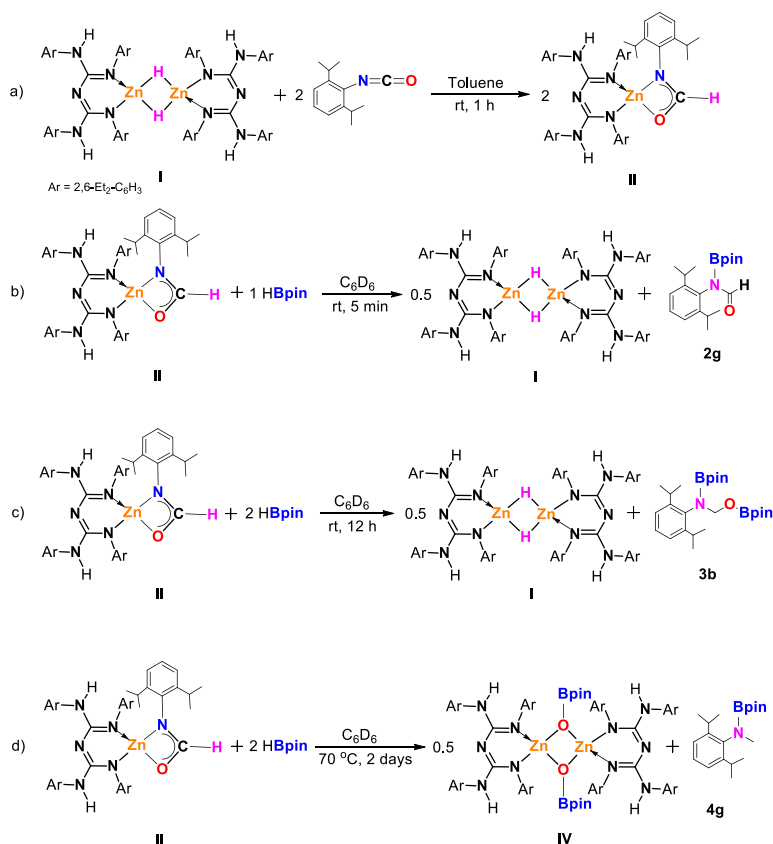
To understand the zinc catalyzed sequential hydroboration of isocyanates to N-boryl formamide, bis(boryl)hemiaminal, and N-boryl methyl amine products, we performed some control experiments. The catalyst **I** treated with two equivalents of DippNCO in toluene at room temperature for 1 h led to zinc formamidate complex (**II**). In this case, the insertion of Zn-H moiety into the carbonyl of RNCO occurred. The intermediate **II** was confirmed by ^1H and $^{13}\text{C}\{^1\text{H}\}$ NMR, IR and mass spectrometric methods.

The ^1H NMR spectrum indicates the formation of zinc formamidate complex by the disappearance of Zn-H (4.52 ppm) resonance and appearance of a new characteristic peak at 7.93 ppm (NCHO), which is well in agreement with NacNac magnesium formamidate complex (7.92 ppm).²⁵ The $^{13}\text{C}\{^1\text{H}\}$ NMR spectrum exhibits a peak at 172.2 ppm, assigned to NCHO. Moreover, the formation of compound **II** was confirmed by the HRMS analysis. It is worthy to note that there have been no reports on structurally characterized molecular zinc hydride insertion into isocyanates, zinc formamidate complexes (*vide infra*). However, Schulz et al. reported zinc amidinato/formamido complexes by zinc hydride reaction with isocyanate.³⁰ Parkin and coworkers reported structurally characterized zinc formate and isocyanate complexes.³¹

Next, a 1:1 stoichiometric reaction between zinc formamidate complex and HBpin has been carried out in C_6D_6 in a J Young valve NMR tube. An immediate formation of compounds **I** and **2g** was

observed by the ^1H and $^{13}\text{C}\{^1\text{H}\}$ NMR spectra. Further, a 1:2 stoichiometric reaction between compound **II** and HBpin was performed in C_6D_6 at room temperature for 12 h in a J Young valve NMR tube.

We noticed the formation of CBG zinc hydride (**I**) and bis-hemiaminal (**3b**). Furthermore, a 1:2 stoichiometric reaction between compound **II** and HBpin has been conducted in C_6D_6 at 70°C for 2 days. We observed the CBG zinc boryloxide (**IV**) and N-boryl amine (**4g**) products



Scheme 3.B.5. Control experiments

by NMR studies (Scheme 3.B.5). Furthermore, the X-ray crystal structures of both zinc compounds **II** and **IV** were determined and are depicted in Figure 3.B.5. To the best of our knowledge, these are the first examples of zinc formamidate and zinc boryl oxide, which were structurally authenticated by X-ray crystallography. Compound **II**'s solid structure revealed a monomeric due

to the steric requirements of one N-Dipp (2,6-*i*Pr₂-C₆H₃) and two N-Dep (2,6-Et₂-C₆H₃) substituents. The C-O bond's cleavage evidences CBG zinc boryl oxide formation either from **II** or N,O- bis hemiaminal species. Like closely related structurally characterized nacnac magnesium boryl complexes,^{25,32} zinc boryl oxide compound **IV** is dimeric.

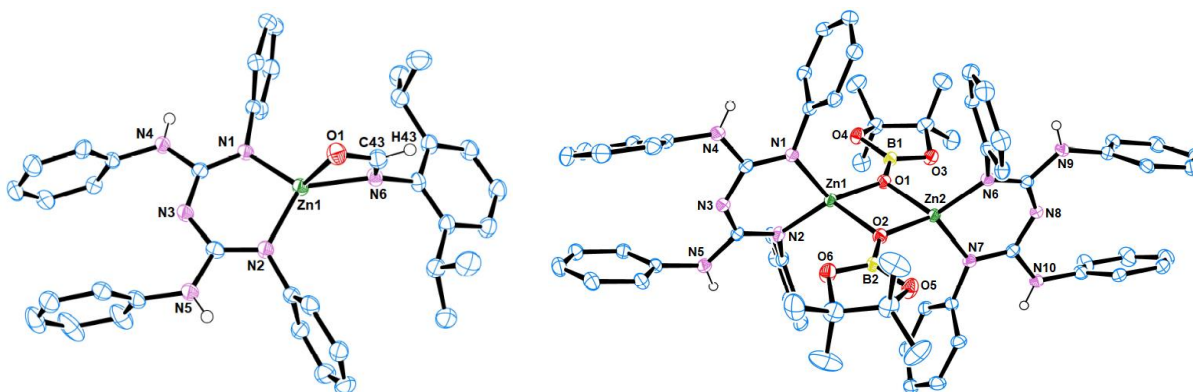
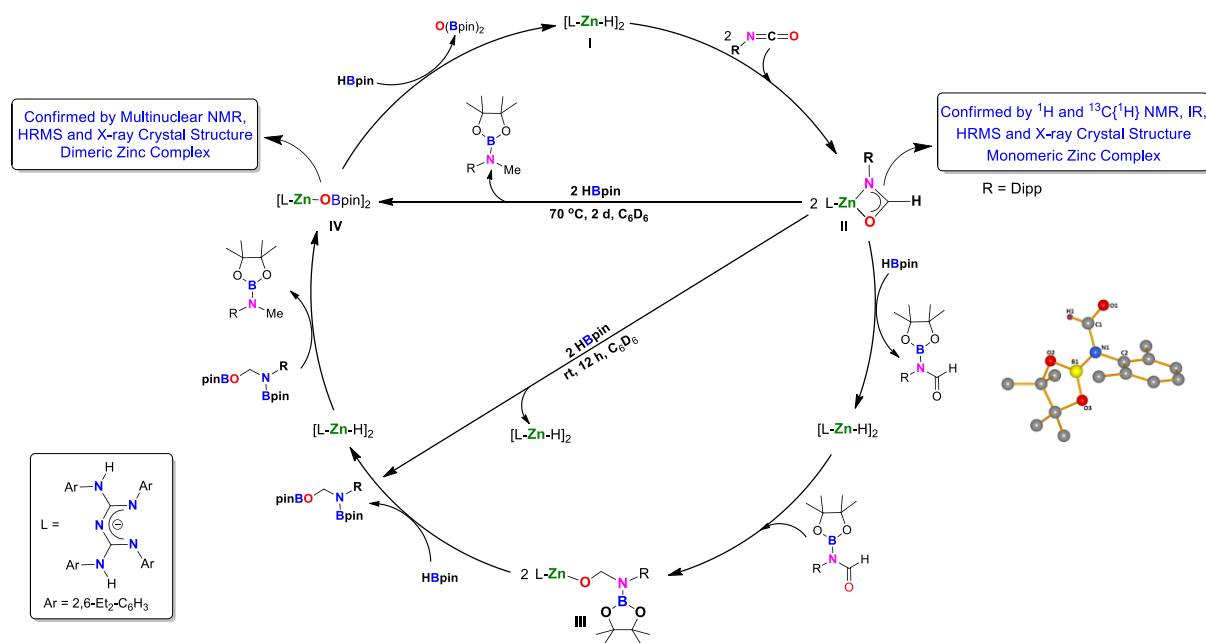


Figure 3.B.5. Molecular structures of **II** (left) and **IV** (right). The thermal ellipsoids are shown at 50% probability, and all the hydrogen atoms (except for H(4), H(5), and H(43) from structure **II** and H(4), H(5), H(9) and H(10) from structure **IV**) and ethyl groups have been removed for clarity. Selected bond lengths (Å) and angles (deg), For **II** (left): Zn1-O1 2.1732(18), Zn1-N1 1.945(2), Zn1-N2 1.9386(19), Zn1-N6 2.0143(19), Zn1-C43 2.4210, O1-C43 1.272(3); O1-Zn1-N1 118.27(8), O1-Zn1-N2 113.67 (7), O1-Zn1-N6 63.95(7), O1-Zn1-C43 31.562(1), N1-Zn1-N6 132.47(8), N1-Zn1-C43 133.101(1), N2-Zn1-N1 97.33(8), N2-Zn1-N6 126.54(8), N2-Zn1-C43 125.296(1), N6-Zn1-C43 32.398(1). For **IV** (right): Zn1-N1 1.956(3), Zn1-N2 1.953(3), Zn2-N6 1.959(3), Zn2-N7 1.954(3), Zn1-O1 2.019(3), Zn1-O2 1.954(2), Zn2-O1 1.963(3), Zn2-O2 2.014(2), Zn1-Zn2 2.9973(5); N1-Zn1-N2 95.76(12), N6-Zn2-N7 96.33(12), O1-Zn1-O2 82.17(10), O1-Zn1-N1 115.20(11), O1-Zn1-N2 119.70(11), O1-Zn2-N6 125.43(12), O1-Zn2-N7 121.13(11), O2-Zn1-N1 121.64(11), O2-Zn1-N2 124.38(11), O2-Zn2-N6 117.83(12), O2-Zn2-N7 115.75(11), Zn1-O1-Zn2 97.66(11), Zn1-O2-Zn2 98.10(11), B1-O1-Zn1 127.8(2), B2-O2-Zn1 134.0(2), B1-O1-Zn2 134.5(2), B2-O2-Zn2 127.9(2).

3.B.2.7. Catalytic Cycle

Based on the above kinetic and control experiments, a catalytic cycle has been proposed for the zinc mediated hydroboration of isocyanates to N-boryl formamide, bis(boryl)hemiaminal, N-boryl methyl amine products (Scheme 3.B.6). In the first step, a reaction between 1:2 stoichiometric

amounts CBG zinc hydride (**I**) and isocyanate (DippNCO) afforded CBG zinc formamidinate complex (**II**). Next, a reaction between intermediate **II** and HBpin afforded the N-boryl formamide and regeneration of a catalyst **I**. Further, catalyst **I** reacts with N-boryl formamide led to the formation of intermediate **III**. The appearance of N-, O-bis(boryl) amine, and regeneration of compound **I** occurred by the reaction of Int **II** and HBpin. Alternatively, the formation of N-, O-bis(boryl) amine, and **I** can be accessed by the direct reaction between int **II** and two equiv. of HBpin in C₆D₆ at rt for 12 h. A reaction between N-, O- bis(boryl) amine, and catalyst **I** allowed the formation of N-boryl methyl amine and CBG zinc boryl oxide, Int **IV**'s establishment.



Scheme 3.B.6. Proposed mechanism

Moreover, a 1:2 stoichiometric ratio of compound **II** and HBpin in C₆D₆ at 70 °C resulted in CBG zinc boryl oxide and N-boryl methyl amine products. Finally, Int **IV** reacts HBpin allowed the regeneration of catalyst **I** and O(Bpin)₂ as a byproduct and closed the catalytic cycle (Scheme 3.B.6).

3.B.3. Conclusion

The zinc catalyzed exceptional chemoselective reduction of isocyanates via hydroboration is described for the first time. A wide range of aryl and cyclic, acyclic, long-chain alkyl isocyanates have been transformed into the corresponding N-boryl formamides. Moreover, diisocyanate could be efficiently converted into either di-N-borylformamide or di-N-boryl methyl amine products. Further, we described an excellent protocol for the catalytic transformation of isocyanates to secondary methyl amines through zinc-mediated C=O bond cleavage (hydrodeoxygenation of isocyanates). More importantly, we have shown intra and intermolecular chemoselective hydroboration of isocyanates over other various reducible functionalities. Mechanistic investigations studies indicate that Zn-H moiety insertion into $\text{RN}=\text{C}=\text{O}$ to afford CBG zinc formamidinato II product and subsequent addition of 1.0 equiv. of HBpin, 2.0 equiv. of HBpin, and 3.0 equiv. of HBpin to yield outcomes, N-boryl formamide, N-, O-bis(boryl) hemiaminal, and N-boryl methyl amine, respectively, via sigma bond metathesis. This is the first report on the metal-catalyzed synthesis of amides through B-H bond activation by using isocyanates as precursors. The catalytic regeneration of the Zn-H bond and C=O bond cleavage open new possibilities for zinc hydrides in catalysis.

3.B.4. General Experimental Methods

All air and moisture sensitive reactions were performed using standard glove box and Schlenk line techniques under an inert atmosphere of nitrogen. Catalysis reactions were conducted in J. Young valve sealed NMR tubes or sealed reaction vials as per the requirement. The ^1H , $^{13}\text{C}\{^1\text{H}\}$, and ^{11}B NMR spectra were recorded on 400 MHz Bruker DPX spectrometer using dried deuterated solvents with chemical shifts given in parts per million. The chemical shift (δ ppm) in ^1H and $^{13}\text{C}\{^1\text{H}\}$ NMR spectra were referenced to the deuterated solvent's residual proton signals and an

external $\text{BF}_3\cdot\text{OEt}_2$ standard for ^{11}B . The solvents used for the synthesis and NMR experiments were dried, distilled, and degassed before use by standard methods. All reagents were purchased from Sigma-Aldrich Co. Ltd., Merck India Pvt. Ltd., TCI chemicals, and Alfa Aesar and were used without further purification. $[\{\text{LZnH}\}_2; (\text{L} = \{(\text{ArNH})(\text{ArN})-\text{C}=\text{N}-\text{C}=(\text{NAr})(\text{NHAr})\}; \text{Ar} = 2,6\text{-Et}_2\text{-C}_6\text{H}_3)]$ (**1**) was synthesized according to literature procedure.²⁷

Synthesis of $[\text{LZnOC}(\text{H})\text{N}(2,6\text{-}^i\text{Pr}_2\text{C}_6\text{H}_3)]$, (I**):** A solution of complex **1** (0.250 g, 25 °C, 0.179 mmol) dissolved in ~10 mL of dry toluene. Also, 2,6-diisopropyl phenyl isocyanate (76.83 μL , 0.359 mmol) was dissolved in ~5 mL of dry toluene in another Schlenk tube. The reaction mixture was stirred for 1 h resulted in the formation of compound **I** was observed by ^1H NMR spectroscopy. Then removed the solvent in vacuum to yield a white crystalline solid a dry hexane was added. The product **I** was crystallized in the form of block shaped crystals suitable for X-ray diffraction at -20 °C after 24 h. (0.216 g, Yield 67 %); Mp °C. ^1H NMR (400 MHz, C_6D_6) δ 7.93 (s, 1H), 7.13 (s, 3H), 7.10 – 7.05 (m, 3H), 7.04 – 6.97 (m, 3H), 6.87 (t, $^3J_{\text{HH}} = 7.6$ Hz, 2H), 6.63 – 6.61 (d, $^3J_{\text{HH}} = 7.6$ Hz, 4H), 5.02 (s, 2H), 3.29 – 3.20 (m, 4H), 2.88 – 2.79 (m, 4H), 2.46 – 2.37 (m, 4H), 2.31 – 2.18 (m, 6H), 1.23 (t, $^3J_{\text{HH}} = 7.5$ Hz, 12H), 0.95 (t, $^3J_{\text{HH}} = 7.6$ Hz, 12H), 0.89 – 0.79 (m, 12H). $^{13}\text{C}\{^1\text{H}\}$ NMR (100 MHz, C_6D_6) δ 172.2, 157.5, 144.2, 142.3, 141.0, 139.3, 138.6, 135.1, 126.3, 126.2, 125.8, 125.4, 125.1, 122.7, 29.8, 27.8, 24.9, 23.7, 14.2, 13.6. HRMS (ESI) m/z : $[\text{M} + \text{Na}]^+$ Calcd for $\text{C}_{55}\text{H}_{72}\text{N}_6\text{OZnNa}$ 919.4951, Found: 919.4988.

Synthesis of $[\text{LZnH}]_2$ & **2g {NMR-Scale}:** The addition of HBpin (8.27 μL , 0.056 mmol) to a J. Young valve NMR tube containing a solution of compound **II** (0.056 mmol) in C_6D_6 resulted in the immediate formation of compound **1** and **2g** was observed by ^1H NMR spectroscopy. NMR Yield: (>99%). ^1H NMR (400 MHz, C_6D_6) δ 9.23 (s, 1H), 7.11 – 7.06 (m, 9H), 6.89 (t, $^3J_{\text{HH}} = 7.5$ Hz, 2H), 6.65 – 6.63 (d, $^3J_{\text{HH}} = 7.9$ Hz, 4H), 4.99 (s, 2H), 4.47 (s, 1H), 3.08 – 2.94 (m, 6H), 2.74

– 2.65 (m, 4H), 2.41 – 2.32 (m, 4H), 2.21 – 2.12 (m, 4H), 1.29 (t, $^3J_{\text{HH}} = 7.5$ Hz, 12H), 1.23 – 1.22 (d, $^3J_{\text{HH}} = 8.0$ Hz, 6H), 1.21 – 1.20 (d, $^3J_{\text{HH}} = 8.1$ Hz, 6H), 0.99 (t, $^3J_{\text{HH}} = 7.6$ Hz, 12H), 0.94 (s, 12H). $^{13}\text{C}\{^1\text{H}\}$ NMR (100 MHz, C_6D_6) δ 164.2, 157.2, 145.5, 142.7, 141.1, 138.9, 135.2, 128.2, 126.7, 126.3, 125.7, 125.2, 123.4, 83.8, 28.8, 24.9, 24.5, 24.2, 23.9, 23.8, 23.7, 14.2. ^{11}B NMR (128 MHz, C_6D_6) δ 25.31.

Synthesis of [LZnH]₂ & 3b {NMR-Scale}: Addition of HBpin (15.02 μL , 0.102 mmol) to a J. Young valve NMR tube containing a solution of compound **I** (0.051 mmol) in C_6D_6 after 12 h at room temperature formation of compound **1** and **3b** was observed by ^1H NMR spectroscopy. NMR Yield: (>99%). ^1H NMR (400 MHz, C_6D_6) δ 7.14– 7.12 (m, 3H), 7.09 (s, 6H), 6.89 (t, $^3J_{\text{HH}} = 7.5$ Hz, 2H), 6.65 – 6.63 (d, $^3J_{\text{HH}} = 7.9$ Hz, 4H), 5.39 (s, 2H), 4.99 (s, 2H), 4.50 (s, 1H), 3.61 – 3.54 (m, 2H), 3.06 – 2.97 (m, 4H), 2.76 – 2.66 (m, 4H), 2.42 – 2.33 (m, 4H), 2.22 – 2.13 (m, 4H), 1.43 – 1.41 (d, $^3J_{\text{HH}} = 8.0$ Hz, 6H), 1.33 – 1.28 (m, 18H), 1.09 (s, 6H), 1.01 (s, 6H), 0.95 (t, $^3J_{\text{HH}} = 7.4$ Hz, 12H), 0.89 (s, 12H). $^{13}\text{C}\{^1\text{H}\}$ NMR (100 MHz, C_6D_6) δ 157.1, 147.4, 142.6, 141.1, 138.8, 137.8, 135.2, 127.1, 126.6, 126.3, 125.7, 125.2, 123.5, 82.5, 81.9, 77.2, 28.2, 24.9, 24.9, 24.2, 24.1, 23.6, 14.3, 14.2. ^{11}B NMR (128 MHz, C_6D_6) δ 24.05, 21.74.

Synthesis of III & 4g {NMR-Scale}: Addition of HBpin (15.02 μL , 0.102 mmol) to a J. Young valve NMR tube containing a solution of compound **I** (0.051 mmol) in C_6D_6 . The reaction mixture was heated at 70 $^\circ\text{C}$ h for 2 days formation of compounds **III** and **4g** was observed by ^1H NMR spectroscopy. NMR Yield: (>99%). ^1H NMR (400 MHz, C_6D_6) δ 7.10 (s, 3H), 7.09 – 7.08 (m, 6H), 6.88 (t, $^3J_{\text{HH}} = 7.6$ Hz, 2H), 6.64 – 6.62 (d, $^3J_{\text{HH}} = 8.0$ Hz, 4H), 5.00 (s, 2H), 3.40 – 3.33 (m, 4H), 3.05 – 2.98 (m, 4H), 2.91 (s, 6H), 2.75 – 2.65 (m, 4H), 2.40 – 2.31 (m, 4H), 2.21 – 2.11 (m, 4H), 1.33 – 1.32 (d, $^3J_{\text{HH}} = 8.0$ Hz, 12H), 1.29 (t, $^3J_{\text{HH}} = 7.5$ Hz, 12H), 1.24 – 1.22 (d, $^3J_{\text{HH}} = 8.0$ Hz, 12H), 1.17 (s, 6H), 1.08 (s, 6H), 1.00 (s, 12H), 0.94 (t, $^3J_{\text{HH}} = 7.4$ Hz, 12H). $^{13}\text{C}\{^1\text{H}\}$ NMR

(100 MHz, C₆D₆) δ 157.2, 146.6, 142.3, 141.3, 141.1, 138.8, 135.1, 126.7, 126.7, 126.3, 125.8, 125.2, 123.6, 82.5, 82.1, 81.5, 37.8, 27.9, 24.9, 24.6, 24.3, 24.2, 24.0, 14.3, 14.2. ¹¹B NMR (128 MHz, C₆D₆) δ 23.95, 21.67. HRMS (ESI) m/z : [M + H]⁺ Calcd for C₉₆H₁₃₃B₂N₁₀O₆Zn₂ 1671.9200, Found: 1671.9248; m/z : [M/2 + H]⁺ Calcd for C₄₈H₆₇BN₅O₃Zn 836.4631, Found: 836.4647.

3.B.4.1. X-ray Crystallography

The single crystal of compound **II** was crystalized from hexane at -20 °C as colorless blocks after 24 h and **IV**, **2d** and **2ee** were crystalized from toluene at rt as colorless blocks after 24 h. The crystal data of compounds **II**, **IV**, **2d** and **2ee** were collected on a Rigaku Oxford diffractometer at 100 K. Selected data collection parameters and other crystallographic results are summarized in Table 3.B.3. The structure was determined using direct methods employed in *ShelXT*,³³ *OleX*,³⁴ and refinement was carried out using least-square minimization implemented in *ShelXL*.³⁵ All non-hydrogen atoms were refined with anisotropic displacement parameters. Hydrogen atom positions were fixed geometrically in idealized positions and were refined using a riding model.

Table 3.B.3. Crystallographic data and refinement parameters for compound **II**, **IV**, **2d** and **2ee**

Compound	II	IV	2d	2ee
Empirical Formula	C ₅₅ H ₇₂ N ₆ OZn	C ₉₆ H ₁₃₂ B ₂ N ₁₀ O ₆ Zn ₂	C ₁₅ H ₂₂ BNO ₃	C ₉ H ₁₁ NO
CCDC	2052422	2052423	2052424	2052425
Molecular mass	898.55	1674.47	275.14	149.19
Temperature (K)	100	100	100	100
Wavelength (Å)	1.54184	1.54184	1.54184	1.54184
Size(mm)	0.2 × 0.18 × 0.17	0.12 × 0.09 × 0.08	0.2 × 0.18 × 0.17	0.14 × 0.11 × 0.09
Crystal system	Monoclinic	Monoclinic	monoclinic	triclinic
Space group	<i>P</i> 2 ₁ / <i>c</i>	<i>I</i> a	<i>C</i> 2/ <i>c</i>	<i>P</i> -1
<i>a</i> (Å)	22.3023(4)	24.9885(2)	23.6454(3)	7.9207(3)
<i>b</i> (Å)	9.2193(2)	25.4418(2)	7.22506(8)	8.0609(3)
<i>c</i> (Å)	24.2773(7)	30.0726(2)	18.5652(2)	12.6145(5)
α (deg)°	90	90	90	78.857(3)
β (deg)°	103.414(2)	109.2370(10)	100.1135(12)	88.033(3)
γ (deg)°	90	90	90	84.057(3)
Volume (Å ³)	4855.5(2)	18051.2(3)	3122.38(6)	785.90(5)
<i>Z</i>	4	8	8	4
Calculated density (g/cm ³)	1.229	1.232	1.171	1.261
Absorption coefficient (mm ⁻¹)	1.040	1.105	0.638	0.658
<i>F</i> (000)	1928.0	7168.0	1184.0	320
Theta range for data collection (deg)°	7.488 to 136.5	3.518 to 75.535	7.596 to 150.938	3.572 to 76.106
Limiting indices	-26 ≤ <i>h</i> ≤ 26, -11 ≤ <i>k</i> ≤ 11, -28 ≤ <i>l</i> ≤ 29	-31 ≤ <i>h</i> ≤ 31, -29 ≤ <i>k</i> ≤ 31, -36 ≤ <i>l</i> ≤ 37	-27 ≤ <i>h</i> ≤ 29, -8 ≤ <i>k</i> ≤ 8, -23 ≤ <i>l</i> ≤ 23	-9 ≤ <i>h</i> ≤ 9, -8 ≤ <i>k</i> ≤ 10, -15 ≤ <i>l</i> ≤ 15
Reflections collected	36289	90258	12568	11849
Independent reflections	8801 [<i>R</i> _{int} = 0.0727, <i>R</i> _{sigma} = 0.0514]	32271 [<i>R</i> _{int} = 0.0298, <i>R</i> _{sigma} = 0.0308]	3162 [<i>R</i> _{int} = 0.0236, <i>R</i> _{sigma} = 0.0176]	3149 [<i>R</i> _{int} = 0.0421, <i>R</i> _{sigma} = 0.0308]
Completeness to theta	99 %	99 %	99 %	99 %
Absorption correction	Empirical	Empirical	Empirical	Empirical
Data / restraints / parameters	8801 / 0 / 580	32271 / 1514 / 2137	3162 / 0 / 188	3149 / 0 / 203
Goodness – of–fit on <i>F</i> ²	1.055	1.053	1.055	1.086
Final <i>R</i> indices [<i>I</i> > 2 σ (<i>I</i>)]	<i>R</i> ₁ = 0.0604, <i>wR</i> ₂ = 0.1658	<i>R</i> ₁ = 0.0367, <i>wR</i> ₂ = 0.1002	<i>R</i> ₁ = 0.0340, <i>wR</i> ₂ = 0.0894	<i>R</i> ₁ = 0.0571, <i>wR</i> ₂ = 0.1705

3.B.5. Appendix: All general experimental information, stoichiometric reactions, analytical data, and spectral data were available in published paper. *Angew. Chem. Int. Ed.* **2021**, *60*, 11991-12000.

3.B.6. References

- (a) Delebecq, E.; Pascault, J.-P.; Boutevin, B.; Ganachaud, F. *Chem. Rev.* **2013**, *113*, 80-118; (b) Braunstein, P.; Nobel, D. *Chem. Rev.* **1989**, *89*, 1927-1945; (c) Ulrich, H. Editor, *Chemistry, and Technology of Isocyanates*, Wiley, **1996**; d) Mitchell, S. M.; Sachinthan, K. A. N.; Pulukkody, R.; Pentzer, E. B. *ACS Macro Lett.* **2020**, *9*, 1046-1059; (e) Jurrat, M.; Pointer-Gleadhill, B. J.; Ball, L. T.; Chapman, A.; Adriaenssens, L. *J. Am. Chem. Soc.* **2020**, *142*, 8136-8141.
- (a) Pace, V.; Monticelli, S.; de la Vega-Hernandez, K.; Castoldi, L. *Org. Biomol. Chem.* **2016**, *14*, 7848-7854; (b) Yang, L.; Huang, H. *Chem. Rev.* **2015**, *115*, 3468-3517; (c) Sasaki, K.; Crich, D. *Org. Lett.* **2011**, *13*, 2256-2259; (d) Miura, T.; Takahashi, Y.; Murakami, M. *Chem. Commun.* **2007**, 3577-3579; (e) Spino, C.; Joly, M.-A.; Godbout, C.; Arbour, M. *J. Org. Chem.* **2005**, *70*, 6118-6121.
- (a) Bruffaerts, J.; von Wolff, N.; Diskin-Posner, Y.; Ben-David, Y.; Milstein, D. *J. Am. Chem. Soc.* **2019**, *141*, 16486-16493; (b) Majewski, M. W.; Miller, P. A.; Oliver, A. G.; Miller, M. J. *J. Org. Chem.* **2017**, *82*, 737-744.
- (a) Nasrollahzadeh, M.; Motahharifar, N.; Sajjadi, M.; Aghbolagh, A. M.; Shokouhimehr, M.; Varma, R. S. *Green Chem.* **2019**, *21*, 5144-5167; (b) Leong, B.-X.; Teo, Y.-C.; Condamines, C.; Yang, M.-C.; Su, M.-D.; So, C.-W. *ACS Catal.* **2020**, *10*, 14824-14833.
- (a) Pattabiraman, V. R.; Bode, J. W. *Nature* **2011**, *480*, 471-479; (b) Valeur, E.; Bradley, M. *Chem. Soc. Rev.* **2009**, *38*, 606-631; c) Gunanathan, C.; Ben-David, Y.; Milstein, D. *Science*

- 2007**, 317, 790-792; (d) Massolo, E.; Pirola, M.; Benaglia, M. *Eur. J. Org. Chem.* **2020**, 4641-4651.
6. (a) Yu, H.; Wu, Z.; Wei, Z.; Zhai, Y.; Ru, S.; Zhao, Q.; Wang, J.; Han, S.; Wei, Y. *Commun. Chem.* **2019**, 2, 15; (b) Chakraborty, S.; Gellrich, U.; Diskin-Posner, Y.; Leitun, G.; Avram, L.; Milstein, D.; *Angew. Chem., Int. Ed.* **2017**, 56, 4229-4233; (c) Wu, Z.; Zhai, Y.; Zhao, W.; Wei, Z.; Yu, H.; Han, S.; Wei, Y. *Green Chem.* **2020**, 22, 737-741.
7. (a) Serrano, E.; Martin, R. *Eur. J. Org. Chem.* **2018**, 3051-3064; (b) Su, Z.; Feng, Y.; Zou, R.; Qiu, X.; Wang, J.; Tao, C. *Chem. Commun.* **2020**, 56, 7483-7486; (c) Derasp, J. S.; Beauchemin, A. M. *ACS Catal.* **2019**, 9, 8104-8109; (d) Fiorito, D.; Liu, Y.; Besnard, C.; Mazet, C. *J. Am. Chem. Soc.* **2020**, 142, 623-632; (e) De Sarkar, S.; Ackermann, L. *Chem. - Eur. J.* **2014**, 20, 13932-13936.
8. Pace, V.; de la Vega-Hernández, K.; Urban, E.; Langer, T. *Org. Lett.* **2016**, 18, 2750-2753.
9. (a) Pace, V.; Castoldi, L.; Holzer, W. *Chem. Commun.* **2013**, 49, 8383-8385; (b) Schaefer, G.; Matthey, C.; Bode, J. W. *Angew. Chem. Int. Ed.* **2012**, 51, 9173-9175.
10. (a) Brand, S.; Causero, A.; Elsen, H.; Pahl, J.; Langer, J.; Harder, S. *Eur. J. Inorg. Chem.* **2020**, 1728-1735; (b) Sadow, A. D. Wiley-VCH Verlag GmbH & Co. KGaA, **2020**, pp. 201-224; (c) Wang, M.; Shi, Z. *Chem. Rev.* **2020**, 120, 7348-7398; (d) Hayrapetyan, D.; Khalimon, A. Y. *Chem. - Asian J.* **2020**, 15, 2575-2587; (e) Wei, D.; Darcel, C. *Chem. Rev.* **2019**, 119, 2550-2610; (f) Tamang, S. R.; Findlater, M. *Molecules* **2019**, 24, 3194; (g) Pollard, V. A.; Fuentes, M. A.; Kennedy, A. R.; McLellan, R.; Mulvey, R. E. *Angew. Chem., Int. Ed.* **2018**, 57, 10651-10655; (h) Obligation, J. V.; Chirik, P. J. *Nat. Rev. Chem.* **2018**, 2, 15-34; (i) Mukherjee, A.; Milstein, D. *ACS Catal.* **2018**, 8, 11435-11469; (j) Nikonov, G. I. *ACS Catal.* **2017**, 7, 7257-7266; (k) Li, W.; Ma, X.; Walawalkar, M. G.; Yang, Z.; Roesky, H. W.; *Coord.*

- Chem. Rev.* **2017**, 350, 14-29; (l) Shegavi, M. L.; Bose, S. K.; *Catal. Sci. Technol.* **2019**, 9, 3307-3336; (m) Zhong, W. Ai, R.; Liu, X.; Liu, Q. *Chem. Rev.* **2019**, 119, 2876-2953; (n) Chong, C. C.; Kinjo, R. *ACS Catal.* **2015**, 5, 3238-3259; (O) Lummis, P. A.; Momeni, M. R.; Lui, M. W.; McDonald, R.; Ferguson, M. J.; Miskolzie, M.; Brown, A.; Rivard, E. *Angew. Chem., Int. Ed.* **2014**, 53, 9347-9351.
11. (a) Leong, B.-X.; Lee, J.; Li, Y.; Yang, M.-C.; Siu, C.-K.; Su, M.-D.; So, C.-W. *J. Am. Chem. Soc.* **2019**, 141, 17629-17636; (b) Franz, D.; Jandl, C.; Stark, C.; Inoue, S. *ChemCatChem* **2019**, 11, 5275-5281; (c) Erken, C.; Kaithal, A.; Sen, S.; Weyhermueller, T.; Hoelscher, M.; Werle, C.; Leitner, W. *Nat. Commun.* **2018**, 9, 1-9.
12. (a) Sarkar, N.; Bera, S.; Nembenna, S. *J. Org. Chem.* **2020**, 85, 4999-5009; (b) Khononov, M.; Fridman, N.; Tamm, M.; Eisen, M. S. *Eur. J. Org. Chem.* **2020**, 3153-3160; (c) Shen, Q.; Ma, X.; Li, W.; Liu, W.; Ding, Y.; Yang, Z.; Roesky, H. W. *Chem. - Eur. J.* **2019**, 25, 11918-11923; (d) Ramos, A.; Antinolo, A.; Carrillo-Hermosilla, F.; Fernandez-Galan, R.; Garcia-Vivo, D. *Chem. Commun.* **2019**, 55, 3073-3076; (e) Rauch, M.; Ruccolo, S.; Parkin, G.; *J. Am. Chem. Soc.* **2017**, 139, 13264-13267; (f) Weetman, C.; Hill, M. S.; Mahon, M. F. *Chem. - Eur. J.* **2016**, 22, 7158-7162.
13. (a) Ojima, I.; Inaba, S.; *J. Organomet. Chem.* **1977**, 140, 97-111; (b) Ojima, I.; Inaba, S.; Nagai, Y. *Tetrahedron Lett.* **1973**, 4363-4366.
14. (a) Luo, J.; Rauch, M.; Avram, L.; Ben-David, Y.; Milstein, D. *J. Am. Chem. Soc.* **2020**, 142, 21628-21633; (b) Howell, H. G. *Synth. Commun.* **1983**, 13, 635-637.
15. Chen, Y. *Chem. - Eur. J.* **2019**, 25, 3405-3439.
16. Cabrero-Antonino, J. R.; Adam, R.; Beller, M. *Angew. Chem. Int. Ed.* **2019**, 58, 12820-12838.

-
17. Ogata, O.; Nara, H.; Fujiwhara, M.; Matsumura, K.; Kayaki, Y. *Org. Lett.* **2018**, *20*, 3866-3870.
18. Magre, M.; Szewczyk, M.; Rueping, M. *Org. Lett.* **2020**, *22*, 3209-3214.
19. Li, Y.; Sorribes, I.; Vicent, C.; Junge, K.; Beller, M. *Chem. - Eur. J.* **2015**, *21*, 16759-16763.
20. Tan, M.; Zhang, Y. *Tetrahedron Lett.* **2009**, *50*, 4912-4915.
21. (a) Finholt, A. E.; Anderson, C. D.; Agre, C. L. *J. Org. Chem.* **1953**, *18*, 1338-1340; (b) Brown, H. C.; Weissman, P. M.; Yoon, N. M. *J. Am. Chem. Soc.* **1966**, *88*, 1458-1463; (c) Cha, J. S.; Brown, H. C. *J. Org. Chem.* **1993**, *58*, 3974-3979; (d) Turnbull, K.; Krein, D. M. *Synthesis* **1999**, *3*, 391-392.
22. Mukherjee, D.; Shirase, S.; Spaniol, T. P.; Mashima, K.; Okuda, J. *Chem. Commun.* **2016**, *52*, 13155-13158.
23. (a) Barger, C. J.; Dicken, R. D.; Weidner, V. L.; Motta, A.; Lohr, T. L.; Marks, T. J. *J. Am. Chem. Soc.* **2020**, *142*, 8019-8028; (b) Lampland, N. L.; Hovey, M.; Mukherjee, D.; Sadow, A. D. *ACS Catal.* **2015**, *5*, 4219-4226; (c) Blondiaux, E.; Cantat, T. *Chem. Commun.* **2014**, *50*, 9349-9352; (d) Li, Y.; Molina de La Torre, J. A.; Grabow, K.; Bentrup, U.; Junge, K.; Zhou, S.; Brückner, A.; Beller, M. *Angew. Chem. Int. Ed.* **2013**, *52*, 11577-11580; (e) Cheng, C.; Brookhart, M.; *J. Am. Chem. Soc.* **2012**, *134*, 11304-11307; (f) Das, S.; Addis, D.; Zhou, S.; Junge, K.; Beller, M. *J. Am. Chem. Soc.* **2010**, *132*, 1770-1771.
24. (a) Ma, M.; Wang, W.; Luo, M.; Xiao, Q.; Xu, L. *CN Pat* 108358959 **2018**; (b) Ma, M.; Xiao, Q.; Cao, X.; Zheng, Y. *CN Pat.* 111410668 **2020**.
25. Yang, Y.; Anker, M. D.; Fang, J.; Mahon, M. F.; Maron, L.; Weetman, C.; Hill, M. S. *Chem. Sci.* **2017**, *8*, 3529-3537.
-

-
26. (a) Wang, X.; Chang, K.; Xu, X. *Dalton Trans.* **2020**, 49, 7324-7327; (b) Uzelac, M.; Yuan, K.; Ingleson, M. J. *Organometallics* **2020**, 39, 1332-1338; (c) Ritter, F.; Spaniol, T. P.; Douair, I.; Maron, L.; Okuda, J. *Angew. Chem., Int. Ed.* **2020**, 59, 23335-23342; (d) Procter, R. J.; Uzelac, M.; Cid, J.; Rushworth, P. J.; Ingleson, M. J. *ACS Catal.* **2019**, 9, 5760-5771; (e) Li, C.; Wang, L.; Wang, M.; Liu, B.; Liu, X.; Cui, D. *Angew. Chem. Int. Ed.* **2019**, 58, 11434-11438; (f) Dawkins, M. J. C.; Middleton, E.; Kefalidis, C. E.; Dange, D.; Juckel, M. M.; Maron, L.; Jones, C. *Chem. Commun.* **2016**, 52, 10490-10492; (g) Sattler, W.; Ruccolo, S.; Rostami Chaijan, M.; Nasr Allah, T.; Parkin, G. *Organometallics* **2015**, 34, 4717-4731; (h) Rit, A.; Spaniol, T. P.; Okuda, J. *Chem. - Asian J.* **2014**, 9, 612-619; (i) Boone, C.; Korobkov, I.; Nikonov, G. I. *ACS Catal.* **2013**, 3, 2336-2340; (j) Wiegand, A.-K.; Rit, A.; Okuda, J. *Coord. Chem. Rev.* **2016**, 314, 71-82; (k) Dagorne, S. *Synthesis* **2018**, 50, 3662-3670; (l) Wang, X.; Zhang, Y.; Yuan, D.; Yao, Y. *Org. Lett.* **2020**, 22, 5695-5700.
27. Sahoo, R. K.; Mahato, M.; Jana, A.; Nembenna, S. *J. Org. Chem.* **2020**, 85, 11200-11210.
28. Li, H.; Goncalves, T. P.; Zhao, Q.; Gong, D.; Lai, Z.; Wang, Z.; Zheng, J.; Huang, K. W. *Chem. Commun.* **2018**, 54, 11395-11398.
29. Hawkeswood, S.; Stephan, D. W. *Dalton Trans.* **2005**, 2182-2187.
30. (a) Schmidt, S.; Schaeper, R.; Schulz, S.; Blaeser, D.; Woelper, C. *Organometallics* **2011**, 30, 1073-1078; (b) Schulz, S.; Eisenmann, T.; Schmidt, S.; Blaeser, D.; Westphal, U.; Boese, R. *Chem. Commun.* **2010**, 46, 7226-7228.
31. Sattler, W.; Parkin, G. *J. Am. Chem. Soc.* **2011**, 133, 9708-9711.
32. (a) Jones, D. D. L.; Matthews, A. J. R.; Jones, C. *Dalton Trans.* **2019**, 48, 5785-5792; (b) Li, J.; Luo, M.; Sheng, X.; Hua, H.; Yao, W.; Pullarkat, S. A.; Xu, L.; Ma, M. *Org. Chem. Front.* **2018**, 5, 3538-3547.
-

33. Sheldrick, G. *Acta Crystallogr. C* **2015**, *71*, 3-8.
34. Dolomanov, O. V.; Bourhis, L. J.; Gildea, R. J.; Howard, J. A. K.; Puschmann, H. *J. Appl. Crystallogr.* **2009**, *42*, 339-341.
35. (a) Sheldrick, G. M. *Acta Crystallogr., Sect. A: Found. Crystallogr.* **2008**, *64*, 112-122; (b) Sheldrick, G. M. *Acta Crystallogr., Sect. A: Found. Adv.* **2015**, *71*, 3-8.

NMR spectra

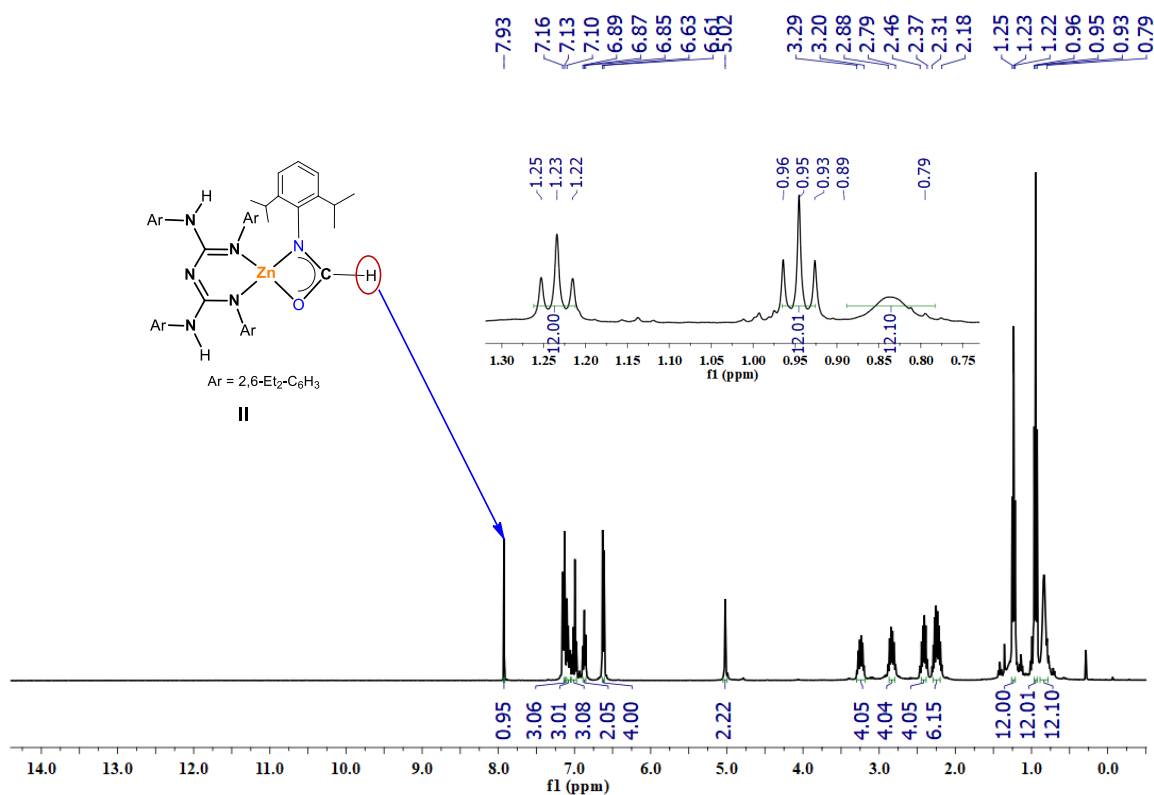


Figure 3.B.6. ^1H NMR (400 MHz, 25°C , C_6D_6) spectrum of $[\text{LZnOC(H)N}(2,6\text{-}^i\text{Pr}_2\text{C}_6\text{H}_3)]$, **II**.

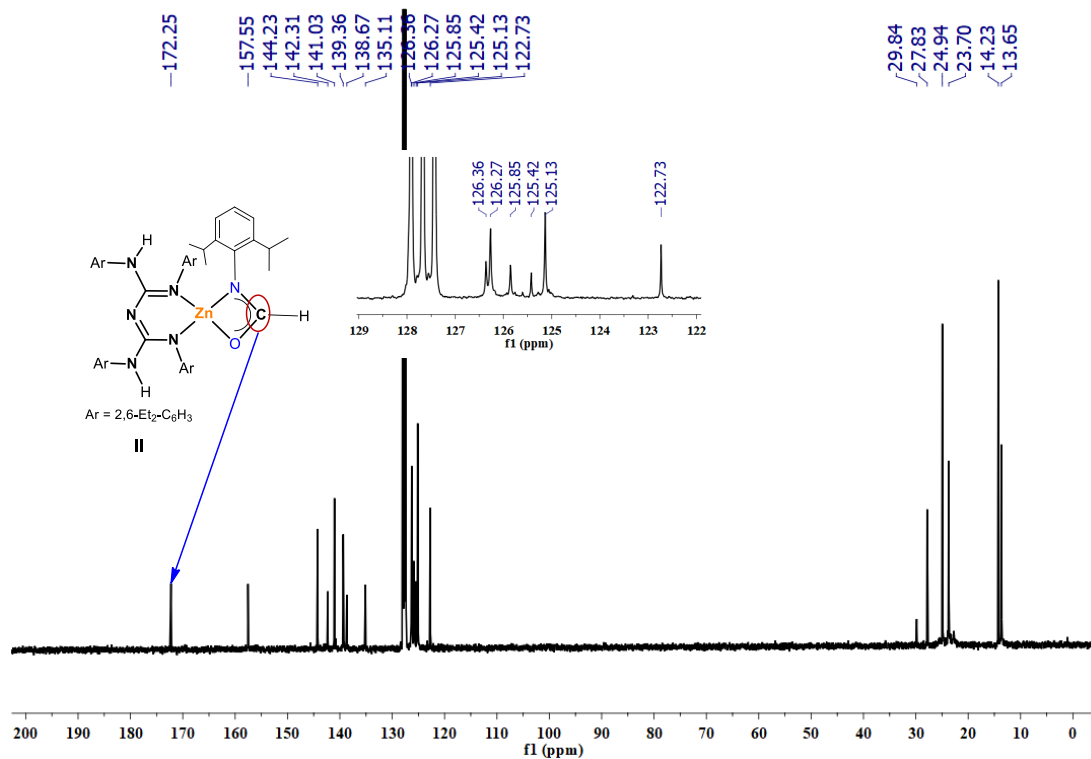


Figure 3.B.7. $^{13}\text{C}\{^1\text{H}\}$ NMR (100 MHz, 25 °C, C_6D_6) spectrum of $[LZnOC(H)N(2,6\text{-}i\text{-Pr}_2\text{C}_6\text{H}_3)]$, II.

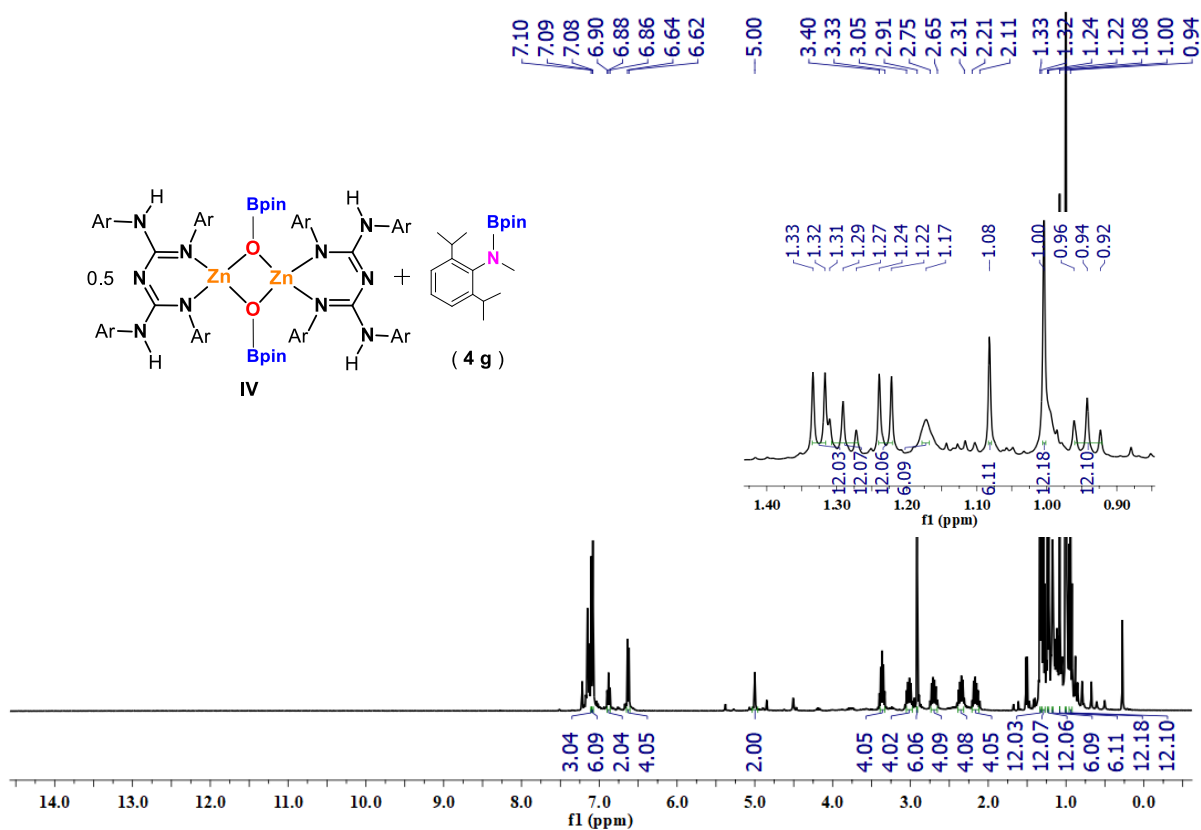


Figure 3.B.8. ^1H NMR (400 MHz, 25 °C, C_6D_6) spectrum of IV and 4g.

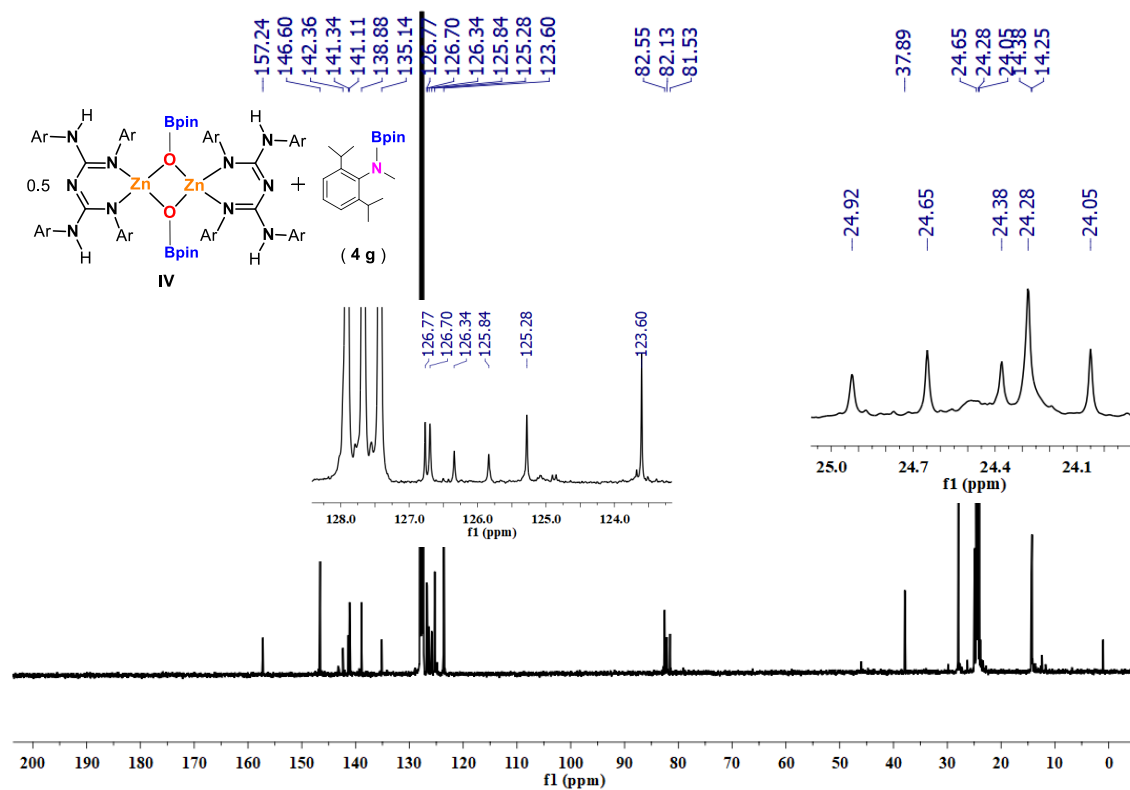


Figure 3.B.9. $^{13}\text{C}\{^1\text{H}\}$ NMR (100 MHz, 25 °C, C_6D_6) spectrum of **IV** and **4g**.

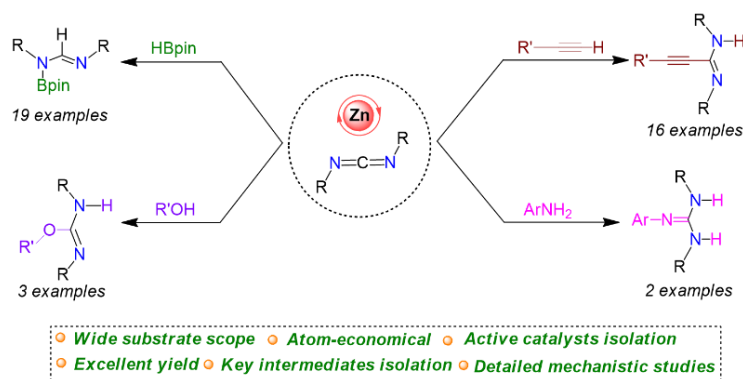
Chapter 4

Zinc Catalyzed Hydroelementation (HE; E = B, C, N, O) of Carbodiimides: Intermediates Isolation and Mechanistic Insights

Published:

Sahoo, R. K.; Patro, A. G.; Sarkar, N.; Nembenna, S. *Organometallics* **2023**, 42, 1746-1758.

Abstract



The conjugated bis-guanidinate (CBG) supported zinc hydride, [$\{LZnH\}_2$; $L = \{(ArHN)(ArN)-C=N-C=(NAr)(NHAr)$; $Ar = 2,6-Et_2-C_6H_3\}$] (**1**) (pre)-catalyzed addition of E-H (E = B, C, N, and O) to carbodiimides is presented. Compound **1** catalyzed the reduction of carbodiimides with pinacolborane (HBpin), terminal alkynes, primary amines, and alcohols, gave a series of N-boryl formamidines, propiolamidines, guanidines, and isoureas with high conversions. All these reactions display good tolerance of functional groups. These reactions proceeded through the active catalysts and intermediate of zinc amidinate (**Zn-1**, **Zn-1'**, and **Zn-3**), zinc alkynyl (**Zn-2**, and **Zn-2'**), zinc anilide (**Zn-4**), and zinc alkoxide (**Zn-5**) complexes, which have been characterized by multinuclear NMR, and HRMS analyses. Moreover, compounds **Zn-1'**, **Zn-2'**, **Zn-4**, and **Zn-5** were confirmed by single-crystal X-ray diffraction studies. Complete catalytic cycles have been proposed based on well-defined intermediates and stoichiometric experiments.

4.1. Introduction

The metal-catalyzed hydroelementation reaction of unsaturated bonds has been an active research area over the past decade.¹ The hydroelementation reaction is used to construct C-heteroatom bonds via hydroboration,² hydrosilylation,³ hydroamination,⁴ hydrophosphination,⁵ hydrothiolation,⁶ hydroalkoxylation⁷ and hydrogenation⁸ of alkenes and alkynes. These reactions have been studied using a wide range of transition, lanthanide, actinide, alkali, and alkaline-earth metal catalysts.⁹ It should be noted that the metal in these reactions does not play a significant role.^{9d}

However, hydroelementation of heterocumulenes has been scarcely investigated using metal catalysts. The hydroelementation of heterocumulenes afforded the corresponding guanidine,¹⁰ propiolamidine,¹¹ and thiourea¹² derivatives, which have been widely used as ligands in coordination compounds,^{10c, 13} material chemistry,¹⁴ and medicinal applications.¹⁵ Thus, developing an atom-efficient, versatile catalyst for the preparation of C-C and C-heteroatom bonds (generally propiolamidine, formamidine, guanidine, and urea) would be significant.

Recently, transition^{2a, 16} and main group^{2b, 17} metal-catalyzed hydroboration of carbodiimides have been developed.¹⁸ To our knowledge, there have been no reports on zinc-catalyzed hydroboration of carbodiimide (CDI) (Figure 4.1A). In 2005, the Hou group introduced rare earth metal-catalyzed hydroalkynylation of carbodiimides to propiolamidines.¹⁹ After that, a few metal-catalyzed conversion of carbodiimides into propiolamidines were reported.^{11, 20} However, zinc-catalyzed hydroalkynylation of carbodiimides is limited (Figure 4.1A).²¹ Roesky^{5a} and Carrillo-Hermosilla²² research groups recently established diethylzinc as a precatalyst for P-H and O-H addition to heterocumulenes, respectively.

As far as the E-H (E = C, N, O, P, and S) bond insertion into carbodiimide is concerned, only a handful of reports are known. Evan,²³ Eisen,²⁴ and Panda²⁵ groups independently reported Th, U, and Ti metal-catalyzed hydroelementation of heterocumulenes (Figure 4.1B). However, the previous reports on the hydroelementation reaction using zinc complexes usually involve one or two kinds of E-H nucleophiles and are limited to a narrow substrate scope.^{5a, 21-22, 26} Therefore, developing a zinc-based versatile catalyst that can exhibit the addition of various E-H (E = B, C, N, O, P, S) moieties to carbodiimide is highly demanding.

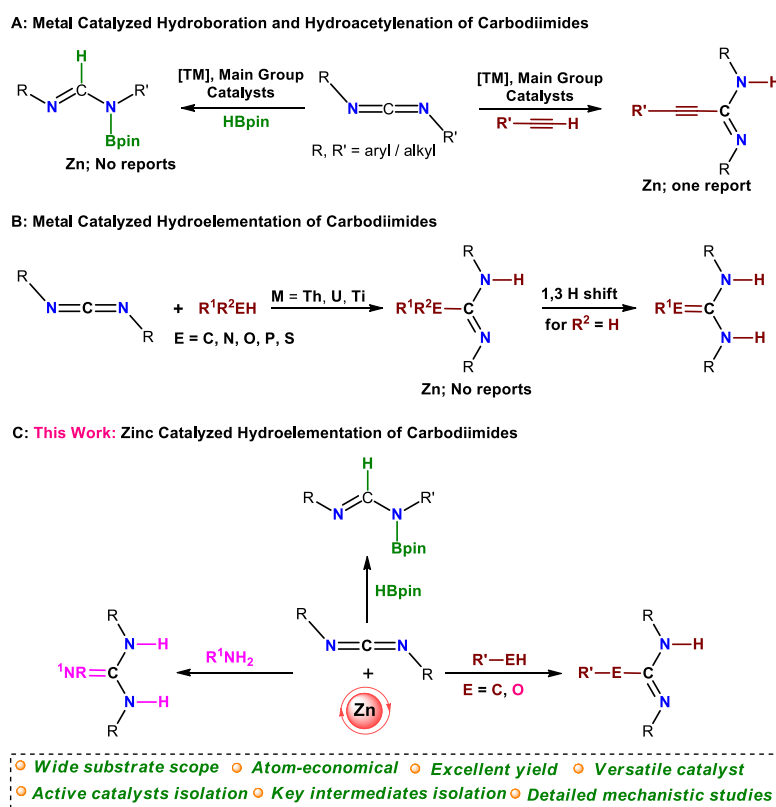


Figure 4.1. Metal-catalyzed E-H addition to carbodiimides

Previously our group reported NacNac analogue, conjugated bis-guanidinate (CBG) stabilized dinuclear zinc hydride complex, $[\{LZnH\}_2]$; $L = \{(ArHN)(ArN)-C=N-C=(NAr)(NHAr)$; $Ar = 2,6-Et_2-C_6H_3\}$ (**1**) and used as an effective catalyst for the B-H addition to a wide range of isocyanates.^{13b, 27}

Herein, we report the first example of zinc-catalyzed hydroboration of a wide range of CDIs, including alkyl-alkyl ($R-N=C=N-R$), aryl-aryl ($Ar-N=C=N-Ar$), alkyl-aryl ($R-N=C=N-Ar$), aryl-aryl' ($Ar-N=C=N-Ar'$), and bis-aryl ($Ar-N=C=N-C_6H_4-N=C=N-Ar$) carbodiimides. Further, the single and effective CBG zinc hydride (**1**) complex performs diverse reactions, such as the addition of pinacolborane (HBpin), terminal alkynes, primary amines, and alcohols (E-H; E = B, C, N, O) to carbodiimides with a broad range of substrate scope. Moreover, we propose catalytic cycles based on structurally characterized zinc-based active catalysts and intermediates (Figure 4.1C).

4.2. Results and Discussion

In a recent study, we reported dinuclear zinc dihydride [$\{LZnH\}_2$; $L = \{(ArHN)(ArN)-C=N-C=(NAr)(NHAr)$; $Ar = 2,6-Et_2-C_6H_3\}$] (**1**) complex chelated by conjugated bis-guanidinate (CBG) ligand.^{13b, 27} The zinc hydride compound (**1**) was used as an efficient catalyst for hydroboration and hydrosilylation reactions of reducible organic functional groups with excellent yields.²⁷ With our ongoing research interest in molecular main-group metal-based catalysts for organic transformation,^{2b, 10a, 10e, 13b, 28} herein, we report the CBG ZnH (**1**) catalyzed E-H (E = B, C, N, O) addition to carbodiimides.

4.2.1. Addition of HBpin to Carbodiimides

Despite the numerous reports on the main group metal-catalyzed hydroboration of unsaturated organic substrates, surprisingly, there have been no reports on zinc-catalyzed hydroboration of carbodiimides to our knowledge. This motivated us to explore B-H's addition to carbodiimide in the presence of zinc compounds. Therefore, we chose *N,N'*-diisopropylcarbodiimide (DIC) (**2a**) as a model substrate and pinacolborane (HBpin) as a hydrogen source. Initial reaction was performed under solvent and catalyst-free conditions, a reaction of **2a** with 1.0 equiv. HBpin

resulted in the formation of a trace amount of N-boryl formamidine product (**3a**) within 4 h (Entry 1 of Table 4.1).

However, adding 10 mol% zinc-hydride catalyst (**1**) to the reaction mixture of **2a** and HBpin affords the corresponding N-boryl formamidine product (**3a**) in 99% conversion, as analyzed by ^1H NMR spectroscopy. A decrease in catalyst loading up to 2 mol% under neat conditions successfully synthesized the N-borylated formamidine **3a** in 4 h (Entry 5 of Table 4.1). Besides, we found no change in the catalytic activity of compound **1** for the B-H addition of DIC (**2a**) when the reactions were performed in different solvents such as benzene, toluene, and hexane (Entries 6-8, Table 4.1). Next, when the catalyst loading further decreased to 0.5 mol% of catalyst **1**, it afforded 94% of the hydroborated product (**3a**).

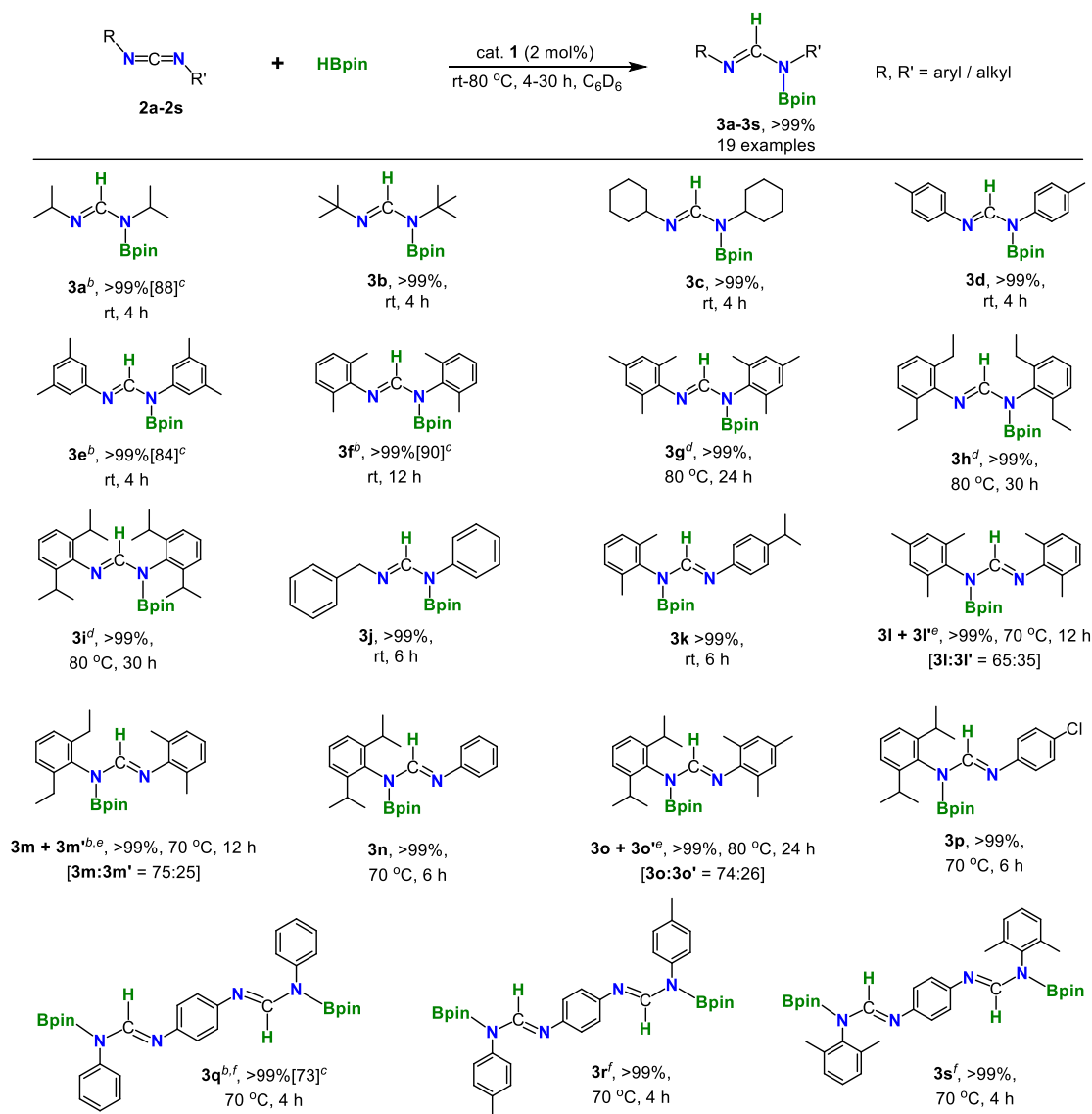
Table 4.1. Optimization table of $[\text{LZnH}]_2$ complex (**1**) catalyzed hydroboration of *N,N'*-diisopropylcarbodiimide (DIC).^a

Reaction scheme: **2a** + HBpin $\xrightarrow{\text{Zn}}$ **3a**

Entries	Cat. (mol%)	Solvent	Time (h)	Conv. (%) ^b
1	-	neat	4	2
2	10	neat	4	>99
3	5	neat	4	>99
4	3	neat	4	>99
5	2	neat	4	>99
6	2	toluene	4	>99
7	2	benzene	4	>99
8	2	hexane	4	>99
9	0.5	neat	4	94

^aReactions were conducted with DIC (0.2 mmol, 1.0 equiv.), pinacolborane (HBpin) (0.2 mmol, 1.0 equiv.), catalyst **1** (2 mol%) in 10 mL sealed vial under dinitrogen and stirred at rt for 4 h. ^bConversion for hydroboration of DIC to N-boryl formamidine (**3a**) was examined by ^1H and $^{13}\text{C}\{^1\text{H}\}$ NMR spectroscopy based on the consumption of starting material and formation of characteristic new proton resonance for (NCHN) moiety.

Further, the substrate scope for carbodiimide hydroboration was widened under optimized catalytic methodology by employing the zinc-hydride (**1**) complex. The results for B-H insertion in various carbodiimides are displayed in Scheme 4.1. In initial substrate screening of alkyl CDIs such as $t\text{BuN}=\text{C}=\text{N}^t\text{Bu}$ and $\text{CyN}=\text{C}=\text{NCy}$, (**2b-2c**), we noticed full conversions of alkyl CDIs into corresponding alkyl N-boryl formamidines **3b-3c** within 4 h using compound **1**.



Scheme 4.1. Hydroboration of carbodiimides catalyzed by $[\text{LZnH}]_2$ complex (**1**)^a

^aReactions were conducted with carbodiimides (0.2 mmol, 1.0 equiv.), pinacolborane (**HBpin**) (0.2 mmol, 1.0 equiv.), catalyst **1** (2 mol%) in 10 mL sealed vial under dinitrogen and stirred at $\text{rt-80 } ^\circ\text{C}$ for 4-30 h.

Conversions for the reduction of CDIs to N-boryl formamidines were examined by ^1H and $^{13}\text{C}\{^1\text{H}\}$ NMR spectroscopy based on the consumption of starting material and formation of characteristic new proton resonance for (NCHN) moiety. ^bFor **3a**, **3e**, **3f**, **3m** + **3m'**, and **3q**, NMR conversion was determined by ^1H NMR spectroscopy using mesitylene as the internal standard. ^cPreparative –scale reaction: 2 mmol of CDI, Catalyst **1** (2 mol%), 2 or 4 mmol of HBpin, rt to 70 °C, 4 h (except **3a**, reaction performed at 5 mmol scale). ^dFor **3g-3i**, 4 mol% of catalyst was used and heated at 80 °C. ^eFor **3l** + **3l'**, **3m** + **3m'**, and **3o** + **3o'**, without brackets, are NMR conversions, and brackets refer to the ratio of regioisomers. ^fFor **3q-3s**, (0.4 mmol, 2 equiv.) HBpin was used and heated at 70 °C for 4 h.

Apart from alkyl CDIs, a series of symmetrical aryl carbodiimides (Ar-N=C=N-Ar), i.e. (*p*-tolyl)N=C=N(*p*-tolyl) (**2d**), (3,5-Me₂Ph)N=C=N(3,5-Me₂Ph) (**2e**), (2,6-Me₂Ph)N=C=N(2,6-Me₂Ph) (**2f**), were also investigated under optimized conditions which afforded the respective monoborylated products R-N=C(H)-N(Bpin)R' (**3d-3f**) in 99% conversions within 4-12 h reaction time intervals. Moreover, the hydroboration of bulkier aryl-aryl symmetrical carbodiimides (2,4,6-Me₃Ph)N=C=N(2,4,6-Me₃Ph) (**2g**), (2,6-Et₂Ph)N=C=N(2,6-Et₂Ph) (**2h**) and (2,6-*i*Pr₂Ph)N=C=N(2,6-*i*Pr₂Ph) (**2i**) provided quantitative amount of corresponding monoborylated products R-N=C(H)-N(Bpin)R (**3g-3i**) at 80 °C with a 4 mol% catalyst loading.

In additional substrate scope, the unsymmetrical *N,N'*-disubstituted aryl-alkyl carbodiimide (Ar-N=C=N-R), ((Benzyl)N=C=N(Phenyl), (**2j**) and aryl-aryl' carbodiimides (Ar-N=C=N-Ar'), **2k**, **2n**, and **2p** were explored under optimized reaction conditions resulted in the formation of single regioisomeric hydroborated products **3j**, **3k**, **3n**, and **3p**, where Bpin moiety is attached to a more hindered nitrogen atom of NCN core, as observed by Eisen and Hill groups.^{16a, 17i} However, for bulkier aryl-aryl' unsymmetrical carbodiimides ArN=C=NAr' (**2l**, **2m**, and **2o**), a mixture of regioisomers of N-boryl formamidines, i.e., Ar(Bpin)-N-C(H)=N-Ar' (**3l**, **3m**, and **3o**) and Ar-N=C(H)-N(Bpin)-Ar' (**3l'**, **3m'**, and **3o'**) were obtained due to competition between two bulky aryl group substituents (-NAr and -NAr') as reported by Eisen group.^{16b} Reports on the hydroboration of bis-aryl CDIs to bis-aryl formamidines are very limited due to the unavailability

of suitable bis-aryl CDIs precursor.^{10a, 29} The bis-aryl CDIs (**2q–2s**), upon treatment with 2.0 equiv of HBpin at 70 °C for 4 h produced quantitative conversions of corresponding N-borylated bis-aryl formamidines (**3q–3s**). These products were confirmed by ¹H NMR spectroscopy, where a single resonance peak of NCHN appeared between 8.13 – 8.51 ppm in C₆D₆. The X-ray diffraction study revealed a new N-B bond between the Bpin unit and the carbodiimide moiety in compound **3q**. The N1-C2 and N2-C2 bond distances in **3q** are 1.2743(17) (Å) and 1.3829(17) (Å), which are comparable to standard N-C double and single bonds, respectively. Moreover, the N1-C2-N2 (123.53(12)°) bond angle of the compound **3q** is acute compared to the N=C=N bond angle of carbodiimide, which confirms the formation of N-boryl formamidine product **3q** (Figure 4.2). To our knowledge, this is the first example of structurally characterized N-borylated bis-aryl formamidine.

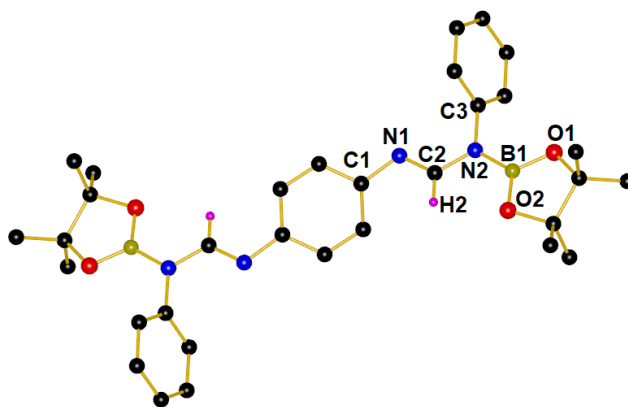


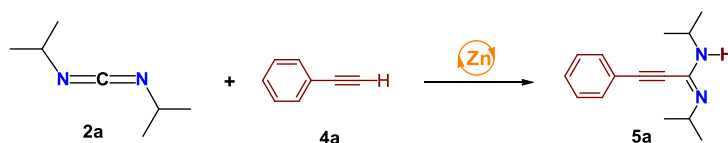
Figure 4.2. Molecular structure of **3q**. The thermal ellipsoids are shown at 50% probability, and all the hydrogen atoms (except for H(2)) are deleted for clarity. Selected bond lengths (Å) and angles (deg): C1-N1 1.4184(17), C2-N1 1.2743(17), N2-B1 1.4370(19), C2-N2 1.3829(17), N2-C3 1.4417(17); N1-C2-N2 123.53(12), C2-N2-B1 119.97(11), C2-N2-C3 118.88(10).

4.2.2. Addition of Alkynes to Carbodiimides (CDIs)

Encouraged by the hydroboration of carbodiimide, we next focused on constructing the C-C bond by hydroacetylenation of CDIs to synthesize propiolamidine derivatives using pre-catalyst **1**. We

selected phenylacetylene (**4a**) as a representative substrate to optimize the catalytic addition of alkyne to carbodiimide. The initial reaction was tested by reaction of substrate **4a** with DIC (**2a**) in the catalyst-free condition in benzene- d_6 at 70 °C for 24 h, no product formation was noticed. Moreover, in the presence of 10 mol% zinc-hydride (**1**) complex at 70 °C, generation of C-C coupled product (*E*)-*N,N'*-diisopropyl-3-phenylpropiolimidamide (**5a**) was detected in ^1H NMR spectrum (Entry 2, Table 4.2). The pre-catalyst loading was decreased up to 3 mol% in C_6D_6 as solvent after 18 h, yielding the quantitative amount of product **5a** (Entry 8, Table 4.2).

Table 4.2. Optimization table of $[\text{LZnH}]_2$ complex (**1**) pre-catalyzed phenylacetylene addition to *N,N'*-diisopropylcarbodiimide (DIC).^a

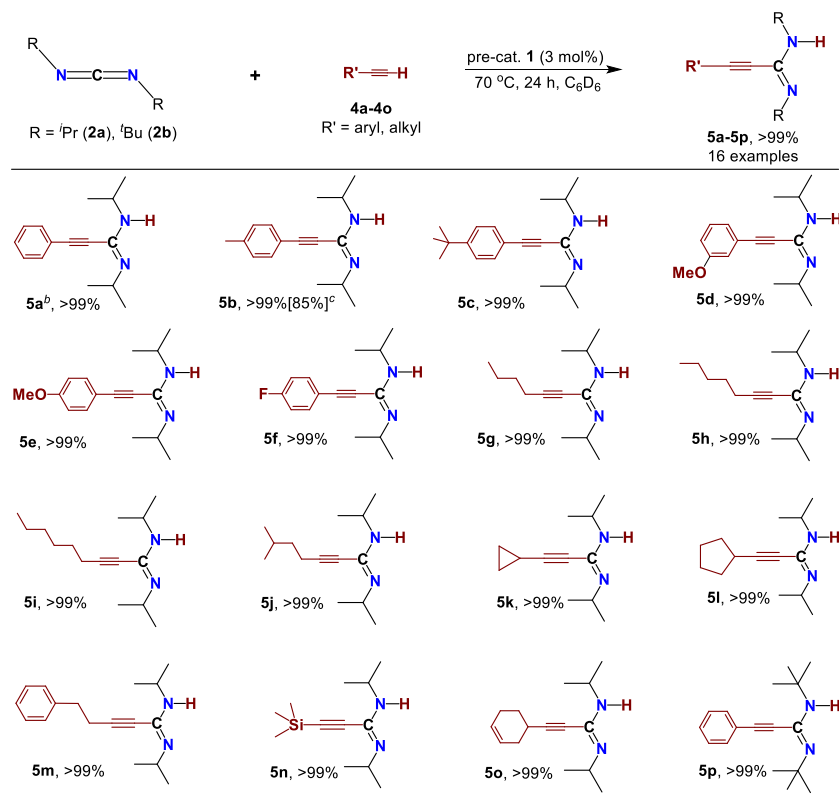


Entries	Cat. (mol%)	Solvent	Temp (°C)	Time (h)	Conv. (%) ^b
1	-	C_6D_6	70	24	-
2	10	C_6D_6	70	24	>99
3	10	C_6D_6	70	18	>99
4	8	C_6D_6	70	18	>99
5	7	C_6D_6	70	18	>99
6	5	C_6D_6	70	18	>99
7	3	C_6D_6	70	24	>99
8	3	C_6D_6	70	18	>99
9	1	C_6D_6	70	18	90

^aReactions were conducted with *N,N'*-diisopropylcarbodiimide (DIC) (0.2 mmol, 1.0 equiv.), phenylacetylene (0.2 mmol, 1.0 equiv.), pre-catalyst **1** (3.0 mol%), in a pressurized J. Young valve NMR tube under dinitrogen and stirred at 70 °C for 24 h. ^bConversion of propiolamidines (**5a**) was examined by ^1H and $^{13}\text{C}\{^1\text{H}\}$ NMR spectroscopy based on the formation of characteristic new proton resonance for the (-NH) moiety of product.

Further lowering in pre-catalyst **1** quantity leads to a decrease in the conversion of **4a** to product **5a** (90%) (Entry 9, Table 4.2). Under the present optimized catalytic conditions, we explored the hydroacetylenation of *N,N'*-diisopropylcarbodiimide (**2a**), and *N,N'*-di-*tert*-butylcarbodiimide (**2b**) with terminal alkynes (**4a-4p**) using CBG zinc hydride pre-catalyst (**1**) in C_6D_6 (Scheme 4.2). In

the initial investigation, the reaction of para- and meta-substituted phenylacetylenes (including electron donating and withdrawing groups) **4b-4f** with diisopropyl carbodiimide afforded the corresponding aryl propiolamidines (**5b-5f**). Furthermore, alkyl (acyclic and cyclic) alkynes **4g-4n** upon treatment with DIC at optimized reaction conditions resulted in the respective alkyl hydroacetylenation products (**5g-5n**) with 99% conversions. More importantly, for substrate 1-ethynylcyclohexene (**4o**), the isolation of relevant propiolamidines, i.e. (*E*)-3-(cyclohex-3-en-1-yl)-*N,N'*-diisopropylpropiolimidamide (**5o**) was noticed with a quantitative conversion with the tolerance of the internal C=C bond. In the end, we examined the addition of phenylacetylene to *N,N'*-di-*tert*-butylcarbodiimide (**2b**), which resulted in the complete formation of hydroacetylenation product (**5p**).



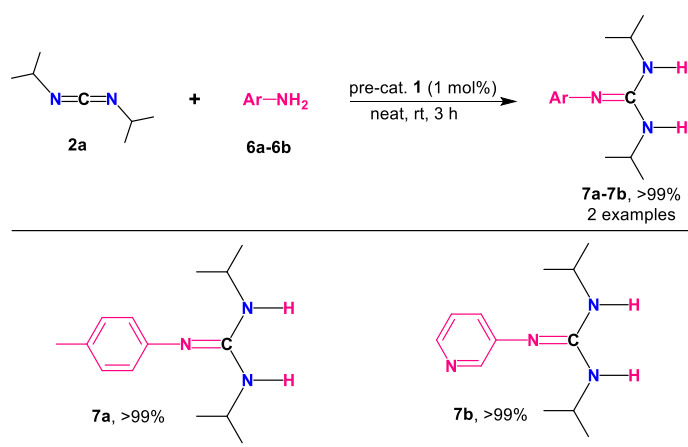
Scheme 4.2. Substrate scope for C-H addition to carbodiimides pre-catalyzed by **1^a**

^aReactions were conducted with carbodiimides (0.2 mmol, 1.0 equiv.), terminal alkynes (0.2 mmol, 1.0 equiv.), pre-catalyst **1** (3.0 mol%), in a J. Young valve sealed NMR tube under dinitrogen and heated at 70

°C of 24 h. Conversion of propiolamidines was examined by ^1H and $^{13}\text{C}\{^1\text{H}\}$ NMR spectroscopy based on the consumption of starting material and formation of characteristic new proton resonance for the (-NH) moiety of products **5a-5p**. ^bFor **5a**, NMR conversion was determined by ^1H NMR spectroscopy using mesitylene as the internal standard. ^cPreparative –scale reaction: 5 mmol of CDI, Catalyst **1** (3 mol%), 5 mmol of 4-ethynyltoluene, 70 °C, 24 h.

4.2.3. Addition of Primary Amines to Diisopropylcarbodiimide

Our group demonstrated catalyst-free guanylation of carbodiimides by using secondary amines.^{10d} However, the Shen group reported that primary aromatic amines did not react with diisopropylcarbodiimide in the absence of a catalyst, even under harsh reaction conditions (100 °C).^{20e} This motivates us to explore the addition of primary aromatic amines (N-H) to carbodiimide in the presence of a zinc compound. Therefore, the addition of 1 mol% pre-catalyst (**1**) to the reaction mixture of an equimolar solution of aryl amines (**6a** or **6b**) and *N,N'*-diisopropylcarbodiimide (**2a**) produced corresponding guanidine derivatives **7a** or **7b** with 99% conversions in neat conditions at room temperature after 3 h. The compounds **7a-7b** were confirmed by ^1H and $^{13}\text{C}\{^1\text{H}\}$ NMR spectroscopy (Scheme 4.3).



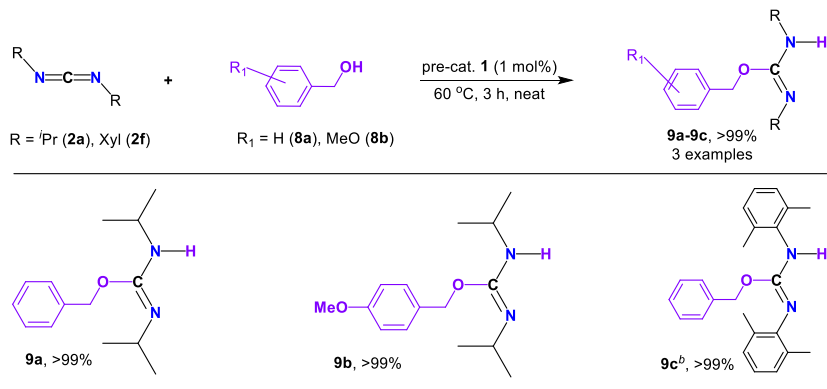
Scheme 4.3. Substrate scope for guanylation of DIC with 1° aryl amines pre-catalyzed by **1**^a

^aReactions were performed with amines (0.2 mmol, 1.0 equiv.), *N,N'*-diisopropylcarbodiimide (0.2 mmol, 1.0 equiv.) pre-cat. (**1**) (1 mol%), in a 10 mL reaction vial under N_2 , stirred at room temperature for 3 h. Conversion for guanylation of DIC with primary amines was confirmed by NMR (^1H and $^{13}\text{C}\{^1\text{H}\}$)

spectroscopy based on the consumption of starting material and formation of characteristic new proton signal for the (-NH) moieties of products **7a-7b**.

4.2.4. Addition of Alcohols to Diisopropylcarbodiimide

A recent literature study confirms that catalytic insertion of O-H (*addition of alcohols*) into carbodiimides is an exciting synthetic route to prepare the isoureas.²²



Scheme 4.4. Substrate scope for alcohol addition to carbodiimide pre-catalyzed by **1**^a

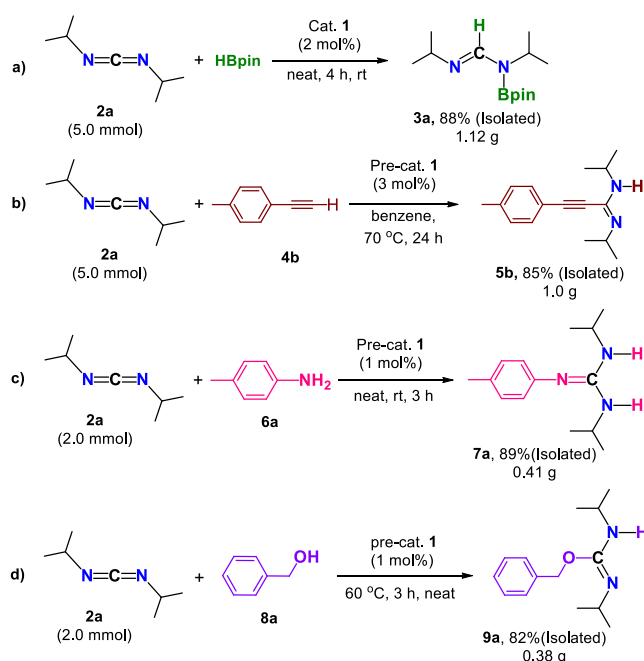
^aReactions were performed with alcohols (0.2 mmol, 1.0 equiv.), carbodiimides (0.2 mmol, 1.0 equiv.), and pre-cat. (**1**) (1 mol%), in a 10 mL reaction vial under N₂, stirred at 60 °C for 3 h. Conversion of isoureas was examined by ¹H and ¹³C{¹H} NMR spectroscopy based on the consumption of starting material and formation of characteristic new proton resonance for the (-NH) moiety of products **9a-9c**. ^bFor **9c**, heated at 70 °C for 4 h.

With our present CBG zinc hydride pre-catalyst (**1**), we explored that the catalytic addition of benzyl alcohol (**8a**) and *p*-methoxy benzyl alcohol (**8b**) to CDIs (**2a** and **2f**) led to the quantitative formation of isourea derivatives **9a-9c** with no trace of any starting material (Scheme 4.4).

4.2.5. Large Scale Reactions

To explore the practical applicability of the present zinc hydride complex, we performed large-scale reactions of carbodiimide with HBpin, 4-ethynyltoluene (**4b**), *p*-toluidine (**6a**) or benzyl alcohol (**8a**).

As demonstrated in Scheme 4.5, a; 5.0 mmol scale reaction of DIC (**2a**) with one equiv. of HBpin, yielded corresponding N-boryl formamidine product **3a** with 88% isolated yield at room temperature after 4 h. On a similar scale, under the standard reaction condition, DIC (**2a**) was treated with one equiv. of 4-ethynyltoluene (**4b**) in benzene afforded corresponding propiolamidine product (**5b**) with 85% isolated yield at 70 °C after 24 h (Scheme 4.5, b). Similarly, 2.0 mmol of DIC (**2a**) reacted with one equiv. of *p*-toluidine or benzyl alcohol at rt to 60 °C for 3 h resulted in the formation of corresponding guanidine derivative (**7a**) or isourea derivative (**9a**) product with 82-89% isolated yield (Scheme 4.5, c-d).



Scheme 4.5. Scale up reactions for E-H addition to DIC.

4.2.6. Stoichiometric Experiments for B-H Addition to Carbodiimides

We performed stoichiometric experiments to investigate the mechanism of zinc hydride catalyzed hydroboration of CDIs. The reaction between catalyst **1** [$\{LZnH\}_2$; $L = \{(ArHN)(ArN)-C=N-C=(NAr)(NHA r)\}$; $Ar = 2,6-Et_2-C_6H_3\}$] and diisopropylcarbodiimides (DIC) in benzene at rt for 1

The $^{13}\text{C}\{^1\text{H}\}$ NMR spectrum shows a peak at 164.5 ppm assigned to NCHN. Next, the zinc amidinate (**Zn-1**) reacted with a stoichiometric amount of HBpin in benzene- d_6 at rt for 30 min, forming catalyst **1** and compound **3a** (Scheme 4.6, ii and Figure 4.3).

Despite several attempts, poor-quality crystals of intermediate **Zn-1** are obtained by crystallization. Therefore, to synthesize and structurally characterize the CBG zinc amidinate complex, catalyst **1** was reacted with *N,N'*-ditertbutylcarbodiimide in benzene at rt for 1 h. Further, zinc amidinate compound $[\text{LZnN}(\text{'Bu})\text{C}(\text{H})\text{N}(\text{'Bu})]$ (**Zn-1'**) was confirmed by NMR, HRMS, and single-crystal diffraction studies (Scheme 4.6, i). The single crystals of compound **Zn-1'** suitable for X-ray diffraction were grown from benzene solution at room temperature. The solid-state structure of compound **Zn-1'** reveals that the CBG zinc amidinate is monomeric, in which zinc centers adopt a distorted tetrahedral geometry bonded to one CBG ligand in *N,N'*-chelated fashion, and other two sites by N-atoms of the formamidine moieties.

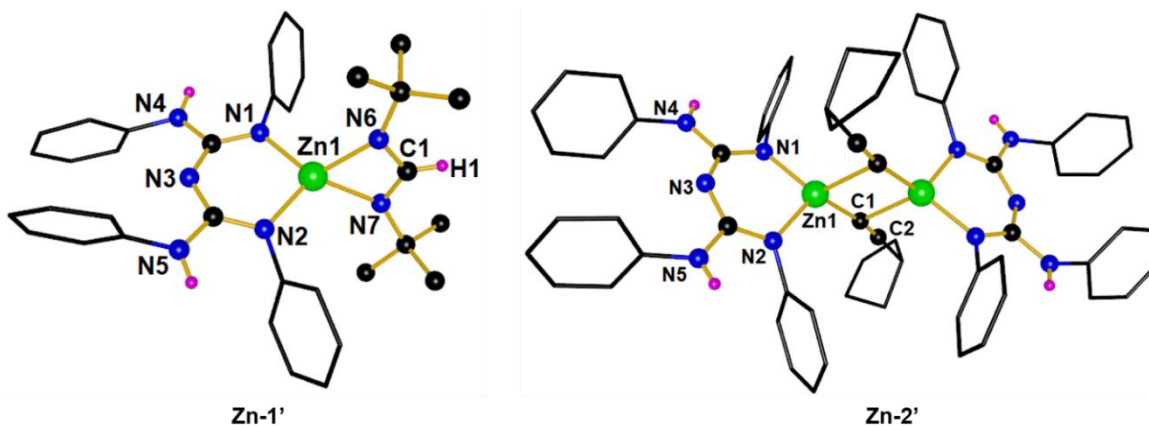


Figure 4.4. Molecular structures of compounds **Zn-1'** (left) and **Zn-2'** (right). The thermal ellipsoids are shown at 50% probability, and all the ethyl groups and hydrogen atoms except those bound to nitrogen atoms and H1 from structure **Zn-1'** are deleted for clarity. Selected bond lengths (Å) and angles (deg) for **Zn-1'** (left): Zn1-N1 1.955(3), Zn1-N2 1.966(3), Zn1-N6 2.056(4), Zn1-N7 2.054(4), N6-C1 1.306(6), N7-C1 1.315(6); N1-Zn1-N2 95.08(15), N1-Zn1-N6 116.78(15), N2-Zn1-N7 118.23(15), N6-Zn1-N7 65.22(15), N6-C1-N7 115.3(4). for **Zn-2'** (right): Zn1-N1 1.958(4), Zn1-N2 1.966(4), Zn1-C1 2.067(5), Zn1-C1' 2.310(4), Zn1-Zn1' 3.0016(11); N1-Zn1-N2 94.81(17), N1-Zn1-C1 116.69(19), N2-Zn1-C1 123.30(18), C1-Zn1-C1' 93.60(17), Zn1-C1-Zn1' 86.40(17).

The compound **Zn-2'** is closely related to previously reported structurally characterized neutral^{30a} and cationic^{30b} zinc amidinate complex (Figure 4.4, left). The Zn1-N6 and Zn1-N7 bond distances in **Zn-1'** are 2.056(4) (Å) and 2.054(4) (Å), which are comparable to Zn–N bond distances of the analogous [(Me₆tren)Zn(ⁱPr)C(H)N(ⁱPr)][B{C₆H₃(CF₃)₂}₄] complex, [Zn–N(5) 2.000(4) Å and Zn–N(6) 2.195(4) Å].^{30b} The N–C–N angle of the compound **Zn-1'** is N6–C1–N7 115.3(4)° which is acute compared to the bond angle in [(Me₆tren)Zn(ⁱPr)C(H)N(ⁱPr)][B{C₆H₃(CF₃)₂}₄] (N5–C16–N6 118.6(4)°).^{30b}

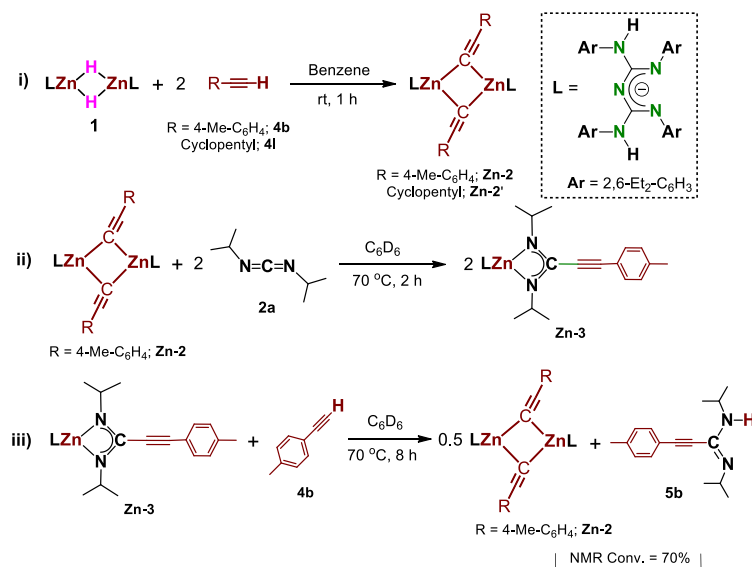
4.2.7. Stoichiometric Experiments for C–H Addition to Carbodiimides

We conducted several stoichiometric experiments to understand the active species involved in the zinc-catalyzed addition of alkynes to CDIs. The reaction of 0.5 equiv. of complex **1** with 1 equiv. 4-ethynyltoluene at room temperature for 1 h yielded the corresponding zinc acetylide complex [LZnC≡C–C₆H₄–*p*–Me]₂ (**Zn-2**) in quantitative yield (Scheme 4.7, i). Further, the addition of 2 equiv. of DIC (**2a**) to **Zn-2** in C₆D₆ at 70 °C for 2 h produced the insertion product, [LZn(NⁱPr)C≡C–C₆H₄–*p*–Me(NⁱPr)], **Zn-3** (Scheme 4.7, ii). Finally, the reaction of compound **Zn-3** with 1 equiv. of 4-ethynyltoluene (**4b**) resulted in the formation of product **5b** and compound **Zn-2** with a 70% conversion in C₆D₆ at 70 °C after 8 h (Scheme 4.7, iii).

Very recently, our group reported structurally characterized CBG zinc acetylide complex, [LZnC≡C–C₆H₄–*p*–Me]₂ (**Zn-2**), by treating low oxidation state Zn(I) dimer, i.e., LZnZnL (L = {(ArNH)(ArN)–C=N–C=(NAr)(NHAr)}; Ar = 2,6-Et₂–C₆H₃) with 4-ethynyltoluene.³¹

In contrast, pre-catalyst **1** was reacted with cyclopentylacetylene in benzene at rt for 1 h to obtain the zinc acetylide complex. The zinc acetylide compound [LZnC≡C–C₅H₉]₂ (**Zn-2'**) was confirmed by NMR, HRMS, and single-crystal diffraction studies (Scheme 4.7, i). The single crystals of compound **Zn-2'** were obtained from a benzene solution at room temperature. The solid-state

structure of compound **Zn-2'** reveals that the CBG zinc acetylide complex is dimeric, in which each zinc center adopts a distorted tetrahedral geometry bonded to one CBG ligand in *N,N'*-chelated fashion, and the other two sites by C-atoms of the bridged acetylene moieties.



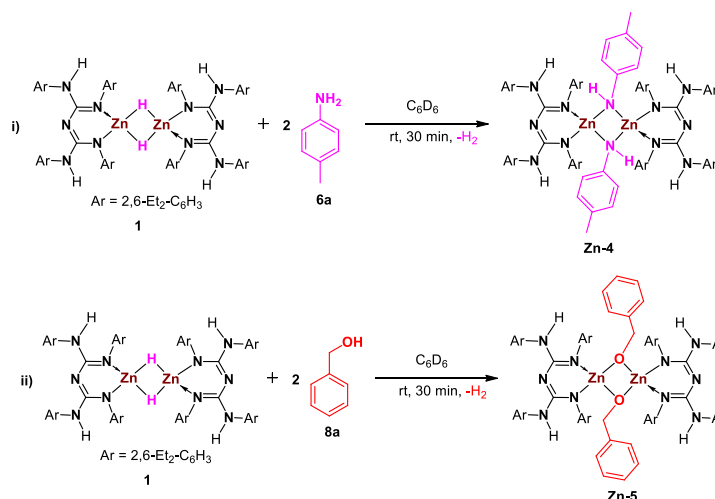
Scheme 4.7. Stoichiometric experiments for hydroacetylation of carbodiimides.

The Zn1–C1 bond distance in compound **Zn-2'** is 2.067(5) Å, which is slightly longer compared to another CBG Zn-alkynyl complex, i.e., $[\text{LZnCC}(\text{C}_6\text{H}_5\text{-4-Me})_2]$ Zn–C = 2.0181(15) Å.³¹ The N1-Zn1-N2 bite angle of the **Zn-2'** is 94.81(17)°, which is comparable to the bond angle in CBG Zn-*p*-tolyl alkynyl complex (N1-Zn1-N2 94.76(5)°) (Figure 4.4, right).³¹

Stoichiometric Experiments for N-H and O-H Addition to Carbodiimide

We conducted stoichiometric experiments to gain further information on the reaction mechanisms of the zinc-catalyzed N-H and O-H addition to CDIs. A reaction between compound **1** and *p*-toluidine (**6a**) was carried out at room temperature for 30 min in C_6D_6 , affording CBG zinc anilide complex, $[\text{LZnNH-C}_6\text{H}_4\text{-}p\text{-Me}]_2$ (**Zn-4**) an excellent conversion. NMR, HRMS, and X-ray single crystal analysis confirmed the formation of compound **Zn-4**. Similarly, compound **1** reacted with benzyl alcohol (**8a**) at the above reaction condition to produce CBG zinc alkoxide complex, $[\text{LZnO-CH}_2\text{-C}_6\text{H}_5]_2$ (**Zn-5**) as confirmed by NMR, HRMS, and X-ray single crystal analysis

(Scheme 4.8). To our knowledge, a few examples of structurally characterized zinc-anilide and zinc alkoxide complexes are known in the literature.³²



Scheme 4.8. Stoichiometric experiments for N-H and O-H addition to carbodiimides

The solid-state structure reveals that the compounds **Zn-4** and **Zn-5** are dimeric in which zinc centers adopt a distorted tetrahedral geometry bonded to one CBG ligand in *N,N'*-chelated fashion, and other two sites by N-atoms of the anilide moieties or O-atoms of the alkoxide moieties (for more details, see Figure 4.5, and Figures S124-S125 and Table 4.3). The zinc anilide complex (**Zn-4**) is closely related to Crimmin's reported structurally characterized NacNac zinc anilide complex.^{32a}

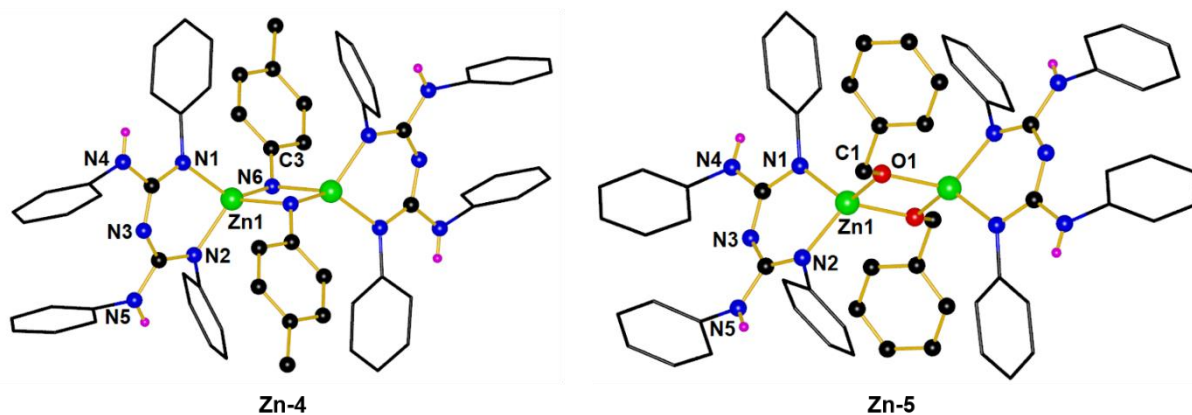
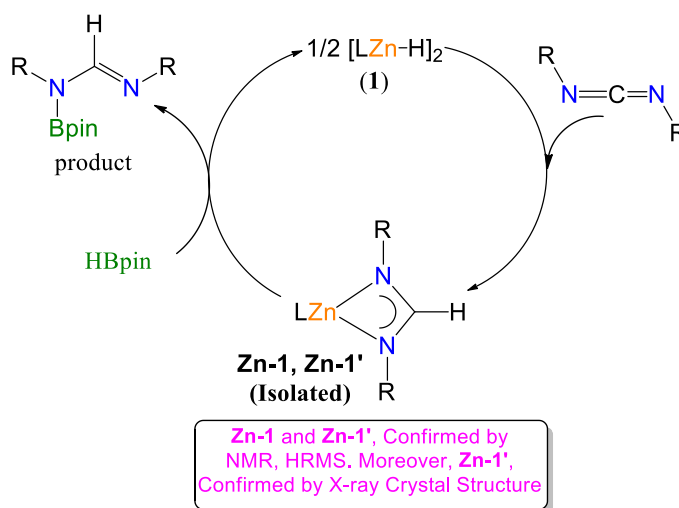


Figure 4.5. Molecular structures of compounds **Zn-4** (left) and **Zn-5** (right). The thermal ellipsoids are shown at 50% probability, and all the ethyl groups and hydrogen atoms except those bound to nitrogen atoms are deleted for clarity. Selected bond lengths (Å) and angles (deg) for **Zn-4** (left): Zn1-N1

1.9962(12), Zn1-N2 1.9838(12), Zn1-N6 2.0044(12), Zn1-N6' 2.1058(12), Zn1-Zn1' 2.9307(3), N6-C3 1.4175(19); N1-Zn1-N2 94.29(5), N1-Zn1-N6 132.57(5), N2-Zn1-N6 114.89(5), N6-Zn1-N6' 89.07(5), Zn1-N6-Zn1' 90.93(5). for **Zn-5** (right): Zn1-N1 1.9798(12), Zn1-N2 1.9800(12), Zn1-O1 1.9708(10), Zn1-O1' 1.9837(10), Zn1-Zn1' 2.9605(4), O1-C1 1.4141(18); N1-Zn1-N2 95.53(5), N1-Zn1-O1 116.19(5), N2-Zn1-O1 123.02(5), O1-Zn1-O1' 83.06(4), Zn1-O1-Zn1' 96.94(4).

4.2.8. Catalytic Cycle for Hydroboration of Carbodiimides

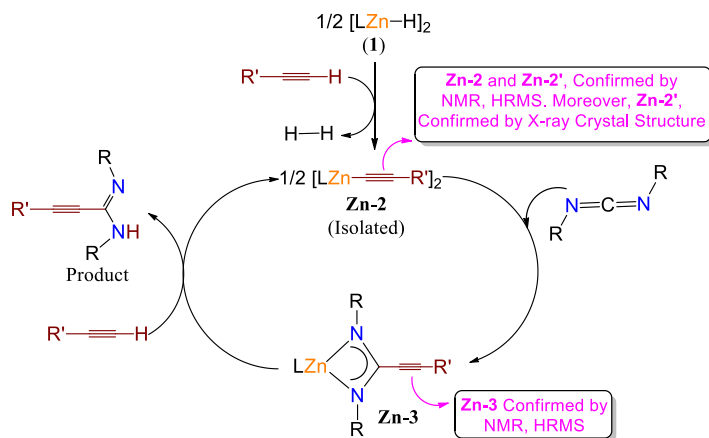
Based on intermediates isolation and stoichiometric experiments, the most plausible mechanism for hydroboration of CDI catalyzed by zinc hydride complex is displayed in Scheme 4.9. Initially, the insertion of the Zn-H moiety of catalyst **1** into the C=N bond of CDI affords the CBG zinc amidinate complex (**Zn-1/Zn-1'**). Finally, the zinc amidinate complex reacts with HBpin via Zn-N/B-H sigma bond metathesis, yielding the N-boryl formamidine product and regeneration of the zinc catalyst (**1**).



Scheme 4.9. Proposed mechanism for CDIs hydroboration catalyzed by compound **1**.

4.2.9. Catalytic Cycles for C, N, and O-H Addition to Carbodiimides

Based upon the above results and previously reported mechanisms in the literature,^{20e, 22, 24a}, the most probable catalytic cycles have been proposed for C-H, N-H, and O-H addition to CDIs in Scheme 4.10.



Scheme 4.10. Proposed mechanism for synthesis of propiolamidines

The reaction of precatalyst **1** with alkynes, amines, and alcohols by H_2 elimination releases corresponding zinc alkynyl (**Zn-2**), zinc anilide (**Zn-4**), and zinc alkoxide (**Zn-5**) complexes. The compounds **Zn-2**, **Zn-4**, and **Zn-5** inserted into carbodiimides give the corresponding inserted zinc complexes (**Zn-3**, **Int A**, and **Int B**). Further, the intermediates **Zn-3**, **Int A**, and **Int B**, independently reacting with an alkyne, amine, and alcohol molecule, afforded the corresponding hydroelementation product and regenerated the active catalyst (**Zn-2**, **Zn-4**, and **Zn-5**).

4.3. Conclusion

In conclusion, we have shown that complex **1** is a highly active (pre)-catalyst for the addition of E-H (E = B, C, N O) moieties to carbodiimides with a broad range of substrate scope under mild conditions. A series of N-boryl formamidines, propiolamidines, guanidines, and isoureas have been synthesized by reacting a wide range of CDI substrates with HBpin (B-H), terminal alkynes (C-H), primary amines (N-H), and alcohols (O-H) substrates. Furthermore, bis-aryl CDIs are efficiently converted into N-borylated bis-aryl formamidines. In all reactions, we noticed good tolerance of other reducible functional groups. More importantly, we have isolated a series of active catalysts and intermediates, i.e., CBG zinc amidinate (**Zn-1**, **Zn-1'**, and **Zn-3**), zinc acetylide (**Zn-2** and **Zn-2'**), zinc-anilide (**Zn-4**), and zinc-alkoxide (**Zn-5**) complexes, which are

thoroughly characterized by NMR, and HRMS analyses. Further, X-ray single-crystal diffraction studies confirmed molecular structures of compounds **Zn-1'**, **Zn-2'**, **Zn-4**, and **Zn-5**; such zinc metal complexes are rare in the literature. The plausible catalytic cycles have been proposed based on the key intermediates isolation and stoichiometric experiments.

4.4. Experimental Section

General Procedures

Unless stated, manipulations were performed under a dinitrogen atmosphere using standard glovebox and Schlenk techniques. NMR spectra were recorded on Bruker 400 MHz NMR spectrometer (400 MHz (^1H), 101 MHz ($^{13}\text{C}\{^1\text{H}\}$), and 128.36 MHz (^{11}B)). ^1H and $^{13}\text{C}\{^1\text{H}\}$ NMR chemical shifts are referenced to residual protons or carbons in the deuterated solvent. ^{11}B was calibrated using the external reference of $\text{BF}_3\cdot\text{Et}_2\text{O}$. Multiplicities are reported as singlet (s), doublet (d), triplet (t), quartet (q), and multiplet (m). Chemical shifts are reported in ppm. Coupling constants are reported in Hz. The crystal data of compounds **Zn-1'** and **Zn-5** are collected on a Rigaku Oxford diffractometer with graphite-monochromated $\text{Cu-K}\alpha$ radiation ($\lambda = 1.54184 \text{ \AA}$) at 100 K. Whereas, the crystal data of compounds **Zn-2'**, **Zn-4**, and **3q** are collected on a Rigaku Oxford diffractometer with $\text{Mo-K}\alpha$ radiation ($\lambda = 0.71073 \text{ \AA}$) at 100 K. Selected data collection parameters, and other crystallographic results are summarized in Table 4.3-4.4. Mass spectrometry analyses were carried out on Bruker micrOTOF-Q II and Waters XevoG2 XS Q-TOF mass spectrometers. The melting points of compounds **Zn-1**, **Zn-1'**, **Zn-2** and **Zn-2'** were measured from the Stuart SMP 10 instrument.

Materials:

Solvents were purified by distillation over Na/ benzophenone. Deuterated chloroform (CDCl_3) was dried on molecular sieves, and benzene- d_6 (C_6D_6) was dried over Na/K alloy and distilled. The

ligand LH and $\{LZnH\}_2$ ($L = \{(ArNH)(ArN)-C=N-C=(NAr)(NHAr)\}$; $Ar = 2,6\text{-Et}_2\text{-C}_6\text{H}_3$]) is prepared according to reported literature procedures.^{13b, 27} For catalysis reactions, 10 mL sealed airtight reaction vials and J. Young valve sealed NMR tubes were oven-dried before being used. Chemicals and reagents were purchased from Sigma-Aldrich Co. Ltd., Merck India Pvt. Ltd., and TCI chemicals were used without any purification.

4.4.1. Stoichiometric Experiments

Synthesis of $[LZnN(^iPr)C(H)N(^iPr)]$, (Zn-1) {Reaction-Scale}: 45 μ L (0.287 mmol) diisopropylcarbodiimide ($^iPr-N=C=N-^iPr$) in ~ 3 mL of benzene was added at room temperature through a cannula transfer to a solution of $[LZnH]_2$ (1**) 0.200 g (0.143 mmol) in 7 mL of benzene and stirred for 1 h. The solvent was removed under a high vacuum resulting in a white solid compound and dried thoroughly to get compound **Zn-1**. (0.192 g, 82 %); m.p. 190-195 °C. 1H NMR (400 MHz, C_6D_6 , 298 K) δ 7.30 (s, 1H), 7.21 – 7.19 (d, $^3J_{HH} = 7.5$ Hz, 4H), 7.14 – 7.10 (d, $^3J_{HH} = 15.0$ Hz, 2H), 6.94 (t, $^3J_{HH} = 7.6$ Hz, 2H), 6.71 – 6.69 (d, $^3J_{HH} = 7.9$ Hz, 4H), 4.98 (s, 2H), 3.30 – 3.19 (m, 6H), 3.05 – 2.95 (m, 4H), 2.43 – 2.34 (m, 4H), 2.20 – 2.10 (m, 4H), 1.39 (t, $^3J_{HH} = 7.5$ Hz, 12H), 1.02 (t, $^3J_{HH} = 7.6$ Hz, 12H), 0.86 – 0.84 (d, $^3J_{HH} = 6.8$ Hz, 12H). $^{13}C\{^1H\}$ NMR (101 MHz, C_6D_6 , 298 K) δ 164.5, 157.6, 143.4, 141.5, 138.5, 135.7, 126.0, 125.4, 125.0, 124.9, 48.2, 25.2, 24.9, 23.3, 14.3, 12.7. HRMS (ASAP/Q-TOF) m/z : $[M]^+$ Calcd for $C_{49}H_{69}N_7Zn$ 819.4906, Found: 819.4935.**

Synthesis of $[LZnN(^tBu)C(H)N(^tBu)]$, (Zn-1') {Reaction-Scale}: 55 μ L (0.287 mmol) tertbutyl carbodiimide ($^tBu-N=C=N-^tBu$) in ~ 3 mL of benzene was added at room temperature through a cannula transfer to a solution of $[LZnH]_2$ (1**) 0.200 g (0.143 mmol) in 7 mL of benzene and stirred for 1 h. The resultant mixture was concentrated to ~ 5 mL under reduced pressure and filtered. Then, the resultant solution was heated to 65 °C for 30 minutes and slowly cooled to room**

temperature. We observed the formation of block-shaped colorless crystals suitable for single-crystal X-ray diffraction within 24 h. (0.180 g, 74 %); m.p. 192-197 °C. ^1H NMR (400 MHz, C_6D_6) δ 7.71 (s, 1H), 7.15 – 7.11 (m, 6H), 6.96 (t, $J = 7.5$ Hz, 2H), 6.73 – 6.71 (d, $J = 7.6$ Hz, 4H), 4.97 (s, 2H), 3.33 – 3.23 (m, 4H), 3.10 – 3.00 (m, 4H), 2.40 – 2.29 (m, 4H), 2.13 – 2.05 (m, 4H), 1.39 (t, $J = 7.6$ Hz, 12H), 1.02 (t, $J = 7.6$ Hz, 12H), 0.97 (s, 18H). $^{13}\text{C}\{^1\text{H}\}$ NMR (101 MHz, C_6D_6 , 298 K) δ 161.0, 157.8, 143.6, 141.6, 138.4, 135.8, 126.1, 125.5, 124.9, 124.6, 49.9, 31.7, 24.9, 23.3, 14.4, 12.5. HRMS (ASAP/Q-TOF) m/z : $[\text{M}]^+$ Calcd for $\text{C}_{51}\text{H}_{74}\text{N}_7\text{Zn}$ 848.5297, Found: 848.5264.

Synthesis of $[\text{LZnC}\equiv\text{C-C}_6\text{H}_4\text{-}p\text{-Me}]_2$, (Zn-2**)** {Reaction-Scale}: 36 μL (0.287 mmol) 4-ethynyltoluene in ~ 3 mL of benzene was added at room temperature through a cannula transfer to a solution of $[\text{LZnH}]_2$ (**1**) 0.200 g (0.143 mmol) in 7 mL of benzene and stirred for 1 h. The solvent was removed under a high vacuum resulting in a white crystalline solid compound and dried thoroughly to get compound **Zn-2**. (0.203 g, 88 %); m.p. 187-192 °C. ^1H NMR (400 MHz, C_6D_6 , 298 K) δ 7.33 – 7.31 (d, $J = 7.7$ Hz, 4H), 7.14 – 7.07 (m, 12H), 6.88 (t, $^3J_{\text{HH}} = 7.5$ Hz, 4H), 6.78 – 6.76 (d, $^3J_{\text{HH}} = 7.5$ Hz, 4H), 6.63 – 6.61 (d, $^3J_{\text{HH}} = 7.6$ Hz, 8H), 5.03 (s, 4H), 3.13 – 3.03 (m, 8H), 2.80 – 2.70 (m, 8H), 2.40 – 2.30 (m, 8H), 2.20 – 2.10 (m, 8H), 1.95 (s, 6H), 1.36 (t, $^3J_{\text{HH}} = 7.5$ Hz, 24H), 0.93 (t, $^3J_{\text{HH}} = 7.6$ Hz, 24H). $^{13}\text{C}\{^1\text{H}\}$ NMR (101 MHz, C_6D_6 , 298 K) δ 157.4, 142.2, 141.0, 139.0, 136.6, 135.1, 131.9, 128.5, 126.4, 126.3, 125.7, 125.2, 122.3, 101.2, 26.2, 24.8, 24.1, 20.8, 14.2. HRMS (ASAP/Q-TOF) m/z : $[\text{M}+\text{H}]^+$ Calcd for $\text{C}_{51}\text{H}_{62}\text{N}_5\text{Zn}$ 808.4297, Found: 808.4210.

Synthesis of $[\text{LZnC}\equiv\text{C-C}_5\text{H}_9]_2$, (Zn-2'**)** {Reaction-Scale}: 33 μL (0.287 mmol) cyclopentylacetylene in ~ 3 mL of benzene was added at room temperature through a cannula transfer to a solution of $[\text{LZnH}]_2$ (**1**) 0.200 g (0.143 mmol) in 7 mL of benzene and stirred for 1 h. The resultant mixture was concentrated to ~ 4 mL under reduced pressure and filtered. Then the

resultant solution was heated to 65 °C for 30 min. and slowly cooled to room temperature. We observed the formation of block-shaped colorless crystals suitable for single-crystal X-ray diffraction within 24 h. (0.175 g, 78 %); m.p. 180-185 °C. ^1H NMR (400 MHz, C_6D_6 , 298 K) δ 7.13 – 7.10 (m, 12H), 6.88 (t, $^3J_{\text{HH}} = 7.5$ Hz, 4H), 6.63 – 6.62 (d, $^3J_{\text{HH}} = 7.6$ Hz, 8H), 5.01 (s, 4H), 3.10 – 2.97 (m, 8H), 2.78 – 2.68 (m, 8H), 2.59 – 2.48 (m, 2H), 2.41 – 2.32 (m, 8H), 2.21 – 2.10 (m, 8H), 1.72 – 1.61 (m, 4H), 1.59 – 1.46 (m, 8H), 1.35 (t, $^3J_{\text{HH}} = 7.5$ Hz, 24H), 1.29 – 1.23 (m, 4H), 0.94 (t, $^3J_{\text{HH}} = 7.6$ Hz, 24H). $^{13}\text{C}\{^1\text{H}\}$ NMR (101 MHz, C_6D_6 , 298 K) δ 157.2, 142.4, 141.0, 138.9, 135.2, 126.4, 126.2, 125.6, 125.2, 34.3, 31.9, 24.9, 24.7, 24.2, 14.2, 14.2. HRMS (ASAP/Q-TOF) m/z : $[\text{M}+\text{H}]^+$ Calcd for $\text{C}_{49}\text{H}_{64}\text{N}_5\text{Zn}$ 786.4453, found: 786.4527.

Synthesis of $[\text{LZn}(\text{N}^i\text{Pr})\text{C}\equiv\text{C}-\text{C}_6\text{H}_4-p\text{-Me}(\text{N}^i\text{Pr})]$, (Zn-3**) {NMR-Scale}:** The addition of diisopropylcarbodiimide (6 μL , 0.038 mmol) to a J. Young valve NMR tube containing a solution of compound **Zn-2** (30 mg, 0.019 mmol) in C_6D_6 , resulted in the formation of compound **Zn-3** at 70 °C after 2 h was observed by ^1H NMR spectroscopy. NMR conversion >99%. ^1H NMR (400 MHz, C_6D_6 , 298 K) δ 7.21 – 7.20 (d, $^3J_{\text{HH}} = 6.9$ Hz, 6H), 7.14 – 7.11 (m, 2H), 6.95 (t, $^3J_{\text{HH}} = 7.6$ Hz, 2H), 6.71 – 6.70 (d, $^3J_{\text{HH}} = 7.6$ Hz, 6H), 5.00 (s, 2H), 4.09 – 4.03 (m, 2H), 3.35 – 3.26 (m, 4H), 3.10 – 3.00 (m, 4H), 2.42 – 2.33 (m, 4H), 2.19 – 2.10 (m, 4H), 1.91 (s, 3H), 1.40 (t, $^3J_{\text{HH}} = 7.6$ Hz, 12H), 1.04 – 1.01 (m, 24H). $^{13}\text{C}\{^1\text{H}\}$ NMR (101 MHz, C_6D_6 , 298 K) δ 157.8, 156.4, 143.5, 141.5, 138.9, 138.5, 135.7, 131.7, 128.9, 126.1, 125.4, 125.0, 124.9, 119.0, 96.8, 78.9, 47.1, 24.9, 24.7, 23.4, 20.9, 14.3, 12.7. HRMS (ASAP/Q-TOF) m/z : $[\text{M}+\text{H}]^+$ Calcd for $\text{C}_{58}\text{H}_{76}\text{N}_7\text{Zn}$ 934.5453, Found: 934.5667.

Synthesis of $[\text{LZnNH}-\text{C}_6\text{H}_4-p\text{-Me}]_2$, (Zn-4**) {NMR-Scale}:** $[\text{LZnH}]_2$ (**1**) (30 mg, 0.021 mmol) and *p*-toluidine (5 mg, 0.043 mmol) were mixed in a J Young valve NMR tube and to that 0.4 mL of benzene- d_6 was added, resulted in the formation of complex **Zn-4** after 30 minutes. Then, the

reaction mixture was heated at 65 °C for 1 h and cooled to room temperature. We observed the formation of block-shaped colorless crystals suitable for single-crystal X-ray diffraction within 24 h. NMR conversion >99%. ^1H NMR (400 MHz, C_6D_6 , 298 K) δ 7.16 (s, 18H), 6.86 (s, 6H), 6.63 – 6.61 (d, $^3J_{\text{HH}} = 7.5$ Hz, 6H), 6.43 – 6.42 (d, $^3J_{\text{HH}} = 7.6$ Hz, 2H), 4.93 (s, 4H), 2.85 – 2.76 (m, 10H), 2.39 – 2.32 (m, 12H), 2.27 (s, 6H), 2.23 – 2.17 (m, 12H), 1.14 (s, 24H), 0.94 (t, $^3J_{\text{HH}} = 7.6$ Hz, 24H). $^{13}\text{C}\{^1\text{H}\}$ NMR (101 MHz, C_6D_6 , 298 K) δ 156.8, 140.9, 138.9, 135.5, 128.9, 126.0, 125.0, 124.9, 122.1, 24.7, 23.3, 20.4, 14.1, 12.6. HRMS (ASAP/Q-TOF) m/z : $[\text{M}+\text{H}]^+$ Calcd for $\text{C}_{49}\text{H}_{63}\text{N}_6\text{Zn}$ 799.4406, found: 799.4371.

Synthesis of $[\text{LZnO-CH}_2\text{-C}_6\text{H}_5]_2$, (Zn-5**) {NMR-Scale}:** $[\text{LZnH}]_2$ (**1**) (30 mg, 0.021 mmol) and benzyl alcohol (5 μL , 0.043 mmol) were mixed in a J Young valve NMR tube and to that 0.4 mL of benzene- d_6 was added, resulted in the formation of complex **Zn-5** after 30 minutes. Then, the reaction mixture was heated at 65 °C for 1 h and cooled to room temperature. We observed the formation of block-shaped colorless crystals suitable for single-crystal X-ray diffraction within 24 h. NMR conversion >99%. ^1H NMR (400 MHz, C_6D_6 , 298 K) δ 7.29 (t, $^3J_{\text{HH}} = 7.6$ Hz, 5H), 7.22 (t, $^3J_{\text{HH}} = 7.5$ Hz, 17H), 6.86 (t, $^3J_{\text{HH}} = 7.5$ Hz, 4H), 6.62 – 6.60 (d, $^3J_{\text{HH}} = 7.6$ Hz, 8H), 4.97 (s, 4H), 4.89 (s, 4H), 2.95 – 2.87 (m, 8H), 2.50 – 2.42 (m, 8H), 2.32 – 2.25 (m, 8H), 2.14 – 2.09 (m, 8H), 1.11 (t, $^3J_{\text{HH}} = 7.6$ Hz, 24H), 0.86 (t, $^3J_{\text{HH}} = 7.6$ Hz, 24H). $^{13}\text{C}\{^1\text{H}\}$ NMR (101 MHz, C_6D_6 , 298 K) δ 157.5, 144.9, 143.7, 140.9, 138.9, 135.4, 125.9, 125.7, 125.5, 125.0, 124.9, 69.2, 24.6, 23.4, 14.0, 12.5. HRMS (ASAP/Q-TOF) m/z : $[\text{M}+\text{H}]^+$ Calcd for $\text{C}_{49}\text{H}_{62}\text{N}_5\text{OZn}$ 800.4246, Found: 800.4255.

4.4.2. X-ray Crystallographic Data

The single crystals of compounds **Zn-1'**, **Zn-2'**, **Zn-4**, **Zn-5** and **3q** are crystallized from benzene at rt as colorless blocks between 24 - 48 h. The crystal data of compounds **Zn-1'** and **Zn-5** are

collected on a Rigaku Oxford diffractometer with graphite-monochromated Cu-K α radiation ($\lambda = 1.54184 \text{ \AA}$) at 100 K. Whereas, the crystal data of compounds **Zn-2'**, **Zn-4**, and **3q** are collected on a Rigaku Oxford diffractometer with Mo-K α radiation ($\lambda = 0.71073 \text{ \AA}$) at 100 K. Selected data collection parameters and other crystallographic results are summarized in Table 4.3-4.4. The structure was determined using direct methods employed in *ShelXT*,³³ *Olex*,³⁴ and refinement was carried out using least-square minimization implemented in *ShelXL*.³⁵ All non-hydrogen atoms were refined with anisotropic displacement parameters. Hydrogen atom positions were fixed geometrically in idealized positions and were refined using a riding model.

Table 4.3. Crystallographic data and refinement parameters for compounds **Zn-1'**, **Zn-2'**, **Zn-4**, and **Zn-5**.

Compound	Zn-1'	Zn-2'	Zn-4	Zn-5
Empirical Formula	C ₅₇ H ₇₉ N ₇ Zn	C ₉₈ H ₁₂₆ N ₁₀ Zn ₂	C ₁₀₀ H ₁₃₆ N ₁₂ Zn ₂	C ₁₀₄ H ₁₂₈ N ₁₀ O ₂ Zn ₂
CCDC	2222780	2222781	2222782	2222784
Molecular mass	927.64	1574.82	1757.04	1680.90
Temperature (K)	100	100	100	100
Wavelength (Å)	1.54184	0.71073	0.71073	1.54184
Size(mm)	0.2 × 0.18 × 0.17	0.2 × 0.18 × 0.17	0.2 × 0.18 × 0.17	0.2 × 0.18 × 0.17
Crystal system	monoclinic	monoclinic	triclinic	triclinic
Space group	<i>P</i> 2 ₁ / <i>n</i>	<i>P</i> 2 ₁ / <i>n</i>	<i>P</i> -1	<i>P</i> -1
<i>a</i> (Å)	11.4388(2)	13.1448(6)	11.1896(2)	12.0396(3)
<i>b</i> (Å)	34.6667(7)	16.2930(5)	14.1614(2)	13.4769(3)
<i>c</i> (Å)	13.5896(3)	20.4106(10)	15.8404(2)	15.2960(4)
α (deg) ^o	90	90	102.7250(10)	91.052(2)
β (deg) ^o	95.902(2)	98.376(5)	96.6800(10)	90.017(2)
γ (deg) ^o	90	90	98.5920(10)	115.692(3)
Volume (Å ³)	5360.33(19)	4324.7(3)	2391.79(6)	2236.04(11)
<i>Z</i>	4	2	1	1
Calculated density (g/cm ³)	1.149	1.209	1.220	1.248
Absorption coefficient (mm ⁻¹)	0.946	0.607	0.556	1.089
<i>F</i> (000)	2000.0	1688.0	940.0	898.0
Theta range for data collection (deg) ^o	7.018 to 136.5	6.55 to 52.744	6.726 to 52.744	7.28 to 136.502
Limiting indices	-13 ≤ <i>h</i> ≤ 13, -41 ≤ <i>k</i> ≤ 40, -12 ≤ <i>l</i> ≤ 16	-16 ≤ <i>h</i> ≤ 16, -20 ≤ <i>k</i> ≤ 20, -25 ≤ <i>l</i> ≤ 25	-13 ≤ <i>h</i> ≤ 13, -17 ≤ <i>k</i> ≤ 17, -19 ≤ <i>l</i> ≤ 19	-10 ≤ <i>h</i> ≤ 14, -16 ≤ <i>k</i> ≤ 16, -18 ≤ <i>l</i> ≤ 18
Reflections collected	44602	46352	45802	32601
Independent reflections	9806 [<i>R</i> _{int} = 0.0693, <i>R</i> _{sigma} = 0.0362]	8825 [<i>R</i> _{int} = 0.0639, <i>R</i> _{sigma} = 0.0434]	9749 [<i>R</i> _{int} = 0.0341, <i>R</i> _{sigma} = 0.0240]	8188 [<i>R</i> _{int} = 0.0434, <i>R</i> _{sigma} = 0.0311]
Completeness to theta	99 %	99 %	99 %	99 %
Absorption correction	Empirical	Empirical	Empirical	Empirical
Data / restraints / parameters	9806 / 0 / 604	8825 / 66 / 498	9749 / 0 / 572	8188 / 0 / 540
Goodness – of–fit on <i>F</i> ²	1.154	1.098	1.070	1.041
Final <i>R</i> indices [<i>I</i> > 2 sigma(<i>I</i>)]	<i>R</i> ₁ = 0.0856, <i>wR</i> ₂ = 0.2471	<i>R</i> ₁ = 0.0991, <i>wR</i> ₂ = 0.3208	<i>R</i> ₁ = 0.0325, <i>wR</i> ₂ = 0.0857	<i>R</i> ₁ = 0.0327, <i>wR</i> ₂ = 0.0873

Table 4.4. Crystallographic data and refinement parameters for compound **3q**.

Compound	3q
Empirical Formula	C ₄₄ H ₅₂ B ₂ N ₄ O ₄
CCDC	2239360
Molecular mass	722.51
Temperature (K)	100
Wavelength (Å)	0.71073
Size(mm)	0.2 × 0.18 × 0.17
Crystal system	triclinic
Space group	P -1
a (Å)	5.9085(2)
b (Å)	9.4320(3)
c (Å)	19.5278(7)
α (deg)°	99.401(3)
β (deg)°	97.313(3)
γ (deg)°	105.067(3)
Volume (Å ³)	1020.15(6)
Z	1
Calculated density (g/cm ³)	1.176
Absorption coefficient (mm ⁻¹)	0.075
F(000)	386.0
Theta range for data collection (deg)°	6.888 to 50.698
Limiting indices	-7 ≤ h ≤ 7, -11 ≤ k ≤ 11, -23 ≤ l ≤ 23
Reflections collected	16274
Independent reflections	3724 [R _{int} = 0.0497, R _{sigma} = 0.0399]
Completeness to theta	99 %
Absorption correction	Empirical
Data / restraints /parameters	3724 / 0 / 248
Goodness – of–fit on F ²	1.043
Final R indices [I>2 sigma(I)]	R ₁ = 0.0398, wR ₂ = 0.0982

4.5. Appendix: All general experimental information, stoichiometric reactions, analytical data, and spectral data were available in published paper. *Organometallics* **2023**, 42, 1746-1758.

4.6. References

1. Zeng, X. *Chem. Rev.* **2013**, *113*, 6864-6900.
2. (a) Bazkiaei, R. A.; Findlater, M.; Gordon, A. E. V. *Org. Biomol. Chem.* **2022**, *20*, 3675-3702; (b) Sarkar, N.; Bera, S.; Nembenna, S. *J. Org. Chem.* **2020**, *85*, 4999-5009; (c) Das, A.; Panda, T. K. *ChemCatChem* **2023**, *15*, e202201011.
3. (a) Iglesias, M.; Fernández-Alvarez, F. J.; Oro, L. A. *ChemCatChem* **2014**, *6*, 2486-2489; (b) Dash, A. K.; Wang, J. X.; Berthet, J. C.; Ephritikhine, M.; Eisen, M. S. *J. Organomet. Chem.* **2000**, *604*, 83-98; (c) Dash, A. K.; Wang, J. Q.; Eisen, M. S. *Organometallics* **1999**, *18*, 4724-4741.
4. (a) Hayes, C. E.; Platel, R. H.; Schafer, L. L.; Leznoff, D. B. *Organometallics* **2012**, *31*, 6732-6740; (b) Ren, W.; Zi, G.; Fang, D.-C.; Walter, M. D. *Chem. Eur. J.* **2011**, *17*, 12669-12682; (c) Stubbert, B. D.; Marks, T. J. *J. Am. Chem. Soc.* **2007**, *129*, 4253-4271; (d) Straub, T.; Haskel, A.; Neyroud, T. G.; Kapon, M.; Botoshansky, M.; Eisen, M. S. *Organometallics* **2001**, *20*, 5017-5035; (e) Haskel, A.; Straub, T.; Eisen, M. S. *Organometallics* **1996**, *15*, 3773-3775.
5. (a) Zhang, B.; Ma, X.; Yan, B.; Ni, C.; Yu, H.; Yang, Z.; Roesky, H. W. *Dalton Trans.* **2021**, *50*, 15488-15492; (b) Koshti, V.; Gaikwad, S.; Chikkali, S. H. *Coord. Chem. Rev.* **2014**, *265*, 52-73; (c) Douglass, M. R.; Stern, C. L.; Marks, T. J. *J. Am. Chem. Soc.* **2001**, *123*, 10221-10238.
6. (a) Wobser, S. D.; Marks, T. J. *Organometallics* **2013**, *32*, 2517-2528; (b) Weiss, C. J.; Wobser, S. D.; Marks, T. J. *J. Am. Chem. Soc.* **2009**, *131*, 2062-2063.
7. Muñoz, M. P. *Org. Biomol. Chem.* **2012**, *10*, 3584-3594.
8. (a) Bauer, H.; Harder, S. In *Early Main Group Metal Catalysis*, **2020**; pp 175-199; (b) Bauer, H.; Thum, K.; Alonso, M.; Fischer, C.; Harder, S. *Angew. Chem. Int. Ed.* **2019**, *58*, 4248-4253;

- (c) Elsen, H.; Färber, C.; Ballmann, G.; Harder, S. *Angew. Chem. Int. Ed.* **2018**, *57*, 7156-7160;
- (d) Elsen, H.; Langer, J.; Ballmann, G.; Wiesinger, M.; Harder, S. *Chem. Eur. J.* **2021**, *27*, 401-411; (e) Friedrich, A.; Eyselein, J.; Elsen, H.; Langer, J.; Pahl, J.; Wiesinger, M.; Harder, S. *Chem. Eur. J.* **2021**, *27*, 7756-7763; (f) Stegner, P.; Färber, C.; Zenneck, U.; Knüpfer, C.; Eyselein, J.; Wiesinger, M.; Harder, S. *Angew. Chem. Int. Ed.* **2021**, *60*, 4252-4258.
9. (a) Barnea, E.; Eisen, M. S. *Coord. Chem. Rev.* **2006**, *250*, 855-899; (b) Bauer, H.; Alonso, M.; Fischer, C.; Rösch, B.; Elsen, H.; Harder, S. *Angew. Chem. Int. Ed.* **2018**, *57*, 15177-15182; (c) Hill, M. S.; Liptrot, D. J.; Weetman, C. *Chem. Soc. Rev.* **2016**, *45*, 972-988; (d) Martin, J.; Knüpfer, C.; Eyselein, J.; Färber, C.; Grams, S.; Langer, J.; Thum, K.; Wiesinger, M.; Harder, S. *Angew. Chem. Int. Ed.* **2020**, *59*, 9102-9112; (e) Penafiel, J.; Maron, L.; Harder, S. *Angew. Chem. Int. Ed.* **2015**, *54*, 201-206.
10. (a) Nayak, D. K.; Sarkar, N.; Sampath, C. M.; Sahoo, R. K.; Nembenna, S. *Z. Anorg. Allgem. Chem.* **2022**, *648*, e202200116; (b) Peddaraao, T.; Baishya, A.; Barman, M. K.; Kumar, A.; Nembenna, S. *New J. Chem.* **2016**, *40*, 7627-7636; (c) Zhang, W.-X.; Xu, L.; Xi, Z. *Chem. Commun.* **2015**, *51*, 254-265; (d) Baishya, A.; Peddaraao, T.; Barman, M. K.; Nembenna, S. *New J. Chem.* **2015**, *39*, 7503-7510; (e) Baishya, A.; Barman, M. K.; Peddaraao, T.; Nembenna, S. *J. Organomet. Chem.* **2014**, *769*, 112-118.
11. Zhang, F.; Zhang, J.; Zhang, Y.; Hong, J.; Zhou, X. *Organometallics* **2014**, *33*, 6186-6192.
12. Bhattacharjee, J.; Sachdeva, M.; Banerjee, I.; Panda, T. K. *J. Chem. Sci.* **2016**, *128*, 875-881.
13. (a) Carrillo-Hermosilla, F.; Fernández-Galán, R.; Ramos, A.; Elorriaga, D. *Molecules* **2022**, *27*, 5962; (b) Peddaraao, T.; Baishya, A.; Sarkar, N.; Acharya, R.; Nembenna, S. *Eur. J. Inorg. Chem.* **2021**, 2034-2046.
14. Smith, R. C.; Protasiewicz, J. D. *J. Am. Chem. Soc.* **2004**, *126*, 2268-2269.

-
15. Zarate, G. S.; Santana, G. A.; Bastida, A.; Revuelta, J. *Curr. Org. Chem.* **2014**, *18*, 2711-2749.
16. (a) Khononov, M.; Fridman, N.; Tamm, M.; Eisen, M. S. *Eur. J. Org. Chem.* **2020**, 3153-3160;
(b) Liu, H.; Kulbitski, K.; Tamm, M.; Eisen, M. S. *Chem. Eur. J.* **2018**, *24*, 5738-5742.
- 17 (a) Yan, B.; He, X.; Ni, C.; Yang, Z.; Ma, X. *ChemCatChem* **2021**, *13*, 851-854; (b) Patel, M.; Desai, B.; Sheth, A.; Dholakiya, B. Z.; Naveen, T. *Asian. J. Org. Chem.* **2021**, *10*, 3201-3232;
(c) Bisai, M. K.; Gour, K.; Das, T.; Vanka, K.; Sen, S. S. *J. Organomet. Chem.* **2021**, 949, 121924; (d) Panda, T. K.; Banerjee, I.; Sagar, S. *Appl. Organomet. Chem.* **2020**, *34*, e5765; (e) Bakewell, C. *Dalton Trans.* **2020**, *49*, 11354-11360; (f) Shen, Q.; Ma, X.; Li, W.; Liu, W.; Ding, Y.; Yang, Z.; Roesky, H. W. *Chem. Eur. J.* **2019**, *25*, 11918-11923; (g) Ding, Y.; Ma, X.; Liu, Y.; Liu, W.; Yang, Z.; Roesky, H. W. *Organometallics* **2019**, *38*, 3092-3097; (h) Rauch, M.; Ruccolo, S.; Parkin, G. *J. Am. Chem. Soc.* **2017**, *139*, 13264-13267; (i) Weetman, C.; Hill, M. S.; Mahon, M. F. *Chem. Eur. J.* **2016**, *22*, 7158-7162; (j) Mukherjee, D.; Shirase, S.; Spaniol, T. P.; Mashima, K.; Okuda, J. *Chem. Commun.* **2016**, *52*, 13155-13158.
18. Ramos, A.; Antiñolo, A.; Carrillo-Hermosilla, F.; Fernández-Galán, R.; García-Vivó, D. *Chem. Commun.* **2019**, *55*, 3073-3076.
19. Zhang, W.-X.; Nishiura, M.; Hou, Z. *J. Am. Chem. Soc.* **2005**, *127*, 16788-16789.
20. (a) Sroor, F. M.; Hrib, C. G.; Hilfert, L.; Busse, S.; Edelman, F. T. *New J. Chem.* **2015**, *39*, 7595-7601; (b) Xu, L.; Wang, Y.-C.; Zhang, W.-X.; Xi, Z. *Dalton Trans.* **2013**, *42*, 16466-16469; (c) Yi, W.; Zhang, J.; Li, M.; Chen, Z.; Zhou, X. *Inorg. Chem.* **2011**, *50*, 11813-11824;
(d) Xu, X.; Gao, J.; Cheng, D.; Li, J.; Qiang, G.; Guo, H. *Adv. Synth. Catal.* **2008**, *350*, 61-64;
(e) Du, Z.; Li, W.; Zhu, X.; Xu, F.; Shen, Q. *J. Org. Chem.* **2008**, *73*, 8966-8972; (f) Zhou, S.; Wang, S.; Yang, G.; Li, Q.; Zhang, L.; Yao, Z.; Zhou, Z.; Song, H.-b. *Organometallics* **2007**,
-

- 26, 3755-3761; (g) Ong, T.-G.; O'Brien, J. S.; Korobkov, I.; Richeson, D. S. *Organometallics* **2006**, *25*, 4728-4730.
21. Martínez, A.; Moreno-Blázquez, S.; Rodríguez-Diéguez, A.; Ramos, A.; Fernández-Galán, R.; Antiñolo, A.; Carrillo-Hermosilla, F. *Dalton Trans.* **2017**, *46*, 12923-12934.
22. Ramos, A.; Carrillo-Hermosilla, F.; Fernández-Galán, R.; Elorriaga, D.; Naranjo, J.; Antiñolo, A.; García-Vivó, D. *Organometallics* **2022**, *41*, 2949-2957.
23. Evans, W. J.; Walensky, J. R.; Ziller, J. W. *Organometallics* **2010**, *29*, 945-950.
24. (a) Liu, H.; Fridman, N.; Tamm, M.; Eisen, M. S. *Organometallics* **2017**, *36*, 3896-3903; (b) Batrice, R. J.; Kefalidis, C. E.; Maron, L.; Eisen, M. S. *J. Am. Chem. Soc.* **2016**, *138*, 2114-2117; (c) Batrice, R. J.; Eisen, M. S. *Chem. Sci.* **2016**, *7*, 939-944; (d) Karmel, I. S. R.; Tamm, M.; Eisen, M. S. *Angew. Chem. Int. Ed.* **2015**, *54*, 12422-12425.
25. Bhattacharjee, J.; Harinath, A.; Banerjee, I.; Nayek, H. P.; Panda, T. K. *Inorg. Chem.* **2018**, *57*, 12610-12623.
26. González, M. J.; López, L. A.; Vicente, R. *Tetrahedron Lett.* **2015**, *56*, 1600-1608.
27. (a) Sahoo, R. K.; Sarkar, N.; Nembenna, S. *Angew. Chem. Int. Ed.* **2021**, *60*, 11991-12000; (b) Sahoo, R. K.; Mahato, M.; Jana, A.; Nembenna, S. *J. Org. Chem.* **2020**, *85*, 11200-11210.
28. (a) Sarkar, N.; Sahoo, R. K.; Mukhopadhyay, S.; Nembenna, S. *Eur. J. Inorg. Chem.* **2022**, e202101030; (b) Khuntia, A. P.; Sarkar, N.; Patro, A. G.; Sahoo, R. K.; Nembenna, S. *Eur. J. Inorg. Chem.* **2022**, e202200209; (c) Barman, M. K.; Baishya, A.; Nembenna, S. *J. Organomet. Chem.* **2019**, *887*, 40-47; (d) Barman, M. K.; Baishya, A.; Nembenna, S. *Dalton Trans.* **2017**, *46*, 4152-4156; (e) Baishya, A.; Peddaraao, T.; Nembenna, S. *Dalton Trans.* **2017**, *46*, 5880-5887; (f) Jakhar, V. K.; Barman, M. K.; Nembenna, S. *Org. Lett.* **2016**, *18*, 4710-4713; (g) Barman, M. K.; Baishya, A.; Nembenna, S. *J. Organomet. Chem.* **2015**, *785*, 52-60; (h)

-
- Barman, M. K.; Baishya, A.; Peddaraao, T.; Nembenna, S. *J. Organomet. Chem.* **2014**, 772-773, 265-270.
29. Hara, M.; Minagawa, K.; Imada, Y.; Arakawa, Y. *ACS Omega* **2021**, 6, 33215-33223.
30. (a) Baishya, A.; Kumar, L.; Barman, M. K.; Biswal, H. S.; Nembenna, S. *Inorg. Chem.* **2017**, 56, 9535-9546; (b) Chamenahalli, R.; Andrews, A. P.; Ritter, F.; Okuda, J.; Venugopal, A. *Chem. Commun.* **2019**, 55, 2054-2057.
31. Sahoo, R. K.; Rajput, S.; Patro, A. G.; Nembenna, S. *Dalton Trans.* **2022**, 51, 16009-16016.
32. (a) Baker, G. J.; White, A. J. P.; Casely, I. J.; Grainger, D.; Crimmin, M. R. *ChemRxiv*. 2022-06-20, DOI: 10.26434/chemrxiv-2022-3tcn2-v2; (b) Wang, C.-H.; Li, C.-Y.; Huang, B.-H.; Lin, C.-C.; Ko, B.-T. *Dalton Trans.* **2013**, 42, 10875-10884.
33. Sheldrick, G. *Acta Crystallogr. C*. **2015**, 71, 3-8.
34. Dolomanov, O. V.; Bourhis, L. J.; Gildea, R. J.; Howard, J. A. K.; Puschmann, H. *J. Appl. Crystallogr.* **2009**, 42, 339-341.
35. (a) Sheldrick, G. M. *Acta Crystallogr., Sect. A: Found. Crystallogr.* **2008**, 64, 112-122; (b) Sheldrick, G. M. *Acta Crystallogr., Sect. A: Found. Adv.* **2015**, 71, 3-8.

NMR Spectra

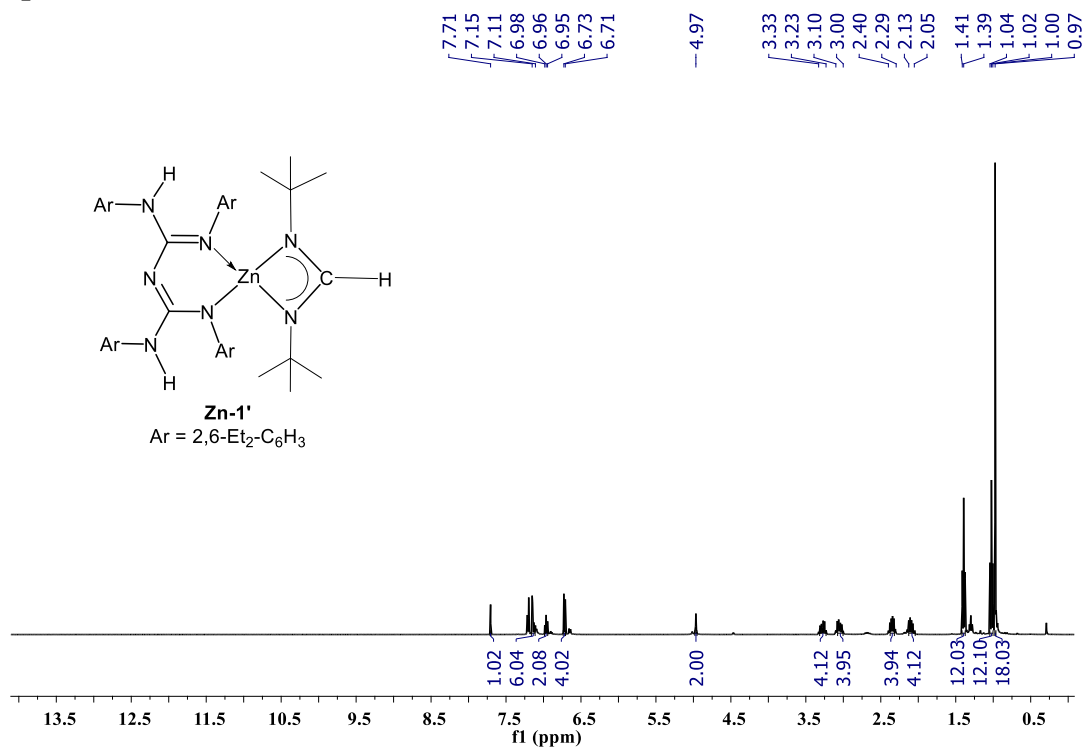


Figure 4.6. ¹H NMR spectrum of compound [LZnN('Bu)C(H)N('Bu)], **Zn-1'** (400 MHz, C₆D₆, 25 °C)

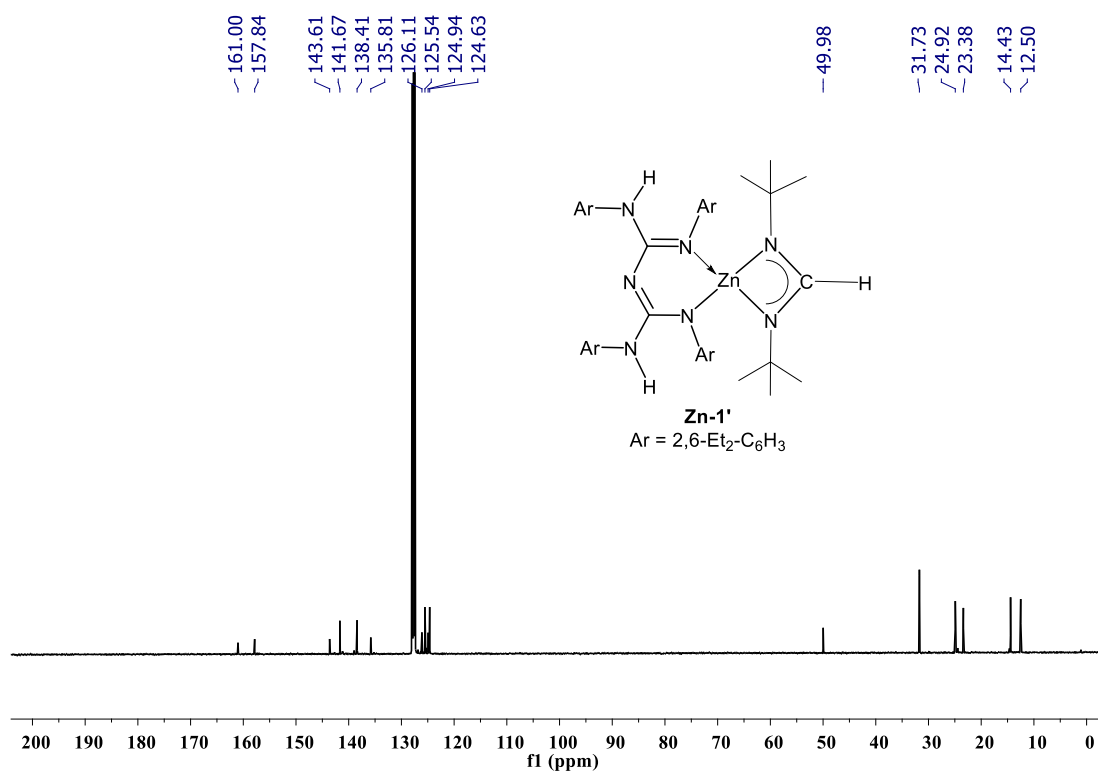


Figure 4.7. ¹³C{¹H} NMR spectrum of compound [LZnN('Bu)C(H)N('Bu)], **Zn-1'** (101 MHz, C₆D₆, 25 °C)

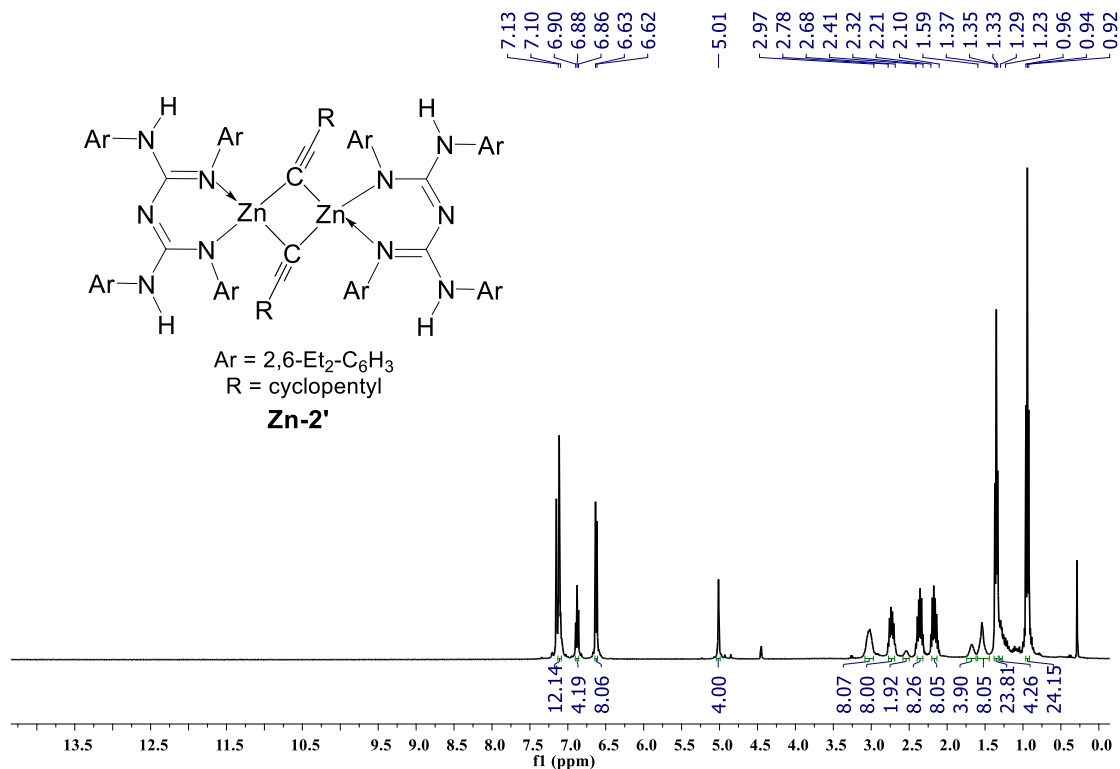


Figure 4.8. ¹H NMR spectrum of compound [LZnC≡C-C₅H₉], **Zn-2'** (400 MHz, C₆D₆, 25 °C)

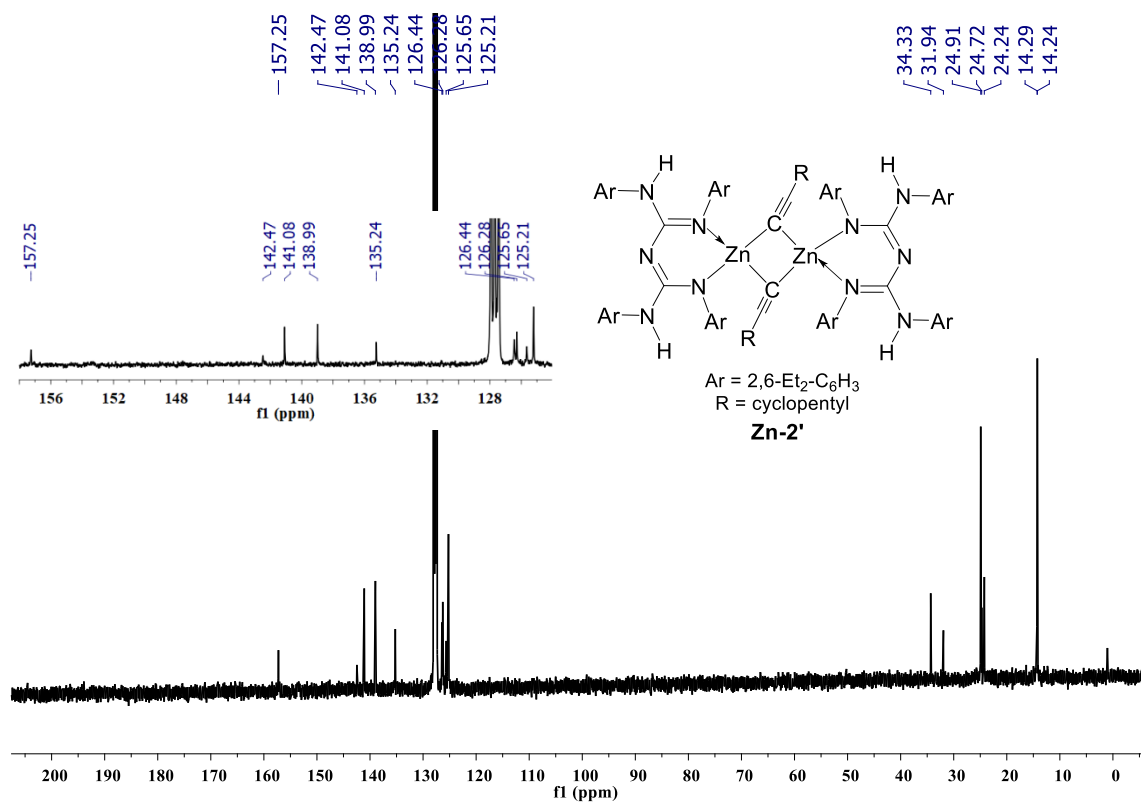


Figure 4.9. ¹³C{¹H} NMR spectrum of compound [LZnC≡C-C₅H₉], **Zn-2'** (101 MHz, C₆D₆, 25 °C)

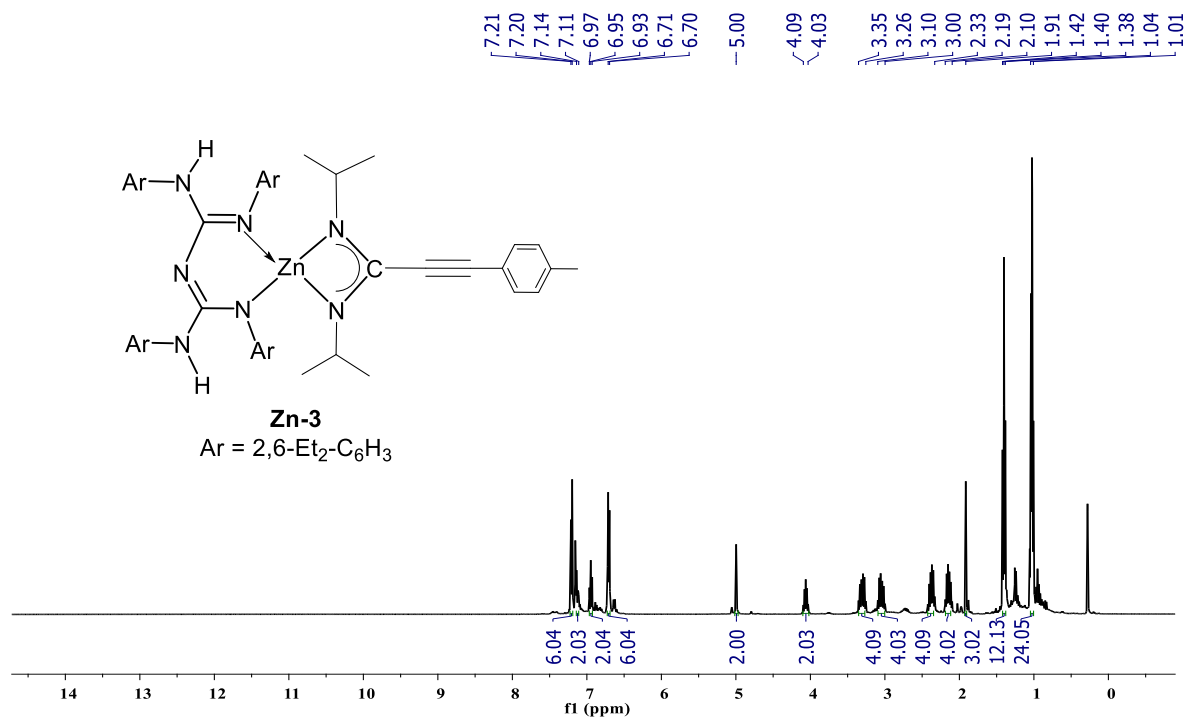


Figure 4.10. ¹H NMR spectrum of compound [LZn(NⁱPr)C≡C-C₆H₄-p-Me(NⁱPr)], **Zn-3** (400 MHz, C₆D₆, 25 °C)

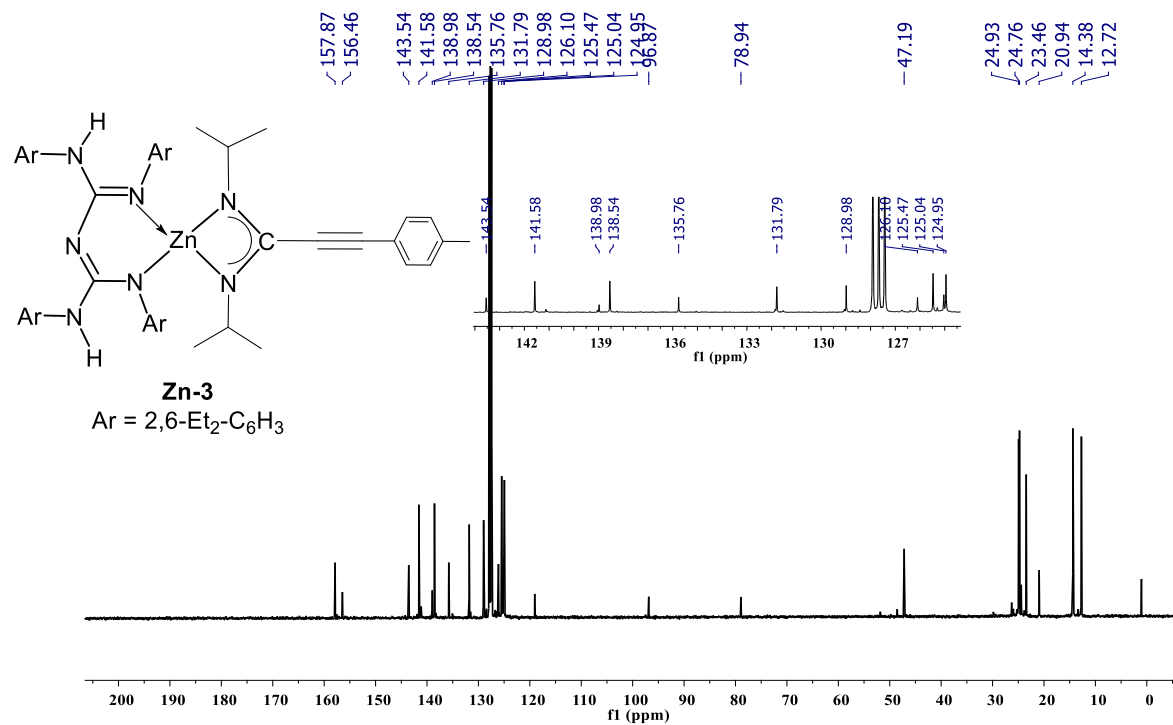


Figure 4.11. ¹³C{¹H} NMR spectrum of compound [LZn(NⁱPr)C≡C-C₆H₄-p-Me(NⁱPr)], **Zn-3** (101 MHz, C₆D₆, 25 °C)

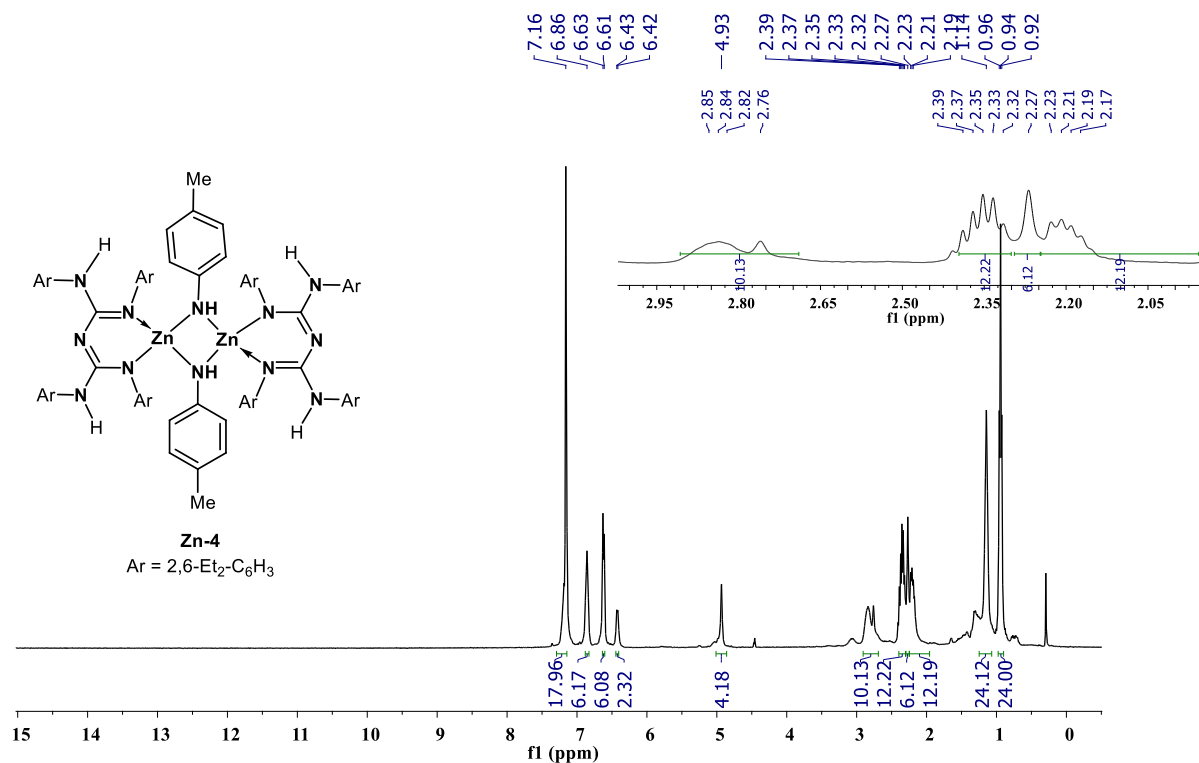


Figure 4.12. ¹H NMR spectrum of compound [LZnNH-C₆H₄-*p*-Me], **Zn-4** (400 MHz, C₆D₆, 25 °C)

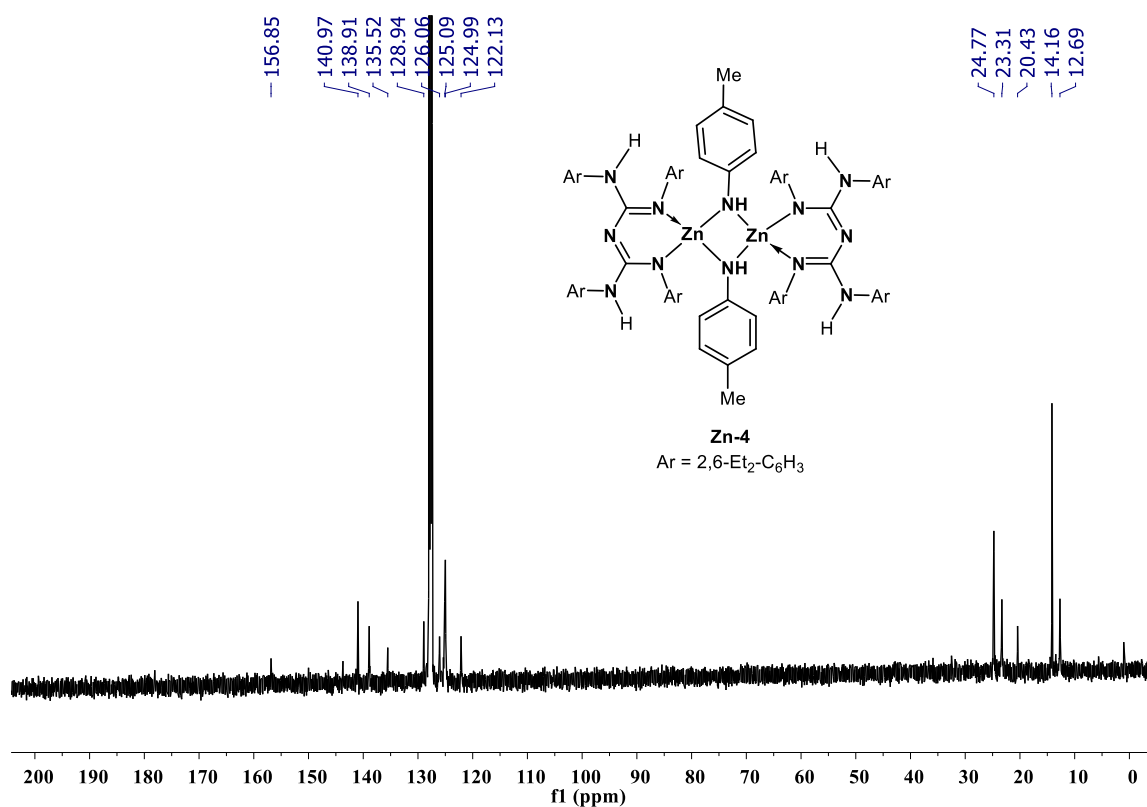


Figure 4.13. ¹³C{¹H} NMR spectrum of compound [LZnNH-C₆H₄-*p*-Me], **Zn-4** (101 MHz, C₆D₆, 25 °C)

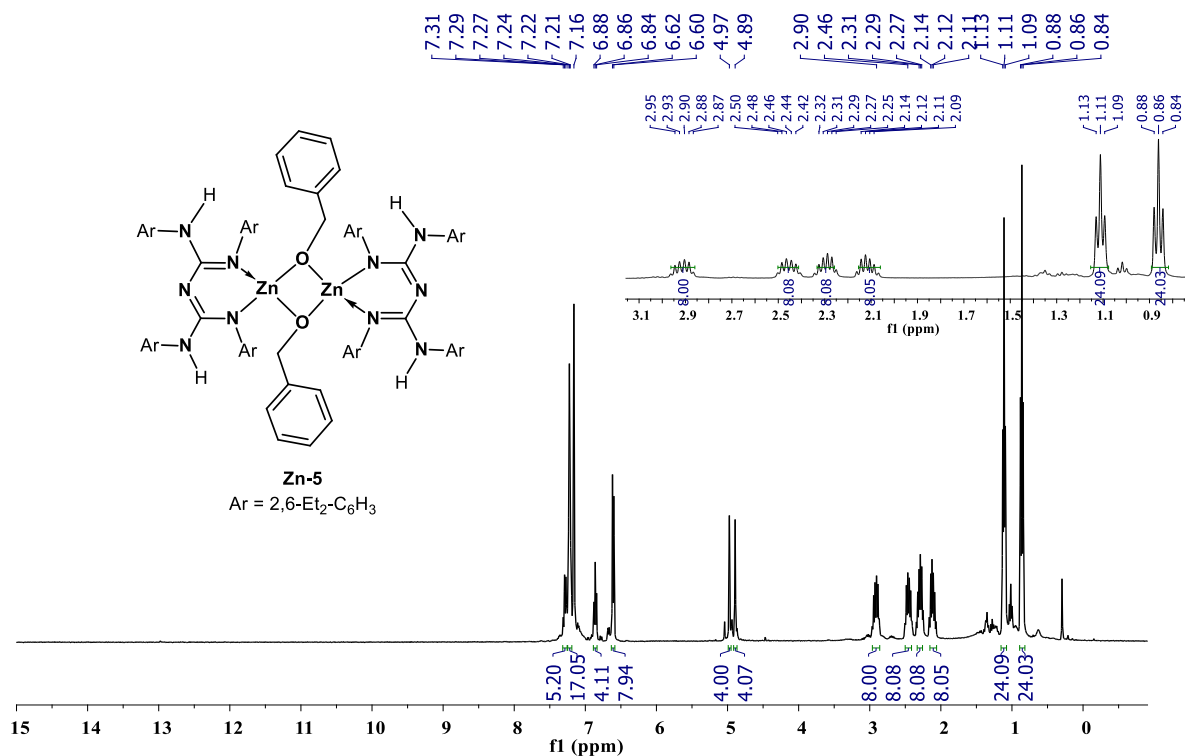


Figure 4.14. ¹H NMR spectrum of compound [LZnO-CH₂-C₆H₅], **Zn-5** (400 MHz, C₆D₆, 25 °C)

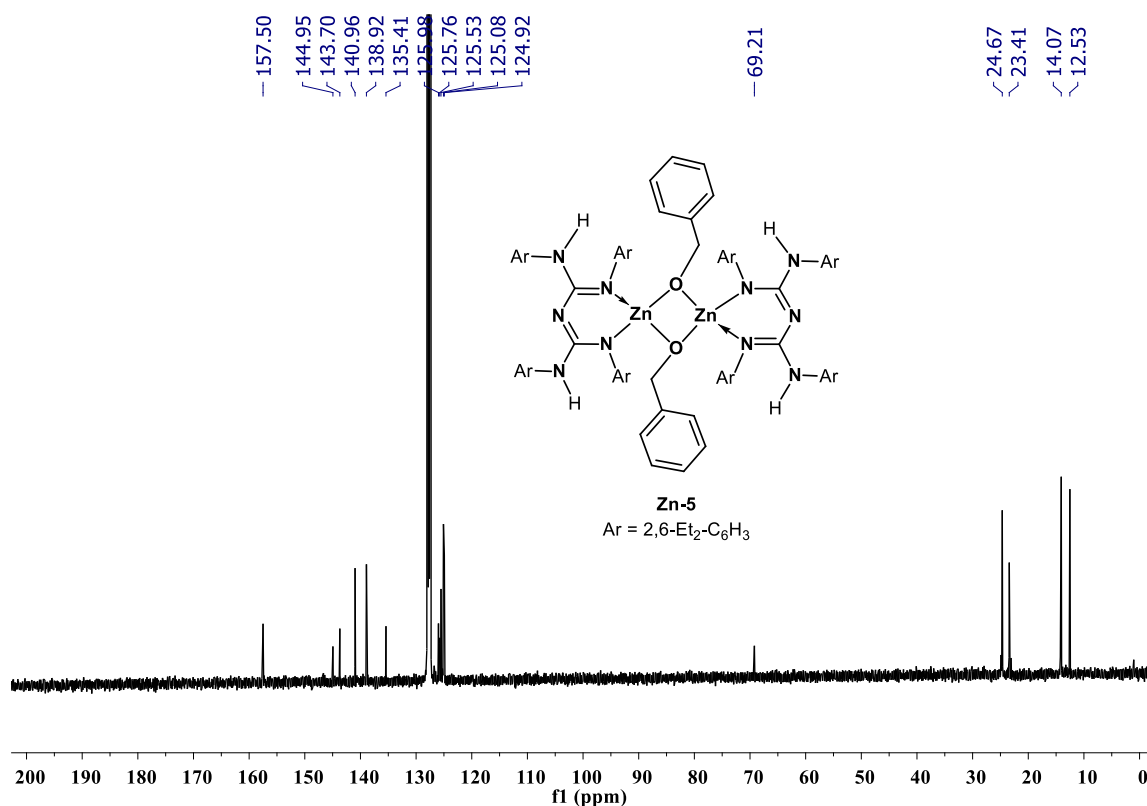


Figure 4.15. ¹³C{¹H} NMR spectrum of compound [LZnO-CH₂-C₆H₅], **Zn-5** (101 MHz, C₆D₆, 25 °C)

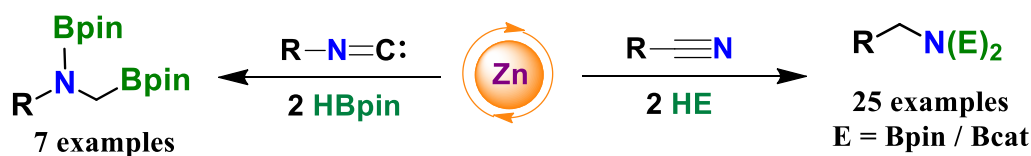
Chapter 5A

Zinc Hydride Catalyzed Dihydroboration of Isonitriles and Nitriles: Mechanistic Studies with the Structurally Characterized Zinc Intermediates

Published:

Sahoo, R. K.; Rajput, S.; Dutta, S.; Sahu, K.; Nembenna, S. *Organometallics* **2023**, DOI: <https://doi.org/10.1021/acs.organomet.3c00281>.

Abstract



- Dihydroboration ● Wide substrate scope ● Excellent conversion
- Mild conditions ● Mechanistic Studies ● Intermediates Isolation

The conjugated bis-guanidinate (CBG)-stabilized zinc hydride, [$\{\text{LZnH}\}_2$; (L = {(ArNH)(ArN)–C=N–C=(NAr)(NHAr)}; Ar = 2,6-Et₂-C₆H₃)] (**Zn-1**) is shown to be a highly active catalyst for the double reduction of isonitriles and nitriles with pinacolborane (HBpin) in this study. A wide array of isonitriles and nitriles, including aryl and alkyl groups, underwent hydroboration to afford exclusively 1,2- and 1,1-diborylated amine products, respectively. A series of stoichiometric reactions were performed to understand the reaction mechanisms. Hydroboration of isonitrile is proceeded through the formation of zinc formimidoyl complex, [$\text{LZnC(H)N}(\text{tBu})_2$] (**Zn-2**), while nitrile hydroboration through zinc vinylidenamido complex, [$\text{LZnNC(H)(C}_6\text{H}_5)_2$] (**Zn-3**). Moreover, compounds **Zn-2** and **Zn-3** are isolated and thoroughly characterized. Such molecular zinc complexes are rare in the literature.

5.A.1. Introduction

The zinc is an earth-abundant, cheaper, readily available, biocompatible, and non-toxic element.¹ Thus, zinc based reagents or molecular compounds are attractive in catalysis.^{1a, 1c, 1d, 2} Zinc-based

compounds have used as catalysts for the hydrofunctionalization of various unsaturated organic compounds.^{1a, 1c, 1d, 3}

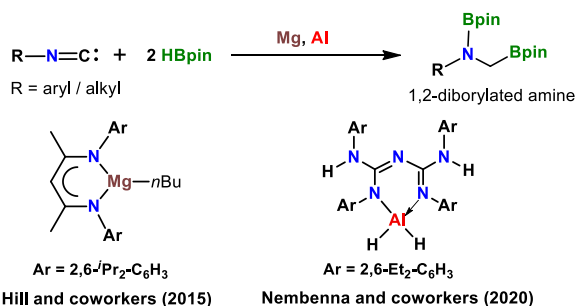
The complete catalytic reduction of the isonitriles ($R-N=C:$) and nitriles ($R-C\equiv N$) affords secondary and primary amines, respectively, which are very useful in synthetic chemistry because of their widespread application in agrochemicals, drug molecules, dyes, and pharmaceutical industries.⁴ In this context, isonitriles reduction is quite an attractive research area. Despite the numerous reports on the metal-catalyzed hydroboration of unsaturated organic substrates,⁵ surprisingly, there are only two reports on the metal-catalyzed hydroboration of isonitrile.^{5i, 6} The first example of isonitrile dihydroboration was introduced by Hill and coworkers by using the *Dipp*NacNac-supported magnesium butyl complex $[CH\{C(Me)NAr\}_2Mg^iBu]$ ($Ar = 2,6\text{-}^iPr_2C_6H_3$) in 2015.⁶ Subsequently, in 2020, the Nembenna group reported aluminum-catalyzed hydroboration of isonitriles to 1,2-diborylated amines, with two examples.⁵ⁱ However, there are no reports on zinc-catalyzed hydroboration of isonitriles (Figure 5.A.1A).

In 2012, Nikonov and co-workers reported the dihydroboration of nitriles using a $(2,6\text{-}^iPr_2C_6H_3N)Mo(H)(Cl)(PMe_3)_3$ complex for the first time.⁷ Since then, there have been numerous reports on transition-, rare-earth, and main-group metal-catalyzed dihydroboration of nitriles to amines.⁵ As far as zinc-catalyzed hydroboration of nitriles is concerned, there are only three reports in the literature. Panda and co-workers reported that organozinc-catalyzed the hydroboration of nitriles.⁸ In 2021, the Xu group established the dihydroboration of nitriles by using NHC-zinc dihydride as a catalyst.⁹ Recently, Baker and co-workers reported that pyridine-thioether-anilido-aryloxy stabilized zinc complex ($Zn(NSNO)$) catalyzed the hydroboration of nitriles (Figure 5.A.1B).¹⁰ Most of the reported protocols suffer from the following disadvantages such as narrow substrate scope and lack of mechanistic details. There have also been no reports on zinc-catalyzed

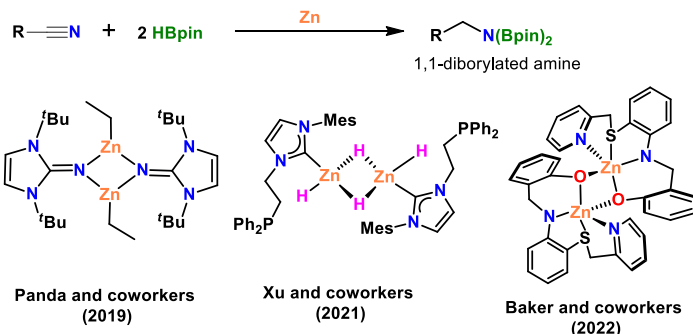
hydroboration of isonitriles. However, a handful of reports on zinc catalyzed dihydroboration of nitriles are known in the literature. Therefore, it is necessary to develop ligand-stabilized zinc complexes containing only C, H, and N elements and use them as active catalysts for the hydroboration of isonitriles and nitriles under mild conditions.

In this paper, we report a ^{Diethyl}CBG (CBG = conjugated bis-guanidinate) zinc hydride complex $[\{LZnH\}_2]$ ($L = \{(ArNH)(ArN)-C=N-C=(NAr)(NHAr)\}$; $Ar = 2,6-Et_2-C_6H_3\}$) (Zn-1) is an effective catalyst for the hydroboration of isonitriles and nitriles with excellent conversions. The most plausible catalytic cycles are proposed based on well-defined intermediates and a series of stoichiometric experiments (Figure 5.A.1C).

A) Metal-Catalyzed Dihydroboration of Isonitriles



B) Zinc-Catalyzed Dihydroboration of Nitriles



C) This Work: Zinc-Catalyzed Dihydroboration of Isonitriles and Nitriles

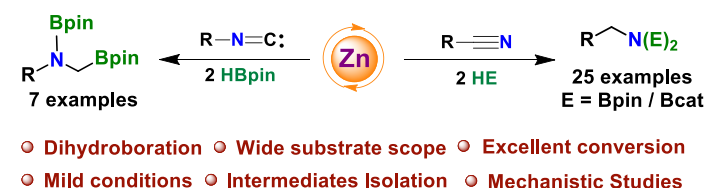


Figure 5.A.1. Metal-catalyzed dihydroboration of isonitriles and nitriles.

5.A.2. Results and Discussion

As previously established by our group, the active zinc catalyst $[LZnH]_2$ ($L = \{(ArNH)(ArN)-C=N-C=(NAr)(NHAr)\}$; $Ar = 2,6-Et_2-C_6H_3$) (**Zn-1**) can be obtained easily by the reaction between $[LZnI]_2$ and $KNH(iPr)BH_3$.^{3f} Moreover, we used complex **Zn-1** as an effective catalyst for the hydroboration of various unsaturated organic substrates.¹¹ Very recently, we also established mechanistic studies of DiethylCBG zinc hydride (**Zn-1**) catalyzed hydrofunctionalization of N-heteroarenes.^{3m}

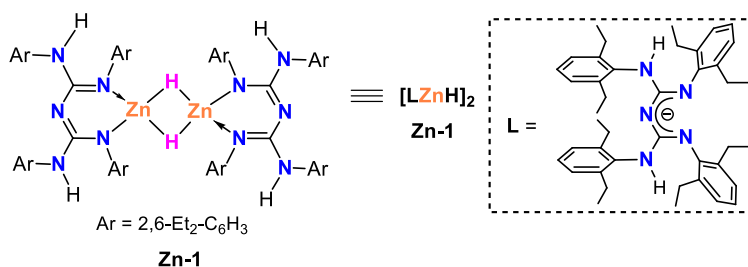
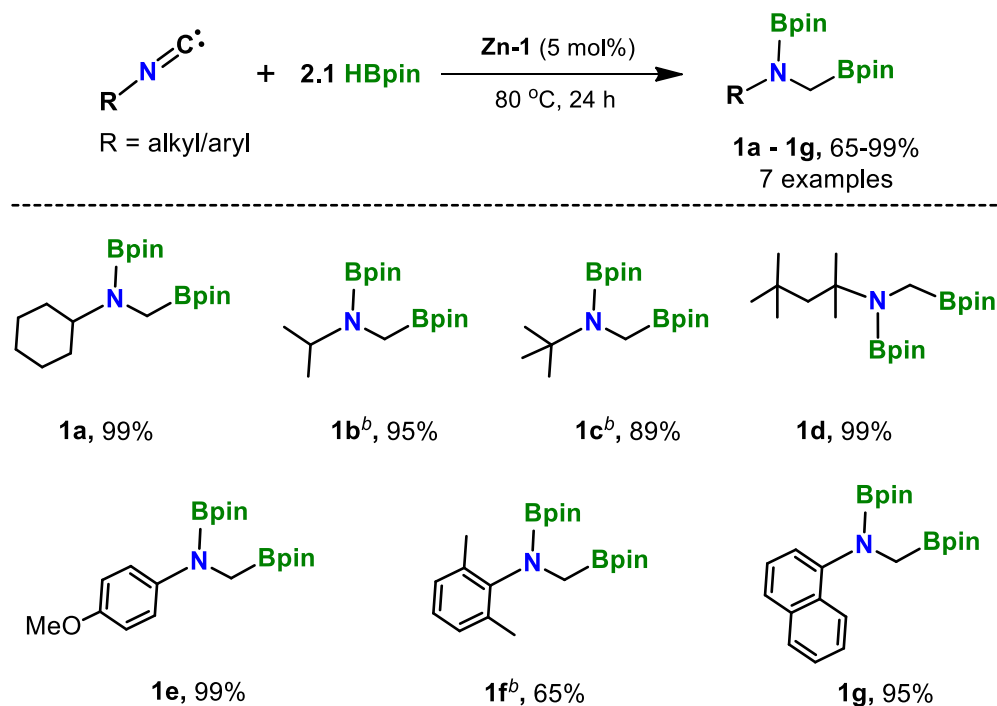


Figure 5.A.2. CBG-based zinc(II) hydride complex (**Zn-1**).

5.A.2.1. Isonitrile Hydroboration

Despite the numerous studies on the zinc-catalyzed hydroboration of unsaturated organic substrates, there have been no reports on the zinc-catalyzed hydroboration of isonitriles to the 1,1-diborylated amines. This motivated us to investigate the hydroboration of isonitriles in the presence of a zinc-based catalyst. An initial trial reaction between 0.2 mmol of cyclohexyl isonitrile and 0.42 mmol of pinacolborane (HBpin) using 10 mol% catalyst **Zn-1** provided quantitative conversion to the corresponding 1,2-diborylated amine product (**1a**) after 36 h at 80 °C. The 1H NMR spectrum evidenced the appearance of a new characteristic singlet peak at 2.85 ppm, corresponding to the methylene (2H) moiety of the product $CyN(Bpin)CH_2Bpin$ (**1a**). Furthermore, by reducing the catalyst loading to 5 mol% in C_6D_6 allowing the reaction to proceed for 24 h at 80 °C, the quantitative amount of product **1a** was observed. Next, when the same

reaction was conducted using a 5 mol% catalyst in solvent-free conditions, we noticed the formation of the desired product **1a** in a quantitative yield. Moreover, decreasing the catalyst loading or shorting the reaction time, affords a lower yield of product **1a**. A control experiment was conducted without a catalyst, resulting in the formation of a trace amount of 1,2-diborylated amine product (**1a**), which confirmed that the role of the catalyst is essential for this transformation. The above result encouraged us to explore the substrate scope of isonitriles. Therefore, under the standard reaction conditions, all alkyl isonitriles, such as isopropyl, tertbutyl, and 1,1,3,3-tetramethylbutyl isocyanides, underwent an effective double reduction with 2.1 equiv. of HBpin, which afforded the 1,2-diborylamines with 89-99% conversions in 24 h at 80 °C (**1b-1d**). However, aryl isonitriles such as 4-methoxyphenyl, xylyl and naphthyl isocyanides reacted with 2.1 equiv. of HBpin to form 65-99% conversions of respective diborylated amine products (Scheme 5.A.1).



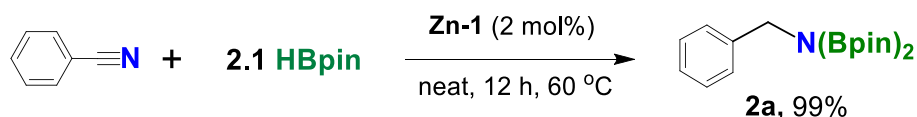
Scheme 5.A.1. Hydroboration of isonitriles catalyzed by **Zn-1** catalyst^a

^aReactions were conducted with isonitriles (0.2 mmol, 1.0 equiv.), pinacolborane (HBpin) (0.42 mmol, 2.1 equiv.), catalyst **Zn-1** (5 mol%), in reaction vial or J. Young Valve NMR tube under N₂ and heated at 80 °C for 24 h. Conversions for the reduction of isonitriles to 1,2-diborylated amines were examined by ¹H and ¹³C{¹H} NMR spectroscopy based on the consumption of starting material and formation of characteristic new proton resonance for (N(Bpin)CH₂Bpin) fraction. ^bFor **1b**, **1c**, and **1e**, NMR conversions were calculated by ¹H NMR spectroscopy using mesitylene as an internal standard.

5.A.2.2. Nitrile Hydroboration

After the success in the dihydroboration of isonitrile and considering the importance of 1,1-diborylated amines for various applications,^{4a, 4c} we aimed to explore the catalytic activity of **Zn-1** for the dihydroboration of nitriles. Accordingly, we chose benzonitrile as a model substrate for optimizing nitrile hydroboration. Initially, the reaction was conducted between benzonitrile and 2.1 equiv. of HBpin in the absence of a catalyst in neat conditions at 60 °C for 12 h, resulting in a trace amount of 1,1-diborylated amine product (**2a**) (Table 5.A.1, entry 1).

Table 5.A.1. Optimization table of **Zn-1** catalyzed hydroboration of benzonitrile^a

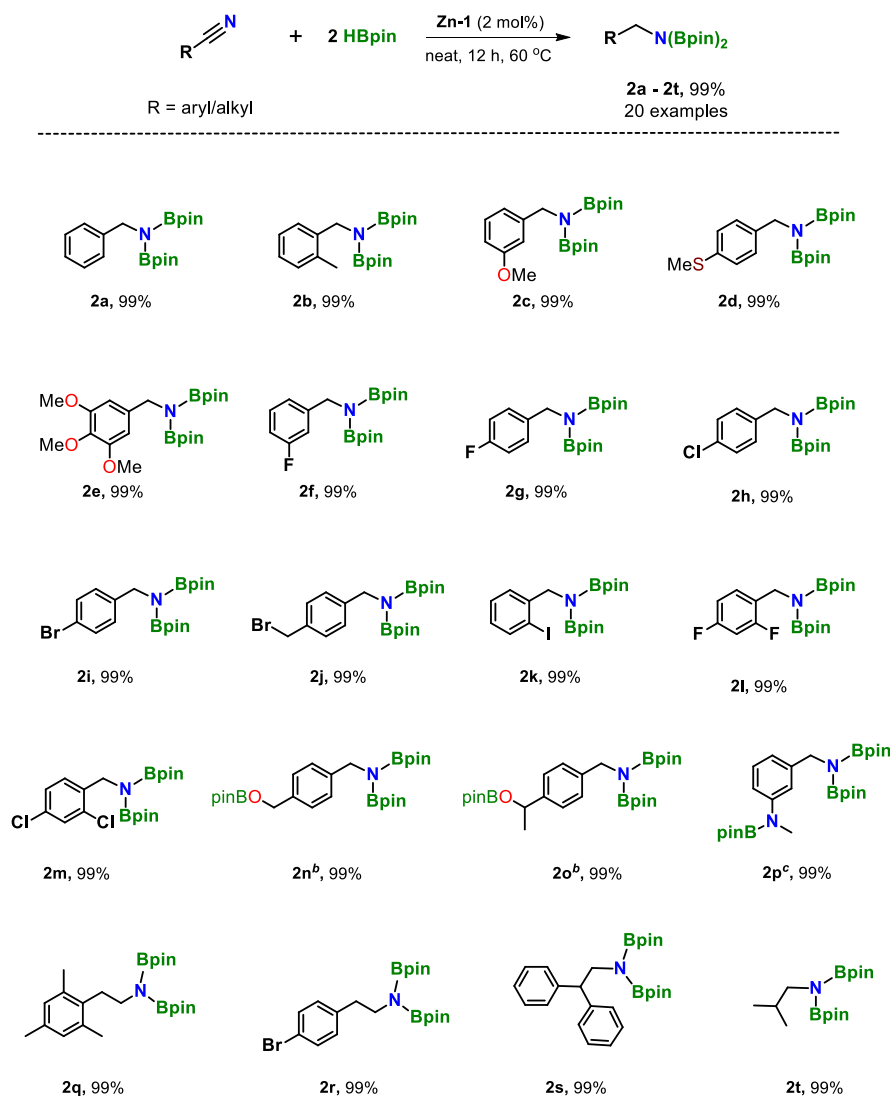


Entries	Cat. (mol%)	Time (h)	Conv. (%) ^b
1	-	12	2
2	10	12	>99
3	5	12	>99
4	3	12	>99
5	2	12	>99
6	1	12	>99
7	1	8	96

^aReactions were conducted with benzonitrile (0.2 mmol, 1.0 equiv.), pinacolborane (HBpin) (0.42 mmol, 2.1 equiv.), catalyst **Zn-1** (2 mol%) in reaction vial under dinitrogen and stirred at 60 °C of 12 h.

^bConversion for the product was examined by ¹H and ¹³C{¹H} NMR spectroscopy based on the consumption of starting material and formation of characteristic new proton resonance for (CH₂N(Bpin)₂) moiety.

However, adding 10 mol% catalyst (**Zn-1**) to the above reaction mixture results in a 99% conversion of the respective 1,1-diborylated amine product (**2a**), as determined by NMR spectroscopy (Table 5.A.1, entry 2). Lowering catalyst loadings by 5, 3, 2, and 1 mol% afforded the complete reduction of benzonitrile into the corresponding diborylated amines (**2a**) within 12 h (Table 5.A.1, entries 3-6).

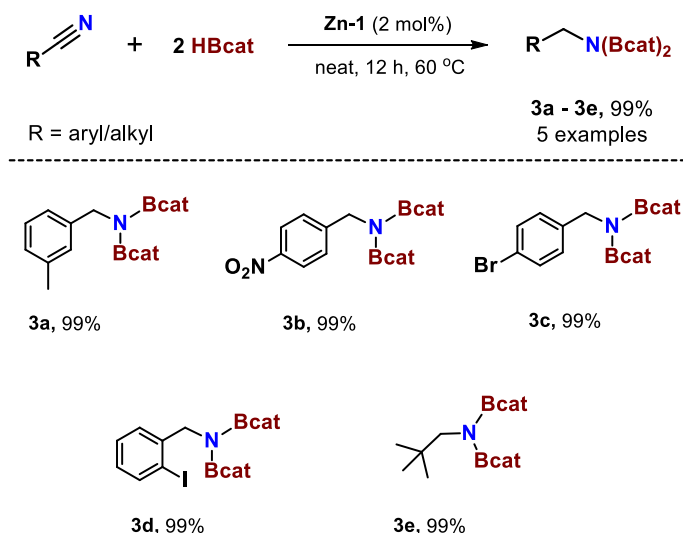


Scheme 5.A.2. Hydroboration of nitriles catalyzed by **Zn-1**^a

^aReactions were conducted with nitrile (0.2 mmol, 1.0 equiv.), pinacolborane (HBpin) (0.42 mmol, 2.1 equiv.), catalyst **Zn-1** (2 mol%) in a reaction vial under dinitrogen and stirred at 60 °C of 12 h. Conversion for the product was examined by ¹H and ¹³C{¹H} NMR spectroscopy based on the consumption of starting material and formation of characteristic new proton resonance for (CH₂N(Bpin)₂) moiety of product **2a-2t**.

^bFor **2n** and **2o** (3.2 equiv.) HBpin was used. ^cFor **2p** (5.1 equiv.) HBpin was used and heated at 70 °C for 36 h.

Furthermore, when the reaction time was shortened from 12 to 8 h at 1 mol% under neat conditions, 96% of the diborylated amine product was obtained (**2a**) (Table 5.A.1, entry 7). After optimizing benzonitrile hydroboration, the substrate scope of nitriles reduction was widened under standard reaction conditions. A broad range of aryl nitriles was converted into corresponding 1,1-diborylated amine products (**2a-2m**) with high conversions (Scheme 5.A.2).



Scheme 5.A.3. Hydroboration of nitriles catalyzed by compound **Zn-1**^a

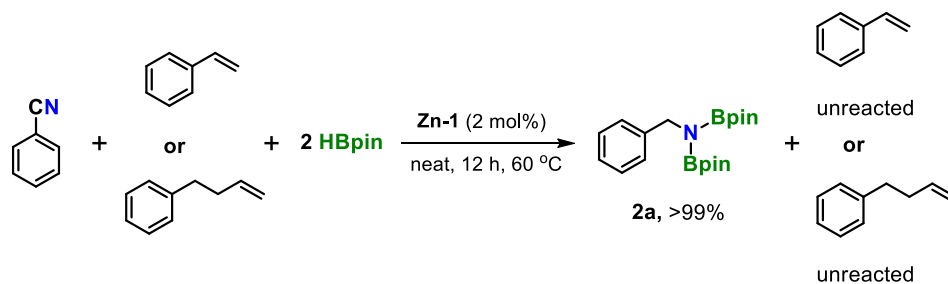
^aReactions were conducted with nitrile (0.2 mmol, 1.0 equiv.), catecholborane (HBCat) (0.42 mmol, 2.1 equiv.), **Zn-1** (2 mol%), in a reaction vial under dinitrogen and stirred at 60 °C for 12 h. Conversions of the product were examined by ¹H and ¹³C{¹H} NMR spectroscopy based on the consumption of starting material and formation of characteristic new proton resonance for (CH₂N(Bcat)₂) moiety of product **3a-3e**.

Next, for substrates bearing the carbonyl functional groups, we noticed that under two equiv. of HBpin, a mixture of products was found due to the high reactivity of the carbonyl groups compared to nitrile functionality. Therefore, when 3.2 equiv. of HBpin were introduced in the reaction

system, both carbonyl and nitrile groups were quantitatively hydroborated into corresponding borylated amine products (**2n** and **2o**). The reaction outcome was similar to the aluminum-based reduction of such nitriles with HBpin.¹² Similarly, 3-cyano phenyl isocyanate reacted with 5.1 equiv. of HBpin gave the respective borylated amine product (**2p**) with >99% conversion. Moreover, the alkyl nitriles were also converted into 1,1-bis(boryl) amine products (**2q-2t**) in quantitative conversions under optimal conditions (Scheme 5.A.2). Further, we examined the hydroboration of nitriles with catecholborane (HBcat) in the presence of **Zn-1** catalyst. Under the standard reaction conditions, we discovered that aryl nitrile with electron-donating and electron-withdrawing substituents was hydroborated to corresponding 1,1-bis(boryl) amine products with excellent conversions (**3a-3d**). We also noticed that alkyl-substituted nitrile, i.e., trimethylacetone nitrile, was quantitatively converted into 1,1-bis(boryl) amine product (**3e**) under optimized conditions (Scheme 5.A.3).

5.A.2.3. Intermolecular Chemoselective Reactions

A chemoselective reaction is an effective tool for preparing desired products in organic chemistry.^{4f} One equiv. benzonitrile, 1 equiv. styrene, and 2.1 equiv. HBpin were treated with catalyst **Zn-1** (2 mol%) under standard reaction conditions for 12 h, which afforded quantitative conversion of product **2a** in preference to styrene (Scheme 5.A.4).

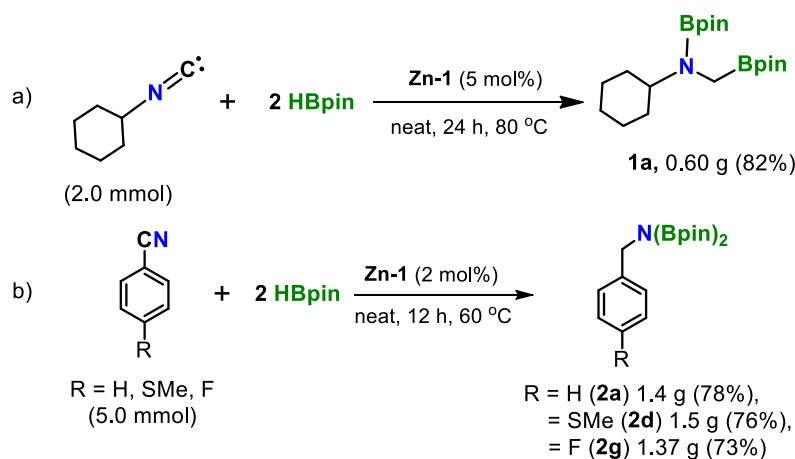


Scheme 5.A.4. Intermolecular chemoselective reactions by **Zn-1** catalyst.

Similarly chemoselective behavior was observed when two-folds of HBpin mixed with an equimolar solution of benzonitrile and 4-phenyl-1-butene, confirming the formation of 1,1-diborylated amine (**2a**) over 4-phenyl-1-butene (Scheme 5.A.4).

5.A.2.4. Scale-up Reactions

To explore the practical applicability of the present zinc hydride complex, we performed large-scale reactions of nitriles with HBpin. As displayed in Scheme 5.A.5a, cyclohexyl isocyanide reacts with 2.1 equiv. of HBpin at a 2.0 mmol scale produces a good yield of 1,1-diborylated amine product **1a** (Scheme 5.A.5a).



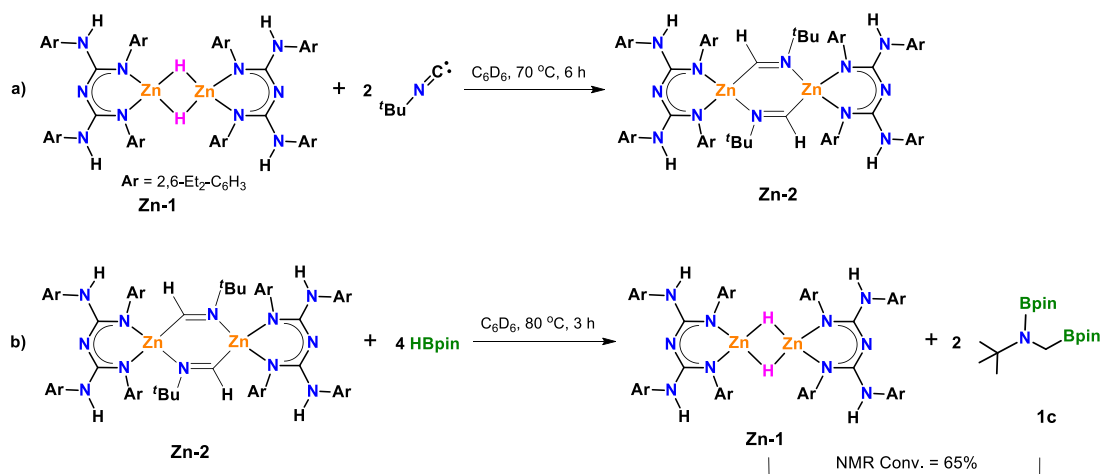
Scheme 5.A.5. Scale-up reactions

Similarly, a 5.0 mmol scale of benzonitrile, 4-(methylthio)benzonitrile, or 4-fluorobenzonitrile with 2.1 equiv. of HBpin under standard conditions afforded complete formation of the 1,2-diborylated amine products **2a**, or **2d**, or **2g** (Scheme 5.A.5b).

5.A.2.5. Stoichiometric Experiments for Hydroboration of Isonitriles and Nitriles

Stoichiometric experiments were conducted to gain more insights into the reaction mechanism. Therefore, we studied the mechanism for zinc hydride-catalyzed hydroboration of isocyanides to 1,2-diborylated amine products. A ratio of 1:2 stoichiometric reaction between a complex **Zn-1** and tert-butyl isocyanide in C_6D_6 at 70 °C for 6 h yielded CBG zinc formimidoyl complex,

[LZnC(H)N(*t*Bu)]₂ (**Zn-2**) via insertion of isocyanide into Zn-*H* moiety. The compound **Zn-2** was characterized by NMR, HRMS, and X-ray diffraction methods. The ¹H NMR spectrum of compound **Zn-2** revealed a characteristic peak at δ 9.59 ppm corresponding to [LZnC(*H*)N(*t*Bu)]₂, which is good in agreement with the reported NacNac stabilized magnesium formimidoyl complex [CH{C(Me)NAr}₂Mg^{*n*}Bu] (Ar = 2,6-*i*Pr₂C₆H₃) at 9.99 ppm, by Hill group.⁶ To our knowledge, this is the first example of a structurally characterized zinc formimidoyl complex. Next, intermediate **Zn-2** is treated with 4 equiv. of HBpin at 80 °C for 3 h, yielding the 1,2-diborylated amine product and the catalyst **Zn-1** with a 65% conversion (Scheme 5.A.6).

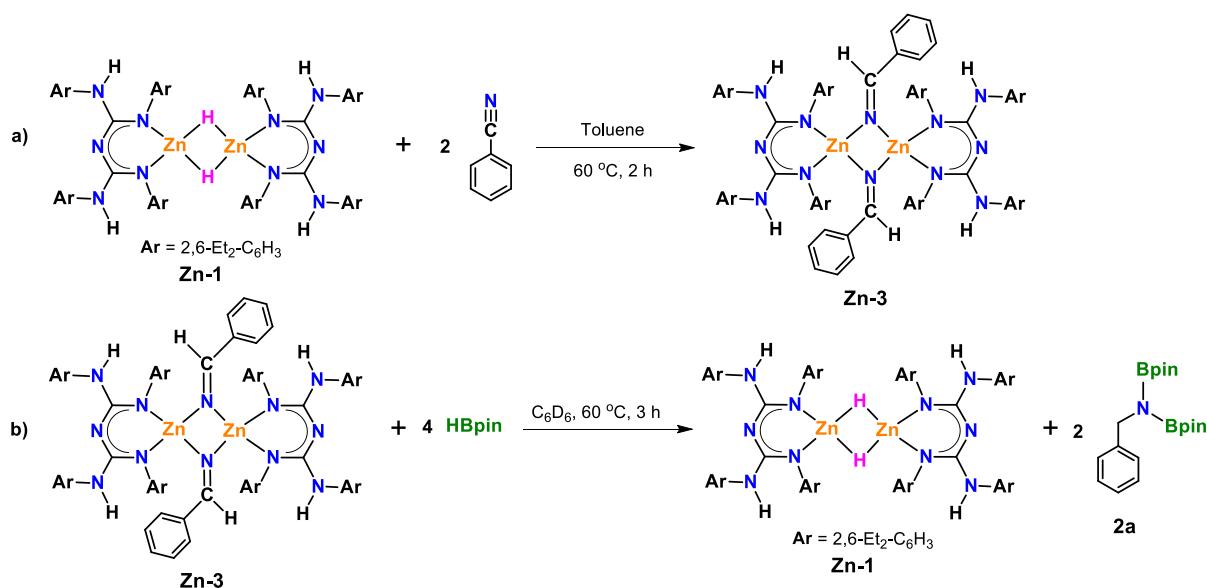


Scheme 5.A.6. Stoichiometric experiments for hydroboration of isocyaniles.

In addition one more example of CBG zinc formimidoyl complex (a mixture of **Zn-2'** (monomer) and **Zn-2''** (dimer)) was prepared by reacting catalyst **Zn-1** with 2,6-dimethyl phenyl isocyanide in C₆D₆ at 70 °C for 6h. Further, the zinc formimidoyl complexes (**Zn-2'** and **Zn-2''**) was confirmed by NMR (¹H and ¹³C{¹H}), and mass studies.

The compound **Zn-2** was grown from a concentrated benzene solution at ambient temperature to give colorless crystals suitable for X-ray diffraction analysis. The X-ray crystal structure for **Zn-2** shows four-coordinate zinc centers with distorted tetrahedral arrangements. The solid-state

structure reveals that the compound **Zn-2** crystallizes as a 6-membered heterocyclic dimer. The zinc atom is bonded by two N atoms from the CBG ligand and other sites occupied by C- and N'-atoms from tert-butyl formimidoyl units. In compound **Zn-2**, Zn1-C1 2.033(4) Å bond length is shorter than previously reported 6-membered heterocyclic dimeric ^{Dipp}NacNacMg-based complex Mg1-C30' 2.179(3) Å.⁶ Likewise, the Zn1'-N6 2.136(3) Å bond length of compound **Zn-2** is comparable to the Mg1-N3 2.109(3) Å bond length of ^{Dipp}NacNacMg-based formimidoyl complex (Figure 5.A.3, left).⁶ To our knowledge, this is the first example of a zinc formimidoyl complex, which is structurally characterized. Furthermore, stoichiometric experiments were performed to better understand the reaction mechanism of zinc-catalyzed nitrile hydroboration. The catalyst **Zn-1** reacted with 2 equiv. of benzonitrile in toluene at 60 °C for 2 h, forming the zinc vinylidenamido complex, **Zn-3** via institution of nitrile into Zn-H moiety.



Scheme 5.A.7. Stoichiometric experiments for hydroboration of nitriles.

The intermediate **Zn-3** was fully characterized by NMR, HRMS, and X-ray analyses. The ^1H NMR spectrum exhibits a sharp signal at δ 9.59 ppm, corresponding to the $\text{Zn-N}=\text{CH-R}$ moiety of compound **Zn-3**. Subsequently, it reacted with 4 equiv. of HBpin at 60 °C for 3 h, forming

compound **2a** and the catalyst **Zn-1** (Scheme 5.A.7). The ^1H NMR spectra show that the disappearance of a peak at δ 9.59 ppm corresponds to the Zn-N=CH-R moiety of compound **Zn-3** and the appearance of a new peak at δ 4.63 ppm corresponding to the $\text{CH}_2\text{N}(\text{Bpin})_2$ moiety of compound **2a** are annotated in Figure 5.A.4. This indicates the formation of compound **2a**.

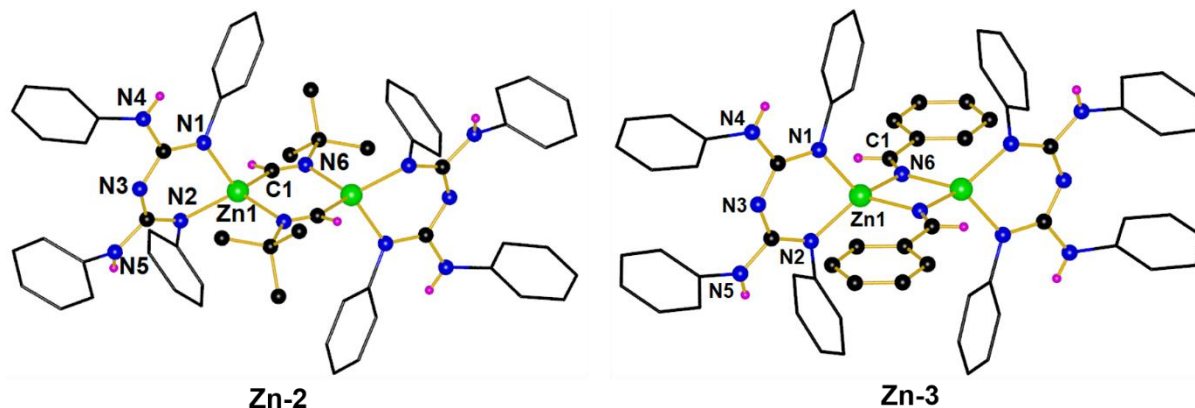


Figure 5.A.3. Molecular structures of compounds **Zn-2** (left), and **Zn-3** (right). The thermal ellipsoids are shown at 50% probability, and all the hydrogen atoms except those bound to nitrogen and C1 atoms are deleted for clarity. Selected bond lengths (Å) and angles (deg), for **Zn-2** (left): Zn1-N1 2.014(2), Zn1-N2 2.013(2), Zn1-C1 2.033(4), Zn1-N6' 2.136(3), Zn1'-N6 2.136(3), N6-C1 1.220(5); N1-Zn1-N2 90.04(10), N1-Zn1-C1 113.29(13), N2-Zn1-C1 107.82(14), C1-Zn1-N6' 113.02(15), Zn1-C1-N6 134.1(3), C1-N6-Zn1' 111.4(3). for **Zn-3** (right): Zn1-N1 1.985(3), Zn1-N2 1.986(3), Zn1-N6 2.027(3), Zn1-N6' 2.048(3), N6-C1 1.178(6); N1-Zn1-N2 94.25(14), N1-Zn1-N6 120.55(13), N2-Zn1-N6 118.09(14), N6-Zn1-N6' 86.15(14), Zn1-N6-Zn1' 93.85(14), Zn1-N6-C1 126.1(3).

The compound **Zn-3** was grown at room temperature from a concentrated benzene solution, yielding colourless crystals suitable for X-ray diffraction analysis. The X-ray structure confirmed that the compound **Zn-3** is dimeric, and the zinc atom has distorted tetrahedral arrangements with coordination number four. According to the solid-state structure of compound **Zn-3**, the zinc atom is coordinated by two N atoms from the CBG ligand and two additional sites from the two bridging N-atoms of the imine moieties.

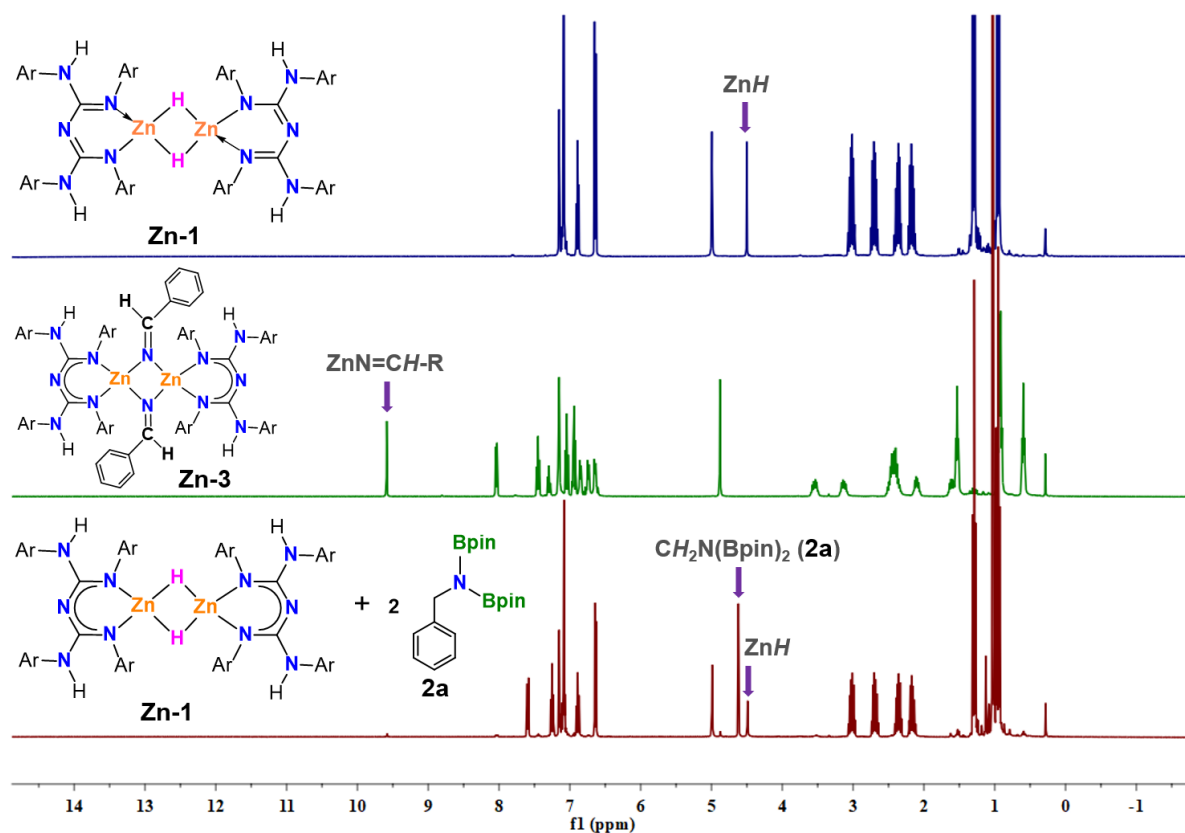


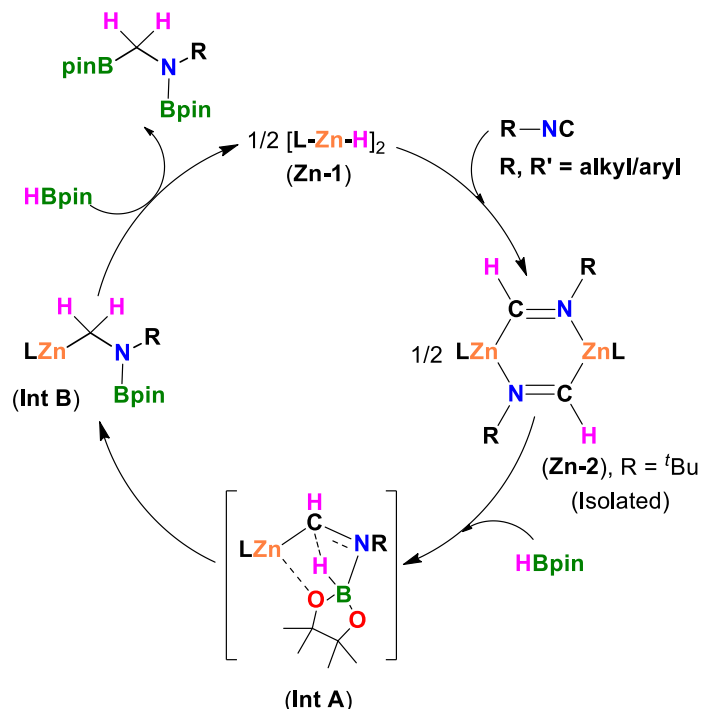
Figure 5.A.4. Annotated ^1H NMR (400 MHz) stack plot of the stoichiometric hydroboration of benzonitrile with **Zn-1** in C_6D_6 . Stacked spectra from top to bottom: LZnH (**Zn-1**); $[\text{LZnNC(H)(C}_6\text{H}_5)]_2$ (**Zn-3**); **Zn-1** + **2a** (compounds were obtained by the addition of 4 equiv. of HBpin to compound **Zn-3** at 60 °C after 3 h).

In compound **Zn-3**, Zn1-N6 2.027(3) Å bond length is similar to previously reported DippNacNac zinc vinylidenamido complex with Zn1-N3 2.053(3) Å.¹³ Further, the bite angle of compound **Zn-3** (N1-Zn1-N2 94.25(14))°, is comparable to DippNacNac zinc vinylidenamido complex (N1-Zn1-N2 90.10(11))° (Figure 5.A.3, right).¹³

5.A.2.6. Catalytic Cycle for Hydroboration of Isonitriles

Scheme 5.A.8 depicts the plausible catalytic cycle for the zinc-hydride catalyzed hydroboration of isonitriles based on the well-defined intermediate isolation, stoichiometric experiments, and previous literature reports.⁶ In the first step, a reaction between catalyst **Zn-1** and isonitrile resulted

in the formation of zinc formimidoyl complex **Zn-2** by inserting the N=C bond of isonitrile into the Zn-H moiety of compound **Zn-1**.



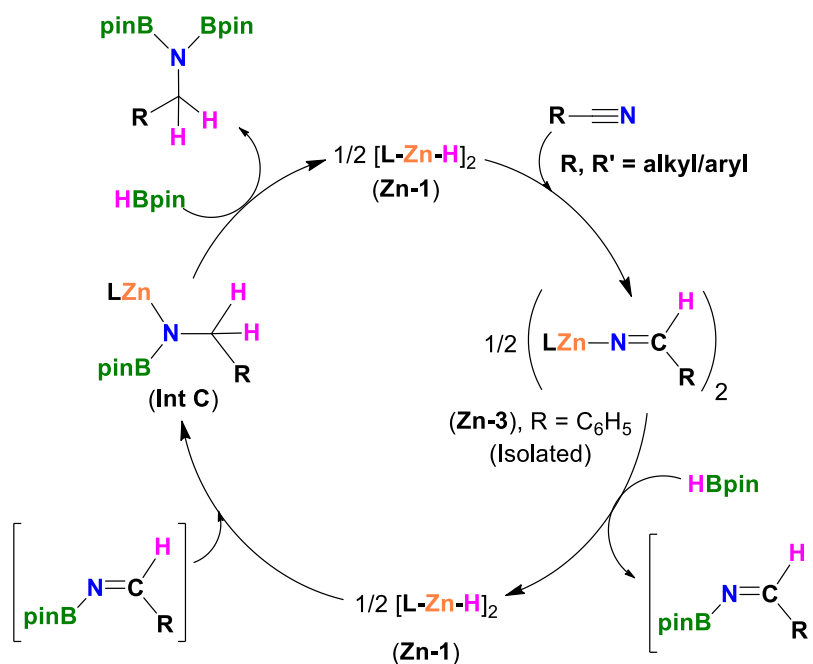
Scheme 5.A.8. Proposed mechanism for hydroboration of isonitriles.

The compound **Zn-2** further reacts with HBpin via **Int A**, giving rise to **Int B**. Further, it is reacted with HBpin via σ -bond metathesis, Zn-C/B-H, resulting in the formation of 1,2-diborylated amine product and renewal of catalyst **Zn-1**.

5.A.2.7. Catalytic Cycle for Hydroboration of Nitriles

Based on stoichiometric experiments, isolation of intermediate, and previous literature reports,⁸⁻¹⁰ the most plausible mechanism for the zinc-hydride catalyzed hydroboration of nitriles is shown in Scheme 5.A.9. Initially, the catalyst **Zn-1** reacts with nitrile to form the corresponding insertion product zinc vinylidenamido **Zn-3**. Next, the compound **Zn-3** reacts with HBpin to possibly produce N-boryl imines and regenerate the catalyst **Zn-1**. Further, a reaction between complex **Zn-1** and N-boryl imines gave the zinc boryl amine (**Int C**). Finally, the reaction of **Int C** with

another molecule of HBpin via σ -bond metathesis produces the 1,1-diborylated amine product with the rebirth of catalyst **Zn-1**.



Scheme 5.A.9. Proposed mechanism for hydroboration of nitriles.

5.A.3. Conclusion

In conclusion, we have shown for the first time that the zinc-catalyzed hydroboration of a wide range of isonitriles with HBpin to 1,2-diborylated amines. Additionally, complex **Zn-1** was successfully employed as an effective catalyst for the hydroboration of nitriles to diboronated amines. Furthermore, we noticed the intermolecular chemoselective reduction of nitriles over other reducible functional groups. In addition, scale-up hydroboration of isonitriles and nitriles has been performed to display the practical utility of the current methodology. We also investigated the reaction mechanism of isonitrile and nitrile hydroboration through the isolation of well-defined intermediates and a series of stoichiometric experiments. Single-crystal X-ray diffraction studies confirm zinc intermediates such as **Zn-2** and **Zn-3** complexes. Further applications and

mechanistic studies of this molecular zinc hydride in other catalytic reactions are being conducted in our laboratory.

5.A.4. General Experimental Methods

General Procedures

Unless stated, manipulations were performed under a dinitrogen atmosphere using standard glovebox and Schlenk techniques. NMR spectra were recorded on Jeol-400 MHz spectrometer and Bruker NMR spectrometers at 400 MHz (^1H), 101 MHz ($^{13}\text{C}\{^1\text{H}\}$), and 128.36 MHz (^{11}B). ^1H NMR and $^{13}\text{C}\{^1\text{H}\}$ NMR chemical shifts are referenced to residual protons or carbons in the deuterated solvent. ^{11}B NMR were calibrated using an external reference of $\text{BF}_3\cdot\text{Et}_2\text{O}$. Multiplicities are reported as singlet (s), doublet (d), triplet (t), quartet (q), and multiplet (m). Chemical shifts are reported in ppm. Coupling constants are reported in Hz. The crystal data were collected on a Rigaku Oxford diffractometer at 100 K. Selected data collection parameters and other crystallographic results are summarized in Table 5.A.2. Mass spectrometry analyses were carried out on Bruker micrOTOF-Q II and Waters XevoG2 XS Q-TOF mass spectrometers. The melting point of compounds **Zn-2** and **Zn-3** were measured from Stuart SMP 10 instrument.

Materials:

Solvents were purified by distillation over Na/ benzophenone. Deuterated chloroform (CDCl_3) was dried on molecular sieves, and benzene- d_6 (C_6D_6) was dried over Na/K alloy and distilled. The ligand LH ($\text{L} = \{(\text{ArNH})(\text{ArN})-\text{C}=\text{N}-\text{C}=(\text{NAr})(\text{NHAr})\}$; $\text{Ar} = 2,6\text{-Et}_2\text{-C}_6\text{H}_3$) and complex $\{\text{LZnH}\}_2$ (**I**) are prepared according to reported literature procedures.^{3f, 3j} For catalysis reactions, J. Young valve NMR tubes or reaction vials, as per the requirement, were properly oven-dried before being used. Chemicals and reagents were purchased from Sigma-Aldrich Co. Ltd., Merck India Pvt. Ltd., and TCI chemicals were used without purification.

5.A.4.1. Stoichiometric Experiments

Synthesis of [LZnC(H)N(ⁱBu)]₂, (Zn-2**) {NMR-Scale}:** Addition of tert-butyl isocyanide (3 μ L, 0.028 mmol) to a J. Young valve NMR tube containing a solution of complex **Zn-1** (0.020 g, 25 $^{\circ}$ C, 0.014 mmol) in C₆D₆ inside the glove box. Then, the reaction mixture was transferred to an oil bath and heated at 70 $^{\circ}$ C for 6 h, resulting in the formation of compound **Zn-2** was observed by ¹H NMR spectroscopy. Then, the reaction mixture was cooled to room temperature. We observed the formation of block-shaped colorless crystals suitable for single-crystal X-ray diffraction within 24 h. NMR conversion >99%. ¹H NMR (400 MHz, C₆D₆, 298 K) δ 9.58 (s, 2H), 7.21 – 7.19 (m, 4H), 7.13 – 7.08 (m, 8H), 6.91 (t, ³J_{HH} = 7.7 Hz, 4H), 6.71 – 6.63 (m, 8H), 4.97 (s, 4H), 3.30 – 3.22 (m, 4H), 3.17 – 3.09 (m, 4H), 2.94 – 2.86 (m, 4H), 2.57 – 2.49 (m, 4H), 2.41 – 2.31 (m, 12H), 2.20 – 2.10 (m, 4H), 1.44 (t, ³J_{HH} = 7.6 Hz, 12H), 1.19 (s, 18H), 1.02 – 0.95 (m, 24H), 0.89 (t, ³J_{HH} = 7.6 Hz, 12H). HRMS (ASAP/Q-TOF) *m/z*: [M+H]⁺ Calcd for C₄₇H₆₅N₆Zn 777.4562, found: 777.4572.

Synthesis of compound Zn-2' and Zn-2'' {NMR-Scale}: Addition of 2,6-dimethylphenyl isocyanide (4 mg, 0.028 mmol) to a J. Young valve NMR tube containing a solution of complex **Zn-1** (0.020 g, 25 $^{\circ}$ C, 0.014 mmol) in C₆D₆ inside the glove box. Then, the reaction mixture was transferred to an oil bath and heated at 70 $^{\circ}$ C for 6 h, resulting in the formation of compounds **Zn-2'** and **Zn-2''** were observed by ¹H and ¹³C{¹H} NMR spectroscopy. For compound **Zn-2'** NMR conversion >99%. ¹H NMR (400 MHz, C₆D₆, 298 K) δ 8.73 (s, 1H), 7.10 – 7.06 (m, 6H), 6.94 – 6.92 (m, 5H), 6.67 – 6.66 (m, 4H), 5.08 (s, 2H), 3.21 – 3.12 (m, 4H), 2.77 – 2.69 (m, 4H), 2.44 – 2.35 (m, 4H), 2.23 – 2.18 (m, 4H), 1.81 (s, 6H), 1.35 (t, ³J_{HH} = 7.6 Hz, 12H), 0.99 (t, ³J_{HH} = 7.5 Hz, 12H). ¹³C{¹H} NMR (101 MHz, C₆D₆) δ 198.6, 159.0, 157.2, 142.3, 141.1, 138.9, 135.1, 126.7, 126.4, 125.9, 125.4, 125.3, 122.2, 24.9, 24.4, 17.9, 14.5, 13.3. HRMS (ASAP/Q-TOF) *m/z*: [M+H]⁺ Calcd for C₅₁H₆₅N₆Zn 825.4562, found: 825.4654.

For compound **Zn-2''** NMR conversion >99%. ^1H NMR (400 MHz, C_6D_6 , 298 K) δ 9.71 (s, 2H), 7.12 – 7.10 (m, 12H), 6.90 – 6.85 (m, 10H), 6.61 – 6.59 (m, 8H), 4.95 (s, 4H), 2.69 – 2.60 (m, 16H), 2.33 – 2.25 (m, 8H), 2.16 – 2.11 (m, 8H), 1.54 (s, 12H), 1.22 (t, $^3J_{\text{HH}} = 7.8$ Hz, 24H), 0.91 (t, $^3J_{\text{HH}} = 7.3$ Hz, 24H). $^{13}\text{C}\{^1\text{H}\}$ NMR (101 MHz, C_6D_6) δ 200.5, 158.9, 156.8, 142.4, 140.9, 138.4, 134.9, 127.7, 126.3, 125.9, 125.7, 125.1, 122.1, 24.8, 23.7, 17.4, 14.2, 14.1.

Synthesis of $[\text{LZnNC}(\text{H})(\text{C}_6\text{H}_5)]_2$, (Zn-3**) {NMR-Scale}:** benzonitrile (37 μL , 0.359 mmol) in ~4 mL of toluene was added at room temperature through a cannula transfer to a solution of **Zn-1** 0.250 g (0.179 mmol) in 8 mL of toluene and stirred at 60 $^\circ\text{C}$ in an oil bath for 2 h. The solvent was removed in a vacuum resulting in a white solid compound and dried thoroughly. The resultant solid was dissolved in benzene (~ 10 mL) and filtered. Further, the solution was heated to 60 $^\circ\text{C}$ and slowly allowed to cool to room temperature, and we observed the formation of colorless block-shaped crystals within 24 h. (0.248 g, 82 %); m.p. 196-201 $^\circ\text{C}$. ^1H NMR (400 MHz, C_6D_6 , 298 K) δ 9.59 (s, 2H), 8.06 – 8.04 (d, $^3J_{\text{HH}} = 7.5$ Hz, 4H), 7.46 (t, $J = 7.6$ Hz, 4H), 7.30 (t, $J = 7.3$ Hz, 2H), 7.16 (s, 2H), 7.05 (t, $J = 7.6$ Hz, 4H), 6.95 (t, $J = 7.5$ Hz, 5H), 6.87 – 6.85 (d, $^3J_{\text{HH}} = 7.8$ Hz, 4H), 6.76 – 6.74 (d, $^3J_{\text{HH}} = 7.9$ Hz, 4H), 6.66 – 6.63 (d, $^3J_{\text{HH}} = 7.5$ Hz, 5H), 4.89 (s, 4H), 3.60 – 3.50 (m, 4H), 3.19 – 3.09 (m, 4H), 2.54 – 2.33 (m, 16H), 2.16 – 2.06 (m, 4H), 1.66 – 1.59 (m, 4H), 1.54 (t, $J = 7.4$ Hz, 12H), 0.96 (q, $J = 7.7$ Hz, 24H), 0.61 (t, $J = 7.5$ Hz, 12H). $^{13}\text{C}\{^1\text{H}\}$ NMR (101 MHz, C_6D_6) δ 169.3, 157.1, 143.7, 140.9, 140.5, 138.9, 138.8, 137.5, 135.8, 131.6, 131.6, 129.8, 128.7, 128.4, 128.0, 126.0, 125.7, 125.3, 124.8, 124.6, 124.1, 24.9, 24.8, 23.1, 22.3, 14.5, 13.8, 12.8, 12.6. HRMS (ASAP/Q-TOF) m/z : $[\text{M}+\text{H}]^+$ Calcd for $\text{C}_{49}\text{H}_{61}\text{N}_6\text{Zn}$ 797.4249, found: 797.4240.

5.A.4.2. X-ray Crystallographic Data

The single crystals of compounds **Zn-2** and **Zn-3** were crystallized from benzene at rt as colorless blocks within 24 h. The crystal data of compounds **Zn-2** and **Zn-3** are collected on a Rigaku Oxford diffractometer with graphite-monochromated Cu-K α radiation ($\lambda = 1.54184 \text{ \AA}$) at 100 K. Selected data collection parameters and other crystallographic results are summarized in Table 5.A.2. The structure was determined using direct methods employed in *ShelXT*,¹⁴ *OleX*,¹⁵ and refinement was carried out using least-square minimization implemented in *ShelXL*.¹⁶ All non-hydrogen atoms were refined with anisotropic displacement parameters. Hydrogen atom positions were fixed geometrically in idealized positions and were refined using a riding model.

Table 5.A.2. Crystallographic data and refinement parameters for compounds **Zn-2** and **Zn-3**.

Compound	Zn-2	Zn-3
Empirical Formula	C ₉₄ H ₁₂₆ N ₁₂ Zn ₂	C ₉₈ H ₁₁₈ N ₁₂ Zn ₂
Molecular mass	1554.80	1594.78
Temperature (K)	100	100
Wavelength (Å)	1.54184	1.54184
Size(mm)	0.2×0.18×0.17	0.2×0.18×0.17
Crystal system	triclinic	triclinic
Space group	P -1	P -1
a (Å)	11.56390(10)	12.7053(4)
b (Å)	12.7891(2)	12.8092(2)
c (Å)	16.2769(2)	15.2063(2)
α (deg)°	76.6120(10)	106.340(2)
β (deg)°	69.7570(10)	109.329(2)
γ (deg)°	65.0060(10)	93.070(2)
Volume (Å ³)	2036.69(5)	2211.33(9)
Z	1	1
Calculated density (g/cm ³)	1.268	1.198
Absorption coefficient (mm ⁻¹)	1.139	1.065
F(000)	834.0	850.0
Theta range for data collection (deg)°	7.666 to 136.5	7.288 to 151.812
Limiting indices	-13 ≤ h ≤ 13, -15 ≤ k ≤ 15, -19 ≤ l ≤ 16	-15 ≤ h ≤ 15, -16 ≤ k ≤ 15, -13 ≤ l ≤ 18
Reflections collected	33910	33385
Independent reflections	7451 [R _{int} = 0.0389, R _{sigma} = 0.0254]	8923 [R _{int} = 0.0475, R _{sigma} = 0.0338]
Completeness to theta	99 %	99 %
Absorption correction	Empirical	Empirical
Data / restraints / parameters	7451 / 2 / 511	8923 / 45 / 513
Goodness – of–fit on F ²	1.137	1.050
Final R indices [I>2 sigma(I)]	R ₁ = 0.0660, wR ₂ = 0.1623	R ₁ = 0.0856, wR ₂ = 0.2346

5.A.5. Appendix: All general experimental information, stoichiometric reactions, analytical data, and spectral data were available in published paper. *Organometallics* **2023**, DOI: <https://doi.org/10.1021/acs.organomet.3c00281>.

5.A.6. References

1. (a) Wu, X.-F. *Chem. Asian J.* **2012**, *7*, 2502-2509; (b) Revunova, K.; Nikonov, G. I. *Dalton Trans.* **2015**, *44*, 840-866; (c) Wiegand, A.-K.; Rit, A.; Okuda, J. *Coord. Chem. Rev.* **2016**, *314*, 71-82; (d) Roy, M. M. D.; Omaña, A. A.; Wilson, A. S. S.; Hill, M. S.; Aldridge, S.; Rivard, E. *Chem. Rev.* **2021**, *121*, 12784-12965; (e) Lennartson, A. *Nat. Chem.* **2014**, *6*, 166-166.
2. Enthaler, S. *ACS Catal.* **2013**, *3*, 150-158.
3. (a) Lortie, J. L.; Dudding, T.; Gabidullin, B. M.; Nikonov, G. I. *ACS Catal.* **2017**, *7*, 8454-8459; (b) Keerthi Krishnan, K.; Ujwaldev, S. M.; Saranya, S.; Anilkumar, G.; Beller, M. *Adv. Synth. Catal.* **2019**, *361*, 381-381; (c) Mandal, S.; Mandal, S.; Geetharani, K. *Chem. Asian J.* **2019**, *14*, 4553-4556; (d) Procter, R. J.; Uzelac, M.; Cid, J.; Rushworth, P. J.; Ingleson, M. J. *ACS Catal.* **2019**, *9*, 5760-5771; (e) Kumar, G. S.; Harinath, A.; Narvariya, R.; Panda, T. K. *Eur. J. Inorg. Chem.* **2020**, 467-474; (f) Sahoo, R. K.; Mahato, M.; Jana, A.; Nembenna, S. *J. Org. Chem.* **2020**, *85*, 11200-11210; (g) Uzelac, M.; Yuan, K.; Ingleson, M. J. *Organometallics* **2020**, *39*, 1332-1338; (h) Wang, X.; Chang, K.; Xu, X. *Dalton Trans.* **2020**, *49*, 7324-7327; (i) Wang, X.; Zhang, Y.; Yuan, D.; Yao, Y. *Org. Lett.* **2020**, *22*, 5695-5700; (j) Sahoo, R. K.; Sarkar, N.; Nembenna, S. *Angew. Chem. Int. Ed.* **2021**, *60*, 11991-12000; (k) Ataie, S.; Hogeterp, S.; Ovens, J. S.; Baker, R. T. *Chem. Commun.* **2022**, *58*, 3795-3798; (l) Shlian, D. G.; Amemiya, E.; Parkin, G. *Chem. Commun.* **2022**, *58*, 4188-4191; (m) Sahoo, R. K.; Sarkar, N.; Nembenna, S. *Inorg. Chem.* **2023**, *62*, 304-317.
4. (a) Hayes, K. S. *Appl. Catal. A* **2001**, *221*, 187-195; (b) Carey, J. S.; Laffan, D.; Thomson, C.; Williams, M. T. *Org. Biomol. Chem.* **2006**, *4*, 2337-2347; (c) Martin, R.; Buchwald, S.

- L. *Acc. Chem. Res.* **2008**, *41*, 1461-1473; (d) Torborg, C.; Beller, M. *Adv. Synth. Catal.* **2009**, *351*, 3027-3043; (e) Pelckmans, M.; Renders, T.; Van de Vyver, S.; Sels, B. F. *Green Chem.* **2017**, *19*, 5303-5331; (f) Shenvi, R. A.; O'Malley, D. P.; Baran, P. S. *Acc. Chem. Res.* **2009**, *42*, 530-541.
5. (a) Haddenham, D.; Pasumansky, L.; DeSoto, J.; Eagon, S.; Singaram, B. *J. Org. Chem.* **2009**, *74*, 1964-1970; (b) Arrowsmith, M.; Hill, M. S.; Kociok-Köhn, G. *Chem. Eur. J.* **2013**, *19*, 2776-2783; (c) Weetman, C.; Anker, M. D.; Arrowsmith, M.; Hill, M. S.; Kociok-Köhn, G.; Liptrot, D. J.; Mahon, M. F. *Chem. Sci.* **2016**, *7*, 628-641; (d) Bismuto, A.; Cowley, M. J.; Thomas, S. P. *ACS Catal.* **2018**, *8*, 2001-2005; (e) Ding, Y.; Ma, X.; Liu, Y.; Liu, W.; Yang, Z.; Roesky, H. W. *Organometallics* **2019**, *38*, 3092-3097; (f) Harinath, A.; Bhattacharjee, J.; Panda, T. K. *Adv. Synth. Catal.* **2019**, *361*, 850-857; (g) Bedi, D.; Brar, A.; Findlater, M. *Green Chem.* **2020**, *22*, 1125-1128; (h) Ghosh, P.; Jacobi von Wangelin, A. *Org. Chem. Front.* **2020**, *7*, 960-966; (i) Sarkar, N.; Bera, S.; Nembenna, S. *J. Org. Chem.* **2020**, *85*, 4999-5009; (j) Das, S.; Maity, J.; Panda, T. K. *Chem. Rec.* **2022**, *22*, e202200192; (k) Pradhan, S.; Sankar, R. V.; Gunanathan, C. *J. Org. Chem.* **2022**, *87*, 12386-12396; (l) Caddick, S.; Judd, D. B.; Lewis, A. K. d. K.; Reich, M. T.; Williams, M. R. V. *Tetrahedron* **2003**, *59*, 5417-5423; (m) Khalimon, A. Y.; Farha, P.; Kuzmina, L. G.; Nikonov, G. I. *Chem. Commun.* **2012**, *48*, 455-457; (n) Chong, C. C.; Kinjo, R. *ACS Catal.* **2015**, *5*, 3238-3259; (o) Geri, J. B.; Szymczak, N. K. *J. Am. Chem. Soc.* **2015**, *137*, 12808-12814; (p) Kaithal, A.; Chatterjee, B.; Gunanathan, C. *J. Org. Chem.* **2016**, *81*, 11153-11161; (q) Ben-Daat, H.; Rock, C. L.; Flores, M.; Groy, T. L.; Bowman, A. C.; Trovitch, R. J. *Chem. Commun.* **2017**, *53*, 7333-7336; (r) Ibrahim, A. D.; Entsminger, S. W.; Fout, A. R. *ACS Catal.* **2017**, *7*, 3730-3734; (s) Banerjee, I.; Anga, S.; Bano, K.; Panda, T. K. *J.*

- Organomet. Chem.* **2019**, *902*, 120958; (t) Ghosh, C.; Kim, S.; Mena, M. R.; Kim, J.-H.; Pal, R.; Rock, C. L.; Groy, T. L.; Baik, M.-H.; Trovitch, R. J. *J. Am. Chem. Soc.* **2019**, *141*, 15327-15337; (u) Kitano, T.; Komuro, T.; Tobita, H. *Organometallics* **2019**, *38*, 1417-1420; (v) Babón, J. C.; Esteruelas, M. A.; Fernández, I.; López, A. M.; Oñate, E. *Organometallics* **2020**, *39*, 3864-3872; (w) Bhattacharjee, J.; Harinath, A.; Bano, K.; Panda, T. K. *ACS Omega* **2020**, *5*, 1595-1606; (x) Nguyen, T. T.; Kim, J.-H.; Kim, S.; Oh, C.; Flores, M.; Groy, T. L.; Baik, M.-H.; Trovitch, R. J. *Chem. Commun.* **2020**, *56*, 3959-3962; (y) Bazkiaei, A. R.; Wiseman, M.; Findlater, M. *RSC Adv.* **2021**, *11*, 15284-15289; (z) Pandey, V. K.; Tiwari, C. S.; Rit, A. *Org. Lett.* **2021**, *23*, 1681-1686; (za) Ataie, S.; Baker, R. T. *Inorg. Chem.* **2022**, *61*, 19998-20007; (zb) Geier, S. J.; Vogels, C. M.; Melanson, J. A.; Westcott, S. A. *Chem. Soc. Rev.* **2022**, *51*, 8877-8922; (zc) Magre, M.; Szewczyk, M.; Rueping, M. *Chem. Rev.* **2022**, *122*, 8261-8312.
6. Weetman, C.; Hill, M. S.; Mahon, M. F. *Chem. Commun.* **2015**, *51*, 14477-14480.
 7. Khalimon, A. Y.; Farha, P.; Kuzmina, L. G.; Nikonov, G. I. *Chem. Commun.* **2012**, *48*, 455-457.
 8. Das, S.; Bhattacharjee, J.; Panda, T. K. *New J. Chem.* **2019**, *43*, 16812-16818.
 9. Wang, X.; Xu, X. *RSC Adv.* **2021**, *11*, 1128-1133.
 10. Ataie, S.; Ovens, J. S.; Tom Baker, R. *Chem. Commun.* **2022**, *58*, 8266-8269.
 11. (a) Sahoo, R. K.; Patro, A. G.; Sarkar, N.; Nembenna, S. *Organometallics* **2023**, DOI: <https://doi.org/10.1021/acs.organomet.2c00610>; (b) Sahoo, R. K.; Patro, A. G.; Sarkar, N.; Nembenna, S. *ACS Omega* **2023**, *8*, 3452-3460.
 12. Sarkar, N.; Bera, S.; Nembenna, S. *J. Org. Chem.* **2020**, *85*, 4999-5009.
 13. Boone, C.; Korobkov, I.; Nikonov, G. I. *ACS Catal.* **2013**, *3*, 2336-2340.

14. Sheldrick, G. *Acta Crystallogr. C* **2015**, 71, 3-8.
15. Dolomanov, O. V.; Bourhis, L. J.; Gildea, R. J.; Howard, J. A. K.; Puschmann, H. *J. Appl. Crystallogr.* **2009**, 42, 339-341.
16. (a) Sheldrick, G. M. *Acta Crystallogr., Sect. A: Found. Crystallogr.* **2008**, 64, 112-122; (b) Sheldrick, G. M. *Acta Crystallogr., Sect. A: Found. Adv.* **2015**, 71, 3-8.

NMR Spectra

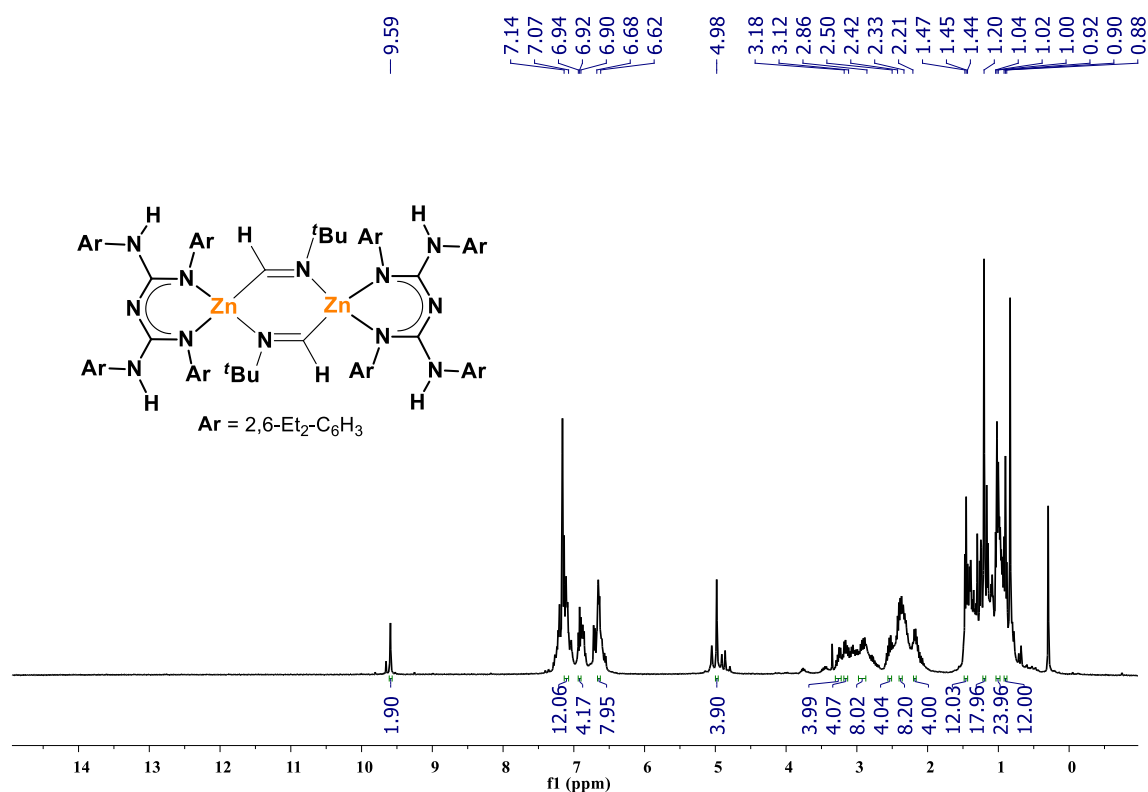


Figure 5.A.5. ¹H NMR spectrum of $[LZnC(H)N(tBu)]_2$ (Zn-2) (400 MHz, C₆D₆).

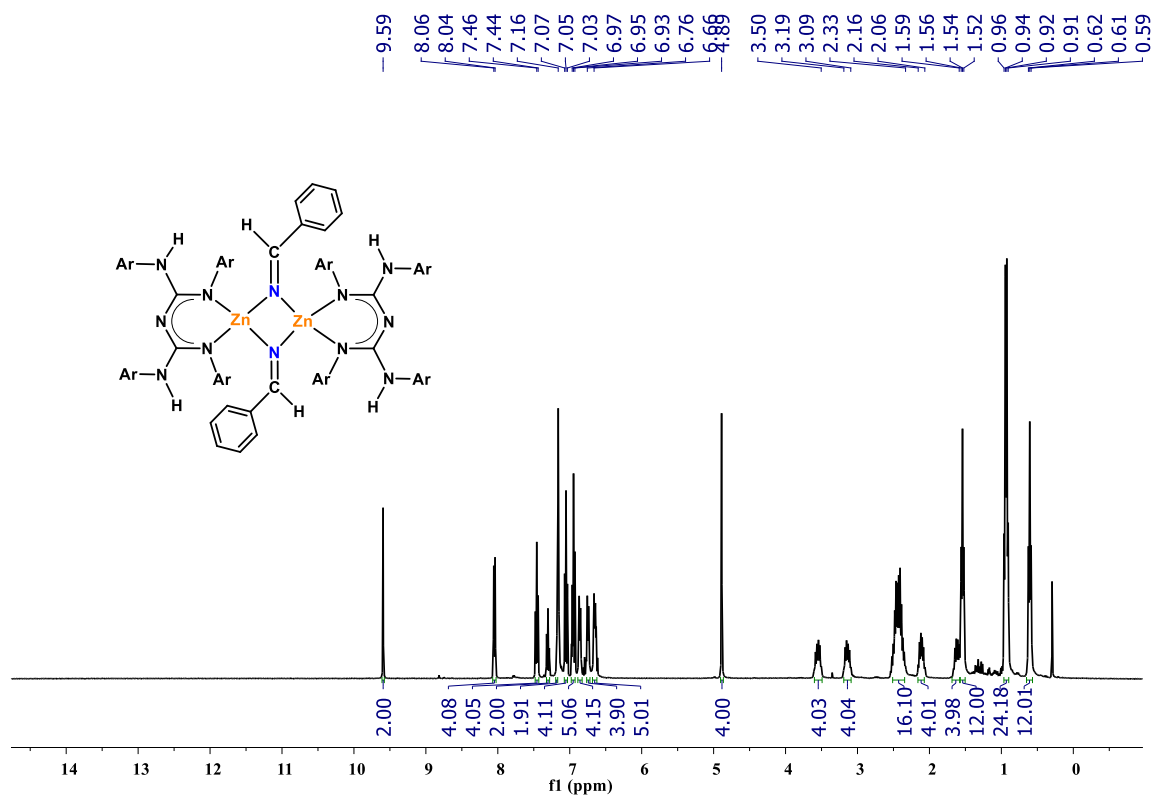


Figure 5.A.6. 1H NMR spectrum of $[L^1ZnNC(H)(4-SMeC_6H_4)]_2$ (**Zn-3**) (400 MHz, C_6D_6).

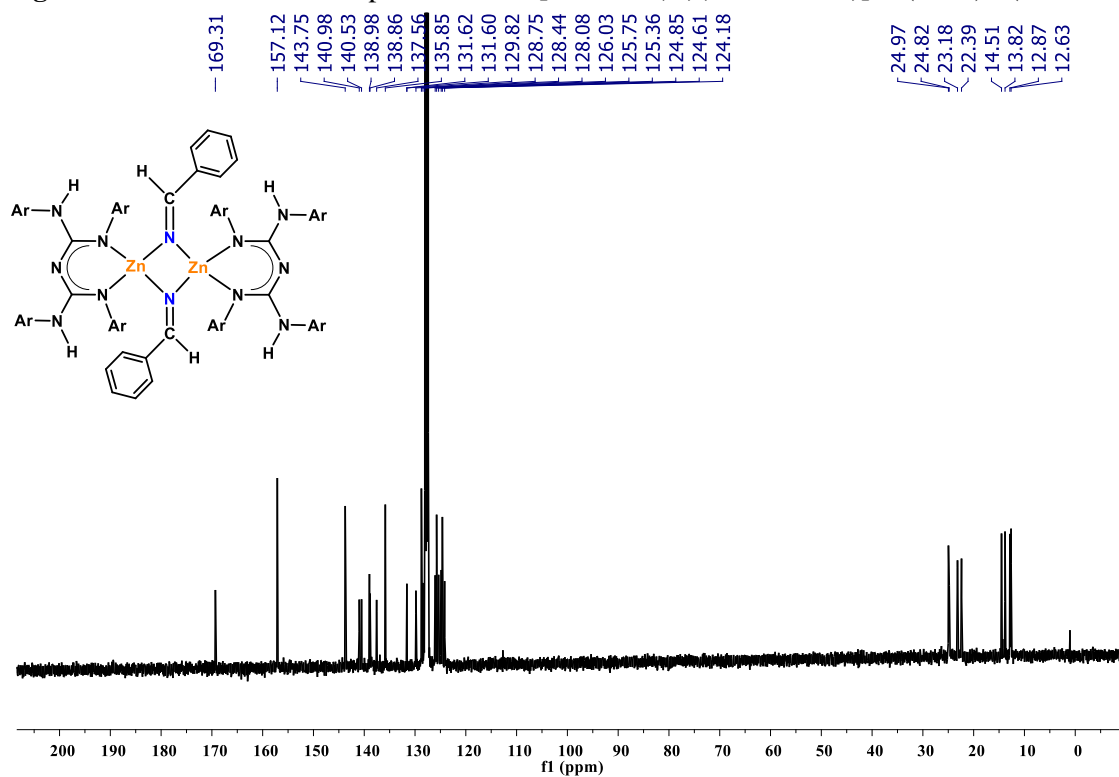


Figure 5.A.7. $^{13}C\{^1H\}$ NMR spectrum of $[L^1ZnNC(H)(4-SMeC_6H_4)]_2$ (**Zn-3**) (101 MHz, C_6D_6).

Chapter 5B

Zinc Catalyzed Chemoselective Reduction of Nitriles to N-Silylimines Through Hydrosilylation: Insights into the Reaction Mechanism

Published:

Sahoo, R. K.; Nembenna, S. *Inorg. Chem.* **2023**, 62, 12213-12222.

Abstract

The *N,N'*-chelated conjugated bis-guanidinate (CBG) supported zinc hydride (**Zn-1**) pre-catalyzed highly challenging chemoselective mono-hydrosilylation of a wide range of nitriles to exclusive N-silylimines and/or *N,N'*-silyldiimines is reported. Furthermore, the effectiveness of pre-catalyst **Zn-1** is compared with another pre-catalyst analogue, i.e., ^{Diethyl}NacNac zinc hydride (**Zn-2**), to know the ligand effect. We observed that pre-catalyst **Zn-1** shows high efficiency and better selectivity than pre-catalyst **Zn-2** for reducing nitriles to N-silylimines. Mechanistic studies indicate the insertion of the C≡N bond of nitrile into the Zn-H to form the zinc vinylidenamido complexes (**Zn-1'** and **Zn-2'**). The active catalysts **Zn-1'** and **Zn-2'** are confirmed by NMR, mass spectrometry, and single-crystal X-ray diffraction analyses. A most plausible catalytic cycle has been explored depending on stoichiometric experiments, active catalysts isolation, and in situ studies. Moreover, the synthetic utility of this protocol was demonstrated.

5.B.1. Introduction

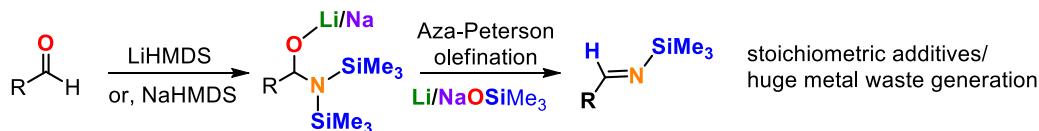
Chemoselective hydrosilylation of unsaturated organic substrates afforded precious organosilicon products, which are valuable precursors for laboratory methodology and industries.¹ Various procedures have been developed for the hydrosilylation of different functional groups such as alkene,^{1e, 1f, 2} alkyne,^{1e, 1f, 3} imine,^{4a-4c} carbonyls,⁴ and carboxylic derivatives.^{4c-4i} Additionally, there are numerous reports on catalytic double hydrosilylation of nitriles to 1,1-disilylamines.^{1h, 4d, 5} However, partial mono-hydrosilylation of nitriles to N-silyl aldimines remains a significant

challenge. Due to N-silylimines being much more reactive than nitriles, these are further reduced to give the disilylamine products.^{5c, 5e, 6} In addition, N-silylimines are very unstable.⁷ These N-silylated imines are suitable precursors in medicinal chemistry, nitrogen-containing organic compounds, and silicon-containing polymers.^{7a, 8} N-silylimines are key intermediates for further functionalization.⁹ N-silylimines can be synthesized by adding a stoichiometric amount of metallo hexamethyldisilylamides to aldehydes (Figure 5.B.1, a)).¹⁰

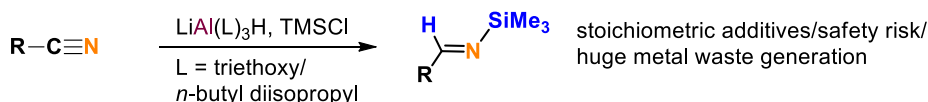
In the traditional method, selective hydrosilylation of nitriles was achieved using mixed metal hydrides [LiAl(L)₃H (L = triethoxy/*n*-butyl diisopropyl)] (Figure 5.B.1, b)).^{7a, 9, 11} Above conventional methods suffer from the following drawbacks such as stoichiometric metal reagents, safety risks, and huge metal waste generation.^{7a, 11} On the other hand, catalytic hydrosilylation of nitriles is also achieved by applying an excessive amount of silanes, which causes over-reduction and yielded disilylamine products.^{5b, 5e} Thus, developing metal-catalyzed selective hydrosilylation of nitriles to N-silylimines under mild conditions is very attractive. The selective synthesis of N-silylimines from nitriles mainly depends upon suitable catalysts and silanes. As far as metal-catalyzed partial reduction of nitriles is concerned, there have been a handful of reports in the literature using transition and main-group metal catalysts.^{4c, 5i, 12} Calas et al. reported the first mono-hydrosilylation of nitriles in 1961 using ZnCl₂ as a catalyst and HSiEt₃ as a silylating reagent with moderate yield under harsh reaction conditions.¹³ The Nikonov,^{12b, 14} Oestreich,¹⁵ and Djukic¹⁶ groups independently reported mono-hydrosilylation of nitriles by using Mo, Ru, and Ir-based catalysts. Since then, non-metals B¹⁷ and P¹⁸ catalyzed selective hydrosilylation of nitriles have also been reported. There are only two reports on zinc-catalyzed hydrosilylation of nitriles to N-silylimines.¹⁹ Recently, the Iwasawa group demonstrated the mono-hydrosilylation of nitriles to imines by using PGa^IP-Rh as a catalyst.²⁰ Unfortunately, most protocols suffer from drawbacks

such as limited substrate scope, low yields, more extended reaction timings, poor functional group tolerance, and lack of selectivity (Figure 5.B.1, c)).

a) Conventional method for the synthesis of N-silylimines from aldehydes



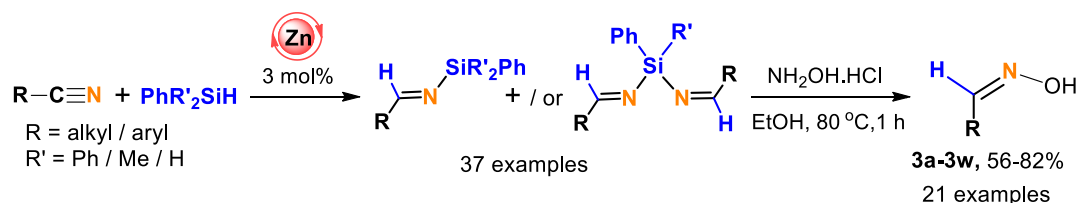
b) Traditional method for the synthesis of N-silylimines from nitriles



c) Metal/non-metal catalyzed mono-hydrosilylation of nitriles to N-silylimines



d) This work: Zinc catalyzed chemoselective hydrosilylation of nitriles to exclusive N-silylimines



- Chemoselective reduction ● Exclusive formation of N-silylimines ● Wide substrate scope
- Mild conditions ● Excellent conversion ● Active catalysts isolation ● Detailed mechanistic studies

Figure 5.B.1. Chemoselective synthesis of N-silylimine

Therefore, developing a new catalyst that works well in mild conditions for the chemoselective hydrosilylation of a wide range of nitriles is highly desirable. Hence, an inexpensive, biocompatible, and earth-abundant main group element, i.e., zinc, is an ideal candidate for the chemoselective reduction of nitriles. Herein, we report conjugated bis-guanidinate (CBG) zinc hydride pre-catalyzed selective mono-hydrosilylation of nitriles to N-silylimines and/or *N,N'*-silyldiimines with excellent conversions (Figure 5.B.1, d)). For the first time, we produce the molecular structures of N- silyl aldimines. The pre-catalyst **Zn-1** shows better catalytic activity

and selectivity than pre-catalyst **Zn-2**. Moreover, the active zinc catalysts $[L^1ZnN=C(H)(4-SMeC_6H_4)]_2$ (**Zn-1'**) and $[L^2ZnN=C(H)(4-SMeC_6H_4)]_2$ (**Zn-2'**) are isolated and structurally characterized.

5.B.2. Results and Discussion

Previously, we investigated the conjugated bis-guanidinate (CBG) supported zinc hydride $[L^1ZnH]_2$; ($L^1 = \{(ArNH)(ArN)-C=N-C=(NAr)(NHAr)\}$; $Ar = 2,6-Et_2-C_6H_3\}$) (**Zn-1**) (Figure 5.B.2), catalyzed hydrofunctionalization of unsaturated organic substrates.²¹ As mentioned, only a few examples of metal-catalyzed chemoselective reduction of nitriles have been reported. Thus, we aimed to examine **Zn-1** as a pre-catalyst for the hydrosilylation of nitriles. Moreover, the pre-catalyst **Zn-1** is compared with the analogue, DiethylNacNac zinc hydride,²² $[L^2ZnH]_2$; (DiethylNacNac (L^2) = $CH\{(CMe)(2,6-Et_2C_6H_3N)\}_2$) (**Zn-2**) for the effective and chemoselective reduction of nitriles to N-silylimines (Figure 5.B.2). We began our investigation by choosing benzonitrile as a substrate and Ph_2SiH_2 as a silane reagent. Initially, 0.3 mmol of nitrile and 0.18 mmol of diphenyl silane were added to a Schlenk tube with 10 mol% of catalyst in ~ 1.5 mL THF affording the quantitative amount of corresponding N-silylimine (**2a**) and N, N'-silyldiimine (**2aa**) after 12 h at 60 °C (Table 5.B.1, entry 2).

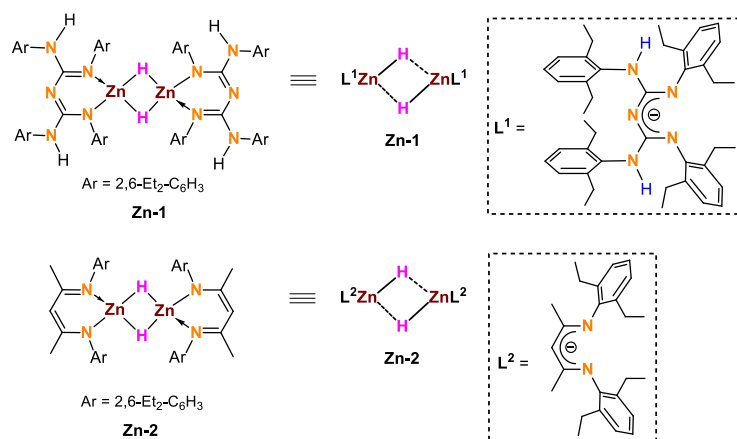


Figure 5.B.2. CBG and NacNac stabilized zinc(II) hydride complexes.

In contrast, a little conversion was observed in the absence of pre-catalyst **Zn-1**, which confirmed that the zinc hydride (**Zn-1**) is responsible for this transformation (Table 5.B.1, entry 1). Moreover, the above reaction was performed by lowering the pre-catalyst loadings (8, 6, 5, and 3 mol%) under the same reaction conditions, resulting in the complete conversion of benzonitrile to the respective N-silylimine (Table 5.B.1, entries 3-6). However, shorter the reaction time (8 h), using 3 mol% pre-catalyst loading, we noticed a 95% conversion of the product (Table 5.B.1, entry 7). Next, when the pre-catalyst loading decreased to 1 mol%, it produced a 65% conversion of the silylated product after 12 h (Table 5.B.1, entry 8).

Table 5.B.1. Optimization of zinc catalyzed chemoselective hydrosilylation of benzonitrile with Ph_2SiH_2 .^a

Reaction scheme: Benzonitrile + 0.6 Ph_2SiH_2 $\xrightarrow[60\text{ }^\circ\text{C}]{\text{Pre-cat./Cat. (x mol\%)}}$ **2a** + **2aa**

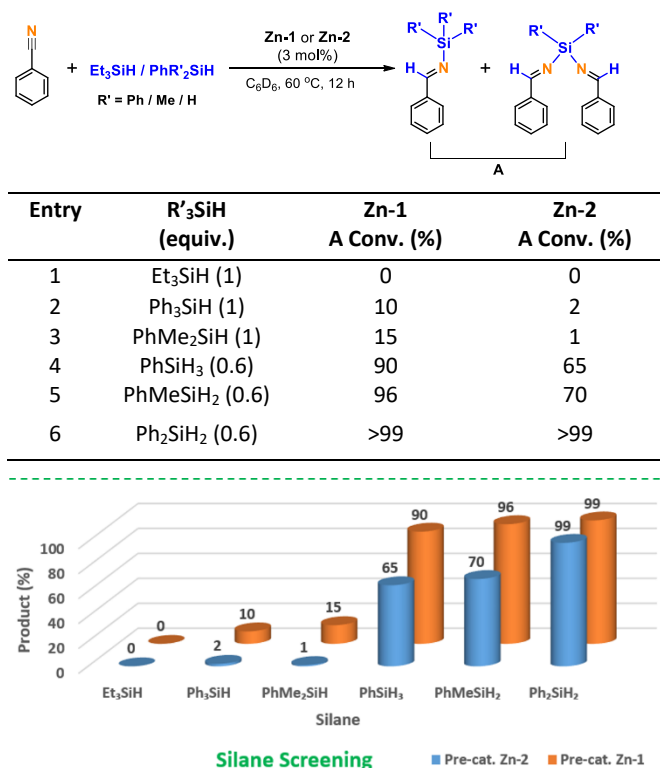
Entry	Pre-cat./Cat.	Time (h)	mol %	Solvent	(2a + 2aa) Conv. (%)
1	---	12	---	THF	<1
2	Zn-1	12	10	THF	>99
3	Zn-1	12	8	THF	>99
4	Zn-1	12	6	THF	>99
5	Zn-1	12	5	THF	>99
6	Zn-1	12	3	THF	>99
7	Zn-1	8	3	THF	95
8	Zn-1	12	1	THF	65
9	Zn-1	12	3	C_6D_6	>99
10	Zn-1	8	3	C_6D_6	90
11	Zn-1	12	3	benzene	>99
12	Zn-2	12	3	THF	>99
13	Zn-1'	12	3	THF	>99
14	Zn-2'	12	3	THF	>99

^aReactions were conducted with benzonitrile (0.3 mmol, 1.0 equiv.), Ph_2SiH_2 (0.18 mmol, 0.6 equiv.), Pre-cat. / Cat. (x mol%), in Schlenk tube or J. Young valve NMR tube under N_2 at 60 °C for 12 h. The NMR

conversion for Si-H addition to benzonitrile was confirmed by ^1H NMR spectroscopy based on the consumption of starting material and formation of characteristic proton signal of *CHN* peak.

Further, using the standard reaction conditions, the above reaction was carried out in other solvents, such as C_6D_6 and benzene. We observed the formation of the required products (**2a** and **2aa**) in a quantitative conversion. Furthermore, we observed a 90% conversion of the product when the reaction time was reduced to 8 h, using 3 mol% pre-catalyst loading in C_6D_6 (Table 5.B.1, entry 10). Notably, no change in the conversion was noticed when the reactions were conducted in the presence of zinc vinylidenamido complexes (**Zn-1'** and **Zn-2'**) under optimized reaction conditions (*vide infra*) (Table 5.B.1, entries 13-14).

Table 5.B.2. Screening of silanes in the hydrosilylation of benzonitrile by pre-catalyst **Zn-1** or **Zn-2**.^a



^aReactions were conducted with benzonitrile (0.3 mmol, 1.0 equiv.), silane (1 or 0.6 equiv.), and pre-cat. **Zn-1** or **Zn-2** (3 mol%), in a J. Young valve NMR tube under N_2 at 60 °C for 12 h. The NMR conversion for Si-H addition to benzonitrile was confirmed by ^1H NMR spectroscopy based on the consumption of starting material and formation of characteristic proton signal of *CHN* peak.

Next, we evaluated the suitable hydrosilane reagent. Accordingly, various commercially available hydrosilanes, such as Et_3SiH , Ph_3SiH , PhMe_2SiH , PhSiH_3 , PhMeSiH_2 , and Ph_2SiH_2 , are used in the hydrosilylation of benzonitrile reactions. We observed diphenyl silane (Ph_2SiH_2) as an ideal hydrosilane reagent for the chemoselective hydrosilylation of nitriles regarding selectivity, efficiency, and cost-effectiveness (Table 5.B.2). A broad range of aryl, heteroaryl, and alkyl nitrile substrates are screened using optimized conditions (Table 5.B.1, entry 6 or 9).

The various nitriles containing electron-donating (**1a–1i**), electron-withdrawing (**1j–1u**), substrate bearing both electron-donating and electron-withdrawing groups (**1v**), heteroaryls (**1w–1x**), alkyl groups (**1y** and **1z**), and alkene group (**1za**) were transformed into corresponding N-silylimines and/or *N,N'*-silyldiimines with high conversions (except **1y** and **1za**) (Table 5.B.3). All nitriles undergo hydrosilylation to produce a mixture of mono- and bis- hydrosilylated products except **1h**, **1u**, **1y**, and **1za**. Where either the exclusive mono-hydrosilylated products, **2y** and **2za** (addition of the one Si-H bond of Ph_2SiH_2 across the $\text{C}\equiv\text{N}$ bond of a nitrile), or the bis-hydrosilylated products, **2h** and **2u** (addition of the two Si-H bonds of Ph_2SiH_2 across the $\text{C}\equiv\text{N}$ bond of two nitriles), were formed. All products were characterized by multinuclear magnetic resonance (^1H , $^{13}\text{C}\{^1\text{H}\}$, and $^{29}\text{Si}\{^1\text{H}\}$) and high-resolution mass spectrometric analyses. More importantly, we have noticed tolerance of alkoxy, halide, nitro, heteroaryl (pyridine and thiophene), and alkene functionalities. In each case, a quantitative conversion of nitriles (**1a–1za**) into their respective N-silylimines was noticed (except **1y** and **1za**).

After workup of N-silylimines afforded good to excellent yields of corresponding oximes (56–82%, **3a–3w** (except **3g** and **3j**), Table 5.B.3). The ^1H and $^{13}\text{C}\{^1\text{H}\}$ NMR spectra for oximes (**3a–3w**) can be found in the Supporting Information. It is noteworthy that compound **Zn-1** can

catalyze the addition of two Si–H bonds of Ph_2SiH_2 across the $\text{C}\equiv\text{N}$ bond of nitriles to afford N,N' -silyldiimines **2aa-2ww**, which upon workup, yielded the corresponding oximes **3a-3w**.

Table 5.B.3. Zinc-catalyzed chemoselective mono-hydrosilylation of nitriles with Ph_2SiH_2 .^a

Entry	R	Conv. (2a-2za)	Conv. (2aa-2zz)	Isolated Yield (3)
1	C_6H_5	2a 60%	2aa 40%	3a 78%
2	2- MeC_6H_4	2b 54%	2bb 46%	3b 72%
3	3- MeC_6H_4	2c 56%	2cc 44%	3c 76%
4	4- MeC_6H_4	2d 56%	2dd 44%	3d 80%
5	2- OMeC_6H_4	2e 84%	2ee 16%	3e 68%
6	3- OMeC_6H_4	2f 58%	2ff 42%	3f 72%
7	4- OMeC_6H_4	2g 54%	2gg 46%	-----
8	4- $\text{SCH}_3\text{C}_6\text{H}_4$	2h 54%	2hh 46%	3h 66%
9	4- $\text{SCH}_3\text{C}_6\text{H}_4^b$	2h 0%	2hh >99%	3h 68%
10	3,4,5- $(\text{MeO})_3\text{C}_6\text{H}_2$	2i 90%	2ii 10%	3i 63%
11	3- FC_6H_4	2j 50%	2jj 50%	-----
12	4- FC_6H_4	2k 89%	2kk 11%	3k 82%
13	2- ClC_6H_4	2l 90%	2ll 10%	3l 80%
14	4- ClC_6H_4	2m 65%	2mm 35%	3m 73%
15	2- BrC_6H_4	2n 90%	2nn 10%	3n 68%
16	3- BrC_6H_4	2o 60%	2oo 40%	3o 70%
17	4- BrC_6H_4	2p 14%	2pp 86%	3p 76%
18	2- IC_6H_4	2q 80%	2qq 20%	3q 63%
19	4- $\text{NO}_2\text{C}_6\text{H}_4$	2r 65%	2rr 35%	3r 65%
20	2,4- $\text{F}_2\text{C}_6\text{H}_3$	2s 85%	2ss 15%	3s 62%
21	2,4- $\text{Cl}_2\text{C}_6\text{H}_3$	2t 85%	2tt 15%	3t 61%
22	2-F,5- BrC_6H_3^b	2u 0%	2uu >99%	3u 78%
23	2-Br,5- MeC_6H_3	2v 44%	2vv 56%	3v 58%
24	2-thiophenyl	2w 78%	2ww 22%	3w 56%
25	4-pyridyl	2x 40%	2xx 60%	-----
26	$i\text{Pr}^c$	2y 44%	2yy 0%	-----
27	$t\text{Bu}$	2z 30%	2zz 70%	-----
28	cyclohexene-1 ^{c,d}	2za 25%	2zaa 0%	-----

^aReactions were conducted with nitriles (0.5 mmol, 1.0 equiv.), Ph₂SiH₂ (0.3 mmol, 0.6 equiv.), pre-cat. **Zn-1** (3 mol%), in Schlenk tube or J. Young valve NMR tube under N₂ and stirred at 60 °C for 12 - 18 h.

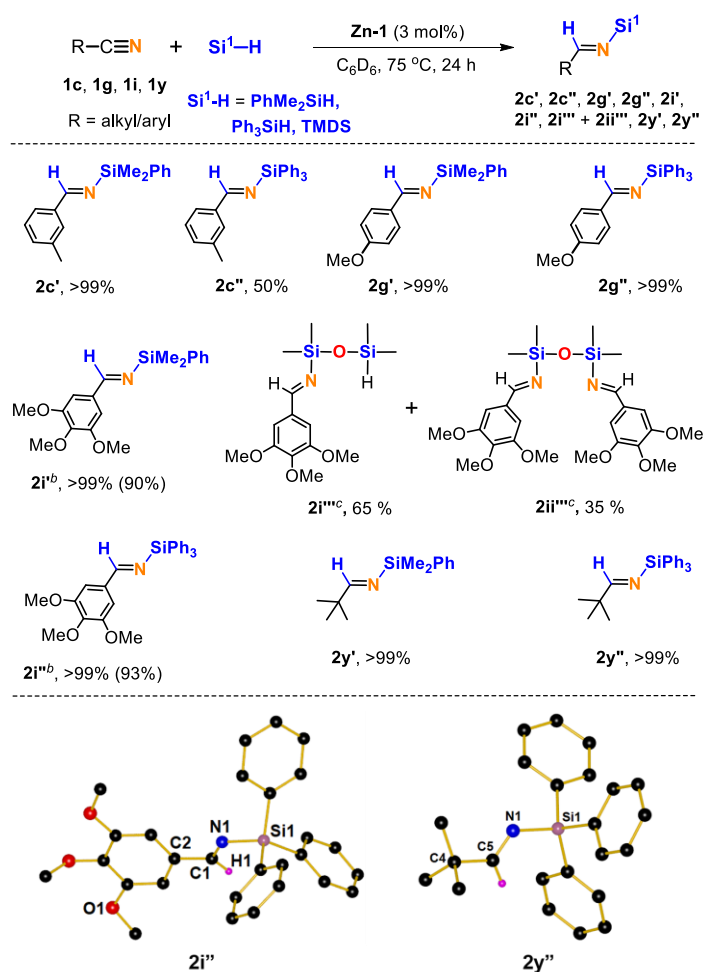
^bFor **1h** (Entry 9) and **1u** (Entry 22), (0.2 mmol, 0.4 equiv.) Ph₂SiH₂ was used and heated at 70 °C for 18 h. The NMR conversion for Si-H addition to nitriles was confirmed by ¹H NMR spectroscopy based on the consumption of starting material and the formation of characteristic proton signals of the CHN peak. ^cFor **2y** and **2za**, NMR conversion was determined by ¹H NMR spectroscopy using mesitylene as an internal standard. ^dFor **1za** (Entry 28) heated at 70 °C for 12 h.

Furthermore, the molecular structures of oximes such as **3h** and **3w** were confirmed by single-crystal X-ray structural analysis. Oximes are an important class of organic compounds with many applications.²³

The pre-catalyst **Zn-1** shows good catalytic performance in catalyzing the chemoselectivity reduction of nitriles using Ph₂SiH₂, which encouraged us to explore different silane reagents such as PhMe₂SiH, Ph₃SiH, and TMDS (1,1,3,3-tetramethyldisiloxane). The 3-methylbenzonitrile (**1c**), 4-methoxybenzonitrile (**1g**), 3,4,5-trimethoxybenzonitrile (**1i**), and alkyl nitrile, i.e., trimethylacetoneitrile (**1y**), were quantitatively converted to corresponding N-silylimine products (**2c'**, **2g'**, **2g''**, **2i'**, **2i''**, **2i'''** + **2ii'''**, **2y'**, **2y''**) (except **2c''**, 50%) after 24 h at 75 °C. The reaction between **1i** and TMDS afforded a mixture **2i'''** + **2ii'''** products. Additionally, the molecular structures of **2i''** and **2y''** were confirmed by single-crystal X-ray structural analysis (for more details, see Scheme 5.B.1). X-ray diffraction study revealed a new N-Si bond between the SiPh₃ unit and the C=N moiety in compounds **2i''** and **2y''**. The N1-C1 (**2i''**) and N1-C5 (**2y''**) bond distances are 1.2698(16) (Å) and 1.2551(19) (Å), respectively, which are comparable to the standard N-C double bond distances. To our knowledge, these are the first examples of structurally characterized N-silyl aldimines.

A mechanism for zinc-catalyzed mono-hydrosilylation of nitriles was investigated to gain more insights into the catalytic applications. Regarding the mono-hydrosilylation of nitriles, a few

research groups have put forward various proposals via metal hydride intermediate formation.^{14a, 16, 18} However, the use of metal hydride catalysts is scarce.¹⁹ In this context, Nikonov and coworkers proposed the mechanism based on kinetics studies.^{19a} The mechanism begins with the coordination of silane to zinc hydride to form an intermediate, followed by a reaction with nitriles via a 6-membered cyclic transition state to produce the desired silylated product. Notably, the authors stated that insertion of the C≡N bond of nitrile into the Zn-H gave the zinc vinylidenamido complex $\text{Dipp}^{\text{NacNac}}\text{Zn-N}=\text{C(H)(Ph)}$ ($\text{Dipp}^{\text{NacNac}} = \text{CH}\{(\text{CMe})(2,6\text{-iPr}_2\text{C}_6\text{H}_3\text{N})\}_2$). Furthermore, the zinc vinylidenamido complex does not react with silanes and is not a potent catalyst.



Scheme 5.B.1. Zinc-catalyzed chemoselective mono-hydrosilylation of nitriles with PhMe_2SiH , Ph_3SiH , and **TMDS**.^a

^aReactions were conducted with nitriles (0.3 mmol, 1.0 equiv.), silanes (PhMe₂SiH, Ph₃SiH or TMS) (0.3 mmol, 1 equiv.), and pre-cat. **Zn-1** (3 mol%), in a J. Young valve NMR tube under N₂ and heated at 75 °C for 24 h. ^bFor **2i'** and **2i''**, a 2 mmol scale was performed under a standard condition in benzene solvent. The NMR conversions for Si-H addition to nitriles were confirmed by ¹H NMR spectroscopy based on the consumption of starting material and formation of characteristic proton signal of *CHN* peak. ^cFor **2i'''** and **2ii'''**, NMR conversion was determined by ¹H NMR spectroscopy using mesitylene as an internal standard.

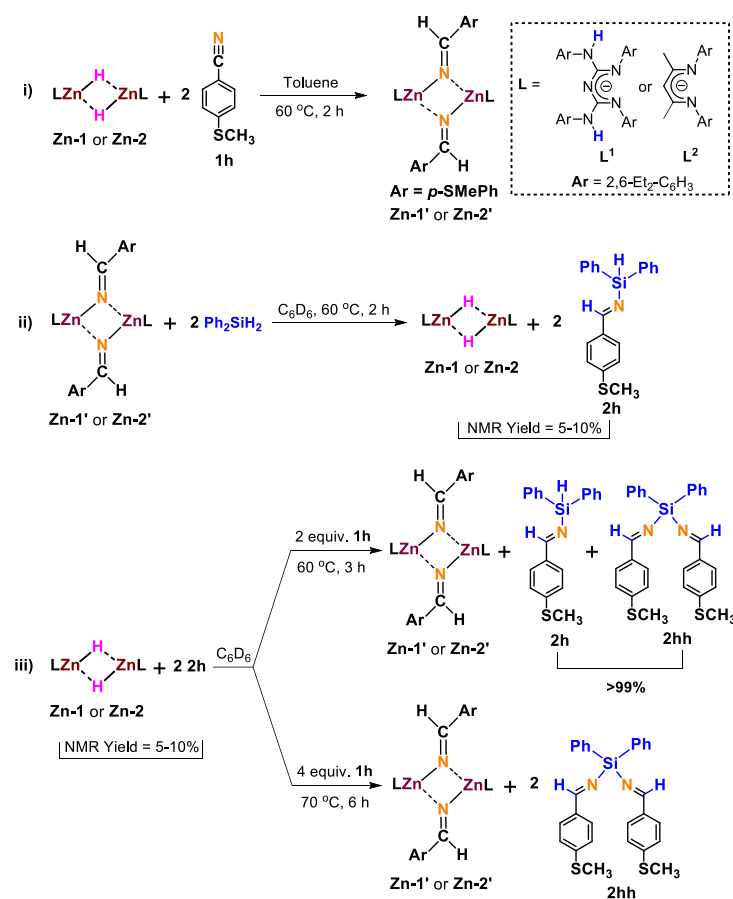
Thus, we carried out more detailed studies such as a series of stoichiometric reactions, active catalysts isolation, and in situ studies to understand the selectivity (effect of ligand) and reaction mechanism of zinc-catalyzed chemoselective hydrosilylation of nitriles to exclusive N-silylimine products. The pre-catalyst **Zn-1** or **Zn-2** reacted with 2 equiv. of 4-(methylthio)benzonitrile (**1h**) produced CBG or NacNac zinc vinylidenamido complex, [L¹ZnN=C(H)(4-SMeC₆H₄)]₂ (**Zn-1'**) or [L²ZnN=C(H)(4-SMeC₆H₄)]₂ (**Zn-2'**) in toluene at 60 °C after 2 h. Multinuclear NMR, HRMS, and X-ray studies confirmed the zinc vinylidenamido complexes **Zn-1'** and **Zn-2'**. In the ¹H NMR spectroscopy, the production of compounds **Zn-1'** and **Zn-2'** was confirmed by complete disappearances of Zn-H resonances and the appearance of a new ZnN=CH singlet peak in the downfield region at 9.53 ppm and 9.34 ppm respectively (Scheme 5.B.2(A), i)).

Further, a 1:2 stoichiometric reaction of catalyst **Zn-1'** with Ph₂SiH₂ undergoes Zn-N/Si-H bond metathesis to produce a 10% conversion of pre-catalyst **Zn-1**, and the hydrosilylated product (**2h**) was observed by ¹H NMR spectroscopy after 2 h at 60 °C. However, the metathesis of ^{Diethyl}NacNac zinc- vinylidenamido (**Zn-2'**) species with Ph₂SiH₂ yielded only a 5% conversion of the mono-hydrosilylated product (**2h**) (Scheme 5.B.2(A), ii)). The formation of product **2h** was confirmed by ¹H NMR spectroscopy as a new N=CH singlet peak appeared at 8.97 ppm. The relative ratio of **2h** and **Zn-1'** or **Zn-2'** did not change after heating at 60 °C up to 12 h. It indicates that the equilibrium position is reached before 2 h. Finally, 2 equiv. 4-(methylthio)benzonitrile (**1h**) was added to the above reaction mixture containing a solution of 5-10% of compounds **Zn-1** or **Zn-2**

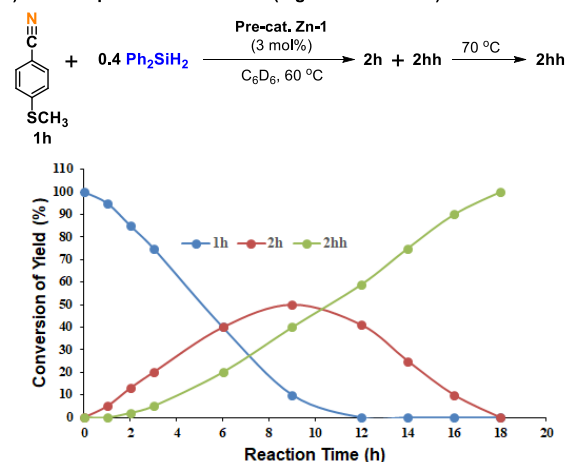
and **2h** in C_6D_6 . The quantitative formation of products **2h** and **2hh** and compound **Zn-1'** or **Zn-2'** were noticed after 3 h, at 60 °C. The 1H NMR spectra confirm the formation of compounds **Zn-1'** or **Zn-2'**, and products **2h** and **2hh** by the appearance of characteristic peaks correspond to $LZnN=CH$ moiety of compound **Zn-1'** (9.53 ppm) and **Zn-2'** (9.34 ppm), and CHN moiety of product **2h** (8.97 ppm) and **2hh** (9.21 ppm) (Scheme 5.B.2(A), iii)).

It is notable that the exclusive quantitative formation of product **2hh** and compound **Zn-1'** or **Zn-2'** were observed when 4 equiv. of **1h** was added to the reaction mixture containing a 5-10% solution of compounds **Zn-1** or **Zn-2** and **2h** (Scheme 5.B.2(A), iii)).

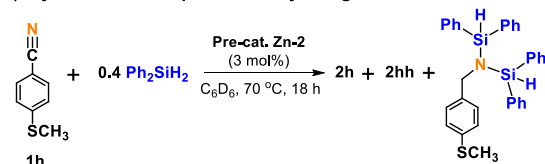
(A) Stoichiometric Experiments



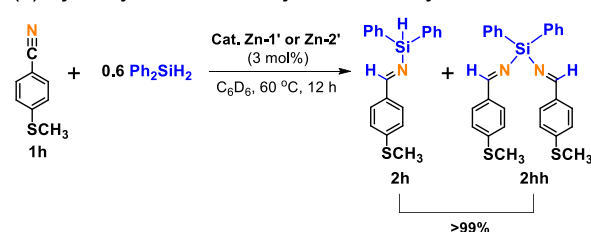
(B) Time-dependent conversion (Figure S7 in the SI)



(C) Synthesis of Compound 2hh by using Pre-cat. Zn-2



(D) Hydrosilylation of Nitriles by an Active Catalyst Zn-1' or Zn-2'



Scheme 5.B.2. Mechanistic studies for partial hydrosilylation of nitriles

According to the study mentioned above, the consumption of Zn-H (**Zn-1** or **Zn-2**) by irreversible reaction with a nitrile is essential for driving the mono- or bis-hydrosilylation of nitrile to completion. The formation of mono- and bis-hydrosilylation products was examined by an *in situ* monitoring of a reaction of 4-(methylthio)benzonitrile (**1h**) with 0.4 equiv. of Ph_2SiH_2 catalyzed by 3 mol% of pre-catalyst **Zn-1** at 60–70 °C over 18 h. The reaction started after 2 h, where the formation of mono-hydrosilylated product N-silylimine, **2h**, was evident by the *CHN* proton signal at δ 8.97 ppm (singlet, C_6D_6). Further, when raised the temperature to 70 °C, the disappearance of the product's **2h** characteristic peak at δ 8.97 ppm and the appearance of a new peak at δ 9.21 ppm corresponding to bis-hydrosilylation product **2hh** was noticed. Finally, after completing 18 h, an exclusive formation of the bis-hydrosilylation product **2hh** was observed (Scheme 5.B.2 (B)), which is in good agreement with the stoichiometric experiments data (Scheme 5.B.2 (A), iii)). Thus, in the initial stage of the reaction, the mono-hydrosilylated product (addition of the one Si-H bond of Ph_2SiH_2 across the $\text{C}\equiv\text{N}$ bond of a nitrile) (**2h**) was observed and added into another nitrile to yield the exclusive bis-hydrosilylated product (addition of the two Si-H bonds of Ph_2SiH_2 across the $\text{C}\equiv\text{N}$ bond of two nitriles) (**2hh**) (Scheme 5.B.2(B)).

Likewise, when the above reaction was conducted in the presence of 3 mol% of pre-catalyst **Zn-2** at 70 °C after 18h, a mixture of compounds **2h**, and **2hh** along with *N, N'*-disilylamine was afforded (Scheme 5.B.2(C)). The above study reveals that pre-catalyst **Zn-1** exhibits better selectivity than pre-catalyst **Zn-2**. Furthermore, isolated zinc vinylidenamido complexes $[\text{L}^1\text{ZnNC(H)(4-SMeC}_6\text{H}_4)]_2$, (**Zn-1'**) and $[\text{L}^2\text{ZnNC(H)(4-SMeC}_6\text{H}_4)]_2$, (**Zn-2'**) (3 mol%) were used in catalysis to confirm the involvement of zinc vinylidenamido species in the catalytic cycle, and excellent conversion of 4-(methylthio)benzonitrile (**1h**) to corresponding N-silylimine was observed at 60 °C after 12 h. This experimental result strongly suggests that the zinc vinylidenamido species (**Zn-**

1' and **Zn-2'**) are involved in the catalytic mono-hydrosilylation of nitriles (Scheme 5.B.2(D)). The active catalysts zinc vinylidenamido derivative **Zn-1'** and **Zn-2'** were crystallized as colorless block-shaped crystals from benzene solution at rt within 2 days. The X-ray diffraction study reveals that compounds **Zn-1'** and **Zn-2'** are dimeric, having distorted tetrahedral geometry. The zinc atom of compounds **Zn-1'** and **Zn-2'** has four coordination sites and is coordinated by two N atoms from ligands (CBG or NacNac) and two bridging N-atoms from imine moieties (Figure 5.B.3).

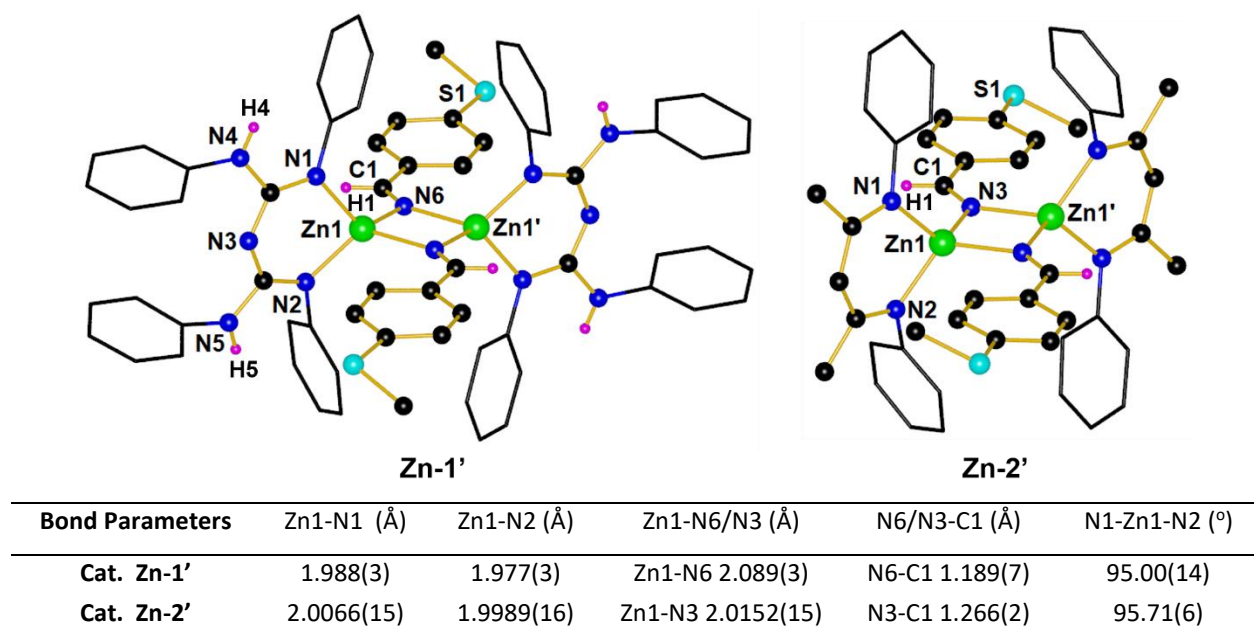
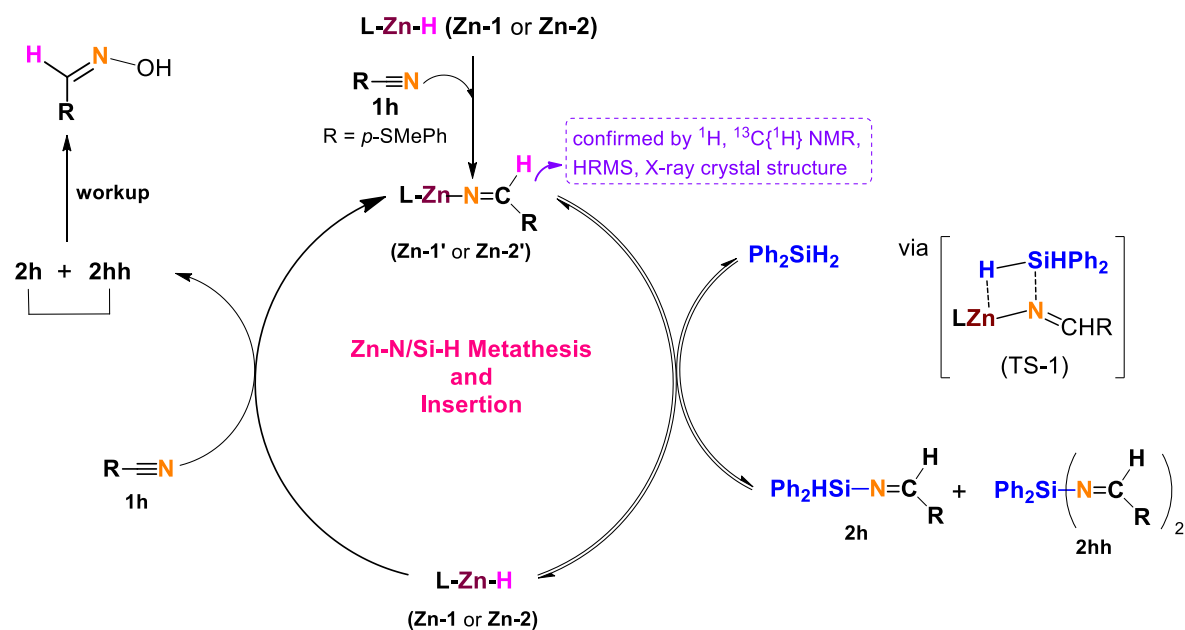


Figure 5.B.3. Molecular structures of compounds **Zn-1'** (left) and **Zn-2'** (right). All the hydrogen atoms (except for H(1), H(4), and H(5) from structure **Zn-1'** and H(1) from structure **Zn-2'**) and ethyl groups are removed for clarity. Comparison of bond parameters of compound **Zn-1'** vs. **Zn-2'** (Selected bond lengths (Å) and angles (°)).

The zinc vinylidenamido complexes are rare in the literature.^{19a} In compound **Zn-1'**, Zn1-N6, 2.089(3) bond distance is slightly longer than the zinc-imino bond distances of compound **Zn-2'**, Zn1-N3 2.0152(15). In contrast, the C1-N6 bond length, 1.189(7) Å of compound **Zn-1'** is significantly shorter than compound **Zn-2'**, C1-N3 1.266(2) Å. Based on the above-mentioned

structural parameter changes (Figure 5.B.3), stoichiometric experiment data (Scheme 5.B.2(A) ii, Scheme 5.B.2(B), and Scheme 5.B.2(C)), and screening of silanes in Table 5.B.2, it suggests that pre-catalyst **Zn-1** has better catalytic activity and selectivity than pre-catalyst **Zn-2** in producing N-silylimines. A most plausible reaction mechanism for chemoselective hydrosilylation of nitriles to N-silylimines has been proposed based on active catalysts isolation, stoichiometric experiments, and *in situ* studies. In the initial stage, the addition of the Zn-H moiety of complex **Zn-1** or **Zn-2** across the C≡N bond of nitrile affords the zinc vinylidenamido derivatives **Zn-1'** or **Zn-2'**. Further, the active catalyst **Zn-1'** or **Zn-2'** reacts with Ph₂SiH₂ via Zn-N/Si-H bond metathesis (TS-1), yielding a 5-10% mixture of N-silylimines and pre-catalyst **Zn-1** or **Zn-2** in an equilibrium position. Finally, a mixture of **Zn-1** or **Zn-2** and N-silylimines reacts with another nitrile molecule, yields the corresponding N-silylimines and regenerates the active catalyst **Zn-1'** or **Zn-2'** with high conversions and closes the catalytic cycle (Scheme 5.B.3). N-silylimines upon reacting with NH₂OH.HCl in ethanol yielded the corresponding oximes.



Scheme 5.B.3. Proposed mechanism for the hydrosilylation of nitriles

5.B.2.1. Synthetic Utility

The N-silylimine products obtained from this reaction were expected to serve as starting materials for other valuable synthetic building blocks.^{7a} Thus, we performed some product transformations to explore the product utility/applicability (Scheme S1).

We found that when mono-hydrosilylation of nitriles (**1a**, **1d**, and **1r**) were performed on a 5.0 mmol scale under standard reaction conditions yielded the corresponding N-silylimines (**2a** + **2aa**, **2d** + **2dd**, **2r** + **2rr**) with quantitative conversions. After the workup of N-silylimines, delivering the respective pure oxime products with good yields (**3a** (74%), **3d** (73%), and **3r** (58%)) (isolated) (Scheme S1, a).²⁰ The borylsilylamines are essential precursors for producing B/Si/N/C ceramics with exceptionally excellent heat-resistant properties. Catalytic dihydroborylsilylation of nitriles is rare.²⁴ In this context, the N-silylimines **2i'** and **2i''** reacted with HBpin in the presence of pre-catalyst **Zn-1** at 75 °C after 24 h, delivered the borylsilylamine derivatives **4a** (>99%) and **4b** (56%) in good conversions (Scheme S1, b).

Like **3a-3w**, the N-silylimines **2i'** and **2i''** under standard reaction conditions, after workup, yielded the respective oximes **3i'** and **3i''** in high yields (Scheme S1, b). *N*-acylimines and *N*-methylenecarbamic esters are essential in organic chemistry, including cycloadditions and natural product synthesis.^{7, 25} Similarly, *N*-sulfonylimines are the necessary starting materials for Diels-Alder chemistry.^{7a, 26} The N-silylimines could also be converted into *N*-acylimine (**5a** or **5b**), *N*-methylenecarbamic ester (**6a**), and *N*-sulfonylimine (**7a** or **7b**) in the presence of pivaloyl chloride or 4-nitrobenzoyl chloride, ethyl chloroformate, and methanesulfonyl chloride or *p*-toluenesulfonyl chloride (Scheme S1, c).

5.B.3. Conclusion

In summary, we have established that the zinc hydride complexes **Zn-1** and **Zn-2** are remarkable pre-catalysts for the selective hydrosilylation of nitriles to N-silylimines. However, pre-catalyst

Zn-1 shows better chemoselective than pre-catalyst **Zn-2**; this implies that the role of the spectator ligand is essential in catalysis. A wide array of nitrile chemoselective reductions produced N-silylimines with good tolerance for other functional groups. The active catalysts **Zn-1'** and **Zn-2'** are isolated and structurally characterized; such examples are scarce in the literature. A plausible complete catalytic cycle has been proposed depending on the isolation of structurally characterized active catalysts, stoichiometric reactions, and *in situ* studies.

In contrast to previously proposed mechanisms, we have established the reaction of zinc vinylidenamido complex with silane, which exists in equilibrium. Upon the addition of nitriles, the exclusive formation of N-silylimines occurs. The synthetic utility of this protocol was demonstrated. Moreover, the zinc hydride-catalyzed selective C \equiv N bond cleavage to C=N opens new possibilities for zinc hydride catalysis in the selective reduction of other organic functionalities. Furthermore, N-silylimines would be ideal precursors for synthesizing metal aldimide complexes; such studies are currently underway in our laboratory.

5.B.4. General Experimental Methods

General Procedures

Unless stated, manipulations were performed under a dinitrogen atmosphere using standard glovebox and Schlenk techniques. NMR spectra were recorded on Jeol-400 MHz spectrometer and Bruker NMR spectrometers at 400 MHz (^1H), 101 MHz ($^{13}\text{C}\{^1\text{H}\}$), 80 MHz ($^{29}\text{Si}\{^1\text{H}\}$). ^1H NMR and $^{13}\text{C}\{^1\text{H}\}$ NMR chemical shifts are referenced to residual protons or carbons in the deuterated solvent. Multiplicities are reported as singlet (s), doublet (d), triplet (t), quartet (q), and multiplet (m). Chemical shifts are reported in ppm. Coupling constants are reported in Hz. The crystal data of compound **Zn-1'** is collected on a Rigaku Oxford diffractometer with graphite-monochromated Cu-K α radiation ($\lambda = 1.54184 \text{ \AA}$) at 100 K. Whereas, the crystal data of compounds **Zn-2'**, **2i''**,

2y”, **3h**, and **3w** are collected on a Rigaku Oxford diffractometer with Mo-K α radiation ($\lambda = 0.71073$ Å) at 100 K. In addition, crystal data for compound **7b** is collected at 298 K using a Rigaku Oxford diffractometer with Mo-K radiation ($\lambda = 0.71073$). Selected data collection parameters and other crystallographic results are summarized in Table 5.B.4-5.B.5. Mass spectrometry analyses were carried out on Bruker micrOTOF-Q II and Waters XevoG2 XS Q-TOF mass spectrometers. The melting points of **Zn-1'** and **Zn-2'** were measured from Stuart SMP 10 instrument.

Materials:

Solvents were purified by distillation over Na/ benzophenone. Deuterated chloroform (CDCl₃) was dried on molecular sieves, and benzene-*d*₆ (C₆D₆) was dried over Na/K alloy and distilled. The ligand L¹(3H) (L¹ = {(ArNH)(ArN)–C=N– C=(NAr)(NHAr)}; Ar = 2,6- Et₂-C₆H₃)] and complex {L¹ZnH}₂ (**Zn-1**) were prepared according to reported literature procedures.²¹ The complex {L²ZnH}₂ ((^{Diethyl}NacNac (L²) = CH{(CMe)(2,6-Et₂C₆H₃N)}₂)] (**Zn-2**) was prepared according to reported literature procedures.²² For catalysis reactions, J. Young valve-sealed NMR tubes or Schlenk tubes, as per the requirement, were properly oven-dried before being used. Chemicals and reagents were purchased from Sigma-Aldrich Co. Ltd., Merck India Pvt. Ltd., and TCI chemicals were used without purification.

5.B.4.1. Stoichiometric Experiments Data.

Synthesis of [L¹ZnNC(H)(4-SMeC₆H₄)]₂, (Zn-1'**) {NMR-Scale}: Addition of 4-(methylthio)benzonitrile (4 mg, 0.028 mmol) to a J. Young valve NMR tube containing a solution of complex **Zn-1** (0.020 g, 25 °C, 0.014 mmol) in C₆D₆. The reaction mixture was heated at 60 °C for 2 h, resulting in the formation of compound **Zn-1'** was observed by ¹H NMR spectroscopy. NMR conversion: (>99%).**

Synthesis of [L¹ZnNC(H)(4-SMeC₆H₄)]₂, (Zn-1'**) {Reaction-Scale}:**

4-(methylthio)benzonitrile 53 mg (0.359 mmol) in ~4 mL of toluene was added at room temperature through a cannula transfer to a solution of [L¹ZnH]₂ (**Zn-1**) 0.250 g (0.179 mmol) in 8 mL of toluene and stirred at 60 °C in an oil bath for 2 h. The solvent was removed in a vacuum resulting in a white solid compound and dried thoroughly. The resultant solid was dissolved in benzene (~ 10 mL) and filtered. Further, the solution was heated to 60 °C and slowly allowed to cool to room temperature, and we observed the formation of colorless block-shaped crystals within 2 days. (0.248 g, 82 %); m.p. 196-201 °C. ¹H NMR (400 MHz, C₆D₆) δ 9.53 (s, 2H), 7.95 – 7.93 (d, ³J_{HH} = 8.2 Hz, 4H), 7.34 – 7.32 (d, ³J_{HH} = 8.2 Hz, 4H), 7.18 – 7.15 (m, 4H), 7.04 (t, ³J_{HH} = 7.6 Hz, 4H), 6.93 (t, ³J_{HH} = 7.5 Hz, 4H), 6.85 – 6.84 (d, ³J_{HH} = 7.4 Hz, 4H), 6.76 – 6.75 (d, ³J_{HH} = 7.4 Hz, 4H), 6.65 – 6.63 (d, ³J_{HH} = 7.4 Hz, 4H), 4.90 (s, 4H), 3.61 – 3.51 (m, 4H), 3.19 – 3.09 (m, 4H), 2.60 – 2.51 (m, 4H), 2.47 – 2.39 (m, 12H), 2.13 – 2.10 (m, 4H), 2.07 (s, 6H), 1.70 – 1.62 (m, 4H), 1.56 (t, ³J_{HH} = 7.5 Hz, 12H), 1.05 (t, ³J_{HH} = 7.5 Hz, 12H), 0.93 (t, ³J_{HH} = 7.4 Hz, 12H), 0.62 (t, ³J_{HH} = 7.5 Hz, 12H). ¹³C{¹H} NMR (100 MHz, C₆D₆) δ 168.5, 157.1, 143.7, 141.7, 141.0, 140.5, 138.8, 137.5, 135.8, 135.6, 128.5, 127.5, 126.0, 125.9, 125.7, 125.3, 125.0, 124.6, 124.1, 25.0, 24.9, 23.1, 22.4, 14.5, 14.4, 14.0, 12.9, 12.6. HRMS (ASAP/Q-TOF) *m/z*: [M + H]⁺ Calcd for C₅₀H₆₃N₆SZn 843.4127, Found: 843.4052.

The reaction between zinc vinylidenamido complex Zn-1' and Ph₂SiH₂ {NMR-Scale}: The addition of Ph₂SiH₂ (5 μL, 0.028 mmol) to a J. Young valve NMR tube containing a solution of compound **Zn-1'** (0.014 mmol) in C₆D₆. The reaction mixture was heated at 60 °C for 2 h resulting in the formation of compounds **Zn-1**, and **2h** with a 10% conversion was observed by NMR spectroscopy. ¹H NMR spectroscopy revealed that the reaction had reached an equilibrium, best evidenced by the integration of resonance for CHN moieties of **2h** and compound **Zn-1'**. After

heating up to 12 h at 60 °C, there was no change in the relative ratio of **2h** and **Zn-1'**, suggesting that the equilibrium position had already been reached before 2 h. NMR conversion: (10%).

Synthesis of compound Zn-1', 2h and 2hh {NMR-Scale}: The addition of 4-(methylthio)benzonitrile 4 mg (0.028 mmol) to a J. Young valve NMR tube containing a solution of compounds **Zn-1** and **2h** (10%) in C₆D₆. The reaction mixture was heated at 60 °C for 3 h resulting in the formation of compounds **Zn-1'**, **2h**, and **2hh** were observed by ¹H NMR spectroscopy. The above study indicates that once 10% of the compounds **2h** and **Zn-1** were formed, they reacted with additional amounts of 4-(methylthio)benzonitrile to form a mixture of products **2h**, **2hh**, and the compound **Zn-1'** in quantitative conversion. It stops the equilibrium reaction between compounds **Zn-1'** and **2h**. NMR conversion: (>99%).

Synthesis of compound Zn-1' and 2hh {NMR-Scale}: The addition of 4-(methylthio)benzonitrile 8 mg (0.056 mmol) to a J. Young valve NMR tube containing a solution of compound **Zn-1** and **2h** (10%) in C₆D₆. The reaction mixture was heated at 70 °C for 6 h resulting in the complete formation of compounds **Zn-1'**, and **2hh** were observed by ¹H and ¹³C NMR spectroscopy. The above study indicates that once 10% of the compounds **2h** and **Zn-1** were formed, they immediately reacted with an additional amount of 4-(methylthio)benzonitrile to form a quantitative amount of product **2hh** and the active catalyst **Zn-1'** NMR conversion: (>99%). ¹H NMR (400 MHz, C₆D₆) δ 9.53 (s, 2H), 9.21 (s, 4H), 7.98 – 7.94 (m, 10H), 7.72 – 7.66 (d, ³J_{HH} = 8.0 Hz, 10H), 7.34 – 7.32 (d, ³J_{HH} = 8.1 Hz, 5H), 7.28 – 7.22 (m, 10H), 7.09 – 7.00 (m, 15H), 6.93 (t, ³J_{HH} = 7.1 Hz, 5H), 6.86 – 6.84 (d, ³J_{HH} = 7.4 Hz, 5H), 6.77 – 6.75 (d, ³J_{HH} = 7.3 Hz, 4H), 6.65 – 6.64 (d, ³J_{HH} = 7.3 Hz, 4H), 4.90 (s, 4H), 3.61 – 3.51 (m, 4H), 3.19 – 3.09 (m, 4H), 2.60 – 2.51 (m, 4H), 2.47 – 2.37 (m, 12H), 2.16 – 2.10 (m, 4H), 2.07 (s, 6H), 1.84 (s, 12H), 1.68 – 1.62 (m, 4H), 1.57 (t, ³J_{HH} = 7.6 Hz, 12H), 1.05 (t, ³J_{HH} = 7.4 Hz, 12H), 0.93 (t, ³J_{HH} = 7.4 Hz, 12H), 0.62 (t, ³J_{HH} =

7.5 Hz, 12H). $^{13}\text{C}\{^1\text{H}\}$ NMR (100 MHz, C_6D_6) δ 172.0, 168.5, 157.1, 144.1, 143.7, 141.7, 141.0, 140.5, 138.8, 137.5, 135.8, 135.7, 135.6, 135.5, 133.8, 130.0, 129.4, 128.5, 126.0, 125.9, 125.8, 125.3, 125.0, 124.6, 124.1, 25.0, 24.9, 23.1, 22.4, 14.5, 14.4, 14.1, 14.0, 12.9, 12.6.

Synthesis of $[\text{L}^2\text{ZnNC}(\text{H})(4\text{-SMeC}_6\text{H}_4)]_2$, (Zn-2'**) {NMR-Scale}:** Addition of 4-(methylthio)benzonitrile (7 mg, 0.047 mmol) to a J. Young valve NMR tube containing a solution of complex **Zn-2** (0.020 g, 25 °C, 0.023 mmol) in C_6D_6 . The reaction mixture was heated at 60 °C for 2 h, resulting in the formation of compound **Zn-2'** observed by ^1H NMR spectroscopy. NMR conversion: (>99%).

Synthesis of $[\text{L}^2\text{ZnNC}(\text{H})(4\text{-SMeC}_6\text{H}_4)]_2$, (Zn-2'**) {Reaction Scale}:**

4-(methylthio)benzonitrile 87 mg (0.586 mmol) in ~4 mL of toluene was added at room temperature through a cannula transfer to a solution of $[\text{L}^2\text{ZnH}]_2$ (**Zn-2'**) 0.250 g (0.293 mmol) in 8 mL of toluene and stirred at 60 °C in an oil bath for 2 h. The solvent was removed in a vacuum resulting in a white solid compound and dried thoroughly. The resultant solid was dissolved in benzene (~ 10 mL) and filtered. Further, the solution was heated to 60 °C and slowly allowed to cool to room temperature, and we observed the formation of colorless block-shaped crystals within 2 days. (0.270 g, 80 %); m.p. 190-195 °C. ^1H NMR (400 MHz, C_6D_6) δ 9.34 (s, 2H), 7.77 – 7.75 (d, $^3J_{\text{HH}} = 8.1$ Hz, 4H), 7.30 – 7.28 (d, $^3J_{\text{HH}} = 8.2$ Hz, 4H), 7.05 – 6.99 (m, 8H), 6.82 – 6.81 (d, $^3J_{\text{HH}} = 6.8$ Hz, 4H), 4.92 (s, 2H), 3.03 – 2.93 (m, 4H), 2.77 – 2.59 (m, 8H), 2.03 – 1.98 (m, 4H), 1.96 (s, 6H), 1.42 (s, 12H), 1.39 (t, $^3J_{\text{HH}} = 7.5$ Hz, 12H), 0.55 (t, $^3J_{\text{HH}} = 7.5$ Hz, 12H). $^{13}\text{C}\{^1\text{H}\}$ NMR (100 MHz, C_6D_6) δ 167.6, 167.1, 147.6, 141.5, 137.7, 135.9, 135.9, 128.7, 127.0, 125.8, 124.3, 124.0, 93.8, 29.8, 23.7, 23.2, 22.4, 14.6, 13.8, 13.4. HRMS (ASAP/Q-TOF) m/z : $[\text{M} + \text{H}]^+$ Calcd for $\text{C}_{33}\text{H}_{42}\text{N}_3\text{SZn}$ 576.2391, Found: 576.2421.

5.B.4.2. X-ray Crystallographic Data

The single crystals of compounds **Zn-1'**, **Zn-2'**, **2i''**, **2y''** and **7b** were crystallized from benzene at rt as colorless blocks after 2 d, and **3h**, and **3w** were crystallized from a mixture of dichloromethane and hexane at rt as colorless blocks after 2 d. The crystal data of compound **Zn-1'** is collected on a Rigaku Oxford diffractometer with graphite-monochromated Cu-K α radiation ($\lambda = 1.54184$ Å) at 100 K. Whereas, the crystal data of compounds **Zn-2'**, **2i''**, **2y''**, **3h**, and **3w** are collected on a Rigaku Oxford diffractometer with Mo-K α radiation ($\lambda = 0.71073$ Å) at 100 K. In addition, crystal data for compound **7b** is collected at 298 K using a Rigaku Oxford diffractometer with Mo-K radiation ($\lambda = 0.71073$). Selected data collection parameters and other crystallographic results are summarized in Table 5.B.4-5.B.5. The structure was determined using direct methods employed in *ShelXT*,²⁷ *Olex*,²⁸ and refinement was carried out using least-square minimization implemented in *ShelXL*.²⁹ All non-hydrogen atoms were refined with anisotropic displacement parameters. Hydrogen atom positions were fixed geometrically in idealized positions and were refined using a riding model.

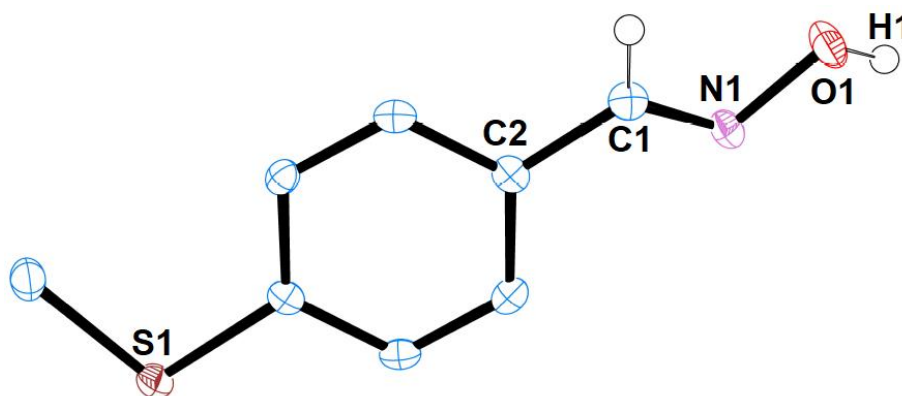


Figure 5.B.4. Molecular structure of **3h**. The thermal ellipsoids are shown at 50% probability, and all the hydrogen atoms (except for H(1), H(1A)) have been removed for clarity. Selected bond lengths (Å) and angles (deg), For **3h**: C1-C2 1.466(2), C1-N1 1.2739(19), N1-O1 1.4137(15); C2-C1-N1 122.03(13), C1-N1-O1 111.09(11).

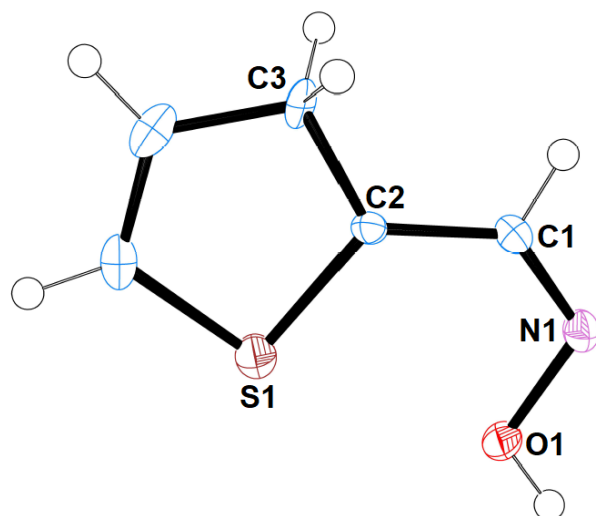


Figure 5.B.5. Molecular structure of **3w**. The thermal ellipsoids are shown at 50% probability. Selected bond lengths (Å) and angles (deg), For **3w**: C1-C2 1.448(5), C1-N1 1.281(5), N1-O1 1.402(4), C2-S1 1.720(4), C2-C3 1.449(5); C2-C1-N1 129.6(3), C1-N1-O1 112.0(3), C3-C2-S1 112.3(3).

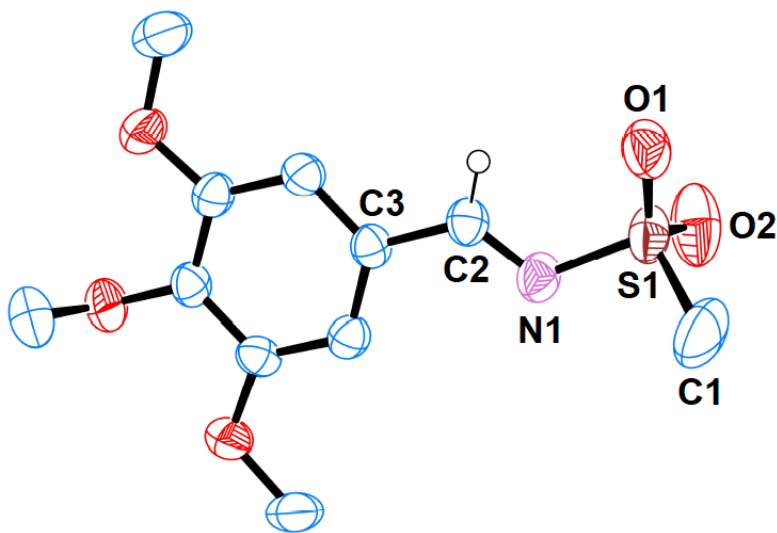


Figure 5.B.6. Molecular structure of **7b**. The thermal ellipsoids are shown at 50% probability. Selected bond lengths (Å) and angles (deg), For **7b**: C2-N1 1.275(2), N1-S1 1.6660(14), C1-S1 1.743(2), C2-C3 1.455(2); C3-C2-N1 122.56(16), C2-N1-S1 116.09(12).

Table 5.B.4. Crystallographic data and refinement parameters for compounds **Zn-1'**, **Zn-2'**, **2i''**, and **2y''**.

Compound	Zn-1'	Zn-2'	2i''	2y''
Empirical Formula	C ₁₀₀ H ₁₂₄ N ₁₂ S ₂ Zn ₂	C ₇₂ H ₈₈ N ₆ S ₂ Zn ₂	C ₂₈ H ₂₇ NO ₃ Si	C ₂₃ H ₂₅ NSi
CCDC	2232417	2232418	2232419	2232416
Molecular mass	1688.96	1232.34	453.59	343.53
Temperature (K)	100	100	100	100
Wavelength (Å)	1.54184	0.71073	0.71073	0.71073
Size(mm)	0.2 × 0.18 × 0.17	0.2 × 0.18 × 0.17	0.2 × 0.18 × 0.17	0.2 × 0.18 × 0.17
Crystal system	triclinic	Monoclinic	monoclinic	triclinic
Space group	P-1	P ₂ ₁ /n	P ₂ ₁ /n	P-1
a (Å)	13.3391(2)	13.5918(3)	6.8325(3)	9.4099(3)
b (Å)	16.1776(2)	15.8628(3)	31.3215(13)	10.0584(4)
c (Å)	21.3848(3)	15.1346(3)	11.3758(5)	11.5742(4)
α (deg)°	84.1774(12)	90	90	106.364(3)
β (deg)°	75.9063(14)	92.465(2)	102.024(4)	97.172(3)
γ (deg)°	87.5292(11)	90	90	106.079(3)
Volume (Å ³)	4451.95(12)	3260.06(11)	2381.06(18)	985.23(7)
Z	2	2	4	2
Calculated density (g/cm ³)	1.260	1.255	1.265	1.158
Absorption coefficient (mm ⁻¹)	1.512	0.846	0.129	0.124
F(000)	1800.0	1308.0	960.0	368.0
Theta range for data collection (deg)°	6.64 to 136.502	6.576 to 50.7	6.932 to 52.742	6.74 to 52.738
Limiting indices	-16 ≤ h ≤ 11, -19 ≤ k ≤ 19, -25 ≤ l ≤ 25	-16 ≤ h ≤ 16, -18 ≤ k ≤ 19, -18 ≤ l ≤ 17	-8 ≤ h ≤ 8, -39 ≤ k ≤ 39, -14 ≤ l ≤ 14	-11 ≤ h ≤ 11, -12 ≤ k ≤ 12, -14 ≤ l ≤ 14
Reflections collected	58859	29147	24735	18840
Independent reflections	16264 [R _{int} = 0.0846, R _{sigma} = 0.0849]	5856 [R _{int} = 0.0511, R _{sigma} = 0.0299]	4860 [R _{int} = 0.0371, R _{sigma} = 0.0264]	4035 [R _{int} = 0.0392, R _{sigma} = 0.0248]
Completeness to theta	99 %	99 %	99 %	99 %
Absorption correction	Empirical	Empirical	Empirical	Empirical
Data/restraints/parameters	16264 / 7 / 1063	5856 / 0 / 377	4860 / 0 / 301	4035 / 0 / 229
Goodness – of–fit on F ²	1.089	1.079	1.037	1.055
Final R indices [I>2 sigma(I)]	R ₁ = 0.0846, wR ₂ = 0.2300	R ₁ = 0.0373, wR ₂ = 0.1071	R ₁ = 0.0328, wR ₂ = 0.0841	R ₁ = 0.0395, wR ₂ = 0.1106

Table 5.B.5. Crystallographic data and refinement parameters for compounds **3h**, **3w**, and **7b**.

Compound	3h	3w	7b
Empirical Formula	C ₈ H ₈ NOS	C ₅ H ₆ NOS	C ₁₁ H ₁₅ NO ₅ S
CCDC	2232420	2232421	2232422
Molecular mass	166.21	128.17	273.30
Temperature (K)	100	100	298
Wavelength (Å)	0.71073	0.71073	0.71073
Size(mm)	0.2 × 0.18 × 0.17	0.2 × 0.18 × 0.17	0.2 × 0.18 × 0.17
Crystal system	monoclinic	orthorhombic	triclinic
Space group	<i>P</i> 2 ₁ / <i>c</i>	<i>Pca</i> 2 ₁	<i>P</i> -1
<i>a</i> (Å)	5.9234(2)	11.4902(4)	7.4747(2)
<i>b</i> (Å)	7.2101(3)	13.6947(4)	10.8452(3)
<i>c</i> (Å)	18.8248(7)	7.3806(2)	17.1096(5)
α (deg) [°]	90	90	98.249(2)
β (deg) [°]	91.375(3)	90	91.218(2)
γ (deg) [°]	90	90	107.891(2)
Volume (Å ³)	803.74(5)	1161.38(6)	1303.11(6)
<i>Z</i>	4	8	4
Calculated density (g/cm ³)	1.374	1.466	1.393
Absorption coefficient (mm ⁻¹)	0.339	0.445	0.261
<i>F</i> (000)	348.0	536.0	576.0
Theta range for data collection (deg) [°]	6.88 to 50.7	6.928 to 52.736	7.238 to 52.736
Limiting indices	-6 ≤ <i>h</i> ≤ 7, -7 ≤ <i>k</i> ≤ 8, -20 ≤ <i>l</i> ≤ 22	-14 ≤ <i>h</i> ≤ 14, -17 ≤ <i>k</i> ≤ 17, -8 ≤ <i>l</i> ≤ 9	-9 ≤ <i>h</i> ≤ 9, -13 ≤ <i>k</i> ≤ 13, -21 ≤ <i>l</i> ≤ 21
Reflections collected	6824	9903	22057
Independent reflections	1466 [<i>R</i> _{int} = 0.0314, <i>R</i> _{sigma} = 0.0255]	2319 [<i>R</i> _{int} = 0.0282, <i>R</i> _{sigma} = 0.0218]	5308 [<i>R</i> _{int} = 0.0410, <i>R</i> _{sigma} = 0.0279]
Completeness to theta	99 %	99 %	99 %
Absorption correction	Empirical	Empirical	Empirical
Data/restraints/parameters	1466 / 0 / 102	2319 / 1 / 147	5308 / 0 / 333
Goodness – of–fit on <i>F</i> ²	1.051	1.140	1.060
Final <i>R</i> indices [<i>I</i> > 2 sigma(<i>I</i>)]	<i>R</i> ₁ = 0.0284, <i>wR</i> ₂ = 0.0779	<i>R</i> ₁ = 0.0360, <i>wR</i> ₂ = 0.1077	<i>R</i> ₁ = 0.0410, <i>wR</i> ₂ = 0.1197

5.B.5. Appendix: All general experimental information, stoichiometric reactions, analytical data, and spectral data were available in published paper. *Inorg. Chem.* **2023**, *62*, 12213-12222.

5.B.6. References

1. (a) Fessenden, R.; Fessenden, J. S. *Chem. Rev.* **1961**, *61*, 361-388; (b) Calas, R. *J. Organomet. Chem.* **1980**, *200*, 11-36; (c) Ruecker, C. *Chem. Rev.* **1995**, *95*, 1009-1064; (d) Marciniak, B. *Appl. Organomet. Chem.* **2000**, *14*, 527-538; (e) Gibson, S. E.; Rudd, M. *Adv. Synth. Catal.* **2007**, *349*, 781-795; (f) Roy, A. K., In *Adv. Organomet. Chem.*, West, R.; Hill, A. F.; Fink, M. J., Eds. Academic Press 2007; Vol. 55, pp 1-59; (g) Campos, J.; Rubio, M.; Esqueda, A. C.; Carmona, E. *J. Label Compd. Radiopharm* **2012**, *55*, 29-38; (h) Huckaba, A. J.; Hollis, T. K.; Reilly, S. W. *Organometallics* **2013**, *32*, 6248-6256; (i) Melen, R. L. *Chem. Soc. Rev.* **2016**, *45*, 775-788; (j) Tanabe, Y.; Nishibayashi, Y. *Coord. Chem. Rev.* **2019**, *389*, 73-93; (k) Kuciński, K.; Stachowiak, H.; Lewandowski, D.; Gruszczyński, M.; Lampasiak, P.; Hreczycho, G. *J. Organomet. Chem.* **2022**, *961*, 122127; (l) Rodríguez, A. M.; Pérez-Ruiz, J.; Molina, F.; Poveda, A.; Pérez-Soto, R.; Maseras, F.; Díaz-Requejo, M. M.; Pérez, P. J. *J. Am. Chem. Soc.* **2022**, *144*, 10608-10614; (m) Liu, Z.; Li, M.; Deng, G.; Wei, W.; Feng, P.; Zi, Q.; Li, T.; Zhang, H.; Yang, X.; Walsh, P. J. *Chem. Sci.* **2020**, *11*, 7619-7625.
2. Tondreau, A. M.; Atienza, C. C. H.; Weller, K. J.; Nye, S. A.; Lewis, K. M.; Delis, J. G. P.; Chirik, P. J. *Science* **2012**, *335*, 567-570.
3. (a) Doyle, M. P.; High, K. G.; Nesloney, C. L.; Clayton, T. W., Jr.; Lin, J. *Organometallics* **1991**, *10*, 1225-1226; (b) Jun, C.-H.; Crabtree, R. H. *J. Organomet. Chem.* **1993**, *447*, 177-187; (c) Takahashi, T.; Bao, F.; Gao, G.; Ogasawara, M. *Org. Lett.* **2003**, *5*, 3479-3481; (d) Trost, B. M.; Ball, Z. T. *J. Am. Chem. Soc.* **2005**, *127*, 17644-17655.

4. (a) Carpentier, J.-F.; Bette, V. *Curr. Org. Chem.* **2002**, *6*, 913-936; (b) Riant, O.; Mostefaï, N.; Courmarcel, J. *Synthesis* **2004**, 2943-2958; (c) Das, K.; Waiba, S.; Jana, A.; Maji, B. *Chem. Soc. Rev.* **2022**, *51*, 4386-4464; (d) Das, S.; Wendt, B.; Möller, K.; Junge, K.; Beller, M. *Angew. Chem. Int. Ed.* **2012**, *51*, 1662-1666; (e) Das, S.; Zhou, S.; Addis, D.; Enthaler, S.; Junge, K.; Beller, M. *Top Catal* **2010**, *53*, 979-984; (f) Addis, D.; Das, S.; Junge, K.; Beller, M. *Angew. Chem. Int. Ed.* **2011**, *50*, 6004-6011; (g) Das, S.; Das, H. S.; Singh, B.; Haridasan, R. K.; Das, A.; Mandal, S. K. *Inorg. Chem.* **2019**, *58*, 11274-11278; (h) Sanagawa, A.; Nagashima, H. *Org. Lett.* **2019**, *21*, 287-291; (i) Das, S.; Addis, D.; Junge, K.; Beller, M. *Chem. Eur. J.* **2011**, *17*, 12186-12192.
5. (a) Weintraub, L.; Oles, S. R.; Kalish, N. *J. Org. Chem.* **1968**, *33*, 1679-1681; (b) Murai, T.; Sakane, T.; Kato, S. *Tetrahedron Lett.* **1985**, *26*, 5145-5148; (c) Murai, T.; Sakane, T.; Kato, S. *J. Org. Chem.* **1990**, *55*, 449-453; (d) Prabhakar, R. N.; Yuko, U.; Hans-Jürgen, L.; Masato, T. *Chem. Lett.* **1992**, *21*, 45-48; (e) Caporusso, A. M.; Panziera, N.; Pertici, P.; Pitzalis, E.; Salvadori, P.; Vitulli, G.; Martra, G. *J. Mol. Catal. A* **1999**, *150*, 275-285; (f) Bornschein, C.; Werkmeister, S.; Junge, K.; Beller, M. *New J. Chem.* **2013**, *37*, 2061-2065; (g) Ito, M.; Itazaki, M.; Nakazawa, H. *ChemCatChem* **2016**, *8*, 3323-3325; (h) Verma, V.; Koperniku, A.; Edwards, P. M.; Schafer, L. L. *Chem. Commun.* **2022**, *58*, 9174-9189; (i) Ganguli, K.; Mandal, A.; Sarkar, B.; Kundu, S. *Tetrahedron* **2020**, *76*, 131439.
6. (a) Corriu, R. J. P.; Moreau, J. J. E.; Pataud-Sat, M. *J. Organomet. Chem.* **1982**, *228*, 301-308; (b) Wei, Y.; Gao, J.; Jiang, L.; Huang, Z.; Bao, Q.; Yuan, Q.; Zhang, L.; Zhou, S.; Wang, S. *Organometallics* **2022**, *41*, 2985-2996.

-
7. (a) Panunzio, M.; Zarantonello, P. *Org. Process Res. Dev.* **1998**, *2*, 49-59; (b) Firsova, Y. N.; Lozinskaya, N. A.; Sosonyuk, S. E.; Proskurnina, M. V.; Zefirov, N. S. *Rev. J. Chem.* **2012**, *2*, 74-104.
8. Shimizu, K.; Minami, Y.; Goto, O.; Ikehira, H.; Hiyama, T. *Chem. Lett.* **2014**, *43*, 438-440.
9. Barluenga, J.; Aznar, F.; Valdés, C. *Angew. Chem. Int. Ed.* **2004**, *43*, 343-345.
10. (a) Chan, L.-H.; Roschow, E. G. *J. Organomet. Chem.* **1967**, *9*, 231-250; (b) Cainelli, G.; Giacomini, D.; Panunzio, M.; Martelli, G.; Spunta, G. *Tetrahedron Lett.* **1987**, *28*, 5369-5372; (c) Gentner, T. X.; Mulvey, R. E. *Angew. Chem. Int. Ed.* **2021**, *60*, 9247-9262; (d) Wang, Z.; Zheng, Z.; Xu, X.; Mao, J.; Walsh, P. J. *Nat. Commun.* **2018**, *9*, 3365; (e) Liu, G.; Walsh, P. J.; Mao, J. *Org. Lett.* **2019**, *21*, 8514-8518.
11. Andreoli, P.; Cainelli, G.; Contento, M.; Giacomini, D.; Martelli, G.; Panunzio, M. *Tetrahedron Lett.* **1986**, *27*, 1695-1698.
12. (a) Khalimon, A. Y.; Simionescu, R.; Kuzmina, L. G.; Howard, J. A. K.; Nikonov, G. I. *Angew. Chem. Int. Ed.* **2008**, *47*, 7701-7704; (b) Peterson, E.; Khalimon, A. Y.; Simionescu, R.; Kuzmina, L. G.; Howard, J. A. K.; Nikonov, G. I. *J. Am. Chem. Soc.* **2009**, *131*, 908-909; (c) Garduño, J. A.; Flores-Alamo, M.; García, J. J. *ChemCatChem* **2019**, *11*, 5330-5338.
13. Calas, R.; Frainnet, E.; Bazouin, A. *C.R. Acad. Sci.* **1961**, *252*, 420-422.
14. (a) Gutsulyak, D. V.; Nikonov, G. I. *Angew. Chem. Int. Ed.* **2010**, *49*, 7553-7556; (b) Shirobokov, O. G.; Kuzmina, L. G.; Nikonov, G. I. *J. Am. Chem. Soc.* **2011**, *133*, 6487-6489; (c) Khalimon, A. Y.; Shirobokov, O. G.; Peterson, E.; Simionescu, R.; Kuzmina, L. G.; Howard, J. A. K.; Nikonov, G. I. *Inorg. Chem.* **2012**, *51*, 4300-4313.
15. Wübbolt, S.; Oestreich, M. *Synlett* **2017**, *28*, 2411-2414.

-
16. Hamdaoui, M.; Desrousseaux, C.; Habbita, H.; Djukic, J.-P. *Organometallics* **2017**, *36*, 4864-4882.
17. Gandhamsetty, N.; Jeong, J.; Park, J.; Park, S.; Chang, S. *J. Org. Chem.* **2015**, *80*, 7281-7287.
18. Pérez, M.; Qu, Z.-W.; Caputo, C. B.; Podgorny, V.; Hounjet, L. J.; Hansen, A.; Dobrovetsky, R.; Grimme, S.; Stephan, D. W. *Chem. Eur. J.* **2015**, *21*, 6491-6500.
19. (a) Boone, C.; Korobkov, I.; Nikonov, G. I. *ACS Catal.* **2013**, *3*, 2336-2340; (b) Rit, A.; Zanardi, A.; Spaniol, T. P.; Maron, L.; Okuda, J. *Angew. Chem. Int. Ed.* **2014**, *53*, 13273-13277; (c) Wiegand, A.-K.; Rit, A.; Okuda, J. *Coord. Chem. Rev.* **2016**, *314*, 71-82.
20. Takaya, J.; Ogawa, K.; Nakaya, R.; Iwasawa, N. *ACS Catal.* **2020**, *10*, 12223-12228.
21. (a) Sahoo, R. K.; Mahato, M.; Jana, A.; Nembenna, S. *J. Org. Chem.* **2020**, *85*, 11200-11210; (b) Peddaraao, T.; Baishya, A.; Sarkar, N.; Acharya, R.; Nembenna, S. *Eur. J. Inorg. Chem.* **2021**, 2034-2046; (c) Sahoo, R. K.; Sarkar, N.; Nembenna, S. *Angew. Chem. Int. Ed.* **2021**, *60*, 11991-12000; (d) Sahoo, R. K.; Sarkar, N.; Nembenna, S. *Inorg. Chem.* **2023**, *62*, 304-317; (e) Sahoo, R. K.; Rajput, S.; Patro, A. G.; Nembenna, S. *Dalton Trans.* **2022**, *51*, 16009-16016; (f) Sahoo, R. K.; Patro, A. G.; Sarkar, N.; Nembenna, S. *Organometallics* **2023**, DOI: <https://doi.org/10.1021/acs.organomet.2c00610>.
22. Sahoo, R. K.; Patro, A. G.; Sarkar, N.; Nembenna, S. *ACS Omega* **2023**, *8*, 3452-3460.
23. (a) Owston, N. A.; Parker, A. J.; Williams, J. M. J. *Org. Lett.* **2007**, *9*, 73-75; (b) Ramón, R. S.; Bosson, J.; Díez-González, S.; Marion, N.; Nolan, S. P. *J. Org. Chem.* **2010**, *75*, 1197-1202; (c) González-Liste, P. J.; Cadierno, V.; García-Garrido, S. E. *ACS Sustainable Chem. Eng.* **2015**, *3*, 3004-3011; (d) Ahmed, S. M.; Hussain, F. H. S.; Quadrelli, P. *Monatsh. Chem.* **2020**, *151*, 1643-1658; (e) Wang, Q.; Gong, H.; Zhang, Y.; Peng, Y.; Chen, H.; Li, M.; Deng, H.; Hao, J.; Wan, W. *Org. Biomol. Chem.* **2021**, *19*, 7867-7874.
-

24. (a) Ito, M.; Itazaki, M.; Nakazawa, H. *Inorg. Chem.* **2017**, *56*, 13709-13714; (b) Itazaki, M.; Nakazawa, H. *Molecules* **2018**, *23*, 2769.
25. Kupfer, R.; Meier, S.; Wuerthwein, E. U. *Synthesis* **1984**, 688.
26. Georg, G. I.; Harriman, G. C. B.; Peterson, S. A. *J. Org. Chem.* **1995**, *60*, 7366.
27. Sheldrick, G. *Acta Crystallogr. C.* **2015**, *71*, 3-8.
28. Dolomanov, O. V.; Bourhis, L. J.; Gildea, R. J.; Howard, J. A. K.; Puschmann, H. *J. Appl. Crystallogr.* **2009**, *42*, 339-341.
29. (a) Sheldrick, G. M. *Acta Crystallogr., Sect. A: Found. Crystallogr.* **2008**, *64*, 112-122; (b) Sheldrick, G. M. *Acta Crystallogr., Sect. A: Found. Adv.* **2015**, *71*, 3-8.

NMR Spectra

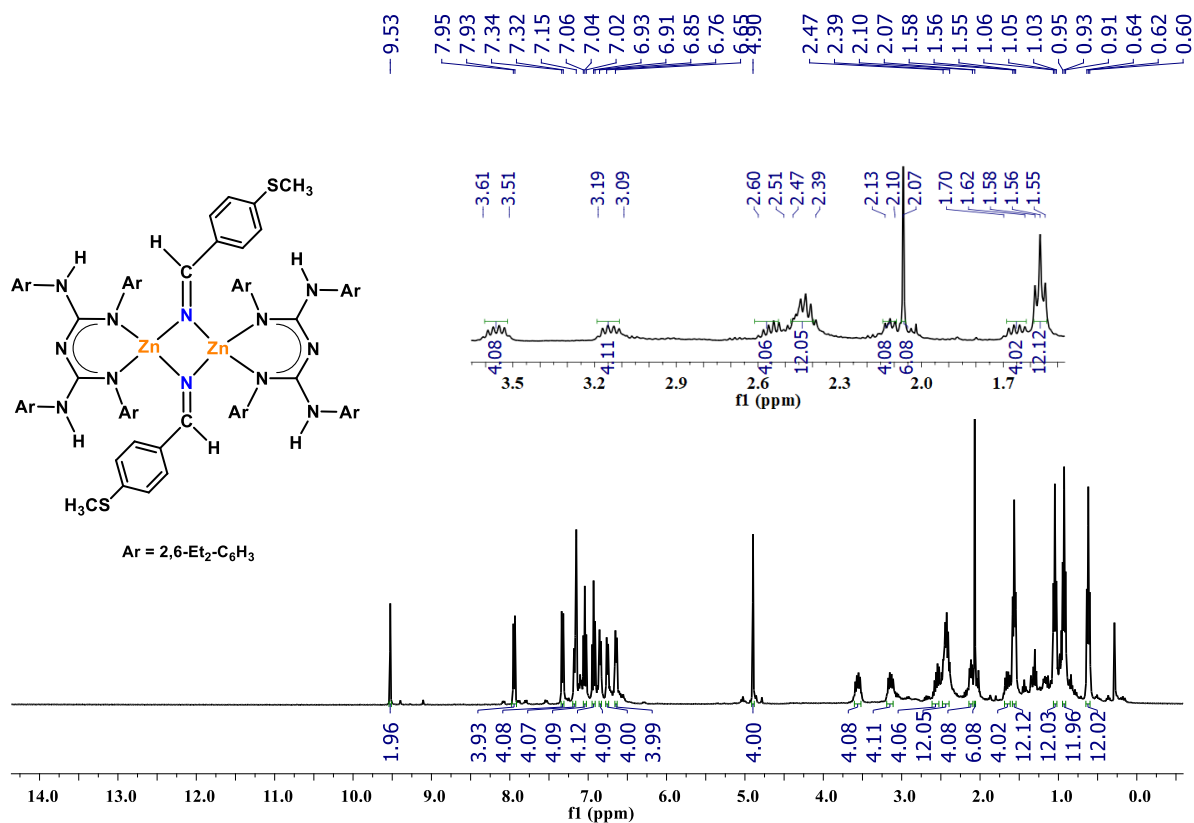


Figure 5.B.7. 1H NMR spectrum of $[L^1ZnNC(H)(4-SMeC_6H_4)]_2$ (**Zn-1'**) (400 MHz, C_6D_6).

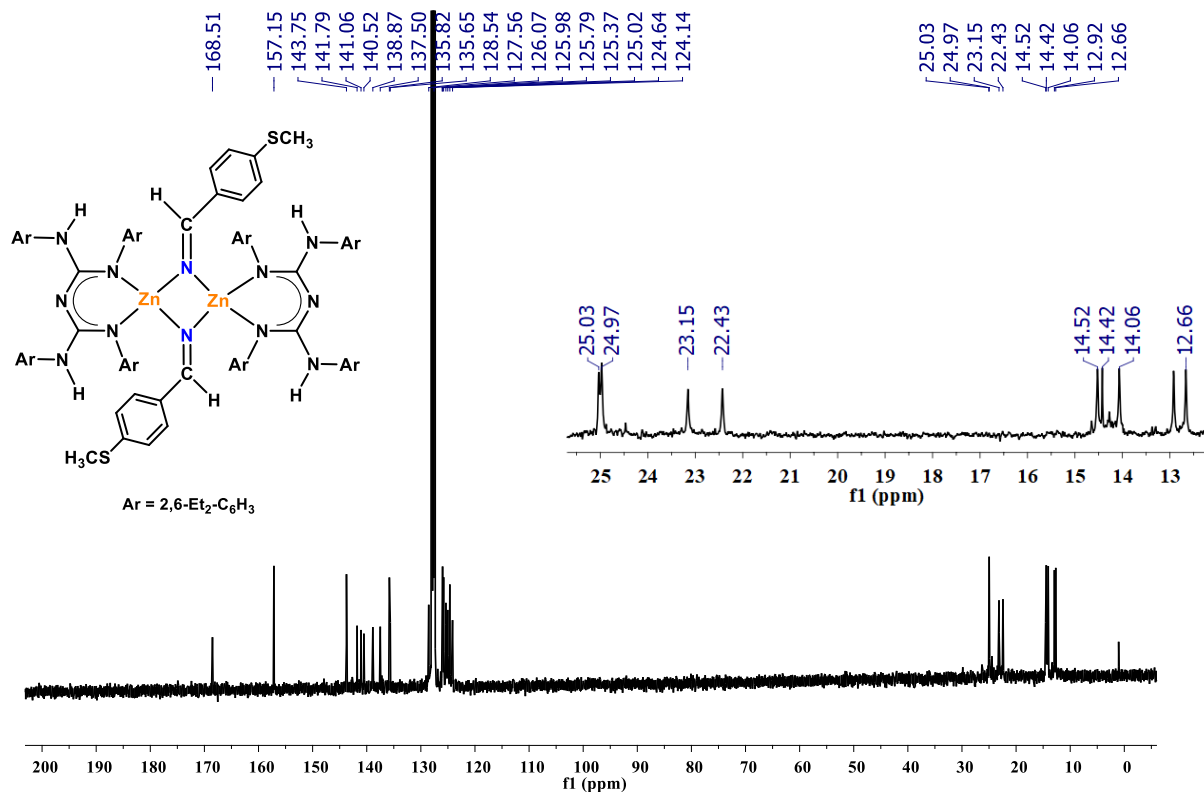


Figure 5.B.8. $^{13}C\{^1H\}$ NMR spectrum of $[L^1ZnNC(H)(4-SMeC_6H_4)]_2$ (Zn-1') (100 MHz, C₆D₆).

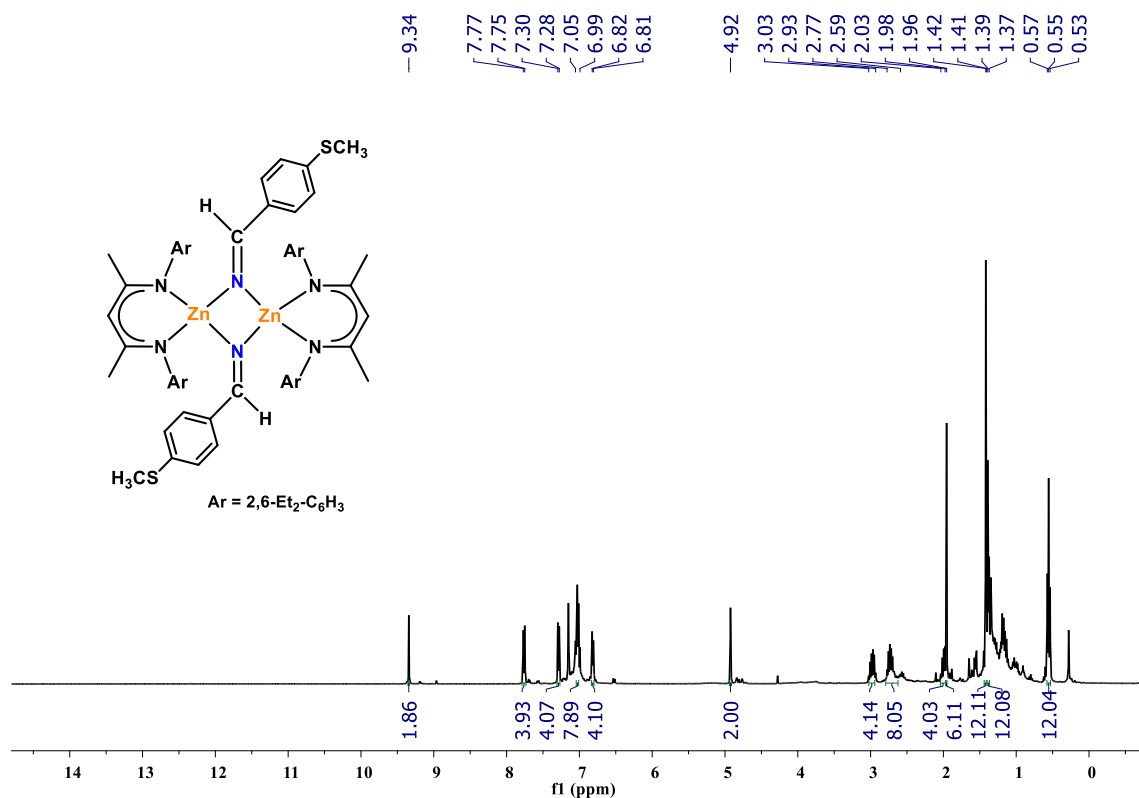


Figure 5.B.9. 1H NMR spectrum of $[L^2ZnNC(H)(4-SMeC_6H_4)]_2$ (Zn-2') (400 MHz, C₆D₆).

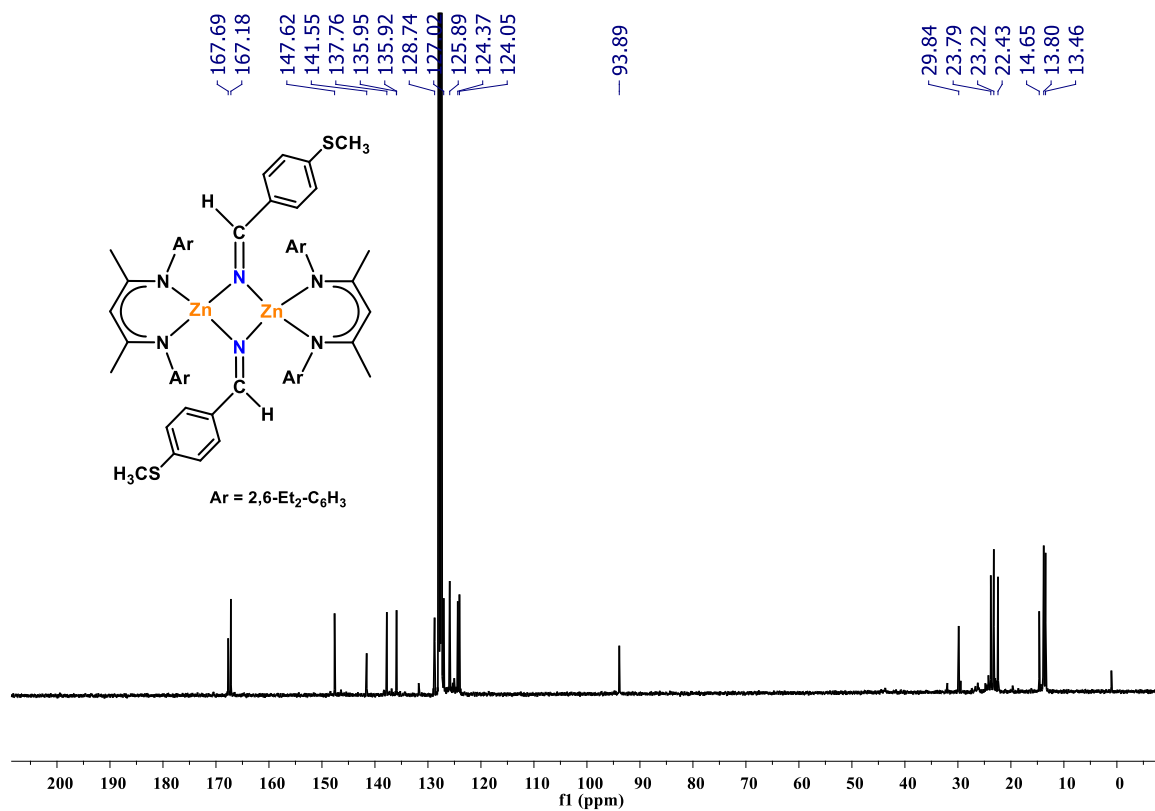


Figure 5.B.10. $^{13}\text{C}\{^1\text{H}\}$ NMR spectrum of $[\text{L}^2\text{ZnNC}(\text{H})(4\text{-SMeC}_6\text{H}_4)]_2$ (Zn-2') (100 MHz, C₆D₆).

Chapter 6

Intermediates, Isolation and Mechanistic Insights into Zinc Hydride Catalyzed 1, 2-Regioselective Hydrofunctionalization of N-Heteroarenes

Published:

Sahoo, R. K.; Sarkar, N.; Nembenna, S. *Inorg. Chem.* **2023**, 62, 304-317.

Abstract

The conjugated bis-guanidinate (CBG) supported zinc hydride, $[\{LZnH\}_2; L = \{(ArHN)(ArN)-C=N-C=(NAr)(NHA r)\}; Ar = 2,6-Et_2-C_6H_3\}$ (**I**) catalyzed highly demanding exclusive 1,2-regioselective hydroboration and hydrosilylation of N-heteroarenes is demonstrated with excellent yields. This protocol is compatible with many pyridines and N-heteroarene derivatives, including electron-donating and withdrawing substituents. The catalytic intermediates such as $[(LZnH) (4\text{-methyl pyridine})]$ **IIA**, $[(L'ZnH) (4\text{-methyl pyridine})]; L' = CH\{(CMe)(2,6-Et_2C_6H_3N)\}_2]$ **IIA'**, $LZn(1,2-DHiQ)(isoquinoline)$ **III**, $[L'Zn(1,2-DHiQ) (isoquinoline)]$ **III'** and $LZn(1,2-(3-MeDHQ))(3\text{-Methylquinoline})$ **V**, were isolated and thoroughly characterized by NMR, HRMS, and IR analyses. Further, X-ray single-crystal diffraction studies confirmed molecular structures of compounds **IIA'**, **III**, and **III'**. The NMR data proved that the intermediate **III** or **III'** reacts with HBpin gave a selected 1,2-addition hydroborated product. Stoichiometric experiments suggest that **V** and **III** independently react with silane, yielding selective 1,2-addition of mono- and bis-hydrosilylated products, respectively. Based on the isolation of intermediates and a series of stoichiometric experiments, plausible catalytic cycles are established. Furthermore, the intermolecular chemoselective hydroboration reaction over other reducible functionalities has been studied.

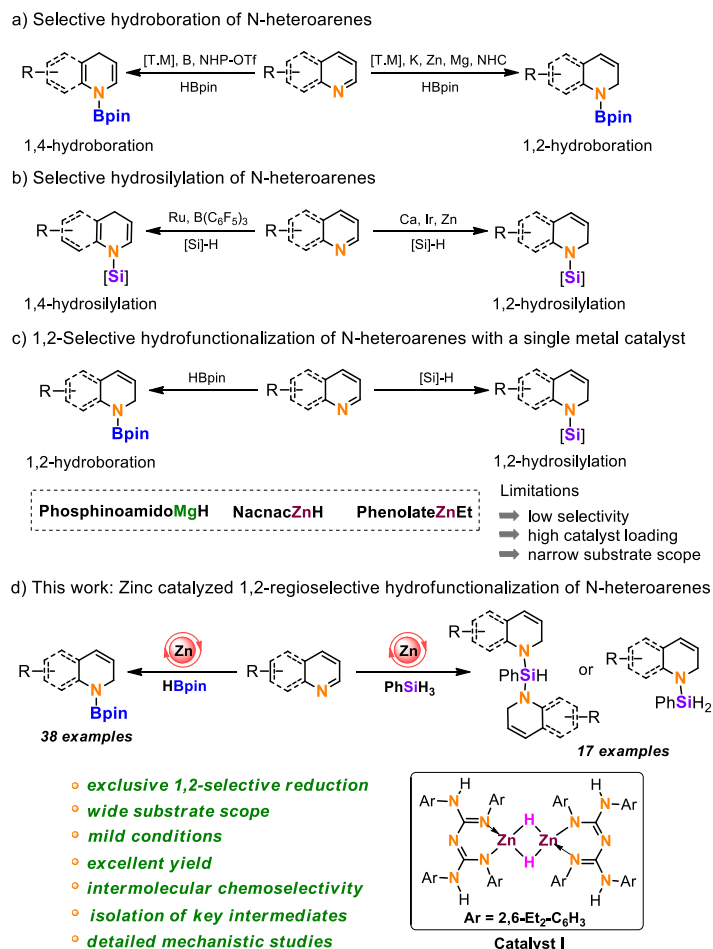
6.1. Introduction

A selective reduction of N-heteroarenes provides precious dihydropyridine (DHP) derivatives,¹ which play an essential role in organic chemistry (natural products), medicines, and biological transformations.² Due to their broad application, many synthetic routes have been developed to prepare selective dihydropyridines.^{1g, 3} Traditionally, stoichiometric metal reagents have been employed for the reduction of pyridines.⁴ Subsequently, metal-catalyzed hydrogenation reactions for selective reduction of N-heteroarenes were established.⁵ These methods often require harsh reaction conditions and lack selectivity.^{4, 5a-5e} Moreover, a large amount of waste is generated in the case of stoichiometric metal reagents.⁴ Thus, the hydrofunctionalization of pyridine with borane or silane as a mild reducing agent for dihydropyridine synthesis would be significant.^{2a, 6} In this context, in 2011, Hill and co-workers reported the β -diketiminato (Nacnac) magnesium alkyl catalyzed hydroboration of pyridine for the first time.⁷ Authors noticed the mixture of 1,2- and 1,4-DHP products.

Since then, metal-free catalysts such as N-heterocyclic phosphonium triflate (NHP-OTf)⁸ and organoboranes ($\text{Ar}^{\text{F}_2}\text{BMe}^9$ and $\text{NH}_4\text{BPh}_4^{10}$) have been used for the selective 1,4-hydroboration of N-heteroarenes with limited substrate scope. Reports on selective 1,4-hydroboration of N-heteroarenes using some transition metal and main group catalysts have been established.^{1c, 11} In 2020, Chang and co-workers reported N-heterocyclic carbene (NHC)-catalyzed selective 1,2-hydroboration of N-heteroarenes.¹² Similarly, regioselective 1,2-addition of B-H or Si-H to N-heteroarenes has been studied over the past years using main group¹³ and transition metal¹⁴ catalysts (Scheme 6.1, a).

In 1998, Harrod, Samuel, and co-workers reported the hydrosilylation of pyridines using a $[\text{Cp}_2\text{TiMe}_2]$ catalyst for the first time.¹⁵ Thereafter, Nikonov¹⁶ and Oestreich¹⁷ groups independently described various cationic ruthenium complexes as catalysts for the 1,4-regio

selective hydrosilylation of N-heteroarenes. As far as 1,2-selective hydrosilylation of N-heteroarenes is concerned, only a few reports are known, including transition and main group metal catalysts.¹⁸⁻²² The research groups of Chang,¹⁸ Gunanathan,¹⁹ Harder,²⁰ Nikonov,²¹ and Yao²² independently reported Ir, Ru, Ca, and Zn metal-catalyzed 1,2-selective hydrosilylation of N-heteroarenes, respectively (Scheme 6.1, b).



Scheme 6.1. Catalytic selective hydrofunctionalization of N-heteroarenes

1,2-dihydropyridines are the necessary starting materials for synthesizing nitrogen-containing natural products and bioactive compounds.^{1e, 23} 1,2-regioselective reactions are kinetically controlled, which typically depend on appropriate catalysts, and reagents.^{2a, 24} There have been only three reports on metal-catalyzed 1,2-selective hydroboration and hydrosilylation of N-

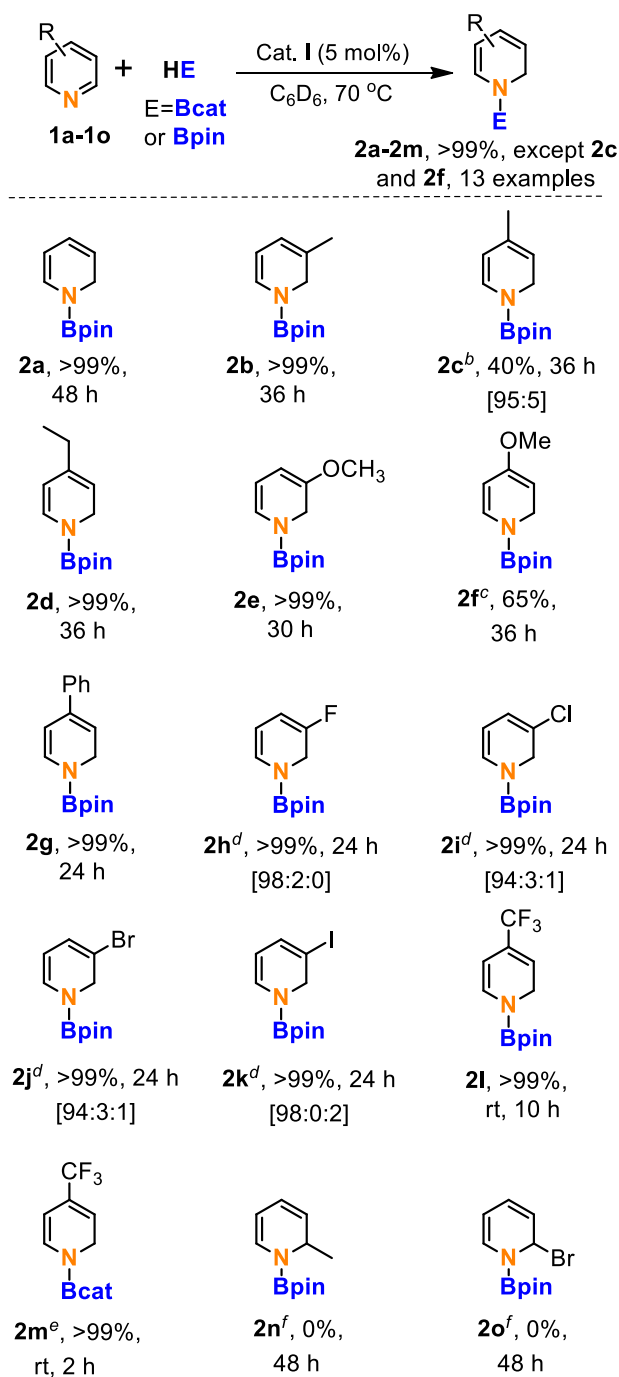
heteroarenes. Stasch and co-workers reported that Mg catalyzed the hydrofunctionalization of pyridines.²⁵ In 2017, the Nikonov group reported that Nacnac zinc hydride catalyzed selective hydrosilylation and hydroboration of N-heteroarenes.²¹ During the preparation of this manuscript, Yao and co-workers reported that Zn(II) catalyzed the hydrofunctionalization of N-heteroarenes (Scheme 6.1, c).²² The above reports suffer from narrow substrate scope, poor selectivity, and high catalyst loadings.^{21-22,25} Hence, using earth-abundant, cheaper, and bio-compatible catalysts under mild conditions for 1,2-regio- and chemoselective hydroboration and hydrosilylation of N-heteroarene reactions are highly desirable.

Herein, we report the zinc hydride catalyzed hydrofunctionalization of N-heteroarenes under mild conditions to yield the respective 1,2-addition products exclusively. A broad range of substrate scope is displayed along with the successful isolation and spectroscopic characterization of intermediates **IIA**, **IIA'**, **III**, **III'**, and **V**. The isolation of intermediates, stoichiometric experiments, and in situ studies support that zinc hydride (**I**) is responsible for 1,2-regioselective hydroboration and hydrosilylation of N-heteroarenes (Scheme 6.1, d). Moreover, the catalytic activity of the β -diketiminato (Nacnac) analogue, conjugated bis-guanidinate (CBG)²⁶ supported dimeric zinc hydride, [$\{LZnH\}_2$; $L = \{(ArHN)(ArN)-C=N-C=(NAr)(NHAr)$; $Ar = 2,6-Et_2-C_6H_3\}$] (**I**), is compared with ^{Diethyl}Nacnac zinc hydride, $\{L'ZnH\}_2$, ((Diethylnacnac (**L'**) = $CH\{(CMe)(2,6-Et_2C_6H_3N)\}_2$) (**I'**), to understand the role of spectator ligand. Compounds **I** and **I'** are efficient catalysts for the 1,2-regioselective hydrofunctionalization of N-heteroarenes. However, compound **I** shows slightly better activity than compound **I'**.

6.2. Results and Discussion

6.2.1. Hydroboration of Pyridines

Our group previously reported a β -diketiminate analogue, conjugated bis-guanidinate (CBG)²⁶ supported dimeric zinc hydride, $[\{LZnH\}_2]$ (**I**); $L = \{(ArHN)(ArN)-C=N-C=(NAr)(NHAr)\}$; $Ar = 2,6-Et_2-C_6H_3\}$, which is obtained by the reaction of $[LZnI]_2$ with $KNH(iPr)BH_3$ in toluene.



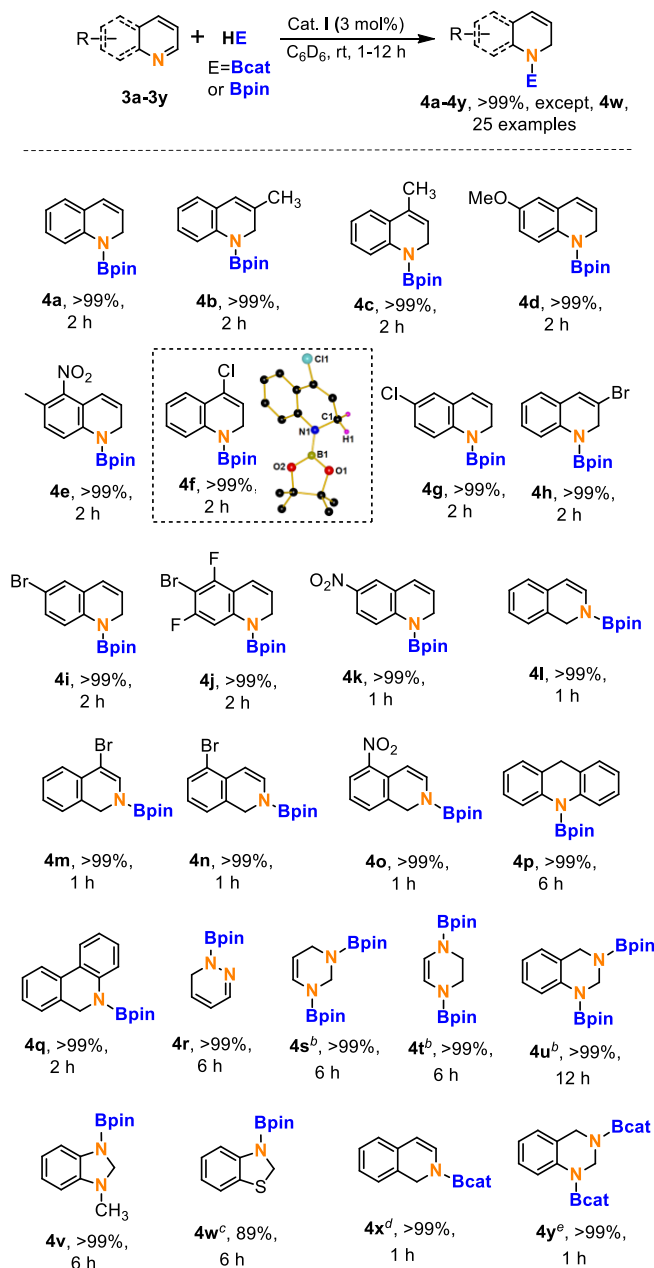
Scheme 6.2. 1, 2-Selective hydroboration of pyridines catalyzed by $[LZnH]_2$ complex (**I**)^a

^aReaction conditions: Pyridines (0.2 mmol, 1.0 equiv.), pinacolborane (0.24 mmol, 1.2 equiv.), catalyst **I** (5 mol%), at 70 °C under N₂. ^{b,c}For **2c** and **2f**, quantities without bracket are NMR yield determined by ¹H NMR spectroscopy using nitromethane as the internal standard. ^bFor **2c**, isomeric ratios are in bracket refer to the ratio of regioisomeric (4-substituted-1,2-pyridine (1,2) and 4-substituted-1,4-pyridine (1,4)). ^dFor **2h**, **2i**, **2j**, and **2k**, quantities without bracket are NMR yield. Isomeric ratios are in brackets refer to the ratio of regioisomeric (3-substituted-1,2-pyridine (1,2) and 3-substituted-1,4-pyridine (1,4) and 5-substituted-1,2-pyridine (1,6)). ^eFor **2m**, catecholborane (0.22 mmol, 1.1 equiv.) was used at room temperature for 2 h. ^fFor **2n** and **2o**, 1.2 equiv. of HBpin was used. The NMR yield was determined by ¹H NMR spectroscopy based on pyridine consumption, and identified the N(Bpin)CH₂ or N(Bcat)CH₂ peak confirmed the product.

We initially studied the reaction of pyridine (0.2 mmol) with pinacolborane (HBpin) (0.24 mmol) in the presence of 5 mol % catalyst **I**, which produced exclusively N-Bpin-1,2- dihydropyridine (**2a**) product after 48 h at 70 °C. In addition, we also reported that zinc hydride catalyzed selective hydroboration of isocyanates²⁷ and hydrofunctionalization of ketones.²⁸ Herein, we report compound **I** catalyzed hydroboration and hydrosilylation of N-heteroarenes. In the absence of catalyst **I**, pyridine did not react with HBpin at 70 °C for 24 h. We observed the donor-acceptor adduct, pyridine·HBpin. Thus, zinc hydride is essential for this transformation.^{6b} A broad range of pyridines, including electron-donating (**1b-1g**) and withdrawing groups (**1h-1l**), were transformed into selective 1,2-hydroborated products (**2b-2l**) with high conversions. We observed that pyridine-bearing meta-substituted electron-withdrawing groups such as 3-fluoropyridine (**1h**), 3-chloropyridine (**1i**), 3-bromopyridine (**1j**), and 3-iodopyridine (**1k**) gave quantitative conversions with shorter reaction timings in comparison to the electron-donating groups **1b-1f**. Similarly, pyridine with a para-substituted electron-withdrawing group, i.e., 4-trifluoromethylpyridine (**1l**), was quantitatively converted into **2l** at room temperature with a shorter reaction time than electron-donating groups **1b-1g**. Nevertheless, for the substrates, 4-methylpyridine (**1c**) and 4-methoxypyridine (**1f**) gave moderate conversion (40 and 65%) of 1,2 reduced products (**2c** and **2f**). The ortho-substituted pyridines, 2-methylpyridine (**1n**) and 2-bromopyridine (**1o**), both failed

to produce 1,2 or 1,4, or 1,6-hydroborated products (no dearomatization). Moreover, a reaction between 4-trifluoromethylpyridine and catecholborane (HBcat) with a 5 mol% catalyst **I** provided the quantitative conversion to the 1,2- selective hydroboration product (**2m**) at room temperature (Scheme 6.2).

6.2.2. Hydroboration of N-Heteroarenes



Scheme 6.3. 1, 2-Selective hydroboration of N-heteroarenes catalyzed by $[LZnH]_2$ complex(**I**)^a

^aReaction conditions: N-heteroarenes (0.2 mmol, 1.0 equiv.), pinacolborane (0.23 mmol, 1.15 equiv.), catalyst **I** (3 mol%), at rt under N₂. ^bFor **4s**, **4t** and **4u** pinacolborane (0.44 mmol, 2.2 equiv) was used. ^cFor **4w**, NMR yield was determined by ¹H NMR spectroscopy using nitromethane as the internal standard. ^dFor **4x**, catecholborane (0.22 mmol, 1.1 equiv) was used. ^eFor **4y**, catecholborane (0.44 mmol, 2.2 equiv.) was used. The NMR yield was determined by ¹H NMR spectroscopy based on N-heteroarenes consumption and identified the N(Bpin)CH₂ or N(Bcat)CH₂ peak confirmed the product.

Moreover, the zinc hydride compound shows excellent activity for the hydroboration of the N-heteroarenes. A wide array of N-heteroarenes are investigated, including quinolines, isoquinoline, acridine, phenanthridine, pyridazine, pyrimidine, pyrazine, imidazole, and thiazole derivatives. The quinoline (**3a**), including electron-donating (**3b-3d**), withdrawing groups (**3f-3k**), and containing both electron-donating as well as withdrawing groups, i.e., **3e**, were quantitatively transformed to corresponding 1,2-dihydroquinoline products (**4a-4k**).

Isoquinoline and its derivatives were fully converted into corresponding 1,2-dihydro isoquinoline derivative products (**4l-4o**) in a shorter reaction time of 1h. In contrast, acridine (**3p**) gave a 1,4-regioselective product **4p** as blocking of ortho position. Phenanthridine and pyridazine were also fully converted into 1,2-selective hydroborated products (**4q-4r**). Heterocycles such as pyrimidine, pyrazine, and quinazoline react with two equivalents of HBpin, providing the double hydroborated products **4s**, **4t**, and **4u** with high yields. N-methyl benzimidazole and 1,3-benzothiazole react with 1.0 equivalent of HBpin to give related products (**4v-4w**) with quantitative conversions (Scheme 6.3).

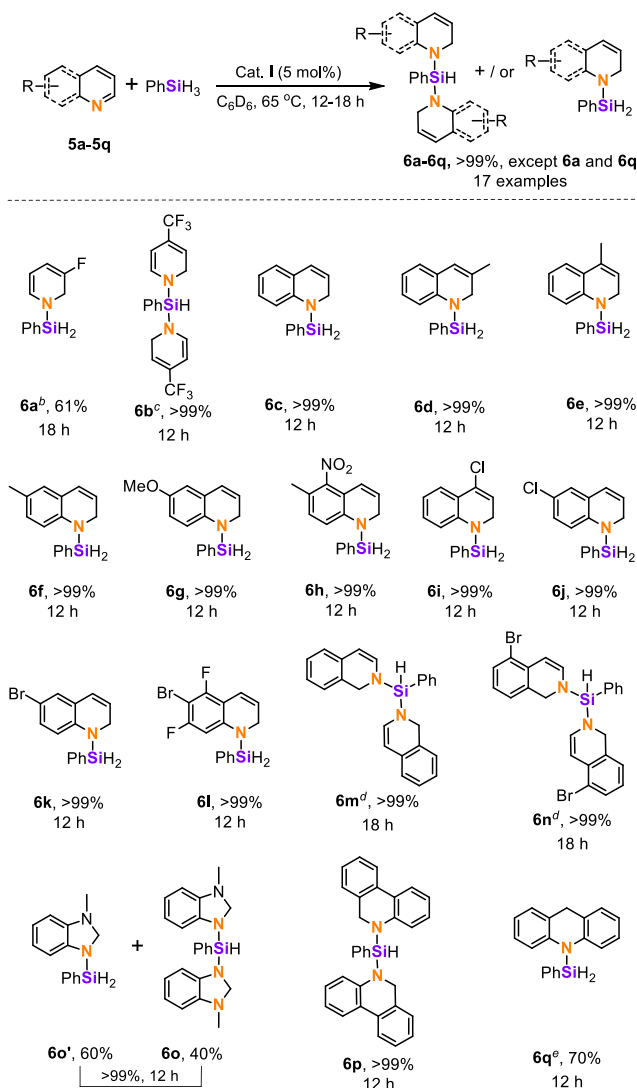
Further, we studied the hydroboration reaction, i.e., HBcat with isoquinoline or quinazoline substrate. The reaction of isoquinoline or quinazoline and HBcat with 3 mol% catalyst **I** provided quantitative conversion to the 1,2- selective hydroboration product (**4x** or **4y**) after 1 h at room temperature. The N-heteroarene derivatives are easily dearomatized compared to pyridines because (i) the resonance stabilization of pyridine core in N-heteroarenes is lower than that of

pyridine, thus probably requiring mild reaction conditions in the case of N-heteroarenes reduction.

(ii) Unlike in N-heteroarenes, more reaction paths lead to poor chemo- and/or regioselectivity in the pyridines; and iii) coordination of pyridine to metal catalyst may lead to catalyst deactivation than N-heteroarenes; because pyridines are more basic than N-heteroarenes.^{13a}

6.2.3. Hydrosilylation of N-Heteroarenes

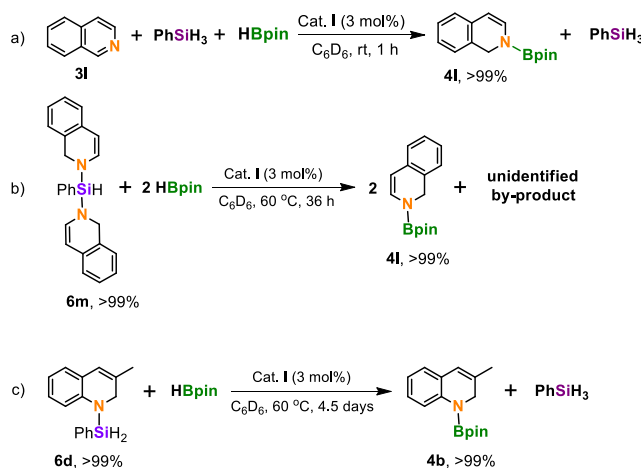
The zinc hydride complex's good catalytic performance in catalyzing the 1,2-regioselective hydroboration of N-heteroarenes encouraged us to explore the more challenging hydrosilylation reaction.



Scheme 6.4. 1, 2-Selective hydrosilylation of N-heteroarenes catalyzed by $[\text{LZnH}]_2$ complex (**I**)^a

^aReaction conditions: N-heteroarenes (0.2 mmol, 1.0 equiv.), phenylsilane (0.11 mmol, 0.55 equiv. or 0.22 mmol, 1.1 equiv.), catalyst **I** (5 mol%), 12–18 h at 65 °C under N₂. The NMR yield was determined by ¹H NMR spectroscopy based on pyridine or N-heteroarenes consumption and identified the N(SiHPh)(CH₂)₂ and N(SiH₂Ph)CH₂ peaks confirmed the product. ^bFor **6a**, heated at 70 °C for 18 h, NMR yield was determined by ¹H NMR spectroscopy using mesitylene as the internal standard. ^cFor **6b** heated at 70 °C for 12 h. ^dFor **6m**, and **6n**, heated at 65 °C for 18 h. ^eFor **6q**, NMR yield was determined by ¹H NMR spectroscopy using mesitylene as the internal standard.

The pyridine derivatives, i.e., 3-fluoropyridine (**5a**) and 4-(trifluoromethyl)pyridine (**5b**), are challenging substrates (due to more aromatically stabilized single-ring molecules) for the hydrosilylation reaction. They gave rewarding results under 5 mol% catalyst loading at 70 °C for 18 h and 12 h, respectively. However, substrate **5a** produces a mono-hydrosilylated product with a 61% yield, while substrate **5b** produces a bis-hydrosilylated product with a quantitative yield. A number of various quinoline derivatives from electron-donating (**5c–5g**), electron-withdrawing (**5i–5l**), and containing both electron-donating and withdrawing groups (**5h**) was reduced by phenylsilane to give mono(hydroquinoline) derivatives (**6c–6l**) with excellent yields.



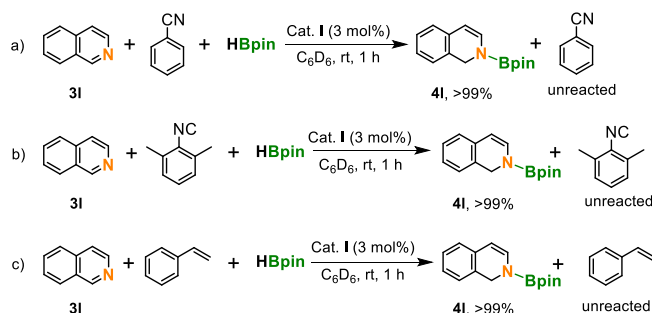
Scheme 6.5. Competitive and exchange reaction between phenylsilane and pinacolborane with N-heteroarenes.

The isoquinoline derivatives (**5m–5n**) and other fused N-heteroarene, i.e., (**5p**), also reacted straightforwardly to produce bis(hydroisoquinoline) derivatives (**6m**, **6n**, and **6p**). However, an

imidazole derivative, i.e., **5o**, reacted with phenylsilane to form a mixture of mono(hydroquinoline) (**6o'**) and bis(hydroquinoline) (**6o**) derivatives with 60% and 40% conversions, respectively. In contrast, substrate **5q** reacted with phenylsilane and afforded 1,4 addition product **6q** with a 70% conversion (Scheme 6.4).

The Yao group reported that N-heteroarenes, upon reaction with phenylsilane, formed exclusive bis-hydrosilylated products in the presence of a 10 mol % catalyst (phenolate ZnEt) at 30 °C for 24 h. However, in the current work, we discovered that quinoline reacted with 1 equiv. of phenylsilane to afford a mono-hydrosilylated product in the presence of a 5 mol% catalyst **I** at 65 °C for 12 h, whereas isoquinoline reacted with 0.5 equiv. of phenylsilane to produce a bis-hydrosilylated product in the presence of a 5 mol% catalyst **I** at 65 °C over 12-18 h. Thus, the formation of mono- and bis-hydrosilylation products depends upon the choice of catalyst, the nature of the substrate, the stoichiometric amount of phenylsilane, and reaction conditions (time, temperature) (*vide infra*).

Next, a one-pot reaction of equimolar quantities of isoquinoline, HBpin, and phenylsilane with catalyst **I** (3 mol %) in C₆D₆ at room temperature for 1 h, was performed. We noticed the formation of hydroborated product **4l** in a quantitative yield (Scheme 6.5, a). When pinacolborane (HBpin) was added to a solution of compound **6m**, resulting in compound **4l** and an unidentified by-product via boryl-silyl exchange reaction (Scheme 6.5, b). Similarly, HBpin addition to a solution of N-silyl-dihydro (3-methylquinoline) (**6d**) yielded the N-boryl-dihydro (3-methylquinoline) (**4b**) and elimination of phenylsilane (Scheme 6.5, c). As shown in Scheme 6.5, competitive and exchange experiments show that Si-N bond formation is reversible, and scrambling occurs when borane is present.



Scheme 6.6. Intermolecular chemoselective reactions.

Further, it has been demonstrated that zinc hydride-catalyzed intermolecular chemoselective reduction of isoquinoline versus other reducible functionalities such as nitrile, isocyanide, and styrene. The reaction of equimolar amounts of isoquinoline, benzonitrile, and HBpin with catalyst **I** (3 mol%) in C_6D_6 at rt for 1 h yielded the quantitative formation of product **4I** in preference to the benzonitrile (Scheme 6.6, a). Likewise, under the same reaction conditions, isoquinoline gave the hydroborated product **4I** over 6-dimethyl phenyl isocyanide (Scheme 6.6, b). Similarly, isoquinoline, styrene, and HBpin were mixed with catalyst **I**, which produced a quantitative conversion of **4I**, in which styrene is unaltered (Scheme 6.6, c). It is important to note that isoquinoline was reduced exclusively in preference to other functionalities.

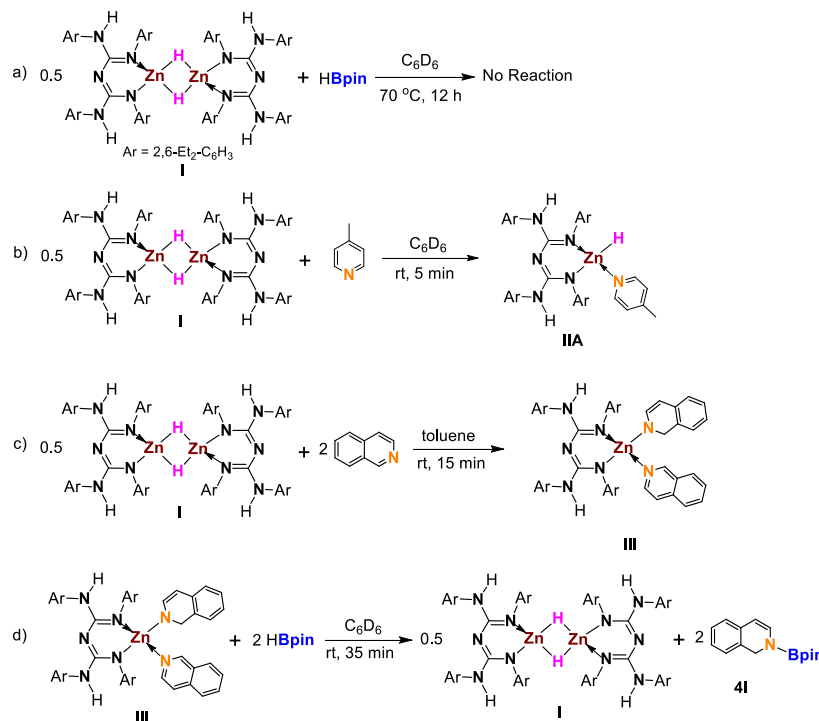
Finally, we compared the catalytic efficiency of CBG-supported zinc hydride complex (**I**) with $DiethylNacnacZnH\{L'ZnH\}_2$, ((Diethylnacnac (L') = $CH\{(CMe)(2,6-Et_2C_6H_3N)\}_2$) (**I'**), Nikonov's and Yao's zinc-based catalysts for the hydroboration and hydrosilylation of N-heteroarenes. The catalytic 1,2-regioselective hydroboration of isoquinoline and pyrimidine substrates was carried out under mild conditions to produce high TON, 16.7, and TOF, $2.8-16.7\ h^{-1}$ compared to $[L'ZnH]_2$ (TON, 14.7-15 and TOF, $2.4-15\ h^{-1}$), **A** (TON, 14.6 and TOF, $2.7\ h^{-1}$) and **B** catalysts (TON, 9.7-10 and TOF, $0.8-6.5\ h^{-1}$).²¹⁻²²

For the hydrosilylation of 4-(trifluoromethyl)pyridine (**5b**), $Diethyl$ CBG zinc hydride (**I**) displayed a TON 10 and TOF $0.8\ h^{-1}$ relative to $DiethylNacnac$ zinc hydride (**I'**) (TON 8.4 and TOF $0.7\ h^{-1}$).

From the optimization table, it appears that the catalytic performance of compound **I** (TON, 10 and TOF, 0.8 h⁻¹) is slightly better than the [L'ZnH]₂, (TON, 9 and TOF, 0.7 h⁻¹) and Yao's zinc catalyst (TON, 7.6 and TOF, 0.3 h⁻¹) for the 1,2-selective hydrosilylation of quinoline (**5c**).²²

6.2.4. Stoichiometric Experiments for 1,2-Regioselective Hydroboration

Stoichiometric experiments are conducted to understand the zinc-catalyzed hydroboration of N-heteroarenes to selective 1,2-hydroborated products. Initially, the 1:2 stoichiometric reaction of catalyst **I** and HBpin in C₆D₆ at 70 °C for 12 h was carried out; we observed that both catalyst **I** and HBpin were intact (no reaction) (Scheme 6.7, a). This ruled out any hidden catalysis involved in the hydroboration reaction.²⁹



Scheme 6.7. Stoichiometric experiments for hydroboration of N-heteroarenes.

The reaction between 0.5 equiv. of [LZnH]₂ (**I**) or [L'ZnH]₂ (**I'**) and 4-methyl pyridine yielded the Lewis acid-base adduct monomeric zinc hydride complex [(LZnH) (4-methyl pyridine)] (**IIa**) or [(L'ZnH) (4-methyl pyridine)] (**IIa'**). Both compounds **IIa** and **IIa'** were characterized by multinuclear (¹H and ¹³C) magnetic resonance spectroscopy and HRMS. Furthermore, the

molecular structure of **IIA'** was confirmed by X-ray single crystal structural analysis (for more details, see Figure 6.1). The ^1H NMR spectra of complexes **IIA** and **IIA'** reveal that the pyridine resonances are shifted downfield in comparison to the free base, indicating a decrease in the overall electron density of pyridine associated with coordination to the zinc center. More interestingly, the Zn-H resonances of compounds **IIA** (4.46 ppm) and **IIA'** (4.37 ppm) appear slightly upfield compared to their dimeric zinc hydrides (compound **I**, i.e., $[\text{LZnH}]_2$ at 4.52 ppm, and compound **I'**, i.e., $[\text{L}'\text{ZnH}]_2$ at 4.41 ppm), which indicate that the compounds **IIA** and **IIA'** are monomeric (Scheme 6.7, b).

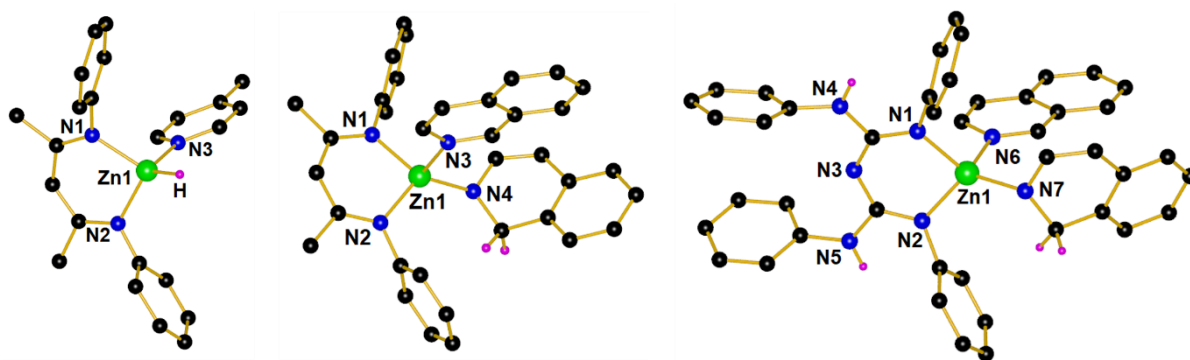


Figure 6.1. Molecular structures of compounds **IIA'** (left), **III'** (middle), and **III** (right). The thermal ellipsoids are shown at 50% probability, and all the hydrogen atoms (except for H from structure **IIA'** and H(48a), and H(48b) from structure **III'** and H(4), H(5), H(7a), and H(7b)) from structure **III**) and ethyl groups are omitted for clarity. Selected bond lengths (Å) and angles (deg), For **IIA'** (left): Zn1–N1 2.0095(15), Zn1–N2 2.0119(15), Zn1–N3 2.1313(16), N1–Zn1–N2 94.54(6), N3–Zn1–N2 100.11(6), N3–Zn1–N1 101.33(6). For **III'** (middle): Zn1–N1 1.968(2), Zn1–N2 1.977(2), Zn1–N3 2.122(2), Zn1–N4 1.946(2), N1–Zn1–N2 98.05(9), N3–Zn1–N4 100.98(9), N3–Zn1–N2 104.19(8), N3–Zn1–N1 103.73(9), N1–Zn1–N4 124.91(9), N2–Zn1–N4 122.19(9). For **III** (right): Zn1–N1 1.9570(18), Zn1–N2 1.9610(18), Zn1–N6 2.1178(19), Zn1–N7 1.981(2), N1–Zn1–N2 94.11(8), N6–Zn1–N7 104.49(8), N6–Zn1–N2 105.69(7), N6–Zn1–N1 103.87(7), N1–Zn1–N7 124.27(8), N2–Zn1–N7 122.17(8).

Next, a reaction of 0.5 equiv. of catalyst **I** with 2.0 equiv. of isoquinoline was performed in toluene; the reaction mixture changed its color from yellow to dark red, resulting in the immediate formation of $[\text{LZn}(1,2\text{-DHiQ})(\text{isoquinoline})]$ (1,2-DHiQ = 1,2-dihydro isoquinoline) **III**, as

displayed in Scheme 6.7, c. In this case, the zinc hydride is shifted deliberately to the 2-position of the isoquinoline, i.e., hydrozincation. Compound **III** was confirmed by NMR, mass spectrometry, and X-ray studies. The ^1H NMR spectrum shows a resonance at 4.08 ppm corresponding to ZnNCH_2 moiety. The $^{13}\text{C}\{^1\text{H}\}$ NMR spectrum exhibits a signal at 53.3 ppm, which refers to the ZnNCH_2 moiety. Moreover, a complete disappearance of the Zn-H peak at 4.52 ppm was noticed. In a similar way, the reaction between 0.5 equiv. of $\{\text{L}'\text{ZnH}\}_2$ (**I'**) and 2.0 equiv. of isoquinoline produced $^{\text{Diethyl}}\text{Nacnac}$ zinc amide complex $[\text{L}'\text{Zn}(1,2\text{-DHQ})(\text{isoquinoline})]$ (**III'**).

The suitable single crystals for X-ray diffraction of compounds **III** and **III'** were obtained from benzene solution at rt as pale orange blocks after 2 days. To our knowledge, compound **III** is the first example of a structurally characterized CBG zinc amide complex. The zinc amide intermediates **III** and **III'** crystallize with the monoclinic system's $P21/c$ and $P21/n$ space groups, respectively. The molecular structures of complexes **III** and **III'** are provided in Figure 6.1.

The zinc atoms in compounds **III** and **III'** adopt distorted-tetrahedral geometries with four coordination sites. The two N atoms coordinate the zinc atom in N, N'-chelating fashion from CBG or Nacnac ligand and other sites occupied by N-atoms from non-dearomatized and dearomatized isoquinolines. The zinc-amido bond distance of compound **III** (Zn1-N7 1.981 (2) Å) is significantly longer than compound **III'** (Zn1-N4 1.946 (2) Å) and $^{\text{Xyl}}\text{NacnacZn}(1,2\text{-DHQ})(\text{quinoline})$ ($\{\text{XylNacnac} = \text{CH}\{(\text{CMe})(2,6\text{-Et}_2\text{C}_6\text{H}_3\text{N})\}_2$ and $(1,2\text{-DHQ} = 1,2\text{-dihydroquinoline})\}$ (Zn-N3 1.949 (2) Å). Further, the N6-Zn1-N7 (104.49 (8°)) bond angle of compound **III** is wider compared to compound **III'** (N3-Zn1-N4 (100.98 (9°))) and $^{\text{Xyl}}\text{NacnacZn}(1,2\text{-DHQ})(\text{quinoline})$ (N3-Zn-N4 (100.61 (8°))). However, the bite angle of compound **III** N1-Zn1-N2 is 94.11 (8°), which is acute compared to the bond angle of compound

III' (N1-Zn1-N2 (98.05 (9)^o)) and ^{Xyl}NacnacZn(1,2-DHQ)(quinoline) (N1-Zn-N2 96.30 (8)^o).²¹

We presume that the changes in structural parameters of intermediate **III** vs. **III'** and ^{Xyl}NacnacZn(1,2-DHQ)(quinoline), the catalyst **I** exhibits slightly better catalytic activity and selectivity than ^{Diethyl}Nacnac and ^{Xyl}Nacnac zinc hydrides (*vide supra*).

Next, a 1:2 stoichiometric ratio of compound **III** and HBpin was carried out in a J. Young valve NMR tube at rt for 35 min. We noticed the color change from dark red to the colorless solution; as a result, the formation of hydroborated product (**4I**) and the zinc hydride complex **I** was observed (Scheme 6.7, d). Likewise, compound **III'** reaction with HBpin in C₆D₆ at room temperature yielded the quantitative amount of hydroborated product (**4I**) and the NacnacZnH complex **I'**.

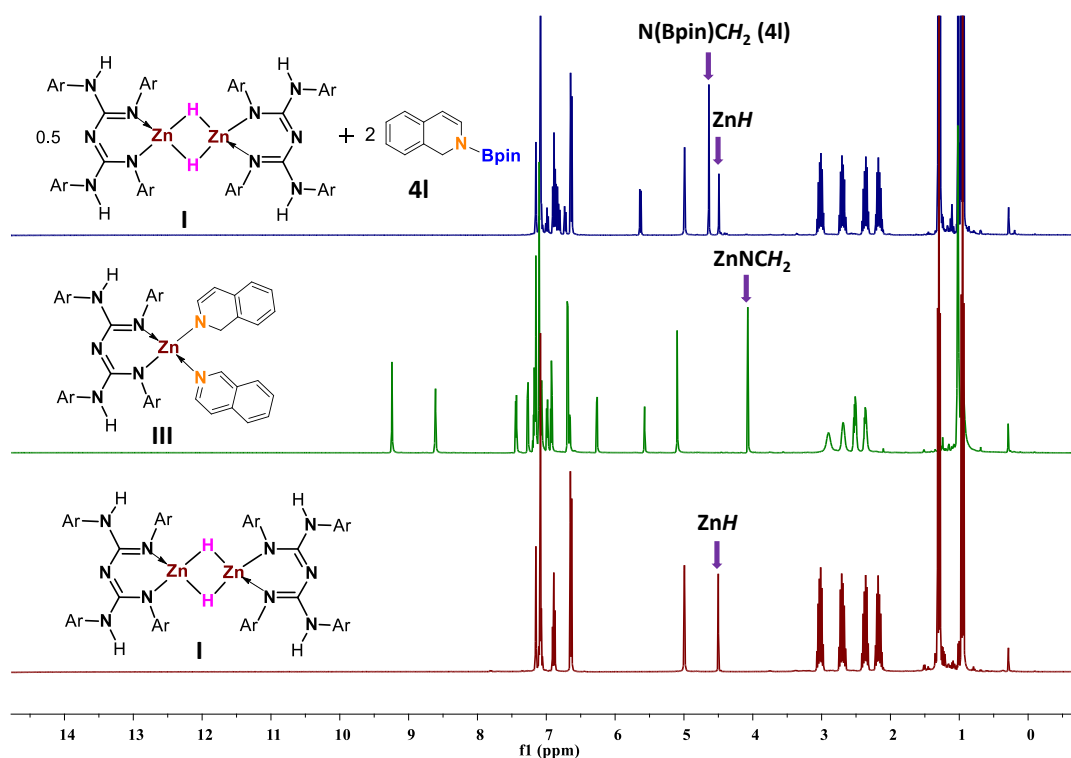


Figure 6.2. Annotated ¹H NMR (400 MHz) stack plot of the stoichiometric hydroboration of isoquinoline with **I** in C₆D₆. Stacked spectra from bottom to top: LZnH (**I**); LZn(1,2-DHiQ)(isoquinoline) (**III**); **I** + **4I** (compounds were obtained by the addition of 2 equiv. of HBpin to compound **III** at room temperature after 35 min).

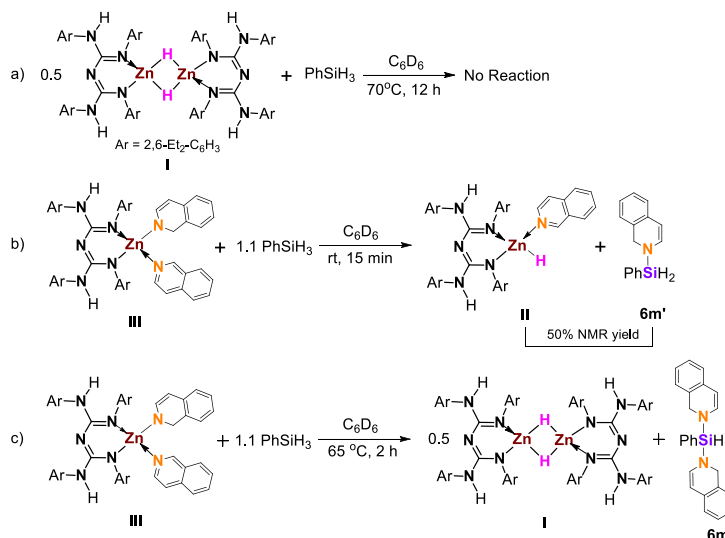
The ^1H NMR spectra indicate that the downfield shift of the methylene proton from 4.08 (ZnNCH₂ moiety of compound **III**) to 4.65 ppm ((N(Bpin)CH₂) of compound **4I**), as shown in Figure 6.2 (top spectrum). ^1H NMR data of stoichiometric experiments provided evidence for the complete catalytic cycle (*vide infra*) of hydroboration of N-heteroarenes are annotated in Figure 6.2. In addition, we performed in situ studies to support the above stoichiometric experiments. Compound **III** was reacted with 2 equiv. HBpin and ^1H NMR spectra recorded from time to time. It provides the hydroborated product (**4I**) and the complex **I**.

6.2.5. Stoichiometric Experiments for Bis-Hydrosilylation

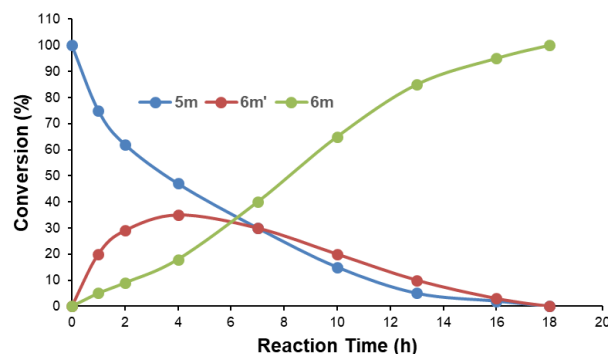
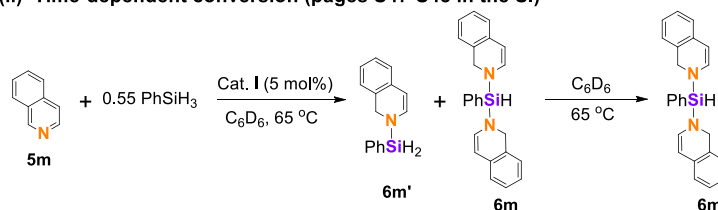
The metal-catalyzed hydrosilylation of N-heteroarene with phenylsilane gave the mono- and bis-1,2-hydrosilylation derivatives. Unfortunately, none of the previous reports¹⁹⁻²² revealed the mechanism for the formation of bis-1,2-hydrosilylation derivatives.

Thus, we were interested in investigating the mechanism for the formation of mono- and bis-1,2-hydrosilylation products. When 0.5 equiv. of catalyst **I** reacted with phenylsilane at 70 °C for 12 h; we observed that both compound **I** and phenylsilane were intact (no reaction) (Scheme 6.8 (i), a). Compound **III** is a common intermediate in hydroboration and hydrosilylation reactions (*vide supra*). Next, intermediate **III** is treated with 1 equiv. of phenylsilane at rt after 15 min. afforded the mono-hydrosilylated product (**6m'**) and intermediate **II** with a 50% conversion observed by multinuclear magnetic resonance spectroscopy (Scheme 6.8 (i), b). The ^1H NMR spectrum indicates the production of compound **6m'** by the appearance of two new peaks, i.e., N(SiH₂Ph)CH₂ at 4.93 and (SiH₂Ph)CH₂ at 4.18 ppm. Similarly, $^{29}\text{Si}\{^1\text{H}\}$ NMR revealed the formation of a **6m'** product by the appearance of a new peak at -21.6 ppm. More interestingly, Zn-*H* of compound **II** appears at 4.47 ppm, slightly upfield compared to compound **I**, i.e., [LZnH]₂ at 4.52 ppm (See, Figure 6.3 and Figure S26).

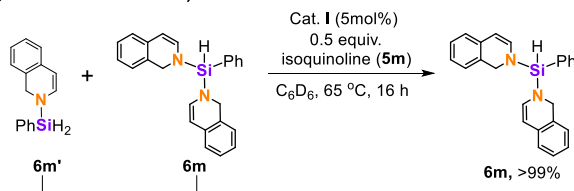
(i) Stoichiometric Experiments



(ii) Time-dependent conversion (pages S47-S48 in the SI)



(iii) Hydrosilylation of isoquinoline (5m) by using 6m' as a silane reagent (pages S49-S50 in the SI)

**Scheme 6.8.** Mechanistic studies for bis-hydrosilylation of N-heteroarenes.

When the same reaction mixture is heated at 65 °C for 2 h, the yellow color changes to a colorless solution. The ^1H NMR spectrum of product **6m** shows the signature methylene peak

(N(SiHPh)CH₂) at 4.23 ppm. This signal appeared in the downfield region compared to the compound **6m'** (N(SiH₂Ph)CH₂, 4.18 ppm) and intermediate **III** (Zn-NCH₂, 4.08 ppm) (Figure 6.3), which confirms the formation of bis-hydrosilylated product **6m** as shown in Scheme 6.8 (i), c.

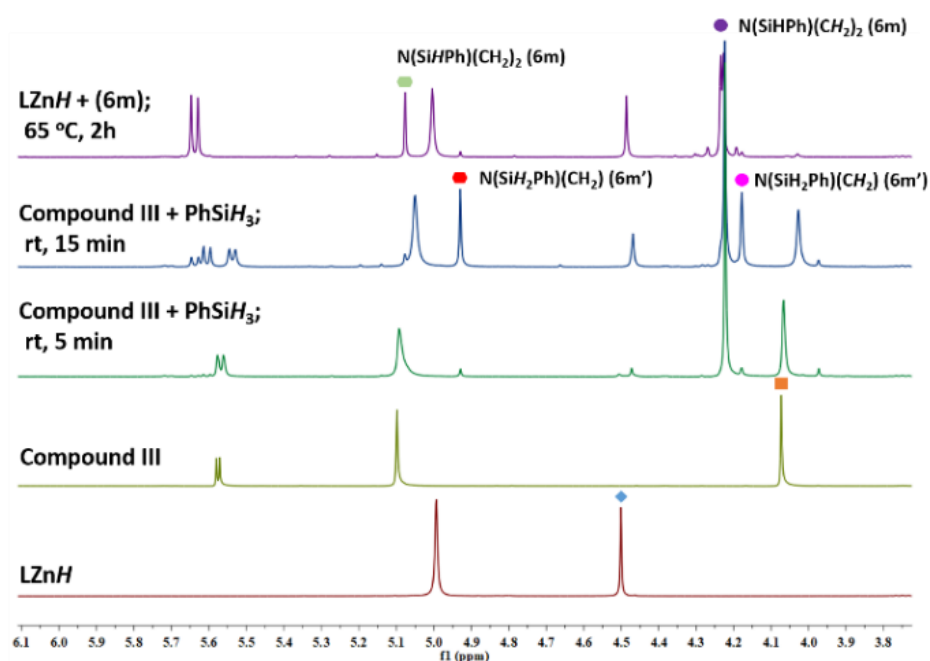


Figure 6.3. Annotated ¹H NMR (400 MHz) stack plot of the stoichiometric hydrosilylation of isoquinoline with catalyst **I** in C₆D₆. Stacked spectra from bottom to top: LZnH (**I**); LZn(1,2-DHiQ)(isoquinoline) (**III**); The addition of 1 equiv. of phenylsilane to compound **III** at room temperature after 5 min; The addition of 1 equiv. of phenylsilane to compound **III** at room temperature after 15 min; LZnH + **6m** (compounds were obtained by the addition of 1 equiv. of phenylsilane to compound **III** at 65 °C after 2 h). ◆ = Zn-H, ■ = Zn-NCH₂ of **III**, ● = N(SiH₂Ph)CH₂ (**6m'**), ● = N(SiH₂Ph)CH₂ (**6m'**). ● = N(SiHPh)(CH₂)₂ (**6m**), ● = N(SiHPh)(CH₂)₂ (**6m**).

This was further supported by the time-dependent reaction profile, as monitored by ¹H NMR, of the reaction of isoquinoline with 0.55 equiv of PhSiH₃ using 5 mol% catalyst **I** at 65 °C over 18 h (Scheme 6.8 (ii)). In the earlier stage of the reaction, substrate **5m** was converted to the mono-hydrosilylated product (**6m'**) up to 7 h, which then slowly converted to the bis-hydrosilylated product (**6m**) between 7 to 18 h. After 18 h, we noticed the exclusive formation of the bis-

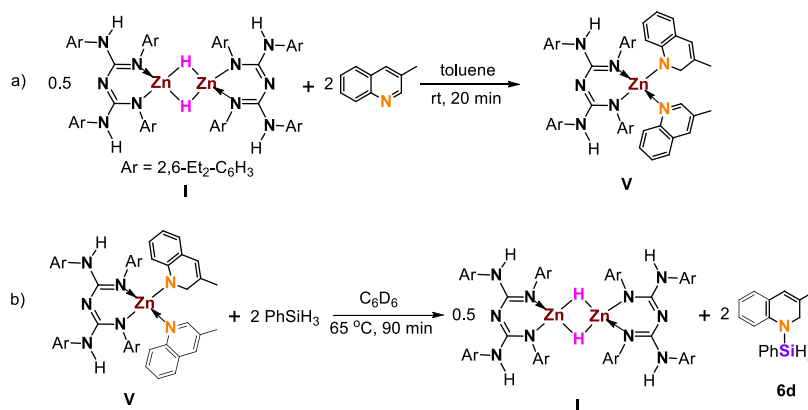
hydrosilylated product (**6m**) (See Scheme 6.8 (ii) and Figures S36-S37). This suggests that the first step of the reaction was forming a mono-hydrosilylated product (**6m'**). Several attempts to generate the exclusive formation of compound **6m'** by the reaction of a 1 equiv. of phenylsilane and isoquinoline (**5m**) in the presence of 5 mol%, **I** resulted in a mixture of **6m'** and **6m**. Thus, resubmitting the isolated compounds (**6m'** and **6m**) to the optimal conditions with 0.5 equiv of isoquinoline led to the formation of the exclusive bis-hydrosilylated product **6m** (See, Scheme 6.8 (iii) and Figures S38-S40). This experimental result indicates that the bis-hydrosilylated product was produced by the hydrosilylation reaction of isoquinoline using **6m'** as a silane reagent, which matched the time-dependent reaction profile and stoichiometric experiments. Hence, monohydrosilylation products are initially formed and then reduced to bis-hydrosilylation products. All the ^1H NMR data of the stoichiometric experiments for selective bis-1,2-hydrosilylation of N-heteroarenes are stacked in Figure 6.3, and $^{29}\text{Si}\{^1\text{H}\}$ NMR stacking is provided in supporting information.

Further, we conducted an in situ experiment for a thorough mechanistic study of bis-1,2-hydrosilylation of N-heteroarenes. Intermediate **III** was reacted with phenylsilane and ^1H and $^{29}\text{Si}\{^1\text{H}\}$ NMR spectra recorded from time to time. After 5 min, ^1H NMR confirms no reaction between compound **III** and phenylsilane (dark red color solution). The $^{29}\text{Si}\{^1\text{H}\}$ NMR spectrum provides a signal at -60.3 ppm for free phenylsilane. Next, the NMR spectra show the production of compound **6m'** after 15 min, while the color changes from dark red to a yellowish solution. The Zn-H peak of intermediate **II** shifted to 4.47 ppm from 4.52 ppm of $[\text{LZnH}]_2$. The ^{29}Si NMR of compound **6m'** (-21.6 ppm) shifted downfield from unreacted phenylsilane (-60.3 ppm). Next, we heated the reaction mixture to 65 °C. The yellowish solution changed to a colorless solution. The disappearance of compound **6m'** was slowly noticed, and the simultaneous appearance of a new

peak at 5.08 ppm corresponding to $\text{N}(\text{SiHPh})(\text{CH}_2)_2$ of bis-hydrosilylated product **6m** was observed after 2 h. The $^{29}\text{Si}\{^1\text{H}\}$ NMR further shifted from -21.6 ppm (compound **6m'**) to -19.2 ppm (**6m**).

6.2.6. Stoichiometric Experiments for Mono-Hydrosilylation

We performed some more stoichiometric experiments to understand the mechanism for zinc hydride-catalyzed mono-1,2-hydrosilylation derivative products (**6a**, **6c-6l**, and **6o'**). The CBG zinc hydride reacted with 3-methyl quinoline in toluene at room temperature for 20 min, resulting in the immediate formation of $[\text{LZn}(1,2\text{-(3-MeDHQ)})(3\text{-methyl quinoline})]$ (1,2-(3-MeDHQ) = 1,2-(3-methyl dihydro quinoline)) **V**, which is analogous to **III** (Scheme 6.9, a). Compound **V** was confirmed by NMR, HRMS, and IR analyses. The ^1H NMR spectrum shows a new peak at 3.74 ppm for the ZnNCH_2 core. In addition, a complete disappearance of the Zn-H peak at 4.52 ppm was noticed. The $^{13}\text{C}\{^1\text{H}\}$ NMR spectrum exhibits a peak at 53.8 ppm, corresponding to ZnNCH_2 moiety.



Scheme 6.9. Stoichiometric experiments for mono-hydrosilylation of N-heteroarenes.

Further, 2.0 equiv. phenylsilane was added to compound **V** in a J. Young valve NMR tube. Next, the temperature was raised from rt to 65 °C. After 90 min, we noticed that the red color changed to a colorless solution and the appearance of a new signal at 5.19 ppm corresponding to the

(N(SiH₂Ph)CH₂) moiety of hydrosilylated product **6d** (Figure 6.4). This indicates the formation of hydrosilylated product **6d**, as shown in Scheme 6.9, b.

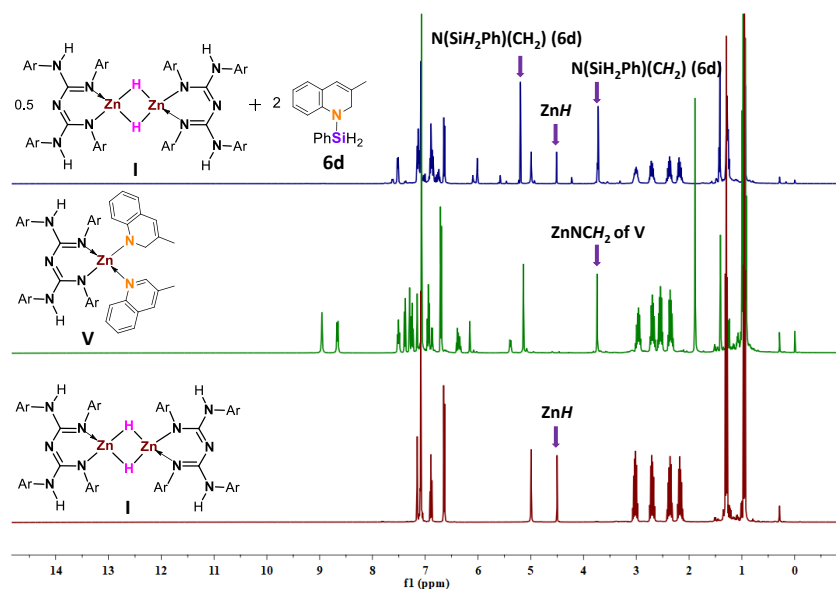


Figure 6.4. Annotated ¹H NMR (400 MHz) stack plot of the stoichiometric hydrosilylation of 3-methylquinoline with catalyst **I** in C₆D₆. Stacked spectra from bottom to top: LZnH (**I**); LZn(1,2-(3-MeDHQ)) (3-Methylquinoline) (**V**); **I** + **6d** (compounds were obtained by the addition of 2 equiv. of phenylsilane to compound **V** at 65 °C after 90 min).

The stacked ¹H NMR spectra of stoichiometric experiments is shown in Figure 6.4. Furthermore, we demonstrated *in situ* studies to understand the specific mechanism of mono-1,2-hydrosilylation of N-heteroarenes. The reaction between phenylsilane and compound **V** was performed in C₆D₆. Further, the progress of the reaction was monitored by ¹H and ²⁹Si NMR spectra from time to time. Very little conversion was observed at ambient temperature for 30 minutes. Next, we elevated the temperature to 65 °C. We noticed a characteristic peak at 5.19 ppm, corresponding to (N(SiH₂Ph)CH₂) moiety of product **6d** in ¹H NMR spectrum.

Finally, after 90 minutes, an exclusive mono-1,2-hydrosilylation product (**6d**) was noticed. The ²⁹Si{¹H} NMR spectrum shows two signals at -26.0 ppm and -60.3 ppm corresponding to compound **6d** and unreacted phenylsilane, respectively.

6.2.7. The Mechanism for 1,2-Regioselective Hydroboration of N-Heteroarenes.

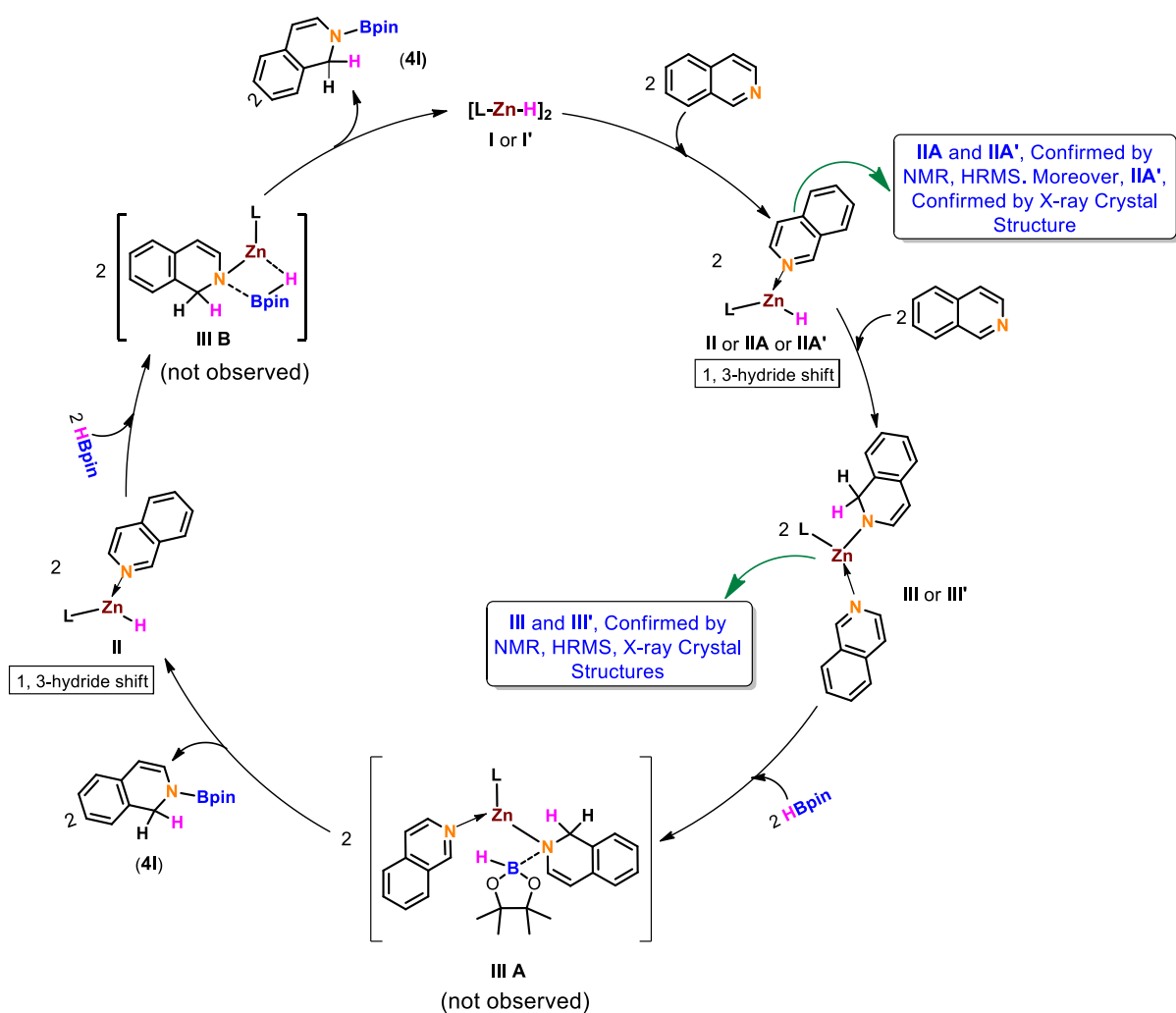
Based on the above isolation of intermediates, stoichiometric experiments, and in situ studies, a possible catalytic cycle is proposed for regioselective 1,2-hydroboration of N-heteroarenes. Initially, isoquinoline coordinated with catalyst **I**, resulting in the formation of compound **II**, which undergoes 1,3-hydride transfer to the C2 position of isoquinoline from Zn-H moiety, followed by treatment with two more equivalents of isoquinoline afforded zinc amide intermediate **III**. After that, a reaction of **III** with HBpin via metathesis reaction (**IIIA**) gives rise to N-boryl dihydro isoquinoline (**4I**) and intermediate **II**. Further, its reaction with 2.0 equivalents of HBpin via σ -bond metathesis reaction (**IIIB**) resulted in the formation of borylated N-heteroarene (**4I**) and the renewal of $[LZnH]_2$ (**I**) (Scheme 6.10).

6.2.8. The Mechanism for 1,2-Regioselective Hydrosilylation of N-Heteroarenes.

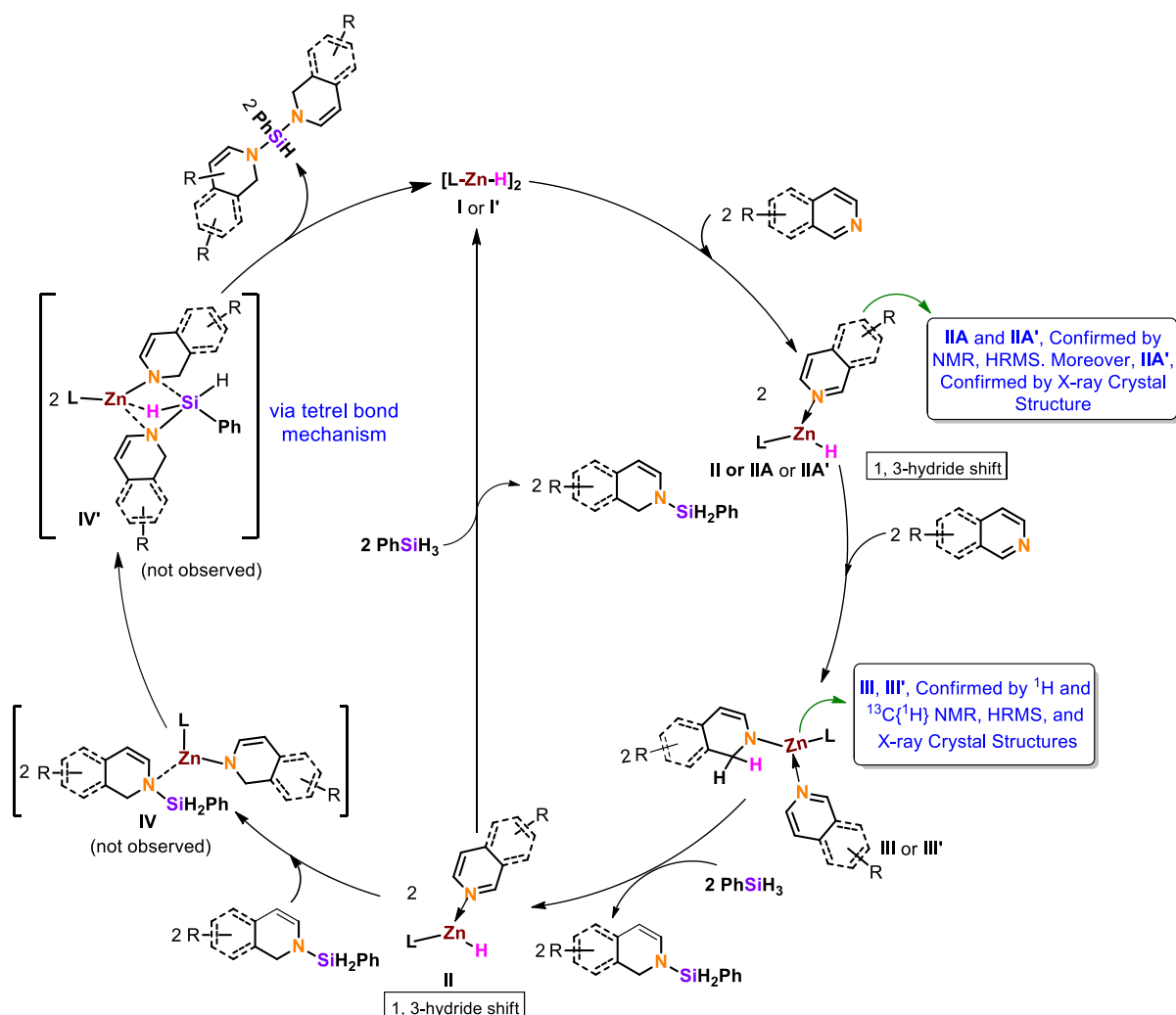
A plausible catalytic cycle is proposed for mono- and bis-hydrosilylation of N-heteroarenes based on intermediates isolation, stoichiometric experiments, and in situ studies. The CBG zinc hydride was treated with 4.0 equivalents of isoquinoline, resulting in the immediate formation of zinc amide intermediate **III** via intermediate **II**. Next, compound **III** reacted with phenylsilane via σ -bond metathesis, resulting in the formation of mono-1,2-hydrosilylated product and intermediate **II**, which undergoes 1,3-hydride transfer followed by reaction with phenylsilane to produce a quantitative amount of mono-1,2- hydrosilylated product and rebirth of catalyst **I** was observed and closed the catalytic cycle for mono-hydrosilylation of N-heteroarenes.

On the other hand, based on the stoichiometric experiments and time-dependent reaction profile studies, we proposed the mechanism for bis-hydrosilylation of N-heteroarenes. Stoichiometric and in situ monitoring experiments suggest mono-hydrosilylation products formed and reinserted into the catalytic cycle for further reduction, leading to the bis-hydrosilylation product. Thus,

intermediate **II** reacted with mono-1,2- hydrosilylated product followed by 1,3-hydride transfer to produce intermediate **IV**, which goes through tetrel bonding³⁰ (**IV'**) followed by σ -bond metathesis to produce bis-hydrosilylated product and renewal of $[LZnH]_2$ (**I**) and closed the catalytic cycle for bis-hydrosilylation of N-heteroarenes (Scheme 6.11). The σ -donation from the lone pair electrons on the N-center of dihydroisoquinoline to the hole region in the silicon atom (Group14 element) of phenylsilane leads to tetrel bonding, in which the silicon atom acts as a Lewis acid (tetrel bonding) .³⁰



Scheme 6.10. Proposed mechanism for the 1,2-regioselective hydroboration of N-heteroarenes



Scheme 6.11. Proposed mechanism for the 1,2-regioselective hydrosilylation of N-heteroarenes

6.3. Conclusion

In summary, we have illustrated the β -diketiminato analogue, CBG stabilized zinc hydride $[LZnH]_2$, as a highly active and regioselective catalyst for the hydrofunctionalization of N-heteroarenes under mild conditions. A broad range of pyridines and N-heteroarenes selectively produces exclusively 1,2-hydroborated or hydrosilylated products. We observed that N-heteroarenes bearing electron-withdrawing groups accelerate the reaction rates. Moreover, pyrazine, pyrimidine, and quinazoline are converted into double hydroborated products. Competitive and exchange experiments show that the formation of Si-N bonds is reversible, and

scrambling occurs when borane is present. Notably, intermolecular hydroboration reactions of isoquinoline (**3I**) with other reducible substrates have been performed, in which nitrile, isocyanide, and alkene functionalities were untouched. Mechanistic studies suggest that zinc hydride moiety insertion in C=N of N-heteroarenes undergoes a 1,3-hydride transfer to furnish CBG zinc amides **III**, **III'**, and **V**. Further addition of HBpin to compound **III** or **III'** produces selective 1,2-hydroborated products. Similarly, the reaction between amide intermediates, either **III** or **V**, with phenylsilane to produce the exclusive 1,2-hydrosilylated product. Finally, a series of stoichiometric experiments structurally characterized intermediates and in situ studies have given evidence for the complete catalytic cycles. More importantly, for the first time, we revealed the mechanism for metal-catalyzed hydrosilylation of N-heteroarenes to exclusively bis-1,2-hydrosilylated products. This study finds that the CBG-ligated zinc hydride's catalytic activities are slightly better than the Nacnac-ligated zinc counterpart. Therefore, it would be helpful to design the ligands in homogeneous catalysis.

6.4. General Experimental Methods

General Procedures

Unless stated, manipulations were performed under a dinitrogen atmosphere using standard glovebox and Schlenk techniques. NMR spectra were recorded on Jeol-400 MHz and Bruker NMR spectrometers at 400 MHz (^1H), 101 MHz ($^{13}\text{C}\{^1\text{H}\}$), 128.36 MHz (^{11}B), and 80 MHz ($^{29}\text{Si}\{^1\text{H}\}$). ^1H NMR and $^{13}\text{C}\{^1\text{H}\}$ NMR chemical shifts are referenced to residual protons or carbons in the deuterated solvent. ^{11}B were calibrated using an external reference of $\text{BF}_3\cdot\text{Et}_2\text{O}$. Multiplicities are reported as singlet (s), doublet (d), triplet (t), quartet (q), and multiplet (m). Chemical shifts are reported in ppm. Coupling constants are reported in Hz. The crystal data were collected on a Rigaku Oxford diffractometer at 100 K. Selected data collection parameters and other

crystallographic results are summarized in Table 6.1. Mass spectrometry analyses were carried out on Bruker micrOTOF-Q II and Waters XevoG2 XS Q-TOF mass spectrometers. Infrared (IR) spectra were recorded in Thermo-Nicolet FT-IR spectrophotometers. The melting points of compounds **III** and **V** were measured from the Stuart SMP 10 instrument.

Materials:

Solvents were purified by distillation over Na/ benzophenone. Deuterated chloroform (CDCl_3) was dried on molecular sieves, and benzene- d_6 (C_6D_6) was dried over Na/K alloy and distilled. The ligand LH ($\text{L} = \{(\text{ArNH})(\text{ArN})-\text{C}=\text{N}-\text{C}=(\text{NAr})(\text{NHAr})\}$; $\text{Ar} = 2,6\text{-Et}_2\text{-C}_6\text{H}_3$) and complex $\{\text{LZnH}\}_2$ (**I**) were prepared according to reported literature procedures.²⁷⁻²⁸ The complex $\{\text{L}'\text{ZnH}\}_2$ [$(^{\text{Diethyl}}\text{nacnac}(\text{L}') = \text{CH}\{(\text{CMe})(2,6\text{-Et}_2\text{C}_6\text{H}_3\text{N})\}_2)$] (**I'**) was prepared by using the same protocol of $\{\text{LZnH}\}_2$ (**I**). For catalysis reactions, J. Young valve-sealed NMR tubes were oven-dried before being used. Chemicals and reagents were purchased from Sigma-Aldrich Co. Ltd., Merck India Pvt. Ltd., and TCI chemicals were used without purification.

6.4.1. Stoichiometric Experiments

Synthesis of [(LZnH) (4-methylpyridine)], (IIA**):** $[\text{LZnH}]_2$ (**I**) (20 mg, 0.0143 mmol) was weighed into J. Young NMR tube dissolved in 0.5 mL C_6D_6 . Next, 4-methylpyridine (3.3 μL , 0.0287 mmol) was quickly added to the solution of **I**. The tube was capped immediately and quickly mixed and monitored by ^1H NMR. The signals in the ^1H NMR spectra of the $[\text{LZnH}]_2$ (**I**)/4-methylpyridine mixture are noticeably shifted from those of the starting materials. The pyridine peaks are shifted downfield, indicating a decrease in the overall electron density of pyridine associated with coordination to the zinc center. It indicates the formation of [(LZnH) (4-methylpyridine)] complex. More interestingly, Zn-H of compound **IIA** appears at 4.46 ppm,

slightly upfield compared to compound **I**, i.e., [LZnH]₂ at 4.52 ppm, which indicates that the Zn-H moiety of compound [(LZnH) (4-methylpyridine)] is monomeric.

NMR Yield: (>99%). ¹H NMR (400 MHz, C₆D₆) δ 8.63–8.62 (d, ³J_{HH} = 8.0 Hz, 2H, 4-methylpy-ArH), 7.14 – 7.07 (m, 6H, ArH), 6.91 (t, ³J_{HH} = 7.6 Hz, 2H, ArH), 6.68–6.66 (d, ³J_{HH} = 8.0 Hz, 4H, ArH), 6.55–6.53 (d, ³J_{HH} = 7.4 Hz, 2H, 4-methylpy-ArH), 5.03 (s, 2H, NH), 4.46 (s, 1H, ZnH), 3.08 – 2.98 (m, 4H, ArCH₂CH₃), 2.76 – 2.67 (m, 4H, ArCH₂CH₃), 2.49 – 2.40 (m, 4H, ArCH₂CH₃), 2.29 – 2.20 (m, 4H, ArCH₂CH₃), 1.66 (s, 4-methylpy-CH₃), 1.23 (t, ³J_{HH} = 7.5 Hz, 12H, ArCH₂CH₃), 0.99 (t, ³J_{HH} = 7.4 Hz, 12H, ArCH₂CH₃). ¹³C{¹H} NMR (101 MHz, C₆D₆) δ 157.0, 149.4, 143.4, 141.1, 138.9, 135.6, 126.5, 126.1, 125.3, 125.2, 124.6, 25.0, 24.2, 20.2, 14.4, 14.3. HRMS (ESI) *m/z*: [M + H]⁺ Calcd for C₄₈H₆₃N₆Zn 787.4406, Found: 787.4388.

Synthesis of [LZn(1,2-DHiQ) (isoquinoline)], (III): Isoquinoline (67.59 μL, 25 °C, 0.575 mmol) in ~3 mL of toluene was added to a solution of complex [LZnH]₂ (**I**) (0.200 g, 25 °C, 0.143 mmol) in ~7 mL of toluene and stirred for 15 min. Then the reaction mixture changed its color immediately from yellow to dark orange. The solvent was removed in a vacuum resulting in a dark orange solid compound, and dried thoroughly. The resultant solid was dissolved in benzene (~ 10 mL) and filtered, and storage of the solution at room temperature gave block-shaped pale orange crystals suitable for single crystal X-ray diffraction within 2 d. (0.185 g, Yield 68 %): Mp 195 – 200 °C. ¹H NMR (700 MHz, C₆D₆) δ 9.25 (s, 2H, iQuin), 8.62–8.61 (d, ³J_{HH} = 7.8 Hz, 2H, iQuin), 7.45–7.44 (d, ³J_{HH} = 8.0 Hz, 2H, iQuin), 7.28–7.27 (d, ³J_{HH} = 8.1 Hz, 2H, ArH), 7.19 – 7.17 (m, 2H, ArH), 7.11 (s, 4H, ArH), 7.07 (t, ³J_{HH} = 7.5 Hz, 2H, ArH), 7.00 – 6.98 (m, 1H, iQuin), 6.93 (t, ³J_{HH} = 7.5 Hz, 2H, ArH), 6.70–6.69 (d, ³J_{HH} = 7.5 Hz, 4H, DHiQ), 6.27–6.26 (d, ³J_{HH} = 7.3 Hz, 1H, DHiQ), 5.59–5.58 (d, ³J_{HH} = 6.8 Hz, 1H, DHiQ), 5.10 (s, 2H, NH), 4.08 (s, 2H, DHiQ), 2.97 – 2.83 (m, 4H, ArCH₂CH₃), 2.75 – 2.62 (m, 4H, ArCH₂CH₃), 2.55 – 2.50 (m, 4H, ArCH₂CH₃),

2.39 – 2.34 (m, 4H, ArCH₂CH₃), 1.02 (t, ³J_{HH} = 7.6 Hz, 12H, ArCH₂CH₃), 0.96 – 0.85 (m, 12H, ArCH₂CH₃). ¹³C{¹H} NMR (101 MHz, C₆D₆) δ 157.3, 153.7, 142.7, 141.2, 140.9, 139.0, 138.1, 136.2, 135.3, 132.0, 128.3, 128.3, 128.2, 128.1, 126.4, 126.3, 126.3, 126.0, 125.6, 125.1, 124.2, 121.8, 119.6, 53.3, 24.9, 23.9, 14.2, 14.0. IR (Nujol mull) ν (cm⁻¹): 3375, 3062, 3015, 2962, 2923, 2793, 1858, 1627, 1594, 1496, 1458, 1427, 1399, 1375, 1352, 1244, 1204, 1111, 1010, 958, 922, 869. HRMS (ESI) *m/z*: [M + H]⁺ Calcd for C₆₀H₇₀N₇Zn 952.4979, Found: 952.4998.

Synthesis of [LZnH]₂ and 4I {NMR-Scale}: The addition of HBpin (16.24 μL, 0.112 mmol) to a J. Young valve NMR tube containing a solution of compound **III** (0.056 mmol) in C₆D₆ resulted in the immediate formation of compound **I** and **4I** were observed by ¹H NMR spectroscopy. NMR Yield: (>99%). ¹H NMR (400 MHz, C₆D₆) δ 7.12 – 7.08 (m, 8H, ArH + DHiQ), 7.02 – 6.98 (m, 1H, DHiQ), 6.92 – 6.81 (m, 8H, ArH + DHiQ), 6.74 – 6.72 (d, ³J_{HH} = 7.5 Hz, 1H, ArH), 6.66 – 6.64 (d, ³J_{HH} = 7.8 Hz, 4H, DHiQ), 5.65 – 5.63 (d, ³J_{HH} = 7.5 Hz, 2H DHiQ), 5.00 (s, 2H, NH), 4.65 (s, 4H, N(Bpin)CH₂), 4.50 (s, 1H, ZnH), 3.07 – 2.98 (m, 4H, ArCH₂CH₃), 2.75 – 2.66 (m, 4H, ArCH₂CH₃), 2.42 – 2.33 (m, 4H, ArCH₂CH₃), 2.22 – 2.13 (m, 4H, ArCH₂CH₃), 1.30 (t, ³J_{HH} = 7.5 Hz, 12H, ArCH₂CH₃), 1.03 (s, 24H, NBpin), 0.96 (t, ³J_{HH} = 7.6 Hz, 12H, ArCH₂CH₃). ¹³C{¹H} NMR (101 MHz, C₆D₆) δ 157.1, 142.7, 141.1, 138.8, 135.2, 133.2, 132.4, 127.2, 126.7, 126.3, 125.8, 125.7, 125.2, 125.1, 123.3, 105.8, 82.9, 45.9, 24.9, 24.3, 24.2, 14.4, 14.2. ¹¹B NMR (128 MHz, C₆D₆) δ 23.77.

Synthesis of [LZnH]₂ and 6m' {NMR-Scale}: {NMR-Scale}: The addition of PhSiH₃ (6.90 μL, 0.056 mmol) to a J. Young valve NMR tube containing a solution of compound **III** (0.056 mmol) in C₆D₆ resulted in the formation of mono-hydrosilylated product (**6m'**) and intermediate **II** with a 50% conversion after 15 min at room temperature was observed by ¹H NMR spectroscopy. NMR

Yield: (50%): ^1H NMR (400 MHz, C_6D_6) δ 4.93 (s, 2H, $\text{N}(\text{SiH}_2\text{Ph})\text{CH}_2$), 4.47 (s, 1H, ZnH (monomeric)), 4.18 (s, 1H, $\text{N}(\text{SiH}_2\text{Ph})\text{CH}_2$). $^{29}\text{Si}\{^1\text{H}\}$ NMR (80 MHz, C_6D_6) δ -21.66.

Synthesis of $[\text{LZnH}]_2$ and **6m {NMR-Scale}:** The addition of PhSiH_3 (6.90 μL , 0.056 mmol) to a J. Young valve NMR tube containing a solution of compound **III** (0.056 mmol) in C_6D_6 resulted in the formation of compound **I** and **6m** after 2 h at 65 $^\circ\text{C}$ were observed by ^1H NMR spectroscopy.

NMR Yield: (>99%). ^1H NMR (400 MHz, C_6D_6) δ 7.46 – 7.44 (d, $^3J_{\text{HH}} = 8.5$ Hz, 2H, ArH), 7.12 – 7.03 (m, 12H, $\text{ArH} + \text{DHiQ}$), 6.97 – 6.86 (m, 6H, $\text{ArH} + \text{DHiQ}$), 6.65 – 6.62 (m, 5H, ArH), 6.32 – 6.31 (d, $^3J_{\text{HH}} = 7.3$ Hz, 2H, DHiQ), 5.65 – 5.63 (d, $^3J_{\text{HH}} = 8.0$ Hz, 2H, DHiQ), 5.08 (s, 1H, $\text{N}(\text{SiHPh})(\text{CH}_2)_2$), 5.00 (s, 2H, NH), 4.49 (s, 1H, ZnH), 4.23 – 4.23 (d, $^3J_{\text{HH}} = 3.1$ Hz, 4H, $\text{N}(\text{SiHPh})(\text{CH}_2)_2$), 3.08 – 2.99 (m, 4H, ArCH_2CH_3), 2.74 – 2.65 (m, 4H, ArCH_2CH_3), 2.42 – 2.32 (m, 4H, ArCH_2CH_3), 2.22 – 2.12 (m, 4H, ArCH_2CH_3), 1.30 (t, $^3J_{\text{HH}} = 7.5$ Hz, 12H, ArCH_2CH_3), 0.96 (t, $^3J_{\text{HH}} = 7.6$ Hz, 12H, ArCH_2CH_3). $^{13}\text{C}\{^1\text{H}\}$ NMR (101 MHz, C_6D_6) δ 157.2, 142.7, 141.1, 138.9, 135.2, 134.9, 134.3, 133.7, 130.9, 130.1, 128.4, 127.5, 127.1, 126.7, 126.3, 125.7, 125.7, 125.3, 124.9, 122.8, 105.3, 46.9, 24.9, 24.3, 14.5, 14.2. $^{29}\text{Si}\{^1\text{H}\}$ NMR (80 MHz, C_6D_6) δ -19.29.

Synthesis of $[\text{LZn}(1,2\text{-(3-MeDHQ)})(\text{3-Methylquinoline})]$, (V**):** 3-Methylquinoline (77 μL , 25 $^\circ\text{C}$, 0.575 mmol) in ~3 mL of toluene was added to a solution of $[\text{LZnH}]_2$ (**I**) (0.200 g, 25 $^\circ\text{C}$, 0.143 mmol) in ~7 mL of toluene and stirred for 20 min. Then the reaction mixture changed its color immediately from yellow to dark red. The solvent was removed in a vacuum resulting in a dark orange oil compound, and dried thoroughly, resulting in compound **V** which was observed by ^1H NMR spectroscopy. (0.178 g, Yield 64 %): Mp 185-190 $^\circ\text{C}$. ^1H NMR (400 MHz, C_6D_6) δ 8.96 (s, 2H, 3-Methylquinoline), 8.67 – 8.65 (d, $^3J_{\text{HH}} = 8.2$ Hz, 2H, 3-Methylquinoline), 7.51 (t, $^3J_{\text{HH}} = 7.5$ Hz, 2H, 3-Methylquinoline), 7.40 – 7.38 (d, $^3J_{\text{HH}} = 7.1$ Hz, 1H, ArH), 7.30 (s, 1H, ArH), 7.25 (t, $^3J_{\text{HH}} = 7.5$ Hz, 2H, ArH), 7.07 (s, 3H, ArH), 6.94 (t, $^3J_{\text{HH}} = 7.3$ Hz, 2H, ArH), 6.88 – 6.86 (m,

1H, 3-MeDHQ), 6.71 – 6.69 (d, $^3J_{\text{HH}} = 7.6$ Hz, 3H, ArH), 6.41 – 6.33 (m, 2H, 3-MeDHQ), 6.16 (s, 1H, 3-MeDHQ), 5.40 – 5.38 (m, 1H, 3-MeDHQ), 5.14 (s, 2H, NH), 3.74 (s, 2H, 3-MeDHQ), 3.01 – 2.92 (m, 4H, ArCH₂CH₃), 2.74 – 2.64 (m, 4H, ArCH₂CH₃), 2.60 – 2.50 (m, 4H, ArCH₂CH₃), 2.40 – 2.30 (m, 4H, ArCH₂CH₃), 1.89 (s, 3H, 3-CH₃-quinoline), 1.41 (s, 3H, 3-CH₃-DHQ), 0.99 – 0.92 (m, 24H, ArCH₂CH₃); $^{13}\text{C}\{^1\text{H}\}$ NMR (101 MHz, C₆D₆) δ 157.4, 154.0, 153.5, 146.0, 144.1, 140.8, 139.4, 135.7, 135.5, 130.6, 129.2, 128.8, 128.7, 128.5, 127.1, 127.0, 126.5, 126.1, 126.1, 125.8, 125.4, 125.0, 123.9, 122.6, 115.6, 112.2, 53.8, 24.9, 23.5, 20.3, 18.0, 14.2, 13.2. IR (Nujol mull) ν (cm⁻¹): 3014, 2959, 2923, 2851, 1514, 1496, 1470, 1458, 1413, 1402, 1353, 1244, 1212. HRMS (ASAP/Q-TOF) m/z : [M]⁺ Calcd for C₆₂H₇₃N₇Zn 979.5219, Found: 979.5206.

Synthesis of [LZnH]₂ and 6f {NMR-Scale}: The addition of PhSiH₃ (6.90 μL , 0.056 mmol) to a J. Young valve NMR tube containing a solution of compound **V** (0.056 mmol) in C₆D₆ resulted in the formation of compound **I** and **6f** after 1.5 h at 65 °C was observed by ^1H NMR spectroscopy. NMR Yield: (>99%). ^1H NMR (400 MHz, C₆D₆) δ 7.53 – 7.51 (d, $^3J_{\text{HH}} = 7.5$ Hz, 2H, ArH), 7.13 (t, $^3J_{\text{HH}} = 6.9$ Hz, 6H, ArH), 7.08 (s, 6H, ArH), 6.91 – 6.85 (m, 10H, , ArH + 3-MeDHQ), 6.76 – 6.72 (m, 2H, 3-MeDHQ), 6.65 – 6.63 (d, $^3J_{\text{HH}} = 8.0$ Hz, 4H, 3-MeDHQ), 6.01 (s, 2H, 3-MeDHQ), 5.19 (s, 4H, N(SiH₂Ph)CH₂), 4.99 (s, 2H, NH), 4.51 (s, 1H, ZnH), 3.72 (s, 4H, N(SiH₂Ph)CH₂), 3.06 – 2.97 (m, 4H, ArCH₂CH₃), 2.75 – 2.66 (m, 4H, ArCH₂CH₃), 2.42 – 2.33 (m, 4H, ArCH₂CH₃), 2.23 – 2.13 (m, 4H, ArCH₂CH₃), 1.42 (s, 6H, 3-CH₃-DHQ), 1.28 (t, $^3J_{\text{HH}} = 7.3$ Hz, 12H, ArCH₂CH₃), 0.95 (t, $^3J_{\text{HH}} = 7.2$ Hz, 12H, ArCH₂CH₃). $^{13}\text{C}\{^1\text{H}\}$ NMR (101 MHz, C₆D₆) δ 157.1, 143.4, 142.7, 141.1, 138.8, 135.2, 134.4, 131.7, 130.2, 128.2, 127.3, 126.6, 126.4, 126.3, 126.2, 125.6, 125.2, 121.8, 120.0, 116.7, 51.0, 24.9, 24.2, 20.2, 20.1, 14.2. $^{29}\text{Si}\{^1\text{H}\}$ NMR (80 MHz, C₆D₆) δ -26.02.

6.4.2. X-ray Crystallographic Data

The single crystals of compounds **IIA'**, **III'**, **III**, and **4f** were crystallized from benzene at rt as colorless blocks after 2 d. The crystal data of compounds **IIA'**, **III'**, **III**, and **4f** were collected on a Rigaku Oxford diffractometer at 100 K. Selected data collection parameters and other crystallographic results are summarized in Table 6.1. The structure was determined using direct methods employed in *ShelXT*,³¹ *OleX*,³² and refinement was carried out using least-square minimization implemented in *ShelXL*.³³ All non-hydrogen atoms were refined with anisotropic displacement parameters. Hydrogen atom positions were fixed geometrically in idealized positions and were refined using a riding model.

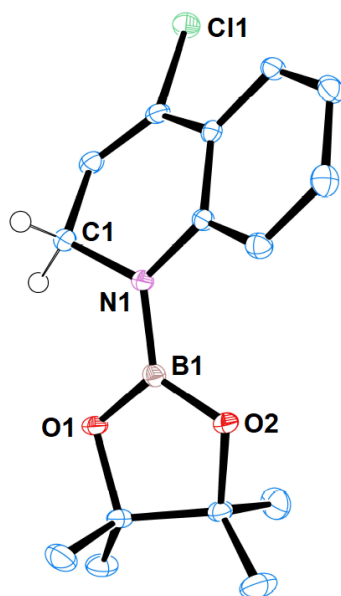


Figure 6.5. The molecular structure of compound **4f**. The thermal ellipsoids are shown at 50% probability, and all the hydrogen atoms except for H(1a) and H(1b) are omitted for clarity. Selected bond lengths (Å) and angles: C1–N1 1.4733(16), N1–B1 1.4238(17), B1–O1 1.3773(17), B1–O2 1.3722(17), C1–N1–B1 119.67(10), N1–B1–O1 121.32(12), N1–B1–O2 124.90(12), O1–B1–O2 113.78(11).

Table 6.1. Crystallographic data and refinement parameters for compounds **IIA'**, **III'**, **III**, and **4f**.

Compound	IIA'	III'	III	4f
Formula	C ₃₁ H ₄₁ N ₃ Zn	C ₄₃ H ₄₇ N ₄ Zn	C ₆₀ H ₆₉ N ₇ Zn	C ₁₅ H ₁₉ BClNO ₂
CCDC	2208799	2206529	2162231	2162235
Mol.mass	521.04	685.21	953.59	291.57
Temperature	100 K	100 K	100 K	100 K
Wavelength	0.71073 Å	0.71073 Å	1.54184 Å	0.71073 Å
Size(mm)	0.2 x 0.1 x 0.1	0.2 x 0.18 x 0.17	0.2 x 0.18 x 0.17	0.2 x 0.18 x 0.17
Crystal system, space group	triclinic, P-1	Monoclinic, P2 ₁ /n	Monoclinic, P2 ₁ /c	Monoclinic, P2 ₁ /n
a (Å)	8.67840(10)	10.4631(5)	14.4694(2)	8.63610(20)
b (Å)	12.6411(2)	17.3820(7)	17.1612(2)	26.4728(7)
c (Å)	13.5970(2)	20.4037(8)	21.7257(2)	12.6812(3)
α (deg)°	77.0800(10)	90	90	90
β (deg)°	85.4300(10)	100.940(4)	109.141(2)	91.599(2)
γ (deg)°	74.2230(10)	90	90	90
Volume (Å ³)	1398.83(4)	3643.4(3)	5096.50(13)	2898.07(12)
Z, Calculated density	2, 1.237 g/cm ³	4, 1.249 g/cm ³	4, 1.243 g/cm ³	8, 1.337 g/cm ³
Absorption coefficient	0.901 mm ⁻¹	0.709 mm ⁻¹	1.016 mm ⁻¹	0.263 mm ⁻¹
F(000)	556.0	1452.0	2032.0	1232.0
Theta range for data collection	6.852 to 52.744 deg.	6.702 to 52.744 deg.	6.714 to 136.49 deg.	6.428 to 50.698 deg.
Limiting indices	-10 ≤ h ≤ 10, -15 ≤ k ≤ 15, -16 ≤ l ≤ 16	-13 ≤ h ≤ 12, -19 ≤ k ≤ 21, -23 ≤ l ≤ 25	-17 ≤ h ≤ 17, -20 ≤ k ≤ 20, -25 ≤ l ≤ 26	-10 ≤ h ≤ 10, -31 ≤ k ≤ 31, -15 ≤ l ≤ 15
Reflections collected	26789	34500	37647	30738
Independent reflections	5702 [R _{int} = 0.0336, R _{sigma} = 0.0223]	7426 [R _{int} = 0.0815, R _{sigma} = 0.0505]	9321 [R _{int} = 0.0518, R _{sigma} = 0.0374]	5304 [R _{int} = 0.0305, R _{sigma} = 0.0188]
Completeness to theta	99.9 %	99.9 %	99.9 %	99.9 %
Absorption correction	Empirical	Empirical	Empirical	Empirical
Data / restraints /parameters	5702 / 2 / 326	7426 / 0 / 439	9321 / 36 / 621	5304 / 0 / 370
Goodness – of–fit on F ²	1.056	1.112	1.042	1.022
Final R indices [I>2 sigma(I)]	R ₁ = 0.0347, wR ₂ = 0.0926	R ₁ = 0.0557, wR ₂ = 0.1342	R ₁ = 0.0536, wR ₂ = 0.1506	R ₁ = 0.0287, wR ₂ = 0.0725

6.5. Appendix: All general experimental information, stoichiometric reactions, analytical data, and spectral data were available in published paper. *Inorg. Chem.* **2023**, *62*, 304–317.

6.6. References

- (a) Wang, D.-S.; Chen, Q.-A.; Lu, S.-M.; Zhou, Y.-G. *Chem. Rev.* **2012**, *112*, 2557–2590; (b) Chatterjee, B.; Gunanathan, C. *J. Chem. Sci.* **2019**, *131*, 118; (c) Yu, H.-C.; Islam, S. M.; Mankad, N. P. *ACS Catal.* **2020**, *10*, 3670–3675; (d) Zhang, F.; Song, H.; Zhuang, X.; Tung, C.-H.; Wang, W. *J. Am. Chem. Soc.* **2017**, *139*, 17775–17778; (e) Park, S. *ChemCatChem* **2020**, *12*, 3170–3185; (f) Zhang, Z.; Huang, S.; Huang, L.; Xu, X.; Zhao, H.; Yan, X. *J. Org. Chem.* **2020**, *85*, 12036–12043; (g) Bull, J. A.; Mousseau, J. J.; Pelletier, G.; Charette, A. B. *Chem. Rev.* **2012**, *112*, 2642–2713; (h) Eisner, U.; Kuthan, J. *Chem. Rev.* **1972**, *72*, 1–42.
- (a) Park, S.; Chang, S. *Angew., Chem. Int. Ed.* **2017**, *56*, 7720–7738; (b) Boll, M. *J. Mol. Microbiol. Biotechnol.* **2005**, *10*, 132–142; (c) Thiele, B.; Rieder, O.; Golding, B. T.; Müller, M.; Boll, M. *J. Am. Chem. Soc.* **2008**, *130*, 14050–14051; (d) Liu, Z.; Chen, L.; Li, J.; Liu, K.; Zhao, J.; Xu, M.; Feng, L.; Wan, R.-z.; Li, W.; Liu, L. *Org. Biomol. Chem.* **2017**, *15*, 7600–7606; (e) Welsch, M. E.; Snyder, S. A.; Stockwell, B. R. *Curr. Opin. Chem. Biol.* **2010**, *14*, 347–361; (f) Michael, J. P. *Nat. Prod. Rep.* **2003**, *20*, 476–493; (g) Katritzky, A. R.; Rachwal, S.; Rachwal, B. *Tetrahedron* **1996**, *52*, 15031–15070; (h) Kung, J. W.; Baumann, S.; von Bergen, M.; Müller, M.; Hagedoorn, P.-L.; Hagen, W. R.; Boll, M. *J. Am. Chem. Soc.* **2010**, *132*, 9850–9856.
- (a) Fu, P.; Brard, L.; Li, Y.-M.; Marks, T. J. *J. Am. Chem. Soc.* **1995**, *117*, 7157–7168; (b) Pape, A. R.; Kaliappan, K. P.; Kuendig, E. P. *Chem. Rev.* **2000**, *100*, 2917–2940; (c) Rochat, R.; Lopez, M. J.; Tsurugi, H.; Mashima, K. *ChemCatChem* **2016**, *8*, 10–20; (d) Revunova, K.; Nikonov, G. I. *Dalton Trans.* **2015**, *44*, 840–866.

-
4. (a) Danishefsky, S.; Cain, P. *J. Org. Chem.* **1975**, *40*, 3606–3608; (b) Birch, A. J.; Karakhanov, E. A. *J. Chem. Soc. Chem. Commun.* **1975**, 480–481; (c) Donohoe, T. J.; McRiner, A. J.; Sheldrake, P. *Org. Lett.* **2000**, *2*, 3861–3863; (d) Danishefsky, S.; Cain, P.; Nagel, A. *J. Am. Chem. Soc.* **1975**, *97*, 380–388; (e) Danishefsky, S.; Cavanaugh, R. *J. Am. Chem. Soc.* **1968**, *90*, 520–521.
 5. (a) Freifelder, M.; Stone, G. R. *J. Org. Chem.* **1961**, *26*, 3805–3808; (b) Adkins, H.; Kuick, L. F.; Farlow, M.; Wojcik, B. *J. Am. Chem. Soc.* **1934**, *56*, 2425–2428; (c) Lunn, G.; Sansone, E. B. *J. Org. Chem.* **1986**, *51*, 513–517; (d) Takasaki, M.; Motoyama, Y.; Higashi, K.; Yoon, S.-H.; Mochida, I.; Nagashima, H. *Chem. Asian J.* **2007**, *2*, 1524–1533; (e) Glorius, F. *Org. Biomol. Chem.* **2005**, *3*, 4171–4175; (f) Vermaak, V.; Vosloo, H. C. M.; Swarts, A. J. *Adv. Synth. Catal.* **2020**, *362*, 5788–5793; (g) Yun, R.; Ma, Z.-W.; Hu, Y.; Zhan, F.; Qiu, C.; Zheng, B.; Sheng, T. *Catal. Lett.* **2021**, *151*, 2445–2451.
 6. (a) Chong, C. C.; Kinjo, R. *ACS Catal.* **2015**, *5*, 3238–3259; (b) McLellan, R.; Kennedy, A. R.; Mulvey, R. E.; Orr, S. A.; Robertson, S. D. *Chem. – Eur. J.* **2017**, *23*, 16853–16861.
 7. Arrowsmith, M.; Hill, M. S.; Hadlington, T.; Kociok-Köhn, G.; Weetman, C. *Organometallics* **2011**, *30*, 5556–5559.
 8. Rao, B.; Chong, C. C.; Kinjo, R. *J. Am. Chem. Soc.* **2018**, *140*, 652–656.
 9. Fan, X.; Zheng, J.; Li, Z. H.; Wang, H. *J. Am. Chem. Soc.* **2015**, *137*, 4916–4919.
 10. Keyzer, E. N.; Kang, S. S.; Hanf, S.; Wright, D. S. *Chem. Commun.* **2017**, *53*, 9434–9437.
 11. (a) Kaithal, A.; Chatterjee, B.; Gunanathan, C. *Org. Lett.* **2016**, *18*, 3402–3405; (b) Tamang, S. R.; Singh, A.; Unruh, D. K.; Findlater, M. *ACS Catal.* **2018**, *8*, 6186–6191; (c) Ji, P.; Feng, X.; Veroneau, S. S.; Song, Y.; Lin, W. *J. Am. Chem. Soc.* **2017**, *139*, 15600–15603; (d) Ji, P.; Sawano, T.; Lin, Z.; Urban, A.; Boures, D.; Lin, W. *J. Am. Chem. Soc.* **2016**, *138*, 14860–

- 14863; (e) Radcliffe, J. E.; Dunsford, J. J.; Cid, J.; Fasano, V.; Ingleson, M. J. *Organometallics* **2017**, *36*, 4952–4960; (f) Hynes, T.; Welsh, E. N.; McDonald, R.; Ferguson, M. J.; Speed, A. W. H. *Organometallics* **2018**, *37*, 841–844; (g) Das, A.; Rej, S.; Panda, T. K. *Dalton Trans.* **2022**, *51*, 3027–3040.
12. Jeong, J.; Heo, J.; Kim, D.; Chang, S. *ACS Catal.* **2020**, *10*, 5023–5029.
13. (a) Gandhamsetty, N.; Park, S.; Chang, S. *J. Am. Chem. Soc.* **2015**, *137*, 15176–15184; (b) Liu, T.; He, J.; Zhang, Y. *Org. Chem. Front.* **2019**, *6*, 2749–2755; (c) Liu, X.; Li, B.; Hua, X.; Cui, D. *Org. Lett.* **2020**, *22*, 4960–4965; (d) Rauch, M.; Ruccolo, S.; Parkin, G. *J. Am. Chem. Soc.* **2017**, *139*, 13264–13267; (e) Mukherjee, D.; Shirase, S.; Spaniol, T. P.; Mashima, K.; Okuda, J. *Chem. Commun.* **2016**, *52*, 13155–13158; (f) Liu, Z.-Y.; Wen, Z.-H.; Wang, X.-C. *Angew. Chem., Int. Ed.* **2017**, *56*, 5817–5820; (g) Jeong, E.; Heo, J.; Park, S.; Chang, S. *Chem. – Eur. J.* **2019**, *25*, 6320–6325; (h) Kucinski, K.; Hreczycho, G. *Green Chem.* **2020**, *22*, 5210–5224; (i) Magre, M.; Szewczyk, M.; Rueping, M. *Chem. Rev.* **2022**, *122*, 9, 8261–8312.
14. (a) Liu, J.; Chen, J.-Y.; Jia, M.; Ming, B.; Jia, J.; Liao, R.-Z.; Tung, C.-H.; Wang, W. *ACS Catal.* **2019**, *9*, 3849–3857; (b) Liu, H.; Khononov, M.; Eisen, M. S. *ACS Catal.* **2018**, *8*, 3673–3677.
15. (a) Harrod, J. F.; Shu, R.; Woo, H.-G.; Samuel, E. *Can. J. Chem.* **2001**, *79*, 1075–1085; (b) Hao, L.; Harrod, J. F.; Lebuis, A.-M.; Mu, Y.; Shu, R.; Samuel, E.; Woo, H.-G. *Angew. Chem., Int. Ed.* **1998**, *37*, 3126–3129.
16. (a) Lee, S.-H.; Gutsulyak, D. V.; Nikonov, G. I. *Organometallics* **2013**, *32*, 4457–4464; (b) Gutsulyak, D. V.; van der Est, A.; Nikonov, G. I. *Angew. Chem., Int. Ed.* **2011**, *50*, 1384–1387.
17. Koenigs, C. D. F.; Klare, H. F. T.; Oestreich, M. *Angew. Chem., Int. Ed.* **2013**, *52*, 10076–10079.

-
18. Jeong, J.; Park, S.; Chang, S. *Chem. Sci.* **2016**, 7, 5362–5370.
 19. Behera, D.; Thiagarajan, S.; Anjalikrishna, P. K.; Suresh, C. H.; Gunanathan, C. *ACS Catal.* **2021**, 11, 5885–5893.
 20. Intemann, J.; Bauer, H.; Pahl, J.; Maron, L.; Harder, S. *Chem. – Eur. J.* **2015**, 21, 11452–11461.
 21. Lortie, J. L.; Dudding, T.; Gabidullin, B. M.; Nikonov, G. I. *ACS Catal.* **2017**, 7, 8454–8459.
 22. Wang, X.; Zhang, Y.; Yuan, D.; Yao, Y. *Org. Lett.* **2020**, 22, 5695–5700.
 23. (a) Dudnik, A. S.; Weidner, V. L.; Motta, A.; Delferro, M.; Marks, T. J. *Nat. Chem.* **2014**, 6, 1100–1107; (b) Pang, M.; Chen, J.-Y.; Zhang, S.; Liao, R.-Z.; Tung, C.-H.; Wang, W. *Nat. Commun.* **2020**, 11, 1249; (c) Oshima, K.; Ohmura, T.; Sugimoto, M. *J. Am. Chem. Soc.* **2012**, 134, 3699–3702.
 24. (a) Bergamaschi, E.; Lunic, D.; McLean, L. A.; Hohenadel, M.; Chen, Y.-K.; Teskey, C. J. *Angew. Chem., Int. Ed.* **2022**, 61, e202114482; (b) Mahatthananchai, J.; Dumas, A. M.; Bode, J. W. *Angew. Chem., Int. Ed.* **2012**, 51, 10954–10990.
 25. Fohlmeister, L.; Stasch, A. *Chem. – Eur. J.* **2016**, 22, 10235–10246.
 26. Peddaraao, T.; Baishya, A.; Sarkar, N.; Acharya, R.; Nembenna, S. *Eur. J. Inorg. Chem.* **2021**, 2034–2046.
 27. Sahoo, R. K.; Sarkar, N.; Nembenna, S. *Angew. Chem., Int. Ed.* **2021**, 60, 11991–12000.
 28. Sahoo, R. K.; Mahato, M.; Jana, A.; Nembenna, S. *J. Org. Chem.* **2020**, 85, 11200–11210.
 29. (a) Bage, A. D.; Nicholson, K.; Hunt, T. A.; Langer, T.; Thomas, S. P. *ACS Catal.* **2020**, 10, 13479–13486; (b) Bage, A. D.; Hunt, T. A.; Thomas, S. P. *Org. Lett.* **2020**, 22, 4107–4112.
 30. (a) Esrafil, M. D.; Mousavian, P. *Molecules.* **2018**, 23, 2642–2661; (b) Cundari, T. R. *Chem. Rev.* **2000**, 100, 807–818; (c) Gao, H.; Müller, R.; Irran, E.; Klare, H. F. T.; Kaupp, M.;

- Oestreich, M. *Chem. – Eur. J.* **2022**, 28, e202104464; (d) Bauza, A.; Mooibroek, T. J.; Frontera, A. *Angew. Chem., Int. Ed.* **2013**, 52, 12317–12321; (e) Wang, C.; Aman, Y.; Ji, X.; Mo, Y. *Phys. Chem. Chem. Phys.* **2019**, 21, 11776–11784.
31. Sheldrick, G. *Acta Crystallogr. C.* **2015**, 71, 3-8.
32. Dolomanov, O. V.; Bourhis, L. J.; Gildea, R. J.; Howard, J. A. K.; Puschmann, H. *J. Appl. Crystallogr.* **2009**, 42, 339-341.
33. (a) Sheldrick, G. M. *Acta Crystallogr., Sect. A: Found. Crystallogr.* **2008**, 64, 112-122; (b) Sheldrick, G. M. *Acta Crystallogr., Sect. A: Found. Adv.* **2015**, 71, 3-8.

NMR Spectra

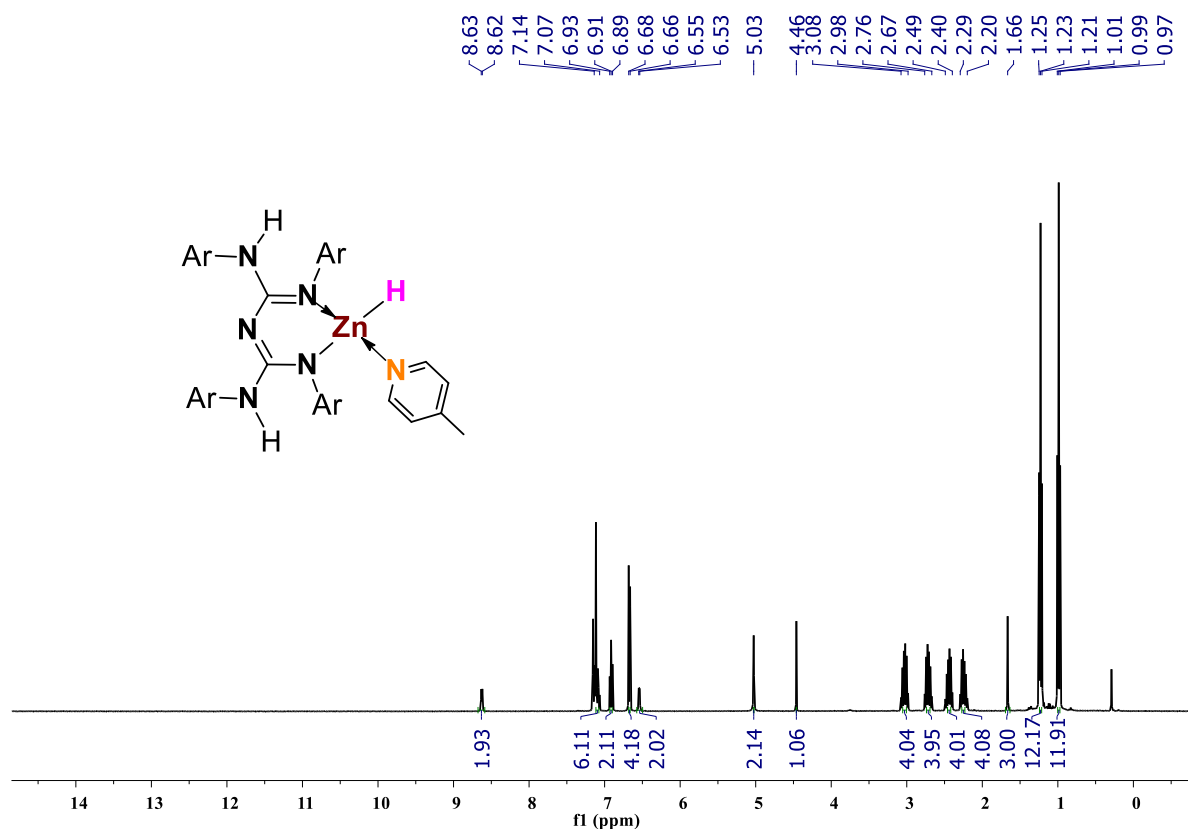


Figure 6.6. ^1H NMR (400 MHz, 25 °C, C_6D_6) spectrum of $[(LZnH)(4\text{-methylpyridine})]$, (IIA).

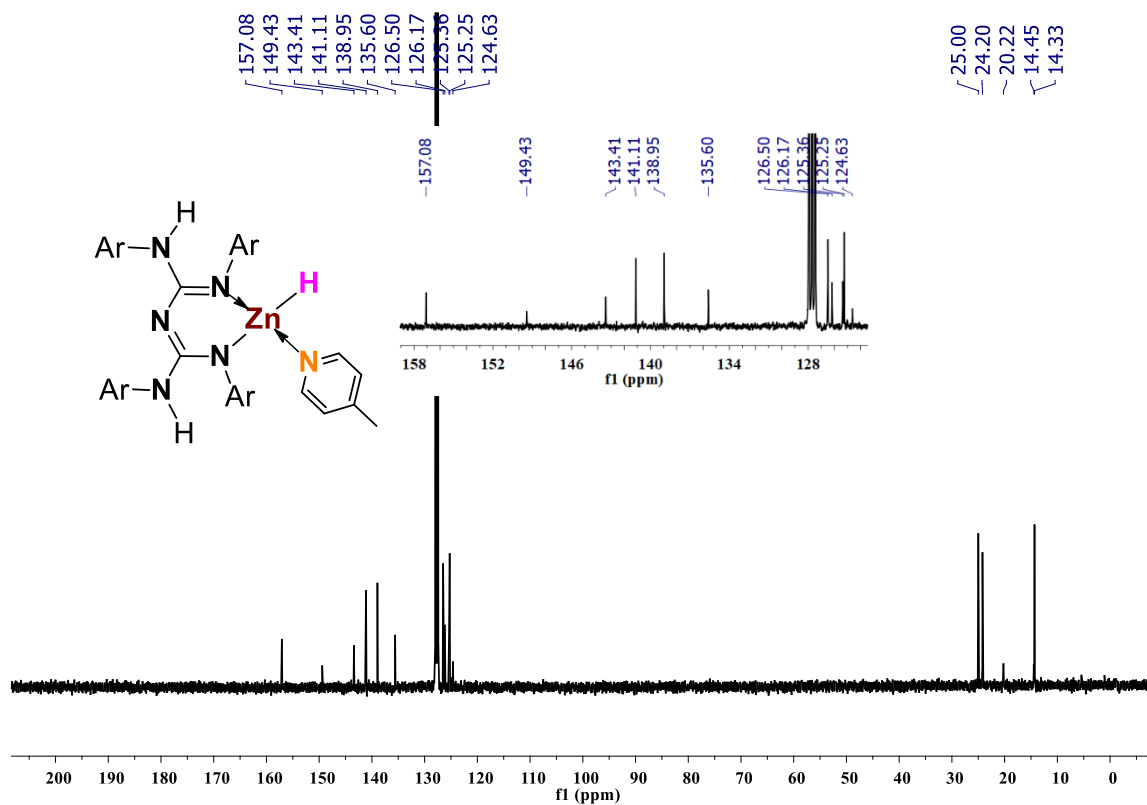


Figure 6.7. $^{13}\text{C}\{^1\text{H}\}$ NMR (100 MHz, 25 °C, C_6D_6) spectrum of [(LZnH)(4-methylpyridine)], (IIA).

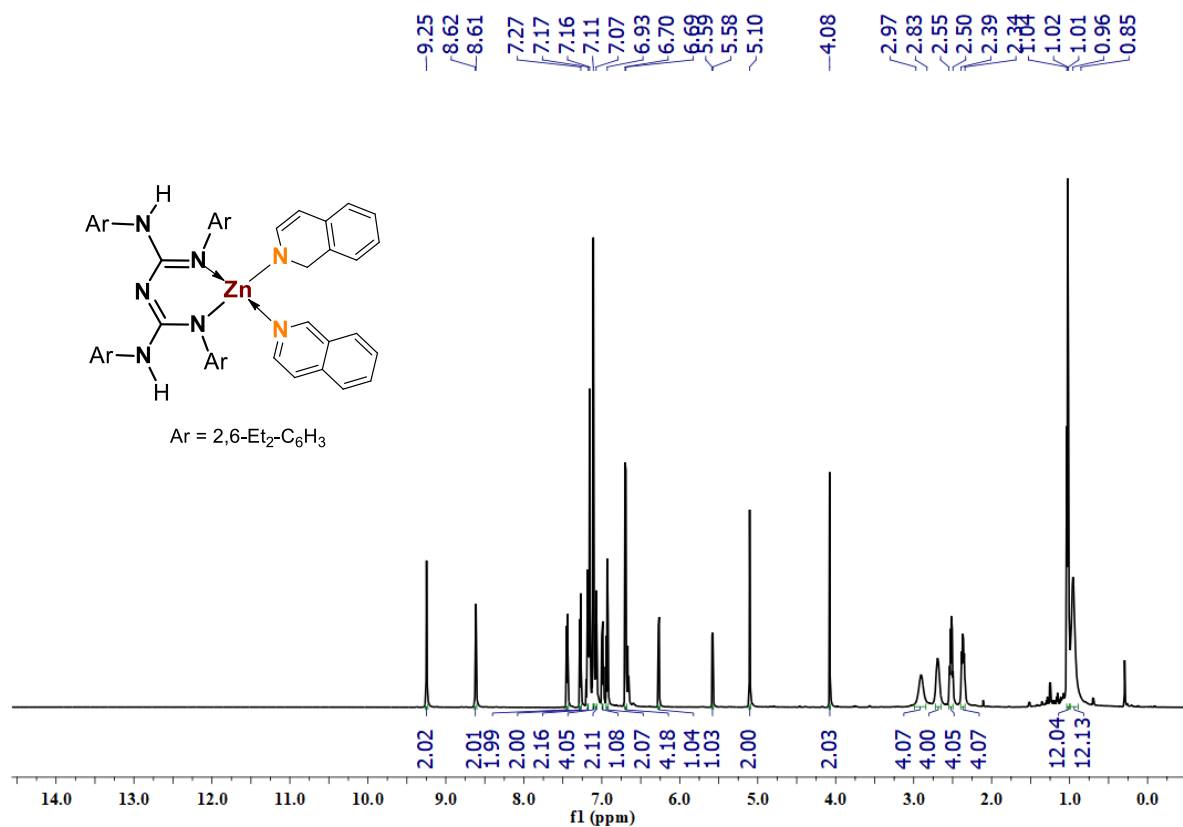


Figure 6.8. ^1H NMR (400 MHz, 25 °C, C_6D_6) spectrum of [LZn(1,2-DHiQ)] (isoquinoline), III.

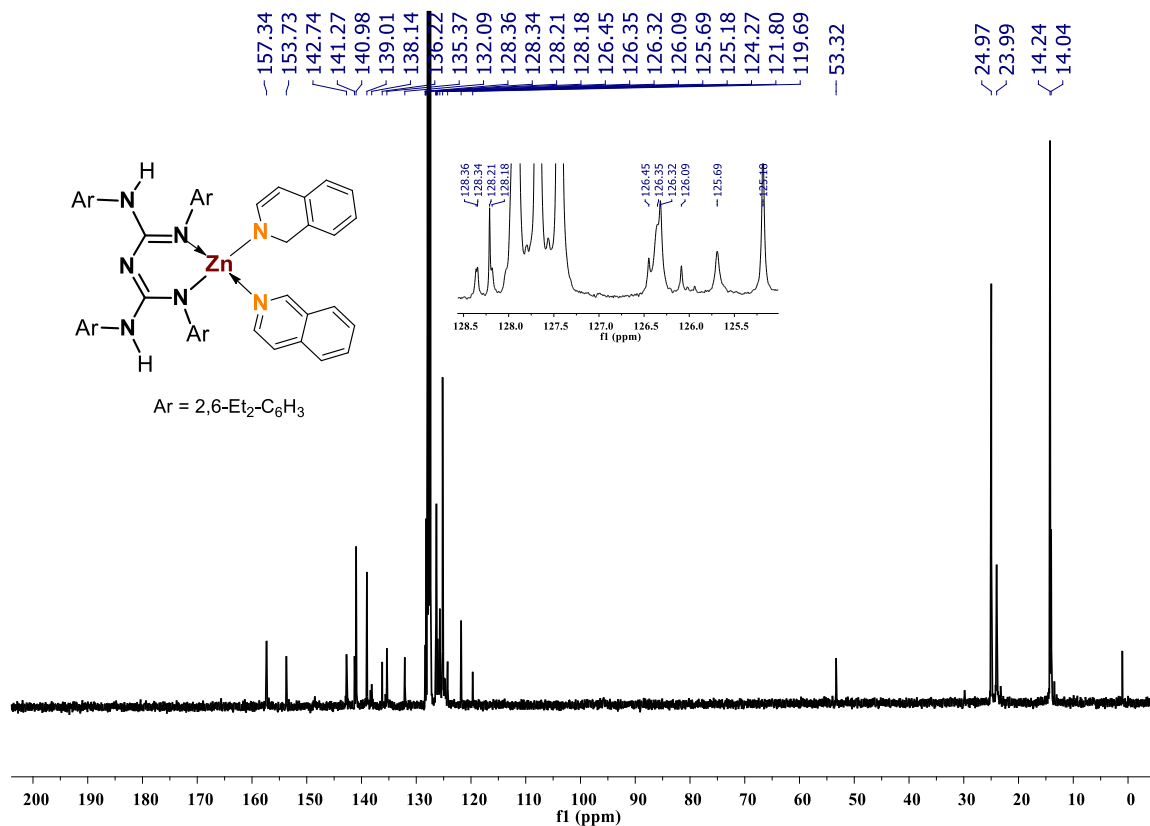


Figure 6.9. ¹³C{¹H} NMR (100 MHz, 25 °C, C₆D₆) spectrum of [LZn(1,2-DHiQ)(isoquinoline)], **III**.

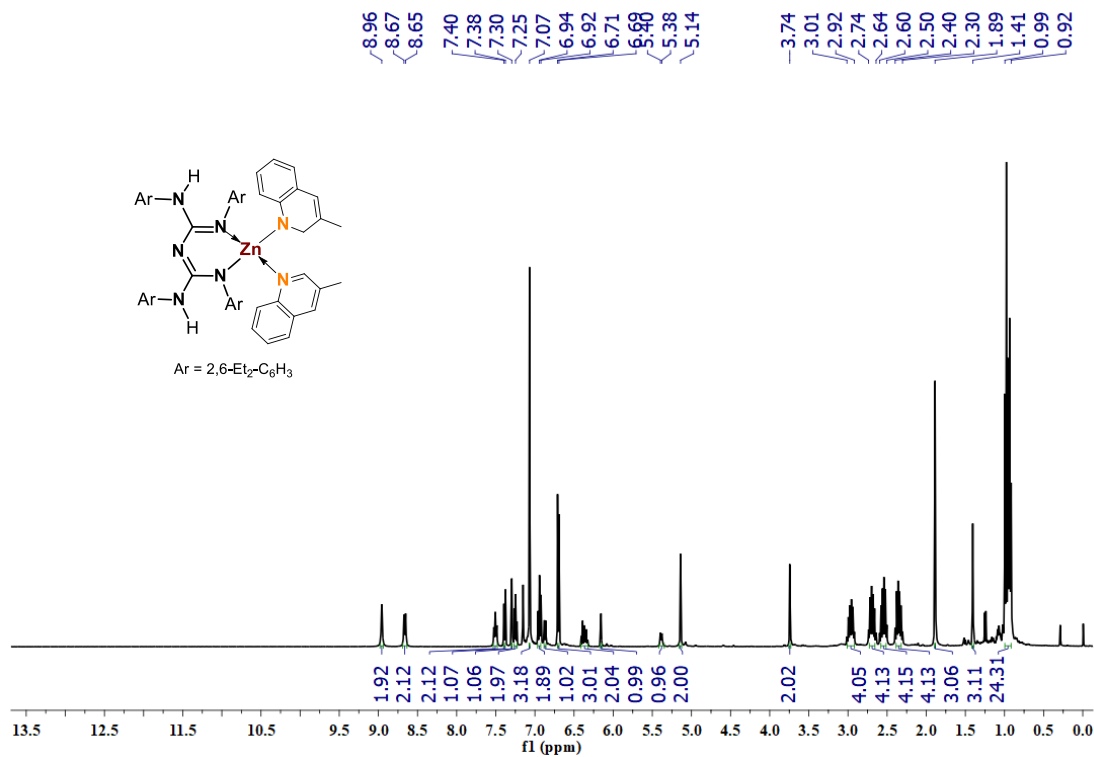


Figure 6.10. ¹H NMR (400 MHz, 25 °C, C₆D₆) spectrum of [LZn(1,2-3-MeDHQ)(3-Methylquinoline)], **(V)**.

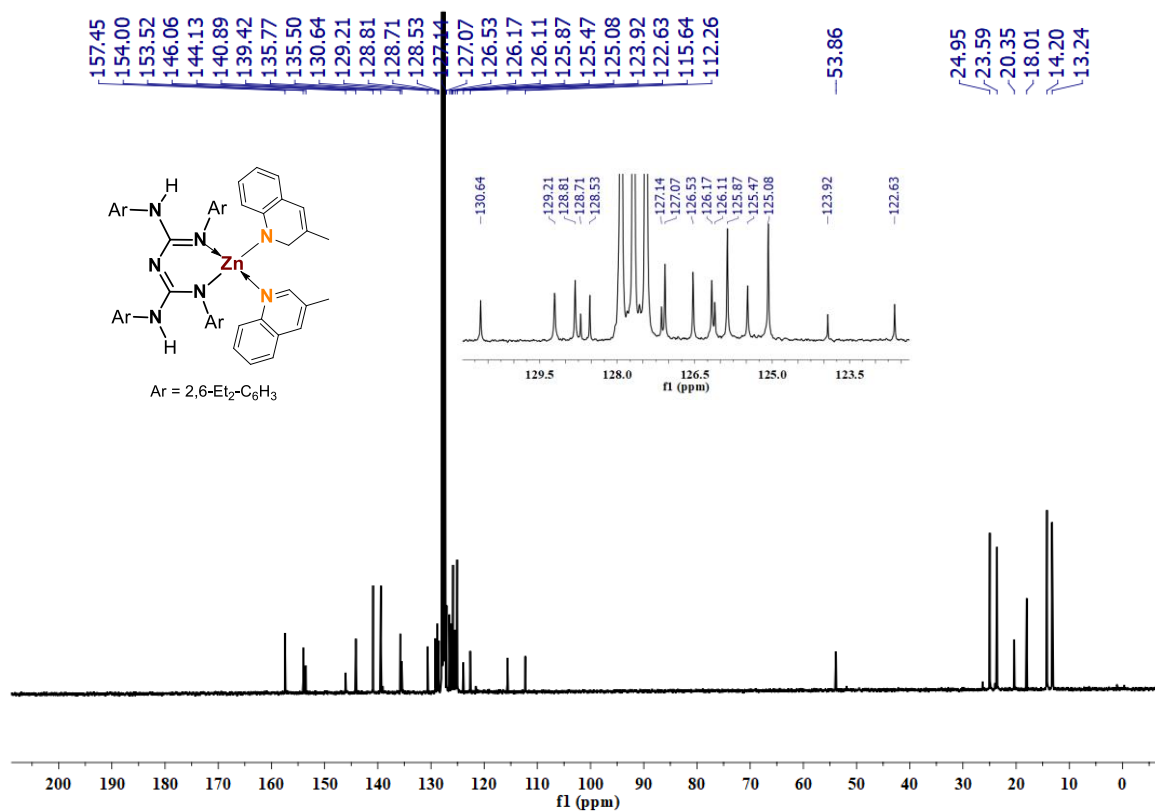


Figure 6.11. $^{13}\text{C}\{^1\text{H}\}$ NMR (100 MHz, 25 °C, C_6D_6) spectrum of $[\text{LZn}(1,2\text{-}3\text{-MeDHQ})]$ (3-Methylquinoline), (V).

Chapter 7

Comparison of Two Zinc Hydride Precatalysts for Selective Dehydrogenative Borylation of Terminal Alkynes: A Detailed Mechanistic Study

Published:

Sahoo, R. K.; Patro, A. G.; Sarkar, N.; Nembenna, S. *ACS Omega* **2023**, 8, 3452-3460.

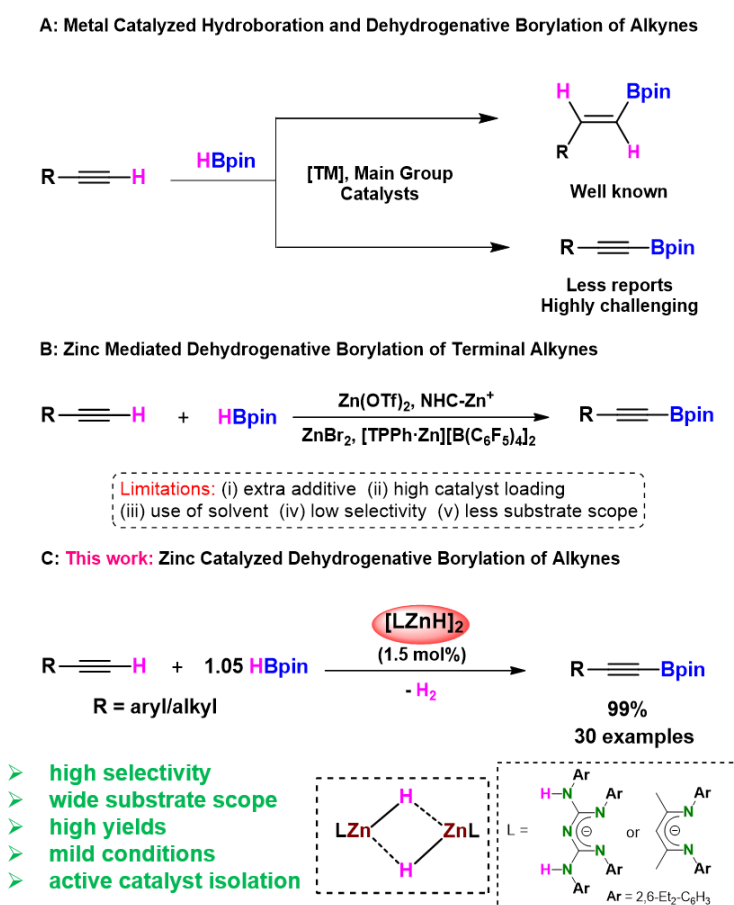
Abstract

The CBG stabilized zinc hydride complex (**I**) precatalyzed chemoselective dehydroborylation of a wide array of terminal alkynes with excellent yields is reported. Further, precatalyst **I** is compared with newly synthesized ^{Diethyl}NacNac zinc hydride precatalyst (**III**) for selective dehydroborylation of terminal alkynes, and it is discovered that precatalyst **I** is more active than **III**. We have studied intra and intermolecular chemoselective dehydroborylation of terminal alkynes over other reducible functionalities such as alkene, ester, isocyanide, nitro, and heterocycles. The highly efficient precatalyst **I** shows the TON, 48.5, and TOF up to 60.5 h⁻¹ in the dehydroborylation of 1-ethynyl-4-fluorobenzene (**1i**). A plausible mechanism for selective dehydrogenative borylation of alkynes has been proposed based on active catalysts isolation and a series of stoichiometric reactions.

7.1. Introduction

A selective dehydrogenative borylation of terminal alkyne produces ubiquitous organoborane products, which play an essential role in many chemical transformations.¹ It also provides valuable intermediates in organic and medicinal chemistry.² Because of its wide application, many methods have been developed to synthesize organoboranes.³ In conventional methods, organoboranes have been synthesized using stoichiometric amounts of organolithium and organomagnesium reagents.³⁻
⁴ The above methods suffer from the following drawbacks: poor functional group tolerance, safety issues, and large quantities of waste material. Therefore, hydroboration reactions using

pinacolborane (HBpin)⁵ or bis(pinacolato)diboron (B₂pin₂)⁶ are efficient routes for synthesizing precious organoborane compounds. As far as zinc-mediated hydroboration of alkynes to vinyl boronates is concerned, in 2013, the Uchiyama group reported hydroboration of alkyne by using diethylzinc and B₂pin₂.⁷ Besides, in 2019, Geetharani and coworkers described Zn(OTf)₂ and [Na][HBEt₃] catalyzed hydroboration of alkynes.^{5d} Compared to well-established hydroboration of alkynes using transition metals,^{5b, 6, 8} main group metal,^{5a, 5c, 5d, 9} and metal-free catalysts,¹⁰ there are fewer reports dehydrogenative borylation of terminal alkynes to alkynyl boronates (Scheme 7.1, A).



Scheme 7.1. Metal-catalyzed dehydroborylation of terminal alkynes.

Ozerov and coworkers revealed the first catalytic dehydrogenative borylation of terminal alkynes using the iridium-based catalyst.¹¹ Subsequently, transition (Cu,¹² Fe¹³) and main group (Al)¹⁴

metal-based catalysts have been utilized for the dehydrogenative borylations. Moreover, a few reports on zinc-mediated dehydrogenative borylation of terminal alkynes are also known in the literature. In 2015, Tsuchimoto and coworkers described $\text{Zn}(\text{OTf})_2$ catalyzed dehydrogenative borylation of terminal alkynes.¹⁵ In 2019, the Ingleson group showed the dehydrogenative borylation of terminal alkyne and hydroboration of alkynyl borate products using NHC zinc cation adducts.¹⁶

After that Ma group reported similar reactions using ZnBr_2 as a catalyst.¹⁷ During the preparation of our manuscript, Dobrovetsky and coworkers demonstrated the zinc cation, $[\text{TPPhZn}^{2+}][\text{B}(\text{C}_6\text{F}_5)_4]_2$ as a catalyst for dehydrogenative borylation and hydroboration of terminal alkynes.¹⁸ All those methods suffer from drawbacks such as high catalyst loading, additive usage, low selectivity, and limited substrate scope. Thus, synthesizing selective dehydrogenative borylation of terminal alkynes by applying an efficient catalyst under mild conditions is highly attractive.

Enhancing the catalytic activities of the molecular metal complex depends upon ligand design, including steric and electronic properties. The main advantage of choosing molecular catalysts is understanding the reaction mechanism by isolating the key intermediates and influencing the selectivity. In this context, molecular main group hydrides, including zinc hydrides, are used as catalysts for various organic transformations (Scheme 7.1, B).¹⁹ Very recently, our group reported conjugated bis-guanidinate (CBG) supported low oxidation state Zn–Zn bonded compounds, i.e., Cp^*ZnZnL and LZnZnL ($\text{Cp}^* = 1,2,3,4,5\text{-pentamethyl cyclopentadienide}$, and $\text{L} = \{(\text{ArNH})(\text{ArN})\text{--C=N--C=(NAr)(NHAr)}\}$; $\text{Ar} = 2,6\text{-Et}_2\text{-C}_6\text{H}_3$) as precatalysts for the dehydroborylation of terminal alkynes under mild condition.²⁰ However, both compounds were prepared by the previously reported zinc(I) dimer, $\text{Cp}^*\text{ZnZnCp}^*$ by Carmona in 2004.²¹

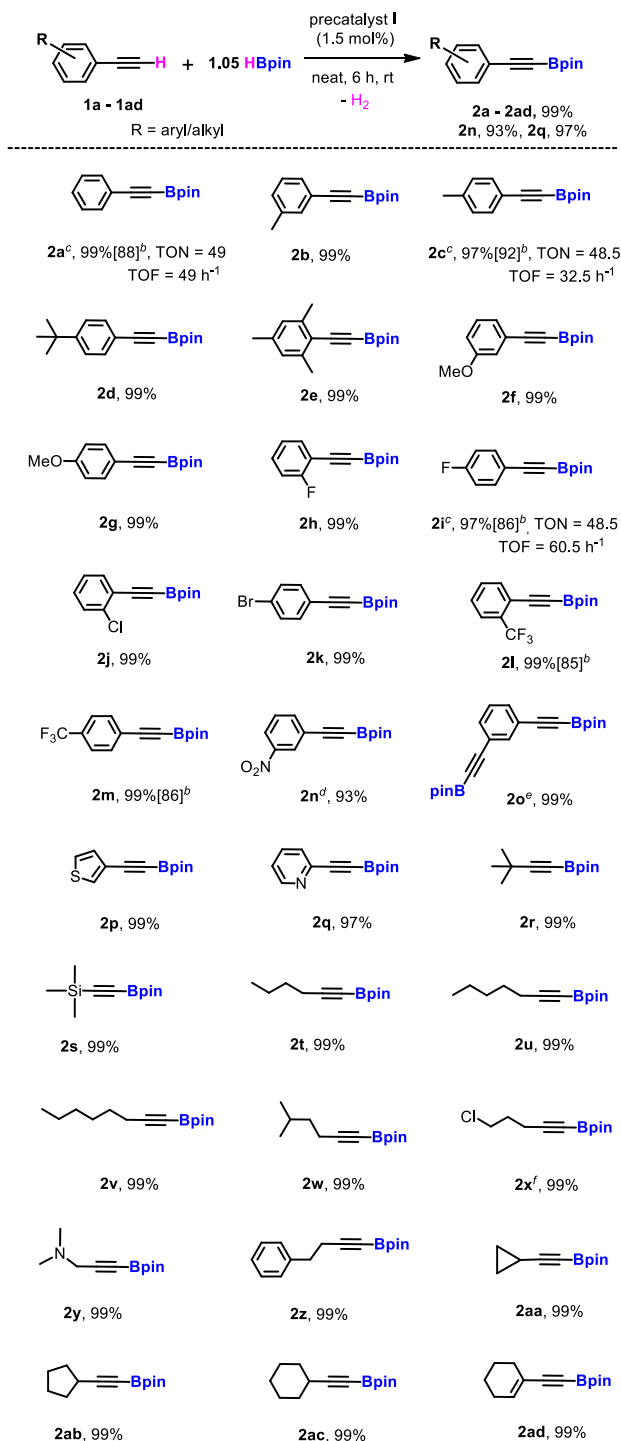
Considering the zinc hydride catalysis, we presumed that easily accessible molecular Zn(II) hydrides would be a better option for dehydroborylation of terminal alkynes. Surprisingly, there have been no reports of molecular zinc hydrides as precatalysts for selective dehydroborylation of terminal alkynes, except Ingleson's sole example.^{16a}

Thus, herein, we report the CBG zinc hydride (**I**) as a precatalyst for selective dehydroborylation of a broad range of terminal alkynes under mild conditions to afford the respective alkynyl boronate products. Further, we describe the isolation and structural characterization of the active catalysts CBG zinc alkynyl **II** and NacNac zinc alkynyl **IV** (Scheme 7.1, C) compounds. Moreover, the zinc hydride (**I**) is compared with NacNac zinc hydride (**III**) to understand the spectator ligand's role and catalytic efficiency and selectivity for the dehydroborylation of terminal alkynes for the first time.

7.2. Results and Discussion

Previously we synthesized the CBG zinc hydride compound **I**, [$\{L^1ZnH\}_2$; ($L^1 = \{(ArNH)(ArN)-C=N-C=(NAr)(NHAr)\}$; Ar = 2,6-Et₂-C₆H₃)], it can be accessed by the reaction of L^1ZnI with $KNH(iPr)BH_3$.^{22, 23} In addition, we published that compound **I** catalyzed the hydroboration of heteroallenes and carbonyl compounds.^{22, 23} As we mentioned, only a handful of examples documented the zinc-catalyzed dehydroborylation of terminal alkynes. Thus, herein we aimed to explore CBG zinc hydride (**I**) catalyzed dehydroborylation of terminal alkynes. Based on the NacNac-supported zinc(II) hydrides established by Roesky,²⁴ Harder^{19a} and other research groups,¹⁹ the corresponding diethyl NacNacZn(II) hydride (**III**) can be prepared in two steps. The reaction of $[L^2ZnEt]_2$ ²⁵ (DiethylNacNac (L^2) = CH{(CMe)(2,6-Et₂C₆H₃N)}₂) with 2.0 equiv. of I₂ in toluene produced $[L^2ZnI]_2$. A reaction between $[L^2ZnI]_2$ and 2.0 equiv. KH in toluene afforded $[L^2ZnH]_2$.

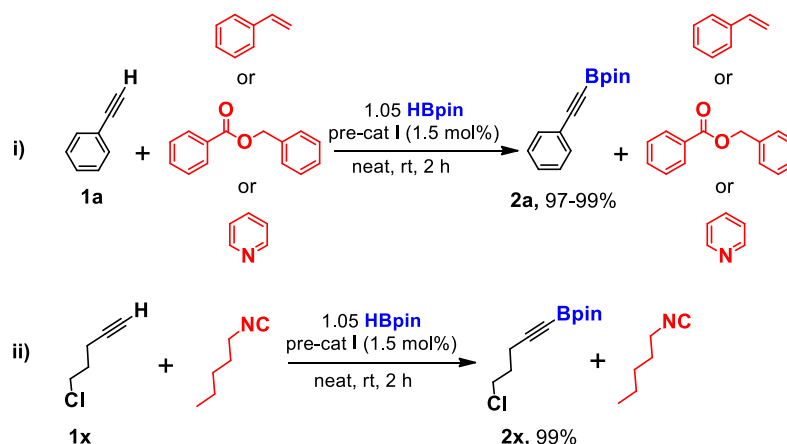
We began our investigation by taking 1:1.05 stoichiometric amounts of phenylacetylene and HBpin with 10 mol% of precatalyst **I** in a neat condition and gave quantitative conversion of borylated alkyne after 6 h at 60 °C.



Scheme 7.2. Dehydrogenative borylation of terminal alkynes catalyzed by [L¹ZnH]₂ precatalyst (**I**)^a

^aReaction conditions: terminal alkynes (0.3 mmol, 1.0 equiv.), pinacolborane (0.315 mmol, 1.05 equiv.), precatalyst **I** (1.5 mol%), at r.t under N₂. ^bPreparative –scale reaction: 1 mmol of terminal alkynes, precatalyst **I** (1.5 mol%), 1.05 mmol of HBpin, 6 h, rt. ^cFor **2a**, **2c**, and **2i** used 1 mol% precatalyst and stirred for 1 h, 1.5 h, and 0.8 h, respectively and the NMR yield was determined by ¹H NMR spectroscopy using mesitylene as the internal standard.. ^dFor **2n**, NMR yield was determined by ¹H NMR spectroscopy using mesitylene as the internal standard. ^eFor **2o**, pinacolborane (0.63 mmol, 2.1 equiv.) was used and stirred for 12 h. ^fFor **2x**, stirred for 2 h. Based on alkyne consumption, the NMR yield was determined by ¹H and ¹¹B NMR spectroscopy and identified the Bpin peak to confirm the product.

After that lowering the precatalyst loadings to 5.0, 3.0, 2.0, and 1.5 mol %, decreasing the temperature from 60 °C to room temperature after 6 h, gave quantitative conversion in neat conditions. Notably, 1 mol% precatalyst loading after 1 h gave a 98% yield, which shows the turnover number (TON), 49, and turnover frequency (TOF), 49 h⁻¹ (Table S1, entry 7/ Table 7.1, entry 1). However, further reduction of the catalyst loading to 0.5 mol % yielded low conversion (75%) (Table S1, entry 8). Moreover, the same reaction in benzene, toluene, and THF using 1.5 mol % of precatalyst **I** produced the desired product **2a** quantitatively. A negligible conversion was noticed in the absence of a precatalyst, **I**, which indicates that a zinc hydride complex is necessary for the dehydroborylation of terminal alkynes. A wide range of aryl, cyclic, and acyclic (long-chain) terminal alkyne substrates were investigated using optimized conditions. The various alkynes, including electron-donating (**1a–1g**) and withdrawing substituents (**1h–1n**), bis(ethynyl)benzene (**1o**), heterocycle systems (**1p** and **1q**), aliphatic alkynes including long-chain (**1r–1z**), and cyclic groups (**1aa–1ad**) were afforded selective alkynyl boronate products with high yields. Moreover, a substrate bearing an electron-donating group, 4-ethynyltoluene (**1c**), exhibits TON 48.5 and TOF 32.5 h⁻¹, while a substrate bearing an electron-withdrawing group, 1-ethynyl-4-fluorobenzene (**1i**), gives TON 48.5 and TOF 60.5 h⁻¹. All alkynyl borates (**2a–2ad**) were confirmed by multinuclear magnetic resonance (¹H, ¹³C{¹H}, and ¹¹B) and HRMS analyses (Scheme 7.2).



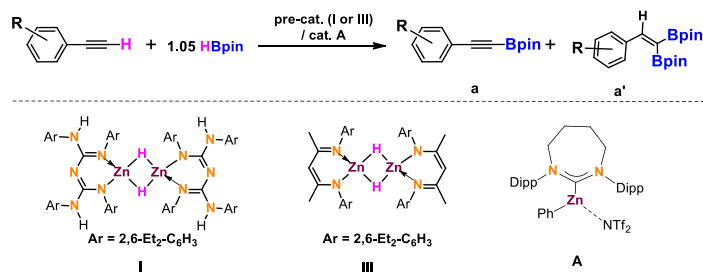
Scheme 7.3. Intermolecular chemoselective reactions.

Next, we decided to conduct some intermolecular chemoselective dehydroborylation of terminal alkynes. Accordingly, equimolar quantities of phenylacetylene, styrene, and HBpin were mixed with precatalyst **I** (1.5 mol%) under neat conditions for 2 h, which afforded the dehydroborylated product **2a** a quantitative yield in preference to styrene.

Likewise, phenylacetylene provided corresponding dehydrogenative borylated product **2a** at the same reaction conditions in a quantitative yield over benzyl benzoate or pyridine. Similarly, equimolar amounts of 5-chloro-1-pentyne (**1x**), 1-pentyl isocyanide and HBpin with 1.5 mol% precatalyst **I** for 2 h produced a corresponding dehydroborylated product (**2x**), in which isocyanide is untouched. We have noticed the excellent tolerance of alkene, ester, pyridine, and isocyanide functionalities in intermolecular chemoselective reactions (Scheme 7.3).

Phenylacetylene (**1a**), 4-ethynyltoluene (**1c**), and 1-ethynyl-4-fluorobenzene (**1i**) substrates were selected to screen the catalytic activity of zinc precatalysts **I**, **III**, and catalyst **A**.^{16b} The catalytic dehydroborylation of phenylacetylene (**1a**) was performed under mild conditions to produce high TON, 49, and TOF, 49 h⁻¹ compared to precatalyst **III** (TON, 35 and TOF, 35 h⁻¹), and catalyst **A** (TON, 16.8 and TOF, 3.4 h⁻¹) (Table 7.1 entries 1-3).

Table 7.1. Comparison of TON and TOF for dehydroborylation of terminal alkynes of selected substrates with precatalysts **I**, **III** and catalyst **A**.



Entry	Substrate	Cat.	Time (h)	Conv. (%)	a/a'	TON	TOF (h ⁻¹)
1	1a	I	1	98	99:<1	49	49
2	1a	III	1	70	98:2	35	35
3	1a	A	5	84	---	16.8	3.4
4	1c	I	1.5	97	99:<1	48.5	32.5
5	1c	III	1.5	70	98:2	35	23.5
6	1c	A	5	90	---	18	3.6
7	1i	I	0.8	97	99:<1	48.5	60.5
8	1i	III	0.8	76	97:3	38	47.5
9	1i	A	5	81	---	16.2	3.2

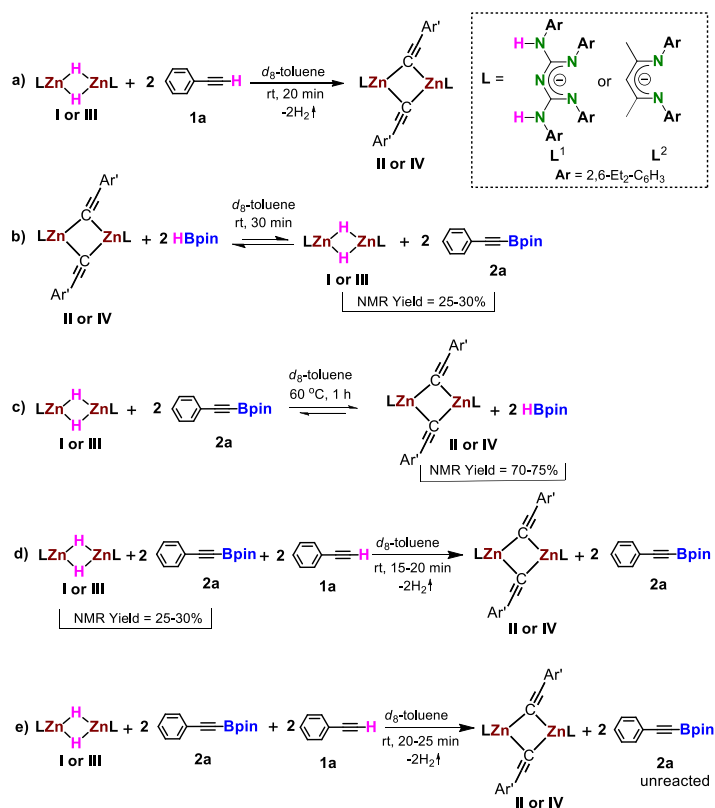
^aReaction conditions: alkyne (0.2 mmol, 1.0 equiv.), pinacolborane (0.21 mmol, 1.05 equiv.), precatalyst **I** or **III** (1 mol%), at r.t under N₂. The NMR yield was determined by ¹H NMR spectroscopy using mesitylene as the internal standard. TON and TOF were calculated for the conversion of product **a**. TON was calculated by dividing the number of moles of the product by the number of moles of catalyst used. TOF was determined by dividing TON by the reaction time. LZnH (**I**) and L'ZnH (**III**), calculating TON and TOF based on monomeric structures.

Similarly, for substrate 4-ethynyltoluene (**1c**), precatalyst **I** displayed a better TON, 48.5, and TOF, 32.5 h⁻¹ compared to precatalyst **III** (TON, 35 and TOF, 23.5 h⁻¹), and catalyst **A** (TON, 18 and TOF, 3.6 h⁻¹)^{16b} (Table 7.1, entries 4-6). Table 7.1, entries 7-9, indicate that compound **I** shows better catalytic performance (TON, 48.5 and TOF, 60.5 h⁻¹) than compound **III** (TON, 38 and TOF, 47.5 h⁻¹), and compound **A** (TON, 16.2 and TOF, 3.2 h⁻¹). As shown in Table 7.1, entries 1-

9, it is evident that precatalyst **I** exhibits better catalytic activity and selectivity than precatalyst **III** and the Ingleson catalyst **A**.

Moreover, we observed a mixture of dehydroborylation and 1,1-borylated products in the presence of precatalyst **III**. It should be noted that Ingleson's catalyst **A** also gave a mixture of products.^{16b} The 1,1-borylated products evidenced by ¹¹B NMR spectroscopy exhibit a characteristic signal in the range of 30-34 ppm. However, exclusively dehydroborylated products are formed in the case of compound **I** as a precatalyst.

We conducted a series of stoichiometric experiments to establish the mechanism of zinc-catalyzed dehydroborylation of terminal alkynes to a selective alkynyl borate product. A reaction between 1:2 stoichiometric amounts of precatalyst **I** and phenylacetylene afforded CBG zinc alkynyl complex (**II**) in *d*₈-toluene at rt after 20 minutes.

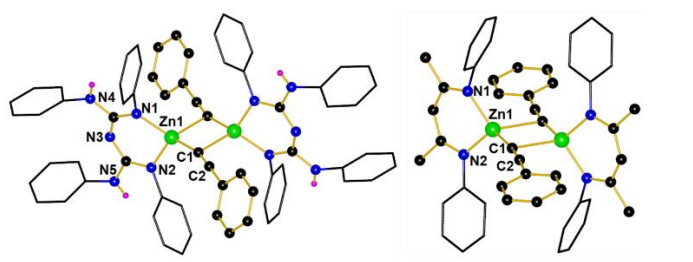


Scheme 7.4. Stoichiometric experiments for dehydroborylation of terminal alkynes

Compound **II** was characterized by NMR, HRMS, IR, and X-ray studies. The ^1H NMR spectrum shows the production of compound **II** by complete disappearances of alkynyl ' $\text{C}\equiv\text{C}-\text{H}$ ' and $\text{Zn}-\text{H}$ resonances (Scheme 7.4a). Next, catalyst **II** reacted with 2 equiv. of HBpin undergoes $\text{Zn}-\text{C} / \text{B}-\text{H}$ bond metathesis to give the desired dehydroboration product (**2a**) and precatalyst **I** with a 30% yield, which was observed by multinuclear NMR spectroscopy. The ^1H and ^{11}B NMR spectra indicate the formation of product **2a** by the appearance of new peaks at 1.03 and 24.5 ppm, corresponding to the *Bpin* moiety of product **2a**.

After prolonged heating up to 24 h at 80 °C showed no change in the relative ratio of **2a** and **II** (does not complete the reaction). It suggests that the equilibrium position has been reached before heating. The reaction mixture contains metathesis products **I**, **2a** and unreacted compound **II**, HBpin, at room temperature, confirming the equilibrium position.

Further, a reaction between compound **I** and **2a** has been performed in d_8 -toluene to confirm the reversible reaction. We noticed the formation of compound **II** with HBpin in 70% conversion, as shown by the characteristic peak of HBpin at 0.98 ppm in ^1H and 27.7 and 29.1 ppm in ^{11}B spectrum. However, $\text{Zn}-\text{H} / \text{C}-\text{B}$ metathesis reaction did not complete even after heating at 80 °C for 24 h; the same ratio of compound **II**: **2a** was observed (Scheme 7.4c). Finally, 2 equiv. of phenylacetylene was added to a J. Young valve NMR tube containing a mixture of compounds **I** and **2a** (30% conversion) in d_8 -toluene. After 15 minutes, the quantitative formation of compounds **2a** and **II** was observed. The ^1H NMR spectra confirm the formation of compound **II** and product **2a** (Scheme 7.4d). Next, equimolar quantities of compounds **I**, **1a** and **2a** were mixed in d_8 -toluene at room temperature for 20 minutes. We notice the exclusive formation of compound **II** (Scheme 7.4e). This study supports the above reactions.



Bond Parameters	Compound II	Compound IV
Zn1-N1 (Å)	1.9612(17)	1.984(4)
Zn1-N2 (Å)	1.9539(16)	1.988(4)
Zn1-C1 (Å)	2.026(2)	1.979(5)
C1-C2 (Å)	1.167(3)	1.213(7)
N1-Zn1-N2 (°)	94.82(7)	97.20(16)

Figure 7.1. Molecular structures of compounds **II** (left) and **IV** (right). All the ethyl groups and hydrogen atoms (except for H(4) and H(5) from structure **II**) are removed for clarity. Comparison of crystal parameters of compound **II** vs. **IV** (Selected bond lengths (Å) and angles (°)).

To further assess the reactivity of precatalysts **I** and **III**, the same stoichiometric experiments were performed with the NacNacZn system. Similarly, $\{L^*ZnH\}_2$ (**III**) reacts with phenylacetylene to produce compound **IV** via deprotonation. However, the metathesis of zinc-alkynyl (**IV**) species with HBpin yielded a 25% conversion (less conversion compared to CBG systems) of the dehydroboration product (**2a**).

Likewise, a reaction between complex **III** and compound **2a** in d_8 -toluene resulted in compound **IV** and HBpin with a 75% conversion. Thus, the subsequent reaction of a mixture of compounds **III** and **2a** with a 25% conversion with additional phenylacetylene (2.0 equiv) produces a quantitative conversion of compounds **2a** and **IV** along with 1,1-diborylated alkenes after 20 minutes (a slightly longer reaction time compared to CBG systems).

Further, we conducted additional stoichiometric experiments to confirm the relative ratio of alkynyl-Bpin and zinc alkynyl complexes (which are in equilibrium) via $^{19}F\{^1H\}$ NMR spectroscopy. The zinc hydride complexes (**I** or **III**) reacted with 4-

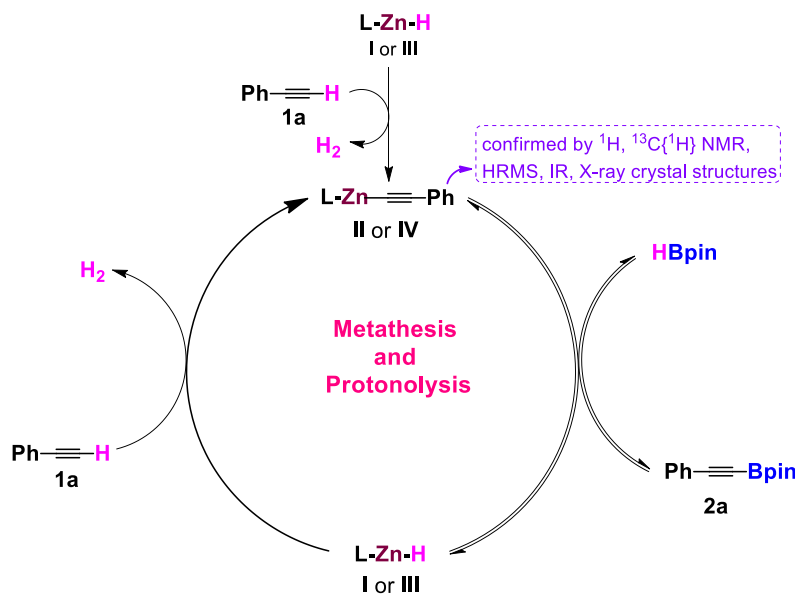
(trifluoromethyl)phenylacetylene (**1m**) afforded corresponding CBG zinc alkynyl complex (**II'**) or NacNac zinc alkynyl complex (**IV'**) in C₆D₆ at rt after 15 minutes. Further, catalyst **II'** reacted with 2 equiv. HBpin yielded the desired dehydroboration product (**2m**) and precatalyst **I** with a 20% conversion, followed by reacting with 2 equiv. of **1m** afforded the quantitative amounts of compounds **2m** and **II'**. However, catalyst **IV'** reacted with 2 equiv. of HBpin yielded the corresponding dehydroboration product (**2m**), precatalyst **III** with a 14% yield, and 1,1-diborylated alkenes product. When prolonged the heating the alkynylborates convert to the 1,1-diborylated alkenes. Moreover, the relative ratio between alkynyl-Bpin and zinc alkynyl complexes is confirmed by ¹⁹F{¹H} NMR spectroscopy. Hence, precatalyst **I** is more active and selective than **III**.

The zinc alkynyl compounds **II** and **IV** were crystallized from a benzene solution and structurally characterized. The solid-state structure of compound **II** or **IV** revealed that the distorted tetrahedral zinc atom is coordinated by two N atoms from the CBG or NacNac ligand and the other two sites from the C-atoms of bridged alkynyl moieties (Figure 7.1). The bond distance of Zn1-C1, 2.026(2) Å in compound **II** is significantly longer than the zinc-alkynyl bond distance of compound **IV**, 1.979(5) Å and NHC zinc-bis alkynyl complex (Zn-C = 1.969(4) and 1.959(4) Å). It suggests compound **II** is more active than compound **IV** and the zinc-bis alkynyl complex established by Ingleson. In contrast, the C1-C2 bond length, 1.167(3) Å of compound **II** is shorter compared to compound **IV**, 1.213(7) Å, and NHC zinc-bis alkynyl complex, 1.197(4) and 1.179(4) Å.^{16b} It revealed that compound **II** is more selective than compound **IV** and zinc-bis alkynyl complex to produce alkynyl boronates (Figure 7.1). Based on the above change in structural parameters (Figure 7.1), stoichiometric experiments data (Scheme 7.4) and comparison of TON and TOF in

Table 7.1 suggest that precatalyst **I** exhibits better catalytic activity and selectivity than precatalyst **III** and the NHC-zinc hydride complex (*vide supra*).^{16b}

Based on the isolation of active catalysts and a series of stoichiometric experiments, a plausible catalytic cycle has been proposed for zinc hydride precatalyzed selective dehydrogenative borylation of terminal alkynes to alkynyl borates. The catalytic cycle involves two steps: i) metathesis and ii) protonolysis. Initially, the zinc hydride complex reacts with the terminal alkyne formation of zinc alkynyl **II** or **IV**.

Next, either **II** or **IV** reacts with HBpin, affording the alkynyl borate and precatalyst LZnH (**I** or **III**) in an equilibrium position via Zn-C / B-H bond metathesis. Next, LZnH reacts with another molecule of terminal alkyne, gives the quantitative amount of corresponding alkynylborate product (**2a**) and regenerates the active catalyst (**II** or **IV**), and closes the catalytic cycle (Scheme 7.5).



Scheme 7.5. Proposed mechanism for the dehydroborylation of terminal alkynes.

7.3. Conclusion

The *N, N'*-chelated, and six-membered dimeric zinc hydride complexes **I** and **III** are used as precatalysts for dehydrogenative borylation of a wide array of terminal alkynes. CBG zinc hydride

I precatalyst is highly efficient and exceptionally selective compared to NacNac zinc hydride **III**. The precatalyst **I** shows excellent tolerance to several functional groups such as halide, alkene, ester, heterocycle, and isocyanide in intra and inter-molecular chemoselective reactions. Most importantly, we isolated and structurally characterized the active catalysts, zinc acetylides **II** and **IV**. Such examples are rare in the literature. The most plausible reaction mechanism has been established based on stoichiometric experiments. We are undertaking further reactivity studies of zinc acetylides and their catalytic applications in our laboratory.

7.4. Experimental Section

Unless stated, manipulations were performed under a dinitrogen atmosphere using standard glovebox and Schlenk techniques. NMR spectra were recorded on Jeol-400 MHz spectrometer and Bruker NMR spectrometers at 400 MHz (^1H), 101 MHz ($^{13}\text{C}\{^1\text{H}\}$), 128.3 MHz (^{11}B), and 377 MHz ($^{19}\text{F}\{^1\text{H}\}$). ^1H NMR and $^{13}\text{C}\{^1\text{H}\}$ NMR chemical shifts are referenced to residual protons or carbons in the deuterated solvent. ^{11}B were calibrated using an external reference of $\text{BF}_3\cdot\text{Et}_2\text{O}$. Multiplicities are reported as singlet (s), doublet (d), triplet (t), quartet (q), and multiplet (m). Chemical shifts are reported in ppm. Coupling constants are reported in Hz. The crystal data of compounds **II** and **IV** were collected on a Rigaku Oxford diffractometer with graphite-monochromated Cu-K α radiation ($\lambda = 1.54184 \text{ \AA}$) and Mo-K α radiation ($\lambda = 0.71073 \text{ \AA}$) respectively at 100 K. Selected data collection parameters, and other crystallographic results are summarized in Table 7.2. Mass spectrometry analyses were carried out on Bruker micrOTOF-Q II and Waters XevoG2 XS Q-TOF mass spectrometers. Infrared (IR) spectra were recorded in Thermo-Nicolet FT-IR spectrophotometers. The melting point of $[\text{L}^2\text{ZnI}]_2$, $[\text{L}^2\text{ZnH}]_2$, **II**, **III**, and **IV** were measured from Stuart SMP 10 instrument.

Solvents were purified by distillation over Na/ benzophenone. Deuterated chloroform (CDCl_3) was dried on molecular sieves, and benzene- d_6 (C_6D_6) was dried over Na/K alloy and distilled. The ligand $\text{L}^1(\text{H})$ ($\text{L}^1 = \{(\text{ArNH})(\text{ArN})-\text{C}=\text{N}-\text{C}=(\text{NAr})(\text{NHAr})\}$; $\text{Ar} = 2,6\text{-Et}_2\text{-C}_6\text{H}_3$)] and complex $\{\text{L}^1\text{ZnH}\}_2$ (**I**) are prepared according to reported literature procedures.^{19, 22-24} Complex $\{\text{L}^2\text{ZnEt}\}_2$ ($\text{L}^2 = \text{Diethyl}^1\text{NacNac}$) was prepared according to reported literature procedures.²⁵ For catalysis reactions, J. Young valve sealed NMR tubes or sealed reaction vials, as per the requirement, were properly oven-dried before being used. Chemicals and reagents were purchased from Sigma-Aldrich Co. Ltd., Merck India Pvt. Ltd., and TCI chemicals were used without purification.

Synthesis of $[\text{L}^1\text{ZnCC}(\text{C}_6\text{H}_5)]_2$, (II**) {Reaction-Scale}:** A solution of $[\text{L}^1\text{ZnH}]_2$ (**I**) 0.250 g (0.179 mmol) in 10 mL of toluene was added to 39.47 μL (0.359 mmol) of phenylacetylene in ~ 5 mL of toluene at room temperature through a cannula transfer and stirred for 2 h. The solvent was then removed in a vacuum, forming a white solid compound, and dried. The resultant solid was dissolved in benzene (~ 10 mL) and filtered. The filtered solution was stored at room temperature and gave block-shaped colorless crystals within two days. (0.240 g, 82 %); m.p. 190 – 195 $^\circ\text{C}$. ^1H NMR (400 MHz, C_6D_6) δ 7.29 – 7.27 (d, $J = 7.8$ Hz, 4H), 7.16 – 7.07 (m, 12H), 6.90 (t, $J = 7.7$ Hz, 4H), 6.85 – 6.81 (d, $^3J_{\text{HH}} = 13.1$ Hz, 6H), 6.65 – 6.63 (d, $^3J_{\text{HH}} = 7.6$ Hz, 8H), 5.07 (s, 4H), 3.18 – 3.09 (m, 8H), 2.77 – 2.67 (m, 8H), 2.40-2.31 (m, 8H), 2.21 – 2.11 (m, 8H), 1.38 (t, $^3J_{\text{HH}} = 7.5$ Hz, 24H), 0.96 (t, $^3J_{\text{HH}} = 7.5$ Hz, 24H). $^{13}\text{C}\{^1\text{H}\}$ NMR (101 MHz, C_6D_6) δ 157.5, 141.9, 141.1, 139.0, 135.0, 131.9, 128.1, 126.7, 126.6, 126.4, 126.0, 125.3, 101.7, 77.4, 24.9, 24.3, 14.5, 14.2. IR (Nujol mull) ν (cm^{-1}): 3024, 2883, 2811, 1996, 1495, 1416, 1327, 1260, 1203, 1091, 1018. HRMS (ASAP/Q-TOF) m/z : $[\text{M} + \text{H}]^+$ Calcd for $\text{C}_{50}\text{H}_{60}\text{N}_5\text{Zn}$ 794.4140, Found: 794.4146.

Synthesis of $[\text{L}^1\text{ZnCC}(\text{C}_6\text{H}_5)]_2$, (II**) {NMR-Scale}:** A solution of complex **I** (0.020 g, 25 $^\circ\text{C}$, 0.014 mmol) in a J. Young valve NMR tube was treated with phenylacetylene (3.07 μL , 0.028

mmol), at room temperature after 20 minutes resulted in the formation of compound **II** with the liberation of H₂ was observed by ¹H NMR spectroscopy. NMR Yield: (>99%). ¹H NMR (400 MHz, *d*₈-toluene) δ 7.24 – 7.15 (m, 5H), 7.09 – 7.01 (m, 8H), 6.97 – 6.90 (m, 5H), 6.87 – 6.79 (m, 8H), 6.61 – 6.59 (d, ³J_{HH} = 9.5 Hz, 8H), 5.04 (s, 4H), 3.18 – 3.01 (m, 8H), 2.78 – 2.63 (m, 8H), 2.37 – 2.26 (m, 8H), 2.22 – 2.11 (m, 8H), 1.38 (t, ³J_{HH} = 7.6 Hz, 24H), 0.95 (t, ³J_{HH} = 7.4 Hz, 24H). ¹³C{¹H} NMR (101 MHz, *d*₈-toluene) δ 157.5, 141.1, 139.0, 131.9, 131.8, 128.3, 128.0, 126.6, 126.3, 126.0, 125.3, 125.2, 77.2, 24.9, 24.3, 14.4, 14.2.

Synthesis of [L^IZnCC(4-CF₃C₆H₄)]₂, (II'**) {NMR-Scale}: A solution of complex **I** (0.020 g, 25 °C, 0.014 mmol) in a J. Young valve NMR tube was treated with 4-(trifluoromethyl)phenylacetylene (**1m**) (4.5 μL, 0.028 mmol), at room temperature after 15 minutes resulted in the formation of compound **II'** with the liberation of H₂ was observed by ¹H NMR spectroscopy. NMR Yield: (>99%). ¹H NMR (400 MHz, C₆D₆) δ 7.13 – 7.05 (m, 12H), 7.00 – 6.98 (d, ³J_{HH} = 8.2 Hz, 4H), 6.94 – 6.89 (m, 8H), 6.66 – 6.64 (d, ³J_{HH} = 7.6 Hz, 8H), 5.07 (s, 4H), 3.17 – 3.08 (m, 8H), 2.76 – 2.67 (m, 8H), 2.40 – 2.30 (m, 8H), 2.21 – 2.11 (m, 8H), 1.39 (t, ³J_{HH} = 7.5 Hz, 24H), 0.96 (t, ³J_{HH} = 7.5 Hz, 24H). ¹³C{¹H} NMR (101 MHz, C₆D₆) δ 157.6, 141.7, 141.1, 139.0, 134.9, 131.9, 126.9, 126.5, 126.2, 125.3, 124.5, 124.5, 124.5, 124.4, 107.7, 105.6, 24.9, 24.4, 14.6, 14.2. ¹⁹F{¹H} NMR (377 MHz, C₆D₆) δ – 62.41. HRMS (ASAP/Q-TOF) *m/z*: [M + H]⁺ Calcd for C₅₁H₅₉F₃N₅Zn 862.4014, Found: 862.4054.**

Synthesis of [L²ZnI]₂: 1 g (1.10 mmol) of [L²ZnEt]₂ dissolved in ~20 mL of dry toluene. Also, 0.56 g (2.20 mmol) of iodine was dissolved in ~10 mL of dry toluene in another Schlenk tube. Then, the iodine solution was added dropwise to the [L²ZnEt]₂ solutions. The reaction mixture was stirred for 12 h; a pale yellow solution was observed during this period. The solution was filtered and evaporated in a high vacuum to get compound [L²ZnI]₂. (0.855 g, 71 %); m.p. 220 – 225 °C.

^1H NMR (400 MHz, CDCl_3) δ 7.05 – 6.99 (m, 6H), 4.98 (s, 1H), 2.52 – 2.35 (m, 8H), 1.70 (s, 6H), 1.12 (t, $J = 7.5$ Hz, 12H). $^{13}\text{C}\{^1\text{H}\}$ NMR (101 MHz, CDCl_3) δ 169.2, 144.2, 136.8, 126.2, 125.6, 95.5, 24.7, 23.5, 14.3. HRMS (ASAP/Q-TOF): m/z Calcd for $\text{C}_{25}\text{H}_{34}\text{IN}_2\text{Zn}$: 553.1058 $[\text{M}+\text{H}]^+$; Found: 553.1049.

Synthesis of $[\text{L}^2\text{ZnH}]_2$, (III): $[\text{L}^2\text{ZnI}]_2$ (1.5 g, 1.36 mmol) and KH (0.06 g, 1.43 mmol) were weighed individually, and both were taken in a Schlenk tube in a glove box under nitrogen conditions. The Schlenk tube was placed in an ice bath, and 20 mL of dry THF was added. Then the reaction mixture was allowed to achieve ambient temperature, followed by stirring at room temperature for 18 h. After evaporation of the solvent under vacuum, the residue was dissolved in toluene (20 mL). The solution was filtered off from precipitated KI and evaporated in a high vacuum to get compound **III**. (890 g, 77 %); m.p. 210 – 215 °C. ^1H NMR (700 MHz, d_8 -toluene) δ 7.02 – 6.99 (m, 12H), 4.93 (s, 2H), 4.26 (s, 2H), 2.60 – 2.55 (m, 8H), 2.45 – 2.39 (m, 8H), 1.59 (s, 12H), 1.16 (t, $J = 7.6$ Hz, 24H). $^{13}\text{C}\{^1\text{H}\}$ NMR (176 MHz, d_8 -toluene) δ 167.2, 146.1, 137.0, 126.4, 125.2, 95.5, 24.7, 22.7, 14.3. IR (Nujol mull) ν (cm^{-1}): 3206, 3018, 3005, 2988, 2833, 2807, 1491, 1470, 1466, 1465, 1401, 1395, 1373. HRMS (ASAP/Q-TOF): m/z Calcd for $\text{C}_{25}\text{H}_{35}\text{N}_2\text{Zn}$: 427.2092 $[\text{M}+\text{H}]^+$; Found: 427.2066.

Synthesis of $[\text{L}^2\text{ZnCC}(\text{C}_6\text{H}_5)]_2$, (IV) {Reaction-Scale}: A solution of $[\text{L}^2\text{ZnH}]_2$ (**III**) 0.250 g (0.293 mmol) in 10 mL of toluene was added to 64.35 μL (0.586 mmol) of phenylacetylene in ~5 mL toluene at room temperature through a cannula transfer and stirred for 2 h. The solvent was then removed in a vacuum, forming a white solid compound and drying thoroughly. The resultant solid was dissolved in benzene (~10 mL) and filtered. The filtered solution was stored at room temperature and gave block-shaped colorless crystals within three days. (0.245 g, 80 %); m.p. 185 – 190 °C. ^1H NMR (400 MHz, C_6D_6) δ 7.09 – 7.06 (m, 4H), 6.96 – 6.93 (m, 12H), 6.69 – 6.63 (m,

6H), 4.80 (s, 2H), 2.57 – 2.48 (m, 8H), 2.40 – 2.30 (m, 8H), 1.46 (s, 12H), 1.09 (t, $J = 7.6$ Hz, 24H). $^{13}\text{C}\{^1\text{H}\}$ NMR (101 MHz, C_6D_6) δ 168.1, 145.5, 136.8, 132.0, 131.9, 128.1, 127.5, 126.5, 125.4, 105.8, 95.5, 77.4, 24.7, 22.8, 14.3. IR (Nujol mull) ν (cm^{-1}): 3410, 2962, 2724, 2669, 2322, 1802, 1580, 1467, 1467, 1369, 1259, 1228, 1162, 1020. HRMS (ASAP/Q-TOF) m/z : $[\text{M} + \text{H}]^+$ Calcd for $\text{C}_{33}\text{H}_{39}\text{N}_2\text{Zn}$ 527.2405, Found: 527.2444.

Synthesis of $[\text{L}^2\text{ZnCC}(\text{C}_6\text{H}_5)]_2$, (IV) {NMR-Scale}: A solution of complex **III** (0.020 g, 25 °C, 0.023 mmol) in a J. Young valve NMR tube was treated with phenylacetylene (5.15 μL , 0.047 mmol), at room temperature after 20 minutes resulted in the formation of compound **IV** with the liberation of H_2 was observed by ^1H NMR spectroscopy. NMR Yield: (>99%). ^1H NMR (700 MHz, d_8 -toluene) δ 7.15 – 7.12 (m, 4H), 7.03 – 7.01 (m, 12H), 6.82 – 6.78 (m, 6H), 4.91 (s, 2H), 2.64 – 2.58 (m, 8H), 2.49 – 2.44 (m, 8H), 1.58 (s, 12H), 1.21 (t, $J = 7.6$ Hz, 24H). $^{13}\text{C}\{^1\text{H}\}$ NMR (176 MHz, d_8 -toluene) δ 167.2, 146.1, 136.6, 127.4, 126.4, 125.2, 95.5, 24.7, 22.7, 14.3.

Synthesis of $[\text{L}^2\text{ZnCC}(4\text{-CF}_3\text{C}_6\text{H}_4)]_2$, (IV') {NMR-Scale}: A solution of complex **III** (0.020 g, 25 °C, 0.023 mmol) in a J. Young valve NMR tube was treated with 4-(trifluoromethyl)phenylacetylene (7.6 μL , 0.047 mmol), at room temperature after 15 minutes resulted in the formation of compound **IV'** with the liberation of H_2 was observed by ^1H NMR spectroscopy. NMR Yield: (>99%). ^1H NMR (400 MHz, C_6D_6) δ 7.06 (m, 14H), 6.92 – 6.91 (d, $^3J_{\text{HH}} = 3.0$ Hz, 6H), 4.94 (s, 2H), 2.68 – 2.59 (m, 8H), 2.49 – 2.40 (m, 8H), 1.59 (s, 12H), 1.21 (t, $^3J_{\text{HH}} = 7.5$ Hz, 24H). $^{13}\text{C}\{^1\text{H}\}$ NMR (101 MHz, C_6D_6) δ 168.3, 145.4, 136.8, 131.9, 126.6, 125.6, 124.5, 124.4, 124.4, 124.4, 107.4, 95.7, 24.8, 22.8, 14.4. $^{19}\text{F}\{^1\text{H}\}$ NMR (377 MHz, C_6D_6) δ – 62.41. HRMS (ASAP/Q-TOF) m/z : $[\text{M} + \text{H}]^+$ Calcd for $\text{C}_{34}\text{H}_{38}\text{F}_3\text{N}_2\text{Zn}$ 595.2278, Found: 595.2230.

7.4.1. X-ray Crystallographic Data

The single crystals of compounds **II** and **IV** were crystallized from Benzene at rt as colorless blocks after 2 d. The crystal data of compounds **II** and **IV** were collected on a Rigaku Oxford diffractometer with graphite-monochromated Cu-K α radiation ($\lambda = 1.54184$ Å) and Mo-K α radiation ($\lambda = 0.71073$ Å) respectively at 100 K. Selected data collection parameters, and other crystallographic results are summarized in Table 7.2. The structure was determined using direct methods employed in *ShelXT*,³⁰ *Olex*,³¹ and refinement was carried out using least-square minimization implemented in *ShelXL*.³² All non-hydrogen atoms were refined with anisotropic displacement parameters. Hydrogen atom positions were fixed geometrically in idealized positions and were refined using a riding model.

Table 7.2. Crystallographic data and refinement parameters for compounds **II** and **IV**.

Compound	II	IV
Empirical Formula	C ₁₀₀ H ₁₁₈ N ₁₀ Zn ₂ 2 (C ₆ H ₆)	C ₆₆ H ₇₆ N ₄ Zn ₂
CCDC	2177018	2177019
Molecular mass	1746.99	1056.16
Temperature (K)	100	100
Wavelength (Å)	1.54184	0.71073
Size(mm)	0.2×0.18×0.17	0.2×0.18×0.17
Crystal system	triclinic	monoclinic
Space group	P -1	P2 ₁ /c
a (Å)	12.0811(3)	17.8516(6)
b (Å)	13.0427(3)	18.4478(7)
c (Å)	16.7425(4)	16.8605(5)
α (deg)°	83.465(2)	90
β (deg)°	86.107(2)	94.032(3)
γ (deg)°	63.721(2)	90
Volume (Å ³)	2349.64(10)	5538.8(3)
Z	1	4
Calculated density (g/cm ³)	1.235	1.2664
Absorption coefficient (mm ⁻¹)	1.041	0.911
F(000)	932.0	2243.1
Theta range for data collection (deg)°	7.592 to 136.478	6.8 to 50.7
Limiting indices	-14 ≤ h ≤ 14, -15 ≤ k ≤ 15, -20 ≤ l ≤ 19	-25 ≤ h ≤ 23, -25 ≤ k ≤ 23, -23 ≤ l ≤ 23
Reflections collected	34507	47199
Independent reflections	8567 [R _{int} = 0.0358, R _{sigma} = 0.0252]	10002 [R _{int} = 0.0776, R _{sigma} = 0.0828]
Completeness to theta	99 %	99 %
Absorption correction	Empirical	Empirical
Data/restraints/parameters	8567 / 7 / 567	10002 / 0 / 661
Goodness – of–fit on F ²	1.016	1.161
Final R indices [I>2 sigma(I)]	R ₁ = 0.0452, wR ₂ = 0.1218	R ₁ = 0.0600, wR ₂ = 0.1655

7.5. Appendix: All general experimental information, stoichiometric reactions, analytical data, and spectral data were available in published paper. *ACS Omega* **2023**, 8, 3452-3460.

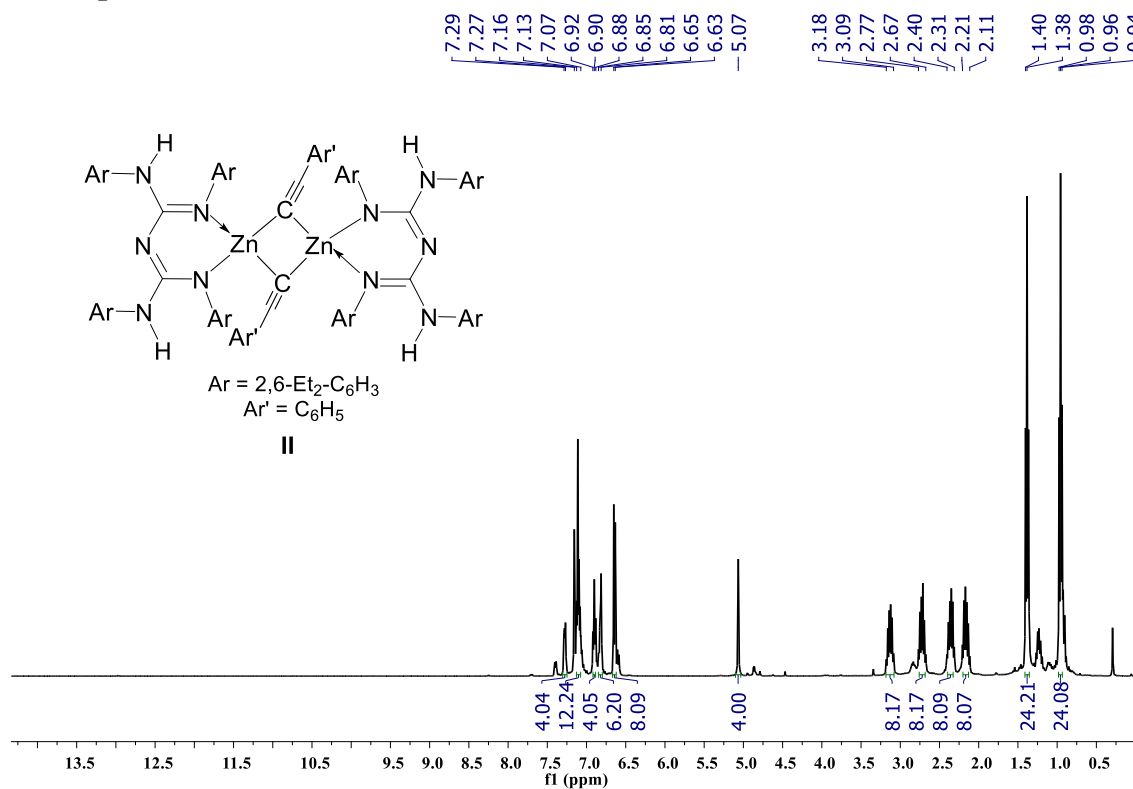
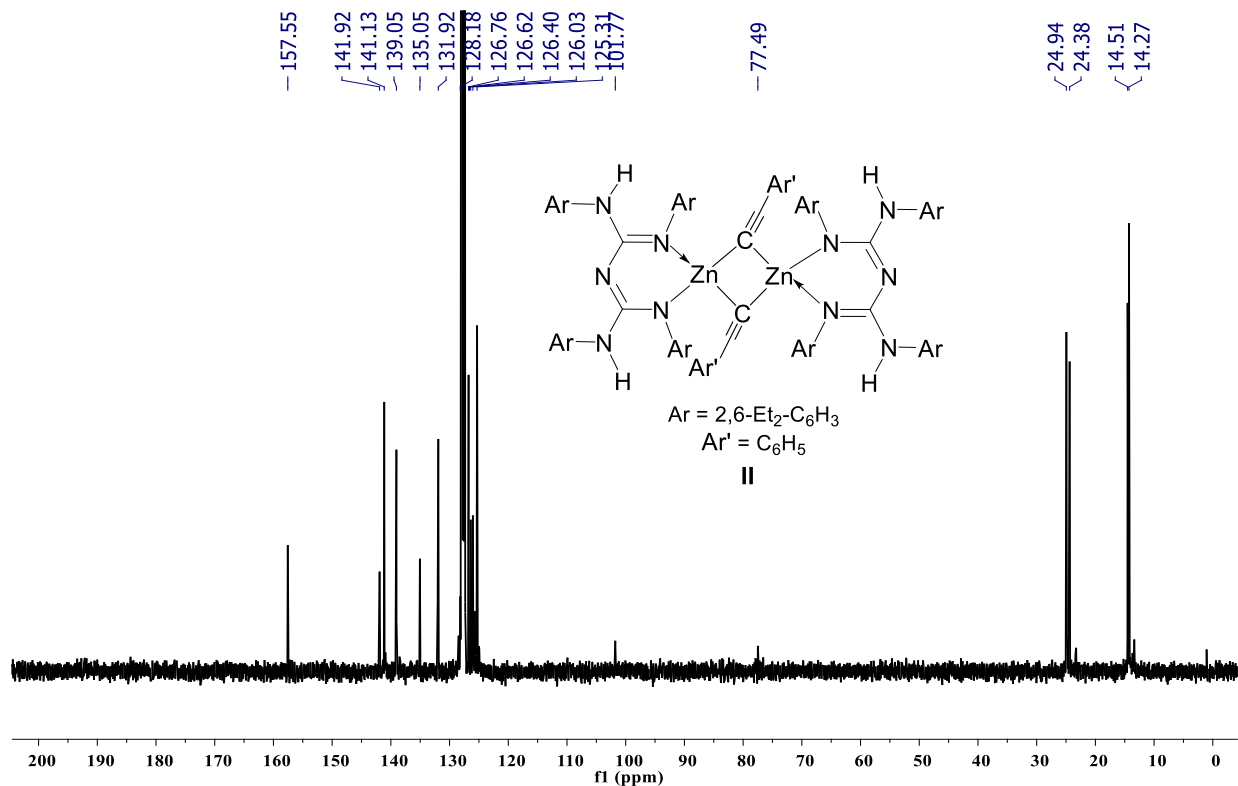
7.6. References

1. (a) Suzuki, A. *Angew. Chem., Int. Ed.* **2011**, *50*, 6722–6737; (b) Lennox, A. J. J.; Lloyd-Jones, G. C. *Chem. Soc. Rev.* **2014**, *43*, 412–443; (c) Hartwig, J. F. *Acc. Chem. Res.* **2012**, *45*, 864–873.
2. Pécharman, A.-F.; Colebatch, A. L.; Hill, M. S.; McMullin, C. L.; Mahon, M. F.; Weetman, C. *Nat. Commun.* **2017**, *8*, 15022.
3. (a) Mkhalid, I. A. I.; Barnard, J. H.; Marder, T. B.; Murphy, J. M.; Hartwig, J. F. *Chem. Rev.* **2010**, *110*, 890–931; (b) Bose, S. K.; Mao, L.; Kuehn, L.; Radius, U.; Nekvinda, J.; Santos, W. L.; Westcott, S. A.; Steel, P. G.; Marder, T. B. *Chem. Rev.* **2021**, *121*, 13238–13341; (c) Tian, Y.-M.; Guo, X.-N.; Braunschweig, H.; Radius, U.; Marder, T. B. *Chem. Rev.* **2021**, *121*, 3561–3597.
4. Brown, H. C.; Bhat, N. G.; Srebnik, M. *Tetrahedron Lett.* **1988**, *29*, 2631–2634.
5. (a) Magre, M.; Maity, B.; Falconnet, A.; Cavallo, L.; Rueping, M. *Angew. Chem., Int. Ed.* **2019**, *58*, 7025–7029; (b) Chen, J.; Shen, X.; Lu, Z. *Angew. Chem., Int. Ed.* **2021**, *60*, 690–694; (c) Li, J.; Luo, M.; Sheng, X.; Hua, H.; Yao, W.; Pullarkat, S. A.; Xu, L.; Ma, M. *Org. Chem. Front.* **2018**, *5*, 3538–3547; (d) Mandal, S.; Mandal, S.; Geetharani, K. *Chem. Asian J.* **2019**, *14*, 4553–4556; (e) Aelterman, M.; Sayes, M.; Jubault, P.; Poisson, T. *Chem. Eur. J.* **2021**, *27*, 8277–8282.
6. (a) Zhong, M.; Gagné, Y.; Hope, T. O.; Pannecoucke, X.; Frenette, M.; Jubault, P.; Poisson, T. *Angew. Chem., Int. Ed.* **2021**, *60*, 14498–14503; (b) Bose, S. K.; Fucke, K.; Liu, L.; Steel, P. G.; Marder, T. B. *Angew. Chem. Int. Ed.* **2014**, *53*, 1799–1803; (c) Neeve, E. C.; Geier, S. J.; Mkhalid, I. A. I.; Westcott, S. A.; Marder, T. B. *Chem. Rev.* **2016**, *116*, 9091–9161; (d) Hemming, D.; Fritzemeier, R.; Westcott, S. A.; Santos, W. L.; Steel, P. G. *Chem. Soc. Rev.* **2018**, *47*, 7477–7494.

-
7. Nagashima, Y.; Takita, R.; Yoshida, K.; Hirano, K.; Uchiyama, M. *J. Am. Chem. Soc.* **2013**, *135*, 18730–18733.
 8. Guo, J.; Cheng, Z.; Chen, J.; Chen, X.; Lu, Z. *Acc. Chem. Res.* **2021**, *54*, 2701–2716.
 9. Sarkar, N.; Bera, S.; Nembenna, S. *J. Org. Chem.* **2020**, *85*, 4999–5009.
 10. Fontaine, F.-G.; Rochette, É. *Acc. Chem. Res.* **2018**, *51*, 454–464.
 11. Lee, C.-I.; Zhou, J.; Ozerov, O. V. *J. Am. Chem. Soc.* **2013**, *135*, 3560–3566.
 12. (a) Romero, E. A.; Jazzar, R.; Bertrand, G. *Chem. Sci.* **2017**, *8*, 165–168. (b) Liu, X.; Ming, W.; Zhang, Y.; Friedrich, A.; Marder, T. B. *Angew. Chem., Int. Ed.* **2019**, *58*, 18923–18927.
 13. Wei, D.; Carboni, B.; Sortais, J.-B.; Darcel, C. *Adv. Synth. Catal.* **2018**, *360*, 3649–3654.
 14. Willcox, D. R.; De Rosa, D. M.; Howley, J.; Levy, A.; Steven, A.; Nichol, G. S.; Morrison, C. A.; Cowley, M. J.; Thomas, S. P. *Angew. Chem., Int. Ed.* **2021**, *60*, 20672–20677.
 15. Tsuchimoto, T.; Utsugi, H.; Sugiura, T.; Horio, S. *Adv. Synth. Catal.* **2015**, *357*, 77–82.
 16. (a) Uzelac, M.; Yuan, K.; Ingleson, M. J. *Organometallics* **2020**, *39*, 1332–1338. (b) Procter, R. J.; Uzelac, M.; Cid, J.; Rushworth, P. J.; Ingleson, M. J. *ACS Catal.* **2019**, *9*, 5760–5771.
 17. Luo, M.; Qin, Y.; Chen, X.; Xiao, Q.; Zhao, B.; Yao, W.; Ma, M. *J. Org. Chem.* **2021**, *86*, 16666–16674.
 18. Jaiswal, K.; Groutchik, K.; Bawari, D.; Dobrovetsky, R. *ChemCatChem* **2022**, *14*, e202200004.
 19. (a) Spielmann, J.; Piesik, D.; Wittkamp, B.; Jansen, G.; Harder, S. *Chem. Commun.* **2009**, 3455–3456. (b) Bose, S. K.; Deibenberger, A.; Eichhorn, A.; Steel, P. G.; Lin, Z.; Marder, T. B. *Angew. Chem., Int. Ed.* **2015**, *54*, 11843–11847. (c) Roy, M. M. D.; Omaña, A. A.; Wilson, A. S. S.; Hill, M. S.; Aldridge, S.; Rivard, E. *Chem. Rev.* **2021**, *121*, 12784–12965. (d) Wiegand, A.-K.; Rit, A.; Okuda, J. *Coord. Chem. Rev.* **2016**, *314*, 71–82. (e) Bayram, M.;

- Gondzik, S.; Bläser, D.; Wölper, C.; Schulz, S. *Z. Anorg. Allg. Chem.* **2016**, 642, 847–852. (f)
- Coles, M. P.; El-Hamruni, S. M.; Smith, J. D.; Hitchcock, P. B. *Angew. Chem., Int. Ed.* **2008**, 47, 10147–10150. (g) Bose, S. K.; Marder, T. B. *Org. Lett.* **2014**, 16, 4562–4565.
20. Sahoo, R. K.; Rajput, S.; Patro, A. G.; Nembenna, S. *Dalton Trans.* **2022**, 51, 16009–16016.
21. Resa, I.; Carmona, E.; Gutierrez-Puebla, E.; Monge, A. *Science* **2004**, 305, 1136–1138.
22. (a) Sahoo, R. K.; Sarkar, N.; Nembenna, S. *Angew. Chem., Int. Ed.* **2021**, 60, 11991–12000; (b) Sahoo, R. K.; Mahato, M.; Jana, A.; Nembenna, S. *J. Org. Chem.* **2020**, 85, 11200–11210.
23. Peddaraao, T.; Baishya, A.; Sarkar, N.; Acharya, R.; Nembenna, S. *Eur. J. Inorg. Chem.* **2021**, 2034–2046.
24. Hao, H.; Cui, C.; Roesky, H. W.; Bai, G.; Schmidt, H.-G.; Noltemeyer, M. *Chem. Commun.* **2001**, 1118–1119.
25. Cheng, M.; Moore, D. R.; Reczek, J. J.; Chamberlain, B. M.; Lobkovsky, E. B.; Coates, G. W. *J. Am. Chem. Soc.* **2001**, 123, 8738–8749.
26. Hu, J.-R.; Liu, L.-H.; Hu, X.; Ye, H.-D. *Tetrahedron* **2014**, 70, 5815–5819.
27. Desrosiers, V.; Garcia, C. Z.; Fontaine, F.-G. *ACS Catal.* **2020**, 10, 11046–11056.
28. Ho, H. E.; Asao, N.; Yamamoto, Y.; Jin, T. *Org. Lett.* **2014**, 16, 4670–4673.
29. Foley, B. J.; Bhuvanesh, N.; Zhou, J.; Ozerov, O. V. *ACS Catal.* **2020**, 10, 9824–9836.
30. Sheldrick, G. *Acta Crystallogr. C.* **2015**, 71, 3–8.
31. Dolomanov, O. V.; Bourhis, L. J.; Gildea, R. J.; Howard, J. A. K.; Puschmann, H. *J. Appl. Crystallogr.* **2009**, 42, 339–341.
32. (a) Sheldrick, G. M. *Acta Crystallogr., Sect. A: Found. Crystallogr.* **2008**, 64, 112–122; (b) Sheldrick, G. M. *Acta Crystallogr., Sect. A: Found. Adv.* **2015**, 71, 3–8.

NMR spectra

Figure 7.2. ^1H NMR (400 MHz, 25 °C, C_6D_6) spectrum of compound **II**.Figure 7.3. $^{13}\text{C}\{^1\text{H}\}$ NMR (100 MHz, 25 °C, C_6D_6) spectrum of compound **II**.

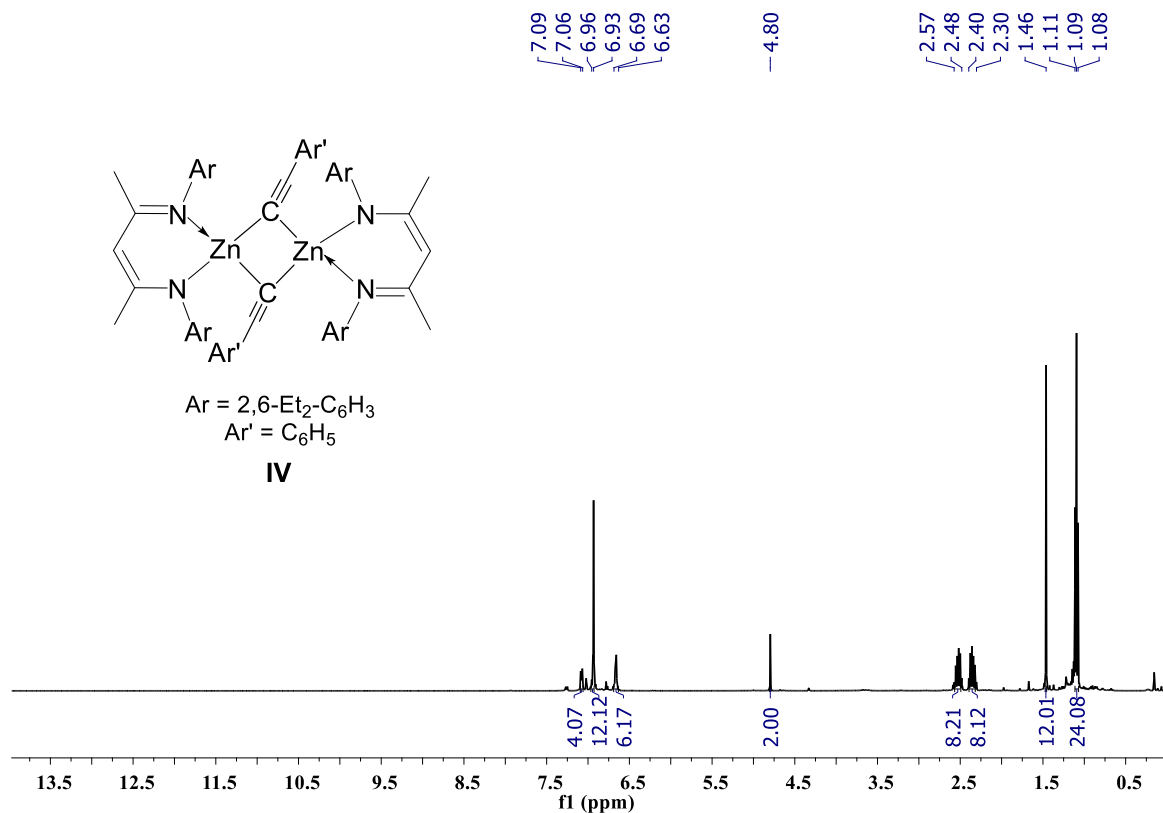


Figure 7.4. ¹H NMR (400 MHz, 25 °C, C₆D₆) spectrum of compound **IV**.

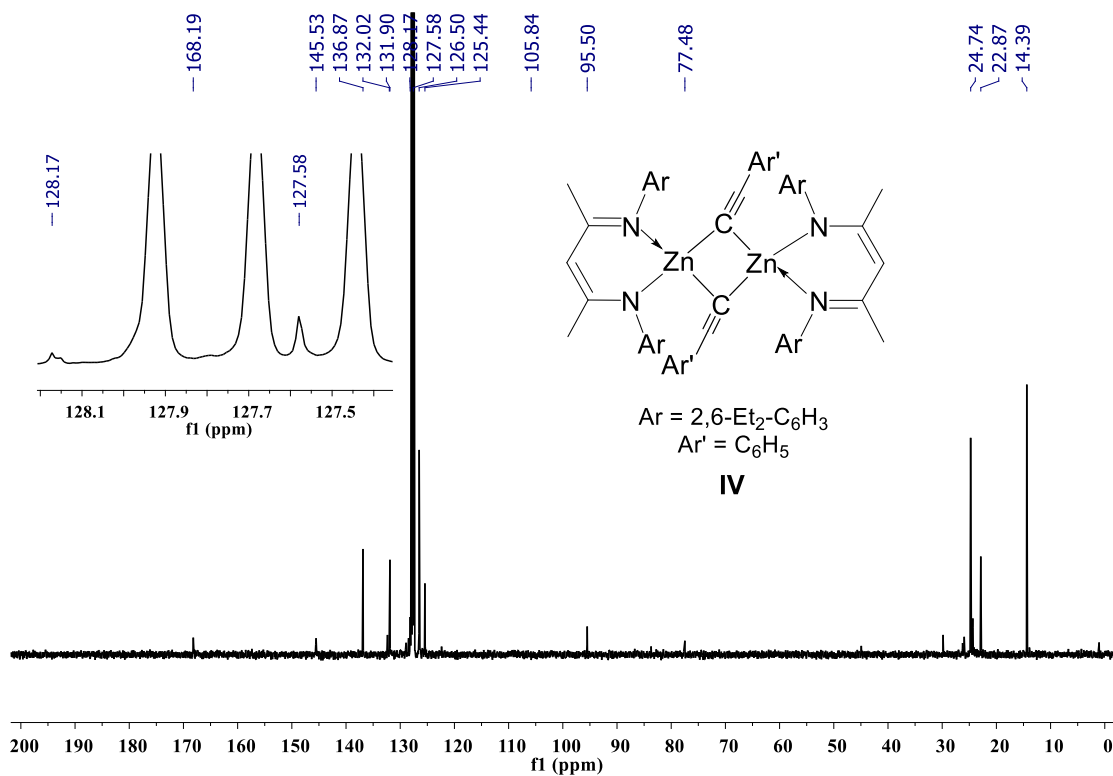
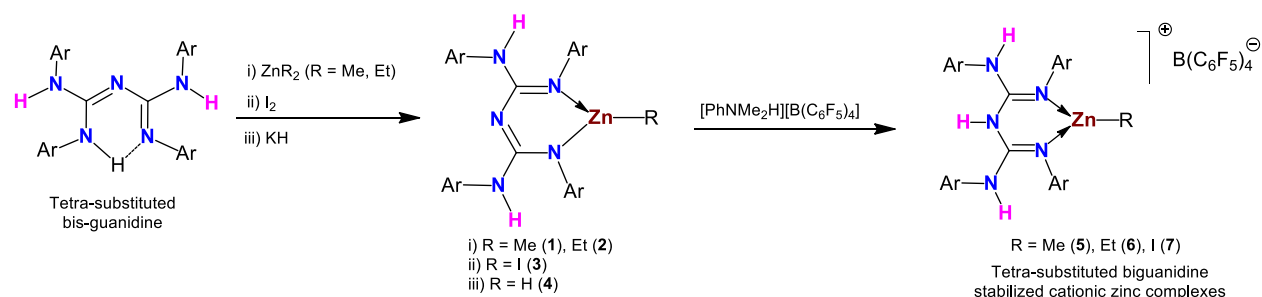


Figure 7.5. ¹³C{¹H} NMR (100 MHz, 25 °C, C₆D₆) spectrum of compound **IV**.

Chapter 8

Conjugated Bis-Guanidine (CBG) Ligand Based Neutral and Cationic Zinc Alkyls, Halide, and Hydride Complexes: Synthesis, Characterization, and Catalytic Application in Cyanosilylation of Ketones

Abstract



● Structurally characterized cationic zinc complexes ● Catalytic application in cyanosilylation of ketones

The N-donor β -diketiminate (NacNac) analogue, i.e., conjugated bisguanidine (CBG) ligand L(3H), was used for the synthesis of mononuclear zinc(II) alkyls [L(2H)ZnR, R = Me (**Zn-1**), Et (**Zn-2**)], iodide [L(2H)ZnI, **Zn-3**], hydride [L(2H)ZnH, **Zn-4**] (L(3H) = {(ArHN)(ArNH)-C=N-C=(NAr)(NHAr)}; Ar=2,6-*i*Pr₂-C₆H₃), complexes with excellent yields. Moreover, the reactions of **Zn-1**, **Zn-2**, and **Zn-3** with [PhNMe₂H][B(C₆F₅)₄] yielded the new category of mononuclear zinc alkyls [L(3H)ZnR][B(C₆F₅)₄], R = Me (**Zn-5**), Et (**Zn-6**) and iodide [L(3H)ZnI][B(C₆F₅)₄] (**Zn-7**) cationic compounds in good yields. All newly isolated and thermally stable zinc complexes (**Zn-1** to **Zn-7**) were well characterized by multinuclear NMR (¹H, ¹³C{¹H}, ¹⁹F{¹H} for (**Zn-5** - **Zn-7**) and ¹¹B for (**Zn-5** - **Zn-7**), HRMS, and single crystal X-ray diffraction studies. Moreover, the well-defined zinc iodide cation (**Zn-7**) [L(3H)ZnI][B(C₆F₅)₄] was further used as catalyst for the synthesis of cyanohydrin enol ether products (RCR'CNOSiMe₃) by TMSCN addition in carbonyl compounds (RCOR', R' = H/ alkyl/aryl) under mild reaction condition. The reaction was highly selective for cyanosilylation of carbonyls with good tolerance of ester substrate with excellent yield.

8.1. Introduction

Over the last few years, zinc complexes have been used as catalysts for various organic transformations in homogeneous and heterogeneous catalytic processes.¹ Although neutral zinc complexes can also be used as catalysts, cationic zinc complexes are more effective than corresponding neutral species due to their enhanced Lewis acidity of the metal centers caused by nucleophilic counter-anions.² In this context, it should be noted that various molecular zinc cations have been synthesized by N-, O- or P- based ligands.²⁻³ Concerning molecular organozinc cations, only a handful of examples were introduced for catalysis application.⁴ In earlier report, Dargorne and coworkers utilized N-heterocyclic (NHC) zinc organocations $[\text{NHC-ZnMe}(\text{THF})_x]^+ [\text{Me}(\text{B}_6\text{F}_5)_3]^-$ (where $x = 1-2$; $\text{NHC} = 1,3-(2,6\text{-}i\text{Pr}_2\text{Ph})_2\text{-}$ or $1,3-(2,4,6\text{-Me}_3\text{Ph})_2\text{-imidazol-2-ylidene}$) for ring-opening polymerization of trimethylene carbonate and cyclic esters (*β -butyrolactone and lactide*) under mild conditions.⁵ Further, in 2015, Roesky and Braun introduced the hydroamination reaction by using structurally characterized zinc organyl compound $[\text{Zn}_2\text{Cp}^*_3]^+ [\text{BAr}^{\text{F}}_4]^-$ (where $\text{BAr}^{\text{F}}_4 = \text{B}(3,5\text{-(CF}_3)_2\text{C}_6\text{H}_3)_4$) as a precatalyst to afford the C-N coupled products.⁶ Later Parkin and Dargorne groups independently described organozinc cations as effective catalysts for the hydrosilylation of carbon dioxide.^{4, 7} Additionally, zinc hydride cations were reported for catalytic hydrosilylation of carbonyl, carbon dioxide, and nitrile functionalities.⁸

In the past few years, cyanosilylation reaction was used to prepare various organic compounds for the chemical industry and agriculture.⁹ For this, trimethylsilyl cyanide (TMSCN) is used as a cyanating reagent compared to HCN (hydrogen cyanide) with carbonyl compounds to afford the cyanohydrin products in high yield.¹⁰ For this, transition and main group molecular metal complexes have been discovered for Si-CN addition to carbonyls.^{9a, 11} Leung and co-workers reported catalyst free cyanosilylation of aldehyde in 2019.¹² It is notable that cyanosilylation of

ketone is difficult compared to aldehyde. Moreover, there are only two reports on zinc-based cyanosilylation of carbonyl groups limited to aldehydes.^{10, 13} In 1978, the Talley group established the first zinc-based cyanosilylation of ketones.¹³ Recently, Pombeiro and co-workers reported multinuclear zinc(II)-arylhydrazone used as catalysts for the cyanosilylation of aldehydes.¹⁰ In this context, Lewis acids are powerful tools for cyanosilylation reactions. However, in main-group catalysis, only a handful of cationic complexes have been reported for TMSCN addition in aldehydes and ketones.¹⁴ Surprisingly, concerning the literature study, we found that no cationic zinc complex was reported for cyanosilylation of aldehydes and ketones. We recently established well-defined CBG-stabilized zinc complexes and used them to catalyze hydrofunctionalization of various challenging organic unsaturated functional groups under mild conditions.¹⁵

Therefore, herein we report the preparation and characterization of conjugated bis-guanidine (CBG) ligand chelated mononuclear zinc alkyls (**Zn-1** and **Zn-2**), iodide (**Zn-3**), and hydride (**Zn-4**) compounds. Moreover, we established the cationic CBG zinc alkyl and halide complexes (**Zn-5** - **Zn-7**). All synthesized zinc compounds are characterized by multinuclear NMR, HRMS, and single-crystal X-ray diffraction studies. Further, we employed well-defined cationic zinc iodide complex $[L(3H)ZnI][B(C_6F_5)_4]$ (**Zn-7**) as a catalyst for the cyanosilylation of a broad range of ketones to cyanohydrin enol ether products.

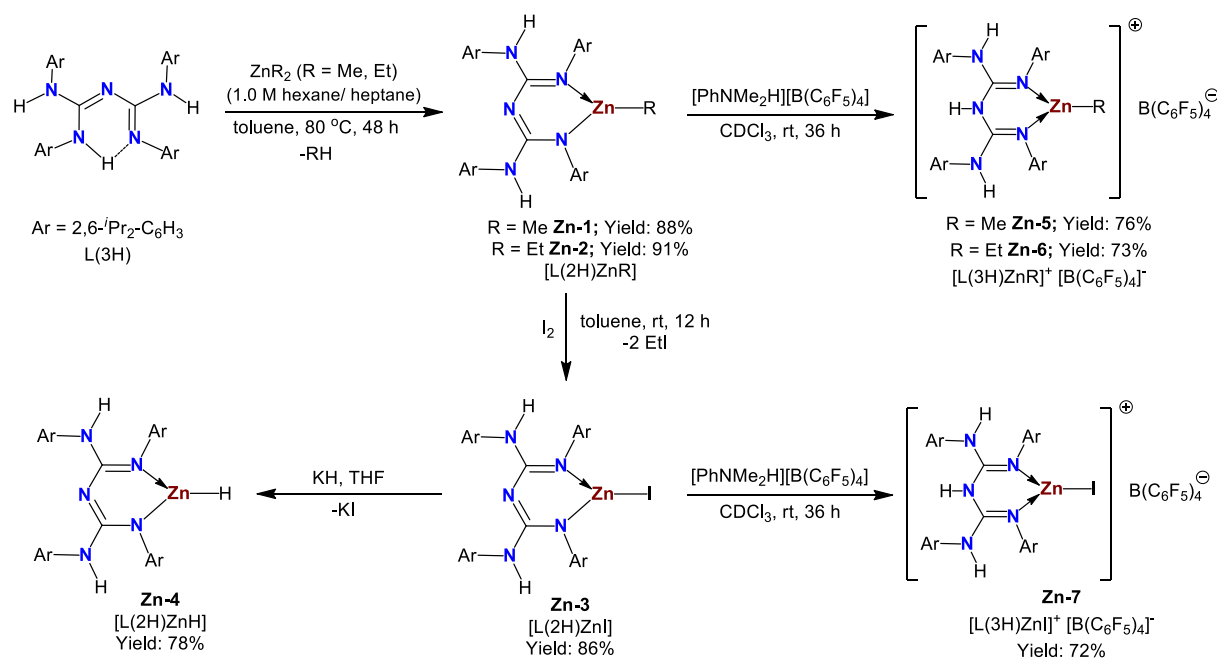
8.2. Results and Discussion

8.2.1. Synthesis and Characterization of CBG Ligated Zinc (II) Alkyls, Halide, Hydride, and their Corresponding Cationic Complexes

In the previous report, we described the synthesis of bulky *Dipp*CBG (conjugated bis-guanidine, L(3H)), (where, L = {(ArHN)(ArNH)-C=N-C=(NAr)(NHAr)}; Ar=2,6-*i*Pr₂-C₆H₃) ligand by reaction of 2.0 equiv. of *Dipp* CDI with 1.0 equiv. of ammonium chloride in ethanol at 80 °C.^{15e}

¹⁶ Our group recently introduced tetra-aryl substituted conjugated bis-guanidinate (CBG) chelated main group and transition metal complexes, including cationic complexes, and studied the catalytic applications.^{11a, 15f, 17} In this work, we have synthesized neutral and cationic zinc alkyls and iodide compounds (**Zn-1** to **Zn-7**) coordinated by N-donor bulkier ^{Dipp}CBG ligand (*a Nacnac analog*) in good yields.

The neutral organo-zinc compounds [L(2H)ZnR, R = Me (**Zn-1**), Et (**Zn-2**)] were synthesized by deprotonation of ligand (LH) with an equimolar solution of dialkylzinc reagent (ZnR₂, R = Me, Et, 1.0 M hexane/heptane) in toluene with 88-91% isolated yields as white solids (Scheme 8.1).



Scheme 8.1. Synthesis of CBG-supported neutral and cationic zinc compounds (**Zn-1** - **Zn-7**).

Further, the reaction of compound (**Zn-2**) with an equivalent amount of I₂ in toluene at rt was conducted, which yielded the brown-colored CBG zinc iodide complex (**Zn-3**) [L(2H)ZnI] in an 86% isolated yield (Scheme 8.1). As already stated, examples of molecular zinc organyl and halide cations were scarce. Along with this, there have been no reports on biguanide-chelated zinc alkyl and iodide cations to our knowledge. Therefore, in an additional experiment, we targeted CBG

organozinc (**Zn-5** to **Zn-6**) and halide (**Zn-7**) cations. Accordingly, the reaction of neutral zinc complexes (**Zn-1** to **Zn-4**) with equiv. quantity of [PhNMe₂H] [B(C₆F₅)₄] reagent in chloroform-d at rt yielded the three coordinate monomeric zinc alkyl cations [L(3H)ZnR]⁺ [B(C₆F₅)₄]⁻ (R = Me (**Zn-5**), Et (**Zn-6**)) and zinc halide cation [L(3H)ZnI]⁺ [B(C₆F₅)₄]⁻ (**Zn-7**) in 72-76% yields (Scheme 8.1).

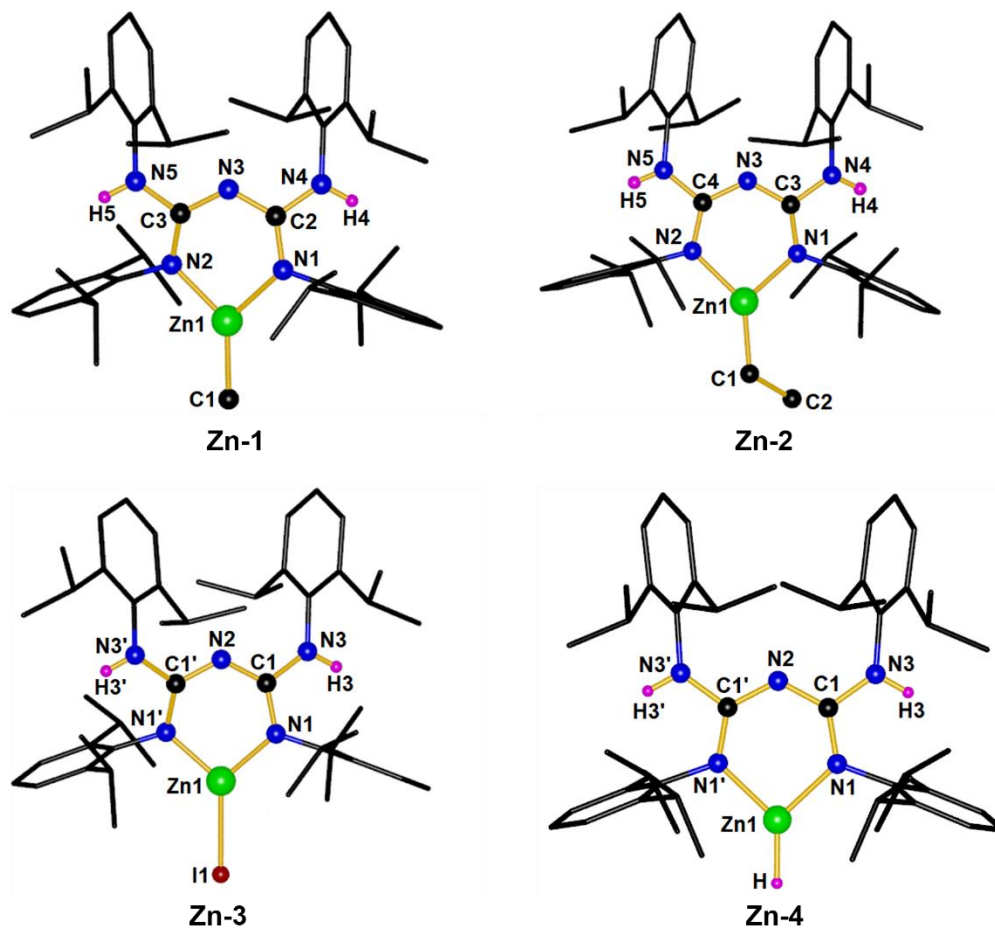


Figure 8.1. Molecular structures of **Zn-1** (upper left), **Zn-2** (upper right), **Zn-3** (lower left), and **Zn-4** (lower right). All the hydrogen atoms (except H(4), H(5), H(3), H(3')) and H) are removed for clarity. Selected bond lengths (Å) and angles (deg), For **Zn-1** (upper left): Zn1-C1 1.9475(17), Zn1-N1 1.9513(11), Zn1-N2 1.9505(11), N2-C3 1.3380(16), N3-C3 1.3390(16), N3-C2 1.3372(16), N1-C2 1.3385(16), N5-C3 1.3705(16), N4-C2 1.3676(16); N1-Zn1-N2 93.89(5), N1-Zn1-C1 131.67(6), N2-Zn1-C1 134.43(6). For **Zn-2** (upper right): Zn1-C1 1.962(4), Zn1-N1 1.955(3), Zn1-N2 1.958(3), C1-C2 1.538(5), N2-C4 1.348(4), N5-C4 1.368(4), N3-C4 1.326(4), N3-C3 1.339(4), N1-C3 1.341(4); N1-Zn1-

N2 94.56(11), N1–Zn1–C1 137.23(13), N2–Zn1–C1 128.03(13), Zn1–C1–C2 115.6(2). For **Zn-3** (lower left): Zn1–I1 2.4427(5), Zn1–N1 1.9111(19), Zn1–N1' 1.9112(19), N1–C1 1.346(3), N2–C1 1.338(2), N3–C1 1.367(3); N1–Zn1–N1' 97.88(11), N1–Zn1–I1 131.07(6), N1'–Zn1–I1 131.06(6). For **Zn-4** (lower right): Zn1–N1 1.9404(13), Zn1–N1' 1.9404(13), N1–C1 1.342(2), N2–C1 1.3438(17), N3–C1 1.3706(19); N1–Zn1–N1' 93.97(7).

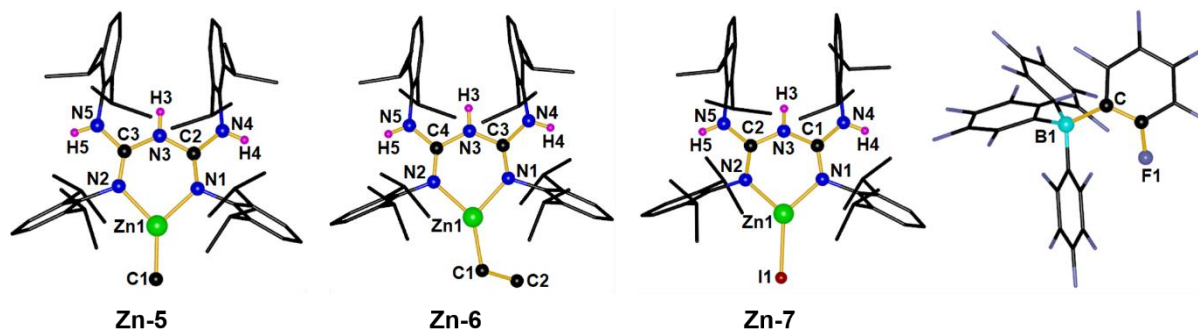


Figure 8.2. Molecular structures of **Zn-5** (left), **Zn-6** (middle), **Zn-7** (right). All the hydrogen atoms (except H(3), H(4), H(5), and anion B(C₆F₅)₄) are removed for clarity. Selected bond lengths (Å) and angles (deg), For **Zn-5** (upper left): Zn1–C1 1.924(7), Zn1–N1 1.988(4), Zn1–N2 1.987(4), N1–C2 1.281(7), N4–C2 1.353(6), N3–C2 1.392(6), N3–C3 1.395(6), N5–C3 1.356(6), N2–C3 1.280(7), B1–C52 1.643(8), C52–C53 1.394(7), C53–F1 1.352(6); N1–Zn1–N2 91.21(18), N1–Zn1–C1 133.8(2), N2–Zn1–C1 134.9(2), B1–C52–C53 128.5(5), C52–C53–F1 121.1(5). For **Zn-6** (upper right): Zn1–C1 2.038(7), Zn1–N1 2.005(4), Zn1–N2 1.994(5), C1–C2 1.425(11), N1–C3 1.257(7), N4–C3 1.361(5), N3–C3 1.395(6), N3–C4 1.361(5), N5–C4 1.351(7), N2–C4 1.276(7), B1–C53 1.643(7), C53–C54 1.397(6), C54–F1 1.356(5), N1–Zn1–N2 90.48(18), N1–Zn1–C1 127.4(2), N2–Zn1–C1 142.1(2), B1–C53–C54 128.3(4), C53–C54–F1 120.4(4). For **Zn-7** (lower): Zn1–I1 2.4317(14), Zn1–N1 1.945(8), Zn1–N2 1.957(8), N1–C1 1.299(12), N4–C1 1.343(11), N3–C1 1.390(11), N3–C2 1.361(12), N5–C2 1.370(12), N2–C2 1.299(12), B1–C51 1.658(15), C51–C52 1.397(18), C52–F1 1.319(13); N1–Zn1–N2 95.6(3), N1–Zn1–I1 135.1(2), N2–Zn1–I1 129.2(2), B1–C51–C52 120.7(9), C51–C52–F1 119.6(9).

All compounds (**Zn-1** to **Zn-7**) were characterized by multinuclear NMR (¹H, ¹³C{¹H}, ¹¹B and ¹⁹F{¹H}), HRMS, and structurally characterized by the single crystal X-ray diffraction technique (Figures 8.1–8.2). The single crystals of compounds **Zn-1**, **Zn-2**, **Zn-3**, and **Zn-4** suitable for X-ray diffraction analysis were crystallized from a concentrated toluene solution at –10 °C, while for compounds **Zn-5**, **Zn-6**, and **Zn-7** the crystals were grown from chloroform solutions.

Compounds **Zn-1**, **Zn-3**, and **Zn-4** were crystallized in the monoclinic system with the P2(1)/c (for **Zn-1**), and C2/c (for **Zn-3** and **Zn-4**), space groups, whereas compound **Zn-2** crystallized in the triclinic with the space group P-1. The selected data collection parameters and structure refinement details of compounds (**Zn-1** to **Zn-7**) are summarized in Tables 8.2-8.3. In all cases, the zinc atom adopts a nearly trigonal planar environment with three coordination sites. The zinc atoms, connected to CBG ligand in N,N'-chelate fashion and other site occupied by alkyls (**Zn-1**, **Zn-2**, **Zn-5**, and **Zn-6**) or iodide (**Zn-3** and **Zn-7**) or hydride (**Zn-4**). Further, solid-state structures confirmed that all compounds **Zn-1–Zn-7** are monomeric and display six-membered metallacycles containing a C2N3Zn ring.

The Zn–C bond lengths in compounds **Zn-1**, **Zn-2**, **Zn-5**, and **Zn-6** lie in the range 1.924(7) Å to 2.038(7) Å and are similar to those reported ligand stabilized neutral and cationic zinc complexes (A–D). A: LZnMe (L' = HC[C(Me)N(2,6-*i*Pr₂C₆H₃)]₂)¹⁸ (Zn(1)–C(6) 1.941(3) Å). B: [L'ZnEt] [L' = HC[C(Me)N(2,6-*i*Pr₂C₆H₃)]₂)¹⁹ (Zn(1)–C(1) 1.963(5) Å). C: [(*a*IDipp)(*n*IDipp)ZnMe]⁺ (Dipp = 2,6-*i*Pr₂C₆H₃)^{4a, 7} (Zn(1)–C(55) 1.997(4) Å). D: (IDipp)Zn–Et⁺ [IDipp = 1,3-bis-(2,6-*i*Pr₂C₆H₃)imidazolin-2-ylidene)]^{4a} (Zn–Et 1.909(5) Å). Also, Zn–N bond distances are comparable to reported zinc alkyl complexes (A–B).

The Zn–I bond length for compounds **Zn-3** and **Zn-7**, i.e., Zn1–I1, are 2.4427(5) Å, and 2.4317(14) Å respectively. These are consistent with the Zn–I bond lengths of previously reported N,N'-chelated DiethylCBG supported zinc iodide complex E: [LZnI]₂; [L¹ = {(ArNH)(ArN)–C=N–C=(NAr)(NHAr)}; Ar = 2,6-*i*Pr₂–C₆H₃)] Zn1–I1 2.5819(15) Å, Zn1–I1' 2.7702(16) Å].^{15f} Similarly, for compound **Zn-4**, the Zn1–N1 bond distance is 1.9404 (13) Å, comparable with the previously reported ^{Dipp}NacNac zinc hydride complex, i.e., 1.950(1) Å.²⁰ The N–Zn–N bite angles in compounds **Zn-1–Zn-7** in the range of 90.48(18)–97.88(11)° that are similar with six-membered

zinc heterocycles [N–Zn–N bite angles in compounds A–B, E: 97.00(8)° (A), 97.07(12)° (B), 95.7(3)° (E).

The bonding mode **I** has been observed for the neutral zinc alkyl (**Zn-1** and **Zn-2**), halide (**Zn-3**), and hydride (**Zn-4**) complexes, while **II** is noticed for the cationic zinc alkyl (**Zn-5** and **Zn-6**) and halide (**Zn-7**) complexes. In bonding mode **I**, the N,N'-chelating scaffold exhibits an LX-type ligand consisting of one σ - and one π -donor property. However, cationic zinc complexes are characterized as an L₂-type ligand consisting of two π -donor properties (Figure 8.3). The above study suggests that in the case of neutral compounds, ligand behaves as monoanionic, whereas cationic complexes ligand acts as neutral.

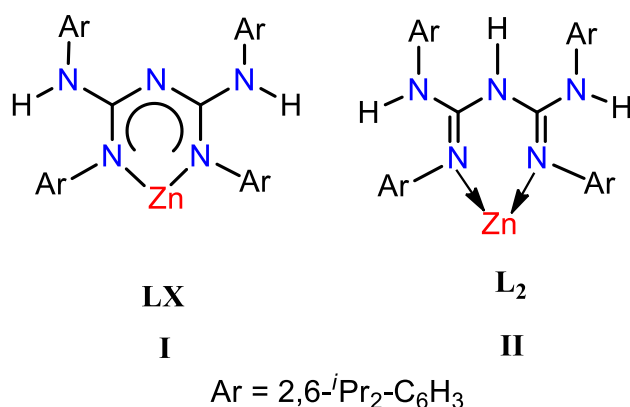
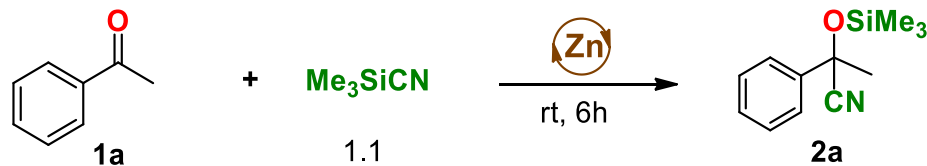


Figure 8.3. Two bonding modes.

8.2.2. TMSCN Addition in Ketones

In the present literature study, we observed that, unlike the B-H addition to carbonyls, only a few main-group molecular metal complexes have been employed for cyanosilylation reactions, which encouraged us to explore trimethylsilyl cyanide (TMSCN) addition across the carbonyl bonds to synthesize the cyanohydrin silyl ether products using CBG stabilized zinc iodide cationic complex (**Zn-7**).

Table 8.1. Optimization table of zinc-catalyzed cyanosilylation of acetophenone^a

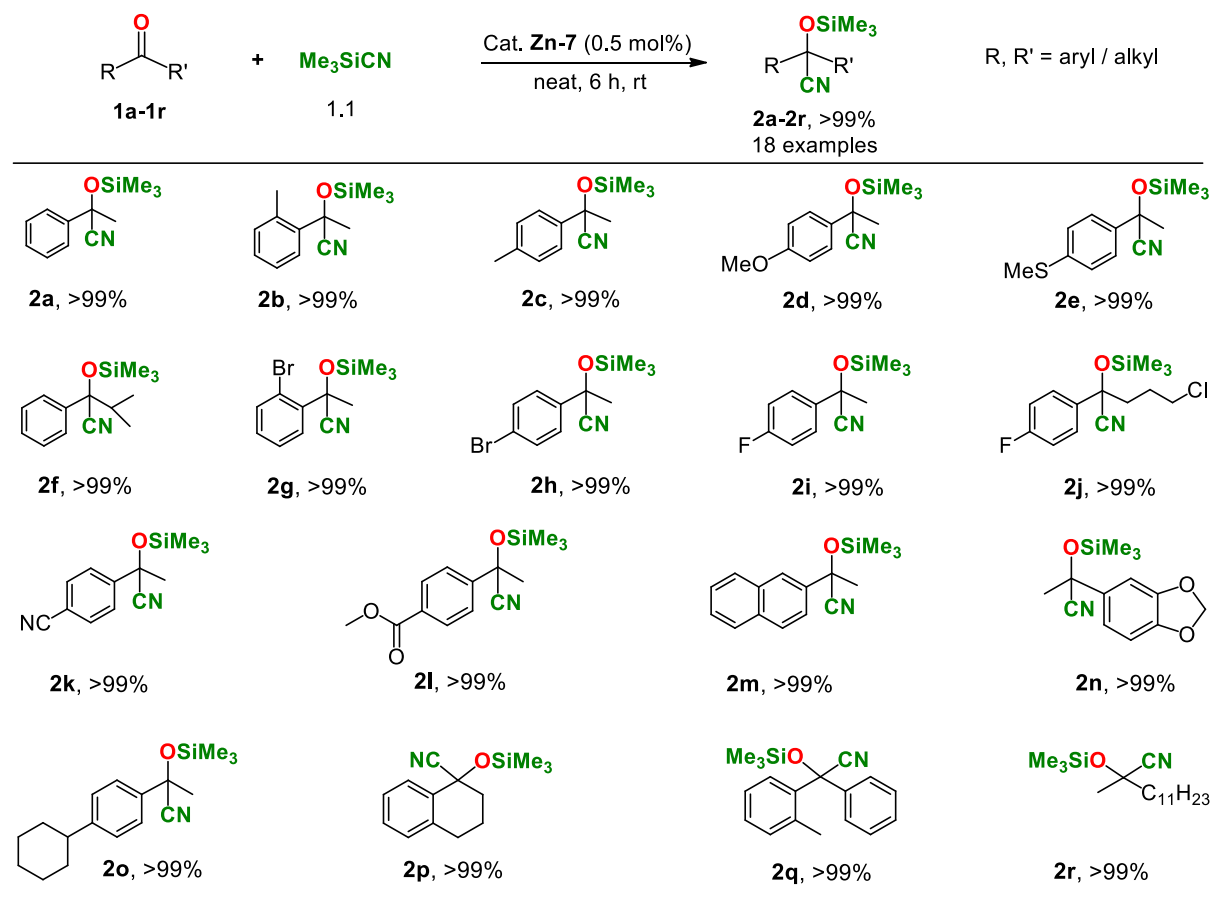
entries	catalysts	mol%	solvent	Conv. (%) ^b
1	-	-	neat	12%
2	Zn-7	5.0	neat	>99%
3	Zn-7	3.0	neat	>99%
4	Zn-7	2.0	neat	>99%
5	Zn-7	1.0	neat	>99%
6	Zn-7	0.5	neat	>99%
7	Zn-7	0.5	toluene	>99%
8	Zn-7	0.5	benzene	>99%
9	Zn-7	0.5	THF	>99%
10	Zn-1	0.5	neat	15
11	Zn-2	0.5	neat	16
12	Zn-3	0.5	neat	18
13	Zn-4	0.5	neat	16
14	Zn-5	0.5	neat	98
15	Zn-6	0.5	neat	98

^aReaction conditions: acetophenone (1.0 equiv., 0.3 mmol), trimethylsilylcyanide (1.1 equiv., 0.33 mmol), catalysts (x mol%) stirred in oven dried reaction vial for 6 h at rt under N₂. ^bConversion was examined by ¹H NMR (400 MHz) spectroscopy based upon consumption of starting material and identified shifting in characteristic proton (PhCMeCNOTMS) resonance signal at (δ) 1.89 ppm in catalytic solution.

In the initial investigation, acetophenone (**1a**) reacted with 1.1 equiv. of TMS-CN in solvent-free and catalyst-free conditions affords only 12% of cyanohydrin product **2a** (Table 8.1, entry 1). We observed that 0.5 mol% of zinc iodide cationic complex (**Zn-7**) is the lowest catalyst load possible for complete conversion of acetophenone into respective silylated product **2a**, both in neat and

solvent like toluene, benzene, THF (Table 8.1, entries 6-9). Eventually, other zinc complexes demonstrate a lower catalytic performance for TMSCN addition in acetophenone (Table 8.1, entries 10-15).

With the final optimization condition for Si-CN addition in acetophenone, next we widen the substrate scope for TMSCN addition in various aryl and alkyl ketones using a zinc catalyst (**Zn-7**).



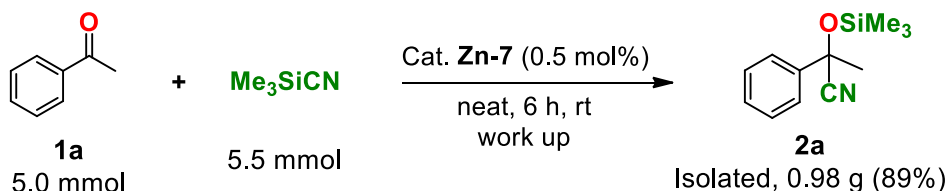
Scheme 8.2. Substrate scope for canosilylation of ketones catalyzed by cationic zinc complex (**Zn-7**)^a

^aReactions were conducted with ketones (0.3 mmol, 1.0 equivalent), trimethylsilylcyanide (0.33 mmol, 1.1 equivalent), and cat. **Zn-7** (0.5 mol%), in a 10 mL reaction vial under N₂ and stirred at rt for 6 h. Conversion for Si-CN addition in ketones was confirmed by NMR (¹H and ¹³C{¹H}) spectroscopy based on the disappearance of starting material and formation of characteristic proton signal for (RCR'CNOSiMe₃).

As shown in Scheme 8.2, complex **Zn-7** catalyzed the complete formation of cyanohydrin products of selected ketones (**2a-2r**, >99%) and showed excellent tolerance of esters (CO₂R) functional group under solvent-free conditions. In our present catalytic system, all tested aryl electron-rich (Me, OMe, and MeS; **1b-1f**) and electron-poor (F, Cl, Br; **1g-1j**) ketones yielded the corresponding cyanohydrin enol ether products (**2b-2j**) under neat conditions. Additionally, for 4-acetylbenzonitrile (**1k**) and 4-acetylphenylacetate (**1l**), we established an intramolecular chemoselective Si-CN addition in carbonyl bond with undisturbed nitrile and ester moiety to afford the quantitative formation of cyanohydrin products (**2k-2l**). In addition, the TMSCN addition in the fused, heterocycle, alkyl, and long-chain ketones **1m-1r**, complete formation of cyanohydrin silyl ether products **2m-2r** with an excellent yield similar to literature reports.

8.2.3. Scale-up Reaction

In additional experiments, the cyanosilylation reaction was conducted at a larger scale under mild conditions to confirm the practical application of the above catalytic reaction (Scheme 8.3). Interestingly, at a 5.0 mmol scale, cyanosilylation of acetophenone with trimethylsilyl cyanide (1.1 equiv.) yielded the respective air-stable cyanohydrin product (**2a**, 0.98 g (89%), Isolated).

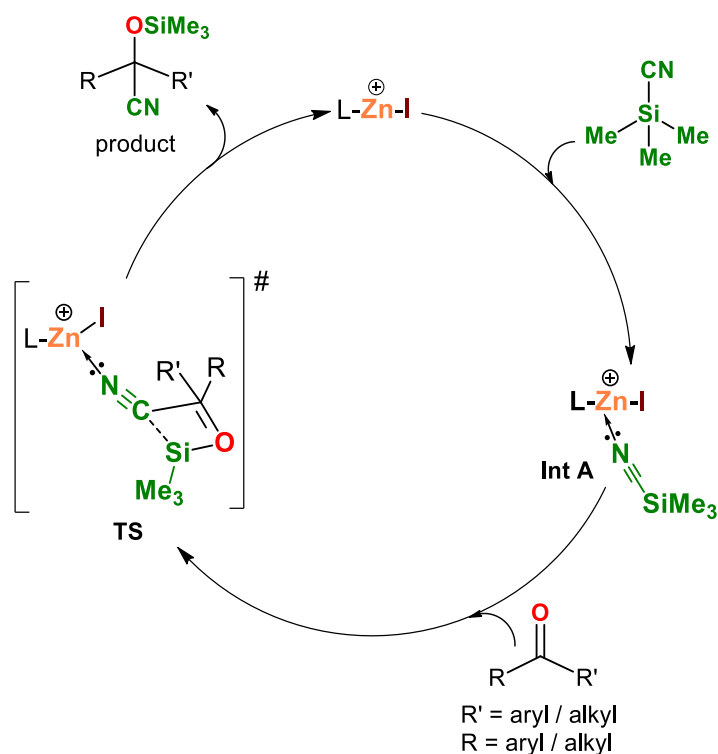


Scheme 8.3. Gram-scale cyanosilylation of benzaldehyde and acetophenone catalyzed by **Zn-7**

8.2.4. Catalytic Cycle for Cyanosilylation of Carbonyls

Based on literature reports of main-group metal catalyzed cyanosilylation of carbonyls, we demonstrate the proposed catalytic cycle of zinc iodide cation (**Zn-7**) catalyzed addition of TMSCN to ketones in Scheme 8.4. In the initial catalytic cycle, TMSCN coordinates with Lewis

acidic zinc center in **Zn-7** to yield the labile adduct (**Int A**). After that reaction of the carbonyl with **Int A** resulted in the corresponding cyanohydrin products and regenerated the catalyst **Zn-7**.



Scheme 8.4. Proposed mechanism for cyanosilylation of carbonyls catalyzed by **Zn-7**.

8.3. Conclusions

In summary, we have described the structurally characterized N-donor CBG chelated mononuclear zinc(II) alkyls, halide, and hydride complexes (**Zn-1** to **Zn-4**). In addition, we have demonstrated the first-time synthesis of cationic zinc methyl, ethyl, and iodide compounds (**Zn-5** to **Zn-7**) coordinated by a tetrasubstituted biguanidine ligand in good yields. Moreover, the zinc iodide cation $[\text{L}(3\text{H})\text{ZnI}]^+ [\text{B}(\text{C}_6\text{F}_5)_4]^-$ (**Zn-7**) was employed for cyanosilylation of a wide range of ketones using TMSCN as a cyanide precursor to synthesize cyanohydrin enol ethers products with excellent yields under solvent-free conditions. We observed that ketone was well-tolerated for reducible ester functional group within the optimized conditions during substrate scope. Currently,

the notable Lewis acidity of the cationic zinc complex opens a new gateway to other challenging organic transformations in main-group metal catalysis.

8.4. Experimental Section

General Procedures

Unless stated, manipulations were performed under a dinitrogen atmosphere using standard Glovebox and Schlenk techniques. NMR spectra were recorded on Bruker NMR spectrometers at 400 MHz (^1H), 101 MHz ($^{13}\text{C}\{^1\text{H}\}$), 128.36 MHz (^{11}B), and 376 MHz ($^{19}\text{F}\{^1\text{H}\}$). ^1H NMR and $^{13}\text{C}\{^1\text{H}\}$ NMR chemical shifts are referenced to residual protons or carbons in the deuterated solvent. ^{11}B and $^{19}\text{F}\{^1\text{H}\}$ were calibrated using an external reference of $\text{BF}_3\cdot\text{Et}_2\text{O}$. Multiplicities are reported as singlet (s), doublet (d), triplet (t), quartet (q), and multiplet (m). Chemical shifts are reported in ppm. Coupling constants are reported in Hz. Mass spectrometry analyses were carried out on Bruker micrOTOF-Q II and Waters XevoG2 XS Q-TOF mass spectrometers. The melting point of **Zn-1** to **Zn-7** were measured from Stuart SMP 10 instrument.

Materials:

Solvents were purified by distillation over Na/ benzophenone. Deuterated chloroform (CDCl_3) dried on molecular sieves, and benzene- d_6 (C_6D_6) dried over Na/K alloy and distilled. The ligand L(3H) ($\text{L} = \{(\text{ArNH})(\text{ArNH})-\text{C}=\text{N}-\text{C}=(\text{NAr})(\text{NHAr})\}$; $\text{Ar} = 2,6\text{-}^i\text{Pr}_2\text{-C}_6\text{H}_3$) is prepared according to the reported literature procedure.^{15e, 16} For catalysis reactions, 10 mL reaction vials, and J. Young valve NMR tubes were properly oven-dried before being used. Chemicals and reagents were purchased from Sigma-Aldrich Co. Ltd., Merck India Pvt. Ltd., and TCI chemicals were used without purification.

Synthesis of [LZnMe] (Zn-1): Dimethylzinc solution (1.41 mL of a 1 M solution in heptane, 1.41 mmol) was added dropwise to a solution of L(3H) (1 g, 1.347 mmol) in toluene (20 mL) at 0 °C.

The reaction mixture was allowed to warm to room temperature and heated at 80 °C for 2 days. The clear solution was concentrated (5 mL) and stored overnight at -10 °C to afford colorless crystals. (Yield 0.72 g, 88%); mp 185-190 °C. ^1H NMR (400 MHz, C_6D_6 , 298 K) δ = 7.20 (brs, 6H, ArH), 6.92 (t, $^3J_{\text{HH}}$ = 8.0 Hz, 2H, ArH), 6.75 – 6.73 (d, $^3J_{\text{HH}}$ = 8.0 Hz, 4H, ArH), 5.28 (s, 2H, NH), 3.44 – 3.41 (m, 4H, $\text{CH}(\text{CH}_3)_2$), 2.95 – 2.91 (m, 4H, $\text{CH}(\text{CH}_3)_2$), 1.33 – 1.31 (d, $^3J_{\text{HH}}$ = 6.8 Hz, 12H, $\text{CH}(\text{CH}_3)_2$), 1.22 – 1.21 (d, $^3J_{\text{HH}}$ = 8.0 Hz, 12H, $\text{CH}(\text{CH}_3)_2$), 1.02 – 1.01 (d, $^3J_{\text{HH}}$ = 8.0 Hz, 12H, $\text{CH}(\text{CH}_3)_2$), 0.77 – 0.75 (d, $^3J_{\text{HH}}$ = 8.0 Hz, 12H, $\text{CH}(\text{CH}_3)_2$), -1.05 (s, 3H, LZnCH_3). HRMS (ASAP/Q-TOF) m/z : $[\text{M}+\text{H}]^+$ Calcd for $\text{C}_{51}\text{H}_{74}\text{N}_5\text{Zn}$ 820.5236, found: 820.5237.

Synthesis of [LZnEt] (Zn-2): Diethylzinc solution (1.41 mL of a 1 M solution in hexane, 1.41 mmol) was added dropwise to a solution of L(3H) (1 g, 1.347 mmol) in toluene (20 mL) at 0 °C. The mixture was allowed to warm to room temperature and heated at 80 °C for 2 days. The clear solution was concentrated (5 mL) and stored overnight at -10 °C to afford colorless crystals. (Yield 0.76 g, 91%); mp 187-192 °C. ^1H NMR (400 MHz, C_6D_6 , 298 K) δ = 7.20 – 7.18 (d, $^3J_{\text{HH}}$ = 8.0 Hz, 4H, ArH), 7.14 – 7.12 (d, $^3J_{\text{HH}}$ = 8.0 Hz, 2H, ArH), 6.95 (t, $^3J_{\text{HH}}$ = 8.0 Hz, 2H, ArH), 6.82 – 6.80 (d, $^3J_{\text{HH}}$ = 8.0 Hz, 4H, ArH), 5.61 (s, 2H, NH), 3.66 – 3.60 (m, 4H, $\text{CH}(\text{CH}_3)_2$), 3.13 – 3.07 (m, 4H, $\text{CH}(\text{CH}_3)_2$), 1.41 – 1.40 (d, $^3J_{\text{HH}}$ = 7.4 Hz, 12H, $\text{CH}(\text{CH}_3)_2$), 1.36 – 1.34 (d, $^3J_{\text{HH}}$ = 8.0 Hz, 12H, $\text{CH}(\text{CH}_3)_2$), 1.17 – 1.15 (d, $^3J_{\text{HH}}$ = 8.0 Hz, 12H, $\text{CH}(\text{CH}_3)_2$), 0.99 (t, $^3J_{\text{HH}}$ = 8.0 Hz, 3H, $\text{LZnCH}_2\text{CH}_3$), 0.81 – 0.79 (d, $^3J_{\text{HH}}$ = 8.0 Hz, 12H, $\text{CH}(\text{CH}_3)_2$), 0.42 (q, $^3J_{\text{HH}}$ = 8.0 Hz, 2H, $\text{LZnCH}_2\text{CH}_3$). $^{13}\text{C}\{^1\text{H}\}$ NMR (100 MHz, C_6D_6 , 298 K) δ = 157.1 (N_3C), 144.9 (Ar-C), 143.6 (Ar-C), 141.4 (Ar-C), 133.1 (Ar-C), 126.4 (Ar-C), 126.2 (Ar-C), 124.0 (Ar-C), 123.9 (Ar-C), 122.2 (Ar-C), 28.3 (Ar- $\text{CH}(\text{CH}_3)_2$), 25.0 (Ar- $\text{CH}(\text{CH}_3)_2$), 24.5 (Ar- $\text{CH}(\text{CH}_3)_2$), 23.2 (Ar- $\text{CH}(\text{CH}_3)_2$), 21.7 (Ar- $\text{CH}(\text{CH}_3)_2$), 11.5 ($\text{LZnCH}_2\text{CH}_3$), -0.7 ($\text{LZnCH}_2\text{CH}_3$). HRMS (ASAP/Q-TOF) m/z : $[\text{M}+\text{H}]^+$ Calcd for $\text{C}_{52}\text{H}_{76}\text{N}_5\text{Zn}$ 834.5392, found: 834.5384.

Synthesis of [LZnI] (Zn-3): Iodine (320 mg, 1.26 mmol) was added to a solution of LZnEt (1 g, 1.20 mmol) in 10 mL of toluene. The brown suspension was stirred at 25 °C for 10 hours until the color had changed to light yellow (all iodine had reacted). The solution was concentrated to 3 mL, and the product was isolated as a light yellow solid. (Yield 0.80 g, 86%); mp 240-245 °C. ¹H NMR (400 MHz, CDCl₃, 298 K) δ = 7.28 (s, 6H, ArH), 6.95 (t, ³J_{HH} = 7.7 Hz, 2H, ArH), 6.78 – 6.76 (d, ³J_{HH} = 8.0 Hz, 4H, ArH), 5.59 (s, 2H, NH), 3.44 – 3.37 (m, 4H, Ar-CH(CH₃)₂), 2.93 – 2.86 (m, 4H, Ar-CH(CH₃)₂), 1.40 – 1.38 (d, ³J_{HH} = 6.8 Hz, 12H, CH(CH₃)₂), 1.37 – 1.36 (d, ³J_{HH} = 6.9 Hz, 12H, Ar-CH(CH₃)₂), 1.09 – 1.07 (d, ³J_{HH} = 6.8 Hz, 12H, Ar-CH(CH₃)₂), 0.76 – 0.74 (d, ³J_{HH} = 6.8 Hz, 12H, Ar-CH(CH₃)₂). ¹³C{¹H} NMR (100 MHz, CDCl₃, 298 K) δ = 157.8 (N₃C), 144.9 (Ar-C), 143.9 (Ar-C), 138.9 (Ar-C), 132.3 (Ar-C), 126.9 (Ar-C), 126.6 (Ar-C), 124.2 (Ar-C), 122.2 (Ar-C), 28.4 (Ar-CH(CH₃)₂), 28.4 (Ar-CH(CH₃)₂), 25.5 (Ar-CH(CH₃)₂), 25.1 (Ar-CH(CH₃)₂), 23.4 (Ar-CH(CH₃)₂), 21.7 (Ar-CH(CH₃)₂). HRMS (ASAP/Q-TOF) *m/z*: [M+H]⁺ Calcd for C₅₀H₇₁N₅ZnI 932.4045, found: 932.4058.

Synthesis of [LZnH] (Zn-4): Individually, LZnI (1.0 g, 1.07 mmol) and KH (45 mg, 1.12 mmol) were weighed and placed in a Schlenk tube under a nitrogen atmosphere. Subsequently, 15 mL of dry THF was added at 0 °C. Then the reaction mixture was stirred at 25 °C for 18 hours. After completing the reaction time intervals, the reaction mixture was evaporated under a vacuum, and the residue was dissolved in toluene. The resultant solution was filtered and evaporated in a high vacuum to afford the desired compound **Zn-4**. (0.63 g, 78 %); m.p. 210 – 215 °C. ¹H NMR (400 MHz, CDCl₃, 298 K) δ = 7.21 – 7.18 (m, 6H, ArH), 7.00 (t, ³J_{HH} = 7.8 Hz, 2H, ArH), 6.85 – 6.83 (d, ³J_{HH} = 8.1 Hz, 4H, ArH), 5.41 (s, 2H, NH), 4.42 (s, 1H, ZnH), 3.63 – 3.56 (m, 4H, Ar-CH(CH₃)₂), 3.14 – 3.07 (m, 4H, Ar-CH(CH₃)₂), 1.42 – 1.40 (d, ³J_{HH} = 6.9 Hz, 12H, CH(CH₃)₂), 1.34 – 1.32 (d, ³J_{HH} = 7.8 Hz, 12H, Ar-CH(CH₃)₂), 1.11 – 1.09 (d, ³J_{HH} = 7.9 Hz, 12H, Ar-

CH(CH₃)₂), 0.87 – 0.85 (d, ³J_{HH} = 7.6 Hz, 12H, Ar-CH(CH₃)₂). ¹³C{¹H} NMR (100 MHz, CDCl₃, 298 K) δ = 158.2 (N₃C), 145.6 (Ar-C), 143.7 (Ar-C), 141.1 (Ar-C), 133.6 (Ar-C), 126.9 (Ar-C), 126.3 (Ar-C), 124.0 (Ar-C), 122.4 (Ar-C), 28.2 (Ar-CH(CH₃)₂), 28.2 (Ar-CH(CH₃)₂), 25.2 (Ar-CH(CH₃)₂), 24.6 (Ar-CH(CH₃)₂), 22.6 (Ar-CH(CH₃)₂), 22.2 (Ar-CH(CH₃)₂). HRMS (ASAP/Q-TOF) *m/z*: [M+H]⁺ Calcd for C₅₀H₇₂N₅Zn 806.5079, found: 806.4998.

Synthesis of [L(3H)ZnMe]⁺ [B(C₆F₅)₄]⁻ (Zn-5): The neutral precursor compound (**Zn-1**) (250 mg, 0.305 mmol) was mixed with an equimolar amount of [PhNMe₂H]⁺[B(C₆F₅)₄]⁻ (0.245 mg, 0.305 mmol) in dry CDCl₃ at room temperature. The reaction mixture was stirred at room temperature for 36 h, followed by the evaporation of volatiles under a high vacuum. The residues were washed with hexane (2*8 mL) and dried under a high vacuum to obtain **Zn-5** as a light greenish powder. (Yield 0.35 g, 76%). Mp: 210-215 °C. ¹H NMR (400 MHz, C₆D₆, 298 K) δ = 7.19 – 7.16 (m, 6H, ArH), 6.93 – 6.89 (m, 2H, ArH), 6.82 – 6.80 (d, ³J_{HH} = 8.0 Hz, 4H, ArH), 5.82 (s, 1H, NH), 5.57 (s, 2H, NH), 3.64 – 3.57 (m, 4H, CH(CH₃)₂), 3.13 – 3.05 (m, 4H, CH(CH₃)₂), 1.53 – 1.51 (d, ³J_{HH} = 6.0 Hz, 12H, CH(CH₃)₂), 1.32 – 1.30 (d, ³J_{HH} = 8.1 Hz, 12H, CH(CH₃)₂), 0.80 – 0.79 (d, ³J_{HH} = 8.0 Hz, 12H, CH(CH₃)₂), 0.74 – 0.72 (d, ³J_{HH} = 8.0 Hz, 12H, CH(CH₃)₂), -0.54 (s, 3H, LZnCH₃). HRMS (ASAP/Q-TOF) *m/z*: [M+H]⁺ Calcd for C₇₅H₇₅BF₂₀N₅Zn 1500.5125, found: 1500.4629.

Synthesis of [L(3H)ZnEt]⁺ [B(C₆F₅)₃]⁻ (Zn-6): The neutral precursor compound (**Zn-2**) (250 mg, 0.3 mmol) was mixed with an equimolar amount of [PhNMe₂H]⁺[B(C₆F₅)₄]⁻ (240 mg, 0.3 mmol) in dry CDCl₃ at room temperature. The reaction mixture was stirred at room temperature for 36 h, followed by the evaporation of volatiles under a high vacuum. The residues were washed with hexane (2*8 mL) and dried under a high vacuum to obtain **Zn-6** as a pale greenish powder. (Yield 0.33 g, 73%). Mp: 213-218 °C. ¹H NMR (400 MHz, C₆D₆, 298 K) δ = 7.41 – 7.34 (m, 6H, ArH),

7.00 – 6.98 (d, $^3J_{\text{HH}} = 8.0$ Hz, 4H, ArH), 6.77 – 6.75 (d, $^3J_{\text{HH}} = 8.0$ Hz, 2H, ArH), 6.53 (s, 1H, NH), 5.96 (s, 2H, NH), 3.09 – 3.03 (m, 4H, CH(CH₃)₂), 2.81 – 2.74 (m, 4H, CH(CH₃)₂), 1.41 – 1.39 (d, $^3J_{\text{HH}} = 4.0$ Hz, 12H, CH(CH₃)₂), 1.30 – 1.28 (d, $^3J_{\text{HH}} = 8.0$ Hz, 12H, CH(CH₃)₂), 1.21 – 1.20 (d, $^3J_{\text{HH}} = 8.0$ Hz, 12H, CH(CH₃)₂), 0.90 – 0.88 (d, $^3J_{\text{HH}} = 8.0$ Hz, 12H, CH(CH₃)₂), 0.47 (t, $^3J_{\text{HH}} = 8.0$ Hz, 3H, LZnCH₂CH₃), 0.13 (q, $^3J_{\text{HH}} = 8.0$ Hz, 2H, LZnCH₂CH₃). ¹³C{¹H} NMR (176 MHz, CDCl₃, 298 K) δ = 150.7 (Ar-C), 146.2 (Ar-C), 142.0 (Ar-C), 134.4 (Ar-C), 131.7 (Ar-C), 129.3 (Ar-C), 129.0 (Ar-C), 125.7 (Ar-C), 125.5 (Ar-C), 125.2 (Ar-C), 112.6 (Ar-C), 29.0 (Ar-CH(CH₃)₂), 28.7 (Ar-CH(CH₃)₂), 24.9 (Ar-CH(CH₃)₂), 24.6 (Ar-CH(CH₃)₂), 22.9 (Ar-CH(CH₃)₂), 21.5 (Ar-CH(CH₃)₂), 10.1 (LZnCH₂CH₃), -0.01 (LZnCH₂CH₃). ¹¹B NMR (128 MHz, CDCl₃, 298 K) δ = -16.64. ¹⁹F{¹H} NMR (377 MHz, CDCl₃, 298 K) δ = -132.5, -163.2, -163.3, -163.3, -166.9, -167.0, -167.0. HRMS (ASAP/Q-TOF) m/z : [M+H]⁺ Calcd for C₇₆H₇₇BF₂₀N₅Zn 1514.5281, found: 1514.4723.

Synthesis of [L(3H)ZnI]⁺ [B(C₆F₅)₄]⁻ (Zn-7): The neutral precursor compound (**Zn-3**) (250 mg, 0.268 mmol) was mixed with an equimolar amount of [PhNMe₂H]⁺[B(C₆F₅)₄]⁻ (215 mg, 0.268 mmol) in dry CDCl₃ at room temperature. The reaction mixture was stirred at room temperature for 36 h, followed by the evaporation of volatiles under a high vacuum. The residues were washed with hexane (2*8 mL) and dried under a high vacuum to obtain **Zn-7** as a pale greenish powder. (Yield 0.31 g, 72 %). Mp: 230-235 °C. ¹H NMR (400 MHz, CDCl₃, 298 K) δ = 7.49 – 7.46 (m, 2H, ArH), 7.42 – 7.41 (d, $^3J_{\text{HH}} = 4.0$ Hz, 4H, ArH), 7.31 – 7.27 (m, 5H, ArH), 7.03 – 7.01 (d, $^3J_{\text{HH}} = 7.8$ Hz, 4H, ArH), 6.85 – 6.82 (m, 4H, ArH + NH), 6.23 (s, 2H, NH), 3.06 – 2.81 (m, 4H, Ar-CH(CH₃)₂), 2.79 – 2.74 (m, 4H, Ar-CH(CH₃)₂), 1.43 – 1.42 (m, 24H, Ar-CH(CH₃)₂), 1.26 – 1.24 (d, $^3J_{\text{HH}} = 8.0$ Hz, 12H, Ar-CH(CH₃)₂), 0.90 – 0.88 (d, $^3J_{\text{HH}} = 6.5$ Hz, 12H, Ar-CH(CH₃)₂). ¹¹B NMR (128 MHz, CDCl₃, 298 K) δ = -16.67. ¹⁹F{¹H} NMR (377 MHz, CDCl₃, 298 K) δ = -132.5,

-163.1, -163.2, -163.3, -166.9, -166.9, -167.0. HRMS (ASAP/Q-TOF) m/z : $[M+H]^+$ Calcd for $C_{74}H_{72}BF_{20}N_5ZnI$ 1612.3934, found: 1612.4288.

8.4.1. X-ray Crystallography

The single crystal of compounds **Zn-1**, **Zn-2**, **Zn-3**, and **Zn-4** were crystalized from toluene at -10 °C as colorless blocks after 24 h and **Zn-5**, **Zn-6** and **Zn-7** were crystalized from benzene or chloroform at rt as pale green blocks after 24 h. The crystal data of compounds **Zn-1**, **Zn-2**, **Zn-3**, **Zn-4**, and **Zn-5** were collected on a Rigaku Oxford diffractometer at 100 K, whereas **Zn-6** and **Zn-7** were collected at 293 K. Selected data collection parameters and other crystallographic results are summarized in Tables 8.2-8.3. The structure was determined using direct methods employed in *ShelXT*,²¹ *OleX*,²² and refinement was carried out using least-square minimization implemented in *ShelXL*.²³ All non-hydrogen atoms were refined with anisotropic displacement parameters. Hydrogen atom positions were fixed geometrically in idealized positions and were refined using a riding model.

Table 8.2. Crystallographic data and refinement parameters for compounds **Zn-1 - Zn-4**.

Compound	Zn-1	Zn-2	Zn-3	Zn-4
Empirical Formula	C ₅₁ H ₇₃ N ₅ Zn	C ₅₂ H ₇₅ N ₅ Zn	C ₅₀ H ₇₀ IN ₅ Zn	C ₅₀ H ₇₁ N ₅ Zn
Molecular mass	821.51	835.60	933.38	807.55
Temperature (K)	100	100	100	100
Wavelength (Å)	1.54184	1.54184	1.54184	0.71073
Size(mm)	0.2 × 0.18 × 0.17	0.2 × 0.19 × 0.17	0.2 × 0.18 × 0.17	0.2 × 0.18 × 0.17
Crystal system	monoclinic	triclinic	monoclinic	monoclinic
Space group	P2 ₁ /c	P-1	C2/c	C2/c
a (Å)	11.02153(12)	10.7771(1)	11.16000(10)	27.6965(13)
b (Å)	20.9515(2)	12.0104(2)	21.0258(2)	10.7068(3)
c (Å)	21.7220(3)	21.3556(2)	21.7420(3)	19.6795(9)
α (deg)°	90	91.713(1)	90	90
β (deg)°	104.6932(12)	104.010(1)	104.4850(10)	127.917(7)
γ (deg)°	90	115.085(1)	90	90
Volume (Å ³)	4851.96(10)	2401.24(6)	4939.55(10)	4603.9(6)
Z	4	2	4	4
Calculated density (g/cm ³)	1.125	1.1556	1.255	1.1650
Absorption coefficient (mm ⁻¹)	0.972	0.990	5.863	0.572
F(000)	1776.0	903.0	1952.0	1745.7
Theta range for data collection (deg)°	8.294 to 151.08	8.22 to 136.5	8.4 to 136.482	7.32 to 52.74
Limiting indices	-13 ≤ h ≤ 12, -25 ≤ k ≤ 23, -26 ≤ l ≤ 22	-13 ≤ h ≤ 10, -14 ≤ k ≤ 14, -24 ≤ l ≤ 26	-13 ≤ h ≤ 13, -25 ≤ k ≤ 20, -26 ≤ l ≤ 22	-34 ≤ h ≤ 38, -14 ≤ k ≤ 14, -25 ≤ l ≤ 24
Reflections collected	37847	34581	18195	28337
Independent reflections	9478 [R _{int} = 0.0275, R _{sigma} = 0.0221]	8766 [R _{int} = 0.0848, R _{sigma} = 0.0502]	4537 [R _{int} = 0.0618, R _{sigma} = 0.0431]	4712 [R _{int} = 0.0393, R _{sigma} = 0.0261]
Completeness to theta	99 %	99 %	99 %	99 %
Absorption correction	Empirical	Empirical	Empirical	Empirical
Data / restraints /parameters	9478 / 0 / 531	8766 / 0 / 540	4537 / 0 / 267	4712 / 0 / 264
Goodness – of–fit on F ²	1.038	1.038	1.048	1.030
Final R indices [I>2 sigma(I)]	R ₁ = 0.0360, wR ₂ = 0.1040	R ₁ = 0.0666, wR ₂ = 0.1805	R ₁ = 0.0459, wR ₂ = 0.1182	R ₁ = 0.0373, wR ₂ = 0.0974

Table 8.3. Crystallographic data and refinement parameters for compounds **Zn-5 - Zn-7**.

Compound	Zn-5	Zn-6	Zn-7
Empirical Formula	C ₈₁ H ₇₇ BF ₂₀ N ₅ Zn	C ₇₇ H ₇₇ BCl ₃ F ₂₀ N ₅ Zn	C ₁₅₃ H ₁₄₇ B ₂ Cl ₁₅ F ₄₀ N ₁₀ Zn ₂
Molecular mass	1576.65	1634.96	3823.71
Temperature (K)	100	293	293
Wavelength (Å)	1.54184	1.54184	1.54184
Size(mm)	0.2 × 0.19 × 0.18	0.13 × 0.1 × 0.08	0.12 × 0.1 × 0.07
Crystal system	Monoclinic	Triclinic	Triclinic
Space group	P21/n	P-1	P-1
a (Å)	17.2919(3)	16.1606(4)	12.4414(2)
b (Å)	24.0736(7)	17.0908(3)	17.3423(2)
c (Å)	19.9128(4)	17.4475(3)	38.6670(4)
α (deg)°	90	76.126(2)	97.2870(10)
β (deg)°	92.305(2)	73.337(2)	96.1580(10)
γ (deg)°	90	78.115(2)	93.3780(10)
Volume (Å ³)	8282.6(3)	4432.88(17)	8205.47(18)
Z	4	2	2
Calculated density (g/cm ³)	1.264	1.225	1.548
Absorption coefficient (mm ⁻¹)	1.183	1.933	6.414
F(000)	3252	1680	3852
Theta range for data collection (deg)°	3.672 to 75.467	3.423 to 72.932	3.227 to 77.133
Limiting indices	-15 ≤ h ≤ 21, -29 ≤ k ≤ 29, -24 ≤ l ≤ 24	-19 ≤ h ≤ 19, -18 ≤ k ≤ 21, -20 ≤ l ≤ 21	-15 ≤ h ≤ 15, -21 ≤ k ≤ 14, -48 ≤ l ≤ 48
Reflections collected	58869	61150	111768
Independent reflections	16665 [R _{int} = 0.0915]	17311 [R _{int} = 0.1031]	33233 [R _{int} = 0.1569]
Completeness to theta	99 %	99 %	99 %
Absorption correction	Empirical	Empirical	Empirical
Data / restraints / parameters	16665 / 706 / 990	17311 / 666 / 982	33233 / 1386 / 2049
Goodness – of–fit on F ²	1.565	1.703	1.072
Final R indices [I>2 sigma(I)]	R ₁ = 0.1410, wR ₂ = 0.4033	R ₁ = 0.1259, wR ₂ = 0.4022	R ₁ = 0.1480, wR ₂ = 0.3736

8.5. References

1. (a) Roy, M. M. D.; Omaña, A. A.; Wilson, A. S. S.; Hill, M. S.; Aldridge, S.; Rivard, E. *Chem. Rev.* **2021**, *121*, 12784-12965; (b) Wiegand, A.-K.; Rit, A.; Okuda, J. *Coord. Chem. Rev.* **2016**, *314*, 71-82; (c) Wu, X.-F.; Neumann, H. *Adv. Synth. Catal.* **2012**, *354*, 3141-3160.
2. Dagorne, S. *Synthesis* **2018**, *50*, 3662-3670.
3. (a) Scheiper, C.; Schulz, S.; Wölper, C.; Bläser, D.; Roll, J. *Z. Anorg. Allg. Chem.* **2013**, *639*, 1153-1159; (b) Chilleck, M. A.; Braun, T.; Herrmann, R.; Braun, B. *Organometallics* **2013**, *32*, 1067-1074; (c) Mukherjee, D.; Ellern, A.; Sadow, A. D. *J. Am. Chem. Soc.* **2010**, *132*, 7582-7583.
4. (a) Specklin, D.; Hild, F.; Fliedel, C.; Gourlaouen, C.; Veiros, L. F.; Dagorne, S. *Chem. Eur. J.* **2017**, *23*, 15908-15912; (b) Rauch, M.; Parkin, G. *J. Am. Chem. Soc.* **2017**, *139*, 18162-18165.
5. Schnee, G.; Fliedel, C.; Avilés, T.; Dagorne, S. *Eur. J. Inorg. Chem.* **2013**, 3699-3709.
6. Chilleck, M. A.; Hartenstein, L.; Braun, T.; Roesky, P. W.; Braun, B. *Chem. Eur. J.* **2015**, *21*, 2594-2602.
7. Specklin, D.; Fliedel, C.; Gourlaouen, C.; Bruyere, J.-C.; Avilés, T.; Boudon, C.; Ruhlmann, L.; Dagorne, S. *Chem. Eur. J.* **2017**, *23*, 5509-5519.
8. (a) Chambenahalli, R.; Andrews, A. P.; Ritter, F.; Okuda, J.; Venugopal, A. *Chem. Commun.* **2019**, *55*, 2054-2057; (b) Rit, A.; Zanardi, A.; Spaniol, T. P.; Maron, L.; Okuda, J. *Angew. Chem. Int. Ed.* **2014**, *53*, 13273-13277; (c) Lummis, P. A.; Momeni, M. R.; Lui, M. W.; McDonald, R.; Ferguson, M. J.; Miskolzie, M.; Brown, A.; Rivard, E. *Angew. Chem. Int. Ed.* **2014**, *53*, 9347-9351.

-
9. (a) Kurono, N.; Ohkuma, T. *ACS Catal.* **2016**, *6*, 989-1023; (b) North, M.; Usanov, D. L.; Young, C. *Chem. Rev.* **2008**, *108*, 5146-5226.
10. Ma, Z.; Aliyeva, V. A.; Tagiev, D. B.; Zubkov, F. I.; Guseinov, F. I.; Mahmudov, K. T.; Pombeiro, A. J. L. *J. Organomet. Chem.* **2020**, *912*, 121171.
11. (a) Khuntia, A. P.; Sarkar, N.; Patro, A. G.; Sahoo, R. K.; Nembenna, S. *Eur. J. Inorg. Chem.* **2022**, e202200209; (b) Sen, N.; Khan, S. *Chem. Asian J.* **2021**, *16*, 705-719; (c) Pahar, S.; Kundu, G.; Sen, S. S. *ACS Omega* **2020**, *5*, 25477-25484; (d) Dasgupta, R.; Das, S.; Hiwase, S.; Pati, S. K.; Khan, S. *Organometallics* **2019**, *38*, 1429-1435; (e) Yadav, S.; Dixit, R.; Vanka, K.; Sen, S. S. *Chem. Eur. J.* **2018**, *24*, 1269-1273; (f) Wang, W.; Luo, M.; Li, J.; Pullarkat, S. A.; Ma, M. *Chem. Commun.* **2018**, *54*, 3042-3044; (g) Harinath, A.; Bhattacharjee, J.; Nayek, H. P.; Panda, T. K. *Dalton Trans.* **2018**, *47*, 12613-12622; (h) Bisai, M. K.; Das, T.; Vanka, K.; Sen, S. S. *Chem. Commun.* **2018**, *54*, 6843-6846; (i) Swamy, V. S. V. S. N.; Bisai, M. K.; Das, T.; Sen, S. S. *Chem. Commun.* **2017**, *53*, 6910-6913; (j) Yang, Z.; Yi, Y.; Zhong, M.; De, S.; Mondal, T.; Koley, D.; Ma, X.; Zhang, D.; Roesky, H. W. *Chem. Eur. J.* **2016**, *22*, 6932-6938; (k) Yang, Z.; Zhong, M.; Ma, X.; De, S.; Anusha, C.; Parameswaran, P.; Roesky, H. W. *Angew. Chem. Int. Ed.* **2015**, *54*, 10225-10229; (l) Karmakar, A.; Hazra, S.; Guedes da Silva, M. F. C.; Pombeiro, A. J. L. *Dalton Trans.* **2015**, *44*, 268-280; (m) Li, Y.; Wang, J.; Wu, Y.; Zhu, H.; Samuel, P. P.; Roesky, H. W. *Dalton Trans.* **2013**, *42*, 13715-13722; (n) Kadam, S. T.; Kim, S. S. *Appl. Organomet. Chem.* **2009**, *23*, 119-123; (o) Zhang, Z.; Chen, J.; Bao, Z.; Chang, G.; Xing, H.; Ren, Q. *RSC Adv.* **2015**, *5*, 79355-79360; (p) Cui, X.; Xu, M.-C.; Zhang, L.-J.; Yao, R.-X.; Zhang, X.-M. *Dalton Trans.* **2015**, *44*, 12711-12716; (q) Saravanan, P.; Anand, R. V.; Singh, V. K. *Tetrahedron Lett.* **1998**, *39*, 3823-3824.
-

-
12. Wang, W.; Luo, M.; Yao, W.; Ma, M.; Pullarkat, S. A.; Xu, L.; Leung, P.-H. *ACS Sustainable Chem. Eng.* **2019**, *7*, 1718-1722.
 13. Gassman, P. G.; Talley, J. J. *Tetrahedron Lett.* **1978**, *19*, 3773-3776.
 14. (a) Rawat, S.; Bhandari, M.; Prashanth, B.; Singh, S. *ChemCatChem* **2020**, *12*, 2407-2411; (b) Sharma, M. K.; Sinhababu, S.; Mukherjee, G.; Rajaraman, G.; Nagendran, S. *Dalton Trans.* **2017**, *46*, 7672-7676.
 15. (a) Sahoo, R. K.; Sarkar, N.; Nembenna, S. *Inorg. Chem.* **2023**, *62*, 304-317; (b) Sahoo, R. K.; Patro, A. G.; Sarkar, N.; Nembenna, S. *Organometallics* **2023**, DOI: <https://doi.org/10.1021/acs.organomet.2c00610>; (c) Sahoo, R. K.; Patro, A. G.; Sarkar, N.; Nembenna, S. *ACS Omega* **2023**, *8*, 3452-3460; (d) Sahoo, R. K.; Rajput, S.; Patro, A. G.; Nembenna, S. *Dalton Trans.* **2022**, *51*, 16009-16016; (e) Sahoo, R. K.; Sarkar, N.; Nembenna, S. *Angew. Chem. Int. Ed.* **2021**, *60*, 11991-12000; (f) Sahoo, R. K.; Mahato, M.; Jana, A.; Nembenna, S. *J. Org. Chem.* **2020**, *85*, 11200-11210.
 16. Peddaraao, T.; Baishya, A.; Sarkar, N.; Acharya, R.; Nembenna, S. *Eur. J. Inorg. Chem.* **2021**, 2034-2046.
 17. (a) Sarkar, N.; Sahoo, R. K.; Mukhopadhyay, S.; Nembenna, S. *Eur. J. Inorg. Chem.* **2022**, e202101030; (b) Sarkar, N.; Mahato, M.; Nembenna, S. *Eur. J. Inorg. Chem.* **2020**, 2295-2301; (c) Sarkar, N.; Bera, S.; Nembenna, S. *J. Org. Chem.* **2020**, *85*, 4999-5009.
 18. Nicasio, A. I.; Montilla, F.; Álvarez, E.; Colodrero, R. P.; Galindo, A. *Dalton Trans.* **2017**, *46*, 471-482.
 19. Cheng, M.; Moore, D. R.; Reczek, J. J.; Chamberlain, B. M.; Lobkovsky, E. B.; Coates, G. *W. J. Am. Chem. Soc.* **2001**, *123*, 8738-8749.

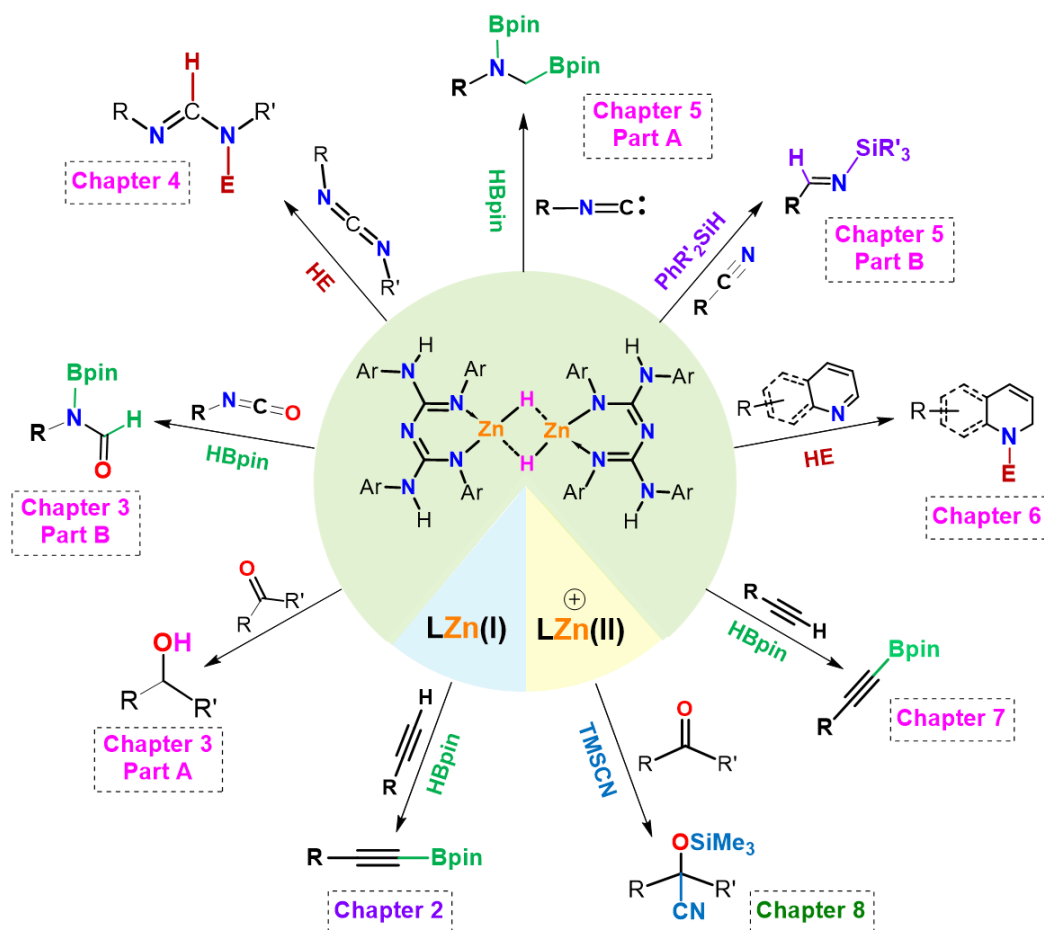
20. Spielmann, J.; Piesik, D.; Wittkamp, B.; Jansen, G.; Harder, S. *Chem. Commun.* **2009**, 3455-3456.
21. Sheldrick, G. *Acta Crystallogr. C.* **2015**, 71, 3-8.
22. Dolomanov, O. V.; Bourhis, L. J.; Gildea, R. J.; Howard, J. A. K.; Puschmann, H. *J. Appl. Crystallogr.* **2009**, 42, 339-341.
23. (a) Sheldrick, G. M. *Acta Crystallogr., Sect. A: Found. Crystallogr.* **2008**, 64, 112-122; (b) Sheldrick, G. M. *Acta Crystallogr., Sect. A: Found. Adv.* **2015**, 71, 3-8.

Thesis Summary

Zinc is a less expensive, non-toxic, and abundant element on the earth's crust than other precious transition or lanthanide elements, thus attracting interest in its use in catalysis. This thesis is based on synthesizing conjugated bis-guanidinate (CBG)-stabilized zinc-based complexes and their application in catalysis. More importantly, investigate the detailed mechanistic insights by isolating the key intermediates.

At first, CBG supported Zn(I) dimers, Zn(II) hydrides, and cations were isolated and thoroughly characterized. Subsequently, Zn(I) dimers are employed as pre-catalysts for the C-H borylation of terminal alkynes. Additionally, the CBG zinc(II) hydride complex has been used for the hydrofunctionalization of ketones and the chemoselective hydroboration of isocyanates. Moreover, the chemoselective reduction of nitriles and isonitriles and 1,2-regioselective hydrofunctionalization of N-heteroarenes were demonstrated by using zinc hydride species. Further, neutral and cationic CBG-stabilized zinc alkyls, halides, and hydride complexes are employed as catalytically active species in the cyanosilylation reactions. Furthermore, we performed various stoichiometric experiments and isolated key intermediates to propose the most probable catalytic cycles.

As a result, the thesis provides excellent guidelines for designing effective catalysts, reducing difficult organic transformations, and understanding the reaction mechanisms.



Zinc Hydride-Catalyzed Hydrofunctionalization of Ketones

Rajata Kumar Sahoo, Mamata Mahato, Achintya Jana, and Sharanappa Nembenna*

Cite This: *J. Org. Chem.* 2020, 85, 11200–11210

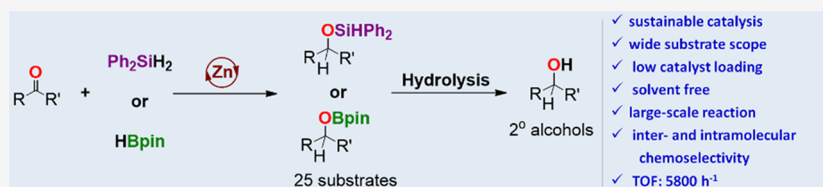
Read Online

ACCESS |

Metrics & More

Article Recommendations

Supporting Information



ABSTRACT: Three new dimeric bis-guanidinate zinc(II) alkyl, halide, and hydride complexes $[\text{LZnEt}]_2$ (1), $[\text{LZnI}]_2$ (2) and $[\text{LZnH}]_2$ (3) were prepared. Compound 3 was successfully employed for the hydrosilylation and hydroboration of a vast number of ketones. The catalytic performance of 3 in the hydroboration of acetophenone exhibits a turnover frequency, reaching up to 5800 h^{-1} , outperforming that of reported zinc hydride catalysts. Notably, both intra- and intermolecular chemoselective hydrosilylation and hydroboration reactions have been investigated.

INTRODUCTION

The catalytic hydrofunctionalization of ketones with silanes or HBpin is undoubtedly a practical methodology for the syntheses of silyl ethers or borate esters, which are extensively utilized as intermediates for the syntheses of alcohols.¹ The design of inexpensive and sustainable homogenous metal catalysts, particularly, metal hydrides, is very desirable. In this context, an earth-abundant, environmentally friendly, cheaper, and biocompatible zinc² element fits the bill entirely.

In 1947, Schlesinger reported the synthesis of zinc dihydride.³ To date, several synthetic routes are available for the preparation of zinc dihydride⁴ (ZnH_2), it is a white solid, for which the exact structure is not clear. Moreover, it is thermally unstable and poorly soluble in organic solvents. This motivated many synthetic chemists to prepare neutral heteroleptic zinc hydrides.⁵ Such zinc hydrides are not only important reducing agents but they can also be model compounds for enzyme mimicking, as precursors in material science and catalysts for various organic transformations.⁶

As far as zinc-catalyzed hydrofunctionalization of carbonyls is concerned, there are reports on zinc-catalyzed hydrosilylation of carbonyls.⁷ Mainly, Parkin et al.,⁸ Nikonov et al.,⁹ Okuda et al.,¹⁰ Rivard et al.,¹¹ Jones et al.,¹² Mösch-Zanetti et al.,¹³ and Venugopal et al.¹⁴ independently reported zinc hydride-catalyzed hydrosilylation of ketones (Figure 1A–G). Surprisingly, examples of zinc-catalyzed hydroboration of ketones are scarce.¹⁵ To our knowledge, there are only two examples on the hydroboration of ketones catalyzed by molecular zinc hydrides (Figure 1D,E).^{11,12} It should be noted that no zinc catalysts are available in literature, which performs for both hydrosilylation and hydroboration of many ketones (bifunctional), except D and E, which are limited to only one substrate. However, very recently, the Baker group

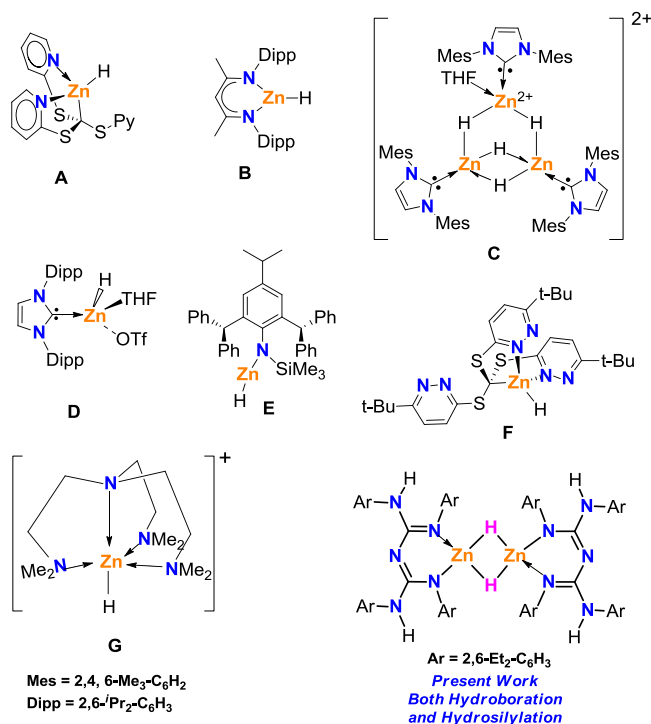


Figure 1. Previously reported selected zinc hydride catalysts for (A–G) hydrosilylation and (D,E) hydroboration of ketones and present work.

Received: May 29, 2020

Published: August 6, 2020

Hydroboration

Zinc Hydride Catalyzed Chemoselective Hydroboration of Isocyanates: Amide Bond Formation and C=O Bond Cleavage

Rajata Kumar Sahoo, Nabin Sarkar, and Sharanappa Nembenna*

Dedicated to Professor Herbert W. Roesky on the occasion of his 85th birthday

Abstract: Herein, a remarkable conjugated bis-guanidinate (CBG) supported zinc hydride, $[(LZnH)_2]$; $L = \{(ArHN)-(ArN)-C=N-C=(NAr)(NHAr)\}$; $Ar = 2,6-Et_2-C_6H_3\}$ (**I**) catalyzed partial reduction of heteroallenes via hydroboration is reported. A large number of aryl and alkyl isocyanates, including electron-donating and withdrawing groups, undergo reduction to obtain selectively N-boryl formamide, bis(boryl) hemiaminal and N-boryl methyl amine products. The compound **I** effectively catalyzes the chemoselective reduction of various isocyanates, in which the construction of the amide bond occurs. Isocyanates undergo a deoxygenation hydroboration reaction, in which the C=O bond cleaves, leading to N-boryl methyl amines. Several functionalities such as nitro, cyano, halide, and alkene groups are well-tolerated. Furthermore, a series of kinetic, control experiments and structurally characterized intermediates suggest that the zinc hydride species are responsible for all reduction steps and breaking the C=O bond.

Introduction

Isocyanates are cheaper and commercially available feedstocks that are very useful in numerous organic transformations.^[1] These are essential precursors for the synthesis of extremely important amides.^[2] In particular, formamides are necessary starting materials to produce useful heterocycles, bioactive compounds, and drugs.^[3] Generally, these formamides can be accessed using formylating agents such as formic acid, formaldehyde, formate, chloral, and carbon dioxide, thereby producing a considerable waste.^[4] Conventional methods for amide bond creation are based on C–N bond-forming strategies utilizing carboxylic acid derivatives and amines.^[5] Formamides can be produced easily by the direct coupling of methanol with amines using organic or inorganic supported metal catalysts (C–N bond formation).^[6] Also, the recent trend of making amides involves metal-catalyzed C–C coupling with isocyanates.^[7]

Pace and co-workers reported the in situ generated Schwartz reagent (Cp_2ZrClH) mediated chemoselective reduction of isocyanates to formamides.^[2a,8] Before this elegant

How to cite: *Angew. Chem. Int. Ed.* **2021**, 60, 11991–12000

International Edition: doi.org/10.1002/anie.202100375

German Edition: doi.org/10.1002/ange.202100375

work, there were reports on amide synthesis by Grignard or other metal reagents and isocyanates' reaction.^[9]

Despite the tremendous work on the metal-catalyzed hydroboration of unsaturated organic molecules,^[10] including heteroallenes such as carbon dioxide^[11] and carbodiimides,^[12] there have been no reports of hydroboration of isocyanates to N-boryl formamides (see below). Nonetheless, to the best of our knowledge, there have been very few reports on selective monohydrosilylation of isocyanates to N-silyl formamide^[13] and hydrogenation of isocyanates to formamides.^[14]

N-methyl amines are key intermediates in the production of fine chemicals, dyes, and natural products.^[15] Typically, the selective N-alkylation of primary amines utilizing CH_3I and $(CH_3)_2SO_4$ is challenging, and usually, over methylation occurs. Other methods are the metal-catalyzed reduction of CO_2 surrogates^[16] and direct amine alkylation with alcohols.^[17] However, these methods suffer from the use of hazardous chemicals and harsh reaction conditions.

Rueping et al. have shown the magnesium catalyzed hydroboration of formamide to N-methyl amine product.^[18] In 2015, Beller and co-workers reported commercially available Karstadt's complex/2,2':6',2''-terpyridine (tpy) catalyzed reductive methylation of amines with carbonates.^[19] In 2009, Zhang et al. reported the metal-free reduction of isocyanates to N-methyl amine using a $Ph_2SiH_2/B(C_6F_5)_3$ catalytic system.^[20] Besides, there have been reports on the reduction of isocyanates by using stoichiometric amounts of metal reagents.^[21]

As far as metal-catalyzed reduction of isocyanates is concerned, as shown in Figure 1, the ideal catalyst for the desired transformations should possess few significant features: a) Partial (chemoselective) reduction of isocyanates via hydroboration, the formation of N-boryl formamide; b) reduction of isocyanates without cleavage of a C=O bond, N-, O-bis(boryl) hemiaminal; c) deoxygenated hydroboration of isocyanates that can lead to the formation of N-boryl methyl amines in which cleavage of C=O bond should occur.

In this context, Okuda group reported magnesium catalyzed dihydroboration of ^{tert}Butyl isocyanate with HBpin to N-, O-bis(boryl) hemiaminal.^[22] The metal-catalyzed deoxygenated reduction of amides to amines^[23] is known, however as far as hydrodeoxygenation (HDO) of isocyanates is concerned, there are only three examples, including recently published two patents and one research paper.^[24] In 2017, Hill and co-workers reported magnesium catalyzed hydroboration of isocyanates to N-boryl methyl amines.^[25] The authors observed N-borylated formamide and N-, O-bis(boryl) hemiaminal species as intermediates during the reductive catalysis.

* R. K. Sahoo, N. Sarkar, Dr. S. Nembenna

School of Chemical Sciences, National Institute of Science Education and Research (NISER), Homi Bhabha National Institute (HBNI) Bhubaneswar, 752050 (India)

E-mail: snembenna@niser.ac.in

Supporting information and the ORCID identification number(s) for the author(s) of this article can be found under: <https://doi.org/10.1002/anie.202100375>.

PAPER

[View Article Online](#)
[View Journal](#) | [View Issue](#)Cite this: *Dalton Trans.*, 2022, **51**, 16009Received 31st August 2022,
Accepted 20th September 2022

DOI: 10.1039/d2dt02846h

rsc.li/dalton

Synthesis of low oxidation state zinc(I) complexes and their catalytic studies in the dehydroborylation of terminal alkynes†

Rajata Kumar Sahoo, Sagrika Rajput, A. Ganesh Patro and
Sharanappa Nembenna[†]*

A new example of a structurally characterized conjugated bis-guanidinate (CBG) supported zinc(I) dimer, *i.e.*, LZnZnL (**3**) (L = {(ArNH)(ArN)–C=N–C=(NAr)(NHAr)}; Ar = 2,6-Et₂-C₆H₃) with a Zn–Zn bond is reported. Moreover, homoleptic (**3**) and heteroleptic (Cp*ZnZnL, **2**, (Cp* = 1,2,3,4,5-pentamethyl cyclopentadienide)) zinc(I) dimers are used as precatalysts in the dehydroborylation of a wide array of terminal alkynes. Furthermore, the active catalyst, CBG zinc acetylide (LZn–C≡C–Ph-4-Me)₂, (**5**), is isolated which is confirmed by X-ray crystal structure analysis. A series of stoichiometric experiments have been performed to propose a plausible reaction mechanism.

Introduction

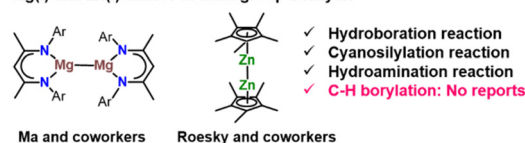
The syntheses of low oxidation state metal–metal bonded complexes have attracted interest in several areas of chemical science due to their unique properties.¹ In 2004, Carmona and coworkers reported the first covalent zinc–zinc bonded complex Cp*₂Zn₂ (Cp* = 1,2,3,4,5-pentamethyl cyclopentadienide).² Later, the synthesis and reactivity studies of low-oxidation state zinc complexes with Zn–Zn bonds showed progress.³ Subsequently, in 2007, Jones and coworkers reported the first example of a β-diketiminato stabilized magnesium(I) dimer with an Mg–Mg bond.⁴ There are only a few reports concerning low oxidation state metal–metal bonded Zn(I) and Mg(I) dimers in catalysis. In 2018, Ma and coworkers reported that a Mg(I) dimer, *i.e.*, (Xyl)NacnacMg)₂, pre-catalyzed the cyanosilylation of ketones.⁵ Afterward, the same group reported the hydroboration of carbonyl compounds such as aldehydes, ketones, esters, carbonates, CO₂, and epoxides using Mg(I) dimers as pre-catalysts.⁶ Furthermore, Ma and coworkers described unsymmetrical β-diketiminato Mg(I) dimers as pre-catalysts for the hydroboration of alkynes and nitriles.⁷ Although mechanisms are unclear, presumably, L'MgH is active species in such hydroboration reactions.⁸

Likewise, a few examples of low oxidation state zinc(I) complexes in catalysis are known. In 2011, Roesky and coworkers demonstrated Cp*₂Zn₂ as a catalyst for the hydroamination reaction for the first time.⁹ Later, the authors compared the catalytic efficiency of Cp*₂Zn₂ with those of Cp*₂Zn and commercially available ZnEt₂ in hydroamination reactions (Scheme 1A).¹⁰ To explore the catalytic activity of the Zn(I) compound, herein, we investigated the Zn(I) pre-catalyzed dehydroborylation of terminal alkynes for the first time. Organoboranes are in high demand because of their wide range of applications in many chemical transformations and provide valuable intermediates in medicinal and organic chemistry.¹¹ Compared to the well-established hydroboration of alkynes,^{8,12} there are few

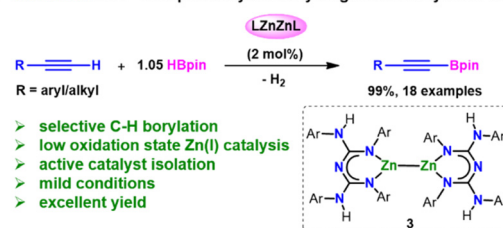
School of Chemical Sciences, National Institute of Science Education and Research (NISER), Homi Bhabha National Institute (HBNI) Bhubaneswar, 752050, India.
E-mail: snembenna@niser.ac.in

† Electronic supplementary information (ESI) available: ¹H and ¹³C{¹H} NMR spectra of compounds **II** and **IV**, stoichiometric experiments, and organoborane products. CCDC 2179810 and 2179805. For ESI and crystallographic data in CIF or other electronic format see DOI: <https://doi.org/10.1039/d2dt02846h>

A. Mg(I) and Zn(I) dimers in main group catalysis



B. This work: Zinc–Zinc precatalyzed dehydrogenative borylation of alkynes



Scheme 1 Low oxidation state metal complexes with the M–M bond in catalysis.

Intermediates, Isolation and Mechanistic Insights into Zinc Hydride-Catalyzed 1,2-Regioselective Hydrofunctionalization of N-Heteroarenes

Rajata Kumar Sahoo, Nabin Sarkar, and Sharanappa Nembenna*



Cite This: *Inorg. Chem.* 2023, 62, 304–317



Read Online

ACCESS |



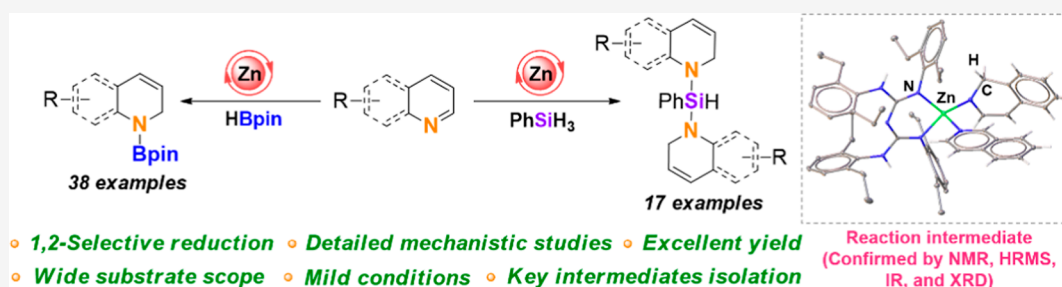
Metrics & More



Article Recommendations



Supporting Information



ABSTRACT: The conjugated bis-guanidinate-supported zinc hydride $[\{LZnH\}_2]$; $L = \{(ArHN) (ArN)-C\equiv N-C\equiv N(Ar) (NHAr)$; $Ar = 2,6-Et_2-C_6H_3\}$ (I)-catalyzed highly demanding exclusive 1,2-regioselective hydroboration and hydrosilylation of N-heteroarenes is demonstrated with excellent yields. This protocol is compatible with many pyridines and N-heteroarene derivatives, including electron-donating and -withdrawing substituents. Catalytic intermediates, such as $[(LZnH) (4\text{-methylpyridine})]$ **IIA**, $[(L'ZnH) (4\text{-methylpyridine})]$ **IIA'**, where $L' = CH\{(CMe) (2,6-Et_2C_6H_3N)_2\}$, $LZn(1,2\text{-DhiQ})$ (isoquinoline) **III**, $[L'Zn(1,2\text{-DhiQ})]$ (isoquinoline) **III'**, and $LZn(1,2\text{-}(3\text{-MeDhQ}))$ (3-methylquinoline) **V**, were isolated and thoroughly characterized by NMR, HRMS, and IR analyses. Furthermore, X-ray single-crystal diffraction studies confirmed the molecular structures of compounds **IIA'**, **III**, and **III'**. The NMR data proved that the intermediate **III** or **III'** reacted with HBpin and gave a selective 1,2-addition hydroborated product. Stoichiometric experiments suggest that **V** and **III** independently reacted with silane, yielding selective 1,2-addition of mono- and bis-hydrosilylated products, respectively. Based on the isolation of intermediates and a series of stoichiometric experiments, plausible catalytic cycles were established. Furthermore, the intermolecular chemoselective hydroboration reaction over other reducible functionalities was studied.

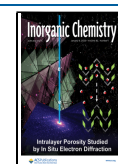
INTRODUCTION

A selective reduction of N-heteroarenes provides precious dihydropyridine (DHP) derivatives,¹ which play an essential role in organic chemistry (natural products), medicines, and biological transformations.² Due to their broad application, many synthetic routes have been developed to prepare selective DHPs.^{1g,3} Traditionally, stoichiometric metal reagents have been employed for the reduction of pyridines.⁴ Subsequently, metal-catalyzed hydrogenation reactions for selective reduction of N-heteroarenes were established.⁵ These methods often require harsh reaction conditions and lack selectivity.^{4,4,5a–e} Moreover, a large amount of waste is generated in the case of stoichiometric metal reagents.⁴ Thus, the hydrofunctionalization of pyridine with borane or silane as a mild reducing agent for DHP synthesis would be significant.^{2a,6} In this context, in 2011, Hill and co-workers reported the β -diketiminato (NacNac) magnesium alkyl-catalyzed hydroboration of pyridine for the first time.⁷ The authors noticed the mixture of 1,2- and 1,4-DHP products.

Since then, metal-free catalysts such as N-heterocyclic phosphonium triflate (NHP-OTf)⁸ and organoboranes ($Ar^F_2BMe^9$ and $NH_4BPh_4^{10}$) have been used for the selective 1,4-hydroboration of N-heteroarenes with limited substrate scope. Reports on selective 1,4-hydroboration of N-heteroarenes using some transition-metal and main-group catalysts have been established.^{1c,11} In 2020, Chang and co-workers reported N-heterocyclic carbene-catalyzed selective 1,2-hydroboration of N-heteroarenes.¹² Similarly, regioselective 1,2-addition of B–H or Si–H to N-heteroarenes has been studied over the past years using main-group¹³ and transition-metal¹⁴ catalysts (Scheme 1a).

Received: September 23, 2022

Published: December 26, 2022



Zinc-Catalyzed Chemoselective Reduction of Nitriles to N-Silylimines through Hydrosilylation: Insights into the Reaction Mechanism

Rajata Kumar Sahoo and Sharanappa Nembenna*



Cite This: *Inorg. Chem.* 2023, 62, 12213–12222



Read Online

ACCESS |



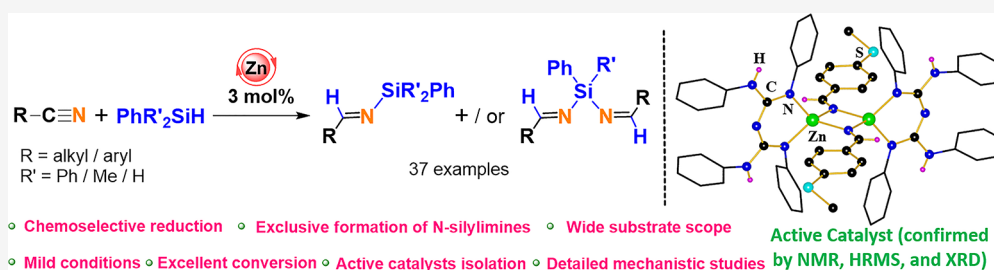
Metrics & More



Article Recommendations



Supporting Information



ABSTRACT: The N,N' -chelated conjugated bis-guanidinate (CBG) supported zinc hydride (**Zn-1**) pre-catalyzed highly challenging chemoselective mono-hydrosilylation of a wide range of nitriles to exclusive N-silylimines and/or N,N' -silyldiimines is reported. Furthermore, the effectiveness of pre-catalyst **Zn-1** is compared with another pre-catalyst analogue, i.e., $Diethyl^{1}NaCNac$ zinc hydride (**Zn-2**), to know the ligand effect. We observed that pre-catalyst **Zn-1** shows high efficiency and better selectivity than pre-catalyst **Zn-2** for reducing nitriles to N-silylimines. Mechanistic studies indicate the insertion of the $C\equiv N$ bond of nitrile into $Zn-H$ to form the zinc vinylidenamido complexes (**Zn-1'** and **Zn-2'**). The active catalysts **Zn-1'** and **Zn-2'** are confirmed by NMR, mass spectrometry, and single-crystal X-ray diffraction analyses. A most plausible catalytic cycle has been explored depending on stoichiometric experiments, active catalysts isolation, and in situ studies. Moreover, the synthetic utility of this protocol was demonstrated.

INTRODUCTION

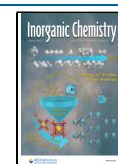
Chemoselective hydrosilylation of unsaturated organic substrates afforded precious organosilicon products, which are valuable precursors for laboratory methodology and industries.¹ Various procedures have been developed for the hydrosilylation of different functional groups such as alkene,^{1e,f,2} alkyne,^{1e,f,3} imine,^{4a–c} carbonyls,⁴ and carboxylic derivatives.^{4c–i} Additionally, there are numerous reports on catalytic double hydrosilylation of nitriles to 1,1-disilylamines.^{1b,4d,5} However, partial mono-hydrosilylation of nitriles to N-silyl aldimines remains a significant challenge. Due to N-silylimines being much more reactive than nitriles, these are further reduced to give the disilylamine products.^{5c,e,6} In addition, N-silylimines are very unstable.⁷ These N-silylated imines are suitable precursors in medicinal chemistry, nitrogen-containing organic compounds, and silicon-containing polymers.^{7a,8} N-silylimines are key intermediates for further functionalization.⁹ N-silylimines can be synthesized by adding a stoichiometric amount of metallo hexamethyldisilylamides to aldehydes (Figure 1a).¹⁰

In the traditional method, selective hydrosilylation of nitriles was achieved using mixed metal hydrides [$LiAl(L)_3H$ ($L = triethoxy/n-butyl diisopropyl$)] (Figure 1b).^{7a,9,11} Above

conventional methods suffer from the following drawbacks such as stoichiometric metal reagents, safety risks, and huge metal waste generation.^{7a,11} On the other hand, catalytic hydrosilylation of nitriles is also achieved by applying an excessive amount of silanes, which causes over-reduction and yielded disilylamine products.^{5b,e} Thus, developing metal-catalyzed selective hydrosilylation of nitriles to N-silylimines under mild conditions is very attractive. The selective synthesis of N-silylimines from nitriles mainly depends upon suitable catalysts and silanes. As far as metal-catalyzed partial reduction of nitriles is concerned, there have been a handful of reports in the literature using transition and main-group metal catalysts.^{4c,5i,12} Calas et al. reported the first mono-hydrosilylation of nitriles in 1961 using $ZnCl_2$ as a catalyst and $HSiEt_3$ as a silylating reagent with moderate yield under harsh reaction conditions.¹³

Received: January 30, 2023

Published: July 23, 2023



Zinc Catalyzed Hydroelementation (HE; E = B, C, N, and O) of Carbodiimides: Intermediates Isolation and Mechanistic Insights

Rajata Kumar Sahoo, Arukela Ganesh Patro, Nabin Sarkar, and Sharanappa Nembenna*

Cite This: *Organometallics* 2023, 42, 1746–1758

Read Online

ACCESS |



Metrics & More

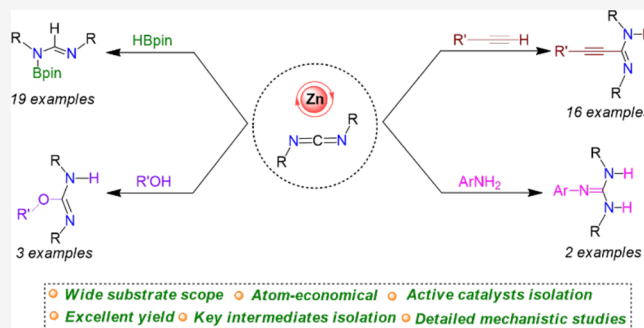


Article Recommendations



Supporting Information

ABSTRACT: The conjugated bis-guanidinate (CBG) supported zinc hydride, $[\{LZnH\}_2; L = \{(ArHN)(ArN)-C=N-C=(NAr)-(NHAr); Ar = 2,6-Et_2-C_6H_3\}]$ (**1**) (pre)-catalyzed addition of E–H (E = B, C, N, and O) to carbodiimides is presented. Compound **1** catalyzed the reduction of carbodiimides with pinacolborane (HBpin), terminal alkynes, primary amines, and alcohols, gave a series of *N*-boryl formamidines, propiolamidines, guanidines, and isoureas with high conversions. All these reactions display good tolerance of functional groups. These reactions proceeded through the active catalysts and intermediate of zinc amidinate (**Zn-1**, **Zn-1'**, and **Zn-3**), zinc alkynyl (**Zn-2**, and **Zn-2'**), zinc anilide (**Zn-4**), and zinc alkoxide (**Zn-5**) complexes, which have been characterized by multinuclear NMR and HRMS analyses. Moreover, compounds **Zn-1'**, **Zn-2'**, **Zn-4**, and **Zn-5** were confirmed by single-crystal X-ray diffraction studies. Complete catalytic cycles have been proposed based on well-defined intermediates and stoichiometric experiments.



INTRODUCTION

The metal-catalyzed hydroelementation reaction of unsaturated bonds has been an active research area over the past decade.¹ The hydroelementation reaction is used to construct C-heteroatom bonds via hydroboration,² hydrosilylation,³ hydroamination,⁴ hydrophosphination,⁵ hydrothiolation,⁶ hydroalkoxylation,⁷ and hydrogenation⁸ of alkenes and alkynes. These reactions have been studied using a wide range of transition, lanthanide, actinide, alkali, and alkaline-earth metal catalysts.⁹ It should be noted that the metal in these reactions does not play a significant role.^{9d}

However, hydroelementation of heterocumulenes has been scarcely investigated using metal catalysts. The hydroelementation of heterocumulenes afforded the corresponding guanidine,¹⁰ propiolamide,¹¹ and thiourea¹² derivatives, which have been widely used as ligands in coordination compounds,^{10c,13} material chemistry,¹⁴ and medicinal applications.¹⁵ Thus, developing an atom-efficient, versatile catalyst for the preparation of C–C and C-heteroatom bonds (generally propiolamide, formamide, guanidine, and urea) would be significant.

Recently, transition^{2a,16} and main group^{2b,17} metal catalyzed hydroboration of carbodiimides have been developed.¹⁸ To our knowledge, there have been no reports on zinc-catalyzed hydroboration of carbodiimide (CDI) (Figure 1A). In 2005, the Hou group introduced rare earth metal-catalyzed hydroalkynylation of carbodiimides to propiolamidines.¹⁹ After that, a few metal-catalyzed conversion of carbodiimides into propiolamidines were reported.^{11,20} However, zinc-catalyzed

hydroalkynylation of carbodiimides is limited (Figure 1A).²¹ Roesky^{5a} and Carrillo–Hermosilla²² research groups recently established diethylzinc as a precatalyst for P–H and O–H addition to heterocumulenes, respectively. As far as the E–H (E = C, N, O, P, and S) bond insertion into carbodiimide is concerned, only a handful of reports are known. Evan,²⁴ Eisen,²⁴ and Panda²⁵ groups independently reported Th, U, and Ti metal-catalyzed hydroelementation of heterocumulenes (Figure 1B). However, the previous reports on the hydroelementation reaction using zinc complexes usually involve one or two kinds of E–H nucleophiles and are limited to a narrow substrate scope.^{5a,21,22,26} Therefore, developing a zinc-based versatile catalyst that can exhibit the addition of various E–H (E = B, C, N, O, P, and S) moieties to carbodiimide is highly demanding.

Previously our group reported a NacNac analogue, conjugated bis-guanidinate (CBG)-stabilized dinuclear zinc hydride complex, $[\{LZnH\}_2; L = \{(ArHN)(ArN)-C=N-C=(NAr)-(NHAr); Ar = 2,6-Et_2-C_6H_3\}]$ (**1**) and used it as an effective catalyst for the B–H addition to a wide range of isocyanates.^{13b,27}

Special Issue: Advances and Applications in Catalysis with Earth-Abundant Metals

Received: December 7, 2022

Published: March 15, 2023



Zinc Hydride-Catalyzed Dihydroboration of Isonitriles and Nitriles: Mechanistic Studies with the Structurally Characterized Zinc Intermediates

Rajata Kumar Sahoo, Sagrika Rajput, Sneha Dutta, Kasturi Sahu, and Sharanappa Nembenna*



Cite This: <https://doi.org/10.1021/acs.organomet.3c00281>



Read Online

ACCESS |



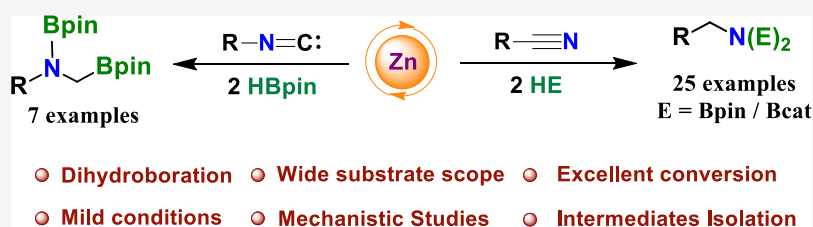
Metrics & More



Article Recommendations



Supporting Information



ABSTRACT: The conjugated bis-guanidinate (CBG)-stabilized zinc hydride, $[\{LZnH\}_2]$ ($L = \{(ArNH)(ArN)-C\equiv N-C\equiv N(Ar)(NHAr)\}$; $Ar = 2,6-Et_2-C_6H_3$) (**Zn-1**), is shown to be a highly active catalyst for the double reduction of isonitriles and nitriles with pinacolborane (HBpin) in this study. A wide array of isonitriles and nitriles, including aryl and alkyl groups, underwent hydroboration to afford exclusively 1,2- and 1,1-diborylated amine products, respectively. A series of stoichiometric reactions were performed to understand the reaction mechanisms. Hydroboration of isonitrile proceeds through the formation of zinc formimidoyl complex, $[LZnC(H)N(tBu)]_2$ (**Zn-2**), while nitrile hydroboration through zinc vinylidenamido complex, $[LZnNC(H)(C_6H_5)]_2$ (**Zn-3**). Moreover, compounds **Zn-2** and **Zn-3** are isolated and thoroughly characterized. Such molecular zinc complexes are rare in the literature.

INTRODUCTION

Zinc is an earth-abundant, cheaper, readily available, biocompatible, and nontoxic element.¹ Thus, zinc-based reagents or molecular compounds are attractive in catalysis.² Zinc-based compounds have been used as catalysts for the hydrofunctionalization of various unsaturated organic compounds.^{2b–d,3}

The complete catalytic reduction of the isonitriles ($R-N\equiv C:$) and nitriles ($R-C\equiv N$) affords secondary and primary amines, respectively, which are very useful in synthetic chemistry because of their widespread application in agrochemicals, drug molecules, dyes, and pharmaceutical industries.⁴ In this context, isonitriles reduction is quite an attractive research area.⁵ Despite the numerous reports on the metal-catalyzed hydroboration of unsaturated organic substrates,⁶ surprisingly, there are only two reports on the metal-catalyzed hydroboration of isonitrile.⁷ The first example of isonitrile dihydroboration was introduced by Hill and coworkers by using the $DippNacNac$ -supported magnesium butyl complex $[CH\{C(Me)NAr\}_2Mg^tBu]$ ($Ar = 2,6-Et_2C_6H_3$) in 2015.^{7b} Subsequently, in 2020, the Nembenna group reported aluminum-catalyzed hydroboration of isonitriles to 1,2-diborylated amines, with two examples.^{7a} However, there are no reports on zinc-catalyzed hydroboration of isonitriles (Figure 1).

In 2012, Nikonov and co-workers reported the dihydroboration of nitriles using a $(2,6-Et_2C_6H_3N)Mo(H)(Cl)(PMe_3)_3$ complex for the first time.⁸ Since then, there have been numerous reports on transition-,^{8,9} rare-earth,^{9b,s,10} and main-group^{9b,n,s,11} metal-catalyzed dihydroboration of nitriles to amines. As far as zinc-catalyzed hydroboration of nitriles is concerned, there are only three reports in the literature. Panda and co-workers reported that organozinc-catalyzed the hydroboration of nitriles.¹² In 2021, the Xu group established the dihydroboration of nitriles by using NHC-zinc dihydride as a catalyst.¹³ Recently, Baker and co-workers reported that pyridine-thioether-anilido-aryloxide stabilized zinc complex ($Zn(NSNO)$) catalyzed the hydroboration of nitriles (Figure 1).¹⁴

Most reported protocols have disadvantages, such as narrow substrate scope and lack of mechanistic details. There have also been no reports on zinc-catalyzed hydroboration of isonitriles. However, few reports on zinc-catalyzed dihydroboration of nitriles are known in the literature. Therefore, it is necessary to

Received: June 20, 2023



Comparison of Two Zinc Hydride Precatalysts for Selective Dehydrogenative Borylation of Terminal Alkynes: A Detailed Mechanistic Study

Rajata Kumar Sahoo, Arukela Ganesh Patro, Nabin Sarkar, and Sharanappa Nembenna*

Cite This: *ACS Omega* 2023, 8, 3452–3460

Read Online

ACCESS |



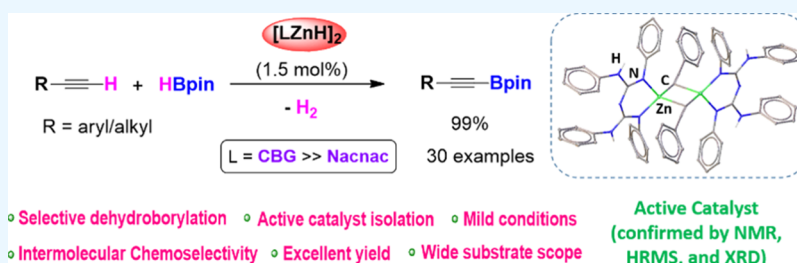
Metrics & More



Article Recommendations



Supporting Information



ABSTRACT: The conjugated bis-guanidinate-stabilized zinc hydride complex (I)-precatalyzed chemoselective dehydroborylation of a wide array of terminal alkynes with excellent yields is reported. Further, precatalyst I is compared with a newly synthesized DiethylNacNac zinc hydride precatalyst (III) for selective dehydroborylation of terminal alkynes, and it is discovered that precatalyst I is more active than III. We have studied intra- and intermolecular chemoselective dehydroborylation of terminal alkynes over other reducible functionalities such as alkene, ester, isocyanide, nitro, and heterocycles. The highly efficient precatalyst I shows a turnover number of 48.5 and turnover frequency of up to 60.5 h⁻¹ in the dehydroborylation of 1-ethynyl-4-fluorobenzene (**1i**). A plausible mechanism for selective dehydrogenative borylation of alkynes has been proposed based on active catalyst isolation and a series of stoichiometric reactions.

INTRODUCTION

A selective dehydrogenative borylation of terminal alkyne produces ubiquitous organoborane products, which play an essential role in many chemical transformations.¹ It also provides valuable intermediates in organic and medicinal chemistry.² Because of its wide application, many methods have been developed to synthesize organoboranes.³ In conventional methods, organoboranes have been synthesized using stoichiometric amounts of organolithium and organomagnesium reagents.^{3,4} The abovementioned methods suffer from the following drawbacks: poor functional group tolerance, safety issues, and large quantities of waste material. Therefore, hydroboration reactions using pinacolborane (HBpin)⁵ or bis(pinacolato)diboron (B₂pin₂)⁶ are efficient routes for synthesizing precious organoborane compounds. As far as zinc-mediated hydroboration of alkynes to vinyl boronates is concerned, Uchiyama and co-workers reported hydroboration of alkyne by using diethylzinc and B₂pin₂.⁷ Besides, Geetharani and co-workers described Zn(OTf)₂- and [Na][HBET₃]-catalyzed hydroboration of alkynes.^{5d} Compared to well-established hydroboration of alkynes using transition metals,^{5b,6,8} main group metal,^{5a,c,d,9} and metal-free catalysts,¹⁰ there are fewer reports on dehydrogenative borylation of terminal alkynes to alkynyl boronates (Scheme 1, A).

Ozerov and co-workers revealed the first catalytic dehydrogenative borylation of terminal alkynes using the iridium-based catalyst.¹¹ Subsequently, transition (Cu,¹² Fe¹³) and main group (Al)¹⁴ metal-based catalysts have been utilized for the dehydrogenative borylations. Moreover, a few reports on zinc-mediated dehydrogenative borylation of terminal alkynes are also known in the literature. Tsuchimoto and co-workers described Zn(OTf)₂-catalyzed dehydrogenative borylation of terminal alkynes.¹⁵ Ingleson and co-workers showed the dehydrogenative borylation of terminal alkyne and hydroboration of alkynyl borate products using NHC zinc cation adducts.¹⁶

After that, Ma and co-workers reported similar reactions using ZnBr₂ as a catalyst.¹⁷ During the preparation of our article, Dobrovetsky and co-workers demonstrated the zinc cation [TPPhZn²⁺][B(C₆F₅)₄]₂ as a catalyst for dehydrogenative borylation and hydroboration of terminal alkynes.¹⁸ All

Received: November 17, 2022

Accepted: December 19, 2022

Published: January 10, 2023

